BIOMATERIALS APPLICATIONS FOR NANOMEDICINE

Edited by **Rosario Pignatello**

INTECHWEB.ORG

Biomaterials Applications for Nanomedicine
Edited by Rosario Pignatello

Published by InTech
Janeza Trdine 9, 51000 Rijeka, Croatia

Copyright © 2011 InTech
All chapters are Open Access distributed under the Creative Commons Attribution 3.0 license, which permits to copy, distribute, transmit, and adapt the work in any medium, so long as the original work is properly cited. After this work has been published by InTech, authors have the right to republish it, in whole or part, in any publication of which they are the author, and to make other personal use of the work. Any republication, referencing or personal use of the work must explicitly identify the original source.

As for readers, this license allows users to download, copy and build upon published chapters even for commercial purposes, as long as the author and publisher are properly credited, which ensures maximum dissemination and a wider impact of our publications.

Notice
Statements and opinions expressed in the chapters are these of the individual contributors and not necessarily those of the editors or publisher. No responsibility is accepted for the accuracy of information contained in the published chapters. The publisher assumes no responsibility for any damage or injury to persons or property arising out of the use of any materials, instructions, methods or ideas contained in the book.

Publishing Process Manager Mirna Cvijic
Technical Editor Teodora Smiljanic
Cover Designer Jan Hyrat
Image Copyright Ali Mazraie Shadi, 2011. Used under license from Shutterstock.com

First published November, 2011
Printed in Croatia

A free online edition of this book is available at www.intechopen.com
Additional hard copies can be obtained from orders@intechweb.org

Biomaterials Applications for Nanomedicine, Edited by Rosario Pignatello
p. cm.
ISBN 978-953-307-661-4

INTECH OPEN ACCESS PUBLISHER

INTECH open

free online editions of InTech
Books and Journals can be found at
www.intechopen.com

Contents

Preface

Scientists who dedicate their research activity to biomaterials pass through the typical dichotomy that often characterizes the basic research.

On one side is the wish of exploring new frontiers of chemistry, physics, biology, medicine, pharmaceutics and all other disciplines to which biomaterials can be applied. Constantly improving of scientific knowledge would feed the freedom of attempting new strategies for producing materials with always tailored and improved characteristics.

On the other side, one should have a look to the different 'official' definitions given for biomaterials. It is evident how the restriction imposed by words would limit the fantasy and effectiveness of fundamental scientific research. Just as an example- biomaterials are defined as a 'nonviable material used in a medical device, intended to interact with biological systems ' (Consensus Conference of the European Society for Biomaterials, 1986), or as 'any substance (other than a drug) or combination of substances, synthetic or natural in origin, which can be used (…) as a whole or as a part of a system which treats, augments, or replaces any tissue, organ, or function of the body (NIH), or even 'a systematically and pharmacologically inert substance designed for implantation within or incorporation with living systems' (Clemson University Advisory Board for Biomaterials).

Essentially, the only common property is that a biomaterial would be different from a biological material, that is produced by a biological system. Clearly, none of the proposed definitions can succeed to cover the whole landscape of properties and applications of these peculiar compounds, but they can only enlighten a particular aspect of their potentials.

A similar situation can be applied for nanomedicine – a research field which often shares technologies and applications with the field of biomaterials – and for which is the gap between 'official' definitions and the originality of published researches even larger.

These considerations have been one of the basis of the present editorial task, that will comprehend three volumes focused on the recent developments and applications of biomaterials. These books collect review articles, original research articles and experimental reports from eminent experts from all over the word, who have been

working in this scientific area for a long time. The chapters are covering the interdisciplinary arena which is necessary for an effective development and usage of biomaterials.

Contributors were asked to give their personal and recent experience on biomaterials, regardless any specific limitation due to fit into one definition or the other.

In our opinion, this will give readers a wider idea on the new and ongoing potentials of different synthetic and engineered macromolecular materials.

In the meantime, another editorial guidance was not to force the selection of papers concerning the market or clinical applications or biomaterial products.

The aim of the book was to gather all results coming from very fundamental studies. Again, this will allow to gain a more general view of what and how the various biomaterials can do and work for, along with the methodologies necessary to design, develop and characterize them, without the restrictions necessarily imposed by industrial or profit concerns.

Biomaterial constructs and supramolecular assemblies have been explored for drug and protein carriers, cell engineering and tissue scaffolds, or to manage the interactions between artificial devices and the body, just to make some examples of the more recent developments.

In this volume of the Biomaterial series have been in particular assembled 21 review articles and papers focusing on the application of new and already known macromolecular compounds to nanotechnology.

The first section of the book deals with chemical and mechanical processing and engineering of biomaterials, tailored towards specific biomedical purposes. The second section presents 6 chapters reporting novel applications of biomaterials to nanomedicine and drug delivery. Finally, 9 chapters have been gathered to show the potential applications of classical and novel biomaterials in different therapeutic and clinical areas.

I am sure that you will find the selected contributions of a great interest and that they will inspire you to broaden your own research within the exciting field of biomaterials development and applications.

Prof. Rosario Pignatello
Department of Pharmaceutical Sciences
Faculty of Pharmacy
University of Catania
Italy

Part 1

Biomaterials Processing and Engineering

1

Bioactive Ceramics as Bone Morphogenetic Proteins Carriers

Sayed Mahmood Rabiee
Babol University of Technology
Iran

1. Introduction

Bone tissue is the component of the skeletal system that provides the supporting structure for the body. Bone has a complex morphology; it is a specialized connective tissue composed of a calcified matrix and an organic matrix. The tissue can be organized in either the dense (compact) or spongy form (cancellous), with pore sizes within the wide range of 1-100 μm (Lane et al., 1999). Although the shape of bone varies in different parts of the body, the physicochemical structure of bone for these different shapes is basically similar. The biochemical composition of bone is precisely composed of two major phases at the nanoscale level namely, organic and inorganic as a good example for a composite. These phases have multiple components which consist of, in decreasing proportions, minerals, collagen, water, non-collagenous proteins, lipids, vascular elements, and cells (Murugan & Ramakrishna, 2005). An overall composition of the bone is given in Table 1.

Inorganic Phases	Wt%	Bioorganic phases	Wt%
Calcium Phosphates (biological apatite)	~ 60	Collagen type I	~ 20
Water	~ 9	None-collagenous proteins	~ 3
Carbonates	~ 4	Primary bone cells	Balance
Citrates	~ 0.9	Other traces	Balance
Sodium	~ 0.7		
Magnesium	~ 0.5		
Other traces	Balance		

Table 1. The biochemical composition of bone (Murugan & Ramakrishna, 2005).

The mineral fraction of bone consists of significant quantities of non-crystalline calcium phosphate compounds and predominantly of a single phase that closely resembles that of crystalline hydroxyapatite ($Ca_{10}(PO_4)_6(OH)_2$) (Hench & Wilson, 1993; Dorozhkin, 2010a). Biological hydroxyapatite also contains other impurity ions as Cl, Mg, Na, K, and F and

trace elements like Sr and Zn (LeGeros, 2002). The apatite in bone mineral is composed of small platelet-like crystals of just 2 to 4 nm in thickness, 25 nm in width, and 50 nm in length (Dorozhkin & Epple, 2002). Bone mineral non-stoichiometry is primarily due to the presence of divalent ions, such as CO_3^{2-} and HPO_4^{2-}, which are substituted for the trivalent PO_4^{3-} ions. Substitutions by CO_3^{2-} and HPO_4^{2-} ions produce a change of the Ca/P ratio, resulting in Ca/P ratio which may vary between 1.50 to 1.70, depending on the age and bone site (Raynaud et al., 2002). When a loss of bony tissue occurs as a result of trauma or by the excision of diseased, healing requires the implantation of bone substitutes. There is a high clinical request for synthetic bone substitution materials, due to the drawbacks such as a prolonged operation time and donor site morbidity in about 10–30% of the cases associated with biological bone grafts (Giannoudis et al., 2005; Beaman et al., 2006; Chu et al., 2007). Biological grafts are generally associated with potential infections. In order to avoid the problems associated with biological bone grafting, there has been a continuous interest in the use of synthetic bone substitute materials. Bioactive ceramics such as calcium phosphates offer alternatives to synthetic bone substitute (Vallet-Regı & lez-Calbet, 2004; Best et al., 2008; Rabiee et al., 2008a). These biomateials with a porous structure not only possess good biocompatibility but also allow the ingrowth of tissues and penetration of biological fluids and form a chemical bond with bone (Lu & Leng, 2005; Rabiee et al. 2008b). Moreover, the Calcium phosphates are freely formed and easily fabricated to satisfy the demands for huge bone and large quantities of bone for bone substitute. For these reasons, the Calcium phosphates have been considered as useful materials for bone repair and replacement. To fabricate a bioactive ceramic bone substitute with various porous configuration, the evidence of tissues ingrowth and biological responses provide obvious advantages in tissue-implant fixation and controlled biodegradation rate for both short-term and long-term implantation purposes (Karageorgiou & Kaplan, 2005, Rabiee et al. 2008b). Many processing technologies have been employed to obtain porous calcium phosphates as bone filler (Rabiee et al., 2007; Best etal. 2008). For example, porous calcium phosphates can be obtained by merging the slurry with a polymer sponge-like mold or polymer beads before sintering. During the sintering, the polymer is completely burnt out, which results in a porous structure. The use of highly porous calcium phosphate induces bone formation inside the implant and increases degradation. Cortical bone has pores ranging from 1 to 100 μm (volumetric porosity 5 to 10%), whereas trabecular bone has pores of 200 to 400 μm (volumetric porosity 70 to 90%). Porosity in bone provides space for nutrients supply in cortical bone and marrow cavity in trabecular bone. Microporosity covers pores sizes smaller than 5 μm for penetration of fluids and Pores larger than 10 μm can be considered as macropores. Macroporous dimensions are reported to play a role in osteoinductive behavior of bone substitutes (Karageorgiou & Kaplan, 2005; Rabiee et al., 2009). Because of the influence of bioactive ceramics on cell behaviour, the bone forming cells are often introduced into these porous ceramics to speed-up tissue ingrowth. The surface of bioactive ceramics is a good substrate for seeding cells (Cao et al., 2010; Rungsiyakull et al., 2010). Bone Tissue engineering typically involves coupling osteogenic cells and/or osteoinductive growth factors with bioactive scaffolds (Buma et al., 2004; Mistry & Mikos, 2005). Some studies have investigated the bone forming capacities of growth factors loaded synthetic bone substitutes. In terms of growth factors, most research has focused on the use of the bone morphogenic proteins (BMPs) (Mont et al. 2004; Termaat et al., 2005). They are

signalling molecules which can induce de novo bone formation at orthotopic and heterotropic sites (Boix et al., 2005). Current examination of alternatives to grafting techniques suggests three possible new approaches to inducing new bone formation: implantation of certain cytokines such as BMPs in combination with appropriate delivery systems at the target site (Liu et al., 2007; Niu et al., 2009); transduction of genes encoding cytokines with osteogenic capacity into cells at repair sites; and transplantation of cultured osteogenic cells derived from host bone marrow (Chu et al., 2007). BMPs have crucial roles in growth and regeneration of skeletal tissues (Nie & Wang, 2007). One primary role of BMPs is to regulate the key elements in the bone induction cascade required for regeneration of skeletal tissues (Schneider et al., 2003). BMPs are bone matrix protein that stimulate mesenchymal cell chemotaxis and proliferation, and promotes the differentiation of these cells into chondrocytes and osteoblasts (Calori et al., 2009; Nie & Wang, 2007). This osteoinductive action of BMPs is well established to be beneficial during the repair bone defects (Termaat et al., 2005). BMPs act locally and therefore must be delivered directly to the site of regeneration via a carrier (Hartman et al., 2005; Chu et al., 2007). Bioactive ceramics can act as vehicle for factor delivery to the surrounding tissues. Future research should be investigated the potentials of these constructs to find a successful alternative for biological bone substitute.

2. Bioactive ceramics

Bioactive ceramics are used in a number of different applications in implants and in the repair and reconstruction of diseased or damaged body parts. Most medical applications of bioactive ceramics relate to the repair of the skeletal system and hard tissue. They include several major groups such as calcium phosphate ceramics, bioactive glasses and glass-ceramics.

2.1 Calcium phosphate ceramics

Calcium phosphate ceramics are very popular implants for medical applications because of their similarity to hard tissue. These bioceramics have been synthesized and used for manufacturing various forms of implants, as well as for solid or porous coatings on other implants. Calcium phosphate compounds exist in several phases. Most of these compounds are used as raw material for synthesis of bioactive ceramics. Different types of calcium phosphate are employed to fabricate implants to accommodate bone tissue regeneration. Table 2 lists the main Ca-P compounds for biomedical applications (Vallet-Reg1 & lez-Calbet, 2004). The atomic ratio of Ca/P in calcium phosphates can be varied between 2 and 1 to produce compounds ranged from calcium tetraphosphate(TTCP) $Ca_4P_2O_9$, hydroxyapatite (HA) $Ca_{10}(PO_4)_6(OH)_2$, octacalcium phosphate (OCP) $Ca_8H_2(PO_4)_6.5H_2O$, tricalcium phosphate (TCP) $Ca_3(PO_4)_2$ to dicalcum phosphate dihydrate (DCPD) $CaHPO_4.2H_2O$ or dicalcum phosphate anhydrus (DCPA) $CaHPO_4$. (Raynaud et al., 2002; Vallet-Reg1 & lez-Calbet, 2004; Dorozhkin, 2010b). Due to their high solubility, the calcium phosphates compounds with a Ca/P ratio less than 1 are not suitable for biological implantation. Hydroxyapatite with Ca/P ratio of 1.667 is much more stable than other calcium phosphates. Under physiological conditions, calcium phosphates degrade via dissolution–reprecipitation mechanisms (Raynaud et al., 2002).

When the dissolution of calcium phosphate is higher than the rate of mineral reprecipitation and tissue regeneration, it is not suitable as a good bone substitute. The dissolution process is dependent on the nature and their thermodynamic stability of calcium phosphate substrate, for example (in order of increasing solubility), HA > TCP > OCP > DCPD or DCPA (Bohner, 2000; Dorozhkin, 2010a). In an ideal situation, a biodegeradable bone substitute is slowly resorbed and replaced by natural bone. TCP with Ca/P ratio of 1.5 is a biodegradable and more resorbed than HA. The use of a mixture of HA and β-TCP, as biphasic calcium phosphate (BCP), has been attempted as bone substitute. The dissolution and resorption rate of BCP can be controlled with ratio of β-TCP/HA (Detsch et al., 2008; De Gabory et al., 2010).

Name	Ca/P	Formula	Acronym
Calcium Dihydrogen Phosphate	0.5	$Ca(H_2PO_4)_2H_2O$	MCP
Dicalcum phosphate dihydrate	1	$CaHPO_4.2H_2O$	DCPD
Dicalcum phosphate anhydrous	1	$CaHPO_4$	DCPA
Octacalcium phosphate	1.33	$Ca_8H_2(PO_4)_6.5H_2O$	OCP
Tricalcium phosphate	1.5	$Ca_3(PO_4)_2$	TCP
Hydroxyapatite	1.67	$Ca_{10}(PO_4)_6(OH)_2$	HA
Tetracalcium phosphate	2	$Ca_4O(PO_4)_2$	TTCP

Table 2. Varius calcium phosphate with their respective Ca/P atomic ratios (Vallet-Regı & lez-Calbet, 2004).

The major limitation to use calcium phosphates is their mechanical properties. Calcium phosphates are used primarily as fillers and coatings (Ooms et al., 2003) because they are brittle with poor fatigue resistance (Teoh, 2000).

2.2 Calcium phosphate cements

Calcium phosphate cements (CPCs) are of interest for bone tissue engineering purposes. Different studies with CPCs have shown that they are highly biocompatible and osteoconductive materials, which can stimulate tissue regeneration (Bohner, 2000; Carey et al., 2005; Ginebra et al., 2006). The main difference between cements when compared to other bioactive ceramics, in the form of ceramic granules or bulk materials, is the injectability and in-situ hardening. Calcium phosphate cements consist of a powder phase and an aqueous liquid, which are mixed together to form a paste that sets after being implanted within the body. Brown and Chow prepared the first CPBC in 1985 contained TTCP and DCPA or DCPD as the solid phase (Brown & Chow, 1985). After mixing with water, the cement components results precipitation of apatite (AP: $Ca_{10-x}(HPO_4)_x(PO4)_{6-x}(OH)_{2-x}$, where $0 \leq x \leq 2$) (Ginebra et al., 2006; Rabiee et al., 2010). There are a variety of different combinations of calcium compounds which are used in the formulation of these bone cements. In general there are two types of CPC: apatite cements and brushite cements. Brushite cement has a lower mechanical strength but a faster biodegradability than the apatite cement. Both types of cement can be applied for bone tissue engineering purposes. (Carey et al., 2005; Rabiee et al., 2010). CPCs as drug delivery systems, where the drugs can be incorporated throughout the whole cement volume. CPCs are suitable materials for local

delivery systems in osseous tissue since they can simultaneously promote bone regeneration and prevent infectious diseases by releasing therapeutic agents. Recent advances in CPC technology have resulted in the enhancement of the handling, application and osteoconductive properties of these cements. These improvements have permitted CPCs to be assayed as carriers for local delivery of drugs and biologically active substances (Ginebra et al., 2006). Drugs, such as antibiotics, antitumors, and growth factors, have been administered to defect regions to induce therapeutic effects (Ginebra et al., 2006; Chu et al. 2007). The success of this idea was favored by the easy incorporation of pharmaceutical and biological substances into the cement solid or liquid phases, the intimate adaptation of the cement paste to bone defects and permits the release of the entrapped substance to the local environment.

2.3 Bioactive glasses & glass-ceramics

Bioactive glasses and glass-ceramics have the ability to bind to hard tissues as was discovered by Hench in 1969 (Hench, 2006). They are used as implants to repair or replace parts of the body; long bones, vertebrae, joints, and teeth. Their clinical success is due to formation of a stable, mechanically strong interface with bone (Hench & Wilson, 1993; Cao et al., 2010). Bioactive materials are typically made of compositions from the Na_2O-CaO, MgO-P_2O_5-SiO_2 system. The composition of the first bioglass Hench made was in weight percent 25% Na_2O, 25% CaO, 5% P_2O_5 and 45% SiO_2 and noted as Bioglass 45S5. Melting and sol- gel processing are two methods for producting glasses. Sol-gel processing has been successfully used in the production of a variety of materials for both biomedical and nonbiomedical applications (Hench, 2006; Ravarian et al., 2010). Sol-gel processing, an alternative to traditional melt processing of glasses, involves the synthesis of a solution (sol), typically composed of metal-organic and metal salt precursors followed by the formation of a gel by chemical reaction or aggregation, and lastly thermal treatment for drying, organic removal, and sometimes crystallization (Saravanapavan & Hench, 2003). Sol-gel-derived bioactive glasses were used because they exhibit high specific area, high osteoconductive properties, and a significant degradability. The sol-gel approach to making bioactive glass materials has produced glasses with enhanced compositional range of bioactivity. When in contact with body fluids or tissues, bioactive glasses develop reactive layers at their surfaces resulting in a chemical bond between implant and host tissue (Hench, 2006). Hench has described a sequence of five reactions that result in the formation of a hydroxy-carbonate apatite (HCA) layer on the surface of these bioactive glasses (Hench, 2006). The dissolution of the glass network, leading to the formation of a silica-rich gel layer and subsequent deposition of an apatite-like layer on the glass surface, was found to be essential steps for bonding of glass to living tissues both through in vivo and in vitro studies (Cao et al., 2010). The use of bioactive glass for load-bearing applications is restricted because of its brittleness. One possibility to overcome this drawback is to crystallize the glass to obtain a glass-ceramic. Glass- ceramics are polycrystalline ceramics made by transformation of the glass into ceramic. The formation of glass ceramics is influenced by the nucleation and growth of small crystals. The nucleation of glass is carried out at temperatures much lower than the melting temperature. Professor Kokubo and his coworkers developed a glass-ceramic containing apatite and wollastonite in a glass matrix (Kokubo et al., 1986). Apatite-wollastonite (A-W) glass-ceramic is one of the most important glass ceramics for use as a bone substitute. The apatite crystals form sites for bone growth; the long wollastonite

crystals reinforce the glass (Liu et al. 2004). Drug and growth factor loading of bioactive glasses and glass ceramics is possible using the sol–gel method. Ziegler et al. introduced Growth factors into a bioactive glass and observed an initial burst of 10%, followed by a delayed boost between day 3 and 8, depending on the type of growth factor (Ziegler et al., 2002).

3. Bone morphogenetic proteins

Bone morphogenetic proteins (BMPs) induce new bone formation by directing mesenchymal stem cells. They are biologically active osteoinductive cytokines that with significant clinical potential. The key steps are proliferation of cells, and finally differentiation into cartilage and then bone. Proliferation was maximal on day 3, chondroblast differentiation was on day 5, and chondrocytes were on day 7. The cartilage hypotrophied on day 9 with vascularization and osteogenesis. On days 10 to 12 maximal alkaline phosphatase activity, a marker of bone formation was observed. Hematopoietic differentiation was observed in the ossicle on day 21. BMP were first characterized in 1965 by Urist as a biologically activator and he has led to various studies for identification of a variety of growth factors that play roles in osteogenesis. The most studied of these are the insulin-like growth factor (IGF), epidermal growth factor (EGF), fibroblast growth factor (FGF), platelet-derived growth factor (PDGF), and the transforming growth factor (TGF) group, of which, the BMPs form a subgroup. There are 15 members of BMPs family in table 3 and Among members of the BMPs, BMP2, 4, and 7 possess a strong ability to induce bone formation (Termaat et al., 2005; Nie & Wang, 2007; Calori et al., 2009).

BMP designation	**Generic Name**
BMP1	bone morphogenetic protein 1
BMP2	bone morphogenetic protein 2
BMP3	bone morphogenetic protein 3 (osteogenic)
BMP4	bone morphogenetic protein 4
BMP5	bone morphogenetic protein 5
BMP6	bone morphogenetic protein 6
BMP7	bone morphogenetic protein 7 (osteogenic protein 1)
BMP8A	bone morphogenetic protein 8a
BMP8B	bone morphogenetic protein 8b (osteogenic protein 2)
BMP9	growth differentiation factor 2 (GDF2)
BMP10	bone morphogenetic protein 10
BMP11	growth differentiation factor 11 (GDF11)
BMP12	growth differentiation factor 7 (GDF7)
BMP13	growth differentiation factor 6 (GDF6)
BMP14	growth differentiation factor 5 (GDF5)
BMP15	bone morphogenetic protein 15

Table 3. The BMPs Family. (Termaat et al., 2005).

4. Bioactive ceramic as carrier for bone marrow cells: case study

This experiment focuses on a tissue engineering strategy for bone regeneration using bone marrow carried by a bioactive ceramic scaffold. To fabricate a bioactive ceramic with porous configuration, the evidence of tissues ingrowth and biological responses provide obvious advantages in tissue-implant fixation and controlled biodegradation rate for both short-term and long-term implantation purposes (Klein et al., 1984; Rabiee et al., 2008c). Many processing technologies have been employed to obtain porous bioceramics as bone substuitute. The method of casting foams has shown suitability to manufacture strong and reliable macro-porous bioceramics that have great potential to replace bone tissue (Rabiee et al., 2007, 2008c). Results obtained with bone substitutes are currently less reliable than with autologous cancellous bone grafting which remains the preferred method for healing bone defects. Bone marrow stromal cells haved proved their ability to induce bone formation (Liu et al., 2007b). So the association of autologous bone marrow and porous bioceramic might be a successful hybrid biomaterial for bone substitute (Liu et al., 2007). The porous sample was fabricated by polyurethane foam reticulate method. The macrostructure of the scaffold was controlled by the porous structure of the polymer substrate. After sintering the ceramic resembled the polymer matrix texture, giving rise to a structure characterized by several macropores, whose size (100 μm <macropores size<200 μm) can assure osteoconduction after implantation (Fig. 1). The total porosity of the porous body was evaluated from the density value calculated as weight/volume and amounted to 64±5%. Details of the preparation method can be found in Ref. (Rabiee et al., 2009).

Fig. 1. SEM micrograph of a macropore in sintered bioactive ceramic.

Synthetic porous ceramic were supplied in the form of cylindrical specimens with a mean diameter of 3.4 ±0.5 mm and a mean length of 6.3±0.7 mm. Under general anesthesia, bone marrow was harvested from one medullar midshaft of the rabbit femur and diluted with 1

cc of saline. The porous ceramic were immersed in the solution for 5 min before implantation. A cavity of 3.5 mm in diameter and 7 mm in depth was drilled manually in the femoral condyles under general anaesthetic conditions and antibiotic protection. After carefully washing with a physiological saline solution, the cavities were filled with porous bioactive ceramic (BC) on one side and with porous bioactive ceramic contain Bone marrow

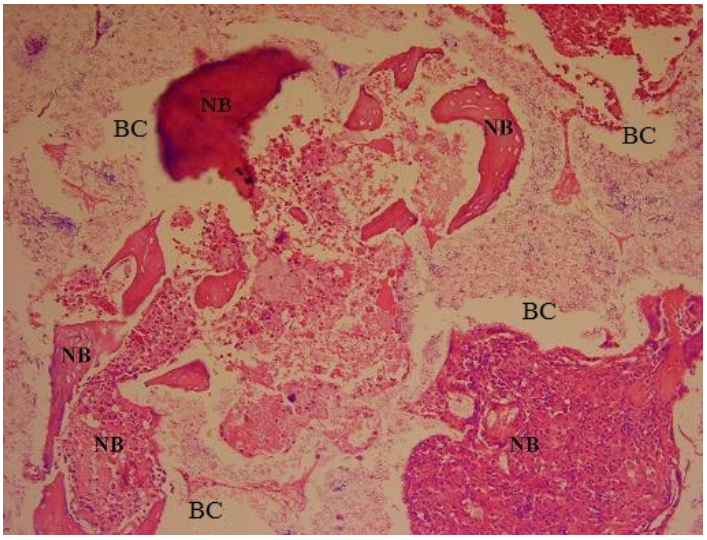

(A)

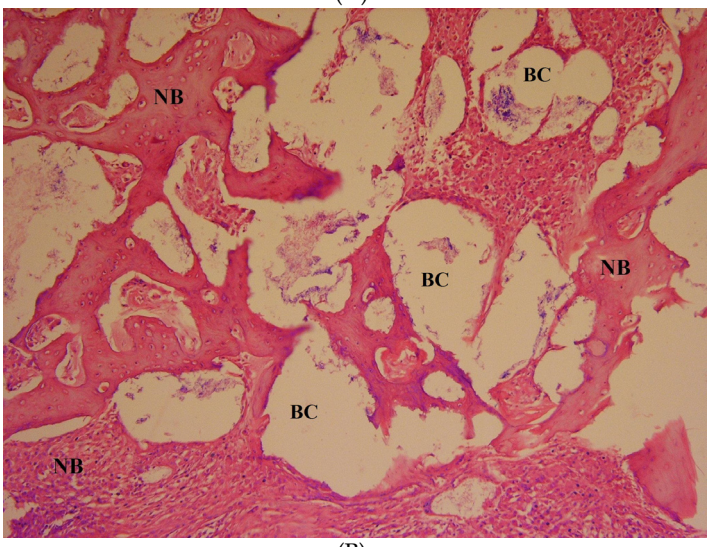

(B)

Fig. 2. Histological section of implants were harvested 3 months after implantation and stained with hematoxylin and eosin at 100x magnification. (A) bioactive ceramic, (B) bioactive ceramic with bone marrow cells. BC=bioactive ceramic, NB= newly formed bone.

(BCBM) on the other side. After 1, 2, 3 and 6 months, animals were killed by an overdose of thiopental sodium and the femoral condyles were removed. Experiments were performed according to the European Guidelines for Care and Use of Laboratory Animals (European Directive 86/609/CEE). During the experiment, all rabbits remained in good health and did not show any wound complications. No inflammatory signs or adverse tissue reaction could be observed. After 3 months, revealed the bridging of the BC and BCBM by host bone. Fig. 2 shows in vivo test results after 3 months. Histological investigations show a higher presence of newly formed bone and a higher osteogenesis in BCBM compared to BC after 3 & 6 months. In general, osteoblasts occurred evidently one month postoperatively, bone marrows began to develop in new bone tissues two months postoperatively, and bone tissues tended to be mature with the development of osteocytes and bone marrows over three months postoperatively.

Ideally, an implant, when placed in an osseous defect, should induce a response similar to that of fracture healing, where by the defect is initially filled with a blood clot which is invaded by mesenchymal cells, osteoblasts and fibroblasts within 2 weeks, followed by extensive bone and osteoid formation at 6 weeks, with complete healing/repair of the cancellous structure by 12 weeks (Orr et al., 2001). [

An equivalent amount of host bone was found in the BC and BCBM treated sites (Fig. 3). No significant difference was seen between BCBM and BC, at month 1 and month 2, but in Group 3 and 6 months, osteoid surface was higher in BCBM than in BC alone ($p<0.05$). BCBM have a stable biomechanical environment conducive to the formation of callus. Data from several sources show the exact effect of bone ingrowth on compressive strength and elastic modulus (Orr et al., 2001; Rabiee et al., 2008b). The porous implant with tissue ingrowth acts a composite structure. The implanted block consists of the mineral matrix of the block, fibrovascular tissue and bony tissue. All of these parameters effect on the compressive strength and modulus.

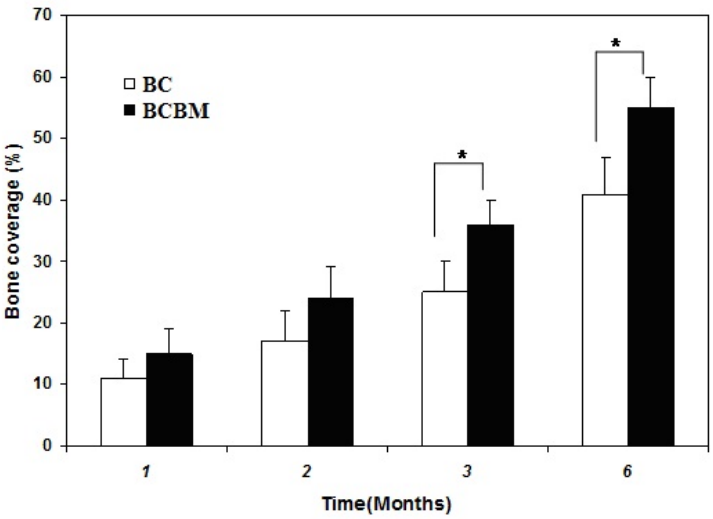

Fig. 3. Histomorphometry of the amount of bone coverage in BC and BCBM at 1, 2, 3 and 6 months after implantation. *$p<0.05$.

Results from mechanical compressive strength and elastic modulus of implanted specimens are presented in Table 4. BC specimens possessed an elastic modulus of 299±21 MPa prior to implantation. Elastic moduli of BC and BCBM became weaker after implantation (Table 4). BC moduli were significantly higher than those of the control at all time points, but no significant difference was apparent between BCBM and control 3 and 6 months after implantation. One example of the influence of a high modulus of elasticity of an implant material on surrounding bone is the dramatic bone loss around certain joint replacement prostheses. This bone loss has been attributed to the stress shielding resulting from the large disparity between the stiffness of the implant and the host bone (Orr et al., 2001).

Time of implantation	Compressive strength (MPa)		Elastic modulus (MPa)	
	BC	BCBM	BC	BCBM
Before implantatiom	6(0.5)	-	299(21)	-
1 months	5.2(0.94)	5.73(1)	268(33)	232(21)
2 months	4.8(0.9)	5.56(1.02)	232(20)	205(19)
3 months	5(0.3)	5.96(0.62)	206(22)	188(16)
6 months	5.1(0.5)	5.76(1.05)	195(17)	171(14)
AC	4.7(0.6)		169(23)	

Table 4. Mechanical properties of BC and BCBM. BC= Bioactive ceramic without bone marrow; BCBM= Bioactive ceramic with bone marrow; AC= anatomic control.

After implantation, BC and BCBM were partly degraded and their compressive mechanical properties decreased or remained at the same level. This could have resulted from two opposing reactions, with the matrix degrading slowly at the same time the amount of bone related to the reduced implant size was increasing. The first results of in vivo tests on rabbits showed good biocompatibility and osteointegration of the synthetic bioactive ceramic with bone marrow, with higher osteoconductive properties and earlier bioresorption, compared to similar synthetic bioactive ceramic without bone marrow samples. Bone marrow improved mechanical properties and bone growth. Bone ingrowth and degradation of the bioactive ceramic allow bone remodeling, which is a prerequisite for a good bone substitute.

5. Acknowledgments

The author would like to thank Prof. Moztarzadeh and Dr Mortazavi for their technical assistance, and Dr Sharifi for organizing the surgery.

6. References

Beaman, F.D., Bancroft, L.W., Peterson, J.J. & Kransdorf, M.J. (2006). Bone Graft Materials and Synthetic Substitutes. *Radiologic Clinics of North America*, Vol. 44, No. 3, pp. 451-461.

Best, S.M., Porter, A.E., Thian, E.S. & Huang, J. (2008). Bioceramics: Past, present and for the future. *Journal of the European Ceramic Society*, Vol. 28, No. 7, pp. 1319-1327.

Bohner, M. (2000). Calcium orthophosphates in medicine: from ceramics to calcium phosphate cements. *Injury*. Vol. 31, pp. 37-47.

Buma, P., Schreurs, W. & Verdonschot, N. (2004). Skeletal tissue engineering from in vitro studies to large animal models. *Biomaterials*, Vol. 25, No. 9, pp.1487–95.

Boix, T., Gómez-Morales, J., Torrent-Burgués, J., Monfort, A., Puigdomènech, P. & Rodríguez-Clemente, R. (2005). Adsorption of recombinant human bone morphogenetic protein rhBMP-2m onto hydroxyapatite. *Journal of Inorganic Biochemistry*, Vol. 99, No. 5, pp. 1043-1050

Brown,W.E., Chow,L.C. (1985). Dental restorative cement pastes. U. S. Patent No. 4518430.

Calori, G.M., Donati, D., Bella C.D. & Tagliabue, L. (2009). Bone morphogenetic proteins and tissue engineering: future directions. *Injury*, Vol. 40, pp. 67-S76

Cao, B., Zhou, D., Xue, M., Li, G., Yang, W., Long, Q. & Ji, L. (2010). Study on surface modification of porous apatite-wollastonite bioactive glass ceramic scaffold. *Applied Surface Science*, Vol. 255, No. 2, pp. 505-508.

Carey, L.E., Xu, H.H.K., Simon Jr, C.G., Takagi, S. & Chow, L.C. (2005). Premixed rapid-setting calcium phosphate composites for bone repair. *Biomaterials,* Vol. 26, pp. 5002–5014.

Chu, T.M.G., Warden, S.J., Turnera, C. H. & Stewart, R.L. (2007). Segmental bone regeneration using a load-bearing biodegradable carrier of bone morphogenetic protein-2. *Biomaterials,* Vol. 28, pp. 459–467.

De Gabory, L., Bareille, R., Stoll, D., Bordenave, L. & Fricain, J. (2010). Biphasic calcium phosphate to repair nasal septum: The first in vitro and in vivo study. *Acta Biomaterialia*, Vol., No. 3, pp. 909-919.

Detsch, R., Mayr, H. & Ziegler, G. (2008). Formation of osteoclast-like cells on HA and TCP ceramics, *Acta Biomaterialia*, Vol. 4, No. 1, pp. 139-148.

Dorozhkin, S.V. & Epple, M. (2002). Biological and medical significance of calcium phosphates. *Angewandte Chemie International Edition*, Vol. 41, pp. 3130–3146.

Dorozhkin, S.V. (2010a). Amorphous calcium (ortho)phosphates. *Acta Biomaterialia*, Vol. 6, No. 12, pp. 4457-4475.

Dorozhkin, S.V. (2010b), Bioceramics of calcium orthophosphates. *Biomaterials,* Vol. 31,Vol. 7, pp. 1465-1485.

Giannoudis, P.V., Dinopoulos, H. & Tsiridis, E. (2005). Bone substitutes: An update. *Injury,* Vol. 36, No. 3, pp. S20-S27.

Ginebra, M.P., Traykova, T.& Planell, J.A. (2006). Calcium phosphate cements as bone drug delivery systems: A review. *Journal of Controlled Release*, Vol. 113, No. 2, pp. 102-110.

Hartman, E.M., Vehof, J.W.M., Spauwen, P.H.M. & Jansen, J.A. (2005). Ectopic bone formation in rats: the importance of the carrier. *Biomaterials,* Vol. 26, No. 14, pp. Pages 1829-1835.

Hench, L.L. (2006). The story of Bioglass*, Journal of Materials Science: Materials in Medicine*, Vol. 17, pp. 967-978.

Hench, L.L. & Wilson J. (1993). An introduction to bioceramics, World Scientific Publishing Co.; Singapore. pp. 245-251.

Karageorgiou, V. & Kaplan, D. (2005). Porosity of 3D biomaterial scaffolds and osteogenesis. *Biomaterials,* Vol. 26, No. 27, pp. 5474-5491.

Klein, C., Driessen, A.A. & De Groot, K. (1984). Relationship between the degradation behavior of calcium phosphate ceramics and their physical chemical characteristics and ultra structural geometry. *Biomaterials*, Vol. 5, pp. 157–160.

Kokubo, T., Ito, S., Sakka S. & Yamamuro, T. (1986). Formation of a high-strength bioactive glass-ceramic in the system MgO-CaO-SiO_2-P_2O_5, *Journal of Materials Science*, Vol. 21, No. 2, pp. 536–540.

Lane, J. M.; Tomin, E., & Bostrom, M.P.G. (1999). Biosynthetic bone grafting. *Clinical Orthopaedics and Related Research*, Vol.65, pp. 107–117.

LeGeros, R.Z. (2002). Properties of osteoconductive biomaterials: calcium phosphates. *Clinical Orthopaedics and Related Research*, Vol. 395, pp. 81–98.

Liu, X., Ding, C. & Chu, P.K. (2004). Mechanism of apatite formation on wollastonite coatings in simulated body fluids. *Biomaterials*, Vol. 25, No. 10, pp. 1755-1761.

Liu, Y., Enggist, L., Kuffer, A.F., Buser, D. & Hunziker, E.B. (2007a). The influence of BMP-2 and its mode of delivery on the osteoconductivity of implant surfaces during the early phase of osseointegration, *Biomaterials,* Vol. 28, pp. 2677–2686

Liu, Y., Cooper, P.R., Barralet J.E. & Shelton, R.M. (2007b). Influence of calcium phosphate crystal assemblies on the proliferation and osteogenic gene expression of rat bone marrow stromal cells. *Biomaterials,* Vol. 28, No. 7, pp. 1393-1403.

Lu, X. & Leng, Y. (2005). Theoretical analysis of calcium phosphate precipitation in simulated body fluid. *Biomaterials*, Vol. 26, pp.1097-1108.

Mistry, A.S. & Mikos, A.G. (2005). Tissue engineering strategies for bone regeneration. *Advances in Biochemical Engineering/Biotechnology*, Vol. 94, pp.1–22.

Mont, M.A., Ragland, P.S., Biggins, B., Friedlaender, G., Patel, T., Cook S, Etienne, G., Shimmin, A., Kildey, R., Rueger, D.C. & Einhorn, T.A. (2004). Use of bone morphogenetic proteins for musculoskeletal applications. An overview. (2004). *Journal of Bone and Joint Surgery*, Vol. 86, pp. 41–55.

Murugan, R. & Ramakrishna, S. (2005). Development of nanocomposites for bone grafting. *Composites Science and Technology* Vol.367, pp. 2385–2406.

Nie, H., & Wang, C. (2007). Fabrication and characterization of PLGA/HAp composite scaffolds for delivery of BMP-2 plasmid DNA. *Journal of Controlled Release*, Vol. 120, No. 1-2, pp. 111-121.

Niu, X., Feng, Q., Wang, M. Guo, X. & Zheng, Q. (2009). Porous nano-HA/collagen/PLLA scaffold containing chitosan microspheres for controlled delivery of synthetic peptide derived from BMP-2. *Journal of Controlled Release*, Vol. 134, No. 2, pp. 111-117.

Ooms, E.M., Wolke, J.G.C., Van de Heuvel, M.T., Jeschke, B. & Jansen, J.A. (2003). Histological evaluation of the bone response to calcium phosphate cement implanted in cortical bone. *Biomaterials,* Vol. 24, No. 6, pp. 989–1000.

Orr, T.E., Villars, P.A., Mitchell, S.L., Hsu, H.P. & Spector, M. (2001). Compressive properties of cancellous bone defects in a rabbit model treated with particles of natural bone mineral and synthetic hydroxyapatite. *Biomaterials*, Vol. 22, pp. 1953-1959.

Rabiee, S.M., Moztarzadeh, F., Salimi-Kenari, H. & Solati-Hashjin, M. (2007). Preparation and properties of a porous calcium phosphate bone graft substitute, *Materials Science- Poland*. Vol. 25, No. 4, pp. 1019-1027.

Rabiee, S. M., Moztarzadeh, F., Solati-Hashjin, M. & Salimi-Kenari, H. (2008a). Porous tricalcium phosphate as a bone substitute. *American Ceramic Society Bulletin*, Vol. 87, No.2, pp.43-45.

Rabiee, S.M., Mortazavi, S.M.J., Moztarzadeh, F., Sharifi, D., Sharifi, Sh., Salimi-Kenari, H., Solati-Hashjin, M. & Bizari, D. (2008b). Mechanical behavior of a new biphasic calcium phosphate bone graft. *Biotechnology and Bioprocess Engineering*. Vol. 13, pp. 204-209.

Rabiee, S.M., Moztarzadeh, F., Salimi-Kenari, H., Solati-Hashjin, M. & Mortazavi, S.M.J. (2008c). Study of Biodegradable Ceramic Bone Graft Substitute, *Advances in Applied Ceramics,* Vol.107, No.4, pp.199-202.

Rabiee, S.M., Mortazavi, S.M.J., Moztarzadeh, F., Sharifi, D., Fakhrejahani, F., Khafaf, A., Houshiar Ahmadi, S.A., Ravarian, R. & Nosoudi, N. (2009). Association of a Synthetic Bone Graft and Bone Marrow Cells as a Composite Biomaterial. *Biotechnology and Bioprocess Engineering*. Vol. 14, pp. 1-5.

Rabiee, S.M., Moztarzadeh, F. & Solati-Hashjin, M. (2010). Synthesis and characterization of hydroxyapatite cement. *Journal of Molecular Structure*, Vol. 969, pp. 172–175.

Ravarian, R., Moztarzadeh, F., Solati-Hashjin, M., Rabiee, S.M., Khoshakhlagh, P. & Tahriri, M. (2010). Synthesis, characterization and bioactivity investigation of bioglass/hydroxyapatite composite, *Ceramics International*, Vol. 36, No. 1, pp. 292-297.

Raynaud, S., Champion, E., Bernache-Assollant, D. & Thomas, P. (2002). Calcium phosphate apatites with variable Ca/P atomic ratio I. Synthesis, characterisation and thermal stability of powders. *Biomaterials,* Vol. 23, pp. 1065-72.

Rungsiyakull, C., Li, Q., Sun, G., Li,W. & Swain, M.V. (2010). Surface morphology optimization for osseointegration of coated implants. *Biomaterials,* Vol. 31, No. 27, pp. 7196-7204.

Schneider, A., Taboas, J.M., McCauley L.K. & Krebsbach, P.H. (2003). Skeletal homeostasis in tissue engineered bone. *Journal of Orthopaedic Research*, Vol. 21, No. 5, pp. 859-864.

Saravanapavan, P. & Hench, L.L. (2003). Mesoporous calcium silicate glasses. II. Textural characterisation. Journal of Non-Crystalline Solids, Vol. 318, No. 1-2, pp. 14-26.

Teoh, S.H. (2000). Fatigue of biomaterials: a review. *International Journal of Fatigue*, Vol. 22, No. 10, pp. 825-837.

Termaat, M.F., Den Boer, F.C., Bakker, F.C., Patka, P. & Haarman, H.J. (2005). Bone morphogenetic proteins. Development and clinical efficacy in the treatment of fractures and bone defects. *Journal of Bone and Joint Surgery*, Vol. 87, No. 6, pp.1367–78.

Vallet-Regı, M., lez-Calbet, J.M.G. (2004). Calcium phosphates as substitution of bone tissues, *Progress in Solid State Chemistry*, Vol. 32, pp. 1–31.

Ziegler, J., Mayr-Wohlfahrt, U., Kessler, S., Breitig, D. & Günther K.P. (2002). Adsorption and release properties of growth factors from biodegradable implants. *Journal of Biomedical Materials Research,* Vol. 59, pp. 422–428.

2

Collagen- vs. Gelatine-Based Biomaterials and Their Biocompatibility: Review and Perspectives

Selestina Gorgieva[1] and Vanja Kokol[1,2]
[1]*University of Maribor, Institute for Engineering Materials and Design, Maribor*
[2]*Center of Excellence NAMASTE, Ljubljana, Slovenia*

1. Introduction

Selection of a starting material, which will somehow mimic a naturally-existing one, is one of the most important points and crucial elements in biomaterials development. **Material biomimetism** is one of those approaches, where restoration of an organ's function is assumed to be obtained if the tissues themselves are imitated (Barrere et al., 2008). However, some of the biopolymers as e.g collagen can be selected from within a group of biomimetic materials, since they already exist, and have particular functions in the human body.

Collagen is one of the key structural proteins found in the extracellular matrices of many connective tissues in mammals, making up about 25% to 35% of the whole-body protein content (Friess, 2000; Muyonga et al., 2004). Collagen is mostly found in fibrous tissues such as tendons, ligaments and skin (about one half of total body collagen), and is also abundant in corneas, cartilages, bones, blood vessels, the gut, and intervertebral discs (Brinckmann et al., 2005). It constitutes 1% to 2% of muscle tissue, and accounts for 6% of strong, tendinous muscle-weight. Collagen is synthesized by fibroblasts, which originate from pluripotential adventitial cells or reticulum cells. Up to date 29 collagen types have been identified and described. Over 90% of the collagen in the body is of type I and is found in bones, skins, tendons, vascular, ligatures, and organs. However, in the human formation of scar tissue, as a result of age or injury, there is an alteration in the abundance of types I and III collagen, as well as their proportion to one another (Cheng et al., 2011).

Collagen is readily isolated and purified in large quantities, it has well-documented structural, physical, chemical and immunological properties, is biodegradable, biocompatible, non-cytotoxic, with an ability to support cellular growth, and can be processed into a variety of forms including cross-linked films, steps, sheets, beads, meshes, fibres, and sponges (Sinha & Trehan, 2003). Hence, collagen has already found considerable usage in clinical medicine over the past few years, such as injectable collagen for the augmentation of tissue defects, haemostasis, burn and wound dressings, hernia repair, bioprostetic heart valves, vascular grafts, a drug –delivery system, ocular surfaces, and nerve regeneration (Lee et al., 2001). However, certain properties of collagen have adversely influenced some of its usage: poor dimensional stability due to swelling in vivo; poor in vivo mechanical strength and low elasticity, the possibility of an antigenic response (Lynn et

al., 2004) causing tissue irritation due to residual aldehyde cross-linking agents, poor patient tolerance of inserts, variability in releasing kinetics, and ineffectiveness in the management of infected sites (Friess, 1998). In addition, there is the high-cost of pure type I collagen, variability in the enzymatic degradation rate when compared with hydrolytic degradation, variability of isolated collagen in cross-link density, fibre size, trace impurities, and side-effects, such as bovine spongeform encephalopathy (BSF) and mineralization. The above-mentioned disadvantages must be considered during collagen use in medical applications (Pannone, 2007).

In this review collagen will be presented and compared to its degradation product, gelatine, taking into account their molecular and submolecular structural properties, possibilities to overcome common problems related to their usage as biomaterial, i.e. the solubility and degradation rate mechanisms, as well as their applications in combination with other types of (bio)polymers.

2. Molecular and submolecular structure of collagen vs. gelatine

2.1 Collagen

The **collagen** rod-shape molecule (or *tropocollagen*) is a subunit of larger collagen fibril aggregates. The lengths of each subunit are approximately 300 nm and the diameter of the triple helix is ~1.5 nm. It is made up of three polypeptide α-chains, each possessing the conformation of a left-handed, polyproline II-type (PPII) helix (Fig. 1). These three left-handed helices are twisted together into a right-handed coiled coil, a triple-helix which represent a **quaternary structure** of collagen, being stabilized by numerous hydrogen bonds and intra-molecular van de Waals interactions (Brinckmann et al., 2005) as well as some covalent bonds (Harkness, 1966), and further associated into right-handed microfibrils (~40 nm in diameter) and fibrils (100-200 nm in diameter), being further assembled into collagen fibres (He et al., 2011) with unusual strength and stability.

The primary structure of collagen shows a strong sequence homology across genus and adjacent family line (Muyonga et a., 2004), thus a distinctive feature of collagen is the regular arrangement of amino acids in each of the three chains of collagen subunits. The sequence of amino acids is characterized by a repetitive unit of glycine (Gly)-proline (Pro)-X or Gly-X- hydroxyproline (Hyp), where Gly accounting for the 1/3 of the sequence, whilst X and Y may be any of various other amino acid residues. However, the X-position is occupied almost exclusively by Pro, whereas Hyp is found predominantly in the Y-position (Gorham, 1991), both constitute of about 1/6 of the total sequence. This kind of regular repetition and high Gly content is found in only a few other fibrous proteins, such as silk fibroin and elastin, but never in globular proteins. Thus the super-coil of collagen is stabilized by hydrogen bonds between Gly and Pro located in neighbouring chains and by an extensive water-network which can form hydrogen bonds between several carbonyl and hydroxyl peptide residues (Brinckmann et al., 2005). Furthermore, amino acids in the X- and Y-positions are able to participate in intermolecular stabilization, e.g. by hydrophobic interactions or interactions between charged residues, mostly coming from Pro and Hyp residues steric repulsion (Brinckmann et al., 2005). This helical part is further flanked by short non-helical domains (9-26 amino acids), the so called telopeptides, which play an important role in fibril formation and natural cross-linking. After spontaneous helix formation, cross-links between chains are formed within the region of the N-terminal telopeptides (globular tail portion of the chains), and then the telopeptides (containing the

cysteine (Cys) and tyrosine (Tyr) of pro-collagen) are shed leaving the rod-like ca. 3150 amino acid containing triple helix. These collagen rods assemble together with a quarter-stagger to form the collagen fibre and the fibres are stabilised by further cross-links.

Type I (Fig. 2) collagen, the predominant genetic type in the collagen family being the major component of tendons, bones and ligaments, is a heterotrimeric copolymer composed of two α1 (I) and one α2 (I) chains, containing approximately 1050 amino acids each. This collagen type contains one-third of Gly, contains no tryptophan (Trp) or Cys, and is very low in Tyr and histidine (His) (Muyonga et al., 2004). Its molecule consist of three domains: amino-terminal nontriple helical (N-telopeptide), central triple helical consisting of more than 300 repeat units and represent more than 95% of polypeptide, and carboxy-terminal nontriple helical (C-telopeptide) (Yamauchi & Shiiba, 2008). New data show that besides the telopeptides, tropocollagens still contain the N- and C-terminal propeptide sequences, called non-collagenous domains (Brinckmann et al., 2005), which are responsible for correct chain alignment and triple helix formation. The propeptides are removed before fibril formation and regulate the fibril formation process. Tropocollagens are staggered longitudinally and bilaterally by inter- and intra-molecular cross-links into microfibrils (4 to 8 tropocollagens) and further into fibrils. This periodic arrangement is characterized by a gap of 40 nm between succeeding collagen molecules and by a displacement of 67 nm. The fibrils organize into fibres which, in turn, can form large fibre bundles, being both stabilized by intermolecular cross-links (Friess, 1998).

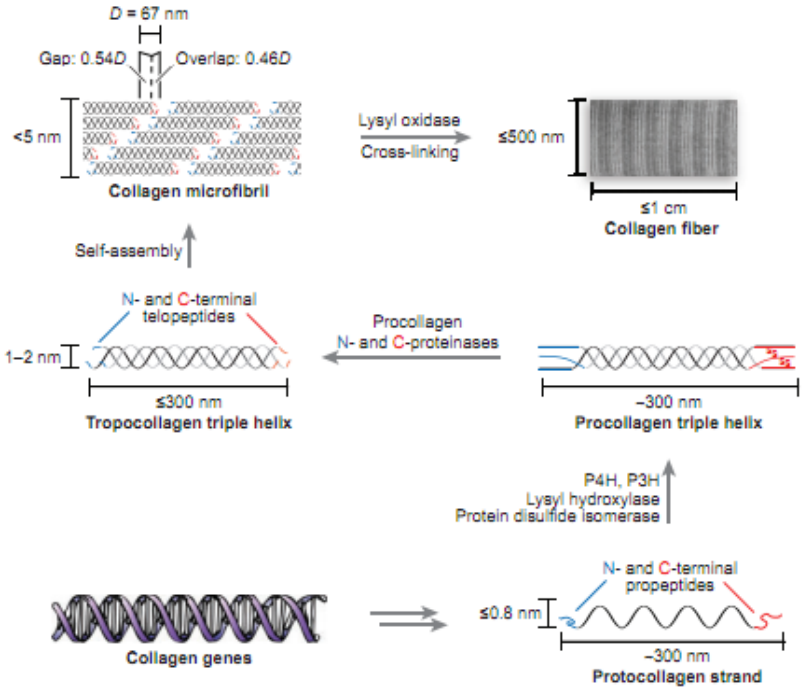

Fig. 1. Biosynthetic route of collagen fibers (Shoulders & Raines, 2009)

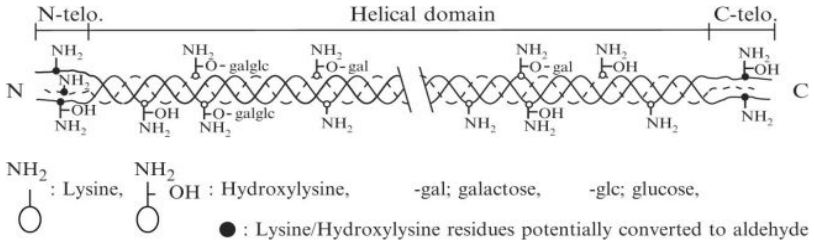

Fig. 2. Structure of type I collagen molecule. (Yamauchi & Shiiba, 2008) and (http://www.kokenmpc.co.jp/english/support/tecnical/collagen/index.html).

Collagen **types I, II, III, and V** (Fig. 3) are called fibril- forming collagens and have large sections of homologous sequences independent of species, among which first three types are known to be chemotactic (Chevallay & Herbage, 2000). Type II collagen, the main component of a nose cartilage , the outside of the ears, the knees and parts of larynx and trachea, is a homotrimer composed of three α1 (II) chain (Shoulders and Rains, 2009), whilst **type III** collagen, present in skin and blood vessels is homotrimer, composed of three α1 (III) chains (Gelse et al., 2003). In **type IV** collagen, being present in basement membrane, the regions with the triple-helical conformation are interrupted with large non-helical domains, as well as with the short non-helical peptide interruption. **Types IX, XI, XII and XIV** are fibril associated collagens with small chains, which contain some non-helical domains. **Type VI** is microfibrillar collagen and **type VII** is anchoring fibril collagen (Samuel et al., 1998).

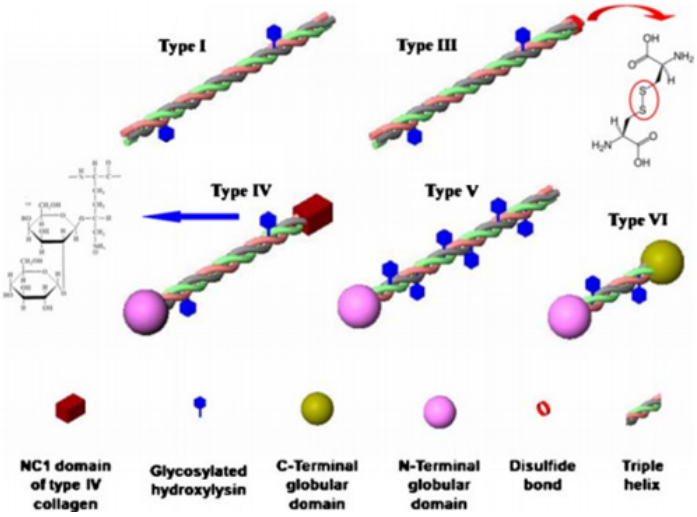

Fig. 3. Schematic presentation of main structural differences between the most abundant collagen types of extracellular matrix in human tissues (Belbachir et al., 2009).

From among all the known collagen types, three-dimensional (3D) model of fibril-forming **type II** collagen was proposed for the development of synthetic collagen tissues and the

study of the structural and functional aspects of collagen (Chen et al., 1995) due its orderly arrangement of triple helix tropocollagen molecules, results in a formation of fibrils having a distinct periodicity. Thus this system also allows the studies of the stereochemistry of all the side-chain groups and specific atomic interactions, and further evaluation of its therapeutic effects on collagen related diseases.

2.1.1 Antigenicity of collagen

A chemical compound that stimulates an immune response is called an antigen, or an immunogen. A host's immune response is not directed toward the entire antigen molecule, but rather to specific chemical groups called epitopes, or antigenic determinants on the molecule, which are responsible for the immunogenic properties of the antigen. Two important characteristic of antigens are **immunogenicity** (specific immune response) and **reactivity** (ability to react with specific antigen) where "complete antigen" possess both characteristics, whilst, "incomplete antigen" do not show immunogenicity, but is able to bind with antibodies (Kokare, 2008). The status of **collagen** as **an animal-derived biomaterial** raise concerns regarding its potential to evoke immune response. Its ability to interact with secreted antibodies (**antigenicity**) and to induce an immune response–process that includes synthesis of the same antibodies (**immunogenicity**), are connected with macromolecular features of a protein, uncommon to the host species, such as collagen with animal origin. When compared with other proteins, collagens are weakly immunogenic, due to evidences of its ability to interact with antibodies (Gorham, 1991). Clinical observations indicate that 2-4 % of the total population posses an inherent immunity (allergy) to bovine type collagen (Cooperman & Michaeli, 1984).

According to Lynn (Lynn et al., 2004), antigenic determinants (epitopes, macromolecular features on an antigen molecule that interact with antibodies) of collagen can be classified into following categories (Fig. 4):

1. Helical- recognition by antibodies is dependent on 3D conformation (i.e., the presence of an intact triple helix).
2. Central- recognitions are located within the triple helical portion of native collagen, but recognition based solely on amino acid sequence and not on 3D conformation. They are often hidden, only interacting with antibodies when the triple helix has unwound, e.g. in denaturated state.
3. Terminal- recognitions are major antigenic determinants (Lee et al., 2001), located in the non-helical terminal regions (telopeptides), but can be eliminated by pepsine treatment leading to atelocollagen (Fig. 5) (Chevallay & Herbage, 2000; Hsu et al., 1999; Kikuchi et al., 2004). Telopeptide cleavage results in collagen whose triple-helical conformation is intact, yet as both the amino and carboxyl telopeptides play important roles in cross-linking and fibril formation, their complete removal results in an amorphous arrangement of collagen molecules and a consequent loss of the banded-fibril pattern in the reconstituted product, and significant increase in solubility (Lynn, 2004).

The possible use of recombinant human collagen (although more expensive) could be a way of removing concerns of species-to-species transmissible diseases (Olsen et al., 2003). However, complete **immunogenic purification** of non-human proteins is difficult, which may result in immune rejection if used in implants. Impure collagen has the potential for xenozoonoses, a microbial transmission from the animal tissue to the human recipient (Canceda et al., 2003). Anyhow, although collagen extracted from animal sources may

present a small degree of antigenicity, it is widely considered acceptable for tissue engineering on humans (Friess, 1998). Furthermore, the literature has yet to find any significant evidence on human immunological benefits of deficient-telopeptide collagens (Wahl & Czernuszka, 2006).

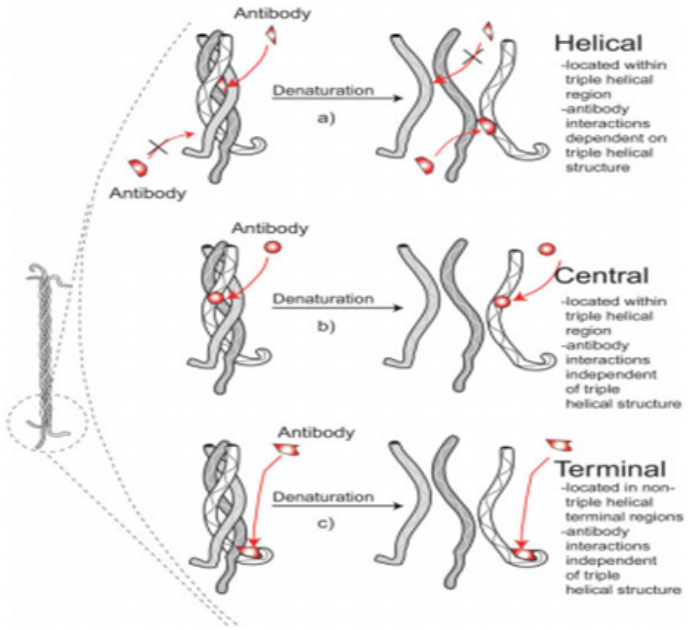

Fig. 4. Classes of antigenic determinants of collagen (Lynn et al., 2004).

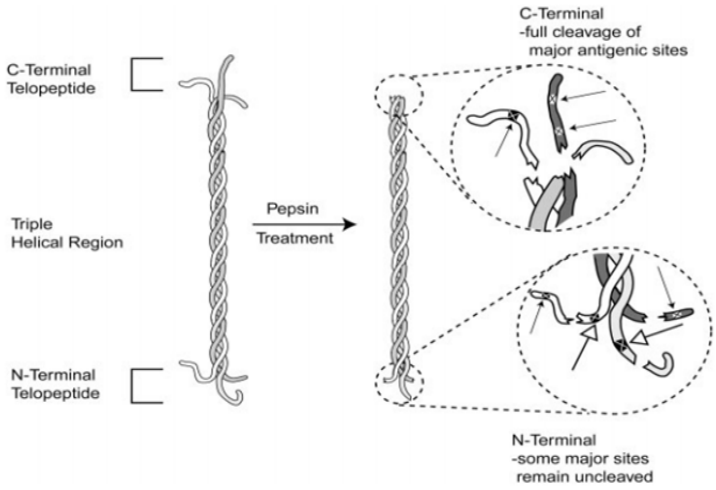

Fig. 5. Telopeptide removal via pepsin treatment (Lynn et al., 2004).

So, atelocollagen produced from type II collagen has demonstrated its potential as a drug carrier, especially for gene delivery (Lee et al., 2001). However, collagen type IV possesses a strong immunogenic character, even after pepsin treatment (Chevallay & Herbage, 2000).
Another approach for rendering the reduction of collagen antigenicity and the immune reaction, has been presented, where the amino and carboxyl side groups are blocked by glutarladehyde cross-linking (Hardin-Young et al., 2000). However, data from studies using glutaraldehyde as the cross-linking agent are hard to interpret because glutaraldehyde treatment is also known to leave behind cytotoxic residues. It is, therefore, possible that the reduced antigenicity associated with glutaraldehyde cross-linking is due to nonspecific cytotoxicity rather than a specific effect on antigenic determinants.

2.2 Gelatine

Gelatine is the product of thermal denaturation or disintegration of insoluble collagen (Gomez-Gullien et al., 2009) with various molecular weights (MWs) and isoionic points (IEPs) depending on the source of collagen and the method of its manufacturing process of recovery from collagen. Collagen exists in many different forms, but gelatine is only derived from sources rich in **Type I collagen** thet generally contains no Cys. Collagen used for gelatine manufacturing can be from different sources, among which anyhow bovine and porcine gelatines are more-widely used. Alternative sources of collagen for gelatine production have been studied in last decade, such as fish skins, bones and fins (Nagai & Suzuki , 2000), sea urchin (Robinson, 1997), jellyfish (Nagai et al., 2000) and bird feet from Encephalopat (Herpandi et al., 2011). However, the amino acid compositions are slightly different among all types of gelatine from different sources. Amino acids from pigskin gelatine and bone gelatines do not contain Cys, but fish scale and bone gelatine instead, which has less content of Gly in comparison with mammalian sources (Zhang et al., 2010). With the exception of gelatine from pigskin origin, all other gelatines do not contain aspartic acid (Asp) and glutamic acid (Glu).
During the **denaturation-hydrolysis process** (Fig. 6), collagen triple-helix organization is hydrolyzed at those sites where covalent cross-links join the three peptides, which in case of type B gelatine produced by partial alkaline hydrolysis of collagen, leads to polydisperse polypeptide mixture with average MW of 40-90 kDa, instead of MW ~ 100 kDa as related to collagen α-chains; the collagen denaturation in its passage to gelatine can be followed polarimetricallly by reduction of specific optical rotation $[\alpha]_D$ of collagen (Cataldo et al., 2008).
As the collagen matures, the cross-links become stabilised, because ε-amino groups of lysine (Lys) become linked to arginine (Arg) by glucose molecules (Mailard reaction), forming extremely stable **pentosidine type cross-links**. During the **alkaline processing,** the alkali breaks one of the initial (pyridinoline) cross-links and as a result, on heating the collagen releases, mainly, denatured α-chains into solution. Once the pentosidine cross-links of the mature animal have formed in the collagen, the main process of denaturation has to be thermal hydrolysis of peptide bonds, resulting in protein fragments being from below 100 kDa to more than 700 kDa, and with IEP between 4,6 and 9. During the **acid process**, the collagen denaturation is limited to the thermal hydrolysis of peptide bonds, with a small amount of α-chain material from acid soluble collagen in evidence. Based on this, gelatine is divided into two main types: **Type A,** which is derived from collagen of pig skin by acid pre-treatment with IEP of 7 - 9, and **Type B,** which is derived from collagen of beef hides or bones by liming (alkaline process) with IEP of 4.6 - 5.4.

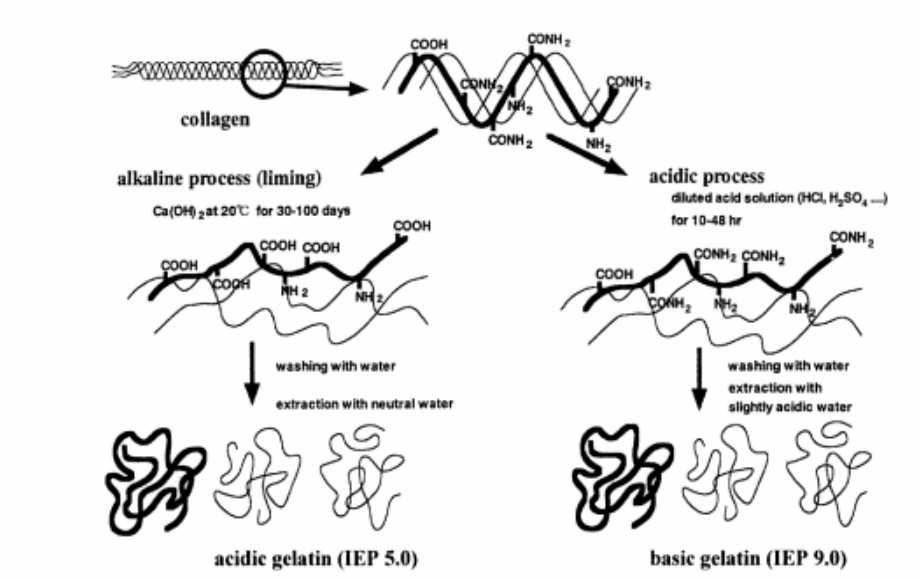

Fig. 6. Two methods for gelatine extraction from tissues containing collagen (Ikada, 2002).

Type A gelatine (dry and ash free) contains 18.5 % nitrogen, but due to the loss of amide groups, **Type B gelatine** contains only about 18% nitrogen. Amino acid analysis of gelatine is variable, particularly for the minor constituents, depending on the raw material and process used, but proximate values by weight are: Gly 21 %, Pro 12 %, Hyp 12 %, Glu 10 %, alanine (Ala) 9 %, Arg 8 %, Asp 6 %, Lys 4 %, serine (Ser) 4 %, leucine (Leu) 3 %, valine (Val) 2 %, phenylalanine (Phe) 2 %, threonine (Thr) 2 %, isoleucine (Ile) 1 %, hydroxylysine (Hyl) 1 %, methionine (Met), His < 1 % and Tyr < 0.5 %. It should be remembered that the peptide bond has considerable aromatic character; hence gelatine shows an absorption maximum at ca. 230 nm.

Collagen is resistant to most proteases and requires special collagenases for its enzyme hydrolysis. Gelatine, however, is susceptible to most proteases, but they do not break gelatine down into peptides containing much less than 20 amino acids (Cole, 2000).

Gelatine forms physical gels in hydrogen-bond friendly solvents above a concentration larger than the chain overlap concentration (~ 2 % w/v). The gelatine sol undergoes a first order thermo-reversible gelation transition at temperatures lower then Tg with is ~30°C, during which gelatine molecules undergo an association-mediated conformational transition from random coil to triple helix. The sol has polydisperse random coils of gelatine molecules and aggregates, whereas in gel state there is propensity of triple helices stabilized through intermolecular hydrogen bonding, during which, three dimensional (3D) interconnected network connecting large fractions of the gelatine chains is formed (Mohanty & Bohidar, 2003, 2005).

On cooling, gelatine chains can rewind, but not within the correct register, and small triple-helical segments formed may further aggregate during gel formation. The lateral aggregation of gelatin triple helix that give rise to collagen fibrils in vivo, does not occur in gelatine gels (Chavez et al., 2006). Hydrogel formation, accompanied by a disorder-order rearrangement in which gelatine chains partially recover the triple helix collagen structure,

leads to forming of renaturated gelatine with amorphous main regions of randomly-coiled gelatine chains interconnected with domains of spatially-ordered microcrystallites, stabilized by hydrogen bonds between N-H of Gly and C=O from Pro. Stabilization of molecular conformation and inter-helix interactions are a consequence of the existence of a highly-ordered hydration shell with water bridges linking two groups within the same or different gelatine chains. Hydrogen bond formation is responsible for the increase in denaturation temperature of the fixed tissue; when compared to the pig-skin and bovine gelatines, which have ~30% Pro and Hyp, fish gelatines possess a lesser percentage of Pro and Hyp (~20 %), the impact of which is thermal stability and shifting by 5-10°C to lower gelling and melting temperatures (Farris et al., 2009) and gel strength (Herpandy et al., 2011).

Despite gelatine being one of the polymers recognized for millennia, questions about its structure and functionality are still being discussed today. The 3D network of gelatine has been defined by several authors using ''fringed micelle'' model in which there are micro-crystallites interconnected with amorphous regions of randomly-coiled segments, whilst other authors propose the existence of local regions of protein quaternary structure, self-limiting in size, which can be triple-helical, only partially triple-helical or also include β-turn and β-sheet motifs (Pena et al., 2010).

2.2.1 Antigenicity of gelatine

Due to modern manufacturing sites and the use of highly advanced, controlled manufacturing processes with numerous purification steps (washing, filtration), heat-treatments including a final ultra-heat treatment (UHT) sterilization step followed by a drying of the gelatine solution, gelatine with highest quality can be prepared in regard to physical, chemical, bacteriological and virological safety.

During Bovine Spongiform Encephalopathy (BSE), all products of bovine origin were under suspicion as being possible transmitters of disease to humans. Thus several studies have been done to demonstrate the capability of certain steps during gelatine production to inactivate BSE infectivity, showing a reduction of SE infectivity for acid demineralization and lime-treatment of 10 and 100 times, respectively. The combined reduction has been found to be 1000 times.

The classical UHT sterilization used in gelatin manufacture should also reduce any residual infectivity 100 times, or more probably 1000 times (Taylor et al., 1994). Washing, filtration, ion exchange and other chemicals or treatments used in the manufacture of gelatine would reduce the SE activity even further (by an assumed ratio of 100 times).

However, it is also a known fact that gelatine is a non-immunogenic material, yet very little research has been done on this theme, thus most knowledge is based on early experiments (Hopkins & Wormall, 1933), where this gelatine property was described to be connected with the absence of aromatic ring. Gelatine non-antigenicity has attracted attention by (Starin, 1918) who, in particular, carried out an extensive investigation, using the precipitin, anaphylactic, complement fixation and meiostagmin reactions, and decided that the injection of gelatine into rabbits, guinea-pigs and dogs failed to produce antibodies by gelatine. This failure of gelatine to incite antibody production has been interpreted in several ways, but the view most commonly held suggests that the non-antigenicity, in this instance, is due to the absence of aromatic groupings, as gelatine is deficient in Tyr and Trp, and contains only a very small amount of Phe. A similar explanation for gelatin´s non-immunogenic property was given by (Kokare, 2008), where is stated that gelatine is non-antigenic because of the absence of aromatic radicals.

3. Cross-linking of collagen vs. gelatine and their immuno response effect

Collagen isolation by pepsin digestion involves de-polymerization of collagen by removing amino and carboxyl- terminal telopeptides containing the intermolecular cross-links. The isolated collagen thus exhibits poor thermal stability, mechanical strength and water resistance, due to the destruction of natural cross-links and assembly structure by neutral salt, acid, alkali, or proteases during the extraction process (Sisson et al., 2009). In order to increase their strength and enzyme resistance, and to maintain their stability during implantation, especially for long term application, collagenous matrices are usually stabilized by cross-linking (Yannas, 1992; Tefft et al., 1997). In addition, cross-linking permits a reduction in the antigenicity of collagen and, in some forms, decreases its calcification (Damnik, 1996).

Method	Collagen	Gelatine
Chemical cross-linking		
Aldehydes e.g. glutaraldehyde (GTA)	Charulatha et al., 2003; Kikuchi et al., 2004; Mu et al., 2010, Ma et al., 2003	Sisson et al.; 2009, Farrist et al.; 2009
Dialdehide starch (DAS)	Mu et al., 2010	Martucci & Ruseckaite, 2009
Acyl azide	Charulatha et al.; 2003, Friess; 1999,	
Diphenylphosphorylazide (DPPA)	Khor, 1997, Roche et al.; 2001	
Carbodiimides, e.g.1-ethyl-3-(3 dimethylamino-propyl)(EDC)	Park et al.; 2002, Pieper et al.; 1999, Kim et al., 2001, Song et al., 2006	Barbetta et al.; 2010, Natu et al.; 2007, Chang et al.; 2007, Kuijpers et al.; 2000
Hexamethylene diisocyanate	Friess, 1999	
Ethylene glycol diglycidyl ether		Vargas et al.; 2008
Polyepoxy compounds	Friess, 1999; Khor, 1997, Zeeman et al., 1999	
Phenolic compounds	Han et al.; 2003; Jackson et al., 2010	Kim et al.; 2005; Zhang et al.; 2010; Pena et al.;2010
Genipin	Ko et al.; 2007; Yan et al., 2010	Yao et al.; 2005, Lien et al.; 2010, Bigi et al., 2002; Chiono et al., 2008; Mi et al., 2005
Citric acid derivative (CAD)		Saito et al., 2004
Enzymatic crosslinking		
Transglutaminase	Jus et al.; 2011	Bertoni et al., 2006; Fuchs et al., 2010, Sztuka & Kolodziejska, 2008
Tyrosinase	Jus et al.; 2011	Chen et al., 2003
Laccasse	Jus et al.; 2011	
Physical crosslinking		
Dehydrothermal treatment (DHT)	Pieper et al., 1999; Tangsadthakun, et al., 2006	Dubruel et. al.; 2007
UV irradiation	Torikai & Shibata, 1999	Bhat & Karim, 2009
γ-radiation	Labout , 1972	Cataldo et al.; 2008

Table 1. Overview over cross-linking methods for collagen vs. gelatine materials

Different ways of collagen (as well as gelatine) cross-linking, **either chemical, enzymatic or physical**, have been carried out and often the method is prescribed by the target application (see Table 1).

Aldehydes have a long tradition as cross-linking reagents. Treatment with **glutaraldehide (GTA)**, in particular, is intensively used. Besides its good efficiency, this cross-linking method is fast, inexpensive and mechanical properties are enhanced (Friess, 1999). Cross-linking reaction occurs between carboxyl groups on the Glu and amine groups of Lys, or Arg forming a Shiff-base as presented on Fig. 7. However, due to the polymerization of GTA, cross-linking is sometimes restricted to the surface of the device and a heterogeneous cross-linking structure can then occur (Cheung et al., 1984). Additionally, GTA is incorporated into the new linkage and unreacted GTA can cause local incompatibility, inflammation or calcification (Luyn et al., 1995), along with limited cell ingrowth (Jayakrishnan et al.; 1996) and cytotoxicity (Sisson et al., 2009) even at concentrations of 3.0 ppm after being released into the host as a result of collagen biodegradation. From other side, glutaraldehide-based cross-linking is the current standard procedure for the production of heart valves, providing the prosthesis with low incidences of thrombo-embolism and satisfactory haemodynamic performance (Everaerts et al., 2007).

Reconstituted collagen membranes cross-linked with **3,3′-dithiobispropionimidate (DTBP)** and **diimidoesters-dimethyl suberimidate (DMS)** (Fig. 8) are shown to be more biocompatible than those treated with GTA (Charulatha & Rajaram, 2001).

Non-toxic, water soluble substances which only facilitate the reaction, without becoming part of the new linkage, are **acyl azides** and carbodiimides. **Carbodiimides, e.g. EDC**, couple carboxyl groups of Glu or Asp with amino groups of Lys or Hyl residues, thus forming stable amide bonds (Fig. 9). Reaction efficacy is increased by addition of **N-hydroxysuccinimde (NHS)** which prevents hydrolysis and rearrangement of the intermediate (Friess, 1999; Gorham, 1991; Olde Damink et al., 1996), thus causing the formation of a coarse structure instead of tougher microstructure, in its absence (Chang & Douglas, 2007). Because EDC can only couple groups within a distance of 1 nm, this treatment enhances intra- and interhelical linkages within or between tropocollagen molecules (Sung et al., 2003), without an inter-microfibrillar cross-links (Zeeman et al., 1999). EDC cross-linked collagens show reduced calcification, with no cytotoxicity and slow enzymatic degradation (Khor, 1997; Pieper et al., 1999).

Some natural non-toxic and biodegradable molecules with favourable biocompatibility have been exploited as protein cross-linkers, such as **D,L-glycceraldehyde** (Sisson et al., 2009), **oxidized alginate** (Balakrishnan & Jayakrishnan, 2005**), dialdehyde starch (DAS** (Mu et al., 2010), Fig. 10) **and genipin**.

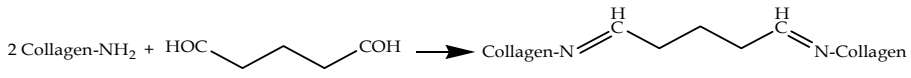

Fig. 7. Crosllinking of collagen with glutaraldehyde (GTA)

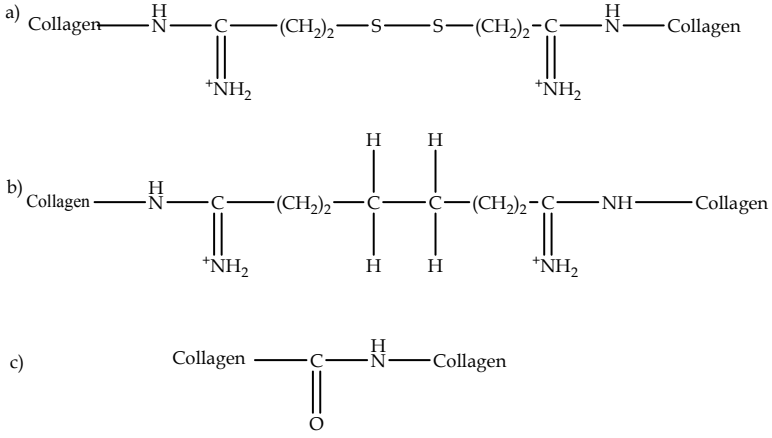

Fig. 8. Structure of cross-links obtained by (a) DTBP, (b) DMS and (c) acyl azide treatments (Charulatha & Rajaram, 2003).

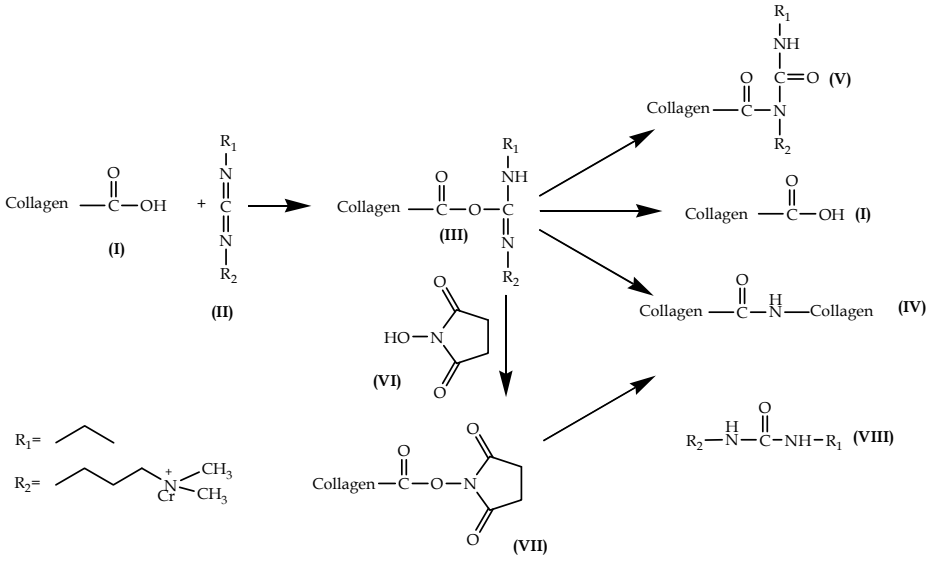

Fig. 9. Crosllinking of collagen with EDC and NHS: (I) collagen, (II) EDC, (III) *O*-acylurea intermediate, (IV.) CO-NH bond formation, (V) N-acylurea intermediate (VI) NHS, (VII) NHS-activated carboxylic group in collagen and (VIII) substituted urea (Damnik et al., 1996).

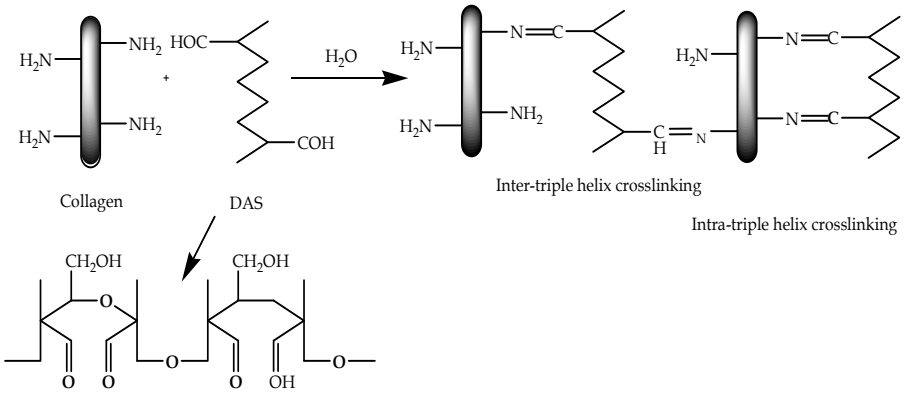

Fig. 10. Cross-linking of collagen with DAS involving Schiff's base formation between ε-amino groups from Lys or Hyl side-groups of collagen and aldehyde groups in DAS (Sission et al., 2009)

Recently, **polyphenols,** such as procyanidin (He, 2011), proanthocyanidin (Kim et al., 2005; Han et al., 2003), caffeic and tannic acids (Zhang et al., 2010), epigallocatehin and epicatehin gallates (Jackson et al., 2010), and other tannins (Pena et al., 2010) have also been used for this purpose, additionally bringing antioxidant activity, pharmacological activity, and therapeutic potential to the biomaterial due their free-radical scavenging capacities. Not only the antioxidant activity of polyphenols, but also their other physiological properties, such as anti-allergenic, anti-inflammatory, antimicrobial, cardioprotective, and anti-thrombotic make these compounds very interesting raw materials for medical applications (Pena et al., 2010). It has been shown that some of them are able to stabilize collagen and protect the chains from collagenase degradation more effectively than glutaraldehyde and carbodiimides, thus extend the implanted material over a longer period, using very low concentration (Jackson et al., 2010). The interactions between protein and polyphenol can involve hydrogen bond, covalent linkage, ionic and hydrophobic bonding. The reaction mechanism involves an initial oxidization of phenolic structures to quinones, which can readily react with nucleophiles from reactive amino acid groups in protein: sulfuhydryl group in Cys, amino group of Lys and Arg, amide group from Asp and Glu, indole ring of Trp and imidazole ring from His (Zhang et al., 2010). Nevertheless, the effect of polyphenol on the microstructure of collagen, i.e. from triple-helixes to fibrils, remains largely unknown. In reaction mechanism between gelatin and tannin are involved hydrogen bonds between hydroxyl groups of tannin and polar groups of gelatin, and hydrophobic interactions between pyrrolidine ring of Pro and pentagalloyl glucose from tannin (Obreque-Slier et al., 2010; Pena et al., 2010).

Anti-inflammatory properties are added values during **genipin**-induced cross-linking, showing to be 10, 000 times less cytotoxic then glutaraldehide which may produce weakly clastogenic responces in CHO-K1 cells (Tsai et al., 2000; Sisson et al., 2009). Moreover, the minimal calcium content of genipin–fixed tissue was detected (Chang, 2001). Genipin is a natural product, being obtained from an iridoid glucoside, geniposide abundantly present in *Genipa Americana* and *Gardenia jasminoides Ellis.* Although the cross-linking mechanism of

genipin with gelatine (or collagen) is insufficiently understood, it is known that genipin reacts with free amino groups of proteins (Fig. 11), such as Lys, Hyl and Arg, forming dark blue colour, thus acting as monomeric or oligomeric bridge which results in a comparable mechanical strength and resistence against enzymatic degradation as the glutaraldehyde–fixed tissues (Mi et al., 2005; Bigi, et al., 2002); the maximum cross-linking percentage when using genipin as a cross-linker enriched in gelatin films, is about 85% (Bigi et al., 2002). Touyama group (Touyama et al., 1994) proposed a mechanism for the reaction of genipin with a methylamine, were, reaction occurred through a nucleophilic attack of the primary amine on the C3 carbon of genipin, causing an opening of the dihydropiran ring. An attack then followed on the resulting aldehyde group by the secondary amine group. The final step in formation of the cross-linking material is believed to be dimerization produced by radical reactions, which indicate that genipin form intra- and intermolecular cross-links that have heterocyclic structure with primary amino group-containing proteins. During cross-linking reaction, genipin introduce intermicrofibrilar cross-links between adjacent collagen microfibrils, which affect the mechanical properties (Sung et al., 2003). The sizes of the interfibrilar cross-links can vary by pH variation, during cross-linking reaction, which is pH dependent: under basic conditions, genipin undergoes ring-opening polymerization, thus enlarging the spaces between fibrils, whilst under basic and neutral conditions, reaction with primary amines occur (Mi et al., 2005). Studies have been also have been conducted using material composed of genipin cross-linked gelatine and tricalcium phosphate, showing no inflammation and biocompatibility of such a composite (Yao et al., 2005). In addition, genipin cross-linking in certain polyelectrolyte multy-layer systems is shown to increase cell-adhesion and the spreading on polymeric films, thus improving tissue-implant interfaces (Hillberg et al., 2009).

Citric acid derivative (CAD) prepared by modification of citric acid carboxylic groups with NHS was introduced for cross-linking of gelatine through its amino groups leading to amide bonds formation (Saitoa et al., 2004).

Several components of **polyepoxy** family have been reported, between which **ethylene glycol diglycidyl ether**, with two epoxide functional groups located on both molecule´s ends, most reactive due to the high energy is associated to the considerable strains that exist within the three-membered ring. For these type of cross-linking agent, the opening of the epoxide ring happen simultaneously to the occurrence of the cross-linking reaction, which can occur within acidic and basic media (Vargas et al., 2008).

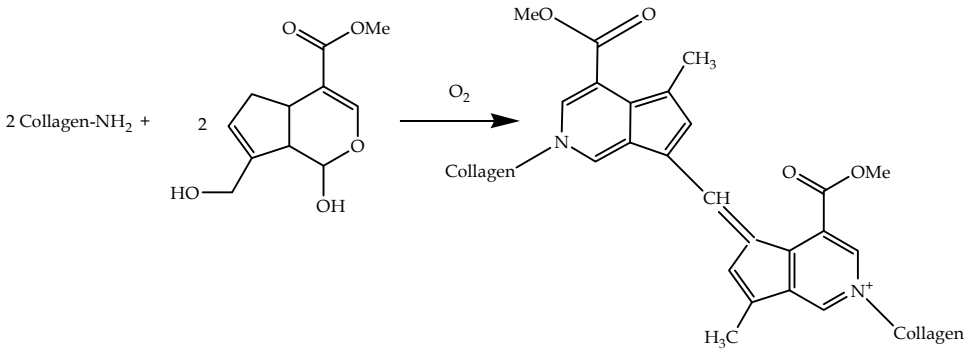

Fig. 11. Reaction between collagen and genipin proposed by (Mi, 2005).

Enzymatic cross-linking was introduced in an attempt to overcome some problems with traditional chemical approaches. The oxidative enzymes tyrosinase and laccase (Jus et al., 2011), as well as acyltransferase-transglutaminase, are capable of creating covalent cross-links in proteinaceous substrates (Fig. 12). Tyrosinases and laccases are capable of converting low-molecular weight phenols or accessible Tyr residues of proteins into quinones-reacitve species capable for non-enzymatic reactions with nucleophiles, such as reactive amino groups of other amino acid residues, without disruption of gelatines coil to helix transitions because of only 0,3% of Tyr residues in gelatine and their location outside of the Gly-X-Y tripeptide repeat region being responsible for gelatine's helix formation (Chen et al., 2003), and thus forming quiet weak gels because of the same reasons. Transglutaminase catalyses the cross-linking of gelatine by formation of isopeptide bonds between the γ-carbonyl group of a Glu residue and ε-amino group of Lys residue, and one molecule of ammonia per cross-link as by-product (Chen et al., 2003; Bertoni et al., 2006; Crescenzi et al., 2002). Presumably transglutaminase-catalyzed cross-linking occurs in the tripeptide repeat region that is responsive for gelatine's helix forming ability (Chen et al., 2003). The acyl-transfer enzyme catalyzes transamidation reactions that lead to the formation of N-ε-(γ-glutamyl)lysine cross-links in proteins (Crescenzi et al., 2002).

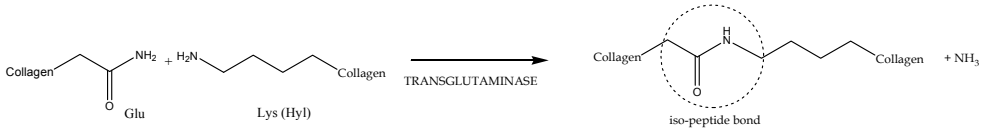

Fig. 12. Chemical cross-linking of Glu-carboxyl and Lys (Hyl)-amino groups in collagen and formation of iso-peptide bond, promote by transglutaminase (Crescenzi et al., 2002).

The treatment by **UV irradiation** only modifies the surface rather than the bulk of the collagen (Mu et al., 2010). Cross-linking of gelatine by UV–irradiation method involve pre-modification of gelatine amino groups (from Lys and Hyl side chains) (Dubruel et al., 2007), commonly by metacrilyc-anhydride (Fig. 13) (Vlierberhe et al., 2009). In subsequent step, water-soluble gelatine-methacrylamide can be cross-linked not only by UV treatment, but, also by a number of suitable polymerization processes, such as redox, thermal, γ-irradiation or e-beam curing (Van Den Bulcke et al., 2000). Prolonged exposure to UV-rays can cause also the denaturation of molecule, which can be minimized by performing the irradiation in deaerated (oxygen-poor) solutions of the gelatine derivatives (Schacht, 2004). Cross-linkage by **electron beam and x-ray** irradiation additional perform sterilization of the substrate.

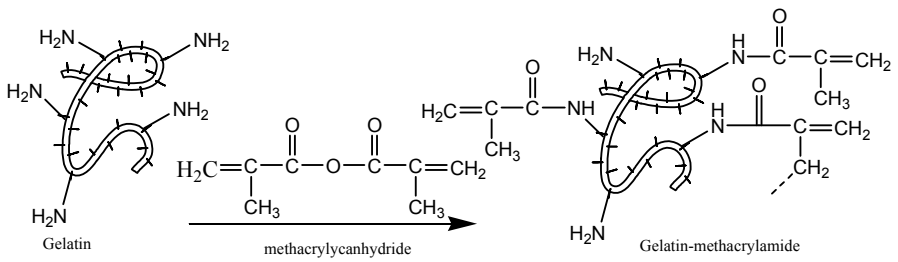

Fig. 13. Derivatization of gelatine amino groups with metacrilycanhydride (Schacht, 2004).

4. Collagen vs. gelatine as biomaterials

Collagen was first employed as a biomaterial in medical surgery in the late 19th century (Burke et al., 1983; Silver et al., 1997). Subsequently, it was used in many other medical applications, e.g. as wound dressings, hemostats or in cardiovascular, plastic or neurosurgery. Most commonly, collagen type I is used in medical devices (Silver et al.; 1997). Device production is uncomplicated and is performed in water without applying high temperatures, resulting in a variety of matrix forms, such as coatings, fibres, films, fleeces, implants, injectable solutions and dispersions, membranes, meshes, powders, sheets, sponges, tapes and tubes. Additionally, its properties can be adapted to desired requirements by additional cross-linking, although shape-instability due to swelling, poor mechanical strength, and low elasticity in vivo, may limit its unrestricted usage. Further limitations are possible antigenic responses, tissue irritations and variations in release kinetics (Sinha & Trehan, 2003). On the other hand, **gelatine** was employed as biomaterials more recently, i.e. tissue engineering from ~ 1970s and in recent years as a cell-interactive coating or micro-carrier embedded in other biomaterials (Dubruel et al., 2007). A non-exhaustive overview of the most recent publications, subdivided by application, for either collagen or gelatine alone or in a combination of other biopolymers is summarized in Table 2 which clearly indicates that gelatine has a wider- application range within the field of both soft and hard-tissue engineering.

Speciality	Collagen application	Gelatine application
Cardiology	heart valves (Everaerts et al., 2007; Taylor et al., 2006; Cox et al., 2010; Tedder et al., 2010)	heart valves– electrospun gelatine-chitosan- polyurethane (Wong et al., 2010) aortic valve –gelatine impregnated polyester graft (Langley et al., 1999) cardiac tissue engineering (Alperin et al., 2005)
Dermatology	soft tissue augmentation (Spira et al., 2004) skin replacement (Lee et al., 2001) artificial skin dermis (Harriger et al., 1998) skin tissue engineering (Ma et al., 2003; Tangsadthakun et al., 2006)	artificial skin (Choi et al., 1999; Lee et al., 2003) soft tissue adhesives (McDermott et al., 2004)
Surgery	hemostatic agent (Cameron, 1978; Browder & Litwin, 1986) plasma expander suture wound dressing and repair (Rao, 1995) skin replacement (artificial skin) nerve repair and conduits blood vessel prostheses (Auger et al., 1998; McGuigan et al., 2006, Amiel et al., 2006)	small intestine (Chiu et al., 2009) liver – chitosan/gelatine scaffold (Jiankang et al., 2007) wound dressing (Tucci & Ricotti, 2001) nerve regeneration - chitosan/gelatin scaffolds (Chiono et al., 2008) blod vesels(Mironov et al., 2005)

Orthopaedic	born, tendon and ligament repair cartilage reconstruction – collagen (Stone, 1997), composite of collagen type II/chondroitin/hyaluronan (Jančar et al., 2007) articular cartilage – collagen/chitosan (Yan et al., 2010)	bone substitute - gelatine/hydroxyapatite (Chang et al., 2007) hard tissue regeneration – gelatine/hydroxyapatite (Kim et al., 2005) cartilage (Lien et al., 2010) cartilage defects regeneration – chitosan/ gelatine (Guo et al., 2006), ceramic/ gelatine (Lien et al.; 2009) bone substitute – gelatine/tricalcium phosphate (Yao et al., 2005)
Ophthalmology	corneal graft (Lass et al., 1986) vitreous implants artificial tears (Kaufman et al., 1994) tape and retinal reattachment contact lenses eye disease treatment (http.....)	ocular inserts (Natu et al., 2007) carriers for intraocular delivery of cell/tissue sheets (Lai et al., 2010) contact lens - chitosan/gelatine (Yuan & Wei, 2004) eye disease treatment (Lai, 2010)
Urology	dialysis membrane hemodialysis (Kon et al., 2004) sphincter repair (Westney et al., 2005)	
Vascular	vascular graft (Yoshida et al., 1996) Vessel replacement, electrospin collagen (Li, 2005) angioplasty	
Others	biocoatings cell culture organ replacement skin test protein , drug and gene delivery (Mahoney & Anseth , 2007) vocal cord regeneration (Hahn et al., 2006) treatment of faecal incontinence (Kumar et al., 1998)	plasma substitutes (Kaur et al., 2002) drug delivery - gelatine/chrodroitin sulphate (Kuijpers et al., 2000) adipose tissue engineering for soft tissue remodelling (Hong et al., 2005)

Table 2. Medical applications of collagen and gelatine

Different research groups have separately evaluated collagen/gelatine-based biomaterials that differ in the applied collagen/gelatine type, cross-linking agents, additives (in the case of composites), pore size, pore geometry, and pore distribution. Beside, only a limited number of cell types have been included in most studies, which makes a meaningful understanding of how one type of (collagen/gelatine) scaffold, with its specific properties, can be applied as a suitable substrate for a variety of cell types, rather difficult. In addition, since the collagen/gelatine-based biomaterial used as scaffolds for in vivo tissue engineering in the form of gels, sponges and woven meshes are required disappear by

resorption into the body after accomplishment of tissue regeneration, different tissues needs may demand biodegradable scaffolds with different physical and chemical characteristics.

4.1 Combination with other biopolymers

Fabrication of scaffolds from single-phase biomaterial with homogeneous and reproducible structures presents a challenge, due their generally-poor mechanical properties, which limit their use. Combination with different natural or synthetic polymers in composites or by introducing of e.g. ceramics is one of today´s approaches for overcoming above mentioned limitations.

Along with **hydroxyapatite (HA), collagen** is one of two major components of the bone, making up 89% of the organic matrix and 32% of the volumetric composition of bone (O´Brien, 2011). HA, being similar to bone mineral in physicochemical properties, is well known for its bioactivity and osteoconductivity in vitro and in vivo. Thus, gelatine/HA composite is a potential temporary biomaterial for hard tissue regeneratation, in view of combining the bioactivity and osteoconductivity of HA with the flexibility and hydrogel characteristics of gelatine (Chang & Douglas, 2007; Kim et al., 2004; Narbat et al., 2006; Wahl & Czernuszka, 2006). Both, collagen and HA devices significantly inhibited the growth of bacterial pathogens, being the most frequent cause of prosthesis-related infection (Carlson et al., 2004).

Modification of the collagen/gelatine scaffold materials by **glycosaminoglycans (hyaluronan and chondroitin sulphate**) was introduced in order to enhance cells migration, adhesion, proliferation and differentiation, and to promote preservation of the differentiated states of the cells, as compared to collagen/gelatine alone (Jancar et al., 2007), as well as for control release of antibacterial agents (van Wachem et al., 2000). Hyaluronic acid is a component of the extracellular matrix of some tissue (cockscomb and vitreous humour) and possesses high capacity lubrication, water-sorption and water retention, whilst chondroitin sulphate is sulfated glycosaminoglycan and is important structural component of cartilage, which provides its resistance to compression (Baeurle et al., 2009).

The better collagen delivery systems, having an accurate release control, can be achieved by adjusting the structure of the collagen matrix or adding **other proteins, such as elastin or fibronectin** (Doillon & Silver, 1986). Thus, a combination of collagen with other polymers, such as collagen/liposome (Kaufman et al., 1994) and collagen/silicone (Suzuki et al., 2000), has been proposed in order to achieve the stability of a system, and the controlled release profiles of incorporated compounds.

The addition of collagen to a **ceramic** structure can provide many additional advantages to surgical applications: shape-control, spatial adaptation, increased particle and defect wall-adhesion, and the capability to favour clot-formation and stabilisation (Scabbia and Trombelli, 2004).

cross-linked **collagen/chitosan** (Kim et al., 2001; Ma et al., 2003; Wang et al., 2003; Chalonglarp et al., 2006) as well as **gelatine/chitosan (**Kim et al., 2005; Chiono et al., 2008) matrices were presented as a promising biomaterial for tissue engineering, to be used in several specific areas, such as drug delivery, wound dressings, sutures, nerve conduit, and matrix templates for tissue engineering. Human connective tissues do not contain chitosan, but it has structural similarity to glucosaminoglycan (GAG), mostly components of ECM. GAG attached to the core protein of proteoglycan consist of repeating disaccharide unit, usually includes an uronic acid component (e.g., D and L-gluconic acid) and a hexoamine component (e.g., N-acetyl-D-glucosamine, which, together with glucosamine build the

copolymer structure of chitosan and N-acetyl-D-galactosamine). Chitosan, because of it cationic nature, can promote cell adhesion, can act as modulator of cell morphology, differentiation, movements, synthesis and function. It is reported that chitosan induces fibroblasts to release interleukin-8, which is involved in migration and proliferation of fibroblasts and vascular endothelial cells, but, also promotes surface-induced thrombosis and embolization, which limits its application in blood-containing biomaterials (Wang et al., 2003). Chitosan addition enhances poor mechanical properties of gelatine and influence on more controllable biodegradation rate. Chitosan, with higher Degree of deacetilation (DD), modified with gelatine, possess more intensive cytocooplatibility, enhance cell proliferation and decline cell apoptosis. From the other hand, a flexible gelatine complex with a rigid chitosan weakens the adhesion via neutralizing cationic sites of chitosan, with suitable negative-charges borne by the gelatine, and as a consequence, a gelatine/chitosan product shows improved cell mobility, migration and multiplication (Mao et al., 2004; Yuan et al., 2004). Thus, networks composed of gelatine and chitosan have been studied extensively due its excellent ability to be processed into porous scaffolds with good cytocompatibility and desirable cellular response (Mao et al., 2004; Wang et al., 2003).

The advantageous properties of collagen for supporting tissue growth have been used in conjunction with the superior mechanical properties of **synthetic biodegradable polymers** to make hybrid tissue scaffolds for bone and cartilage. Collagen has also been used to improve cells´ interactions with electrospun nanofibers of poly (hydroxyl acids), such as poly(lactic acid), poly(glycolic acid), poly(ε-caprolactone), and their copolymers (Pachence et al., 2007).

Novel **gelatine/alginate** sponge serving as an drug carrier for silver sulfadiazine and gentamicin sulphate, used for wound healing (Choi et al., 1999). Alginate is known as a hydrophilic and biocompatible polysaccharide, and is commonly used in medical applications, such as wound dressing, scaffolds for hepatocyte culture, and surgical and dental materials. It's content in the above-mentioned sponge cause increasing in porosity, resulting in enhanced water uptake ability.

4.2 Mechanism of collagen degradation

4.2.1 In vitro degradation

Degradation of collagen requires water and enzyme penetration, and the digestion of linkages. Collagen swells to a certain extent by exposure to water, but due to its special sterical arrangement (triple helical conformation), native collagen can only be digested completely by specific collagenases and pepsin-cleaving enzymes being able to cleave collagen in its undenatured helical regions at physiological pH and temperature (Harrington, 1996; Sternlicht & Werb, 2001). Included are collagenases which cleave once across all three chains, such as tissue collagenases, as well as collagenases making multiple scissions per chain, such as collagenase from *Clostridium histolyticum* (CHC) (Seifter et al., 1971) whilst non-specific proteinases, such as pepsin, which can only attack the telopeptides or denatured helical regions of collagen (Weiss, 1976) are responsible for further degradation down to amino acids.

CHC types of collagenase are only present in tissue at very low- levels and tightly- bound to collagen (Woessner, 1991), while tissue collagenases cleavie to all types of collagen, with no preference for a special collagen substrate (Welgus et al.,; 1983). Depending on the collagen type, about 150-200 cleaves per chain can be made (Seifter et al., 1971).

To date, seven forms of CHC are known (Mookhtiar et al., 1992). All seven enzymes contain zinc and calcium and consist of one polypeptide chain with one active site. The zinc (II) atom is located in the active site and is therefore essential for catalysis, whereas the calcium (II) atoms are required to stabilize the enzyme conformation and, consequently, the enzymatic activity (Bond et al., 1984). On the basis of their primary and secondary structures, their substrate specifities and their method of attack, CHCs can be divided into two classes. Class I contains α-, β-, γ-, and η-collagenase, and firstly attacks the collagen triple-helix near the ends. After cleavage at the C-terminal end, a cut near the N-terminus follows, before collagen is successively degraded into smaller fragments. Class II consists of δ-, ε- and ζ- collagenase and cleaves the tropocollagen in its centre, to producing two fragments. Further digestion of the bigger fragment follows (Mookhtiar et al., 1992). Consequently, class II CHC better resembles tissue collagenases, which cleaves collagen into TCA and a TCB fragment (Seifter et al., 1971; Welgus et al., 1980).
Collagen fibrils are degraded in a non-specific manner, with no preferential cleavage site in the interior or at the ends of fibrils (Paige et al.; 2002). It was concluded that collagenase is too large to penetrate into the fibrils, so digestion can only occur at the fibrils` surface (Okada et al., 1992; Paige et al., 2002). Hence, the degradation rate is directly correlated to those substrate molecules available on the surface. If collagen forms fibres and fibre-bundles, and the tropocollagens within becomes inaccessible, the degradation rate is reduced even more (Steven, 1976).

4.2.2 In vivo degradation

In vivo, degradation of collagen is more complex than in vitro. Collagen implants are infiltrated by various inflammatory cells, e.g. fibroblasts, macrophages or neutrophils, which cause contraction of the implant and secret collagen-degrading enzymes, activators, inhibitors, and regulatory molecules. Infiltration depends on properties of the implant, such as collagen nature, shape, porosity and degree of cross-linking, implantation site and individual enzyme levels (Gorham, 1991). Collagen is degraded by endopeptidases from the four major classes (Table 3): mettaloproteinases, serine proteases, cysteine proteases and aspartic proteases, although, non-enzymatic degradation mechanisms, e.g. hydrolysis, participate in collagen breakdown (Okada et al., 1992). Connective tissue, for example, is digested by the interplay between four different classes of proteinases, which are either stored within cells or released when required, while for degradation of the extracellular matrix, MMPs are mainly responsible. Cystein and aspartic proteinases (cathepsins) degrade connective tissue intracellularly at acidic pH (3-5) values, whereas serine and matrix metalloproteinases (MMP) act extracellularly at neutral pH values (Shingleton et al., 1996). Anyhow, cathepsins also play a major role in intracellular digestion of phagocytosed material, by cleaving telopeptide containing cross-links, and under certain conditions they can also act extracellularly by cleaving triple-helical regions, which is followed by denaturation of solubilised triple-helix and further degradation by proteases (such as gelatinases type MMP-2 and 9), due to susceptibility of individual α-chains (Baley, 2000).
MMP enzymes represent a family of structurally and functionally related zinc- and calcium-containing endopeptidases which degrade almost all extracellular matrix and basement membrane proteins (Wall et al., 2002; Bailey, 2000). To date, 24 different MMPs and 4 tissue inhibitors of metalloproteinases (TIMP) are characterized (Yoshizaki et al., 2002). According to their primary structure and substrate specify, MMPs are divided into five sub-classes.

Five major MMPs have been identified in humans, namely fibroblast collagenase (MMP1), gelatinase A (MMP-2), gelatinase B (MMP-9), neutrophil collagenase (MMP-8) and stromelysine (MMP-3) (Netzel-Arnett et al., 1991). Besides collagenase 4MMP-8, which is stored in specific granules of neutrophils, and membrane-type MMPs (MT-MMP), which are integral membrane cell glycoproteins, all other MMPs are synthesized if required (Imai et al., 1998) and able to cleave native triple-helical fibrilar collagens.

Enzyme class	Cellular source	Substrate	Activator
Matrix metalloproteinases			
Collagenases			
• MMP-1	Connective tissue cells Monocytes/macrophages	Native triple helix	MMP-3 Plasmin
• MMP-8	Neutrophilis	Native triple helix	MMP-3/NE
• MMP-13 (Rodent MMP-1)	as MMP-1	as MMP-q plus telopeptides	Plasmin MMP-2/3 MT-MMP
Gelatinases	Most cell types	Native type IV gelatin	
• MMP-2			MMP-1/2 MT-MMP
• MMP-9	Connective tissue cells Neutriphilis/monocytes	as MMP-2	Plasmin MMP-2/3
Stromelysins	Connective tissue cells		
• MMP-3	Macrophages	Collagen types III,IV and IX	Plasmin Cathepsin G
• MMP-10	Macrophages	Aggrecan	
Cystine proteinases		as MMP-3	as MMP-3
• Cathepsins	Lysosomal		
• B,L,C,H,N and S			
• K		Telopeptide	Cathepsin D
Serine proteinases		Bone/triple helix plus telopeptides	Low pH
• Neutrophil elastase	Granulocytes		
• Cathepsin G		Telopeptides/triple helix	
Aspartic proteases			
• Cathepsin D		Telopeptide	
		Telopeptide	

Table 3. Major collagen degrading enzymes (Bailey, 2001).

The mechanism of collagen degradation by MMPs is not totally resolved. One of hypothesis is that collagen is actually unwound by MMPs (Chung et al., 2004). Collagenases bind and locally unwind the triple-helical structure before hydrolysing the peptide bonds. According

to these, MMP-1 preferentially interact with the Gly-Leu on α2 (I) chain residues and with Gly-Ileu on α1 chain and cleaves the three α chains in succession, generating two triple-helical fragments of ¾ and ¼ the molecule length, which show lower denaturation temperature then physiological one, and they both denaturate, producing random polypeptide gelatine chains (Baley, 2000), which are further degraded by gelatinases (MMP-2 and MMP-9) and other nonspecific enzymes as schematically presented on Fig. 14.

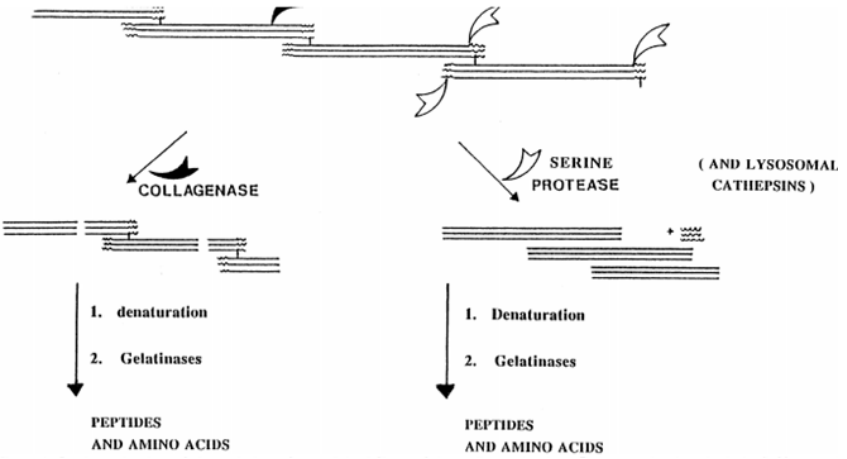

Fig. 14. Dual degradation mechanism of cross-linked fibers in the collagen implant. These mechanism include (left) neutral collagenase cleaving the three chains of the triple-helix and (right) the acid cathepsins and neutral serine proteases cleaving the nonhelical terminal regions (telopeptides) containing the intermolecular cross-links (Bailey, 2001).

Existence of locally unfolded states in collagen molecule has been also suggested (Escat, 2010), according to which, folded structure of collagen cannot fit into the catalytic site, since collagen triple-helix has a diameter of approximately 15 Å, whiles catalytic domain of MMPs has a catalytic site of only 5 Å wide. Beside, scissile bond, cleaved by collagenases is buried in collagen structure when collagen is exposed to solvent, which make it inaccessible for scission. Local unfolding is collagen triple-helix property, which occur without presence of collagenases, but necessary for collagen degradation in collagenase presence. In addition, immino-poor regions in collagen are thought to carry biological information, such as cell recognition or protein binding sites (Brodsky & Persikov, 2005), but may play also an important role in collagen degradation (Fields, 1991).

MMP expression is induced by various cytokines, e.g. interleukin-1, and growth factors (Shingleton et al., 1996). MMPs are secreted as latent inactive pro-enzymes (zymogens) which have to be activated before they have complete proteolytic activity (Overall, 1991). Four amino acids (three His and one Cys) are coordinated to the zinc atom in the active centre of zymogens (Birkedal-Hansen et al., 1993), being proposed by a "cysteine switch model". The linkage to the Cys residue is thought to be cleaved and a water molecule, which must be the fourth substituent in the active enzyme can bind (Nagase et al., 1999). In vivo, zymogens are activated by removal of a pro-peptide by proteinases, like plasmin or stromelysin, followed by a second activation step provoked by proteinases or autocatalysis

(Shingleton et al., 1996). Additionally, activation is controlled by TIMPs, which can prevent activation of zymogens and/or action of activated MMPs. In vitro, trypsin and organomercurials can be used for activation as well (Overall, 1991). Physical agents unfold the structure, the zinc-cysteine contact breaks and the propeptide is cleaved auto-catalytically (Woessner, 1991).
Tissue collagenases cleave tropocollagen at one single site, producing TCA and TCB fragments about three-quarters and one-quarter of the original molecule size. After this initial cleavage, the helical fragments spontaneously denature at body temperature and are subsequently further digested by other proteinases (Mallya et al., 1992). This secondary degradation can take place extracellularly or intracellularly after phagocytosis (Harris, et al., 1974). Apart from collagenases, gelatinases play an important role in collagen degradation. Besides, with any further degradation of initially-cleaved collagen, gelatinases can degrade native collagen type I, IV, V and VII (Overall, 1991). Furthermore, levels of gelatinases are considered to be a good index whether inflammation is present or not, because high concentrations are only available when a normal remodeling process is disrupted (Trengove et al., 1999).

4.2.3 Immunological response of collagen-based biomaterials

As already mentioned, the implantation of biomaterials often initiates acute inflammatory responses, which sometimes can cause chronic inflammatory response. Measuring the intensities and duration of the immune responses against implanted biomaterials is important for biocompatibility evaluation. The tissue response towards implanted biomaterials (also called the foreign body reaction) is influenced by morphology and composition of the biomaterial and the place where biomaterial is implanted (Ye et al., 2010; Jansen et al., 2008; Wang et al., 2008). Inflammation reaction is manifested by secretion of large amount of antibodies (secreting B cells and T cells with cytotoxic activity) and cytokines, in presence of foreign materials (as scaffolds) or pathogens. The microenvironment of the implant further changes, so, determination of immunological response after in vivo implantation is based of measuring the level of pro-inflammatory cytokine secretions and antibody secretions, and monitoring the population changes of immune cells (Song et al., 2006; Hardin-Young et al., 2000).
According to (Luttikhuizen et al., 2007), collagen-based scaffolds are mainly infiltrated by Giant cells that phagocytose and degrade the collagen bundles, until the material is completely disposed of. This is a chronic inflammatory reaction, which last until the material is completely degraded, after which the cells that are involved disappear.
As an alternative for collagens isolated from calf skin and bond, as a risk-carry materials of bovine spongiform encephalophaty and transmissible spongiform encephalopathy, novel **forms of acid-soluble collagen**, extracted from jellyfish was proposed (Song et al., 2006), because of their differences in amino acid composition: jellyfish collagen had higher content of Gln (glutamine) and Glu, lower Pro content, small Tyr content, comparing with bovine and also contains Cys, which is not common for bovine collagen.

4.2.4 New sources of gelatine

Currently gelatine for food and used by the pharmaceutical industry is derived almost exclusively from **animal products**. About 55,000 tons of animal-sourced gelatine is used each year. Recently, an advance toward turning corn plants into natural factories producing

high-grade gelatine in a safe and inexpensive manner has been introduced as an alternative, enabling the development of a variety of gelatines with specific MWs and properties tailored to suit various needs. Beside, **plant-derived recombinant gelatine** would address concerns about the possible presence of infectious agents in animal by-products and the lack of traceability of the source of the raw materials currently used to make gelatine. Resourcing plant materials to recover and purify recombinant gelatine has remained a challenge because only very low levels accumulate at the early stages of the development process. Furthermore, since recently, gelatines are also produced biotechnologically by the use of recombinant DNA technology, which opens the possibility to manipulate the amino acid sequence of gelatines, and thereby to functionalize them for specific purposes. The biotechnological production of recombinant gelatine also eliminates the risk of prion contaminations, which are possible, present in non-recombinant animal source gelatines (Sutter et al., 2007). Thus, many commercial recombinant collagens already exist on the market and are becoming commonly used in the development of medical soft and hard tissue repair applications (Pannone, 2007).

5. Conclusion

This review presents the characteristic properties of both fibrous proteins including biocompatibility, non-immunogenicity, their capacities for modification at the molecular level, thus rendering or tuning their functional (surface/interfacial, mechanical, topological and morphological) properties, characteristic gelation (sol-gel transition) and gel-forming abilities and, finally, their bio-absorbability and biodegradability. In addition, their expanding applications for biomaterials are compared, with emphasis on the importance of understanding their suitability, as defined biomaterials with specific properties, for certain cell types. Finally, new perspectives for further study and development indicated, providing satisfactory interaction and imitation of biological functions.

6. References

Alperin, C., Zandstra, P.W. & Woodhouse, K.A. (2005). Polyurethane films seeded with embryonic stem cell derived cardiomycytes for use in cardiac tissue engineering applications. *Biomaterials,* Vol. 26, No. 35, pp. (7377-7386)

Amiel, G.E., Komura, M., Shapira, O., Yoo, J.J., Yazdani, S., Berry, J., Kaushai, S., Bischoff, J., Atala, A. & Soker, S. (2006). Engineering of blood vessels from acellular collagen matrices coated with human endothelial cells. *Tissue Engineering,* Vol. 12, No. 8, pp. (2355-2365)

Auger, F.A., Rouabhia, M. Goulet, F., Berthod, F., Moulin, V. & Germain, L. (1998). Tissue-engineered human skin substitutes developed from collagen-populated hydrated gels: clinical and fundamental applications. *Medical and Biologycal Engineering & Computing,* Vol. 36, No. 6, pp. (801-812)

Baeurle, S.A., Kiselev, M.G., Makarova, E.S. & Nogovitsin, E.A. (2009). Effect of the counterion behaviour on the frictional-compressive properties of chondroitin sulphate solutions. *Polymer,* Vol 50, No. 7, pp. (1805-1813)

Balakrishnan,B. & Jayakrishnan, A. (2005). Self-cross-linking biopolymers as injectable in situ forming biodegradable scaffolds. *Biomaterials,* Vol. 26, No.18, pp. (3941-3951)

Bailey, A.J.(2001).The fate of collagen implants in tissue defects. *Wound Repair and Regenration,* Vol. 8, pp. (5-12)

Barrere, F., Mahmood, T.A., de Groot, K., van Blitterswijak, C.A. (2008). Advanced biomaterials for skeletal tissue regeneration: Instructive and smart functions. *Material science and Engineering,* Vol. 59, No. 1-6, pp. (38-71)

Barbetta, A., Rizzitelli, G., Bedini, R., Pecci, R. & Dentini, M.(2010). Porous gelatin hydrogels by gas-in-liquid foam templating. *Soft Matter,* Vol. 6, pp. (1785-1792)

Belbachir, K., Noreen, R., Gouspillou, G. & Petibois, C. (2009). Collagen types analysis and differentiation by FTIR spectroscopy. *Analytical and Bioanalytical Chemistry*, Vol.395, No. 3, pp. (829-837)

Bertoni, F., Barbani,N., Giusti, P & Giardelli, G. (2006). Transglutaminase reactivity with gelatine: perspective applications in tissue engineering. *Biotechnology Letters,* Vol.28, pp. (697-702)

Bigi,A., Cojazzi,G., Panzavolta, S., Roveri,N. & Rubini, K. (2002). Stabilization of gelatin films by crosslinking with genipin. *Biomaterials,* Vol.23, pp. (4827-4832)

Birkedal-Hansen,H., Moore,W.G., Bodden,M.K., Windsor,L.J., BirkedalHansen,B., DeCarlo,A. & Engler, J.A. (1993). Matrix Metalloproteinases: a Review. *Critical Reviews in Oral Biology and Medicine : an Official Publication of the American Association of Oral Biologists*, Vol. 4, pp.(197 – 250)

Bhat, R. & Karim, A.A. (2009). Ultraviolet irradiation improves gel strength of fish gelatin. *Food Chemistry,* Vol. 113, No. 4, pp. (1160-1164)

Bond, M.D. & Van Wart, H.E. (1984). Relationship Between the Individual Collagenases of Clostridium Histolyticum: Evidence for Evolution by Gene Duplication. *Biochemistry*, Vol.23, pp. (3092 – 3099)

Brinckmann, J., Notbohm, H., Mueller,P.K. & Editors. (2005). *Collagen: Primer in Structure, Processing and Assembly,* Springer-Verlag Heidelberg, ISBN-10 3-540-23272-9, The Netherlands

Browder, I.W., & M.S. Litwin. (1986). Use of absorbable collagen for hemostasis in general surgical patients. The American Surgeon, Vol. 52, No. 9, pp. (492-494)

Brodsky, B. & Persikov, A.V. (2005). Molecular structure of the collagen triple helix. *Advances in Protein Chemistry,* Vol. 70, pp. (301-309)

Browder, I.W. & Litwin, M.S. (1986). Use of absorbable collagen for hemostasis in general patients. *Americal Surgeon,* Vol. 52, No. 9, pp. (492-494)

Burke, K.E., Naughton, G., Waldo, E. & Cassai, N. (1983). Bovine Collagen Implant: Histologic Chronology in Pig Dermis. *Journal of Dermatologic Surgery and Oncology*, Vol. 9, pp. (889 – 895)

Cameron, W.J. (1978). A new topical hemostatic agent in gynecologic surgery. *Obstet Gynecology,* Vol. 51, No. 1, pp. (118-122)

Cancedda, R., Dozin, B., Giannoni, P. & Quarto, R. (2003). Tissue engineering and cell therapy of cartilage and bone. *Matrix Biology*, Vol. 22, No.1, pp. (81-91)

Carlson, G.A., Dragoo, J.L., Samimi, B., Bruckner, D.A, Bernard, G.W., Hedrick, M. & Benhaim, P. (2004) Bacteriostatic properties of biomatrices against common orthopaedic pathogens. *Biochemical and Biophysical Research Communications,* Vol. 321, No. 2, pp. (472-478)

Cataldo, F., Ursini, O., Lilla, E. & Angelini, G. (2008). Radiation-induced crosslinking of collagen gelatin into a stable hydrogel. *Journal of Radioanalytical and Nuclear Chemistry,* Vol. 275, No. 1, pp. (125-131)

Chalonglarp, T., Sorada, K., Neeracha, S., Tanom, B. & Siriporn, D.(2006). Properties of Collagen/Chitosan Scaffolds for Skin Tissue Engineering. *Journal of Metals, Materials and Minerals,* Vol. 16, pp. (37-44)

Chang, M.C. & Douglas, W.H. (2007). Cross-linking of hydroxyapatite/gelatin nanocomposite using imide-based zero-length cross-linker. *Journal of Materials Science: Materials for Medicine,* Vol.18, pp. (2045-2051)

Charulatha, V. &. Rajaram , A. (1997). Crosslinking density and resorption of dimethyl suberimidate treated collagen. *Journal of Biomedical Materials Research*, Vol.36, pp. (478–486)

Chang, Y. Tsai CC, Liang HC, Sung HW. (2001). Reconstruction of the RVOT with a bovine jugular vein graft fixed with a naturally occurring crosslinking agent (genipin) in a canine model. *Journal of Thoracic and Cardiovascular Surgery,* Vol.122, No. 6, pp. (1208–1218)

Charulatha, V. &. Rajaram, A. (2001). Dimethyl 3,3′-dithiobispropionimidate: a novel crosslinking reagent for collagen. *Journal of Biomedical Materials Research*, Vol. 54, pp. (122–128)

Charulatha, V. &. Rajaram, A. (2003). Influence of different crosslinking treatments on the physical properties of collagen membranes. *Biomaterials,* Vol. 24, No. 5, pp. (759-767)

Chavez, F.V., Hellstrand, E. & Halle, B. (2006). Hydrogen Exchange and Hydration Dynamics in Gelatin Gels. *Journal of Physical Chemistry B*, Vol. 110, No. 43, pp. (21551-21559)

Chen,T., Embree, H.D., Brown,E.M., Taylor, M.M. & Payne, G.F. (2003). Enzyme-catalyzed gel formation of gelatin and chitosan: potential for in situ appplications. *Biomaterials*, Vol. 24, pp. (2831-2841)

Chen, J.M., Sheldon, A., & Pincus, M.R. (1995). Three dimensional energy-minimized model of human type II smith collagen microfibrill. *Journal of Biomolecular Structure & Dinamics*, Vol. 12, pp. (1129 –1156)

Cheng,W.,Yan-hua,R., Fang-gang,N. & Guo-an,Z. (2011). The content and ration of type I and type III collagen in skin differ with age and injury. *African Journal of Biotechnology,* Vol. 10, No. 13, pp. (2524-2529)

Cheung, D.T., Perelman,N., Ko, E.C. & Nimni,M.E.(1984). Mechanism of Crosslinking of Proteins by Glutaraldehyde III. Reaction With Collagen in Tissues. *Connective Tissue Research*, Vol.13, No. 2, pp. (109 – 115)

Chevallay, B. & Herbage, D. (2000). Collagen-based biomaterials as 3D scaffold for cell cultures: applications for tissue engineering and gene therapy, *Medical & Biological Engineering & Computing*, Vol. 38, No.2, pp. (211-218)

Chiono, V., Pulieri, E., Vozzi, G., Ciardelli, G., Ahluwalia, A. & Paolo Giusti, P.(2008). Genipin-crosslined chitosan/gelatin blends for biomedical applications. *Journal of Material Science: Materials in Medicine,* Vol. 19, No. 2, pp. (889-898)

Chiu, C.H., Shin, H.C., Jwo, S.C. & Hsieh, M.F. (2010). Effect of Crosslinkers on Physical Properties of Gelatin Hollow Tubes for Tissue Engineering Application. *World Congress on Medical Physics and Biomedical Engineering,* Vol. 25, No. 10, pp.(293-296)

Choi, Y.S., Hong, S.R., Lee, Y.M., Song, K.W., Park,M.H. & Young Soo Nam, Y.S. (1999). Study of gelatin-containing artificial skin: I. Preparation and characteristics of novel gelatin-alginate sponge. *Biomaterials,* Vol. 20, pp. (409-417)

Chung, L., Dinakarpandian, D., Yoshida, N., Fields, J.L.L., Fields, G. B., Visse, R. & Nagase, H.(2004). Collagenase unwinds triple-helical collagen prior to peptide bond hydrolysis. *The European Molecular Biology Organization Journal,* Vol. 23, pp. (3020-3020)

Collagen Corneal Shields, Available online: http://www.uic.edu/com/eye/LearningAboutVision/EyeFacts/CollagenCornealShields.shtml

Collagen: The Body´s Cellular Fabric, Available online: http://www.kokenmpc.co.jp/english/support/tecnical/collagen/index.html)

Cole, B. (1999). Gelatin, In: *Wiley Encyclopedia of Food Science and Technology (second edition),* Francis,F.J, John Wiley & Sons, ISBN: 0-471-19285-6, New York

Cooperman, L. & Michaeli, D. (1984). The immunogenicity of injectable collagen. 1. 1-year prospective study, Journal of the American Academy of Dermatology, Vol.10, No. 4, pp. (647-651)

Cox, M.A.J., Kortsmit, J., Driessen, N., Bouten, C.V.C. & Baaijens, F.P.T. (2010). Tissue-Engineered Heart Valves Develop Native-like Collagen Fiber Architecture, *Tissue Engineering Part A*, Vol. 16, No. 5, pp. (1527-1537)

Crescenzi V, Francescangeli A, Taglienti A. (2002). A new gelatine-based hydrogels via enzymatic networking. *Biomacromolecules,* Vol. 3, pp. (1384–1391)

Damnik, O., L.H.H., Dijkstra, P.J., van Luyn, M.J.A, van Wachem, P.B, Nieuwenhuis, P. & Feijen, J. (1996). Cross-linking of dermal sheep collagen using a water-soluble carbodiimide, *Biomaterials*, Vol. 17, No. 8, pp. (765-773)

Doillon, C.J. & Silver, F.H. (1986). Collagen — based wound dressing effects of hyaluronic acid and fibronectin on wound healing. *Biomaterials*, Vol. 7, pp. (3 –8)

Dubruel, P., Unger, R., Van Vlierberghe, S., Cnudde, V., Jacobs, P.J.S, Schacht, E. & Kirkpatrick, C.J. (2007). Porous Gelatin Hydrogels: 2. In Vitro Cell Interaction Study. *Biomacromolecules,* Vol. 8, pp. (338-344)

Escat, R.S. (2010). The role of Unfolded States in Collagen Degradation, PhD thesis Massachusetts Institute of Technology

Everaerts, F., Torrianni, M., Hendriks, M., Feijen, J. (2007). Quantification of carboxyl groups in carbodiimide cross-linked collagen sponges. *Journal of Biomedical Materials Research, Part A,* Vol. 83A, No. 4, pp. (1176-1183)

Farris,S., Schaich,K.M., Liu,L.S., Piergiovanni, L. & Yam, K.L. (2009). Development of polyon-complex hydrogels as an alternative approach for the production of bio-based polymers for food packaging applications. A review. *Trends in Food Science ¸Technology*, Vol. 20, pp. (316-332)

Farrist, S., Song, J. & Huang, Q. (2009). Alternative Reaction mechanism for the Cross-Linking of Gelatin with Glutaraldehyde. *Journal of Agricultural & Food Chemistry*, Vol. 58, No. 2, pp. (998-1003)

Fields, G.B. (1991). A model for interstitial collagen catabolism by mammalian collagenase. *Journal of Theoretical Biology,* Vol. 153, No. 4, pp. (585-602)

Fuchs, S., Kutscher, M., Hertel, T., Winter, G., Pietzsch, M. & Coester, C. (2010). Transglutaminase: new isights into gelatin nanoparticle cross-linking. *Journal of Microencapsulation,* Vol. 27, No. 8, pp. (747-754)

Friess, W. (1998). Collagen-biomaterial for drug delivery. *European Journal of Pharmaceutics and Biopharmaceutics,* Vol.45, No. 2, pp. (113 – 136)

Friess, W. (1999). *Drug Delivery Systems Based on Collagen,* Shaker Verlag, ISBN, 3-8265-6994-6, Aachen

Gelse, K., Poschl, E., Aigner, T. (2003). Collagens-structure, function, and biosynthesis. *Advanced Drug Delivery Reviews*, Vol. 55, No.12, pp. (1531-1546)

Gomez-Guillen, M. C., Perez-Mateos, M., Gomez-Estaca, J., Lopez-Caballero, E., Gimenez, B., & Montero, P. (2009). Fish gelatin: a renewable material for developing active biodegradable films. *Trends in Food Science & Technology*, Vol. 20, No. 1, pp. (3-16)

Gorham, S.D. (1991). Collagen as a biomaterial. In: *Biomaterials,* Byron D, Stockton Press, New York, 55-122

Guo, T., Zhao, J., Chang, J., Ding, Z., Hong, H., Chen, J. & Zhang, J. (2006). Porous chitosan-gelatin scaffold containing plasmid DNA encoding transforming growth factor-β1 for chrondrocytes proliferation. *Biomaterials*, Vol. 27, No. 7, pp. (1095-1103)

Hahn, M.S., Kobler, J.B., Zeitels, S.M . & Langer, R. (2006). Quantitative and comparative studies of the vocal fold extracellular matrix II: collagen. *The Annals of Otology, Rhinology & Laringhology,* Vol. 115, No. 3, pp. (225-232)

Han, B., Jaurequi, J., Tang, B.W. & Marcel E. Nimni (2003). Proanthocyanidin: A natural crosslinking reagent for stabilizing collagen matrices, *Journal of Biomedical Materials Research Part A,* Vol 65A, No. 1, pp. (118-124)

Hardin, J.Y., Carr, R.M., Dowing, G.J., Condon, K.D. & Termin,P.L. (2000). Modification of Native Collagen Reduces Antigenicity but Preserves Cell Compatibility, *Biotechnology and Bioingeneering,* Vol. 49, No. 6, pp. (675-682)

Harriger, M.D., Supp, A.P., Warden , G.D. & Boyce, S.T. (1998). Glutaraldehyde crosslinking of collagen substrates inhibits degradation in skin substitutes grafted to athymic mice. *Journal of Biomedical research* ,Vol.5 pp. (137-145)

Harrington,D.J. (1996). Bacterial Collagenases and Collagen-Degrading Enzymes and Their Potential Role in Human Disease. *Infection and Immunity*, Vol.64, pp. (1885-1891)

Harris,E.D., Jr. & Krane,S.M.(1974). Collagenases(Second of Three Parts). *The New England Journal of Medicine,* Vol. 291, pp. (605 – 609)

Harkness, R.D. (1966). Collagen. *Science Progress*, Vol. 54, pp. (257-274)

He, L., Mu, C., Ski, J., Zhang, Q., Shi, B & Lin, Q. (2011). Modification of collagen with a natural cross-linker, procyanidin. *International Journal of Biological Macromolecules,* Vol. 48, No. 2, pp. (354-359)

Herpandi, Huda, N. & Adzitey,F. (2011). Fish Bone and Scale as a Potential Source of Halal Gelatin. *Journal of Fisheries and Aquatic Science,* Vol. 6, No. 4, pp. (379-389)

Hillberg, A.L., Christina A. Holmes, C.A. & Maryam Tabrizian, M.(2009). Effect of genipin cross-linking on the cellular adhesion properties of lyer-by –lyer assembled plyelectrolyte films. *Biomaterials* , Vol. 30, No. 27, pp. (4463-4470)

Hopkins, S.J. & Wormall, A. (1933). Phenyl isocyanate protein compounds and their immunological properties. *Biochemical Journal,* Vol. 27, pp. (740-753)

Hsu, F.Y., Chueh, S.C. & Wang, J.Y. (1999). Microspheres of hydroxyapatite/reconstituted collagen as supports for osteoblast cell growth. *Biomaterials,* Vol.20, No. 20, pp. (1931-1936)

Ikada, Y. (2002). Biological Materials, In: *Integrated Biomaterials Science,* Barbucci,R. Kluwer Academic /Plenium Publishers, ISBN: 978-0-306-46678-6, New York, USA

Imai,S., Konttinen,Y.T., Jumppanen,M., Lindy,O., Ceponis,A., Kemppinen,P., Sorsa,T., Santavirta,S., Xu,J.W. & Lopez-Otin,C. (1998). High Levels of Expression of Collagenase-3 (MMP-13) in Pathological Conditions Associated With a Foreign-Body Reaction. *Journal of Bone and Joint Surgery*, Vol. 80, pp. (701 – 710)

Jackson, J.K., Zhao, J., Wong, W. & Burt, H.B. (2010). The inhibition of collagenase induced degradation of collagen by the galloyl-containing polyphenols tannic acid, epigallocatechin gallate and epicatechin gallate. *Journal of Materials Science: Materials for Medicine,* Vol.2, pp. (1435-1443)

Yan, L.P., Wang, Y.J., Ren, L., Wu, G., Caridade, S.G., Fan,J.B., Wang, L.Y., Ji, P.H., Oliveira, J.M., Oliveira, J.T., Mano, J.F. & Reis, R.L. (2010). Genipin-cross-linked collagen/chitosan miomimetic scaffolds for articular cartilage tissue engineering applications. *Journal of Biomedical Materials Research Part A*, 95A, No. 2, pp. (465-475)

Jancar, J., Slovnikova, A., .Amler,E., Krupa, P., Kecova,H., Planka, L., Gal,P. & Necas, A. (2007). Mechanical Response of Porous Scaffolds for Cartilage Engineering. *Physiologycal Research,* Vol. 56, No. 1, pp. (17-25)

Jansen, R.G., van Kuppevelt, T.H., Daamen,W.F., Kuijpers-Jagtman, A.M. & Von den Hoff, J.W. (2008). Tissue reactions to collagen scaffolds in the oral mucosa and skin of rats: Environmental and mechanical factors. *Archives of Oral Biology*, Vol. 53, pp. (376-387)

Jayakrishnan, A. & Jameela,S.R. (1996). Glutaraldehyde as a Fixative in Bioprostheses and Drug Delivery Matrices. *Biomaterials*, Vol. 17, No. 5, pp. (471 – 484)

Jiankang, H., Dichen, L., Yaxiong, L., Bo, Y., Hanxiang, Z., Qin, L., Bingegg, L. & Yi, L. (2009). Preparation of chitosan-gelatin hybrid scaffolds with well-organized microstructures for hepatic tissue engineering. *Acta Biomaterialia,* Vol. 5, No. 1, pp. (453-461)

Jus, S., Stachel, I., Schloegl,W., Pretzler,M., Friess,W., Meyer,M., Birner-Gruenberg, R., & Guebitz,G.M. (2011). Cross-linking of collagen with laccases and tyrosinases. *Materials Science and Engineering C,* Vol. 31, No. 5, pp. (1068-1077)

Kaufman, H.E., Steinemann, T.L., Lehman, E., Thompson, H.W., Varnell, E.D., Jacob-La Barre, J.T. & Gerhardt, B.M. (1994). Collagen based drug delivery and artificial tears. *Journal of Ocular Pharmacology*, Vol.10, No.1, pp. (17 –27)

Kaur, M., Jumel, K., Hardie, K.R., Hardman, A., Meadows, J. & Melia, C.D. (2002). Determining the molar mass of a plasma substitute succinylated gelatin by size exclusion chromatography –multi- angle laser light scattering , sedimentation equilibrium and conventional size exclusion chromatography. *Journal of Chromatography A,* Vol. 957, No. 2, pp. (139-148)

Khor, E. (1997). Methods for the Treatment of Collagenous Tissues for Bioprostheses. *Biomaterials,* Vol. 18, No. 2, pp. (95 – 105)

Kikuchi, M., Matsumoto, H.N., Yamada, T., Koyama, Y., Takakuda, K. & Tanaka, J. (2004). Glutaraldehyde crosslinked hydroxyapatite/collagen self-organized nanocomposites. *Biomaterials,* Vol. 25, No. 1, pp. (63-69)

Kim, H.W., Knowles, J.C. & Kim, H.E. (2004). Hydroxyapatite and gelatin composite foams processed via novel freeze-drying and crosslinking for use as temporary hard tissue scaffolds. *Journal of Biomedical Materials Research Part A*, Vol. 72, No. 2, pp. (136-145)

Kim, S.E., Cho, Y.W., Kang, E.J., Kwon, I.C., Lee, E.B., Kim, J.H., Chung, H & Jeong, S.Y. (2001). Three-Dimensional Porous Collagen/Chitosan Complex Sponge for Tissue Engineering. *Fibers and Polymers*, Vol. 2, No. 2, pp. (64-70)

Kim, S., Nimni, M.E., Yang, Z. and Han, B. (2005*). Chitosan/gelatin-based films crosslinked by proanthocyanidin.* Journal of Biomedical Materials Research Part B: Applied Biomaterials, *Vol. 75B,* No. 2, pp. (442-450)

Ko, C.S., Wu, C.H., Huang, H.H. & Chu, I.M. (2007). Genipin Cross-linking of Type II Collagen-chondroitin Sulfate-hyaluronan Scaffold for Articular Cartilage Therapy. *Journal of Medical and Biological Engineering,*Vol. 27, No. 1, pp. (7-14)

Kokare, C.R. (2008). *Pharmaceutical Microbiology-Principles and Applications,* Nirali Prakashan, ISBN NO.978-81-85790-61-2, Pune, India

Kon, T., Mrava, G.L, Weber, D.C. & Nose, Y. (2004). Collagen membrane for hemodialysis. *Journal of Biomedical Materials Research Part A,* Vol. 4, No. 1, pp. (13-23)

Kuijpers, A.J., Engbers, G.H., Krijqsveld, J., Zaat, S.A., Dankert, J. & Feijen, J. (2000). Cross-linking and characterization of gelatin matrices for biomedical applications. *Journal of Biomaterials scince. Polymer Edition,* Vol. 11, No. 3, pp. (225-243)

Kumar, D., Benson, M.J. & Bland, J.E. (1998). Glutaraldehyde cross-linked collagen in the treatment of faecal incontinence. *British Journal of Surgery,* Vol. 85, No. 7, pp. (978-979)

Labout, J.J.M. (1972). Gamma-radiation in Collagen Solutions Influence of Solutes on the Gelatin Dose. *International Journal of Radiation Biology,* Vo. 21, No. 5, pp. (483-492)

Lai, J.Y. & Li,Y.T. (2010). Functional Assesment of Cross-Linked Porous Gelatin Hydrogels for Bioingeneered Cell Sheet Carriers, *Biomacromolecules*, Vol. 11, No. 5, pp. (1387-1397)

Lass, J.H., Ellison, R.R., Wong, K.M. & Klein, L. (1986). Collagen degradation and synthesis in experimental corneal crafts. *Experimental Eye Research,* Vol. 42, No. 3, pp. (201-210)

Langley, S.M., Rooney,S.J., Hay, M.J.R.D., Spencer,J.M.F., Lewis,M.E., Pagano, D., M Asif, M., Goddard, J.R., Tsang,V.T., Lamb, R.K., Monro, J.L., Livesey, S.A. & Bonser, R. S. (1999). Replacement of the proximal aorta and aortic valve using a composite bileaflet prosthesis and gelatin-impregnated polyester graft (Carbo-seal): early results in 143 patients. *The Journal of Thoracic and Cardiovascular Surgery,* Vol. 118, pp. (1014-1020)

Lee, C.H., Singla, A. & Lee, Y. (2001). Biomedical applications od collagen. *International Journal of Pharmaceuticals,* Vol. 221, No. 1-2, pp. (1-22)

Lee, S.B., Jeon, H.W., Lee, Y.W., Lee, Y.M., Song, K.W., Park, M.H., Nam, Y.S. & Ahn, H.C. (2003.)*Bio-artificial skin composed of gelatin and (1-->3), (1-->6)-betaglucan.* Biomaterials , Vol. 24, No. 14, pp. (2503-2511)

Li, M., Mondrinos, M.J., Gandhi, M.R., Ko, F.K., Weiss, A.S. & Lelkes, P.I. (2005). Electrospun protein fibers as matrices for tissue engineering. *Biomaterials,* Vol. 26, No. 30, pp. (5999-6008)

Lien, S. M., Chien, C. H. & Huang, T. J. (2009). A novel osteochondral scaffold of ceramic – gelatin assembly for articular cartilage repair. *Materials Science & Engineering: C,* Vol. 29, No. 1, pp. (315-321)

Lien, S., Li, W. & Huang, T. (2010). Genipin-crosslinked gelatin scaffolds for articular cartilage with a novel crosslinking method. *Materials Science & Engineering C,* Vol. 28, No. 1, pp. (36-43)

Liu, H., Peptan, I., Clark, P. & Mao, J. (2005). Ex Vivo Adipose Tissue Engineering by Human Marrow Stomal Cell Seeded Gelatin Sponge. *Annals of Biomedical Engineering,* Vol. 33, No. 4, pp. (511-517)

Luttikhuizen,D.T., Dankers, P.Y., Harmsen, M.C., van Luyn, M.J.A. (2007). Material dependent differences in inflammatory gene expression by giant cells during the foreign body reaction. *Journal of Biomedical Materials Research Part A*, Vol. 83 , pp. (879-886)

Lynn, A. K., Yannas, L.V. & Bonfield, W. (2004). Antigenicity and Immunogenicity of Collagen. *Journal of Biomadical Materials Research Part B: Applied Biomaterials B,* Vol.71B, No.2, pp. (343-354)

Ma, L., Gao, C., Mao, Z., Zhou, J., Shen, J., Hu, X. & Han,C. (2003). Collagen/chitosan porous scaffolds with improved biostability for skin tissue engineering. *Biomaterials*, Vol. 24, pp. (4833-4841)

Mahoney, M.J. & Anseth, K.S. (2007). Contrasting effects of collagen and bFGF-2 on neural cell function in degradable synthetic PEG hydrogels. *Journal of Biomedical Materials Research Part A,* Vol. 81A, No. 2, pp. (269-278)

Mallya,S.K., Mookhtiar,K.A. & Van Wart,H.E. (1992). Kinetics of Hydrolysis of Type I, II, and III Collagens by the Class I and II Clostridium Histolyticum Collagenases. *Journal of Protein Chemistry,* Vol. 11, pp. (99 – 107)

Mao, J.S., Cui,Y.L., Wang, X.H., Sun, Y., Yin, Y.Y, Zhao, H.M. & Yao, K.D.(2004). A preliminary study on chitosan and gelatin polyelectrolyte complex cytocompatibility by cell cycle and apoptosis analysis. *Biomaterials,* Vol. 25, pp. (3973-3981)

McDermott, M.K., Chen, T., Williams, C.M., Markley, K.M. & Payne, G.F. (2004). Mechanical properties of biomimetic tissue adhesive based on the microbial transglutaminase-catalysed crosslinking of gelatin. *Biomacromolecules,* Vol. 5, No. 4, pp. (1270-1279)

McGuigan, A.P. & Sefton, M.V. (2006). Vascularized organoid engineered by modular assembly enables blood perusion. *Proceedings of the National Academy of Sciences of the Unated States of America,* Vol. 103, No. 31, pp. (11461-11466)

Mi, F.L., Shyu,S.S & Peng C.K. (2005). Caracterization of ring-opening polymerization of genipin and pH dependent cross-linking reactions between chitosan and genipin. *Journal of Polymer Science Part A: Polymer Chemistry,* Vol.43, No.10, pp. (1985-2000)

Mironov, V., Kasyanov, V. & Markwald, R.R. 8Nanotechnology in vascular tissue engineering: from nanoscaffolding towards rapid vessel biofabrication. *Trends in Biotechnology,* Vol. 26, No. 6, pp. (338-344)

Martucci, J.F. & Ruseckaite, R.A. (2009). Biodegradation of three.layer films based on gelatin under indoor soil condiions. *Polymer Degradation & Stability,* Vol. 94, No. 8, pp. (1307-1313)

Mohanty, B & Bohidar, H.B. (2003). Systematic of Alcohol-Induced Simple Coacervation in Aqueous Gelatin Solutions. *Biomacromolecules,* Vol. 4, No. 4 , pp. (1080-1086)

Mohanty, B., & Bohidar, H.B. (2005). Microscopic structure of gelatin coacervates. *International Journal of Biological Macromolecules* , Vol. 36, No. 1-2, pp. (39-46)

Mohanty, B., & Bohidar, H.B. (2005). Microscopic structure of gelatin coacervates. *International Journal of Biological Macromolecules*, Vol. 36, No. 1-2, pp. (39-46)

Mookhtiar, K.A. & Van Wart,H.E. (1992).Clostridium Histolyticum Collagenases: a New Look at Some Old Enzymes. *Matrix (Stuttgart*), Vol. 1, pp. (116 – 126)

Muyonga, J.H., Cole, C.G.B. & Duodu, K.G.(2004). Characterization of acid soluble collagen from skins of young and adult Nile perch (Lates niloticus). *Food Chemistry*, Vol. 85, No. 1, pp. (81-89)

Mu, C., Liu,F., Cheng,Q., Li,H., Wu, B., Zhang, G. & Lin, W. (2010). Collagen Cryogel Cross-Linked by Dialdehyde Starch, *Macromolecular Materials and Engineering,* Vol. 295, No. 2, pp. (100-107)

Nagai, T., & Suzuki, N. (2000). Isolation of collagen from fish waste material-skin, bone and fins. *Food Chemistry,* Vol. 68, No. 3, pp. (277-281)

Nagai, T., Worawattanamateekul, W., Suzuki, N., Nakamura, T., Ito, T., Fujiki, K., Nakao, M. & Yano, T. (2000). Isolation and characterization of collagen from rhizostomous jellyfish (*Rhopilema asamushi)*. *Food chemistry,* Vol. 70, No. 2, pp. (205-208)

Nagase,H. & Woessner,J.F., Jr. (1999). Matrix Metalloproteinases. *Journal of Biological Chemistry*, Vol. 274, pp. (21491 – 21494)

Narbat, M.K., Orang, F., Hashtjin, M.S. & Goudarzi, A. (2006). Fabrication of Porous Hydroxyapatite-Gelatin Composite Scaffolds for Bone Tissue Engineering. *Iranian Biomedical Journal*, Vol. 10, No. 4, pp. (215-223)

Natu, M.V., Sadinha, J.P., Correia, I.J. & Gil, M.H. (2007). Controlled release gelatin hydrogels and liophilisates with potential application as ocular inserts. *Biomedical Materials,* Vol. 2, pp. (241-249)

Netzel-Arnett,S., Mallya,S.K., Nagase,H., Birkedal-Hansen,H. & Van Wart,H.E. (1991). Continuously Recording Fluorescent Assays Optimized for Five Human Matrix Metalloproteinases. *Analytical Biochemistry,* Vol.195, pp. (86 – 92)

Obregue-Slier, E., Solis, R.L., Neira, A.P. & Marin, F.Z. (2010). Tannin-protein interaction is more closely associated with astringency than tannin-protein precipitation: experience with two oenological tannins and a gelatin. *International Journal of Food Science & Technology,* Vol. 45, No. 12, pp. (2629-2636)

Okada,T., Hayashi,T. & Ikada,Y. (1992). Degradation of Collagen Suture in Vitro and in Vivo. *Biomaterials,* Vol. 13, pp. (448 – 454)

Olsen, D., Yang, C., Bodo, M., Chang, R., Leigh, S., Baez, J., Carmichael, D., Perala, M., Hamalainen, E.R., Jarvinen, M. & Polarek, J. (2003). Recombinant collagen and gelatin for drug delivery. *Advanced Drug Delivery Reviews*, Vol. 55, No. 12, pp. (1547-1567)

Overall, C.M. (1991). Recent Advances in Matrix Metalloproteinase Research. *Trends in Glycoscience and Glycotechnology,* Vol. 3, pp. (384 – 400)

Pachence, J.M., Bohrer, M.P. & Kohn, J. (2007). Biodegradable Polymers, In: *Principles of Tissue Engineeting,* Lanza, R., Langer, R. &Vacanti, J., pp. (323-358), Elsevier Academic Press, ISBN-13:978-0-12-370615-7, Burlington, USA

Paige, M.F., Lin, A.C. & Goh, M.C. (2002). Real-Time Enzymatic Biodegradation of Collagen Fibrils Monitored by Atomic Force Microscopy. *International Biodeterioration & Biodegradation,* Vol. 50, pp. (1 – 10)

Pannone, P.J. (2007).*Trends in biomaterials research (first edition),* Nova Science Publishers, ISBN-13: 978-1600213618, New York

Park, S.N., Lee, H.J., Lee, K.H. & Suh, H. (2003). Biological characterization of EDC-crosslinked collagen-hyaluronic acid matrix in dermal tissue restoration. *Biomaterials,* Vol. 24, No. 9, pp. (1631-1641)

Pena, C., Caba, K., Eceiza, A., Ruseckaite, R. & Mondragon, I. (2010). Enhancing water repellence and mechanical properties of gelatin films by tannin addition. *Bioresourse Technology,* Vol. 101, pp. (6836-6842)

Pieper,J.S., Oosterhof,A., Dijkstra,P.J., Veerkamp,J.H. & Van Kuppevelt,T.H. (1999). Preparation and Characterization of Porous Crosslinked Collagenous Matrixes Containing Bioavailable Chondroitin Sulfate. *Biomaterials,* Vol. 20, pp. (847 – 858)

Rao, K.P. (1995). Recent developments of collagen-based materials for medical applications and drug delivery systems. *Journal of biomaterials sicence. Polymer edition,* Vol. 7, No. 7, pp. (623-645)

Roche, S., Ronziere, M.C., Herbage, D & Freyria, A.M. (2001). Native and DPPA cross-linked collagen sponges seeded with fetal bovine spiphyseal chondrocytes used for cartilage tissue engineering. *Biomaterials,* Vol. 22, No. 1, pp. (9-18)

Robinson, J.J (1997). Comparative Biochemical Analysis of Sea Urchin Peristome and Rat Tail Tendon Collagen. *Comparative Biochemistry and Physiology Part B: Biochemistry and Molecular Biology,* Vol. 117, No. 2, pp. (307-313)

Saitoa, H., Taguchic,T., Kobayashic,H., Kataokac, K., Tanakac, J., Murabayashia, S. & Mitamuraa, Y. (2004). Physicochemical properties of gelatin gels prepared using citric acid derivative. *Material Science and Engineering C* , Vol. C24, No. 6-8, pp. (781-785)

Samuel, C.S., Coghlan, J.P. & Bateman, J.F. (1998).Effects of relaxin, pregnancy and parturition on collagen metabolism in the rat public symphysis. *Journal of Endocrinology*, Vol. 159, No.1, pp. (117–125)

Schacht, E.H. (2004). Polymer chemistry and hydrogel systems. *Journal of physics: Conference Series,* Vol. 3, pp. (22-28)

Seifter, S., & Harper, E. (1971). Collagenases, In*: The Enzymes* Vol. 3,*P*. Boyer, Academic Press, NewYork

Silver, F.H. & Garg,A.K. (1997). Collagen. Characterization, Processing, and Medical Applications. *Drug Targeting and Delivery*, Vol. 7, pp. (319 – 346)

Sinha,V.R. & Trehan, A. (2003). Biodegradable Microspheres for Protein Delivery. *Journal of Controlled Release*, Vol. 90, No. 3, pp. (261 – 280)

Sisson, K., Zhang, C., Farach-Carson, M.C., Chase, D.B. & Rabolt,J.F. (2009). Evaluation of Cross-Linking Methods for Electrospun Gelatin on Cell Growth and Viability. *Biomacromolecules, Vol. 10, No. 7, pp. (1675-1680)*

Song, E., KimS.Y., Chun,T., Byun, H.J & Lee,Y.M. (2006). Collagen Scaffolds derived from a marine source and their biocompatibility. *Biomaterials,* Vol 27, No. 15, (2951-2961)

Sung, H.W., Chang, W.H., Ma, C.Y. & Lee, M.H. (2003).Crosslinking of biological tissues using genipin and/or carbodiimide. *Journal of Biomedical Materials Research Part A,* Vol. 64A, No. 3, pp. (427-438)

Sutter, M., Siepmann,J., Hennink, W.E. & Jiskoot, W.(2007). Recombinant gelatin hydrogels for the sustained release of proteins. *Journal of Controlled Release*, Vol. 119, No.3, pp. (301-312)

Suzuki, S., Kawai, K., Ashoori, F., Morimoto, N., Nishimura, Y. & Ikada, Y. (2000). Long-term follow-up study of artificial dermis composed of outer silicone layer and inner collagen sponge. *British Journal of Plastic Surgery,* Vol. 53, No.8, pp. (659 –666)

Shingleton, W.D., Hodges, D.J., Brick, P. & Cawston,T.E. (1996). Collagenase: a Key Enzyme in Collagen Turnover. *International Journal of Biochemistry & Cell Biology*, Vol. 74, pp. (759 – 775)

Shoulders, M.D. & Raines, R.T. (2009). Collagen structure and stability. *Annual Review of Biochemistry,* Vol. 78, pp. (929-958)

Spira, M., Liu, B., Xu, Z., Harrell, R. & Chanhadeh, H. (2004). Human amnion collagen for soft tissue augmentation-biochemical characterizations and animal observations. *Journal of Biomedical Materials Research,* Vol. 28, No. 1, pp. (91-96)

Starin, W.A. (1918). The Antigenic Properties of Gelain. *The Journal of Infectious Diseases,* Vol. 23, No. 2, pp. (139-158)

Stone, K.R., Steadman, J.R., Rodkey, W.G. & Li, S.T. (1997). Regeneration of Meniscal Cartilage With Use of a Collagen Scaffold. Journal of Bone and Joint Surgery, Vol. 79-A, No. 12, pp. (1770-1777)

Sztuka, K. & Kolodziejska, I. (2008). Effect of transglutaminase and EDC on biodegradation of fish gelatin and gelatin-chitosan film. *European Food Research & Technology,* Vol. 226, No. 5, pp. (1127-1133)

Tangsadthakun, C., Kanokpanont, S., Sanchavanakit, N., Banaprasert, T. & Damrongsakkul, S. (2006). Properties of Collagen/Chitosan Scaffolds for Skin Tissue Engineering. *Journal of Metals, Materials and Minerals,* Vol. 16, No. 1, pp. (37-44)

Taylor, P.M., Cass, A.E.G. & Yacoub, M.H. (2006). Extracellular matrix scaffolds for tissue engineering heart valves. *Process in Pediatric Cardiology,* Vol. 21, No. 2, pp. (219-225)

Tedder, M.E., Liao,J., Weed,B., C. Stabler, C., H. Zhang, H., A. Simionescu,A. & Simionescu,D. (2009). Stabilized collagen scaffolds for heart valve tissue engineering. *Tissue Engineering Part A,* Vol. 15, No. 6, pp. (1257-1268)

Tefft, S., Bentz, H., & Estridge, T.D. (1997). Collagen and heparin matrices for growth factor delivery. *Journal of Control Release,* Vol.48, No. 1, pp. (29–33)

Touyama, R.,Takeda, Y., Inoue, K., Kawamura, I., Yatsuzuka, M., Ikumoto, T., Shingu, T., Yokoi, T.I.& Inouye, H. (1994). Studies on the blue pigments produced from genipin and methlylamine. I. Structures of the brownish-red pigments, intermediates leading to the blue pigments. *Chemical and Pharmaceutical Bulletin,* Vol. 42, pp. (668-673)

Toricai, A. & Shibata, H. (1999). Effect of ultraviolet radiation on photodegradation of collagen. *Journal of Applied Polymer Science,* Vol. 73, No. 7, pp. (1259-1265)

Trengove,N.J., Stacey,M.C., MacAuley,S., Bennett,N., Gibson,J., Burslem,F., Murphy,G. & Schultz,G. (1999). Analysis of the Acute and Chronic Wound Environments: the Role of Proteases and Their Inhibitors. *Wound Repair and Regeneration,* Vol. 7, pp. (442 – 452)

Tsai, C.C., Huang, R.N., Sung, H.W. & Liang, H.C. (2000). In vitro evaluation of the genotoxicity of a naturally occurring agent (genipin) for biologic tissue fixation. *Journal of Biomedical Materials Research,* Vol. 52, No. 1, pp. (58-65)

Tucci, M.G. & Ricotti, G. (2001). Chitosan & Gelatin as Engineered Dressing for Wound Repair. *Journal of Bioactive andCompatiblePolymers,* Vol. 16, pp. (144-157)

Van Den Bulcke, A.I., Bogdanov, B., De Rooze, N., Schacht,E.H., Cornellssen, M.& Berghmans, H. (2000). Structural and Rheological Properties of Methacrylamide Modified Gelatin Hydrogels. *Biomacromolecules,* Vol. 1, pp. (31-38)

Van Luyn, M.J.A., van Wachem, P.B., Dijkstra, P.J., L.H.H., Damink, O & Feijen, J. (1995). Calcification of subcutaneously implanted collagen in relation to cytotoxicity, cellular interactions and crosslinking. *Journal of Materials Scinecne: Materials in Medicine,* Vol. 6, No. 5, pp. (288–296)

Van Wachem,P.B., Zeeman,R., Dijkstra,P.J., Feijen, J., Hendriks, M., Cahalan, P.T. & van Luyn, V.J. (1999). Characterization and biocompatibility of epoxy-crosslinked dermal sheep collagens. *Journal of Biomedical Materials Research,* Vol.47, No. 2, pp. (270–277)

Van Wachem ,P.B., van Luyn, M.J.A., Brouwer, L.A., Engbers, G.H.M., Krijgsveld, J., Zaat, S.A.J., Dankert, J. & Feijen,J. (2000). In vitro and in vivo evaluation of gelatin-chrondroitin sulphate hydrogels for controlled release of antibacterial proteins. *Biomaterials*, Vol. 21, pp. (1763-1772)

Vargas, G.,Acevedo, J.L.,Lopez,J. & Romero,J. (2008). Study of cross-linking of gelatin by ethylene glycol diglycidyl ether. *Materials Letters,* Vol. 62, pp. (3656-3658).

Vlierberhe,V.S., Dubruel, P., Lippens, E., Cornelissen, M. & Schacht, E. (2009). Correlation Between Cryigenic Parameters and Physico-Chemical Properties of Porous Gelatin Cryogels. *Journal of Biomaterial Science,* Vol. 20, pp. (1417-1438)

Wahl , D.A. & Czernuszka, J.T. (2006). Collagen-hydroxyapatite composites for hard tissue repair. *European Cells and Materials,* Vol. 11, pp. (43-56)

Wall, S.J., Bevan,D., Thomas,D.W., Harding,K.G., Edwards,D.R & Murphy,G. (2002). Differential Expression of Matrix Metalloproteinases During Impaired Wound Healing of the Diabetes Mouse. *Journal of Investigative Dermatology*, Vol. 119, pp. (91 – 98)

Wang, X., Yu, X., Yan, Y. & Zhang, R.(2008). Liver tissue responses to gelatin and gelatin/chitosan gels. *Journal of Biomedical Materials Research A,* Vol. 87, No. 1, pp. (62-80)

Wang, X.H., Li, D.P., Wang, W.J., Feng, Q.L., Cui, F.Z., Xu, Y.X., Song, X.H. & Van Der Werf, M.. (2003). Crosslinked collagen/chitosan matrix for artificial livers. *Biomaterials*, Vol. 24, pp. (3213-3220)

Welgus ,H.G., Jeffrey,J.J., Stricklin,G.P., Roswit,W.T. & Eisen,A.Z. (1980). Characteristics of the Action of Human Skin Fibroblast Collagenase on Fibrillar Collagen. *Journal of Biological Chemistry,* Vol. 255, pp. (6806 – 6813)

Welgus, H.G., Kobayashi,D.K. & Jeffrey, J.J. (1983). The Collagen Substrate Specificity of Rat Uterus Collagenase. *Journal of Biological Chemistry*, Vol. 258, pp. (14162 – 14165)

Weiss, J.B. (1976). Enzymic Degradation of Collagen. *International Review of Connective Tissue Research*, Vol. 7, pp. (101 – 157)

Westney, O.L., Bevan-Thomas, R., Palmer, J.L., Cespedes, R.D. & McGuire, E.J. (2005). Transurethral collagen injections for male intrinsic sphincter deficiency: the University of Texas-Houston experience. *The Journal of Urology,* Vol. 174, No. 3, pp. (994–997)

Woessner, J.F. (1991).Matrix Metalloproteinases and Their Inhibitors in Connective Tissue Remodeling. *The Journal of the Federation of Americal Societies for Experimental Biology,* Vol. 5, pp. (2145 – 2154)

Wong, C., Shital, P., Chen, R., Owida, A. & Morsi, Y. (2010). Biomimmetic alactrospun gelatin-chitosan polyurethane for heart valve leaflets. *Journal of Mechanics in Medicine and Biology,* Vol. 10, No. 4, pp. (563-576)

Yamauchi, M. & Shiiba, M. (2008). Lysine Hydroxylation and Crosslinking of Collagen, In: *Post-translational Modifications of Proteins,* Kannicht, C., Springer, Humana Press, ISBN: 9781588297198, New York

Yan, L.P., Wang, Y.J., Ren, L., Wu, G., Caridade, S.G., Fan, J.B., Wang, L.Y, Ji, P.H., Oliveira, J.M., Oliveira, J.T., Mano, J.F. & Reis, R.L. (2010). Genipin-cross-linked collagen /chitosan biomimetic scaffolds for articular cartilage tissue engineering applications. *Journal of Biomedical Materials Research Part A,* Vol. 95A, No. 2, pp. (465-475)

Yannas, I.V.(1992). Tissue regeneration by use of collagen–glycosaminoglycan co-polymers. *Clinical Materials,* Vol. 9, No. 3-4, pp. (179–187)

Yao, C.H., Lui B.S., Hsu S.H., Chen Y.S.(2005). Cavarial Bone Response to Tricalcium Phosphate-Genipin Crosslinked Gelatin Composite. *Biomaterials,* Vol. 26, pp. (3065-3074)

Yoshida, H., Sasajima, T., Goh, K., Inaba, M. Otani, N. & Kubo, Y. (1996). Early results of a reinforced biosynthetic ovine collagen vascular prosthesis for small arterial reconstruction. *Surgery Today,* Vol. 26, No. 4, pp. (262-266)

Yoshizaki, T., Sato,H. & Furukawa,M. (2002). Recent Advances in the Regulation of Matrix Metalloproteinase 2 Activation: From Basic Research to Clinical Implication (Review). *Oncology Reports,* Vol. 9, pp. (607 – 611)

Ye, Q., Xing, Q., Ren, Y., Harmsen, M.C. & Bank, R.A. (2010). ENDO180 andMT1-MMP are involved in the phagocytosis of collagen scaffolds by macrophages and is regulated by interferon-gamma. *European Cells and Materials,* Vol. 20, pp. (197-209)

Yuan, Y., Zhang, P., Yanq, Y., Wang, X, Gu, X. (2004). The interaction of Schwann cells with chitosan membranes and fibers in vitro. *Biomaterials*, Vol. 25, No. 18, (4273–4278)

Yuan, S.X., Wei, T.T. (2004). New Contact Lens Based on Chitosan/Gelatin Composites. *Journal of Bioactive and Compatible Polymers,* Vol. 19, No. 6, pp. (467-479)

Zeeman, R., Dijkstra,P.J., Van Wachem,P.B., Van Luyn,M.J.A., Hendriks,M., Cahalan,P.T. & Feijen,J. (1999). Successive Epoxy and Carbodiimide Crosslinking of Dermal Sheep Collagen. *Biomaterials,* Vol. 20, pp. (921 – 931)

Zhang, F., Xu, S. & Wang, Z. (2010). Pre-treatment optimization and properties of gelatin from freshwater fish scales. *Food and Bioproducts Processing*, doi: 10.1016/j.fbp.2010.05.003 (Article in press)

Zhang,X, Do, M.D., Casey,P., Sulistio, A., Qiao, G.G., Lundin, L. , Lillford, P. & Kosarju, S. (2010). Chemical crosslinking of gelatin with natural phenolic compounds as studied by high-resolution NMR spectroscopy. *Biomacromolecules,* Vol. 11, No. 4, pp. (1125–1132)

3

Hydrogel Scaffolds Contribute to the Osteogenesis and Chondrogenesis in the Small Osteochongral Defects

Miroslav Petrtyl et al.*
Laboratory of Biomechanics and Biomaterial Engineering, Department of Mechanics, Faculty of Civil Engineering, Czech Technical University in Prague
Czech Republic

1. Introduction

Hyaline cartilage shows only a limited response to self-repair (Hunter, 1743). Many people are stricken with degenerative osteochondral defects. Modern therapies of osteochondral defects are focused (for example) on the transplantation of osteochondral autografts, rushed spongiosa with collagen, chondrocytes and many others. The insertion of a crushed autologous bone graft has been reported as a possible therapy. However, the regenerative biomechanical (material) quality was less than 70% of healthy cartilage for fragments and controls (Kleemann et al., 2006). The transplantation of autologous osteochondral 3D-cylinders is one of several surgical therapies (Horas, 2003). During operations osteochondral defects are filled with material of a natural histological structure. However, the subchondral bone plates are interrupted and the biomechanical stability between the original tissue and the transplanted tissue is different. Provision of a long-term functional stability of inanimate implants in live surroundings is a complex and quite uneasy task. The development of replacements for a human subchondral bone and articular cartilage follows the path of a proposal and investigation of such materials whose mechanical properties are very similar to the biomechanical properties of a bone/cartilage tissue and whose biophysical and biochemical interactions with the surrounding living tissue neither cause necroses, nor lead to any initiation of other pathological processes. The biophysical and biochemical fixation of replacements and/or scaffolds to the tissue depends dominantly: (a) on the biomechanical properties and biochemical environments of the implants and the tissue; (b) on the stress–strain distributions in the tissue and the replacement, (c) on the organization and stability of

*Jaroslav Lisal[1], Ladislav Senolt[2], Zdenek Bastl[3], Zdenek Krulis[4], Marketa Polanska[2], Hana Hulejova[2], Pavel Cerny[5] and Jana Danesova[1]
[1]*Laboratory of Biomechanics and Biomaterial Engineering, Department of Mechanics, Faculty of Civil Engineering, Czech Technical University in Prague*
[2] *Institute of Rheumatology, The First Faculty of Medicine, Charles University in Prague*
[3] *J. Heyrovsky Institute of Physical Chemistry, Academy of Sciences of the Czech Republic*
[4] *Institute of Macromolecular Chemistry, Academy of Sciences of the Czech Republic*
[5] *ORTOTIKA, s.r.o., Prague, Czech Republic*

collagen molecules adsorbed to modified surfaces of COC-blend replacements and (d) on the chondrogenesis on the hydrogel scaffold.
Our activities were aimed at forming new articular cartilage and subchondral bone using biocompatible and bioconductive polymer replacements.

2. Methods

Finding the optimal biomechanical, biophysical and biochemical conditions for chondrogenesis is a very complicated and difficult task. The aim of our research is to assess the principal conditions improving the treatment of osteochondral defects. We have been focused preferentially on the application of biomaterials with material properties close to the natural properties of the relevant tissue. Special attention has been focused on the surface modification of the COC-blend by the action of nitrogen and/or oxygen microwave plasma, the application of type I collagen, the application of chitosan and the influence of the vertical position of replacements in the localities of osteochondral defects.

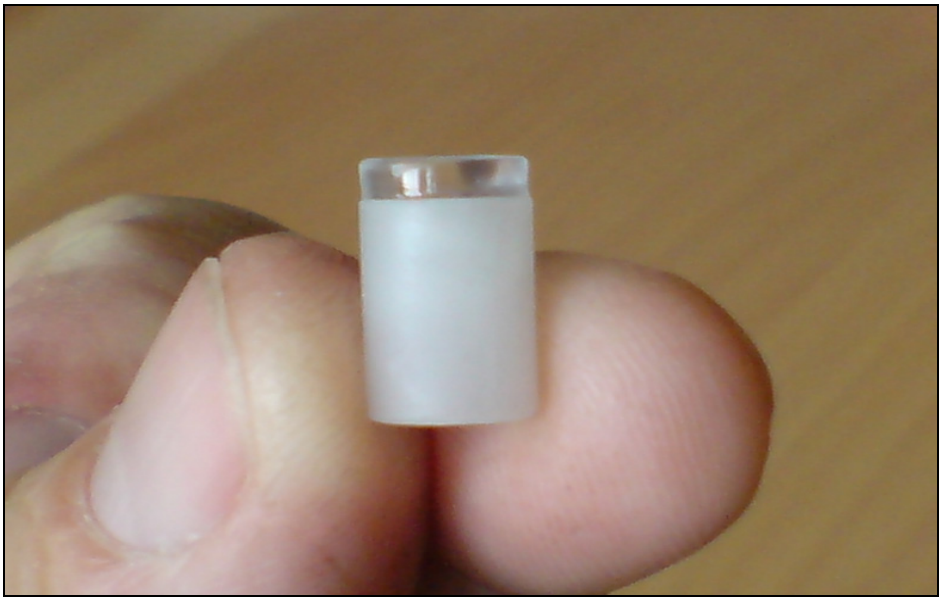

Fig. 1. Bi-component replacement of the subchondral bone (in the distal part, nontransparent material) and the articular cartilage scaffold (partly, in the proximal part, transparent hydrogel)

The presumed concept applies a substitute consisting of two supporting polymer components (see Fig. 1.). One of them (the lower element) is composed of a polycycloolefinic (blend) material (with the modulus of elasticity E = 0.5–3 GPa, the diameter of 8 mm, and the length of 10–12 mm, Krulis et al., 2006), while the upper hydrogel scaffold element of poly (2-hydroxyethylmethacrylate) has the relative modulus of deformation $E_{r,\mathrm{def}}$ = 1.5 MPa, the diameter of 8 mm and the thickness of the upper plate of 1.1– 1.3 mm, Fig. 2. The COC-blend substance was made with spherical/ellipsoidal pores (with a diameter of 0.6–1.5 μm), Fig. 3.

Fig. 2. Poly (2-hydroxyethylmethacrylate) scaffolds – upper parts of hybrid replacements

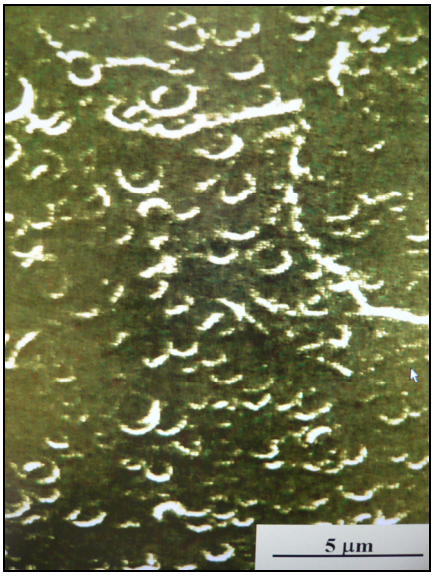

Fig. 3. Surface of COC-blend with designed pores with diameters ranging from 0.6 to 1.5 µm

In order to improve the bonding between the polymer blend and collagen, the surface of the polymer matrix was modified by the action of a nitrogen and/or oxygen microwave plasma. The plasmatic modification resulted in a significant increase of surface hydrophilicity demonstrated by a decrease of water contact angle.

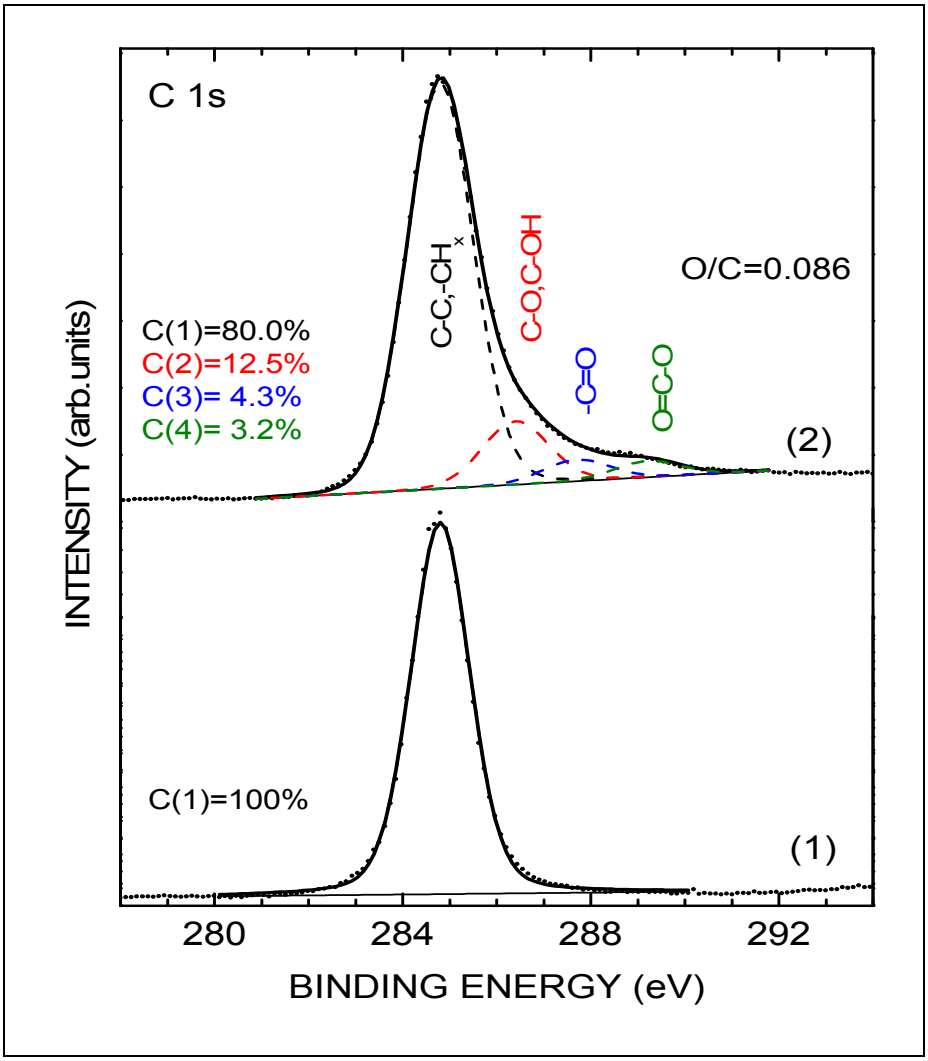

Fig. 4. Spectra of C 1s electrons of (1) unmodified and (2) plasma-modified surface of polymer blend

The plasma modification was carried out in a MW reactor equipped with the SLAN I OV 425 (Plasma Consult) magnetron operand at 300 W, 80 Pa, a gas flow of 15 scm/min and with exposure times of 15 min. For water contact angle measurements, the SEE System was used (Milli-Q water droplet volume 2 μL).

After optimizing conditions for the surface modification with regard to achieving the highest hydrophilicity of the surface, the samples were examined by the XPS method with the aim of identifying their chemistry and the population of individual chemical groups present on the surface. After plasmatic treatment (Spirovova et al., 2007), the components with higher values of binding energy occurred in the C 1s spectra of electrons (see Fig. 4.).

The aging of modified surfaces was also studied by XPS and by water contact angle measurements. The adsorption of collagen I on untreated and treated polymers was studied by XPS and AFM methods. XPS measurements were carried out using the ESCA 310 spectrometer. Electrons were excited by Al Kα monochromatized radiation. For the visualization of surface topography, the AFM Nanoscope IIIa (Digital Instruments) in the tapping mode was used.
The upper components of the replacement were made of poly-hydroxyethylmethacrylate with chitosan without any additional plasma surface treatment. Osteochondral defects (depth: 12 mm, diameter: 8 mm) were created in each lateral and medial tibial condyle of the right and left knees in 6 adult pigs. Histological analyses of the cartilage matrix were accomplished after 6 and 4 months.

Fig. 5. Total operative time was less than eight minutes per two osteochondral defects in knee joint

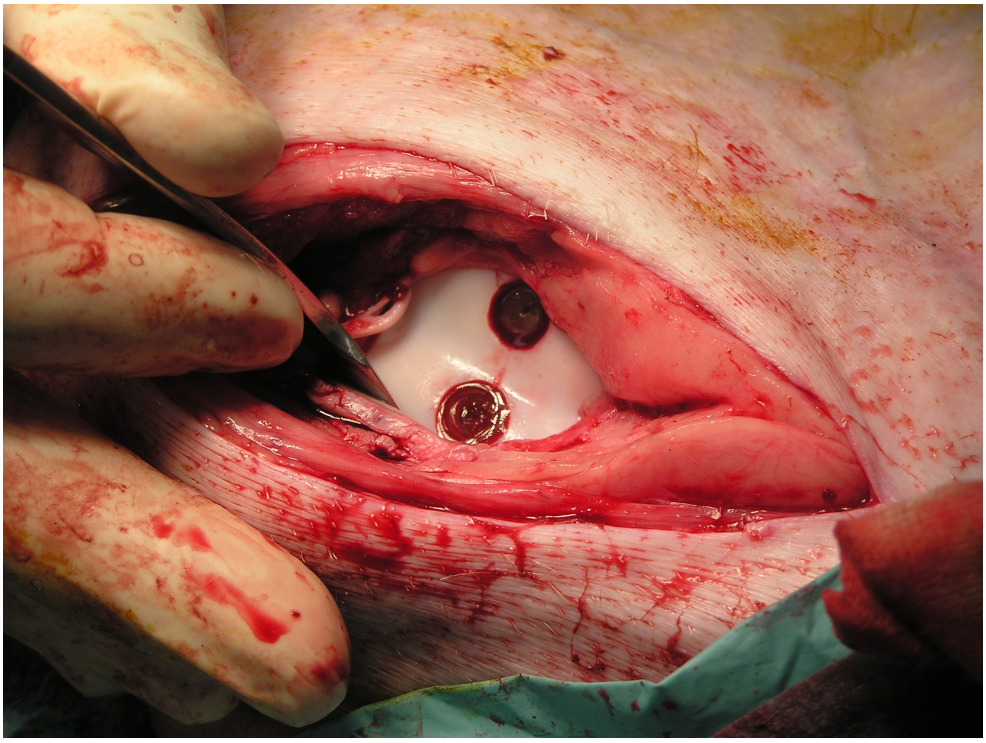

Fig. 6. Implantation of replacements. The lower hydrogel scaffold has been allocated approximately 1 mm under the articular surface and the upper one has been allocated ca 2.5 mm under the articular surface

3. Results

The replacements developed and plasmatically modified/unmodified under in vivo conditions have been proven as bioactive, bioconductive and biotolerant materials. It is well known that collagen adsorption promotes cell adhesion and proliferation.

The measured spectra of C 1s electrons showed the presence of components belonging to C–O, C=O and O–C=O functionalities (see Fig. 4.). For examining the collagen adsorption, table samples whose surface composition did not change with time were used. The presence of adsorbed collagen was indicated by the presence of the spectrum of N 1s electrons in the spectrum and its morphology was visualized by the AFM method. It was observed that on untreated, hydrophobic smooth polymer surfaces comparable or larger amounts of collagen are adsorbed than on hydrophilic surfaces, but immobilized collagen tends to form aggregates on hydrophobic surfaces. On hydrophilic, plasma-modified surfaces, more homogeneous coverage by collagen is observed.

The developed subchondral bone around the COC blend had the same quality as a natural healthy one (Petrtyl et al., 2008). The new subchondral bone mineralized perfectly. The mediator C+TGF films (made from type I collagen and from growth hormones TGF-β) applied on the COC-blend surface contribute to the creation of stable encapsulation (Fig. 7.,

Fig. 8.). Verifying the C+TGF films on the COC surface (in vitro) showed very good cell proliferation and cell differentiation. The modified surface exhibits enhanced adsorption of collagen and improvement of its adhesion. Stronger bonding explains a higher quantity, better organization and better stability of collagen molecules adsorbed on oxidized surfaces.
The polymer replacements installed into artificially executed osteochondral defects of porcine tibial condyles, including both modified and non-modified implants, demonstrated a perfect tolerability and appeared to heal into the existing subchondral bone without any displacement or evidence for necrosis. Histological findings and morphological changes of osteochondral samples did not demonstrate any pathological features. The top surfaces of the bi-component replacements were overgrown with viable new articular cartilage (Fig. 7.) or with articular cartilage and partly with fibrocartilage (Fig. 9.).

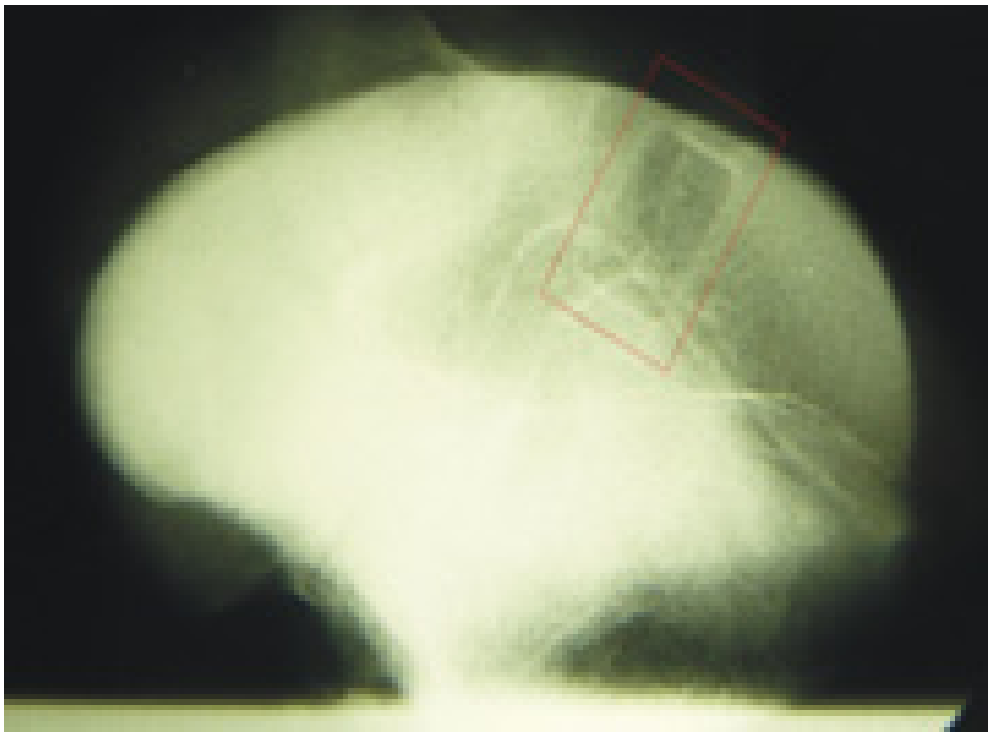

Fig. 7. X-ray stability analyses of replacement + scaffold with the new articular cartilage. Excellent stability of replacement in the subchondral bone without necrosis

Fig. 8. X-ray analyses of the encapsulated COC-blend replacements in the subchondral bone by collagen (I. type)

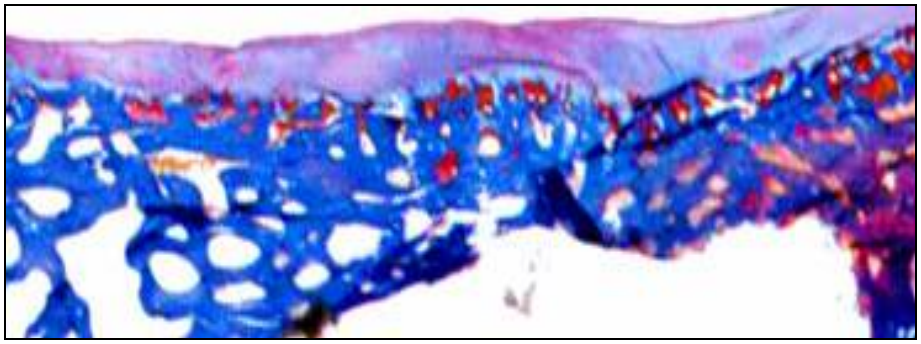

Fig. 9. Tissue bridge from articular cartilage and subchondral/spongy bone across the HEMA scaffold

The biomechanical in vivo environments have particularly potent regulatory effects on chondrogenesis, both in terms of proliferation and the new matrix synthesis. The matrix synthesis is regulated by mechanical stimuli and depends on the initial high stability of subchondral bone COC-blend replacements.

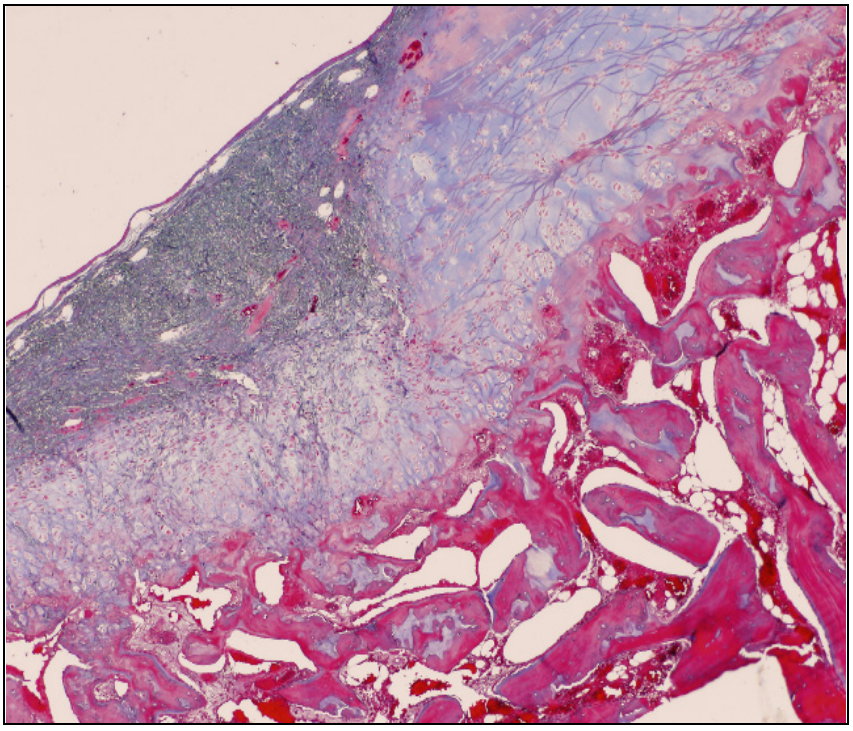

Fig. 10. Top surfaces of the hydrogel scaffold were overgrown with subchondral bone (the lower layer), with viable new articular cartilage (the medial layer) and partly by fibrocartilage (the upper small part)

4. Discussion

The leading strategies in the treatment of osteochondral defects are to minimize the operative trauma by minimally invasive procedures, to stimulate chondro/osteogenesis and/or to regenerate the tissues. Operative approaches are becoming ever smaller. Current and future concepts are based on a better understanding of biomechanical conditions and local mechanisms of healing, tissue regeneration and prophylaxis.
The local application of growth factors is investigated in clinical practice and has a great potential in treatment. The reason for a limited acceptance in clinical use may be that the applied proteins are expensive and with limited availability, and considerable quantities have to be implanted locally (Raschke, Fuchs & Stange, 2006).

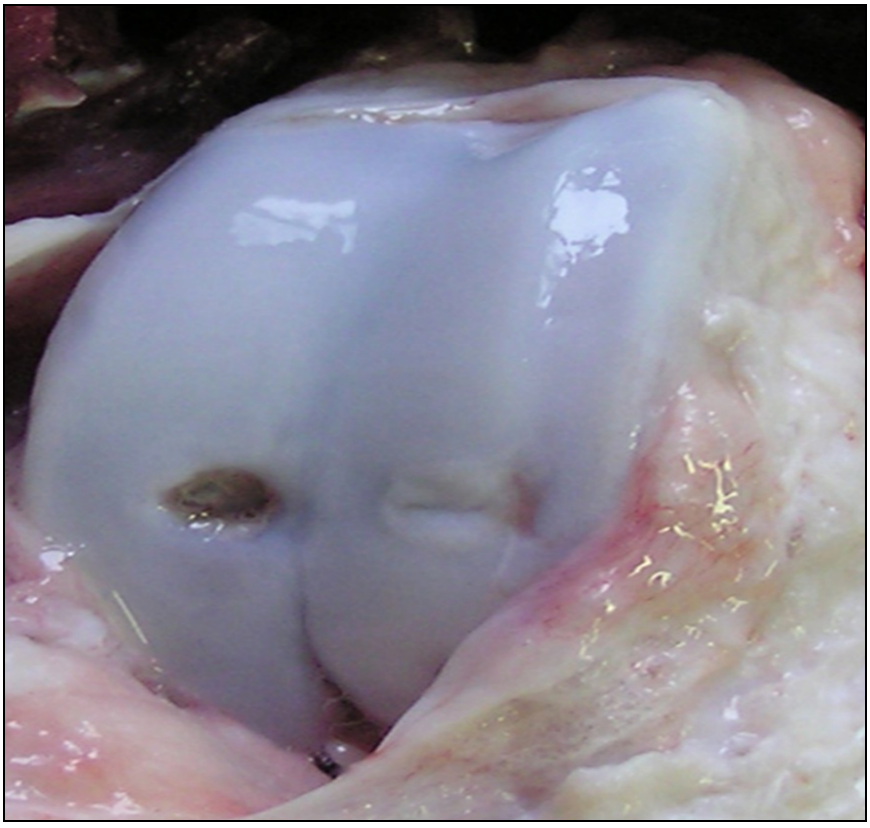

Fig. 11. New articular cartilage after 12-week chondrogenesis (the right tibial condyle) and the control defect (the left tibial condyle)

Other relatively new innovative techniques include *the stem cell therapy*. The application of autologous stem cells taken out and re-transplanted can also be used for healing (Raschke, Fuchs & Stange, 2006). However, this manner of treatment depends on the appropriate biomechanical and biochemical conditions of the tissue. The healing of osteochondral defects is controlled both mechanically and biologically. The processes of

osteo/chondrogenic differentiation are slightly promoted by mechanical effects (Bader et al., 2006). The cells are very sensitive to small strains. The physiological balance between the microstrain magnitude and biochemical stimulation can be easily disrupted when the subchondral/spongy bone is pathologically a soft one. In the case of an unstable subchondral bone and spongy bone, the articular surface of cartilage is affected by small sags (Petrtyl et al., 2008).

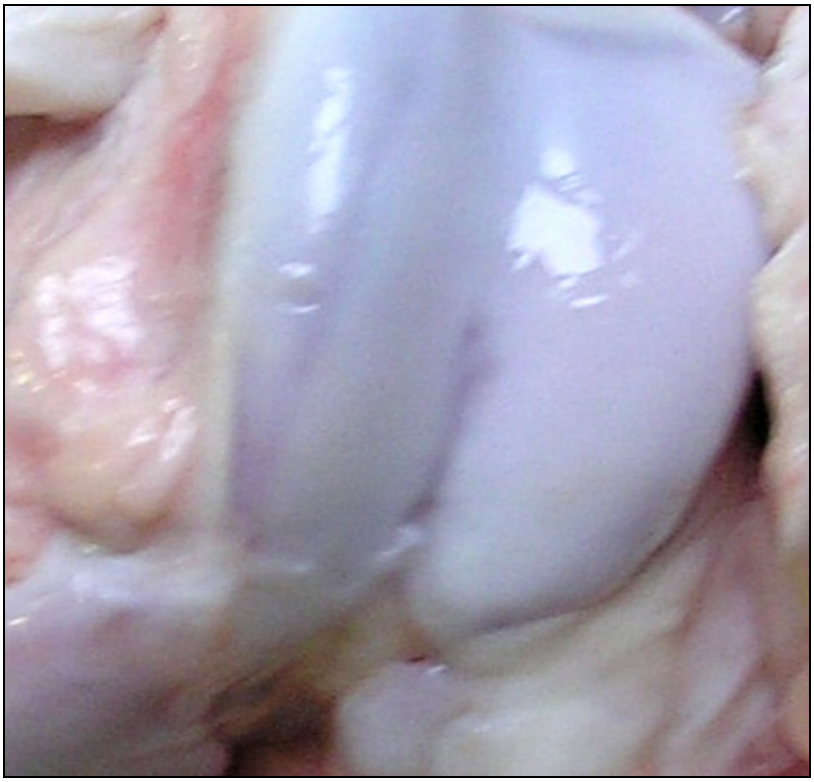

Fig. 12. Chondrogenesis after 20 weeks (in both the left and right tibial condyles). The application of chitosan (0.3% liquid, pH 5.5), TGF-β (1.2 mg/l ml PBS) type I collagen (0.3%), surface plasmatic modification of COC-blend

The regeneration of osteochondral defects treated with crushed bone grafts is in verified cases accompanied by the presence of soft regenerated tissue (Kleemann et al., 2006). The regeneration of osteochondral defects treated with crushed bone grafts remains incomplete still after three months. However, the inserted bone graft can be completely absorbed. After six months, the connective tissue within the defect is transformed into a bone and fibrocartilage tissue through enchondral ossification. The surface of the regenerated joint area is rough and irregular. The regenerate mechanical quality was 61%–70% of healthy cartilage for treatment and control, respectively. Although this method was reported as successful in the clinical treatment, it failed to enhance the quality of regenerated defects in the case of a sheep study (Kleemann et al., 2006). It must be noted that the stability of

biomaterials substituting pathological subchondral/spongy bone tissues is the fundamental condition for the regeneration of osteochondral defects.
Osteoarthrosis is the result of pathological biological processes and high biomechanical effects that destabilize the natural tissue degradation and synthesis of articular cartilage (Dieppe, 1998). The decrement of hyaluronic acid (HA, hyaluronate) concentrations and the descent of its molecular mass are the principal causes of chondral defects. The application of intraarticular injections of hyaluronan upgrades the quality of articular cartilage through the synovial liquid (Balasz & Delinger, 1993). This is a therapeutic experiment for effective temporary elimination of pains (Petrella, Di Silvestro & Hidebrandt, 2002; Dahlberg, Lohmander & Ryd, 1994). Good clinical results have been obtained after the treatment of deep chondral defects in the knee with autologous chondrocytes implantation using 3D hyaluronan-based scaffolds (Hyalograft C), (Podskubka et al., 2010). Some scaffolds can effectively increase the initial bearing capacity of newly created tissue. It is also the fundamental condition for successful chondrogenesis.
From the previous small/non-invasive methods of treatments it is apparent that the quality of microstructures and continuous biomechanical properties of the subchondral bone play an important role in the morphology and the quality of chondrogenesis. Chondrogenesis depends very sensitively on the initial stability of biomaterials implanted into the subchondral bone. Vertical displacements and rotations of COC-blend replacements shortly after implantations must be eliminated. The initial integrity of biomaterials substituting the subchondral bone, the initial bearing capacity and the vertical position of these replacements have a major influence on chondrogenesis. The initial biomechanical stiffness of materials (substituting the subchondral bone) has a fundamental influence on the quality of new articular cartilage.

5. Conclusion

With regard to these initial requirements, acceleration of the stability of COC-blend replacements in the subchondral bone is a requisite of advisable conditions for the tissue genesis.
The stability of COC-blend replacements in the subchondral bone can be ensured by:

1. plasmatic modification of the COC-blend surface by the action of a nitrogen and/or oxygen microwave plasma;
2. surface spherical/ellipsoidal pores with the diameter of < 0.5, 1.5 > μm in the COC-blend;
3. application of both type I collagen (0.3%) and growth hormones TGF-β (1.2 mg/1 ml PBS) on the COC-blend surface;
4. application of chitosan (0.3% liquid, pH 5.5) on the hydrogel surface.

The bearing capacities of subchondral bone COC-blend replacements considerably contribute to the genesis of a new extracellular cartilage matrix (Fig. 11. and Fig. 12.). Histological analyses demonstrated the healing process with partial (12 weeks) or complete (20 weeks) spongy bone + cartilage bridging (in vivo) (Fig. 9. and Fig. 10.).
The COC-blend copolymers and hydrogel [poly (2-hydroxyethylmethacrylate)] scaffolds can be suggested as a reliable reconstructive alternative for local osteochondral defects and effective support for the creation of new hyaline cartilage having an articular surface without fibrillation.

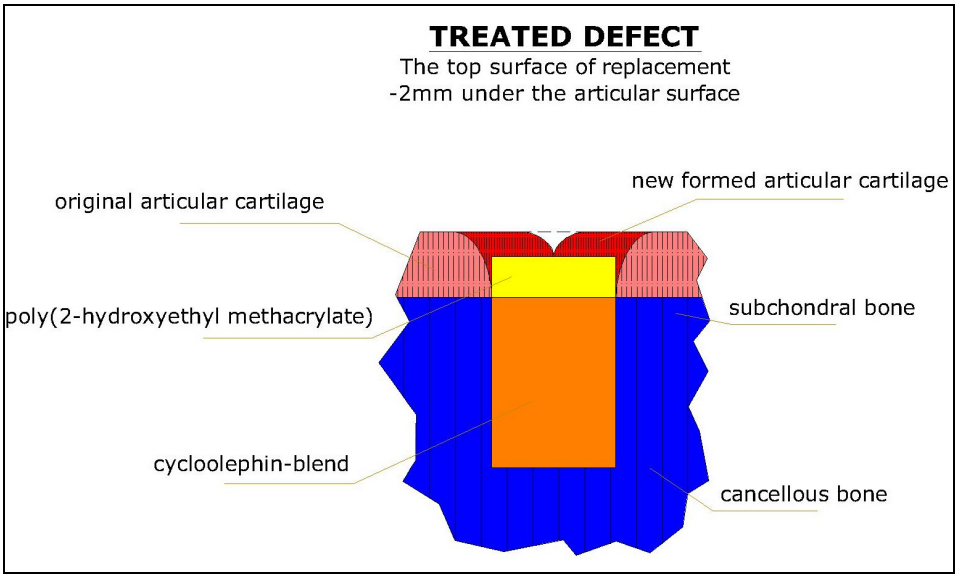

Fig. 13. New articular cartilage is formed over the hydrogel scaffold. Its surface is approximately 1–1.5 mm above the tide

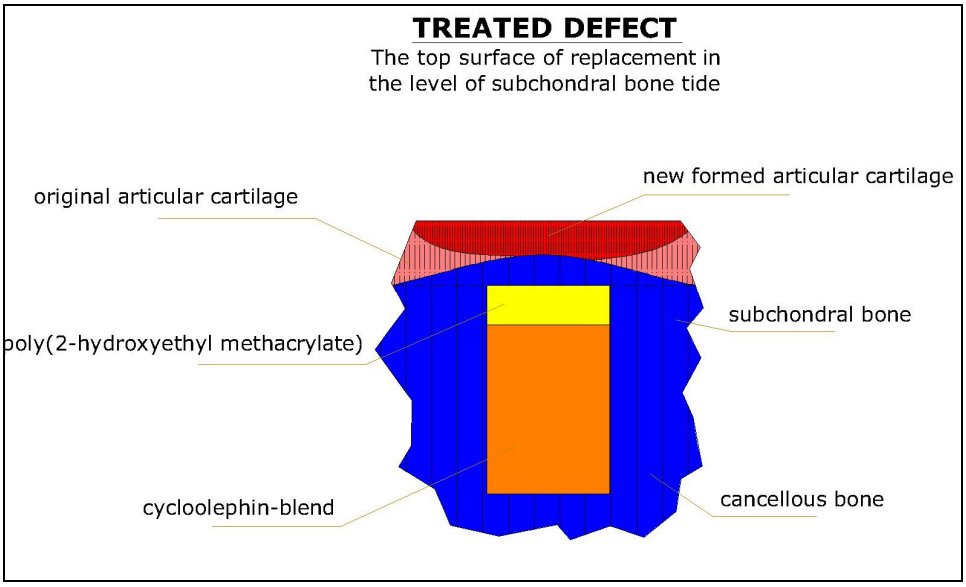

Fig. 14. New subchondral bone and new articular cartilage are formed over the hydrogel scaffold. The top plane of hydrogel surfaces is allocated approximately 0.5 mm under the indigenous level of the tidemark

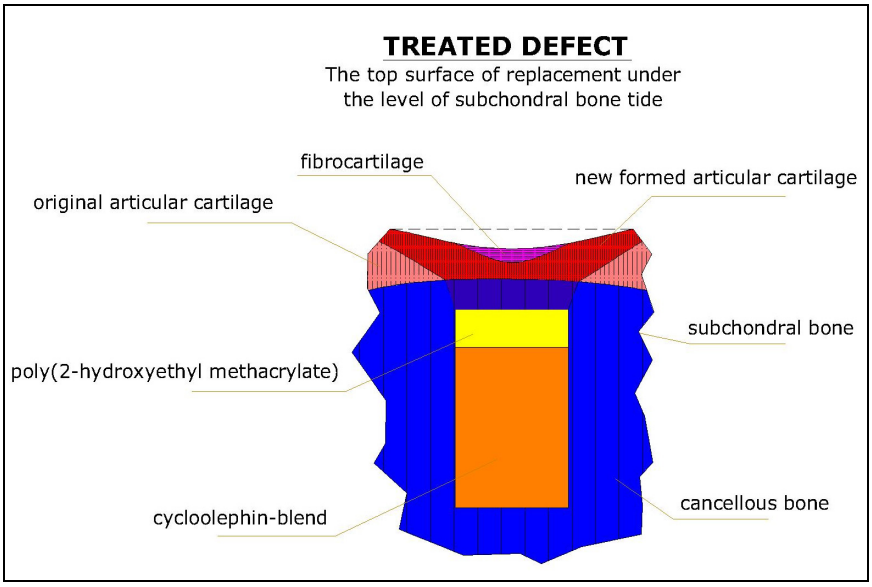

Fig. 15. New subchondral bone and new articular cartilage with peripheral fibrocartilage are formed over the hydrogel scaffold. The surface of hydrogel scaffold is allocated approximately 2 mm under the indigenous level of the tidemark. The articular surface has a sag profile

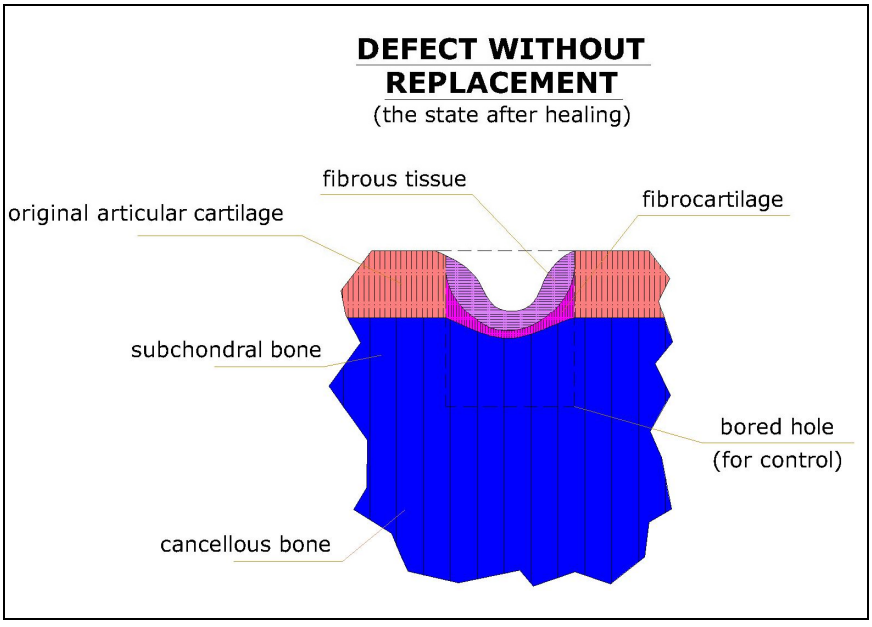

Fig. 16. Control defects are filled with both fibrous and fibrocartilage tissues

With regard to the conditions mentioned previously, the new articular cartilage is formed over the hydrogel scaffold when its surface is approximately 1–1.5 mm above the tidemark (see Fig. 13.). If the hydrogel surfaces are allocated approximately 0.5 mm under the indigenous level of the tidemark, then a new subchondral bone and new articular cartilage are formed over the hydrogel scaffold (Fig. 14.). A new subchondral bone and new articular cartilage with peripheral fibrocartilage are also formed over the hydrogel scaffold when the top surface of the hydrogel scaffold is allocated approximately 2 mm under the indigenous level of the tidemark. The articular surface has a sag profile (Fig. 15.). Control defects are filled with both fibrous and fibrocartilage tissues (Fig. 16.).

6. Acknowledgment

This research has been supported by the GAČR grant No. 106/06/0761 and by the MŠMT grant No.: VZ-6840770012. An extraordinary acknowledgement belongs to Professor C. Povýšil, Dr. Sc., M.D., from the Institute of Pathology of the First Faculty of Medicine, Charles University in Prague, and to MVDr. S. Špelda, PhD, from the Military Hospital and Faculty of Medicine in Hradec Králové.

7. References

Bader, D.L.; Pingguan-Murphy, B., van de Logt, V. & Knight, M. (2006). Intracellular signalling pathways of chondrocytes in 3D constructs subjected to physiological loading, *Proceedings of The Interaction of Mechanics and Biology in Knee Joint Restoration and Regeneration*, Center for Musculoskeletal Surgery, Charité, Berlin, June 2006

Balasz, E.A. & Denlinger, S.L. (1993). Viscosupplementation: a new concept in the treatment of osteoarthritis, Journal of Rheumatology, Vol. 20, Suppl. 39, pp. 3-9, ISSN 1499-2752

Dahlberg, L.; Lohmander, L.S. & Ryd, L. (1994). Intraarticular injections of hyaluronan in patients with cartilage abnormalities and knee pain, *Arthritis and rheumatism*, Vol. 37, No. 4, (April 1994), pp. 521-528, ISSN 0004-3591

Dieppe, p. (1998). Osteoarthritis, *Acta Orthopaedica Scandinavica*, Vol. 69, No. S281, pp. 2-5, ISSN 0001-6470

Horas, U.; Pelinkovic, D.; Herr, G.; Aigner, T. & Schnettler, R. (2003). Autologous chondrocyte implantation and osteochondral cylinder transplantation. *Journal of Bone and Joint Surgery (American)*, Vol. 85, No. 2, (February 2003), pp. 185-192, ISSN 1535-1386

Hunter, W. (1743). On the structure and diseases of articulating cartilage, In: *Phil Trans Roy Soc*, 42B, 514–521

Kleemann, R. (2006). Mechanical influences on cartilage regeneration, *Proceedings of The Interaction of Mechanics and Biology in Knee Joint Restoration and Regeneration*, Center for Musculoskeletal Surgery, Charité, Berlin, June 2006

Krulis, Z.; Stary, Z.; Horak, Z. & Petrtyl, M. (2006). Thermoplastic polymer composition for skeletal replacements and method of production, Patent Application No. 2006-70, Industrial Property Office, Prague, Czech Republic

Petrella, R.J.; DiSilvestro, M.D. & Hidebrand, C. (2002). Effects of hyaluronate sodium on pain and physical functioning in osteoarthritis of the knee: a randomized, double-

blind, placebo-controlled clinical trial, *Arch. Intern. Med.,* Vol. 162, No. 2, (February 2002), pp. 292-298, ISSN 0003-9926

Petrtyl, M.; Senolt, L.; Hulejova, H.; Cerny, P.; Krulis, Z.; Bastl, Z. & Horak, Z. (2008). Treatment of osteoarthritis by hybrid polymer replacement, *Proceedings of 6th International Workshop for Musculoskeletal and Neuronal Interactions - ISMNI*, Cologne, Germany, May 2008

Podskubka, A.; Vaculik, J.; Povysil, C.; Masek, M. & Sprindrich J. (2010). Autologous chondrocytes implantation in the treatment of the knee chondral defects, Findings in one, three and five years, *Ortopedie*, Vol. 4, No. 3, pp. 25

Raschke, M.J.; Fuchs, T. & Stange, R. (2006). Future concepts in healing stimulation, *Proceedings of The Interaction of Mechanics and Biology in Knee Joint Restoration and Regeneration*, Center for Musculoskeletal Surgery, Charité, Berlin, June 2006

Spirovova, I.; Janda, P.; Krulis, Z.; Petrtyl, M. & Bastl, Z. (2007). Surface modification of COC-LLDPE copolymer by ion beams, plasma, ozone and excimer laser radiation, *Proceedings of Abstr. 12th European Conference on Applications of Surface and Interface Analysis*, Brussels, Belgium, September 2007

4

Development and Applications of Varieties of Bioactive Glass Compositions in Dental Surgery, Third Generation Tissue Engineering, Orthopaedic Surgery and as Drug Delivery System

Samit Kumar Nandi[1], Biswanath Kundu[2] and Someswar Datta[2]
[1]Department of Veterinary Surgery and Radiology, West Bengal University of Animal and Fishery Sciences, Kolkata,
[2]Bioceramics and Coating Division, Central Glass and Ceramic Research Institute, Kolkata,
India

1. Introduction

Bioactive glass is composed mainly of silica, sodium oxide, calcium oxide and phosphates. The bone-bonding reaction results from a series of reactions in the glass and its surface (Hench & Wilson, 1984). When granules of bioactive glass are inserted into bone defects, ions are released in body fluids and precipitate into a bone-like apatite on the surface, promoting the adhesion and proliferation of osteogenic cells (Ohtsuki et al., 1991; Neo et al., 1993) which is partially replaced by bone after long time implantation (Neo et al., 1994). The ion leaching phenomenon involves the exchange of monovalent cations from the glass, such as Na+ or K+, with H3O+ from the solution, and thus causes an increase in the pH of the solution. It is known that osteoblasts prefer a slightly alkaline medium (Ramp *et al.,* 1994; Kaysinger & Ramp, 1998), but it is also known that severe changes in pH can inhibit osteoblast activity and cause cell necrosis or apoptosis (Brandao-burch et al., 2005; Frick et al., 1997; El-ghannam et al., 1997). Bioactive glass with a macroporous structure has the properties of large surface areas, which are favourable for bone integration. The behaviour of bioactive glass is dependent on the composition of the glass (Brink, 1997; Brink et al., 1997), the surrounding pH, the temperature, and the surface layers on the glass (Andersson et al., 1988; Gatti & Zaffe, 1991). The porosity provides a scaffold on which newly-formed bone can be deposited after vascular in growth and osteoblast differentiation. The porosity of bioglass is also beneficial for resorption and bioactivity (De Aza et al., 2003). In push-out tests the strength of the chemical bond between bioactive glass and the host tissue has been measured to be at least ten times higher than the contact osteogenesis (Anderson et al., 1992). Its high modulus and brittle nature makes its applications limited, but it has been used in combination with poly-methylmethacrylate to form bioactive bone cement and with metal implants as a coating to form a calcium-deficient carbonated calcium phosphate layer. Certain bioactive glass are strong enough to function in stress-bearing sites in the head and

neck (e.g., mandible replacement); however, such implants cannot be easily contoured in the operating room, and screws cannot be easily placed into bioactive glass blocks because they defy drilling and have a tendency to fragment during creation of screw holes.

2. Bioactive glass materials

Legendary Prof. L. L. Hench of University of Florida, USA discovered in 1969 that some compositions of glasses can bond chemically with bone when implanted to living tissues. Many researchers later on discovered some other ceramics, glass-ceramics and composites also have the same property (De Groot, 1983, 1988; De Groot et al., 1990; De Groot & LeGeros, 1988; Ducheyne et al., 1980; Gross et al., 1988; Gross and Strunz, 1985; Hench, 1987, 1988; Hench & Ethridge, 1982; Hench et al., 1971; Hench & Wilson, 1984; Holand et al., 1985; Hulbert et al., 1987; Jarcho, 1981; Kitsugi et al., 1989; Kokubo et al., 1986; Kokubo et al., 1982; Nakamura et al., 1985; Wilson et al., 1981; Yamamuro et al., 1990b; Yamamuro et al., 1988; Yoshii et al., 1988). He defined these glasses as 'bioactive glass' and since then it has been used mostly as a reconstructive material for damaged hard tissues such as bone (Hench, 2006; Hench et al., 1971). Some more specialized compositions of bioactive glass will bond to soft tissues and bone (Wilson & Nolletti, 1990; Wilson et al., 1981; Yamamuro et al., 1990a). General characteristics of these bioactive glasses are a time-dependent, kinetic modification of the surface that occurs when implanted *in vivo* (Gross et al., 1988; Hench, 1988), the surface forms biologically active hydroxycarbonate apatite (HCA) layer providing bonding interface with tissues. The advantage is that it is possible to design this glass to get a controlled rate of degradation and bonding to the tissue. The HCA phase that forms on these implants is very similar chemically and structurally to the mineral phase in bone and thus responsible for interfacial bonding. These bioactive materials develop an adherent interface with tissues that resists significant mechanical forces. In some cases this interfacial strength of adhesion is equivalent to or greater than the cohesive strength of the implant material or the tissue bonded to bioactive implant. The rapid reaction at the surface leads to a fast bonding with the living tissues, but, due to the mainly two-dimensional structure of the glass network, the mechanical properties are relatively low. It may be noted that small changes in the composition can lead to very different properties and thus has added advantage of its versatility in contact with different living tissues, on range of properties depending on the implantation site of the prosthesis.

Certain compositional range of bioactive glass containing SiO_2, Na_2O, CaO, and P_2O_5 like ordinary soda-lime-silica glasses in specific proportions shows bonding to bone (Table 1).Three key compositional features of these glasses distinguish them from traditional Na_2O-CaO-SiO_2 glasses: (1) less than 60 mol. % SiO_2, (2) high-Na_2O and high-CaO content, and (3) high-CaO/P_2O_5 ratio. As known, SiO_2/Al_2O_3 act as glass network former, CaO/MgO/P_2O_5 is the network modifier and Na_2O/K_2O is the fluxing agent. These compositional features made the surface highly reactive when exposed to aqueous medium. Very popular 45S5 bioactive silica glasses are based upon 45 wt. % SiO_2, S as the network former, and a 5 to 1 molar ratio of Ca to P. Glasses with very lower molar ratios of Ca to P (in the form of CaO and P_2O_5) do not bond to bone (Hench and Paschall, 1973). Different substitutions in the 45S5 compositions of 5-15 wt. % B_2O_3 for SiO_2, or 12.5 wt. % CaF_2 for CaO or crystallizing the various bioactive glass compositions to form glass-ceramics were found to have no measurable effect on the ability of the material to form a bone bond (Hench & Paschall, 1973). But, addition of small 3 wt. % Al_2O_3 to the 45S5 formula prevents bonding

Sl. No.	Name of the composition	All are in weight %											
		SiO_2	P_2O_5	CaO	$Ca(PO_3)_2$	CaF_2	MgO	MgF_2	Na_2O	K_2O	Al_2O_3	B_2O_3	Ta_2O_5 / TiO_2
1.	45S5 Bioglass ® (Hench et al., 1971)	45	6	24.5	-	-	-	-	24.5	-	-	-	-
2.	45S5.4F Bioglass ® (Hench et al., 1986; Hench et al., 1971)	45	6	14.7	-	9.8	-	-	24.5	-	-	-	-
3.	45B15S5 Bioglass ® (Hench and Paschall, 1974; Hench et al., 1975)	30	6	24.5	-	-	-	-	24.5	-	-	15	-
4.	52S4.6 Bioglass ® (Hench and Clark, 1982)	52	6	21	-	-	-	-	21	-	-	-	-
5.	55S4.3 Bioglass ® (Hench and Clark, 1982)	55	6	19.5	-	-	-	-	19.5	-	-	-	-
6.	KGC Ceravital ® (Gross et al., 1988)	46.2	-	20.2	25.5	-	2.9	-	4.8	0.4	-	-	-
7.	KGS Ceravital ® (Gross et al., 1988)	46	-	33	16	-	-	-	5	-	-	-	-
8.	KGy213 Ceravital ® (Gross et al., 1988)	38	-	31	13.5	-	-	-	4	-	7	-	6.5
9.	A/W glass-ceramic (Kokubo et al., 1986)	34.2	16.3	44.9	-	0.5	4.6	-	-	-	-	-	-
10.	MB glass-ceramic (Holand et al., 1985)	19-52	4-24	9-3	-	-	5-15	-	3-5	3-5	12-33	-	-
11.	S45P7 (Andersson et al., 1988)	45	7	22	-	-	-	-	24	-	-	2	-
12.	S53P4 (Zehnder et al., 2004)	53	4	20	-	-	-	-	23	-	-	-	-
13.	13-93 (Fu et al., 2008)	53	4	20	-	-	5	-	6	12	-	-	-
14.	4-Mar (Zhang et al., 2008)	50.5	1	22.5	-	-	6	-	5	15	-	-	-
15.	18-04 (Zhang et al., 2008)	54.5	4	20	-	-	4.5	-	15	-	-	2	-
16.	23-04 (Zhang et al., 2008)	56.25	1	20	-	-	4.5	-	5	11.25	-	2	-
17.	H2-02 (Munukka et al., 2008)	53	2	22	-	-	4.5	-	6	11	0.5	1	-

Sl. No.	Name of the composition	All are in mole %												
		SiO_2	P_2O_5	CaO	$Ca(PO_3)_2$	CaF_2	MgO	MgF_2	Na_2O	K_2O	Al_2O_3	B_2O_3	Ta_2O_5/ TiO_2	ZnO
18.	CEL-2 (Vitale-Brovarone et al., 2009)	45	3	26	-	-	7	-	15	4	-	-	-	-
19.	55S (Loty et al., 2001)	55	4	41	-	-	-	-	-	-	-	-	-	-
20.	H (Linati et al., 2005)	46.2	2.6	26.9	-	-	-	-	24.3	-	-	-	-	-
21.	HZ5 (Linati et al., 2005)	44.4	2.5	25.9	-	-	-	-	23.4	-	-	-	-	3.8
22.	HZ10 (Linati et al., 2005)	42.5	2.4	4.8	-	-	-	-	22.5	-	-	-	-	7.8
23.	HZ20 (Linati et al., 2005)	38.8	2.2	22.6	-	-	-	-	20.5	-	-	-	-	15.9

Table 1. Different compositions of bioactive glass materials

(Andersson et al., 1990; Greenspan & Hench, 1976; Gross et al., 1988; Gross and Strunz, 1985; Hench & Clark, 1982; Hench & Paschall, 1973). Gross and co-workers found that a range of low-alkali (0-5 wt. %), bioactive silica glass-ceramics (Ceravital ®) also bond to bone (Gross et al., 1981; Gross et al., 1988; Gross et al., 1986a; Gross et al., 1986b; Gross & Strunz, 1985; 1980). Also small additions of Al_2O_3, Ta_2O_5, TiO_2, Sb_2O_3 or ZrO_2 inhibit bone bonding (Table 1). A two-phase silica-phosphate glass-ceramic composed of apatite ($Ca_{10}(PO_4)_6(OH1F_2)$) and wollastonite ($CaO.SiO_2$) crystals (termed A/W glass-ceramic by the Kyoto University team, Japan) and a residual SiO_2 glassy matrix, also bonds with bone with very high interfacial bond strength (Kitsugi et al., 1989; Kokubo et al., 1986; Kokubo et al., 1982; Nakamura et al., 1985; Yamamuro et al., 1988; Yoshii et al., 1988). But, addition of $A1_2O_3$ or TiO_2 to the A/W glass-ceramic inhibits bone bonding, while a second phosphate phase, β-whitlockite ($3CaO.P_2O_5$) does not. Multiphase machinable bioactive silica phosphate glass-ceramic containing phlogopite ($(Na,K)Mg_3(AlSi_3O_{l0})F_2$), mica and apatite crystals, developed by the Freidrich Schiller University, Jena, Germany, bonds to bone despite presence of alumina in the composition (Holand et al., 1985). $A1^{3+}$ ions incorporated within the crystal phase did not alter the surface reaction kinetics of the material (Vogel et al., 1990). Some other compositions of bioactive glass have been developed at Abo Akademi, Turku, Finland, for coating onto dental alloys (Andersson et al., 1988; Andersson et al., 1990; Kangasniemi & Yti-Urpo, 1990).

Prof. Hench has recently published the history leading to the development of bioactive glass from the discovery of classical 45S5 Bioglass® composition to successful clinical applications and tissue engineering (Hench, 2006). High amounts of Na_2O and CaO as well as relatively high CaO/P_2O_5 ratio make the glass surface highly reactive in physiological environments (Hench, 1991). Other bioactive glass compositions developed over few years contain no sodium or have additional elements incorporated in the silicate network such as fluorine (Vitale-Brovarone et al., 2008), magnesium (Vitale-Brovarone et al., 2005; Vitale-Brovarone et al., 2007), strontium (Gentleman et al., 2010; O'Donnell & Hill, 2010; Pan et al., 2010), iron (Hsi et al., 2007), silver (Balamurugan et al., 2008; Bellantone et al., 2002; Blaker et al., 2004;

Delben et al., 2009), boron (Gorriti et al., 2009; Liu et al., 2009a; Liu et al., 2009b; Munukka et al., 2008), potassium (Cannillo & Sola, 2009) or zinc (Aina et al., 2009; Haimi et al., 2009).
Introduction of Ag_2O into bioactive glass compositions minimize the risk of microbial contamination by antimicrobial activity of the leaching Ag^+ ions has been reported (Blaker et al., 2004; Saravanapavan et al., 2003). In the reports synthesis by sol-gel process also allowed tailoring of the textural characteristics of the matrix in order to obtain a controlled Ag^+ delivery system. Introduction of B_2O_3 into the $CaO–SiO_2$ system on the other hand enhanced the bioactivity, for more soluble boric compounds increased the supersaturating of Ca ions in the SBF (simulated body fluid) solution and water-corrosive borosilicate glass forms Si–OH groups that act as nucleation sites for the apatite layer (Ryu et al., 2003). Zn-substituted bioactive glass creates a template for osteoblast proliferation and differentiation by the interaction between the Zn and inorganic phosphate at the surface of the bioactive glass. Addition of Zn has synergistic effect on cell attachment which also maintains the pH of SBF within the physiological limit by forming zinc hydroxide in the solution. Limited amounts of Zn in the bioactive glass system stimulate early cell proliferation and promote differentiation as assessed by the *in vitro* biocompatibility experimentation. Now, compositional dependence of bone bonding and soft-tissue bonding for the Na_2O-CaO-P_2O_5-SiO_2 glasses (constant 6 wt. % of P_2O_5) is presented in Fig. 1. Compositions at the middle of the diagram form a bond with bone (region A). Region A is termed as the bioactive-bone bonding boundary. Silica glasses within region B (such as bottle, window or slide glasses of microscope) behave as nearly inert materials and elicit a fibrous capsule at the implant-tissue interface. Glasses within region C are resorbable and disappear within maximum 1 day of implantation. Glasses within region D are not technically realistic and have not been tested as implants. The collagenous constituent of soft tissues can strongly adhere to the bioactive silica glasses which lie within the compositional range marked as E (Fig. 1).
Very briefly, bioactive glass can be made either by conventional melt-quenching (Chen et al., 2008b; Guarino et al., 2007; Hench & Polak, 2002; Hutmacher et al., 2007; Jones, 2007; Jones, 2009; Misra et al., 2006) or by modern sol-gel method (Balamurugan et al., 2007; Radha & Ashok, 2008). Sol-gel process involves synthesis of solution (sol), typically composed of metal-organic and metal salt precursors followed by formation of gel by chemical reaction or aggregation and finally thermal treatment for drying, organic removal and sometimes crystallization (Olding et al., 2001). This particular method is a low temperature preparative method and glasses produced by this method may have some porous structure too with high specific surface area (Sepulveda et al., 2001). There are diversified application potential of different bioactive glass which have been discussed many authors and will be presented in the subsequent sections. But, bone tissue engineering is a very exotic future clinical application of these materials. Both micron-sized and nano-scale particles deployed recently (Brunner et al., 2006; Delben et al., 2009; Vollenweider et al., 2007) are considered to be the part of this application field which also include fabrication of composite materials, e.g., combination of biodegradable polymers and bioactive glass (Liu et al., 2008; Lu et al., 2003; Misra et al., 2010a; Misra et al., 2010b; Misra et al., 2008; Yang et al., 2001). Bioactive glass-ceramics on the other hand belong to the group of Class A bioactive materials which are characterized by both osteoconduction (growth of bone at the implant surface) and osteoinduction (activation and recruitment of osteoprogenitor cells by the material itself

stimulating bone growth on the surface of the material) (Hench, 2006; Hench, 1998; Jones, 2007; Thompson & Hench, 1998). In contrast, Class B bioactive materials exhibit only osteoconductivity. A recent review summarizing research on Ca-Si-based ceramics is also available (Wu, 2009). As far as bioactive glass-ceramics are concerned, these are partially crystallized glasses produced by heating the parent bioactive glass above its crystallization temperature, usually at about 610-630° C (Boccaccini, 2005; Boccaccini et al., 2007; Brunner et al., 2006; Jones, 2007). Glass-ceramics obtained by a sintering process, it is found that during the incidence of crystallization and densification, the microstructure of the parent glass shrinks, porosity is reduced and the solid structure gains mechanical strength (Thompson & Hench, 1998). But, brittleness and low fracture toughness remain a major problem of these materials. The limited strength and low fracture toughness (i.e., resistance to fracture crack propagation) of bioactive glass has so far prevented their use for load-bearing implants (Boccaccini, 2005; Hench, 2006; Thompson & Hench, 1998; Thompson, 2005). Subsequently, the repair and regeneration of large bone defects at load-bearing anatomical sites remains a clinical/orthopedic challenge (Fu et al., 2010; Kanczler & Oreffo, 2008).

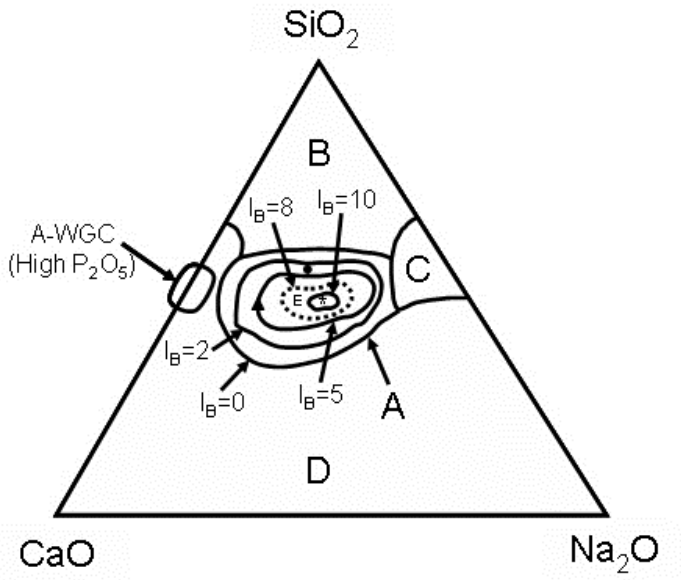

Fig. 1. Compositional dependence of bone bonding and soft tissue bonding of bioactive glass and glass ceramics. All compositions in region A have a constant 6 wt. % of P_2O_5. A-WGC (apatite-wollastonite glass-ceramic) has higher P_2O_5 content (Table 1). Region E (soft tissue boding) is inside the dashed line where I_B>8 [* 45S5 Bioglass ®, ▲ Ceravital®, ● 55S4.3 Bioglass ®, and (---) soft-tissue bonding; $I_B=100/t_{0.5bb}$, where $t_{0.5bb}$ is the time to have more than 50% of the implant surface bonded to the bone and I_B is bioactivity index, i.e. the level of bioactivity of a specific material can be related to the time for more than 50% of the interface to be bonded (Hench, 1988; Hench, 1991)]

2.1 Reaction kinetics

When a bioactive glass is immersed in an aqueous solution, like SBF (simulated body fluid) or TBS (tris buffer solution), there are three distinguishing reactions could be identified (Andersson et al., 1992; Hench, 1991, 1996, 1998; Hench & Andersson, 1993) (Fig. 2):

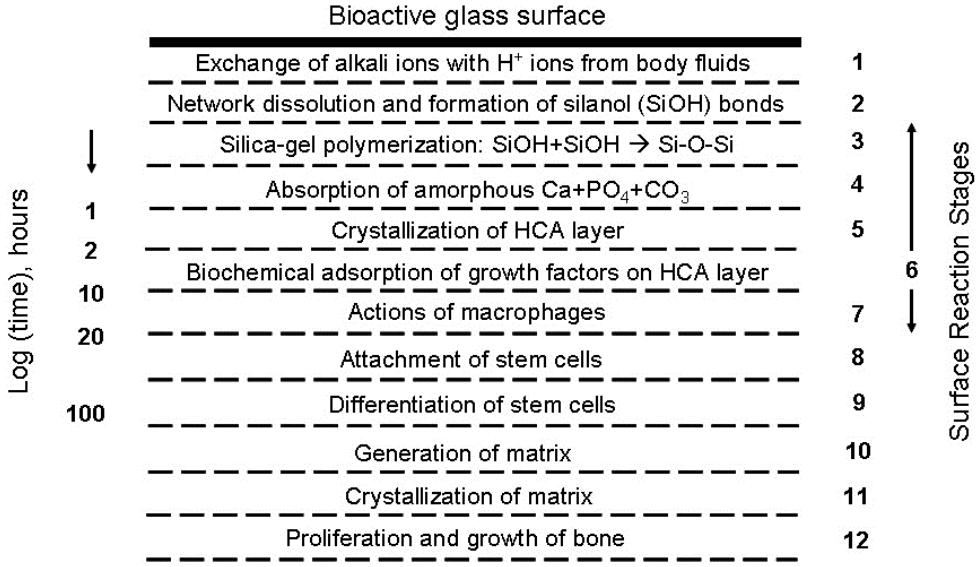

Fig. 2. Sequence of interfacial reactions kinetics involved in forming a bond between bone and a bioactive glass [modified after (Hench, 1998) and (Gerhardt & Boccaccini, 2010)].

1. Leaching and formation of silanols: Glass network releases alkali or alkaline earth elements exchanging cations with H^+ or H_3O^+ cations proceeding from the solution. These modifying ions lead to high values of the interfacial pH, usually more than 7.4.
2. Dissolution of the glass network: -Si-O-Si-O-Si- bonds break through the action of hydroxyl ions. Breakdown of the silica network releases locally silicic acid $[Si(OH)_4]$. If there is more than 60% of silica, the dissolution rate decreases as this increases the number of bridging oxygens in the structure of the glass. The hydrated silica (Si-OH) formed on the glass surface by these reactions undergoes rearrangement by polycondensation of neighboring silanols, resulting in a silica rich gel layer.
3. Precipitation: Calcium and phosphate ions released from the glass together with those from solution form a calcium-phosphate rich layer (CaP) on the surface. This phosphate is initially amorphous, then crystallizes to a hydroxycarbonate apatite (HCA) structure by incorporating carbonate anions from solution within the amorphous CaP phase. The mechanism of nucleation and growth of HCA appears to be the same *in vivo* and *in vitro* and is accelerated by the presence of hydrated silica. These stages do not depend on the presence of the tissue and they are observed in distilled water as well as SBF or tris-buffer solution. The following additional series of reactions is needed to get a bond with the tissue:
4. Absorption of biological moieties in the SiO_2-HCA layer
5. Action of macrophages

6. Attachment of stem cells
7. Differentiation of stem cells
8. Generation of matrix
9. Mineralisation of matrix

This model as proposed by Prof. Hench is widely accepted but has some limitations too. As for example the first stage of the reaction relies on the rapid exchange of the Na^+ ions released from the glass with the protons of the solution, although bioactive glass have been produced without sodium. The index as given in Fig. 1 is also not predictive of the influence of the silica mole fraction on the reactivity of the glass. Some parameters like network connectivity based on the inorganic polymer model for glasses could be considered to describe the behavior of a bioactive glass (Bovo, 2007). The closer the glass composition to the boundary of Fig. 1, the slower is the bonding rate. Usually, the thickness of the bonding zone is proportional to I_B. As the thickness of this zone increases, the failure strength decreases. Further, it was found that if they break after implantation and the broken surfaces stay in contact with SBF, they may self-repair fusing themselves through their apatite surface layers (Bovo, 2007). Again, bioactive glass produced by Ebisawa et al. with a molecular formula of $CaO.SiO_2$ (Ebisawa et al., 1990) could not account for the bioactivity, the model of which proposed by Prof. Hench (Hill, 1996).

Concepts such as cross-link density or network connectivity can be applied to describe their structure if silicate glasses are considered to be inorganic polymers of silicon cross-linked by oxygen (Ray, 1978). The network connectivity of a glass is defined as the average number of additional cross-linking bonds (more than two) for elements other than oxygen that form the network backbone. The calculation of network connectivity of a glass network is based on the relative numbers of network-forming oxide species (those which contribute "bridging" or cross-linking oxygen species) and network-modifying species (those which result in the formation of "non-bridging" species) present (Wallace et al., 1999). The network connectivity of a glass can be used to predict various physical properties of the glass, including its solubility (Hill, 1996). The silicate structural units in a glass of low network connectivity are probably of low molecular mass and are capable of going into solution. Thus, glass solubility increases as network connectivity is reduced. So, glasses of low network connectivity are potentially bioactive (Wallace et al., 1999). Lockyer et al. determined the effect of substituting sodium oxide for calcium oxide on some glass properties (Lockyer et al., 1995). Most studies on bioactive glass systems have been carried out on a weight per cent basis. But, mole per cent substitutions are known to have more significance on a structural level. Weight percent basis has the effect of hiding the composition-property relationships of bioactive glass as there is no account taken of the degree of disruption of the glass network (Lockyer et al., 1995; Strnad, 1992). Fig. 3 represents a highly disrupted glass network. It can be seen that for every mole of calcium oxide removed from the glass network, one mole of sodium oxide must be added in order to maintain the same number of non-bridging oxygen species and, thus the same network connectivity value. So, a substitution on weight per cent basis produces a change in the relative number of non-bridging oxygen species and bridging oxygen species, with consequent change in network connectivity. Work carried out by Wallace et al. uses the concepts of network connectivity for the purposes of designing bioactive glass compositions for control of the physical, chemical and biological properties of bioactive glass (Wallace et al., 1999).

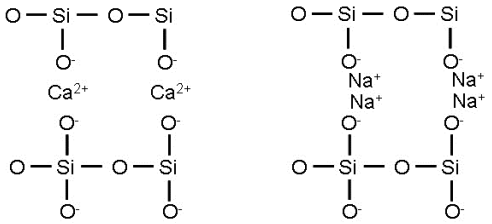

Fig. 3. Representation of glass structure (Wallace et al., 1999)

2.2 Fabrication

Properties of bioactive glass and glass-ceramics are dependent on fabrication methods and the heat-treatment used. Many scaffold fabrication techniques have been reported in the literature, e.g., foam replication methods, salt or sugar leaching, thermally induced phase separation, microsphere emulsification sintering, electrospinning for nano-fibrous structures, computer aided rapid prototyping techniques (Yang et al., 2002; Yun et al., 2007), textile and foam coating methods (De Diego et al., 2000; Francis et al., 2010; Mohamad Yunos et al., 2008) and biomimetic approach (Oliveira et al., 2003; Taboas et al., 2003). All of these methods were done to optimize the structure, properties and mechanical integrity of scaffolds. The design and incorporation of nano-topographic features on the scaffold surface architecture, in order to mimic the nanostructure of natural bone, is also becoming a significant area of research in bone tissue engineering (Berry et al., 2006; Jones, 2009; Stevens & George, 2005; Webster & Ahn, 2007). Also, comprehensive reviews of the general state-of-the art in scaffold manufacturing and optimization are available (Boccaccini & Blaker, 2005; Guarino et al., 2007; Hutmacher et al., 2007; Mohamad Yunos et al., 2008; Rezwan et al., 2006; Yang et al., 2001).

Pores of bioactive glass and glass-ceramics could be formed by the addition of suitable porogens, such as polymeric materials and foaming agents (Karlsson et al., 2000). Rainer et al. prepared bioactive glass foams for mimicking bone tissue engineering scaffolds using *in situ* foaming of bioactive glass-loaded polyurethane foam (Rainer et al., 2008). Inspired by this fabrication technique, the bioactive materials were prepared with three-dimensional processing and showed promising applications in reconstructive surgery tailored to each single patient. Polyethylene glycol 4000 ($HO(C_2H_4O)$-nH) with particles sizes of 5-500 μm was used as foaming agent for preparing porous bioactive glass ceramic (Lin et al., 1991). This group has also reported the compatibility of porous bioactive glass ceramic with animal tissues. The microstructures of the implant were distributed uniformly in the material, which provided channels for bone in-growth and improved the microscopic bioresorption. Organic polymers were found to be an alternate attractive choice for generating desired pores and porosity due to the complete degradation at temperatures above 600° C. These organic polymers are abundant in natural environment, also available as biomass such as dry and wet woods and crops. This can be obtained from wastes in many related industries too such as food processing and wood finishing manufactures (Sooksaen et al., 2008). It was reported that textural properties (pore size, pore volume, pore structure) of biomaterials may have complex influences on the development of the apatite layer in bioactive glass. Increasing the specific surface area and pore volume of bioactive glass may greatly accelerate the apatite formation and therefore enhance the bioactive behavior (Vallet-Regí et al., 2003).

Sl. No.	Glass composition or system	Reference	Fabrication method adopted	Particle size of starting glass powder
1	45S5	(Ochoa et al., 2009)	Polymer foam replication	< 5 µm
2	SiO_2-CaO-CaF_2-Na_2O-K_2O-P_2O_5-MgO	(Vitale-Brovarone et al., 2008)	Polymer foam replication	< 32 µm
3	SiO_2-P_2O_5-CaO-MgO-Na_2O-K_2O	(Vitale-Brovarone et al., 2009b; Vitale-Brovarone et al., 2007)	Polymer foam replication	< 30 µm
4	SiO_2-P_2O_5-CaO-MgO-Na_2O-K_2O	(Renghini et al., 2009)	Polymer foam replication	-do-
5	45S5	(Chen et al., 2008a)	Polymer foam replication	10-20 µm
6	SiO_2-Na_2O-CaO-MgO	(Vitale-Brovarone et al., 2005)	Starch consolidation	< 100 µm
7	SiO_2-P_2O_5-B_2O_3-CaO-MgO-K_2O-Na_2O	(Moimas et al., 2006)	Compaction and sintering of melt-spun fibers	75 µm (fibre diameter)
8	SiO_2-CaO-Na_2O-K_2O-P_2O_5-MgO-CaF_2	(Baino et al., 2009)	Polymer porogen bakeout	< 106 µm
9	45S5	(Boccaccini et al., 2007)	Polymer foam replication	20-50 µm
10	SiO_2-Na_2O-K_2O-MgO-CaO-P_2O_5	(Fu et al., 2007)	Slip casting	255-325 µm
11	SiO_2-Na_2O-K_2O-MgO-CaO-P_2O_5	(Fu et al., 2008)	Polymer foam replication	< 5-10 µm
12	SiO_2-Na_2O-K_2O-MgO-CaO-P_2O_5	(Fu et al., 2010)	Freeze casting	< 5 µm
13	SiO_2-CaO-K_2O	(Vitale Brovarone et al., 2006)	Polymer porogen burn-off	< 106 µm
14	SiO_2-TiO_2-B_2O_3-P_2O_5-CaO-MgO-K_2O-Na_2O	(Haimi et al., 2009)	Compaction and sintering of melt-spun fibers	75 µm (fibre diameter)
15	45S5	(Deb et al., 2010)	Polymer porogen bakeout	45-90 µm
16	45S5	(Bretcanu et al., 2008)	Polymer foam replication	< 5 µm
17	SiO_2-Na_2O-K_2O-MgO-CaO-P_2O_5; 45S5	(Brown et al., 2008)	Densification and sintering of melt-spun fibers	25-40 µm (fibre diameter)

18	45S5	(Chen et al., 2006b)	Polymer foam replication	≈ 5 μm
19	45S5	(Chen et al., 2006a)	Polymer foam replication	5-10 μm
20	45S5	(Chen et al., 2007)	Polymer foam replication	≈ 10 μm
21	SiO_2-P_2O_5-CaO-MgO-Na_2O-K_2O	(Vitale-Brovarone et al., 2010)	Polymer burn-off, foam replication	Not applicable
22	45S5	(Vargas et al., 2009)	Polymer foam replication	< 5 μm
23	SiO_2-Na_2O-CaO-P_2O_5-B_2O_3-TiO_2	(Ghosh et al., 2008)	Polymer porogen bakeout	Not applicable
24	SiO_2-Na_2O-CaO-P_2O_5-B_2O_3-TiO_2	(Nandi et al., 2009)	Polymer porogen bakeout	Not applicable
25	SiO_2-CaO-P_2O_5-Al_2O_3	(Mahmood et al., 2001)	Manual free-forming of melt- spun fibers	8-30 μm (fibre diameter)
26	SiO_2-CaO-Na_2O-P_2O_5-K_2O-MgO-B_2O_3	(Mantsos et al., 2009)	Polymer foam replication	Not applicable
27	SiO_2-CaO-Na_2O-K_2O-MgO-P_2O_5-B_2O_3	(Miguel et al., 2010)	Densification and sintering of melt-spun fibers	75 μm (fibre diameter)

Table 2. Summary of recent studies performed on silicate bioactive glass-ceramic scaffolds

2.3 Clinical relevance

For bioactive glass-ceramics, recent developments related to bone tissue engineering scaffolds have been used to remove the gap of load-bearing large bone defects by inter-playing between architectures and components carefully designed from comprehensive levels, i.e., from the macro-, meso-, micrometer down to the nanometer scale (Deville et al., 2006), including both multifunctional bioactive glass composite structures and advanced bioactive glass-ceramic scaffolds exhibiting oriented microstructures, controlled porosity and directional mechanical properties (Baino et al., 2009; Bretcanu et al., 2008; Fu et al., 2010; Fu et al., 2008; Vitale-Brovarone et al., 2010). As summarized in Table 2 [reproduced from (Gerhardt & Boccaccini, 2010)], most of the studies have mainly investigated the mechanical properties, in vitro and cell biological behavior of glass-ceramic scaffolds (Baino et al., 2009; Boccaccini et al., 2007; Bretcanu et al., 2008; Brown et al., 2008; Chen et al., 2007; Chen et al., 2006a; Chen et al., 2008a; Chen et al., 2006b; Deb et al., 2010; Fu et al., 2010; Fu et al., 2007; Fu et al., 2008; Ghosh et al., 2008; Haimi et al., 2009; Klein et al., 2009; Kohlhauser et al., 2009; Mahmood et al., 2001; Mantsos et al., 2009; Miguel et al., 2010; Moimas et al., 2006; Nandi et al., 2009; Ochoa et al., 2009; Renghini et al., 2009; Vargas et al., 2009; Vitale-Brovarone et al., 2009a; Vitale-Brovarone et al., 2010; Vitale-Brovarone et al., 2009b; Vitale-Brovarone et al., 2008; Vitale-Brovarone et al., 2004; Vitale-Brovarone et al., 2005; Vitale-Brovarone et al., 2007; Vitale Brovarone et al., 2006). Scaffolds with compressive strength (Baino et al., 2009; Fu et al., 2010) and elastic modulus values (Fu et al., 2010; Fu et al., 2008) in magnitudes far above that of cancellous bone and close to the lower limit of cortical bone have been realized.

3. Bioactive glass in dental surgery and cranio-maxillofacial augmentation

The increasing need for biomedical devices, required to face dysfunctions of natural tissues and organs caused by traumatic events, diseases and simple ageing, has drawn attention onto new materials that could be able to positively interact with the human body. Biomaterials play a significant role in dental, craniofacial and maxillofacial reconstruction. Their ever-increasing ease of use, long 'shelf-life' and safety enables them to be used efficiently and play an important role in reducing operating times (Gosain & Persing, 1999; Chim & Gosain, 2009). The ideal biomaterial in such reconstruction should be biocompatible with surrounding tissue without elucidating a foreign body reaction, radiolucent, easily shaped or molded, strong enough to endure trauma, stable over time, able to maintain volume, and osteoactive (Gosain & Persing, 1999; Damien & Parsons, 1991; Costantino et al., 1992; Jackson & Yavuzer, 2000; Gosain, 2003).

Abnormality of the craniofacial skeleton may bring in from various causes, including tumor resection, severe infection, trauma, or congenital deformity. Restoring appropriate contour and support in the cranio-orbital region following loss or removal of bone may be quite challenging to the Craniofacial and Neurosurgeons. Since the late 1800's when Muller described using calvarial bone grafts for reconstruction, they have remained the gold standard [Muller, 1890]. Autologous bone grafting provides a rich amount of native tissue that has a high possibility of osseous integration with little risk of rejection or infection long-term, in addition to safety and security (Manson et al., 1986). Although autogenous bone is the ideal material to primarily reconstruct large skull bone defects (Barone & Jimenez, 1997; Goodrich et al., 1992; Weber et al., 1987), it has some drawbacks in reconstruction including donor site morbidity, prolonged operating times, limited availability, and difficulty to contour (Nickell et al., 1972; Whitaker *et al.,* 1979; Jackson *et al.,* 1983). In the pediatric surgery, bone grafts may be relatively easily contoured and curved while, in adults, it is often difficult to achieve the precise three dimensional contours normally found in the cranio-orbital region (Ducic, 2001). Research was then initiated by reconstructive surgeons to find alternative means of reconstruction with alloplasts. In reality, alloplast reconstruction of the calvarium dates back to the year 2000 B. C. in ancient Peru when a gold plate was used to disguise a trephination defect (Grana *et al*., 1954). Since then, various alloplasts have been used in craniofacial reconstruction. The most commonly utilized material has been methylmethacrylate. Although, it suffers from several potential drawbacks including lack of osseointegration, secondary infection, plate fracture, erosion of the underlying recipient bone, necrosis of surrounding tissues during setting as it forms during an exothermic reaction with temperatures reaching 110° C, and difficulty shaping once polymerization occurs (Ducic , 2002; Costantino et al., 2000; Smith et al., 1999).

In the past century, other metallic materials, such as silver, tantalum, stainless steel or titanium and calcium phosphate based materials like hydroxyapatite cement, calcium orthophosphate cements, porous granular hydroxyapatite, marine coral-based calcium carbonate were used for reconstruction purposes. The present endeavor deals with the application of bioactive glass based material in dental, craniofacial and maxillofacial reconstruction. Bioactive glass (BG) is biocompatible, osteoconductive, form a strong bond with living tissue via the formation of a hydroxyapatite layer on their surface (Meffert et al., 1985; Schepers et al., 1991; Hench et al., 1971) and have been used to repair hard tissues in a variety of craniofacial, maxillofacial, and periodontal applications (Hench, 1991). It has also been established that BG has good mechanical properties and a higher bioactivity in comparison to hydroxyapatite (Mardare et al., 2003; Ghosh et al., 2008)

BG particulate, for example, is used in a variety of dental procedures (Shapoff et. al., 1997), and many BG compositions can be formed into scaffolds for tissue engineering (Jones et al., 2007). Surface reactivity, however, is not their only mechanism of action as BG also releases ions that promote the osteoblast phenotype (Effah Kaufmann et al., 2000; Jell et al., 2008). In vitro studies have established that BG stimulates osteoprogenitors to differentiate to mature osteoblasts that produce bone-like nodules (Tsigkou et al., 2007; 2009). Bioactive glass was used in dentistry as a bioactive material in endosseous ridge maintenance implants (ERMI) as early as in 1986. Dicor® was the first glass-ceramic that allowed the manufacture of inlays and crowns where the major crystalline phase in the glass ceramic was mica (Grossman, 1991). A new glass-ceramic was developed by sol-gel technique having resemblance with commercial leucite based fluorapatite dental glass-ceramic. The produced material has prospective application in dental restorations and it is anticipated to exhibit better control of composition, microstructure and properties due to the intrinsic advantages of the sol-gel preparation method (Chatzistavrou et al., 2009). Recent studies indicated that rhenanite glass-ceramics can be utilized in dentistry (Holand et al., 2006). In a study, bioactive glass coated titanium alloy dental implants were compared with hydroxyapatite implants in human jaw bone and observed that bioactive glass coated implants were as equally successful as hydroxyapatite in achieving osseointegration and supporting final restorations (Mistry et al., 2011). Bioglass was mixed with phosphoric acid and irradiated with $CO_{(2)}$ laser could occlude the dentinal tubule orifices with calcium-phosphate crystals where the application of $CO_{(2)}$ laser potentially improved the mechanical organization of these crystals (Bakry et al., 2011). In another study, radio-opaque nanosized bioactive glass was used for root canal application particularly for dressing or filling material (Mohn et al., 2010). A modified bioglass formula was used as a pulp capping agent where the incidence of properly positioned dentin bridge formation was higher and the incidence of extruded dentin bridge formation was reduced (Stanley et al., 2001). A new treatment for localized aggressive periodontitis using enamel matrix proteins and bioactive glass resulted in the successful treatment of intrabony defects (Miliauskaite et al., 2007; Zietek et al., 1998). Bioactive glass was used in the treatment of intrabony defects in patients with generalized aggressive periodontitis (Mengel et al., 2006), in patients with moderate to advanced periodontitis with excellent outcome in mandibular molar Class II furcations (Yukna et al., 2001), molar furcation invasions (Anderegg et al., 1999), periodontal intrabony defects (Zamet et al., 1997) and in experimental periodontal wound healing in animal model (Karatzas et al., 1999). The effects of a recombinant mouse amelogenin (rM179) on the growth of apatite crystals nucleated on a bioactive glass (45S5 type Bioglass) surface were investigated with a view to gaining a better understanding of the role of amelogenin protein in tooth enamel formation and of its potential application in the design of novel enamel-like biomaterials (Wen et al., 1999). A fibre-reinforced bioglass composite is a promising material for dental applications where fibre significantly increases strength and toughness (Gheysen et al., 1983). PerioGlas, a silicate-based synthetic biomaterial was used for regeneration of peri-implant infrabony defects where new bone eventually reaches the implant, and osseointegration occurs with incorporation of the PerioGlas particles (Johnson et al., 1997).

Bioactive glass has been used in cranio-maxillofacial reconstruction especially on the repair of periodontal and alveolar ridge defects (Quinones & Lovelace, 1997; Han et al., 2002; Sy, 2002; Throndson & Sexton, 2002; Norton & Wilson, 2002; Knapp et al., 2003) although its use is also extended for successful reconstruction of other areas of the head and neck (Scotchford et al., 2011). Bioactive glass has been utilized for the repair of orbital floor

fractures with maintenance of globe position (Kinnunen et al., 2000; Aitasalo et al., 2001) and elevation of the floor of the maxillary sinus floor (Tadjoedin et al., 2002) in combination with autogenous iliac bone. Bioactive glass particles (Nova Bone, Porex Surgical) mixed with autogenous bone particles has also been used to cranial vault reconstruction (Gosain, 2003), in clinical studies in the treatment of cystic defects, ridge augmentations, apical resections, extraction sites, periodontal osseous defects and sinus lifts and augmentation (Furusawa T, Mizunuma, 1997; Low et al., 1997; Lovelace et al., 1998; Galindo-Moreno et al., 2008; Klongnoi et al., 2006). Bioactive glass posed some complications when used as a ceramic implant for contour restoration of the facial skeleton.

4. Bioglass as bone graft substitute

The management of fractures remains an incessant challenge for trauma and orthopedic surgeons. Although, majority of fractures heal uncomplicated, 5–10% of patients meet problems due to bone defects or impaired fracture healing, or a combination of both (Einhorn, 1995). Bone grafts fill voids and offer support, and therefore may augment the biological repair of the defect. Bone grafting is a widespread surgical procedure, carried out in approximately 10% of all skeletal reconstructive surgery cases (Schnettler & Markgraf, 1997).

Bone healing differs from any other soft tissue since it heals through the generation of new bone rather than by forming fibrotic tissue. Osteogenesis, osteoinduction, osteoconduction and adequate blood and nutrient supply are the four critical elements of bone regeneration along with the final bonding between host bone and grafting material which is called osteointegration (Hing, 2004). Osteoprogenitor cells living within the donor graft, may survive during transplantation, could potentially proliferate and differentiate to osteblasts and eventually to osteocytes which represent the ''osteogenic'' potential of the graft (Cypher & Grossman, 1996; Giannoudis et al., 2005). ''Osteoinduction'' conversely is the stimulation and activation of host mesenchymal stem cells from the surrounding tissue, which differentiate into bone-forming osteoblasts. This process is mediated by a cascade of signals and the activations of several extra and intracellular receptors the most important of which belong to the TGF-beta superfamily (Urist, 1965; Cypher & Grossman, 1996). Osteoconduction describes the facilitation and orientation of blood-vessel and the creation of the new Haversian systems into the bone scaffold [Burchardt, 1983; Constantino & Freidman, 1994]. At last, ''osteointegration'' describes the surface bonding between the host bone and the grafting material (Constantino & Freidman, 1994).

The most desirable form of bone substitute is the autologous bone graft for their superior osteoconduction, ease of incorporation, lack of immunological reactions, contains living bone cells that offer osteogenesis and growth factors that stimulate osteoinduction (Cypher & Grossman, 1996; Naber et al., 1972; Marciani et al., 1977). However, massive replacements of bone are not easily achieved by bone autografts as autogenous bone is limited in availability, and may result in the donar site morbidity (Mankin et al., 1976). Moreover, harvesting the autograft requires an additional surgery at the donar site that can result in its own 8–39% risk of complications, such as inflammation, risk of extensive blood loss infection, nerve and urethral injury, pelvic instability, cosmetic disadvantages and chronic pain (Banwart et al., 1995; Constantino & Freidman, 1994; Patka et al., 1998; Younger & Chapman, 1989; Summers & Eisenstein, 1989; Ross et al., 2000; Seiler & Johnson, 2000;

Skaggs et al., 2000). Furthermore, autografting is normally not recommended for elderly or pediatric patients or for patients with malignant or infectious disease (Bridwell et al., 1994; Gau et al., 1991; McCarthy et al., 1986). An allograft is preferred in some cases but the possible immune response and disease transmission may be detrimental for the recipient (Asselmeier et al., 1993; Stevenson & Horowitz, 1992; Chapman et al., 1997; Gazdag et al., 1995), so their use is suboptimal.

Despite the benefits of autografts and allografts, the limitations of each have necessitated the pursuit of alternatives biomaterials. The ideal bone composite material with composition and mechanical properties equivalent to that of bone should have adequate biocompatibility, tailorable biodegradability, ability to initiate osteogenesis; in short, the graft should closely mimic the natural bone. Biodegradability together with biocompatibility and suitable mechanical properties are found only in a small group of materials. The aim of the present chapter was to provide a comprehensive overview of literature data of bioactive glass as bone substitutes for use in trauma and orthopedic surgery.

Bioactive glasses exhibit osteoinductive and osteoconductive properties (Giannoudis et al., 2005) and can be manufactured into microspheres, fibers and porous implants. They are bioactive, as they interact with the body. Bioactivity depends upon the SiO2 content; the bonding between bone and glass is most excellent if the bioactive glass contains 45–52% SiO2 (Valimaki & Aro, 2006). The combination of hydroxyapatite with bioglass result in better composite bioactivity and biocompatibility compared to hydroxyapatite alone (Cholewa-Kowalska et al., 2009). They have significantly greater mechanical strength when compared to calcium phosphate preparations. After contact with body fluids, a silicate- rich layer is formed leading to mechanical strong graft–bone bonding. Above this, a hydroxyapatite layer will form, which directs new bone formation together with protein absorption. The extracellular proteins magnetize macrophages, mesenchymal stem cells and osteoprogenitor cells. Consequently, the osteoprogenitor cells proliferate into matrix-producing osteoblasts (Valimaki & Aro, 2006; Hench & Paschall, 1973). Mechanical properties of bioactive glass are not optimal, and therefore other ceramic components are sometimes added to the bioactive glass for reinforcement. Mechanical capability and biological absorbability of SiO(2)-CaO bioactive glass may also be improved by incorporating Na(2)O into bioactive glass, which can result in the formation of a hard yet biodegradable crystalline phase from bioactive glass when sintered by sol-gel process (Chen et al., 2010). In another study, mechanical properties of potassium fluorrichterite ($KNaCaMg(5)Si(8)O(22)F(2)$) glass-ceramics may be improved by either increasing the concentration of calcium (GC5) or by the addition of P(2)O(5) (GP2) that has potential as a load bearing bioceramic for fabrication of medical devices intended for skeletal tissue repair (Bhakta et al., 2010; Bandyopadhyay-Ghosh et al., 2010). A new porous bioactive glass has been developed by foaming with rice husks and sintering at 1050 degrees C for 1 hour that provides sufficient mechanical support temporarily while maintaining bioactivity, and that can biodegrade at later stages is achievable with the developed 45S5 bioglass-derived scaffolds (Wu et al., 2009).

In experimental cancellous bone defects in rat models, bioactive glass was found biocompatible, and the filler effect was greater with bioactive glass than with autogenous bone (Heikkila et al., 1995). Bioglass was found to trigger new bone formation by allogenic demineralized bone matrix, and the biocompatibility of the glass was verified by the absence of adverse cellular reactions (Erdemli et al., 2010; Pajamaki et al., 1993a, 1993b).

Biocompatibility and osteogenesis of biomimetic bioglass-collagen composite scaffolds alone and in combination with phosphatidylserine were also studied and confirmed that the composite scaffolds fulfill the basic requirements of bone tissue engineering scaffold and have the potential to be applied in orthopedic and reconstructive surgery (Marelli et al., 2010; Xu et al., 2011). Addition of hyaluronic acid and mesenchymal stem cell in the aforesaid scaffold further enhanced the healing of the bone defect (Xu et al., 2010). Bone-bonding response significantly enhanced with the micro-roughening of the bioactive glass surface, but the glass composition affected the intensity of the response (Itala et al., 2003). Bioactive glass have shown no or only mild inflammatory responses in the surrounding tissue in histological in vivo studies and in 6 months, the glass fiber scaffolds are completely resorbed (Moimas et al., 2006). In an experimental critical size bone defect model in goat, porous bioactive glass promoted bone formation over the extension of the defect and offers interesting potential for orthopedic reconstructive procedures (Nandi et al., 2009). Bioglass has been investigated extensively in bone tissue engineering but there has been relatively little previous research on its application to soft-tissue engineering. In a study, bioactive glass incorporated into scaffold was able to increase neovascularization that is extremely beneficial during the engineering of larger soft-tissue constructs (Day et al., 2004). Irrespective of soft and hard tissue healing necessitates enhanced neovascularization which can be induced by localized low concentration bioglass delivery and may offer an alternative approach to costly growth factors and their potential side-effects in bone regeneration (Leu et al., 2009).

The first reports on clinical applications of bioactive glass materialize in the 1980s (Reck, 1981). Screw augmentation with bioactive glass was evaluated in 37 Weber type B ankle fractures with no information of screw loosening within a period of 2 years (Andreassen et al., 2004). Bioactive glass have been clinically used in vertebroplasty (Middleton et al., 2008; Palussiere et al., 2005), treatment of an unstable distal radius fracture (Smit et al., 2005), tympanoplastic reconstruction (Reck, 1983), as filling material in benign tumour surgery (Heikkila et al., 1995), for reconstruction of defects in facial bones [Suominen & Kinnunen, 1996], for treatment of periodontal bone defects (Villaca et al., 2005; Leonetti et al., 2000), in obliteration of frontal sinuses (Suonpaa et al., 1997; Peltola et al., 2000a, 2000b), in repairing orbital floor fractures (Kinnunen et al., 2000; Aitasalo et al., 2001), in lumbar fusion (Ido et al., 2000), reconstruction of the maxillary sinus (Scala et al., 2007), in cementless metal-backed acetabular cups (Hedia et al., 2006) and for reconstruction of the iliac crest defect after bone graft harvesting (Asano et al., 1994). The combination of a thermoplastic, viscous carrier with a granular bioglass scaffold allowed for the delivery of allergenic mesenchymal stem cells in a clinically manageable form that enhanced bone formation at early stages of canine alveolar repair (Mylonas et al., 2007).

5. Bioactive glass in drug delivery system

In recent years wide spread research has been initiated with new advanced drug delivery systems with better drug control and prolonged action. The drug delivery process is of paramount importance in assuring that a certain molecule will reach without decomposition or secondary reactions at the right place to perform its task with efficiency. The drug is introduced as part of an inert matrix, from which it should be released in a controlled way and where it should be distributed uniformly. Smart delivery systems that can be utilized

for the delivery of antibiotics, insulin, anti-inflammatory drugs, anticancer drugs, hormones and vaccines are yet to be developed, which are responsive to normal physiological process. Significant consideration is paid on the use of microspheres as carriers for proteins and drugs. The main benefit of microspheres over the more traditional macroporous block orthopaedic scaffolds is that microspheres possess not only better drug-delivery properties, but also the potential to fill the bone defects with irregular and complex shapes and sizes (Wu et al., 2004). The interstitial space between the particles of the microspheres is imperative for effective and functional bone regeneration (Malafaya et al., 2008; Luciani et al., 2008; Hsu et al., 1999), as they permit for both bone and vascular ingrowths. Several difficulties are encountered when macromolecules are incorporated in polymer devices e.g. protein drugs when impregnated may denature within the polymer matrix causing a loss of biological activity and probable changes in immunogenicity (Langer, 1990a, 1980b). This may happen due to degradation of the drug by the solvents or the temperature involved in the fabrication of the polymeric devices. Presently, ceramics have gained major recognition as bone substitute materials in dentistry and medicine as ceramics are biocompatible, resorbable and porous, attempts have been made to exploit them as delivery systems for drugs, chemicals and biologicals (Bajpai & Benghuzzi, 1988; Bajpai, 1994; Lasserre & Bajpai, 1998).

5.1 Drug delivery of antibiotics for treatment of osteomyelitis

Treatment of orthopaedic infections with antibacterial agents by oral or intravenous route often leads the clinicians to be distrustful about patient outcome (Walenkamp, 1997); as the condition is frequently associated with poor vascular perfusion accompanied by infection of the surrounding tissue (Mader et al., 1993). Subsequent to surgical debridement, it is essential to maintain a highly effective concentration of the antibiotic in the infected area for a sufficient period of time (usually 4–6 weeks) to allow the healing process to complete (Kanellakopoulou & Giamarellos-Bourboulis, 2000).

Treatment of osteomyelitis with local biodegradable antibiotic delivery systems has become a common practice in orthopaedic surgery. Biodegradable implants could provide high local bactericidal concentrations in tissue for the prolonged time needed to completely eradicate the infection and the likelihood to match the rate of implant biodegradability according to the type of infection treated (Kanellakopoulou & Giamarellos-Bourboulis, 2000). Biodegradation also makes surgical removal of the implant unnecessary. The implant can also be used initially to obliterate the dead space and, eventually to guide its repair. Porous block of bioactive glass has been studied for drug delivery applications of antibiotics for treatment of osteomyelitis in animal model (Nandi et al., 2009; Kundu et al., 2011). The glass ceramic block exists in two forms: one with porosity of 20-30 % and the other of 70 %. Excellent results were observed in infected arthroplasty after 2 years of treatment and the implanted material triggered osteogenesis so as to produce a complete radiological replacement of the osseous defect (Kawanabe et al., 1998). It has been observed that locally produced pure or bioglass reinforced plaster of Paris, hydroxyapatite and sodium alginate with cephazoline antibiotic are promising biomaterials for treatment of osteomyelitis and mainly because of economical reasons and availability, may be an alternative in clinical practice, especially for developing countries (Heybeli et al., 2003). Glass reinforced hydroxyapatite with sodium ampicillin, a broad spectrum antibiotic has been successfully applied for treatment of periodontitis (Queiroz et al., 2001). Gentamicin sulfate impregnated bioactive SiO2-CaO-P2O5 glass implants are good carriers for local gentamicin release into

the local osseous tissue, where they show excellent biocompatibility and bone integration. Moreover, these implants are able to promote bone growth during the resorption process (Mes eguer-Olmo et al., 2006; Arcos et al., 2001). Antimicrobial activity of bioactive glass (BG) as a controlled release device for tetracycline hydrochloride and an inclusion complex formed by tetracycline and b-cyclodextrin has been investigated in mice model where there is prolonged period of release of antibiotic due to presence of cyclodextrin. It has been observed that there was an initial burst of 12%, followed by a sustained release over 80 days and a total release of 22–25%. (Dominguesa et al., 2004). The effectiveness of a degradable and bioactive borate glass has been compared with the clinically used calcium sulfate in the treatment of osteomyelitis of rabbits, as a carrier for vancomycin and proved to have excellent biocompatibility and to be very effective in eradicating osteomyelitis and simultaneously stimulating bone regeneration, avoiding the disadvantages of vancomycin loaded calcium sulphate (Zongping et al., 2009). Chitosan-bonded mixture of borate bioactive glass particles with teicoplanin (antibiotic) combining sustained drug release with the ability to support new bone ingrowth, could provide a method for treating chronic osteomyelitis *in vitro* and *in vivo* (Wei-Tao et al., 2010; Xin et al., 2010). In another study, well-ordered mesoporous bioactive glass impregnated with gentamycin has been carried out *in vitro* as a bioactive drug release system for preparation of bone implant materials vis-à-vis treatment of osteomyelitis (Xia & Chang, 2006; Zhu & Kaskel, 2009). Mesoporous bioactive glass (MBGs) with different compositions impregnated tetracycline has been prepared and their drug release behaviors have been studied (Zhao et al., 2008). Recently, an unique multifunctional bioactive composite scaffold mainly 45S5 Bioglass-based glass–ceramic scaffolds has been investigated with the potential to enhance cell attachment and to provide controlled delivery of gentamicin for bone tissue engineering (Francis et al., 2010). Composite materials composed of borate bioactive glass and chitosan (designated BGC) were investigated *in vitro* and *in vivo* as a new delivery system for teicoplanin in the treatment of chronic osteomyelitis induced by methicillin-resistant *Staphylococcus aureus* (MRSA) and demonstrated that this system is effective in treating chronic osteomyelitis by providing a sustained release of teicoplanin, in addition to participating in bone regeneration (Jia et al., 2010).

5.2 Bioactive glass delivery of growth factors

Bone regeneration is a coordinated cascade of events regulated by several hormones, cytokines and growth factors (Carano & Filvaroff, 2003; El-Ghannam, 2005; Hsiong & Mooney, 2000). Bioactive glass is regarded as high-potential scaffolds due to their osteoconductive properties (Thomas et al., 2005). The bone bonding ability is based on the chemical reactivity of the bioactive glass in which silicon bonds are broken and finally a CaP-rich layer is deposited on top of the glass which crystallizes to hydroxycarbonate apatite (HCA). To improve the biodegradability of this implant, porosity is introduced (Karageorgiou & Kaplan, 2005) which also helps to bone ingrowth, though pore sizes should be large enough. This porosity is occasionally called macroporosity while the bioglass implants can encompass a micro or nanoporosity of their own. Interconnectivity of the pores is of paramount necessity for tissue engineered bone constructs which implies generation of overlapping pore connection into the scaffolds. In bone tissue engineering growth factors are also introduced to accelerate tissue ingrowth. However, due to variation in potency and efficacy of individual growth factors, each study claimed different levels of bone healing. Growth factors like bone morphogenic protein-2&7 (BMP-2&7), transforming growth factor

(TGF-β), basic fibroblast growth factor (bFGF), insulin like growth factor-1&2 (IGF-1&2) and vascular endothelial growth factor (VEGF) are commonly introduced into these scaffolds due to their osteoinductive properties and vascularization (Seeherman & Wozney, 2005; Ginebra et al., 2006; Jansen et al., 2005). This increases the clinical significant amount high above normal values inside the human body and increases the cost of a single implant considerably, therefore diminishing a possible use of the material. The most appropriate technique for growth factor delivery is still under debate. Bioactive glass stimulates fibroblasts to secrete significantly increased amounts of angiogenic growth factors and can induce infiltration of a significantly increased number of blood vessels into tissue engineering scaffolds (Day, 2005; Day et al., 2004). Therefore it has a number of potential applications in therapeutic angiogenesis (Keshaw et al., 2005).
PLGA polymeric system coated bioactive glass with VEGF has been investigated in the rat critical-sized defect with resultant enhanced angiogenesis and additive bone healing effects (Leach et al., 2006). An additional study in which BMP-4 and VEGF were concertedly delivered confirmed that combination of two growth factors promoted greater bone formation as compared to single factor treatment group (Huang et al., 2005). These results delineate a promising approach to enhance bone healing in hypovascularized defects that commonly occur after removal of bone tumors by radiation therapy. Sol-gel silica-based porous glass (xerogel) was used as a novel carrier material for recombinant human transforming growth factor-β1 (TGF-β1) and is capable of eliciting bone tissue reactivity that may serve as an effective bone graft material for the repair of osseous defects (Nicoll et al., 1997). A delivery system consisting of collagen Type I gel, Recombinant human BMP-2 (rhBMP-2) and 45S5 Bioglass microspheres seem to be a promising system for bone regeneration (Bergeron et al., 2007). Bovine bone morphogenetic protein has been delivered in bioactive glass on demineralized bone matrix grafts in the rat muscular pouch with effective outcome (Pajamaki et al., 1993).

6. Bioglass as coating of implants

In the present days, metallic materials gained considerable dimension as medical and dental devices due to their mechanical properties (Roessler et al., 2002). Implants are usually prepared of metals such as titanium alloys, cobalt alloys and SS 316L (García et al., 2004). The need to diminish costs in public health services has constrained the use of SS as the most economical option for orthopedic implants (Meinert et al., 1998; Fathi et al., 2003), because of its comparative low cost, ease of fabrication, ready availability and reasonable corrosion resistance. However, this material is prone to localized attack in long term use due to the hostile biological effects (Yılmaz et al., 2005). Besides, the corrosion of the metallic implants is imperative because it could adversely affect the biocompatibility and the mechanical integrity. Large concentrations of metallic cations coming from the implant can result in biologically unwanted reactions and might lead to the mechanical failure of the implant. Titanium and Ti-alloys are commonly used materials for *in vivo* applications, due to their good physical and mechanical properties such as low density, high corrosion resistance and mechanical resistance. Nevertheless, titanium and other alloying metal ions as aluminium and vanadium, release from the implants being accumulated in the nearby tissues, due to the aggressive action of the biological fluids (Hodgson et al., 2002; Zaffe et al., 2003; Yue et al., 2002; Finet et al., 2000; Milosev et al., 2000). The lack of interaction with the biological environment prevents the implant from integrating with the surrounding hard tissue.

The perfection of the interface between bone and orthopaedic or dental implants is still considered as a challenge because the formation and maintenance of viable bone closely apposed to the surface of biomaterials are indispensable for the stability and clinical success of non-cemented orthopaedic/dental implants. It has been addressed to create a suitable environment where the natural biological potential for bone functional regeneration can be encouraged and maximized (Carlsson et al., 1994; Wennerberg et al., 1996; Larsson et al., 1996; Buser et al., 1998). Implant osseointegration depends on various factors viz. surface structure, biomechanical factors and biological response (Carlsson et al., 1994; Chappard et al., 1999). At the present time, osseointergation is defined not only as the absence of a fibrous layer around the implant with an active response in terms of integration to host bone, but also as a chemical (bonding osteogenesis) or physico-chemical (connective tissue osteogenesis) bond between implant and bone (Branemårk et al., 1983; Albrektsson, 1993) which in turn, depends on the biomineralization into the surrounding tissue. Biomineralization is normally happens when the bony injury or normal bone tissue in cellular level takes place. The process starts with the osteolysis through the osteoclastic cells from the vicinity as well as from the systemic source. This is instantaneously followed by formation of a protein-rich matrix in the localized area (injury site) which ultimately being mineralized with the inorganic ions viz. calcium and phosphorous from the serum and the localized tissues. Once the nucleation of bone formation takes place at a very faster rate (approx. 10 days), then routinely further bone formation with the incorporation of above-mentioned inorganic ions are found from the serum (Weiner, 1986). Further, implant loosening/migration is an unanswered complication associated with internal fixation. This problem may be overcome by modifying the implant/bone interface for improved osseous integration. Improved osseous integration may be obtained by the use of hydroxyapatite (HAp), b-tri calcium phosphate (b-TCP) and their composite coatings as nominally HAp to enhance the osteoconductivity of metallic implant (Thomas et al., 1987; Filiaggi, et al., 1991; Rivero et al., 1988). These coatings have been shown to promote osseointegration by stimulating bone growth onto the surface (Dey et al., 2011).

Apart from calcium phosphate coating of metallic implants, extensive research has been initiated with bioglass as coatings for metallic implants because of their controlled surface reactivity and good bone bonding ability (Hench and Andersson, 1993; Hench, 1993; Ferraris et al., 1996). These coatings accomplish two purposes: improving the osseointegration of the implants, and shielding the metal against corrosion from the body fluids and the tissue from the corrosion products of the alloys. Unfortunately, most of the attempts to coat metallic implants with bioactive glass have had poor success. The explanation behind is due to poor adhesion of the coating and/or degradation of the glass properties during the coating procedure (typically enameling, or flame or plasma spray coating) (Hench & Andersson, 1993). Bioactive glass can be used to coat titanium alloys by different methods such as conventional enamelling, sputtering techniques, vacuum plasma spray and subsonic thermal spraying technique (STS) (Ferraris et al., 1996; Verné et al., 2000; Jana et al., 1995; Gomez-Vega et al., 2000; Li et al., 2007). These implants can offer several advantages, in terms of the high mechanical properties of the metallic substrate combined with the bioactivity of the coating aside from good protection of the substrate from corrosion. Bioactive glass and nanohydroxyapatite (BG-nHA) on titanium-alloy orthopaedic implants and surrounding bone tissue in vivo was evaluated and observed that these coatings could enhance the osteointegration of orthopaedic implant (Xie et al., 2010). Bioglass coating of the three-dimensional Ti scaffolds by the radio frequency magnetron sputtering technique

determines an in vitro increase of the bone matrix elaboration and may potentially have a clinical benefit (Saino et al., 2010). Biocompatible yttrium-stabilized zirconia (YSZ) in the form of nanoparticles and bioactive Bioglass (45S5) in the form of microparticles were used to coat Ti6Al4V substrates by electrophoretic deposition with potential applications in the orthopedics (Radice et al., 2007). Fluorapatite glass LG112 can be used as a sputtered glass coating on roughened surfaces of Ti6Al4V for possible future use for medical implants (Bibby et al., 2005). However, the Ti-alloys used in the fabrication of prosthetic implants are very reactive, and the glass/metal reactions that occur during firing are unfavorable to adhesion and bioactivity. Thus, coating titanium with bioactive glass is challenging. Besides, tremendous care should be taken in storing and/or shipping HA- or BG-coated Ti6A14V implants due to loss of bonding strength in low and high humidity (Chern et al., 1993). Bioactive glass comprising of SiO_2-Na_2O-K_2O-CaO-MgO-P_2O_5 system has been formulated to coat orthopedic metallic implants by enameling and now have been utilized for coatings on commercial dental implants approximately 100 μm thick (Lopez-Esteban et al., 2003). Due to the peculiar softening properties of these materials, bioactive glass and glass-ceramics do imply a good alternative to hydroxyapatite, commonly used as bioactive coating on metallic prostheses in order to improve their adhesion to the bone. Further, bioglass coated implants exhibited greater bone ingrowth compared to hydroxyapatite coated and control implants in animal model and they maintained their mechanical integrity over time (Wheeler et al., 2001). In a study, multilayered bioactive glass-ceramic coatings on a Ti6Al4V alloy screws was conducted for dental applications with layers of controlled thickness (Verné et al., 2004). A biocompatible composite implant system was developed by coating bioglass onto cobalt-chromium alloy substrates where thin, adherent bioglass coating provides the ability of bonding directly to bone, while the underlying metal substrate gives the composite implants adequate strength to be used in load bearing applications (Lacefield & Hench, 1986). Improvement of the alumina/bone interface in Alumina on alumina total hip arthroplasty can be done by coating with sol-gel derived bioactive glass (Hamadouche et al., 2000). Polyurethane (PUR) and polyurethane/poly(d, l-lactide) acid (PUR/PDLLA) based scaffolds coated with Bioglass particles have potential to be used as bioactive, biodegradable scaffolds in bone tissue engineering (Bil et al., 2007).

7. Bioactive glasses' in biomolecular engineering with special referencing to third generation biomaterials

Third generation biomaterials should be biocompatible, resorbable, and also bioactive eliciting specific cellular responses at the molecular level (Hench & Polak, 2002). Three-dimensional porous structures that stimulate cells' invasion, attachment and proliferation, as well as functionalized surfaces with peptide sequences that mimic the ECM components so as to trigger specific cell responses are being developed (Agrawal & Ray, 2001; Hutmacher et al., 1996; Temenoff & Mikos, 2000).

Tissue engineering applications and development of third generation biomaterials emerged at the same time. Tissue engineering is the promising therapeutic approach that combines cells onto resorbable scaffolds for in situ tissues regeneration and has emerged as an alternative potential solution to tissue transplantation and grafting. Tissue engineering is a multidisciplinary field that applies principles of life sciences and engineering towards the development of biological substitutes employing three fundamental "tools", namely cells, scaffolds and growth factors (GFs) for the restoration, maintenance or improvement of

tissue form and function (Langer & Vacanti, 1993). The common limitations associated with the application of allografts, autografts and xenografts include donor site insufficiency, rejection, diseases transfer, harvesting costs and post-operative morbidity (Fernyhough et al., 1992; Banwart et al., 1995; Goulet et al., 1997). Tissue engineering and regenerative medicine has made a new horizon in repairing and restoring organs and tissues using the natural signaling pathways and components such as stem cells, growth factors and peptide sequences among others, in amalgamation with synthetic scaffolds (Hardouin et al., 2000). Apart from the basic tissue engineering triad (cells, signaling and scaffold), angiogenesis and nutrients delivery should be taken into account as they both play vital role to stimulate tissue regeneration. Although tissue engineering emerged as a very dazzling option to overcome many existing problems related to the current use of autografts, allografts and xenografts, its implementation as part of a routine treatment for tissue replacement is controversial. Despite such limitations, tissue engineering is a very promising approach that opens newer vista of study and research in the field of regenerative medicine.

Scaffolds of three-dimensional porous structures need to achieve the following criteria in order to be used in tissue engineering [Spaans et al., 2000; Boccaccini et al., 2008].

- must be biocompatible and bio-resorbable at a controllable degradation and resorption rate as well as provide the control over the appropriation
- must possess well defined microstructure with an interconnected porous network, formed by a combination of macro and micro pores to allow proper tissue ingrowth, vascularization and nutrient delivery.
- must have proper mechanical properties to regenerate bone tissue in load-bearing sites.
- must keep its structural integrity during the first stages of the new bone formation.

The amalgamation of bioactivity and biodegradability is most likely the pertinent characteristics that include third-generation biomaterials. The bioactivation of surfaces with specific biomolecules is an influential means that allows cell guidance and stimulation towards a particular response. The endeavor is to mimic the ECM environment and function in the developed scaffold by coupling specific cues in its surface. Thus, cell behavior including adhesion, migration, proliferation and differentiation into a particular lineage will be influenced by the biomolecules attached to the material surface. In addition, pore distribution, interconnectivity and size are of paramount significance in order to assurance of proper cell proliferation and migration, as well as tissue vascularization and diffusion of nutrients.

The concept of using bioactive glass substrates as templates for in vitro synthesis of bone tissue for transplantation by assessing the osteogenic potential has been investigated (Xynos et al., 2000; Phan et al., 2003; Chen et al., 2008; Brown et al., 2008) and confirmed that Bioglass scaffolds have potential as osteoconductive tissue engineering substrates for maintenance and normal functioning of bone tissue (Bretcanu et al., 2009). Human primary osteoblast-like cells cultured in contact with different bioactive glass suggested that bioglass not only induces osteogenic differentiation of human primary osteoblast-like cells, but can also increase collagen synthesis and release. The newly formulated bioactive gel-glass seems to have potential applications for tissue engineering, inducing increased collagen synthesis (Bosetti et al., 2003; Jones et al., 2007). Bone marrow is a combination of hematopoietic, vascular, stromal and mesenchymal cells capable of skeletal repair/regeneration with the ability of bone marrow cells to differentiate into osteoblasts and osteoclasts which is imperative in tissue regeneration during fracture healing, or for successful osteointegration of implanted prostheses, and in bone remodelling. Bone marrow cell culture systems with

bioactive glass seem to be useful and induce osteogenic differentiation and cell mineralization (Bosetti & Cannas, 2005). In another study, bioglass granules in combination with expanded periosteal cells in culture were investigated in rabbit large calvarial defects with increased ossification (Moreira-Gonzalez et al., 2005).

Bioresorbable and bioactive tissue engineering composite scaffolds based on bioactive glass (45S5 Bioglass(R)) particles and macroporous poly(DL-lactide) (PDLLA) and polylactide-co-glycolide (PLAGA) with osteoblasts (HOBs) cells have tremendous potential as scaffolds for guided bone regeneration (Roether et al., 2002; Lu et al., 2005; Yang et al., 2006;), for intervertebral disc tissue repair (Wilda & Gough, 2006; Helen & Gough, 2008). In another study, the cellular response of fetal osteoblasts to bioactive resorbable composite films consisting of a poly-D,L-lactide (PDLLA) matrix and bioactive glass 45S5 particles in the absence of osteogenic factors stimulates osteoblast differentiation and mineralization of the extracellular matrix, demonstrating the osteoinductive capacity of the composite (Tsigkou et al., 2007).

Revision cases of total hip implants are complicated by the considerable amount of bone loss. New materials and/or approaches are desirable to provide stability to the site, stimulate bone formation, and eventually lead to fully functional bone tissue. Porous bioactive glass have been developed as scaffolds for bone tissue engineering. The incorporation of tissue-engineered constructs utilizing these scaffolds seeded with osteoprogenitor cells or culture expanded to form bonelike tissue on the scaffold prior to implantation has been conducted in large, cortical bone defects in the rat (Livingston et al., 2002).

Bioglass-incorporated alginate hydrogels encapsulated with murine embryonic stem cells have potential implications and applications for tissue engineering where bioglass substrates could be used for the production of bioengineered bone both in vitro and in vivo and bioglass-incorporated alginate hydrogels can be injected directly into the defect area (Zhang et al., 2009). One of the major factors in the therapeutic accomplishment of bone tissue engineered scaffolds is the capacity of the construct to vascularise after implantation. For improving vascularization, porous bioactive glass-ceramic construct combination of co-culture human umbilical vein endothelial cells (HUVECS) with human osteoblasts (HOBS) may promote vascularization and facilitate tissue regeneration (Deb et al., 2010).

8. Conclusion

During the past decades, there has been a major breakthrough in development of biomedical materials including various ceramic materials for bone and dental repair as well as implantable drug delivery systems. Both increases in life expectancy and the social obligations to provide a better quality of life appeared to be the vital factors to this development. Significant attention has been paid towards the use of synthetic graft materials in bone tissue and dental repair and development of new implant technologies has led to the design concept of novel bioactive materials. Bioactive glass inducing active biomineralization in vivo have been a high demand in the development of clinical regenerative medicine. Originally, it was thought for bone repair and bone regeneration via tissue engineering (TE), but eventually has become a very attractive biomaterials of choice having implications in: dental, maxillofacial and ear implants, drug delivery system, injectable for treatment of enuresis, to activate genes for maintaining the health of tissues as they age, third generation TE scaffolds for soft connective tissue regeneration and repair,

hybrid inorganic/organic bioactive scaffolds, anti-microbial effect for wound dressing, molecular modeling of the interaction of surface sites with amino acids, coating of metallic implants, effective carriers of growth factors, bioactive peptides etc.. In the coming future, bioactive glass may be explored by the scientists/researchers/clinicians in a better way and dimension for wellbeing of human kind.

9. References

Agrawal, CM. & Ray, RB. (2001). Biodegradable polymeric scaffolds for musculoskeletal tissue engineering. *Journal of Biomedical Materials Research*, 55(2): 141-150

Aina, V., Malavasi, G., Fiorio Pla, A., Munaron, L. & Morterra, C. (2009) 'Zinc-containing bioactive glasses: Surface reactivity and behaviour towards endothelial cells', *Acta Biomaterialia*, 5(4): 1211-1222.

Aitasalo, K., Kinnunen, I., Palmgren, J. & Varpula, M. (2001). Repair of orbital floor fractures with bioactive glass implants. *J. Oral. Maxillofac. Surg.,* 59(12):1390-1395.

Albrektsson, T. (1993). On long-term maintenance of the osseointegrated response. *Australian Pros. J.*, 7: 15-24.

Anderegg, C.R., Alexander, D.C. & Freidman, M. (1999). A bioactive glass particulate in the treatment of molar furcation invasions. *J. Periodontol.,* 70(4):384-7.

Anderson, O.H., Liu, G., Kangasniemi, K. & Juhanoja, J. (1992). Evaluation of the acceptance of glass in bone. Journal of Materials Science: *Materials in Medicine,* 3(2):145-150.

Andersson, O.H., Karlsson, K.H., Kangasniemi, K. & Xli-Urpo, A. (1988). Models for physical properties and bioactivity of phosphate opal glasses. *Glastechnische Berichte*, 61(10):300-305.

Andersson, Ö.H., Liu, G., Kangasniemi, K. & Juhanoja, J. (1992) 'Evaluation of the acceptance of glass in bone', *Journal of Materials Science: Materials in Medicine*, 3(2): 145-150.

Andersson, Ö.H., Liu, G., Karlsson, K.H., Niemi, L., Miettinen, J. & Juhanoja, J. (1990) 'In vivo behaviour of glasses in the SiO_2-Na_2O-CaO-P_2O_5-Al_2O_3-B_2O_3 system', *Journal of Materials Science: Materials in Medicine*, 1(4): 219-227.

Andreassen, G.S., Hoiness, P.R., Skraamm, I., Granlund, O. & Engebretsen, L. (2004). Use of a synthetic bone void filler to augment screws in osteopenic ankle fracture fixation. *Arch. Orthop. Trauma. Surg*., 124:161–5.

Arcos, D., Ragel, CV. & Vallet-Regí, M. (2001). Bioactivity in glass/PMMA composites used as drug delivery system. *Biomaterials*, 22(7): 701-708

Asano, S., Kaneda, K., Satoh, S., Abumi, K., Hashimoto, T. & Fujiya, M. (1994). Reconstruction of an iliac crest defect with a bioactive ceramic prosthesis. *Eur. Spine J.*, 3(1):39-44.

Asselmeier, M.A., Caspari, R.B. & Bottenfield, S. (1993). A review of allograft processing and sterilization techniques and their role in transmission of the human immunodeficiency virus. *Am. J. Sports Med*., 21:170–5.

Baino, F., Verné, E. & Vitale-Brovarone, C. (2009) '3-D high-strength glass-ceramic scaffolds containing fluoroapatite for load-bearing bone portions replacement', *Materials Science and Engineering: C*, 29(6): 2055-2062.

Bajpai, PK. (1994). Using ceramics as drug delivery devices. *Biomedical Engineering - Applications, Basis and Communications,* 6(4): 64-70.

Bajpai, PK. & Benghuzzi HA. (1988). Ceramic systems for long-term delivery of chemicals and biologicals. *Journal of Biomedical Materials Research*, 22(12): 1245-1266.

Bakry, A.S., Takahashi, H., Otsuki, M., Sadr, A., Yamashita, K. & Tagami, J. (2011). CO2 laser improves 45S5 bioglass interaction with dentin. *J. Dent. Res.*, 90(2):246-50.

Balamurugan, A., Balossier, G., Laurent-Maquin, D., Pina, S., Rebelo, A.H.S., Faure, J. & Ferreira, J.M.F. (2008) 'An in vitro biological and anti-bacterial study on a sol-gel derived silver-incorporated bioglass system', *Dental Materials*, 24(10): 1343-1351.

Balamurugan, A., Balossier, G., Michel, J., Kannan, S., Benhayoune, H., Rebelo, A.H.S. & Ferreira, J.M.F. (2007) 'Sol gel derived SiO_2-CaO-MgO-P_2O_5 bioglass system - Preparation and *in vitro* characterization', *Journal of Biomedical Materials Research Part B: Applied Biomaterials*, 83B(2): 546-553.

Bandyopadhyay-Ghosh, S., Faria, P.E., Johnson, A., Felipucci, D.N., Reaney, I.M., Salata, L.A., Brook, I.M. & Hatton, P.V. (2010). Osteoconductivity of modified fluorcanasite glass-ceramics for bone tissue augmentation and repair. *J. Biomed. Mater. Res. A.*, 94(3):760-8.

Banwart, JC., Asher, MA. & Hassanein, RS. (1995). Iliac crest bone graft harvest donor site morbidity. A statistical evaluation. *Spine*, 20(9): 1055-1060.

Barone, C.M. & Jimenez, D.F. (1997). Split-thickness calvarial grafts in young children. *The Journal of craniofacial surgery*, 8(1):43-47.

Bellantone, M., Williams, H.D. & Hench, L.L. (2002). 'Broad-Spectrum Bactericidal Activity of Ag_2O-Doped Bioactive Glass', *Antimicrob. Agents Chemother.*, 46(6): 1940-1945.

Bergeron, E., Marquis, ME., Chrétien, I. & Faucheux, N. (2007). Differentiation of preosteoblasts using a delivery system with BMPs and bioactive glass microspheres. *J. Mater. Sci. Mater. Med.* 18(2): 255-63.

Berry, C.C., Dalby, M.J., Oreffo, R.O.C., McCloy, D. & Affrosman, S. (2006) 'The interaction of human bone marrow cells with nanotopographical features in three dimensional constructs', *Journal of Biomedical Materials Research Part A*, 79A(2): 431-439.

Bhakta, S., Pattanayak, D.K., Takadama, H., Kokubo, T., Miller, C.A., Mirsaneh, M., Reaney, I.M., Brook, I., van Noort, R. & Hatton, P.V. (2010). Prediction of osteoconductive activity of modified potassium fluorrichterite glass-ceramics by immersion in simulated body fluid. *J. Mater. Sci. Mater. Med.,* 21(11):2979-88.

Bibby, JK., Bubb, NL., Wood DJ. & Mummery, PM. (2005). Fluorapatite-mullite glass sputter coated Ti6Al4V for biomedical applications. *J. Mater. Sci. Mater. Med.*, 16(5): 379-85.

Bil, M., Ryszkowska, J., Roether, JA., Bretcanu, O. & Boccaccini, AR. (2007). Bioactivity of polyurethane-based scaffolds coated with Bioglass. *Biomed. Mater.,* 2(2): 93-101.

Blaker, J.J., Nazhat, S.N. & Boccaccini, A.R. (2004) 'Development and characterisation of silver-doped bioactive glass-coated sutures for tissue engineering and wound healing applications', *Biomaterials*, 25(7-8): 1319-29.

Boccaccini, A.R. (2005) 'Ceramics', in Hench, L.L. & Jones, J.R. (Eds.): *Biomaterials, Artificial Organs and Tissue Engineering*, Woodhead Publishing Limited CRC Press, Cambridge, U. K., pp. 26-36.

Boccaccini, A.R. & Blaker, J.J. (2005). 'Bioactive composite materials for tissue engineering scaffolds', *Expert Review of Medical Devices*, Vol. 2, No. 3, pp. 303-317.

Boccaccini, A.R., Chen, Q., Lefebvre, L., Gremillard, L. & Chevalier, J. (2007) 'Sintering, crystallisation and biodegradation behaviour of Bioglass (R)-derived glass-ceramics', *Faraday Discussions*, 136: 27-44.

Boccaccini, AR., Roelher, JA., Hench, LL., Maquet, V. & Jérome, RA. (2008). Composites approach to tissue engineering. 26th Annual Conference on Composites, Advanced Ceramics, Materials, and Structures: B: *Ceramic Engineering and Science Proceedings*, 23(4): 805-816.

Bosetti, M. & Cannas, M. (2005). The effect of bioactive glasses on bone marrow stromal cells differentiation. *Biomaterials*, 26(18): 3873-9.

Bosetti, M., Zanardi, L., Hench, L. & Cannas, M. (2003). Type I collagen production by osteoblast-like cells cultured in contact with different bioactive glasses. *J. Biomed. Mater. Res. A.*, 64(1): 189-95.

Bovo, N. (2007) 'Structure-properties relationships in bioactive glasses for PAA-based polyalkenoate cements': *Departament de Ciència dels Materials i Enginyeria Metallúrgica*, Universitat Politècnica de Catalunya, Barcelona, Spain.

Brandao-Burch, A., Utting, JC., Orriss, IR. & Arnett, TR. (2005). Acidosis inhibits bone formation by osteoblasts in vitro by preventing mineralisation. *Calcified Tissue International*, 77: 167-174.

Branemårk, PI., Adell, R., Albrektsson, T., Lekholm, U., Lundkvist, S. & Rockler, B. (1983). Osseointegrated titanium fixtures in the treatment of endentulosness. *Biomaterials,* 4: 25-28.

Bretcanu, O., Misra, S., Roy, I., Renghini, C., Fiori, F., Boccaccini, AR. & Salih, V. (2009). In vitro biocompatibility of 45S5 Bioglass-derived glass-ceramic scaffolds coated with poly(3-hydroxybutyrate). *J. Tissue Eng. Regen. Med.,* 3(2): 139-48.

Bretcanu, O., Samaille, C. & Boccaccini, A. (2008) 'Simple methods to fabricate Bioglass andlt;sup>®</sup>-derived glass–ceramic scaffolds exhibiting porosity gradient', *Journal of Materials Science*, 43(12): 4127-4134.

Bridwell, KH., O'Brien, MF., Lenke, LG., Baldus, C. & Blanke, K. (1994). Posterior spinal fusion supplemented with only allograft bone in paralytic scoliosis. Does it work? *Spine*, 19: 2658—66.

Brink, M. (1997). The influence of alkali & alkaline earths on the working range for bioactive glasses. *Journal of biomedical materials research*, 36(1):109-117.

Brink, M., Turunen, T., Happonen, R.P. & Yli-Urpo, A. (1997). Compositional dependence of bioactivity of glasses in the system Na2O-K2O-MgO-CaO-B2O3-P2O5-SiO2. *Journal of biomedical materials research*, 37(1):114-121.

Brown, R.F., Day, D.E., Day, T.E., Jung, S., Rahaman, M.N. & Fu, Q. (2008) 'Growth and differentiation of osteoblastic cells on 13-93 bioactive glass fibers and scaffolds', *Acta Biomaterialia*, Vol. 4(2): 387-396.

Brunner, T.J., Grass, R.N. & Stark, W.J. (2006) 'Glass and bioglass nanopowders by flame synthesis', *Chemical Communications*, 13: 1384-1386.

Burchardt, H. (1983). The biology of bone graft repair. *Clin. Orthop. Relat. Res.*, 174: 28–42.

Buser, D., Nydegger, T., Hirt, HP., Cochran, DL. & Nolte, LP. (1998). Removal torque values of titanium implants in the maxilla of miniature pigs. *Int. J. Oral Maxillofac. Implants,* 13: 611-619.

Cannillo, V. & Sola, A. (2009) 'Potassium-based composition for a bioactive glass', *Ceramics International*, 35(8): 3389-3393.

Carano, RA. & Filvaroff, EH. (2003). Angiogenesis and bone repair, *Drug Discov. Today* 8: 980–989.

Carlsson, L., Regner, L., Johansson, C., Gottlander, M. & Herberts, P. (1994). Bone response to hydroxyapatite-coated and commercially pure titanium implants in the human arthritic knee. *J. Orthop. Res*., 12: 274-285.

Chapman, M.W., Bucholz, R. & Cornell, C. (1997). Treatment of acute fracture with collagen-calcium phosphate graft material. *J. Bone Joint Surg*., 79-A: 143-147.

Chappard, D., Aguado, E., Huré, G., Grizon, F. & Basle, MF. (1999). The early remodeling phases around titanium implants: a histomorphometric assessment of bone quality in a 3- and 6-month study in sheep. *Int. J. Oral. Maxillofac. Implants*, 14: 189-196.

Chatzistavrou, X., Hatzistavrou, E., Kantiranis, N., Papadopoulou, L., Kontonasaki, E., Chrissafis, K., Petros, K., Konstantinos, M., Paraskevopoulos, A. & Boccaccini, R. (2009). Novel glass-ceramics for dental application by sol-gel technique. *Key Engineering Materials*, 396-398: 153-156.

Chen, Q., Rezwan, K., Armitage, D., Nazhat, S. & Boccaccini, A. (2006a) 'The surface functionalization of 45S5 Bioglass (R)-based glass-ceramic scaffolds and its impact on bioactivity', *Journal of Materials Science: Materials in Medicine*, 17(11): 979-987.

Chen, Q.Z., Efthymiou, A., Salih, V. & Boccaccini, A.R. (2008a) 'Bioglass®-derived glass–ceramic scaffolds: Study of cell proliferation and scaffold degradation in vitro', *Journal of Biomedical Materials Research Part A*, 84A (4): 1049-1060.

Chen, Q.Z., Li, Y., Jin, L.Y., Quinn, J.M. & Komesaroff, PA. (2010). A new sol-gel process for producing Na(2)O-containing bioactive glass ceramics. *Acta Biomater.,* 6(10):4143-53.

Chen, Q.-Z., Rezwan, K., Françon, V., Armitage, D., Nazhat, S.N., Jones, F.H. & Boccaccini, A.R. (2007) 'Surface functionalization of Bioglass®-derived porous scaffolds', *Acta Biomaterialia*, 3(4): 551-562.

Chen, Q.Z., Thompson, I.D. & Boccaccini, A.R. (2006b). '45S5 Bioglass®-derived glass-ceramic scaffolds for bone tissue engineering', *Biomaterials*, 27(11): 2414-2425.

Chen, X., Meng, Y., Li, Y. & Zhao, N. (2008b). 'Investigation on bio-mineralization of melt and sol-gel derived bioactive glasses', *Applied Surface Science*, 255(2): 562-564.

Chern, LJ., Liu, ML. & Ju, CP. (1993). Environmental effect on bond strength of plasma-sprayed hydroxyapatite/bioactive glass composite coatings. Technical note. *Dent. Mater*., 9(4): 286-7.

Chim, H. & Gosain, A.K. (2009). Biomaterials in craniofacial surgery: experimental studies and clinical application. *The Journal of craniofacial surgery*, 20(1):29-33.

Cholewa-Kowalska, K., Kokoszka, J., Laczka, M., Niedźwiedzki, L., Madej, W. & Osyczka, A.M. (2009). Gel-derived bioglass as a compound of hydroxyapatite composites. *Biomed. Mater*., 4(5):055007.

Constantino, P.D. & Freidman, C.D. (1994). Synthetic bone graft substitutes. *Otolaryngol. Clin. North Am.,* 27: 1037—73.

Costantino, P.D., Friedman, C.D., Jones, K., Chow, L.C. & Sisson, G.A. (1992). Experimental hydroxyapatite cement cranioplasty. *Plastic and reconstructive surgery*, 90(2):174-185.

Costantino, PD., Chaplin, JM., Wolpoe, ME., Catalano, PJ., Sen, C., Bederson, JB. & Govindaraj, S. (2000). Applications of fast-setting hydroxyapatite cement: cranioplasty. *Otolaryngol Head Neck Surg*., 123(4): 409-412.

Cypher, T.J. (1996). Grossman JP. Biological principles of bone graft healing. *J. Foot Ankle Surg.,* 35: 413–7.

Damien, C.J. & Parsons, J.R. (1991). Bone graft and bone graft substitutes: a review of current technology and applications. *J. Appl. Biomater*., 2(3):187-208.

Day, R.M., Boccaccini, A.R., Shurey, S., Roether, J.A., Forbes, A., Hench, L.L. & Gabe, S.M. (2004). Assessment of polyglycolic acid mesh and bioactive glass for soft-tissue engineering scaffolds. *Biomaterials*, 25(27):5857-66.

Day, RM. (2005). Bioglasss stimulates the secretion of angiogenic growth factors and angiogenesis. *Tissue Eng*., 11(5-6): 768-77.

Day, RM., Boccaccini, AR., Shurey, S., Roether, JA., Forbes, A., Hench, LL. & Gabe, SM. (2004). Assessment of polyglycolic acid mesh and bioactive glass for soft tissue engineering scaffolds. *Biomaterials*, 25 (27): 5857–66.

De Aza, P.N., Luklinska, Z.B., Santos, C., Guitian, F. & De Aza, S. (2003). Mechanism of bone-like formation on a bioactive implant in vivo. *Biomaterials,* 24(8):1437-1445.

De Diego, M.A., Coleman, N.J. & Hench, L.L. (2000). 'Tensile properties of bioactive fibers for tissue engineering applications', *Journal of Biomedical Materials Research*, 53(3): 199-203.

De Groot, K. (1983). *Bioceramics of Calcium Phosphate*. CRC Press, Boca Raton, FL.

De Groot, K. (1988). 'Effect of porosity and physico-chemical properties on the stability, resorption and strength of calcium phosphate ceramics', in Ducheyne, P. & Lemons, J. (Eds.): *Bioceramics: Material Characteristics Versus In Vivo Behaviour*, Annals of New York Academy of Sciences, New York.

De Groot, K. & LeGeros, R.Z. (1988) 'Significance of porosity and physical chemistry of calcium phosphate ceramics', in Ducheyne, P. & Lemons, J. (Eds.): *Bioceramics: Material Charactersitics Versus In Vivo Behaviour*, Annals of New York Academy of Sciences, New York, pp. 268-277.

De Groot, K., Klein, C.P.A.T., Wolke, J.G.C. & De Blieck-Hogervorst, J. (1990) 'Chemistry of calcium phosphate bioceramics', in Yamamuro, T., Hench, L.L. & Wilson, J. (Eds.): *Handbook of Bioactice Ceramics*, CRC Press, Boca Raton, FL, pp. 3-15.

Deb, S., Mandegaran, R. & Di Silvio, L. (2010) 'A porous scaffold for bone tissue engineering/45S5 Bioglass and lt;supandgt;®and lt;/supandgt; derived porous scaffolds for co-culturing osteoblasts and endothelial cells', *Journal of Materials Science: Materials in Medicine*, 21(3): 893-905.

Delben, J., Pimentel, O., Coelho, M., Candelorio, P., Furini, L., Alencar dos Santos, F.b., de Vicente, F.b. & Delben, A. (2009) 'Synthesis and thermal properties of nanoparticles of bioactive glasses containing silver', *Journal of Thermal Analysis and Calorimetry*, 97(2): 433-436.

Deville, S., Saiz, E., Nalla, R.K. & Tomsia, A.P. (2006) 'Freezing as a Path to Build Complex Composites', *Science*, 311(5760): 515-518.

Dey, A., Nandi, SK., Kundu, B., Kumar, C., Mukherjee, P., Roy, S., Mukhopadhyay, AK., Sinha, MK. & Basu, D. (2011). Evaluation of hydroxyapatite and β-tri calcium phosphate microplasma spray coated pin intra-medullary for bone repair in a rabbit model. *Ceramic International*, 37 (4): 1377-1391

Dominguesa, ZR., Cortes, ME., Gomes, TA., Diniz, HF., Freitas, CS. Gomes, JB., Faria, AMC. & Sinisterra, RD. (2004). Bioactive glass as a drug delivery system of tetracycline and tetracycline associated with b-cyclodextrin. *Biomaterials*, 25 (2004): 327–333

Ducheyne, P., Hench, L.L., Kagan, A., 2nd, Martens, M., Bursens, A. & Mulier, J.C. (1980) 'Effect of hydroxyapatite impregnation on skeletal bonding of porous coated implants', *J. Biomed. Mate.r Res.*, 14(3): 225-37.

Ducic, Y. (2001). Three-dimensional alloplastic orbital reconstruction in skull base surgery. *The Laryngoscope*, 111(7):1306-1312.

Ducic, Y. (2002). Titanium mesh and hydroxyapatite cement cranioplasty: a report of 20 cases. *J. Oral Maxillofac. Surg.*, 60(3):272-276.

Ebisawa, Y., Kokubo, T., Ohura, K. & Yamamuro, T. (1990) 'Bioactivity of CaO·SiO_2-based glasses: *In vitro* evaluation', *Journal of Materials Science: Materials in Medicine*, 1(4): 239-244.

Effah Kaufmann, E.A., Ducheyne, P. & Shapiro, I.M. (2000). Evaluation of osteoblast response to porous bioactive glass (45S5) substrates by RT-PCR analysis. *Tissue Eng.*, 6(1):19–28.

Einhorn, T.A. (1995). Enhancement of fracture-healing. *J. Bone Joint Surg. Am.*, 77:940–56.

El-Ghannam, A. (2005). Bone reconstruction: from bioceramics to tissue engineering, *Expert Rev. Med. Devices*, 2: 87–101.

El-Ghannam, A., Ducheyne, P. & Shapiro, IM. (1997a). Formation of surface reaction products on bioactive glass and their effects on the expresssion of the osteoblastic phenotype and the deposition of mineralized extracellular matrix. *Biomaterials*, 18: 295-303.

Erdemli, O., Captug, O., Bilgili, H., Orhan, D., Tezcaner, A. & Keskin, D. (2010). In vitro and in vivo evaluation of the effects of demineralized bone matrix or calcium sulfate addition to polycaprolactone-bioglass composites. *J. Mater. Sci. Mater. Med.*, 21(1):295-308.

Fathi, MH., Salehi, M., Saatchi, A., Mortazavi, V. & Moosavi, SB. (2003). In vitro corrosion behavior of bioceramic, metallic, and bioceramic-metallic coated stainless steel dental implants. *Dent. Mater.*, 19(3): 188-198.

Fernyhough, JC., Schimandle, JJ., Weigel, MC., Edwards, CC. & Levine, AM. (1992). Chronic donor site pain complicating bone graft harvesting from the posterior iliac crest for spinal fusion. *Spine*, 17(12): 1474-1480.

Ferraris, M., Rabajoli, P., Brossa, F. & Paracchini, L. (1996). Vacuum plasma spray deposition of titanium particle/glass-ceramic matrix biocomposites. *Journal of the American Ceramic Society*, 79(6): 1515-1520.

Filiaggi, M., Pilliar, RM. & Coombs, NA. (1991). Characterization of the interface in the plasma-sprayed HA coating/Ti-6AI-4V implant system. *Journal of Biomedical Materials Research*, 25: 1211-29.

Finet, B., Weber, G. & Cloots, R. (2000). Titanium release from dental implants: An in vivo study on sheep. *Materials Letters*, 43(4):159-165.

Francis, L., Meng, D., Knowles, J.C., Roy, I. & Boccaccini, A.R. (2010) 'Multi-functional P(3HB) microsphere/45S5 Bioglass®-based composite scaffolds for bone tissue engineering', *Acta. Biomaterialia*, 6(7): 2773-2786.

Frick, KK., Jiang, L., & Bushinsky, DA. (1997). Acute metabolic acidosis inhibits the induction of osteoblastic egr-1 and type 1 collagen. *Am. J. Physiol. (Cell Physiol.)*, 272: C1450-C1456

Fu, Q., Rahaman, M.N., Bal, B.S. & Brown, R.F. (2010) 'Preparation and in vitro evaluation of bioactive glass (13–93) scaffolds with oriented microstructures for repair and regeneration of load-bearing bones', *Journal of Biomedical Materials Research Part A*, 93A (4): 1380-1390.

Fu, Q., Rahaman, M.N., Bal, B.S., Huang, W. & Day, D.E. (2007) 'Preparation and bioactive characteristics of a porous 13–93 glass, and fabrication into the articulating surface of a proximal tibia', *Journal of Biomedical Materials Research Part A*, 82A (1): 222-229.

Fu, Q., Rahaman, M.N., Sonny Bal, B., Brown, R.F. & Day, D.E. (2008) 'Mechanical and in vitro performance of 13-93 bioactive glass scaffolds prepared by a polymer foam replication technique', *Acta Biomaterialia*, 4(6): 1854-1864.

Furusawa, T. & Mizunuma, K. (1997). Osteoconductive properties and efficacy of resorbable bioactive glass as a bone-grafting material. *Implant dentistry*, 6(2):93-101.

Galindo-Moreno, P., Avila, G., Fernández-Barbero, J.E., Mesa, F., O'Valle-Ravassa, F. & Wang, H.L. (2008). Clinical and histologic comparison of two different composite grafts for sinus augmentation: a pilot clinical trial. *Clin. Oral. Implants Res.*, 19(8):755-9.

García, C., Ceré, S. & Durán, A. (2004). Bioactive coatings prepared by sol-gel on stainless steel 316L. *Journal of Non-Crystalline Solids*, 348: 218-224

Gatti, A.M. & Zaffe, D. (1991). Short-term behaviour of two similar active glasses used as granules in the repair of bone defects. *Biomaterials*, 12(5):497-504.

Gau, YL., Lonstein, JE., Winter, RB., Koop, S. & Denis, F. (1991). Luque—Galveston procedure for correction and stabilization of neuromuscular scoliosis and pelvic obliquity: a review of 68 patients. *J. Spinal Disord*. 4: 399—410.

Gazdag, A.R., Lane, J.M., Glaser, D. & Forster, R.A. (1995). Alternatives to autogenous bone graft: efficacy and indications. *J. Am. Acad. Orthop. Surg.*, 3: 1-8.

Gentleman, E., Fredholm, Y.C., Jell, G., Lotfibakhshaiesh, N., O'Donnell, M.D., Hill, R.G. & Stevens, M.M. (2010) 'The effects of strontium-substituted bioactive glasses on osteoblasts and osteoclasts in vitro', *Biomaterials*, 31(14): 3949-3956.

Gerhardt, LC. & Boccaccini, A.R. (2010) 'Bioactive glass and glass-ceramic scaffolds for bone tissue engineering', *Materials*, 3(7): 3867-3910.

Gheysen, G., Ducheyne, P., Hench, L.L. & de Meester, P. (1983). Bioglass composites: a potential material for dental application. *Biomaterials,* 4(2):81-4.

Ghosh, SK., Nandi, SK., Kundu, B., Datta, S., De, DK., Roy, SK. & Basu, D. (2008) 'In vivo response of porous hydroxyapatite and β-tricalcium phosphate prepared by aqueous solution combustion method and comparison with bioglass scaffolds', *Journal of Biomedical Materials Research Part B: Applied Biomaterials*, 86B (1): 217-227.

Giannoudis, P.V. (2005). Dinopoulos H, Tsiridis E. Bone substitutes: an update. *Injury*, 36(Suppl. 3): S20–7.

Ginebra, MP., Traykova, T. & Planell, JA. (2006). Calcium phosphate cements as bone drug delivery systems: a review, *J. Control. Release*., 113: 102–110.

Gomez-Vega, JM., Saiz, E., Tomsia, AP., Marshall, GW. & Marshall, SJ. (2000). Bioactive glass coatings with hydroxyapatite and Bioglass particles on Ti-based implants. 1. Processing. *Biomaterials*, 21(2): 105-111.

Goodrich, J.T., Argamaso, R. & Hall, C.D. (1992). Split-thickness bone grafts in complex craniofacial reconstructions. *Pediatric neurosurgery*, 18(4):195-201.

Gorriti, MF., López, JMP., Boccaccini, AR., Audisio, C. & Gorustovich, A.A. (2009) 'In vitro Study of the Antibacterial Activity of Bioactive Glass-ceramic Scaffolds', *Advanced Engineering Materials*, 11(7): 67-B70.

Gosain, A.K. (2003). Biomaterials in facial reconstruction. *Operative Techniques in Plastic and Reconstructive Surgery*, 9(1):23-30.

Gosain, A.K. & Persing, J.A. (1999). Biomaterials in the face: benefits and risks. *The Journal of craniofacial surgery*, 10(5):404-414.

Goulet, JA., Senunas, LE., DeSilva, GL. & Greenfield, ML. (1997). Autogenous iliac crest bone graft. Complications and functional assessment. *Clinical Orthopaedics and Related Research,* 339: 76-81.

Grana, F., Rocca, ED. & Grana, L. (1954). Las trepanaciones craneanas en el Peru en a epoca prehispanica. Lima, Peru: Imprenta Santa Maria,

Greenspan, DC. & Hench, LL. (1976). 'Chemical and mechanical behavior of bioglass-coated alumina', *J Biomed Mater Res*, 10(4): 503-9.

Gross, U. & Strunz, V. (1985) 'The interface of various glasses and glass ceramics with a bony implantation bed', *J Biomed Mater Res*, Vol. 19, No. 3, pp. 251-71.

Gross, U., Brandes, J., Strunz, V., Bab, I. & Sela, J. (1981) 'The ultrastructure of the interface between a glass ceramic and bone', *J Biomed Mater Res*, Vol. 15, No. 3, pp. 291-305.

Gross, U., Kinne, R., Schmitz, H.J. & Strunz, V. (1988) 'The response of bone to surface active glass/glass-ceramics', *CRC Critical Reviews on Biocompatibility*, Vol. 4, p. 2.

Gross, U., Roggendorf, W., Schmitz, H.J. & Strunz, V. (1986a) 'Testing procedures for surface reactive biomaterials', in Christel, P., Meunier, A. & Lee, A.J.C. (Eds.): *Biological* and *Biomechanical Performance of Biomaterials*, Elsevier, Amsterdam, Netherlands, p. 367.

Gross, U., Schmitz, H.J., Strunz, V., Schuppan, D. & Termine, J. (1986b) 'Proteins at the interface of bone-bonding and non-bonding glass-ceramics': *Transaction of the Twelfth Annual Meeting of the Society for Biomaterials*, Society for Biomaterials, Algonquin, IL, p. 98.

Gross, U.M. & Strunz, V. (1980) 'The anchoring of glass ceramics of different solubility in the femur of the rat', *J Biomed Mater Res*, Vol. 14, No. 5, pp. 607-18.

Grossman, D.G. (1991). In: *International Symposium on Computer Restorations,* IL: Quintessenz, Chicago, p. 103.

Guarino, V., Causa, F. & Ambrosio, L. (2007) 'Bioactive scaffolds for bone and ligament tissue', *Expert Review of Medical Devices*, Vol. 4, pp. 405-418.

Haimi, S., Gorianc, G., Moimas, L., Lindroos, B., Huhtala, H., Räty, S., Kuokkanen, H., Sándor, G.K., Schmid, C., Miettinen, S. & Suuronen, R. (2009) 'Characterization of zinc-releasing three-dimensional bioactive glass scaffolds and their effect on human adipose stem cell proliferation and osteogenic differentiation', *Acta Biomaterialia*, Vol. 5, No. 8, pp. 3122-3131.

Hamadouche, M., Meunier, A., Greenspan, DC., Blanchat, C., Zhong, JP., La Torre, GP. & Sedel, L. (2000). Bioactivity of sol-gel bioactive glass coated alumina implants. *J. Biomed. Mater. Res.* 52(2): 422-9.

Han, J., Meng, H. & Xu, L. (2002). Clinical evaluation of bioactive glass in the treatment of periodontal intrabony defects. *Zhonghua kou qiang yi xue za zhi = Zhonghua kouqiang yixue zazhi = Chinese journal of stomatology,* 37(3):225-227.

Hardouin, P., Anselme, K., Flautre, B., Bianchi, F., Bascoulenguet, G. & Bouxin, B. (2000). Tissue engineering and skeletal diseases. *Joint Bone Spine,* 67(5): 419-424.

Hedia, H.S., El-Midany, T.T., Shabara, M.A. & Fouda, N. (2006). Design optimization of cementless metal-backed cup prostheses using the concept of functionally graded material. *Biomed. Mater.*, 1(3):127-33.

Heikkila, J.T., Aho, H.J., Yli-Urpo, A., Happonen, R.P. & Aho, A.J. (1995). Bone formation in rabbit cancellous bone defects filled with bioactive glass granules. *Acta orthopaedica Scandinavica*, 66(5):463-467.

Heikkila, J.T., Mattila, K.T., Andersson, O.H., Yli-Urpo, A. & Aho, A.J. (1995). Behaviour of bioactive glass in human bone, In: *Bioceramics 8*, Hench, L.L. & Wilson, J., pp. 35-41, Elsevier Science, Oxford, U. K.

Helen, W. & Gough, JE. (2008). Cell viability, proliferation and extracellular matrix production of human annulus fibrosus cells cultured within PDLLA/Bioglass composite foam scaffolds in vitro. *Acta. Biomater.,* 4(2): 230-43.

Hench, L. (2006) 'The story of Bioglass', *Journal of Materials Science: Materials in Medicine*, Vol. 17, No. 11, pp. 967-978.

Hench, L.L. (1987) 'Cementless fixation', in Pizzoferrato, A., Marchetti, P.G., Ravaglioli, A. & Lee, A.J.C. (Eds.): *Biomaterials and Clinical Applications*, Elsevier, Amsterdam, Netherl&s, p. 23.

Hench, L.L. (1988) 'Bioactive ceramics', in Ducheyne, P. & Lemons, J. (Eds.): *Bioceramics: Materials Characteristics Versus In Vivo Behaviour*, Annals of New York Academy of Sciences, New York, p. 54.

Hench, L.L. (1991) 'Bioceramics: From Concept to Clinic', *Journal of the American Ceramic Society*, Vol. 74, No. 7, pp. 1487-1510.

Hench, L.L. (1996) 'Biomaterials Science: An Introduction to Materials in Medicine', in Ratner, B.D., Hoffman, A.S., Schoen, F.J. & Lemons, J.E. (Eds.), Academic Press, San Diego, p. 73.

Hench, L.L. (1998) 'Bioceramics', *Journal of the American Ceramic Society*, Vol. 81, No. 7, pp. 1705-1728.

Hench, L.L. & Andersson, Ö.H. (1993) 'Bioactive glasses', in Hench, L.L. & Wilson, J. (Eds.): *An Introduction to Bioceramics Vol. 1*, World Scientific Publishing, Singapore, pp. 41-62.

Hench, L.L. & Clark, A.E. (1982) 'Chapter 6: Adhesion to bone', in Williams, D.F. (Ed.): *Biocompatibility of Orthopaedic Implants*, CRC Press, Boca Raton, FL.

Hench, L.L. & Ethridge, E.C. (1982) *Biomaterials: An interfacial approach*. Academic Press, New York.

Hench, L.L. & Paschall, H.A. (1973) 'Direct chemical bond of bioactive glass-ceramic materials to bone and muscle', *J Biomed Mater Res*, Vol. 7, No. 3, pp. 25-42.

Hench, L.L. & Paschall, H.A. (1974) 'Histochemical responses at a biomaterial's interface', *J Biomed Mater Res*, Vol. 8, No. 3, pp. 49-64.

Hench, L.L., Paschall, H.A., Allen, W.C. & Piotrowski, G. (1975) 'Interfacial behavior of ceramic implants', *National Bureau of Standards Special Publication*, Vol. 415, pp. 19-35.

Hench, L.L. & Polak, J.M. (2002) 'Third-generation biomedical materials', *Science*, Vol. 295, No. 5557, pp. 1014-1017.

Hench, L.L. & Wilson, J. (1984) 'Surface-active biomaterials', *Science*, Vol. 226, No. 4675, pp. 630-6.

Hench, L.L., Spilman, D.B. and Nolletti, D. (1986) 'Fluoride Bioglasses (R)', in Christel, P., Meunier, A. & Lee, A.J.C. (Eds.): *Biological and Biomechanical Performance of Biomaterials*, Elsevier, Amsterdam, Netherlands, pp. 99-104.

Hench, L.L., Splinter, R.J., Allen, W.C. & Greenlee, T.K. (1971) 'Bonding mechanisms at the interface of ceramic prosthetic materials', *Journal of Biomedical Materials Research*, Vol. 5, No. 6, pp. 117-141.

Hench, LL. (1993). Bioactive glasses. In: Hench, LL. & Wilson, J., *An Introduction to Bioceramics,* World Scientific, London.

Heybeli, N., Oktar, FN., Ozyazgan, S., Akkan, G. & Ozsoy, S. (2003). Low-cost antibiotic loaded systems for developing countries. *Technol. Health Care.*, 11(3): 207-16.

Hill, R. (1996) 'An alternative view of the degradation of bioglass', *Journal of Materials Science Letters*, Vol. 15, No. 13, pp. 1122-1125.

Hing, K.A. (2004). Bone repair in the twenty-first century: biology, chemistry or engineering? *Philos. Transact. A Math. Phys. Eng. Sci.*,362: 2821–50.

Hodgson, AWE., Mueller, Y., Forster, D. & Virtanen, S. (2002). Electrochemical characterisation of passive films on Ti alloys under simulated biological conditions. *Electrochimica Acta.*, 47(12):1913-1923.

Holand, W., Rheinberger, V., Apel, E., Van 't Hoen, C., Holand, M., Dommann, A., Marcel, O., Corinna, M. & Ursula, GH. (2006). Clinical applications of glass-ceramics in dentistry. *Journal of materials science*, 17(11): 1037-1042.

Holand, W., Vogel, W., Naumann, K. & Gummel, J. (1985) 'Interface reactions between machinable bioactive glass-ceramics and bone', *J Biomed Mater Res*, Vol. 19, No. 3, pp. 303-12.

Hsi, C.-S., Cheng, H.-Z., Hsu, H.-J., Chen, Y.-S. & Wang, M.-C. (2007) 'Crystallization kinetics and magnetic properties of iron oxide contained $25Li_2O$-$8MnO_2$-20CaO-

$2P_2O_5$-$45SiO_2$ glasses', *Journal of the European Ceramic Society*, Vol. 27, No. 10, pp. 3171-3176.

Hsiong, SX. & Mooney, DJ. (2006). Regeneration of vascularized bone. *Periodontol*, 41: 109–122.

Hsu, FY., Chueh, SC. & Wang, YJ. (1999). Microspheres of hydroxyapatite/reconstituted collagen as supports for osteoblast cell growth. *Biomaterials*, 20(20): 1931-1936.

Huang, YC., Kaigler, D., Rice, KG., Krebsbach, PH. & Mooney, DJ. (2005). Combined angiogenic and osteogenic factor delivery enhances bone marrow stromal cell-driven bone regeneration. *J. Bone Miner. Res.,* 20: 848–857.

Hulbert, S.F., Bokros, J.C., Hench, L.L., Wilson, J. & Heimke, G. (1987) 'Ceramics in clinical applications: Past, present and future', in Vincenzini, P. (Ed.): *High Tech Ceramics*, Elsevier, Amsterdam, Netherlands, pp. 189-213.

Hutmacher, D., Hürzeler, MB. & Schliephake, H. (1996). A review of material properties of biodegradable and bioresorbable polymers and devices for GTR and GBR applications. *International Journal of Oral and Maxillofacial Implants,* 11(5): 667-678.

Hutmacher, D.W., Schantz, J.T., Lam, C.X.F., Tan, K.C. & Lim, T.C. (2007) 'State of the art and future directions of scaffold-based bone engineering from a biomaterials perspective', *Journal of Tissue Engineering and Regenerative Medicine*, Vol. 1, No. 4, pp. 245-260.

Ido, K., Asada, Y., Sakamoto, T., Hayashi, R. & Kuriyama, S. (2000). Radiographic evaluation of bioactive glass-ceramic grafts in postero-lateral lumbar fusion. *Spinal Cord,* 38(5):315-318.

Itala, A., Koort, J., Ylanen, H.O., Hupa, M. & Aro, H.T. (2003). Biologic significance of surface microroughing in bone incorporation of porous bioactive glass implants. *J. Biomed. Mater. Res. A.*, 67(2): 496-503.

Jackson, I.T. & Yavuzer, R. (2000). Hydroxyapatite cement: an alternative for craniofacial skeletal contour refinements. *British journal of plastic surgery*, 53(1):24-29.

Jackson, I.T., Pellett, C. & Smith, J.M. (1983). The skull as a bone graft donor site. *Annals of plastic surgery*, 11(6):527-532.

Jana, C., Nisch, W. & Grimm, G. (1995). Production and characterization of thin films of Bioverit-type glasses deposited by RF magnetron sputtering, In: Vincenzini, P., *Advances in Science and Technology, Vol12 (Materials in Clinical applications)*. p. 257-262, Faenza: Techna

Jansen, JA., Vehof, JWM., Ruhé, PQ., Kroeze-Deutman, H., Kuboki, Y., Takita, H., Hedberg E.L. & Mikos, AG. (2005). Growth factor-loaded scaffolds for bone engineering. *J. Control. Release,* 101: 127–136.

Jarcho, M. (1981) 'Calcium phosphate ceramics as hard tissue prosthetics', *Clin Orthop Relat Res*, No. 157, pp. 259-78.

Jell, G., Notingher, I., Tsigkou, O., Notingher, P., Polak, JM., Hench, LL. & Stevens, MM. (2008). Bioactive glass-induced osteoblast differentiation: a noninvasive spectroscopic study. J. Biomed. Mater. Res., 86(1): 31–40.

Johnson, M.W., Sullivan, S.M., Rohrer, M. & Collier, M. (1997). Regeneration of peri-implant infrabony defects using PerioGlas: a pilot study in rabbits. *Int. J. Oral Maxillofac. Implants.*, 12(6):835-9.

Jones, J.R. (2007) 'Bioactive ceramics and glasses', in Boccaccini, A.R. & Gough, J.E. (Eds.): *Tissue Engineering Using Ceramics and Polymers Vol. 1*, Woodhead Publishing Limited CRC Press, Cambridge, U. K., pp. 52-71.

Jones, J.R. (2009) 'New trends in bioactive scaffolds: The importance of nanostructure', *Journal of the European Ceramic Society*, Vol. 29, No. 7, pp. 1275-1281.

Jones, J.R., Gentleman, E. & Polak, J. (2007). Bioactive glass scaffolds for bone regeneration. *Elements*, 3(6):393–9.

Jones, JR., Tsigkou, O., Coates, EE., Stevens, MM., Polak, JM. & Hench, LL. (2007). Extracellular matrix formation and mineralization on a phosphate-free porous bioactive glass scaffold using primary human osteoblast (HOB) cells. *Biomaterials*, 28(9): 1653-63.

Kanczler, J.M. & Oreffo, R.O. (2008) 'Osteogenesis and angiogenesis: the potential for engineering bone', *Eur Cell Mater*, Vol. 15, pp. 100-14.

Kanellakopoulou, K. & Giamarellos-Bourboulis, EJ. (2000). Carrier systems for the local delivery of antibiotics in bone infections. *Drugs*, 59(6): 1223–32.

Kangasniemi, K. & Yti-Urpo, A. (1990) 'Biological response of glasses in the SiO_2-Na_2O-CaO-P_2O_5-B_2O_3 system', in Yamamuro, T., Hench, L.L. & Wilson, J. (Eds.): *Handbook of Bioactive Ceramics Vol. I*, CRC Press, Boca Raton, FL, pp. 97-108.

Karageorgiou, V. & Kaplan, D. (2005). Porosity of 3D biomaterial scaffolds and osteogenesis, *Biomaterials*, 26: 5474–5491.

Karatzas, S., Zavras, A., Greenspan, D. & Amar, S. (1999). Histologic observations of periodontal wound healing after treatment with PerioGlas in nonhuman primates. *Int. J. Periodontics Restorative Dent.*, 19(5):489-99.

Karlsson, K.H., Ylänen, H. & Aro, H. (2000) 'Porous bone implants', *Ceramics International*, Vol. 26, No. 8, pp. 897-900.

Kawanabe, K., Okada, Y., Matsusue, Y., Iida, H. & Nakamura, T. (1998). Treatment of osteomyelitis with antibiotic-soaked porous glass ceramic. *The Journal of bone and joint surgery* 80(3): 527-530.

Kaysinger, KK. & Ramp, WK. (1998). Extracellular pH modulates the activity of cultured human osteoblasts. *Cell Biochem.*, 68: 83-89

Keshaw, H., Forbes, A. & Day, Richard M. (2005). Release of angiogenic growth factors from cells encapsulated in alginate beads with bioactive glass. *Biomaterials*, 26(19): 4171-4179

Kinnunen, I., Aitasalo, K., Pollonen, M. & Varpula, M. (2000). Reconstruction of orbital floor fractures using bioactive glass. *J. Craniomaxillofac. Surg.*, 28(4):229-234.

Kitsugi, T., Yamamuro, T. & Kokubo, T. (1989) 'Bonding behavior of a glass-ceramic containing apatite and wollastonite in segmental replacement of the rabbit tibia under load-bearing conditions', *J Bone Joint Surg Am*, Vol. 71, No. 2, pp. 264-72.

Klein, M., Goetz, H., Pazen, S., Al-Nawas, B., Wagner, W. & Duschner, H. (2009) 'Pore characteristics of bone substitute materials assessed by microcomputed tomography', *Clinical Oral Implants Research*, Vol. 20, No. 1, pp. 67-74.

Klongnoi, B., Rupprecht, S., Kessler, P., Thorwarth, M., Wiltfang, J. & Schlegel, KA. (2006). Influence of platelet-rich plasma on a bioglass and autogenous bone in sinus augmentation. An explorative study. *Clin. Oral. Implants Res.*, 17(3):312-20.

Knapp, C.I., Feuille, F., Cochran, D.L. & Mellonig, J.T. (2003). Clinical and histologic evaluation of bone-replacement grafts in the treatment of localized alveolar ridge defects. Part 2: bioactive glass particulate. *Int. J. Periodontics Restorative Dent.,* 23(2):129-37.

Kohlhauser, C., Hellmich, C., Vitale-Brovarone, C., Boccaccini, A.R., Rota, A. & Eberhardsteiner, J. (2009) 'Ultrasonic Characterisation of Porous Biomaterials Across Different Frequencies', *Strain*, Vol. 45, No. 1, pp. 34-44.

Kokubo, T., Ito, S., Sakka, S. & Yamamuro, T. (1986) 'Formation of a high-strength bioactive glass-ceramic in the system MgO-CaO-SiO_2-P_2O_5', *Journal of Materials Science*, Vol. 21, No. 2, pp. 536-540.

Kokubo, T., Shigematsu, M., Nagashima, Y., Tashiro, M., Nakamura, T., Yamamuro, T. & Higashi, S. (1982) 'Apatite- and wollastonite-containg glass-ceramics for prosthetic application', *Bulletin of the Institute for Chemical Research, Kyoto University*, Vol. 60, No. 3-4, pp. 260-268.

Kundu, B., Nandi, SK., Dasgupta, S., Datta, S., Mukherjee, P., Roy, S., Singh, AK., Mandal, TK., Das, P., Bhattacharya, R. & Basu, D. (2011). Macro-to-micro porous special bioactive glass and ceftriaxone-sulbactam composite drug delivery system for treatment of chronic osteomyelitis: an investigation through in vitro and in vivo animal trial. *J. Mater. Sci. Mater. Med.,* 22(3):705-20.

Lacefield, WR. & Hench, LL. (1986). The bonding of Bioglass to a cobalt-chromium surgical implant alloy. *Biomaterials*, 7(2): 104-8.

Langer, R. (1980). Polymeric delivery systems for controlled drug release. *Chemical Engineering Communications*, 6(1-3): 1-48.

Langer, R. (1990). New methods of drug delivery. *Science*, 249(4976): 1527-1533.

Langer, R. & Vacanti, JP. (1993). Tissue Engineering. Science, 260(5110): 920-926

Larsson, C., Thomsen, P., Aronsson, BO., Rodahl, M., Lausmaa, J., Kasemo, B. & Ericson, LE. (1996). Bone response to surface-modified titanium implants: studies on the early tissue response to machined and electropolished implants with different oxide thicknesses. *Biomaterials*, 17: 605-616.

Lasserre, A. & Bajpai, PK. (1998). Ceramic drug-delivery devices. *Critical reviews in therapeutic drug carrier systems,* 15(1): 1-56.

Leach, JK., Kaigler, D., Wang, Z., Krebsbach, PH. & Mooney, DJ. (2006). Coating of VEGF-releasing scaffolds with bioactive glass for angiogenesis and bone regeneration, *Biomaterials*, 27: 3249–3255.

Leonetti, J.A, Rambo, H.M. & Throndson, R.R. (2000). Osteotome sinus elevation and implant placement with narrow size bioactive glass. *Implant dentistry*, 9(2):177-182.

Leu, A., Stieger, S.M., Dayton, P., Ferrara, K.W. & Leach. J.K. (2009). Angiogenic response to bioactive glass promotes bone healing in an irradiated calvarial defect. *Tissue Eng. Part A,* 15(4):877-85.

Li, M., Zhang, R., Wang, J. & Yang, S. (2007). Study of different biocomposite coatings on Ti alloy by a subsonic thermal spraying technique. *Biomed. Mater.,* 2(1): 1-5.

Lin, F.-H., Huang, Y.-Y., Hon, M.-H. & Wu, S.-C. (1991) 'Fabrication and biocompatibility of a porous bioglass ceramic in a Na_2O-CaO-SiO_2-P_2O_5 system', *Journal of Biomedical Engineering*, Vol. 13, No. 4, pp. 328-334.

Linati, L., Lusvardi, G., Malavasi, G., Menabue, L., Menziani, M.C., Mustarelli, P. & Segre, U. (2005) 'Qualitative and quantitative structure-property relationships analysis of multicomponent potential bioglasses', *The Journal of Physical Chemistry B*, Vol. 109, No. 11, pp. 4989-4998

Liu, A., Hong, Z., Zhuang, X., Chen, X., Cui, Y., Liu, Y. & Jing, X. (2008) 'Surface modification of bioactive glass nanoparticles and the mechanical and biological properties of poly(l-lactide) composites', *Acta Biomaterialia*, Vol. 4, No. 4, pp. 1005-1015.

Liu, X., Huang, W., Fu, H., Yao, A., Wang, D., Pan, H. & Lu, W. (2009a) 'Bioactive borosilicate glass scaffolds: improvement on the strength of glass-based scaffolds for tissue engineering', *Journal of Materials Science: Materials in Medicine*, Vol. 20, No. 1, pp. 365-372.

Liu, X., Huang, W., Fu, H., Yao, A., Wang, D., Pan, H., Lu, W., Jiang, X. & Zhang, X. (2009b) 'Bioactive borosilicate glass scaffolds: in vitro degradation and bioactivity behaviors', *Journal of Materials Science: Materials in Medicine*, Vol. 20, No. 6, pp. 1237-1243.

Livingston, T., Ducheyne, P. & Garino, J. (2002). In vivo evaluation of a bioactive scaffold for bone tissue engineering. *J. Biomed. Mater. Res.*, 62(1): 1-13.

Lockyer, M.W.G., Holland, D. & Dupree, R. (1995) 'NMR investigation of the structure of some bioactive and related glasses', *Journal of Non-Crystalline Solids*, Vol. 188, No. 3, pp. 207-219.

Lopez-Esteban, S., Saiz, E., Fujino, S., Oku, T., Suganuma, K. & Tomsia, AP. (2003). Bioactive glass coatings for orthopedic metallic implants. *J. Eur. Ceram. Soc.*, 23(15): 2921-2930.

Loty, C., Sautier, J.M., Tan, M.T., Oboeuf, M., Jallot, E., Boulekbache, H., Greenspan, D. & Forest, N. (2001) 'Bioactive glass stimulates *in vitro* osteoblast differentiation and creates a favorable template for bone tissue formation', *Journal of Bone and Mineral Research*, Vol. 16, No. 2, pp. 231-239.

Lovelace, T.B., Mellonig, J.T., Meffert, R.M., Jones, A.A., Nummikoski, P.V. & Cochran, D.L. (1998). Clinical evaluation of bioactive glass in the treatment of periodontal osseous defects in humans. *Journal of periodontology*, 69(9):1027-1035.

Low, S.B., King, C.J. & Krieger, J. (1997). An evaluation of bioactive ceramic in the treatment of periodontal osseous defects. *The International journal of periodontics and restorative dentistry*, 17(4):358-367.

Lu, H.H., El-Amin, S.F., Scott, K.D. & Laurencin, C.T. (2003) 'Three-dimensional, bioactive, biodegradable, polymer–bioactive glass composite scaffolds with improved mechanical properties support collagen synthesis and mineralization of human osteoblast-like cells in vitro', *Journal of Biomedical Materials Research Part A*, Vol. 64A, No. 3, pp. 465-474.

Lu, HH., Tang, A., Oh, SC, Spalazzi, JP. & Dionisio, K. (2005). Compositional effects on the formation of a calcium phosphate layer and the response of osteoblast-like cells on polymer-bioactive glass composites. *Biomaterials*, 26(32): 6323-34.

Luciani, A., Coccoli, V., Orsi, S., Ambrosio, L. & Netti, PA. (2008). PCL microspheres based functional scaffolds by bottom-up approach with predefined microstructural properties and release profiles. *Biomaterials*, 29(36):4800-4807.

Mader, JT., Landon, GC. & Calhoun, J. (1993). Antimicrobial treatment of osteomyelitis. *Clin. Orthop. Relat. Res.*, 295: 87–95.

Mahmood, J., Takita, H., Ojima, Y., Kobayashi, M., Kohgo, T. & Kuboki, Y. (2001) 'Geometric Effect of Matrix upon Cell Differentiation: BMP-Induced Osteogenesis Using a New Bioglass with a Feasible Structure', *Journal of Biochemistry*, Vol. 129, No. 1, pp. 163-171.

Malafaya, PB., Santos, TC., Van Griensven, M. & Reis, RL. (2008). Morphology, mechanical characterization and in vivo neo-vascularization of chitosan particle aggregated scaffolds architectures. *Biomaterials*, 29(29): 3914-3926.

Mankin, H.J., Fogelson, F.S., Thrasher, Z.A. & Jaffer, F. (1976). Massive resection and allograft transplantation in the treatment of malignant bone tumours. *N. Engl. J. Med*., 294: 1247-1250.

Manson, P.N., Crawley, W.A. & Hoopes, J.E. (1986). Frontal cranioplasty: risk factors and choice of cranial vault reconstructive material. *Plastic and reconstructive surgery*, 77(6):888-904.

Mantsos, T., Chatzistavrou, X., Roether, J.A., Hupa, L., Arstila, H. & Boccaccini, A.R. (2009) 'Non-crystalline composite tissue engineering scaffolds using boron-containing bioactive glass and poly(D,L-lactic acid) coatings', *Biomed Mater*, Vol. 4, No. 5, p. 055002.

Marciani, R.D., Gonty, A.A., Giansanti, J.S. & Avila, J. (1977). Autogenous cancellous marrow bone graft in irradiated (i) long mandibles. *Oral. Surg*., 43: 365-368.

Mardare, CC., Mardare, AI., Fernandes, JR. & Joanni, ED. (2003). Imposition of bioactive glass-ceramic thin-films by RF magnetron sputtering. *J. European. Ceram. Soc.*, 23:1027–1030.

Marelli, B., Ghezzi, C.E., Barralet, J.E., Boccaccini, A.R. & Nazhat, S.N. (2010). Three-dimensional mineralization of dense nanofibrillar collagen-bioglass hybrid scaffolds. *Biomacromolecules*, 11(6):1470-9.

McCarthy, R.E., Peek, R.D., Morrissy, R.T. & Hough, Jr A.J. (1986). Allograft bone in spinal fusion for paralytic scoliosis. *J. Bone Joint Surg. Am*., 68: 370—5.

Meffert, R.M., Thomas, J.R., Hamilton, K.M. & Brownstein, C.N. (1985). Hydroxylapatite as an alloplastic graft in the treatment of human periodontal osseous defects. *Journal of periodontology*, 56(2):63-73.

Meinert, K., Uerpmann, C., Matschullat, J. & Wolf, GK. (1998). Corrosion and leaching of silver doped ceramic IBAD coatings on SS 316L under simulated physiological conditions. *Surface and Coatings Technology*, 103-104: 58-65.

Mengel, R., Schreiber, D. & Flores-de-Jacoby, L. (2006). Bioabsorbable membrane and bioactive glass in the treatment of intrabony defects in patients with generalized aggressive periodontitis: results of a 5-year clinical & radiological study. *J. Periodontol.*, 77(10):1781-7.

Meseguer-Olmo, L., Ros-Nicolás, M., Vicente-Ortega, V., Alcaraz-Baños, M., Clavel-Sainz, M., Arcos, D., Ragel, C., Vallet-Regí, M. & Meseguer-Ortiz, C. (2006). A bioactive

sol-gel glass implant for in vivo gentamicin release. Experimental model in Rabbit. *Journal of Orthopaedic Research,* 24: 454–460.

Middleton, E.T., Rajaraman, C.J., O'Brien, D.P., Doherty, S.M. & Taylor, A.D. (2008). The safety and efficacy of vertebroplasty using Cortoss cement in a newly established vertebroplasty service. *Br. J. Neurosurg.,* 22:252–6.

Miguel, B.S., Kriauciunas, R., Tosatti, S., Ehrbar, M., Ghayor, C., Textor, M. & Weber, F.E. (2010) 'Enhanced osteoblastic activity and bone regeneration using surface-modified porous bioactive glass scaffolds', *Journal of Biomedical Materials Research Part A*, Vol. 94A, No. 4, pp. 1023-1033.

Miliauskaite, A., Selimovic, D. & Hannig, M. (2007). Successful management of aggressive periodontitis by regenerative therapy: a 3-year follow-up case report. *J. Periodontol.*, 78(10):2043-50.

Milosev, I., Metikos-Hukovic, M. & Strehblow, HH. (2000). Passive film on orthopaedic TiAlV alloy formed in physiological solution investigated by X-ray photoelectron spectroscopy. *Biomaterials,* 21(20): 2103-2113.

Misra, S.K., Ansari, T., Mohn, D., Valappil, S.P., Brunner, T.J., Stark, W.J., Roy, I., Knowles, J.C., Sibbons, P.D., Jones, E.V., Boccaccini, A.R. & Salih, V. (2010a) 'Effect of nanoparticulate bioactive glass particles on bioactivity and cytocompatibility of poly(3-hydroxybutyrate) composites', *Journal of The Royal Society Interface*, Vol. 7, No. 44, pp. 453-465.

Misra, S.K., Ansari, T.I., Valappil, S.P., Mohn, D., Philip, S.E., Stark, W.J., Roy, I., Knowles, J.C., Salih, V. & Boccaccini, A.R. (2010b) 'Poly(3-hydroxybutyrate) multifunctional composite scaffolds for tissue engineering applications', *Biomaterials*, Vol. 31, No. 10, pp. 2806-2815.

Misra, S.K., Mohn, D., Brunner, T.J., Stark, W.J., Philip, S.E., Roy, I., Salih, V., Knowles, J.C. & Boccaccini, A.R. (2008) 'Comparison of nanoscale and microscale bioactive glass on the properties of P(3HB)/Bioglass® composites', *Biomaterials*, Vol. 29, No. 12, pp. 1750-1761.

Misra, S.K., Valappil, S.P., Roy, I. & Boccaccini, A.R. (2006) 'Polyhydroxyalkanoate (PHA)/Inorganic Phase Composites for Tissue Engineering Applications', *Biomacromolecules*, Vol. 7, No. 8, pp. 2249-2258.

Mistry, S., Kundu, D., Datta, S. & Basu, D. (2011). Comparison of bioactive glass coated and hydroxyapatite coated titanium dental implants in the human jaw bone. *Australian Dental Journal*, 56: 68–75.

Mohamad Yunos, D., Bretcanu, O. & Boccaccini, A. (2008) 'Polymer-bioceramic composites for tissue engineering scaffolds', *Journal of Materials Science*, Vol. 43, No. 13, pp. 4433-4442.

Mohn, D., Zehnder, M., Imfeld, T. & Stark, W.J. (2010). Radio-opaque nanosized bioactive glass for potential root canal application: evaluation of radiopacity, bioactivity and alkaline capacity. *Int. Endod. J.*, 43(3):210-7.

Moimas, L., Biasotto, M., Di Lenarda, R., Olivo, A. & Schmid, C. (2006). Rabbit pilot study on the resorbability of three-dimensional bioactive glass fibre scaffolds. *Acta biomaterialia Mar.*, 2(2):191-199.

Moimas, L., Biasotto, M., Lenarda, R.D., Olivo, A. & Schmid, C. (2006) 'Rabbit pilot study on the resorbability of three-dimensional bioactive glass fibre scaffolds', *Acta Biomaterialia*, Vol. 2, No. 2, pp. 191-199.

Moreira-Gonzalez, A., Lobocki, C., Barakat, K., Andrus, L., Bradford, M., Gilsdorf, M. & Jackson, IT. (2005). Evaluation of 45S5 bioactive glass combined as a bone substitute in the reconstruction of critical size calvarial defects in rabbits. *J. Craniofac. Surg*. 16(1): 63-70.

Muller, W. (1890). Zur frage der tempoaren schadelresektion an stele der trepanation. *Zentralbl. Chir.,* 4:65.

Munukka, E., Leppäranta, O., Korkeamäki, M., Vaahtio, M., Peltola, T., Zhang, D., Hupa, L., Ylänen, H., Salonen, J., Viljanen, M. & Eerola, E. (2008) 'Bactericidal effects of bioactive glasses on clinically important aerobic bacteria', *Journal of Materials Science: Materials in Medicine*, Vol. 19, No. 1, pp. 27-32.

Mylonas, D., Vidal, M.D., De Kok, I.J., Moriarity, J.D. & Cooper, L.F. (2007). Investigation of a thermoplastic polymeric carrier for bone tissue engineering using allogeneic mesenchymal stem cells in granular scaffolds. *J. Prosthodont*., 16(6):421-30.

Naber, C.L., Reid, O.M. & Hammer, J.E. III. (1972). Gross and histologic evaluation of an autogenous bone graft. 57th month post operatively. *J. Periodontal*., 43: 702.

Nakamura, T., Yamamuro, T., Higashi, S., Kokubo, T. & Itoo, S. (1985) 'A new glass-ceramic for bone replacement: evaluation of its bonding to bone tissue', *J Biomed Mater Res*, Vol. 19, No. 6, pp. 685-98.

Nandi, S.K., Kundu, B., Datta, S., De, D.K. & Basu, D. (2009) 'The repair of segmental bone defects with porous bioglass: An experimental study in goat', *Research in Veterinary Science*, Vol. 86, No. 1, pp. 162-173.

Nandi, SK., Kundu, B., Mukherjee, P., Mandal, TK., Datta, S., De, DK. & Basu, D. (2009). In vitro and in vivo release of cefuroxime axetil from bioactive glass as an implantable delivery system in experimental osteomyelitis. *Ceram. Int*., 35(8): 3207-3216.

Neo, M., Nakamura, T., Ohtsuki, C., Kasai, R., Kokubo, T. & Yamamuro, T. (1994). Ultrastructural study of the A-W GC-bone interface after long-term implantation in rat and human bone. *Journal of biomedical materials research,* 28(3):365-372.

Neo, M., Nakamura, T., Ohtsuki, C., Kokubo, T. & Yamamuro, T. (1993). Apatite formation on three kinds of bioactive material at an early stage in vivo: a comparative study by transmission electron microscopy. *Journal of biomedical materials research,* 27(8):999-1006.

Nickell, W.B., Jurkiewicz, M.J. & Salyer, K.E. (1972). Repair of skull defects with autogenous bone. *Arch. Surg*., 105(3):431-433.

Nicoll Steven, B., Radin, S., Santos, EM., Tuan, RS. & Ducheyne, P. (1997). *In vitro* release kinetics of biologically active transforming growth factor-β1 from a novel porous glass carrier. *Biomaterials*, 18 (12): 853-859

Norton, M.R. & Wilson, J. (2002). Dental implants placed in extraction sites implanted with bioactive glass: human histology and clinical outcome. *The International journal of oral and maxillofacial implants*, 17(2):249-257.

Ochoa, I., Sanz-Herrera, J.A., GarcÃa-Aznar, J.M., DoblarÃ©, M., Yunos, D.M. & Boccaccini, A.R. (2009) 'Permeability evaluation of 45S5 BioglassÂ®-based scaffolds for bone tissue engineering', *Journal of Biomechanics*, Vol. 42, No. 3, pp. 257-260.

O'Donnell, M.D. & Hill, R.G. (2010) 'Influence of strontium and the importance of glass chemistry and structure when designing bioactive glasses for bone regeneration', *Acta Biomaterialia*, Vol. 6, No. 7, pp. 2382-2385.

Ohtsuki, C., Kushitani, H., Kokubo, T., Kotani, S. & Yamamuro, T. (1991). Apatite formation on the surface of Ceravital-type glass-ceramic in the body. *Journal of biomedical materials research*, 25(11):1363-1370.

Olding, T., Sayer, M. & Barrow, D. (2001) 'Ceramic sol-gel composite coatings for electrical insulation', *Thin Solid Films*, Vol. 398-399, pp. 581-586.

Oliveira, A.L., Mano, J.F. & Reis, R.L. (2003) 'Nature-inspired calcium phosphate coatings: present status and novel advances in the science of mimicry', *Current Opinion in Solid State and Materials Science*, Vol. 7, No. 4-5, pp. 309-318.

Pajamaki, K.J., Andersson, O.H., Lindholm, T.S., Karlsson, K.H. & Yli-Urpo, A. (1993). Induction of new bone by allogeneic demineralized bone matrix combined to bioactive glass composite in the rat. *Annales chirurgiae et gynaecologiae*, 207:137-143.

Pajamaki, K.J., Andersson, O.H., Lindholm, T.S., Karlsson, K.H., Yli-Urpo, A. & Happonen, R.P. (1993). Effect of bovine bone morphogenetic protein and bioactive glass on demineralized bone matrix grafts in the rat muscular pouch. *Annales chirurgiae et gynaecologiae,* 207:155-161.

Palussiere, J., Berge, J., Gangi, A., Cotton, A., Pasco, A., Bertagnoli, R., Hans, J., Paolo, C. & Hervé, D. (2005). Clinical results of an open prospective study of a bis-GMA composite in percutaneous vertebral augmentation. *Eur. Spine J.*, 14: 982–91.

Pan, H.B., Zhao, X.L., Zhang, X., Zhang, K.B., Li, L.C., Li, Z.Y., Lam, W.M., Lu, W.W., Wang, D.P., Huang, W.H., Lin, K.L. & Chang, J. (2010) 'Strontium borate glass: potential biomaterial for bone regeneration', *Journal of The Royal Society Interface*, Vol. 7, No. 48, pp. 1025-1031.

Patka, P., Haarman, H.J. & Bakker, F.C. (1998). Bone transplantation and bone replacement materials. *Ned. Tijdschr. Geneeskd.*,142: 893–6.

Peltola, M., Suonpaa, J., Aitasalo, K., Maattanen, H., Andersson, O., Yli-Urpo, A. & Laippala, P. (2000). Experimental follow-up model for clinical frontal sinus obliteration with bioactive glass (S53P4). *Acta. Otolaryngol Suppl* 543: 167-169.

Peltola, MJ., Suonpaa, JT., Andersson, H., Maattanen, HS., Aitasalo, KM., Yli-Urpo, A. & Laippala, PJ. (2000). In vitro model for frontal sinus obliteration with bioactive glass S53P4. *Journal of Biomedical Materials Research*, 53(2): 161-166.

Phan, PV., Grzanna, M., Chu, J., Polotsky, A., El-Ghannam, A., Van Heerden, D., Hungerford, DS. & Frondoza, CG. (2003). The effect of silica-containing calcium-phosphate particles on human osteoblasts in vitro. *J. Biomed Mater. Res, A.* 67(3): 1001-8

Queiroz, AC., Santos, JD., Monteiro, FJ., Gibson, IR. & Knowles, JC. (2001). Adsorption and release studies of sodium ampicillin from hydroxyapatite and glass-reinforced hydroxyapatite composites. *Biomaterials*, 22 (11): 1393-1400

Quinones, C.R. & Lovelace, T.B. (1997). Utilization of a bioactive synthetic particulate for periodontal therapy & bone augmentation techniques. *Pract. Periodont. Aesthet. Dent*., 9:1-7.

Radha, G. & Ashok, K. (2008) 'Bioactive materials for biomedical applications using sol-gel technology', *Biomedical Materials*, Vol. 3, No. 3, p. 034005.

Radice, S., Kern, P., Bürki, G., Michler, J. & Textor, M. (2007). Electrophoretic deposition of zirconia-Bioglass composite coatings for biomedical implants. *J. Biomed. Mater. Res. A*, 82(2): 436-44.

Rainer, A., Giannitelli, S.M., Abbruzzese, F., Traversa, E., Licoccia, S. & Trombetta, M. (2008) 'Fabrication of bioactive glass-ceramic foams mimicking human bone portions for regenerative medicine', *Acta Biomaterialia*, Vol. 4, No. 2, pp. 362-369.

Ramp, WK., Lenz, LG. & Kaysinger, KK. (1994). Medium pH modulates matrix, mineral, and energy metabolism in cultured chick bones and osteoblast-like cells. *Bone Miner*., 24(1): 59-73.

Ray, N.H. (1978) *Inorganic Polymers*. Academic Press, London.

Reck, R. (1981). Tissue reactions to glass ceramics in the middle ear. *Clin. Otolaryngol. Allied Sci., 6*:63–5.

Reck, R. (1983). Bioactive glass ceramic: a new material in tympanoplasty. *The Laryngoscope,* 93(2):196-199.

Renghini, C., Komlev, V., Fiori, F., Verné, E., Baino, F. & Vitale-Brovarone, C. (2009) 'Micro-CT studies on 3-D bioactive glass-ceramic scaffolds for bone regeneration', *Acta Biomaterialia*, Vol. 5, No. 4, pp. 1328-1337.

Rezwan, K., Chen, Q.Z., Blaker, J.J. & Boccaccini, A.R. (2006) 'Biodegradable and bioactive porous polymer/inorganic composite scaffolds for bone tissue engineering', *Biomaterials*, Vol. 27, No. 18, pp. 3413-3431.

Rivero, DP., Fox, J., Skipor, AK., Urban, RN. & Galante, JO. (1988). Calcium phosphate-coated porous titanium implants for enhanced skeletal fixation, *Journal of Biomedical Materials Research* 22: 191-201.

Roessler, S., Zimmermann, R., Scharnweber, D., Werner, C. & Worch, H. (2002). Characterization of oxide layers on Ti6Al4V and titanium by streaming potential and streaming current measurements. *Colloids and Surfaces B: Biointerfaces*, 26(4): 387-395.

Roether, JA., Gough, JE., Boccaccini, AR., Hench, LL., Maquet, V. & Jérôme, R. (2002). Novel bioresorbable and bioactive composites based on bioactive glass and polylactide foams for bone tissue engineering. *J. Mater. Sci. Mater. Med.*, 13(12): 1207-14.

Ross, N., Tacconi, L. & Miles, J.B. (2000). Heterotopic bone formation causing recurrent donor site pain following iliac crest bone harvesting. *Br. J. Neurosurg*., 14: 476—9.

Ryu, H.S., Seo, J.H., Kim, H., Hong, K.S., Park, H.J., Kim, D.J., Lee, J.H., Lee, D.H., Chang, B.S. & Lee, C.K. (2003) 'Bioceramics 15', Trans Tech Publications Limited, Zurich-Uetikon, p. 261.

Saino, E., Maliardi, V., Quartarone, E., Fassina, L., Benedetti, L., De Angelis, MG., Mustarelli, P., Facchini, A. & Visai, L. (2010). In vitro enhancement of SAOS-2 cell calcified matrix deposition onto radio frequency magnetron sputtered bioglass-coated titanium scaffolds. *Tissue Eng. Part A*., 16(3): 995-1008.

Saravanapavan, P., Gough, J.E., Jones, J.R. & Hench, L.L. (2003) 'Antimicrobial macroporous gel-glasses: Dissolution and cytotoxicity', *Key Engineering Materials*, Vol. 254-256, pp. 1087-1090.

Scala, M., Gipponi, M., Pasetti, S., Dellachá, E., Ligorio, M., Villa, G., Margarino, G., Giannini, G. & Strada, P. (2007). Clinical applications of autologous cryoplatelet gel for the reconstruction of the maxillary sinus. A new approach for the treatment of chronic oro-sinusal fistula. *In Vivo.*, 21(3):541-7.

Schepers, E., de Clercq, M., Ducheyne, P. & Kempeneers, R. (1991). Bioactive glass particulate material as a filler for bone lesions. *Journal of oral rehabilitation*, 18(5):439-452.

Schnettler, R. (1997). Markgraf E. Knochenersatzmaterialen und Wachstumsfaktoren. Thieme: Stuttgart

Scotchford, C.A., Shataheri, M., Chen, P.S., Evans, M., Parsons, A.J., Aitchison, G.A., Efeoglu, C., Burke, J.L., Vikram, A., Fisher, S.E. & Rudd, C.D. (2011). Repair of calvarial defects in rats by prefabricated, degradable, long fibre composite implants. *J. Biomed. Mater. Res. A.*, 96(1):230-8.

Seeherman, H. & Wozney, JM. (2005). Delivery of bone morphogenic proteins for orthopedic tissue regeneration. *Cytokine Growth Factor Rev.*, 16: 329–345.

Seiler, J.G. & Johnson, J. (2000). Iliac crest autogenous bone grafting: donor site complications. *J. South Orthop. Assoc.*, 9: 91—7.

Sepulveda, P., Jones, J.R. & Hench, L.L. (2001) 'Characterization of melt-derived 45S5 and sol-gel-derived 58S bioactive glasses', *Journal of Biomedical Materials Research*, Vol. 58, No. 6, pp. 734-740.

Shapoff, C.A., Alexander, D.C. & Clark, A.E. (1997). Clinical use of a bioactive glass particulate in the treatment of human osseous defects. *Compend. Contin. Educ. Dent.*, 18(4):352–4.

Skaggs, DL., Samuelson, MA., Hale, JM., Kay, RM. & Tolo, VT. (2000). Complications of posterior iliac crest bone grafting in spine surgery in children. *Spine*, 25: 2400—2

Smit, R.S., van der Velde, D. & Hegeman, J.H. (2008). Augmented pin fixation with Cortoss for an unstable AO-A3 type distal radius fracture in a patient with a manifest osteoporosis. *Arch. Orthop. Trauma. Surg.*, 128:989–93.

Smith, A.W., Yousefi, J. & Jackson, I.T. (1999). Screw fixation of methylmethacrylate in the craniofacial area. *Eur J Plast Surg.*, 22:17-21.

Sooksaen, P., Suttiruengwong, S., Oniem, K., Ngamlamiad, K. & Atireklapwarodom, J. (2008) 'Fabrication of porous bioactive glass-ceramics via decomposition of natural fibres', *Journal of Metals, Materials and Minerals*, Vol. 18, No. 2, pp. 85-91.

Spaans, CJ., Belgraver, VW., Rienstra, O., de Groot, JH., Veth, RP. & Pennings, AJ. (2000). Solvent-free fabrication of micro-porous polyurethane amide and polyurethane-urea scaffolds for repair and replacement of the knee-joint meniscus. *Biomaterials*, 21(23): 2453-2460.

Stanley, H.R., Clark, A.E., Pameijer, C.H. & Louw. N.P. (2001). Pulp capping with a modified bioglass formula (#A68-modified). *Am. J. Dent.*, 14(4):227-32.

Stevens, M.M. & George, J.H. (2005) 'Exploring and Engineering the Cell Surface Interface', *Science*, Vol. 310, No. 5751, pp. 1135-1138.

Stevenson, S. & Horowitz, M. (1992). The response to bone allografts. *J. Bone Joint Surg. Am*., 74:939–50.

Strnad, Z. (1992) 'Role of the glass phase in bioactive glass-ceramics', *Biomaterials*, Vol. 13, No. 5, pp. 317-321.

Summers, B.N. & Eisenstein, S.M. (1989). Donor site pain from the ilium: a complication of lumbar spine fusion. *J. Bone Joint Surg. Br*., 71-B: 677—80.

Suominen, E. & Kinnunen, J. (1996). Bioactive glass granules and plates in the reconstruction of defects of the facial bones. Scandinavian journal of plastic and reconstructive surgery. *Nordisk plastikkirurgisk forening and Nordisk klubb for handkirurgi*, 30(4):281-289.

Suonpaa. J., Sipila, J., Aitasalo, K., Antila, J. & Wide, K. (1997). Operative treatment of frontal sinusitis. *Acta Otolaryngol. Suppl*., 529:181-183.

Sy, I.P. (2002). Alveolar ridge preservation using a bioactive glass particulate graft in extraction site defects. *General dentistry*, 50(1):66-68.

Taboas, J.M., Maddox, R.D., Krebsbach, P.H. & Hollister, S.J. (2003) 'Indirect solid free form fabrication of local and global porous, biomimetic and composite 3D polymer-ceramic scaffolds', *Biomaterials*, Vol. 24, No. 1, pp. 181-194.

Tadjoedin, E.S., de Lange, G.L., Lyaruu, D.M., Kuiper, L. & Burger, E.H. (2002). High concentrations of bioactive glass material (BioGran) vs. autogenous bone for sinus floor elevation. *Clinical oral implants research*, 13(4):428-436.

Temenoff, JS. & Mikos, AG.(2000). Review: tissue engineering for regeneration of articular cartilage. *Biomaterials*, 21(5): 431-440.

Thomas, KA., Kay, JF., Cook, SD. & Jarcho, M. (1987). The effect of surface macrotexture & hydroxylapatite coating on the mechanical strengths and histologic profiles of titanium implant materials. *Journal of Biomedical Materials Research*, 21: 1395-414.

Thomas, MV., Puleo, DA. & Al-Sabbagh, M. (2005). Bioactive glass three decades on, *J. Long-Term Eff. Med. Implants*, 15 (6): 585–597.

Thompson, I. & Hench, L. (1998) 'Mechanical properties of bioactive glasses, glass-ceramics and composites', *Proceedings of the Institution of Mechanical Engineers, Part H: Journal of Engineering in Medicine*, Vol. 212, No. 2, pp. 127-136.

Thompson, I.D. (2005) 'Biocomposites', in Hench, L.L. and Jones, J.R. (Eds.): *Biomaterials, Artificial Organs and Tissue Engineering*, Woodhead Publishing Limited CRC Press, Cambridge, U. K., pp. 48-58.

Throndson, R.R. & Sexton, S.B. (2002). Grafting mandibular third molar extraction sites: a comparison of bioactive glass to a nongrafted site. *Oral surgery, oral medicine, oral pathology, oral radiology, and endodontics*, 94(4):413-419.

Tsigkou, O., Hench, L.L., Boccaccini, A.R., Polak, J.M. & Stevens, M.M. (2007). Enhanced differentiation and mineralization of human fetal osteoblasts on PDLLA containing bioglass composite films in the absence of osteogenic supplements. *J. Biomed. Mater. Res. A*., 80(4):837–51.

Tsigkou, O., Jones, J.R., Polak, J.M. & Stevens, M.M. (2009). Differentiation of fetal osteoblasts and formation of mineralized bone nodules by 45S5 bioglass conditioned medium in the absence of osteogenic supplements. *Biomaterials*, 30(21): 3542–50.

Urist, M.R. (1965). Bone: formation by autoinduction. *Science*,150: 893–9.

Valimaki, V.V. & Aro, H.T. (2006). Molecular basis for action of bioactive glasses as bone graft substitute. *Scand. J. Surg.*, 95:95–102.

Vallet-Regí, M., Ragel, C.V. & Salinas, Antonio J. (2003) 'Glasses with Medical Applications', *European Journal of Inorganic Chemistry*, Vol. 2003, No. 6, pp. 1029-1042.

Vargas, G.E., Mesones, R.V., Bretcanu, O., López, J.M.P., Boccaccini, A.R. & Gorustovich, A. (2009) 'Biocompatibility and bone mineralization potential of 45S5 Bioglass®-derived glass-ceramic scaffolds in chick embryos', *Acta Biomaterialia*, Vol. 5, No. 1, pp. 374-380.

Verné, E., Fernández, Vallés C., Vitale Brovarone, C., Spriano, S. & Moisescu, C. (2004). Double-layer glass-ceramic coatings on Ti6Al4V for dental implants. *J. Eur. Ceram. Soc*. 24(9): 2699-2705.

Verné, E., Ferraris, M., Jana, C. & Paracchini, L. (2000). Bioverit® I base glass/Ti particulate biocomposite: "In situ" vacuum plasma spray deposition. *J. Eur. Ceram. Soc.,* 20(4): 473-479.

Verné, E., Ferraris, M., Ventrella, A., Paracchini, L., Krajewski, A. & Ravaglioli, A. (1998). Sintering and plasma spray deposition of bioactive glass-matrix composites for biomedical applications. *J. Eur. Ceram. Soc*., 18(4): 363-372.

Villacam J,H., Novaes, A.B. Jr., Souza, S.L., Taba, M. Jr., Molina, G.O. & Carvalho, T.L. (2005). Bioactive glass efficacy in the periodontal healing of intrabony defects in monkeys. *Brazilian dental journal*, 16(1):67-74.

Vitale Brovarone, C., Verné, E. & Appendino, P. (2006) 'Macroporous bioactive glass-ceramic scaffolds for tissue engineering', *Journal of Materials Science: Materials in Medicine*, Vol. 17, No. 11, pp. 1069-1078.

Vitale-Brovarone, C., Baino, F. & VernÃ©, E. (2010) 'Feasibility and Tailoring of Bioactive Glass-ceramic Scaffolds with Gradient of Porosity for Bone Grafting', *Journal of Biomaterials Applications*, Vol. 24, No. 8, pp. 693-712.

Vitale-Brovarone, C., Baino, F. & Verné, E. (2009b) 'High strength bioactive glass-ceramic scaffolds for bone regeneration', *Journal of Materials Science: Materials in Medicine*, Vol. 20, No. 2, pp. 643-653.

Vitale-Brovarone, C., Baino, F., Bretcanu, O. & Verné, E. (2009a) 'Foam-like scaffolds for bone tissue engineering based on a novel couple of silicate-phosphate specular glasses: synthesis and properties', *Journal of Materials Science: Materials in Medicine*, Vol. 20, No. 11, pp. 2197-2205.

Vitale-Brovarone, C., Miola, M., Balagna, C. & Verné, E. (2008) '3D-glass-ceramic scaffolds with antibacterial properties for bone grafting', *Chemical Engineering Journal*, Vol. 137, No. 1, pp. 129-136.

Vitale-Brovarone, C., Nunzio, S.D., Bretcanu, O. & Verné, E. (2004) 'Macroporous glass-ceramic materials with bioactive properties', *Journal of Materials Science: Materials in Medicine*, Vol. 15, No. 3, pp. 209-217.

Vitale-Brovarone, C., Vernè, E., Bosetti, M., Appendino, P. & Cannas, M. (2005) 'Microstructural and *in vitro* characterization of SiO_2-Na_2O-CaO-MgO glass-ceramic bioactive scaffolds for bone substitutes', *Journal of Materials Science: Materials in Medicine*, Vol. 16, No. 10, pp. 909-917.

Vitale-Brovarone, C., Verné, E., Robiglio, L., Appendino, P., Bassi, F., Martinasso, G., Muzio, G. & Canuto, R. (2007) 'Development of glass-ceramic scaffolds for bone tissue engineering: Characterisation, proliferation of human osteoblasts and nodule formation', *Acta Biomaterialia*, Vol. 3, No. 2, pp. 199-208.

Vogel, W., Hohland, W., Naumann, K., Vogel, J., Carl, G., Gotz, W. & Wange, P. (1990) 'Glass-ceramics for medicine and dentistry', in Yamamuro, T., Hench, L.L. & Wilson, J. (Eds.): *Handbook of Bioactive Ceramics Vol. I*, CRC Press, Boca Raton, FL, p. 353.

Vollenweider, M., Brunner, T.J., Knecht, S., Grass, R.N., Zehnder, M., Imfeld, T. & Stark, W.J. (2007) 'Remineralization of human dentin using ultrafine bioactive glass particles', *Acta Biomaterialia*, Vol. 3, No. 6, pp. 936-943.

Walenkamp, GHIM. (1997). Chronic osteomyelitis. *Acta. Orthop. Scand.*, 68(5): 497–506.

Wallace, K.E., Hill, R.G., Pembroke, J.T., Brown, C.J. & Hatton, P.V. (1999) 'Influence of sodium oxide content on bioactive glass properties', *Journal of Materials Science: Materials in Medicine*, Vol. 10, No. 12, pp. 697-701.

Weber, R.S., Kearns, D.B. & Smith, R.J. (1987). Split calvarium cranioplasty. *Archives of otolaryngology--head and neck surgery,*113(1):84-89.

Webster, T.J. & Ahn, E.S. (2007) 'Nanostructured biomaterials for tissue engineering bone': *Tissue Engineering II Vol. 103*, Springer, Berlin, Germany, pp. 275-308.

Weiner, S. (1986). Organization of extracellularly mineralized tissues: A comparative study of biological crystal growth. *CRC Crit. Rev. Biochem.*, 20: 365-408.

Wei-Tao, J., Xin, Z., Chang-Qing, Z., Xin, L., Wen-Hai, H., Mohamed, NR. & Day, DE. (2010). Elution characteristics of teicoplanin-loaded biodegradable borate glass/chitosan composite. *International Journal of Pharmaceutics,* 387(1-2): 184-186

Wei-Tao, J., Xin, Z., Shi-Hua, L., Xin, L., Wen-Hai, H., Mohamed, NR., Day, DE., Chang-Qing, Z., Zong-Ping, X. & Jian-Qiang, W. (2010). Novel borate glass/chitosan composite as a delivery vehicle for teicoplanin in the treatment of chronic osteomyelitis. Acta Biomaterialia 6: 812–819

Wen, H.B., Moradian-Oldak, J. & Fincham, A.G. (1999). Modulation of apatite crystal growth on Bioglass by recombinant amelogenin. *Biomaterials*, 20(18):1717-25.

Wennerberg, A., Albrektsson, T. & Andersson, B. (1996). Bone tissue response to commercially pure titanium implants blasted with fine and coarse particles of aluminum oxide. *Int. J. Oral Maxillofac. Implants*, 11: 38-45.

Wheeler, DL., Montfort, MJ. & McLoughlin, SW. (2001). Differential healing response of bone adjacent to porous implants coated with hydroxyapatite and 45S5 bioactive glass. *J. Biomed. Mater. Res.*, 55(4): 603-12.

Whitaker, L.A., Munro, I.R., Salyer, K.E., Jackson, I.T., Ortiz-Monasterio, F. & Marchac, D. (1979). Combined report of problems and complications in 793 craniofacial operations. *Plastic and reconstructive surgery*, 64(2):198-203.

Wilda, H. & Gough. JE. (2006). In vitro studies of annulus fibrosus disc cell attachment, differentiation and matrix production on PDLLA/45S5 Bioglass composite films. *Biomaterials*, 27(30): 5220-9.

Wilson, J. & Nolletti, D. (1990) 'Bonding of soft tissues of Bioglass (R)', in Yamamuro, T., Hench, L.L. & Wilson, J. (Eds.): *Handbook of Bioactive Ceramics Vol. I, Bioactive Glasses and Glass-Ceramics*, CRC Press, Boca Raton, FL, pp. 283-302.

Wilson, J., Pigott, G.H., Schoen, F.J. & Hench, L.L. (1981) 'Toxicology and biocompatibility of bioglasses', *J Biomed Mater Res*, Vol. 15, No. 6, pp. 805-17.

Wu, C. (2009) 'Methods of improving mechanical and biomedical properties of CaSi-based ceramics and scaffolds', *Expert Review of Medical Devices*, Vol. 6, No. 3, pp. 237-241.

Wu, S.C., Hsu, H.C., Hsiao, S.H. & Ho, W.F. (2009). Preparation of porous 45S5 Bioglass-derived glass-ceramic scaffolds by using rice husk as a porogen additive. *J. Mater. Sci. Mater. Med.,* 20(6):1229-36.

Wu, TJ., Huang, HH., Lan, CW., Lin, CH., Hsu, FY. & Wang, YJ. (2004). Studies on the microspheres comprised of reconstituted collagen and hydroxyapatite. *Biomaterials*, 25(4): 651-658.

Xia, W. & Chang, J. (2006). Well-ordered mesoporous bioactive glasses (MBG): A promising bioactive drug delivery system. *Journal of Controlled Release,* 110(3): 522-530

Xie, XH., Yu, XW., Zeng, SX., Du, RL., Hu, YH., Yuan, Z., Lu, EY., Dai, KR. & Tang, TT. (2010). Enhanced osteointegration of orthopaedic implant gradient coating composed of bioactive glass and nanohydroxyapatite. *J. Mater. Sci. Mater. Med*., 21(7): 2165-73.

Xin, Z., WeiTao, J., YiFei, G., Wei, X., Xin, L., DePing, W., ChangQing, Z., WenHai, H., Mohamed, NR., Day, DE. & Nai, Z. (2010). Teicoplanin-loaded borate bioactive glass implants for treating chronic bone infection in a rabbit tibia osteomyelitis model. *Biomaterials* 31(22): 5865-5874

Xu, C., Su, P., Chen, X., Meng, Y., Yu, W., Xiang, A.P. & Wang, Y. (2011). Biocompatibility and osteogenesis of biomimetic Bioglass-Collagen-Phosphatidylserine composite scaffolds for bone tissue engineering. *Biomaterials*, 32(4):1051-8.

Xu, C., Su, P., Wang, Y., Chen, X., Meng, Y., Liu, C., Yu, X., Yang, X., Yu, W., Zhang, X. & Xiang, A.P. (2010). A novel biomimetic composite scaffold hybridized with mesenchymal stem cells in repair of rat bone defects models. *J. Biomed. Mater. Res. A*., 95(2):495-503.

Xynos, ID., Hukkanen, MV., Batten, JJ., Buttery, LD., Hench, LL. & Polak, JM. (2000). Bioglass 45S5 stimulates osteoblast turnover and enhances bone formation In vitro: implications and applications for bone tissue engineering. *Calcif. Tissue Int.,* 67(4): 321-9.

Yamamuro, T., Hench, L.L. & Wilson, J. (1990a) *Bioactive glasses and glass-ceramics Vol. I*. CRC Press, Boca Raton, FL.

Yamamuro, T., Hench, L.L. & Wilson, J. (1990b) *Calcium phosphate and hydroxylapatite ceramics Vol. II*. CRC Press, Boca Raton, FL.

Yamamuro, T., Shikata, J., Kakutani, Y., Yoshii, S., Kitsugi, T. & Ono, K. (1988) 'Novel methods for clinical applications of bioactive ceramics', in Ducheyne, P. and Lemons, J.E. (Eds.): *Bioceramics: Material Characteristics Versus In Vivo Behaviour*, Annals of New York Academy of Sciences, New York, p. 107.

Yang, S., Leong, K.-F., Du, Z. & Chua, C.-K. (2001) 'The Design of Scaffolds for Use in Tissue Engineering. Part I. Traditional Factors', *Tissue Engineering*, Vol. 7, No. 6, pp. 679-689.

Yang, S., Leong, K.-F., Du, Z. & Chua, C.-K. (2002) 'The Design of Scaffolds for Use in Tissue Engineering. Part II. Rapid Prototyping Techniques', *Tissue Engineering*, Vol. 8, No. 1, pp. 1-11.

Yang, XB., Webb, D., Blaker, J., Boccaccini, AR., Maquet, V., Cooper, C. & Oreffo, RO. (2006). Evaluation of human bone marrow stromal cell growth on biodegradable polymer/bioglass composites. *Biochem. Biophys. Res. Commun.*, 342(4): 1098-107.

Yılmaz, S., Ipek, M., Celebi, GF. & Bindal, C. (2005). The effect of bond coat on mechanical properties of plasma-sprayed Al2O3 and Al2O3-13 wt% TiO2 coatings on AISI 316L stainless steel. *Vacuum*, 77(3): 315-321.

Yoshii, S., Kakutani, Y., Yamamuro, T., Nakamura, T., Kitsugi, T., Oka, M., Kokubo, T. & Takagi, M. (1988) 'Strength of bonding between A-W glass-ceramic and the surface of bone cortex', *J Biomed Mater Res*, Vol. 22, No. 3 Suppl, pp. 327-38.

Younger, E.M. & Chapman, M.W. (1989). Morbidity at bone graft donor sites. *J. Orthop. Trauma.*, 3: 192–5.

Yue, TM., Yu, JK., Mei, Z. & Man, HC. (2002). Excimer laser surface treatment of Ti-6Al-4V alloy for corrosion resistance enhancement. *Materials Letters*, 52(3): 206-212.

Yukna, R.A., Evans, G.H., Aichelmann-Reidy, M.B. & Mayer, E.T. (2001). Clinical comparison of bioactive glass bone replacement graft material and expanded polytetrafluoroethylene barrier membrane in treating human mandibular molar class II furcations. *J. Periodontol.,* 72(2):125-33.

Yun, H.-s., Kim, S.-e. & Hyeon, Y.-t. (2007) 'Design and preparation of bioactive glasses with hierarchical pore networks', *Chemical Communications*, No. 21, pp. 2139-2141.

Zaffe, D., Bertoldi, C. & Consolo, U. (2003). Element release from titanium devices used in oral and maxillofacial surgery. *Biomaterials*, 24(6): 1093-1099.

Zamet, J.S., Darbar, U.R., Griffiths, G.S., Bulman, J.S., Brägger, U., Bürgin, W. & Newman, H.N. (1997). Particulate bioglass as a grafting material in the treatment of periodontal intrabony defects. *J. Clin. Periodontol.,* 24(6):410-8.

Zhang, J., Wang, M., Cha, JM. & Mantalaris, A. (2009). The incorporation of 70s bioactive glass to the osteogenic differentiation of murine embryonic stems cells in 3D bioreactors. *J. Tissue Eng. Regen. Med.* 3(1): 63-71.

Zhao, L., Yan, X., Zhou, X., Zhou, L., Wang, H., Tang, J. & Yu, C. (2008). Mesoporous bioactive glasses for controlled drug release. *Microporous and Mesoporous Materials*, 109(1-3): 210-215

Zhu Yufang & Kaskel Stefan. 2009. Comparison of the in vitro bioactivity and drug release property of mesoporous bioactive glasses (MBGs) and bioactive glasses (BGs) scaffolds. Microporous and Mesoporous Materials. 118 (1-3): 176-182

Zietek, M., Radwan-Oczko, M., Konopka, T. & Kozłowski, Z. (1998). Use of the BIOGRAN preparation in surgical treatment of periodontal disease. *Polim. Med.,* 28(3-4):63-9.

Zongping, Xie., Xin, Liu., Weitao, Jia., Changqing, Z., Wenhai, H. & Jianqiang, W. 2009. Treatment of osteomyelitis and repair of bone defect by degradable bioactive borate glass releasing vancomycin. *Journal of Controlled Release*, 139(2): 118-126

5

Elasticity of Spider Dragline Silks Viewed as Nematics: Yielding Induced by Isotropic-Nematic Phase Transition

Linying Cui[1], Fei Liu[2] and Zhong-can Ou-Yang[2]
[1]*Department of Physics, Tsinghua University, Beijing,*
[2]*Center for Advanced Study, Tsinghua University, Beijing, China*

1. Introduction

Spider dragline silk (SDS), the main structural web silk regarded as the "spider's lifeline", exhibits a fascinating combination of high tensile strength and high extensibility (1). Its toughness is over 10 times that of Kevlar, the material for making bullet-proof suits (2). In addition, SDS has a unconventional sigmoidal shaped stress-strain curve and shape memory capability after the tension and torsion test (3; 4) (Figure 1). All these intriguing properties have aroused the broad interest of scientists to understand the underlying deformation mechanism of SDS.

Leaving the open question of why SDS is that mechanically superb aside, people have already started to produce artificial SDS for numerous applications. Various methods to spin artificial SDS have been explored. These include conventional wet spinning of regenerated SDS obtained through forced silking (5; 6), solvent spinning of recombinant SDS protein analogue produced via bacteria and yeast cell cultures doped with chemically synthesized artificial genes (6; 7), and spinning of silk monofilaments from aqueous solution of recombinant SDS protein obtained by inserting the silk-producing genes into mammalian cells (6; 8). The applications also cover a broad biomedical range. For example, the silk-silica fusion proteins was used for bone regeneration by combining the self-assembling domains of SDS (*Nephila clavipes*) as scaffolds and the silaffin-derived R5 peptide of *Cylindrotheca fusiformis* that is responsible for silica mineralization (6; 9). Improved cell adhesion and proliferation of mouse osteoblast (MC3T3-E1) cells was achieved with films composed of *B. mori* fibroin and recombinantly produced proteins based upon *N. clavipes* SDS (incorporating the RGD integrin recognition sequence) *in vitro* (6; 10). SDS based antibacteria materials was also demonstrated by incorporating silk proteins with inorganic antibacteria nanoparticles such as silver nanoparticles (11) and titanium dioxide nanoparticles (12). In addition, silk films are promising candidates for biocompatible coatings for biomedical implants. For instance, gold nanoparticles, silver nanoparticles, and transition metal oxides/sulfides were dip-coated by SDS proteins and showed novel electrical, magnetic, optical properties, and at the same time, biocompatibility (6; 13–16).

Going back to the fundamental question of the structure-property relation of SDS, several experimental studies have been carried out to determine the supra-molecular structure of

SDS (17–22). X-ray diffraction patterns showed that there are many well oriented beta-sheet nanocrystals in the silk, with the long axis of the beta-sheet parallel to the silk axis (17–19). And polarized FTIR spectroscopy and Raman spectroscopy revealed more structures beyond the beta-sheet nanocrystal, including beta-coils, beta-turns, alpha-helices or the more compact and left-handed 3(1)-helices, all of which have quite low orientation in un-stressed SDS (1; 23–26). NMR data also suggested that there are two regions in SDS, a highly oriented beta-sheet nanocrystal region and a poorly oriented polypeptide chain region (22; 27; 28).Furthermore, these structural study results were confirmed by the protein sequence analysis (20; 29). Based on all these results, it is generally accepted that SDS is semicrystalline polymer with beta-sheet nanocrystals embedded in the amorphous region, which was a polypeptide chain network (23; 24; 30) (Figure 2(a)). The beta-sheet nanocrystals were always highly oriented to the axis of SDS, while the polypeptide chain network exhibited random orientation under zero external stress (19). When SDS was subjected to external tension stress, the orientation of the components in the polypeptide chain network was observed to increase significantly as the strain increased (17; 25; 28).

A few models were proposed (18; 23; 30; 31) to understand the structure-property relation of SDS based upon deformation theories of polymers and composite materials. For example, the model by Termonia (23) treated SDS as a hydrogen-bonded amorphous matrix embedded with stiff crystals as cross-links. In the interfacial region, an extremely high modulus is required to get SDS's overall behavior on deformation. While in the model of Porter and Vollrath (30; 31), parameters linking to chemical compositions and morphological order were used to interpret thermo-mechanical properties of SDS. But some parameters such as ordered/disordered fractions are difficult to be obtained from experiments. A recent model (18) connecting deformations on the macroscopic and molecular length scales still did not consider the change of the orientation of nanocomposites during deformation. Especially, as pointed out by Vehoff *at al.* recently (32), basic polymer theories such as the freely jointed chain, the freely rotating chain and the worm-like chain, as well as a hierarchical chain model of the spider capture silk (33) could not reproduce the sigmoidal shape or even the steep initial regime of SDS (Fig. 2(a)) (32). While nonlinear polymer theories can give a general description of the entire deformation process of the silk, some special conditions are invoked (30; 31) and the uniqueness in SDS is not taken into account. In one word, a more natural and unified description for the extraordinary properties of SDS as a model biomaterial still seems to be lacking.

Quite a few works (4; 17; 19; 22; 34–37) have pointed out that SDS is liquid crystalline material and liquid crystal (LC) phase plays a vital role in both its spinning process and mechanical properties. In the spinning process, the spider's 'spinning dope' is liquid crystalline, which make it possible to efficiently spin a thread from large silk protein molecules (4; 38–40). Specifically, in the spider's gland and duct the molecules form a nematic phase (4; 38) — a phase that makes the silk solution flow as a liquid but maintain some of the orientational order characteristic of a crystal, with the long axes of neighboring molecules aligned approximately parallel to one another. In the final extrusion stage of the spinning process, the liquid crystal phase is even more enhanced and frozen into the beta-sheet structure of the silk: The forming thread stretches, narrows and pulls away from the walls of the duct, which bring the dope molecules into better alignment and into a more extended conformation to facilitate hydrogen bonds formation to give the anti-parallel beta conformation of the final thread (4; 38). The final silk contains 40 vol % anti-parallel beta-nanocrystals highly aligned to the silk axis as a frozen LC phase from the spinning process (31).

For the solid SDS, the LC phase transition is an important feature in SDS's deformation process and contributes a lot to the silk's combination of high strength and high extensibility, as well as the shape memory property. In the unstressed state of SDS, the polypeptide chain network has random orientation (25) with many components present, such as beta-coils, beta-turns, alpha-helices or the more compact and left-handed 3(1)-helices (1; 22–24; 26). All of these structures have elongated shapes and the tendency to form LC phase (41). Under increasing tensile stress, the orientations of the elongated components increase substantially as revealed by polarized FTIR spectroscopy and DECODER (direction exchange with correlation for orientation distribution evaluation and reconstruction) NMR (25; 28). The sigmoidal shape of the stress-strain curve (Figure 1(a)) indicates that a LC phase transition takes place at the yield point, resulting in the huge extensibility of SDS after the yield point.
Although some work proposed SDS to be a biological LC elastomer together with the silkworm's silk (37), a detailed description of the deformation mechanism of SDS from the LC point of view is lacking. We constructed an analytical LC model. The polypeptide chain network is set to be in the isotropic state at the beginning with the tendency to transit into the LC phase. Under external stress, the Maier-Saupe theory (42) of nematic LC is employed to monitor the change of the orientation of the polypeptide chain network. We show that during deformation SDS undergoes significant increase of the orientation of the chain network, with a force-induced isotropic-nematic phase transition at the yield point which especially facilitates the extension of the SDS after the yield point. The comprehensive agreement between theory and experiments on the stress-strain curve strongly indicates SDS to belong to LC materials. Especially, the remarkable yielding elasticity of SDS is understood for the first time as the force-induced isotropic-nematic phase transition of the chain network. The present theory also predicts a drop of the stress in supercontracted SDS, an early found effect of humidity on the mechanical properties in many silks (30; 32; 43).

2. Model

Because the beta-sheet nanocrystal has high orientation along the silk axis as spun and deforms much smaller than that of the bulk (17), we will neglect the deformation and rotation of the beta-sheet nanocrystal under external stress and focus on the deformation change of the amorphous polypeptide chain network in the current work. This assumption is also supported by the observations that SDS's high extensibility results primarily from the disordered region (18; 20; 21), and that the deformation of the beta-sheet nanocrystal is at least a factor of 10 smaller than that of the bulk (17).
We take the polypeptide chain network in the amorphous region of SDS as a molecular LC field with each chain section corresponding to a mesogenic molecule (i.e. a molecule having the tendency to form liquid crystal phase under specific conditions); see Fig. 2. Following the LC continuum theory in the absence of forces, the potential of a mesogenic molecule takes the Maier-Saupe interaction form (42)

$$V(\cos\theta) = -aS(\frac{3}{2}\cos^2\theta - \frac{1}{2}), \tag{1}$$

where θ is the angle between the long axis of the molecule and the silk axis (the z-axis), which is also the direction of $\hat{\mathbf{n}}$ (Fig. 2 (b)). a is the strength of the mean field. S is the orientation

order parameter of the LC, defined as the average of second Legendre polynomial (41)

$$S = \left\langle \frac{3}{2}\cos^2\theta - \frac{1}{2} \right\rangle. \tag{2}$$

We notice that the Maier-Saupe potential has been used by Pincus and de Gennes when investigating LC phase transition in a polypeptide solution (44). Using the LC potential to describe the interaction between the segments of the polypeptide chain network is a good mean-field approach because a large part of the polypeptide chain network bears alpha helix and beta coil structures (20; 24), which tend to form a LC phase due to their elongated shape (41). When a uniform force field **f** along z-axis is applied, the potential of a molecule is written as

$$U(\cos\theta) = V - fl\cos\theta, \tag{3}$$

where l denotes the length of the mesogenic molecule.
From the definition of the order parameter S, we get a self-consistency equation

$$\begin{aligned} S = {} & \textstyle\int_{-1}^{1}(\frac{3}{2}\cos^2\theta - \frac{1}{2})\exp(\frac{3aS}{2k_BT}\cos^2\theta + \alpha\cos\theta)d\cos\theta \\ & \Big/ \textstyle\int_{-1}^{1}\exp(\frac{3aS}{2k_BT}\cos^2\theta + \alpha\cos\theta)d\cos\theta\ , \end{aligned} \tag{4}$$

with $\alpha = fl/k_BT$. The solution of the above equation may not be unique, in order to obtain physically sound solution we need to apply the free energy minimization criterion (41) given by

$$F_{MS} = -k_BT\ln Z + \frac{1}{2}aS^2, \tag{5}$$

where Z is the partition function $Z = \int_{-1}^{1} e^{-U(\cos\theta)/k_BT}d\cos\theta$, and the second term at the right-hand side corrects for the double counting arising from the mean field method (45).
The orientation function S was calculated numerically at different temperatures $T^* = T/T_{ni}$ and forces f, and the results were shown in Fig. 3(b). Here $T_{ni} = a/(4.541k_B)$ is the isotropic-nematic transition temperature in the absence of forces (42). At temperatures below T_{ni} the molecules have spontaneous nematic order, and the force does not induce further order significantly. While for the molecules initially in paranematic state (i.e. an isotropic state close to the nematic state), the applied force field will induce a first-order phase transition — S jumps discontinuously to a higher value at a certain critical force $f_C(T^*)$. At even higher temperatures, nematic field is weaker and the effect of the force is less dramatic.
To compare with experiment data, we give the expressions of stress and strain in our model. Apparently, the stress σ of the bulk is $\sigma \equiv F/A = Nf$: F is the force on the surface of the bulk, A is the area of the surface, and N is the number of molecules per area. The strain ε of the bulk is defined as $\varepsilon = [L(f) - L_0]/L_0$, where $L(f)$ is the length of the bulk along z-axis when the force field **f** is applied and we can take it as $L(f) = \langle l|\cos\theta|\rangle$, and $L_0 = L(f = 0) = l/2$. Then the strain ε is $\varepsilon = 2\langle|\cos\theta|\rangle - 1$. The curve of ε versus σ at different temperatures is shown in Fig. 3(c). At temperatures below T_{ni}, the strain grows smoothly with the stress. For temperatures just above T_{ni}, the strain grows with the stress in an almost linear way under small forces, then a jump in the strain occurs at the critical force $f_C(T^*)$, after which the strain increases smoothly with the stress again. At higher temperatures, the nematic field is weaker

and the jump is replaced by a smooth increase in strain, with a plateau in a certain range of force.

In our model, the reduced temperature T^* is an essential parameter, which needs to be chosen specifically in order to predict the stress-strain curve of SDS. Because the silk solution is in LC state at ambient temperature (4; 34; 35) while for the solid silk the orientation of the polypeptide chain network is very low (25), it is likely that the solid polypeptide chain network still has a high tendency to form LC state and is in paranematic state under zero loading. Namely, the isotropic-nematic transition temperature $T_{\rm ni}$ of the chain network is slightly lower than the room temperature T_r, i. e. T^* is just above 1. Actually, the curves of $T^* = 1.01$ and 1.02 agree well with the experimental stress-strain curve of SDS, with a steep linear relation at the beginning and more abrupt increase of the strain after the yield point. Due to viscoelasticity (46), defects and polydomain effects (45), the real SDS exhibit a smoother strain increase after the yield point, while the non-viscoelastic and defect-free LC model predicts an abrupt increase of the strain. From the curves of $T^* = 1.01$ and 1.02, we get the estimation of the yield strain $\varepsilon_y \approx 0.04$, the yield stress $\sigma_y = \alpha N {\rm k_B} T/l \approx 8.4$MPa, and the Young's modulus at the linear region $E \equiv \sigma_y/\varepsilon_y \approx 210$MPa, given $\alpha \sim 0.2$, $N/l \sim 10{\rm nm}^{-3}$, and ${\rm k_B}T_r \sim 4.1$pNnm. These estimations well agree with the experimental results for the low reeling speed SDS, with the yield strain $\varepsilon_y \approx 0.04$, the yield stress $\sigma_y \approx 10$MPa, and the Young's modulus at the linear region $E \approx 250$MPa (Fig. 3(d)) (19).

3. Discussion

The stress-strain curve of paranematic state in the LC model well explains the main features of the stress-strain curve of SDS: With low loading, entropy is dominating and the polypeptide chain network is isotropic. Mesogenic molecules only respond individually to the external stress field by rotating a little bit to the stress direction on average, so the increase of the strain is small and the Young's modulus is high. As the stress increases, the competition between the entropy and the mesogenic molecule potential (including the LC field and the external force field) in the free energy expression (Eq. 3 and 5) begins to favor the potential field. At the point when the potential begins to dominate over the entropy, the isotropic-nematic phase transition of the mesogenic molecule network (i.e. the polypeptide chain network) occurs. Mesogenic molecules start to rotate collectively to the stress direction to form the nematic LC phase. Since all components in the polypeptide chain network tend to align parallel to the silk axis, the length of the silk increases substantially under a constant stress, resulting in the plateau following the transition initiation point which is called the yield point. Due to viscoelasticity (46), defects and polydomain effects (45), the real SDS has a smoother plateau in the stress-strain curve with the same fact that the majority of the SDS's extensibility results from the softening plateau after the yield point. When the stress increases further, the orientation of the network grows rapidly, as observed by polarized FTIR spectroscopy and DECODER (direction exchange with correlation for orientation distribution evaluation and reconstruction) NMR (25; 28). Finally, the shape memory property of SDS in the tension test can be understood as a reverse phase transition process when the external stress decreases to zero.

In the LC model, we predict an isotropic-nematic phase transition at the yield point. Several experimental observations do support a significant increase of the orientation of the elongated components in the amorphous region with various strain. For example, a polarized FTIR spectroscopy measurement (25) showed that the orientation of some components in the

amorphous region increased by 0.3 when the strain reached 24%. A NMR study also suggested the alignment of the components in the amorphous region became poor in the strain relaxation process (28). Further experimental work needs be done to track the orientation change of the polypeptide chain network in the deformation process of SDS in order to better understand its LC character.

We notice that our results agree much better with the mechanical properties of the silks produced by low reeling speed. That is because a high reeling speed will induce a low orientation in the amorphous region, which is not taken into account in the current work.

In addition to describing the stress-strain relation of SDS, our LC model can also qualitatively account for the drop of the stress in wet SDS, *i.e.* the supercontracted SDS. Take L_0 and R_0 as the initial length and radius of the silk, and L and R as those under stress. Under the assumption of volume conservation we have $\pi R_0^2 L_0 = \pi R^2 L$, so $R/R_0 = \sqrt{1/(1+\varepsilon)}$. The free energy of the bulk can be written as

$$\begin{aligned} F &= V - f_{ext}(L - L_0) + 2\pi RL\gamma \\ &= V - f_{ext}(L - L_0) + 2\pi R_0 L_0 \gamma \sqrt{1+\varepsilon}, \end{aligned} \tag{6}$$

where V is the internal energy of the bulk, f_{ext} is the external force on the bulk and γ is the surface energy coefficient. Minimizing F with respect to ε, we get

$$\sigma = \frac{f_{ext}}{\pi R_0^2} = \frac{1}{\pi R_0^2 L_0}\frac{\partial V}{\partial \varepsilon} + \frac{\gamma}{R_0\sqrt{1+\varepsilon}}. \tag{7}$$

When the silk is immersed in water, the surface energy coefficient γ increases, so with the same stress σ we need a bigger strain. Thus our theory can predict the softening of supercontracted silk, an effect observed in many experiments (30; 32; 43; 47; 48).

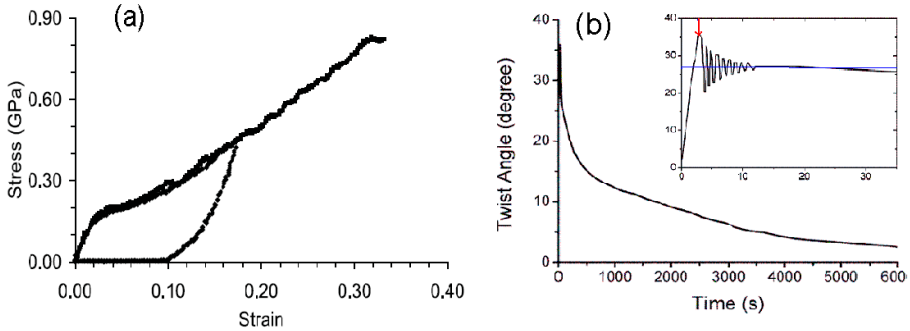

Fig. 1. (a). The stress-strain curves of a spider silk in a deformation cycle and during strain to break. (31) (b). Relaxation dynamics of a torsion pendulum for a spider silk thread. Inset: zoom of the start of the self-relaxation dynamics. The red arrow indicates the end of the excitation and the start of the free relaxation period. Blue line, new equilibrium position. (3)

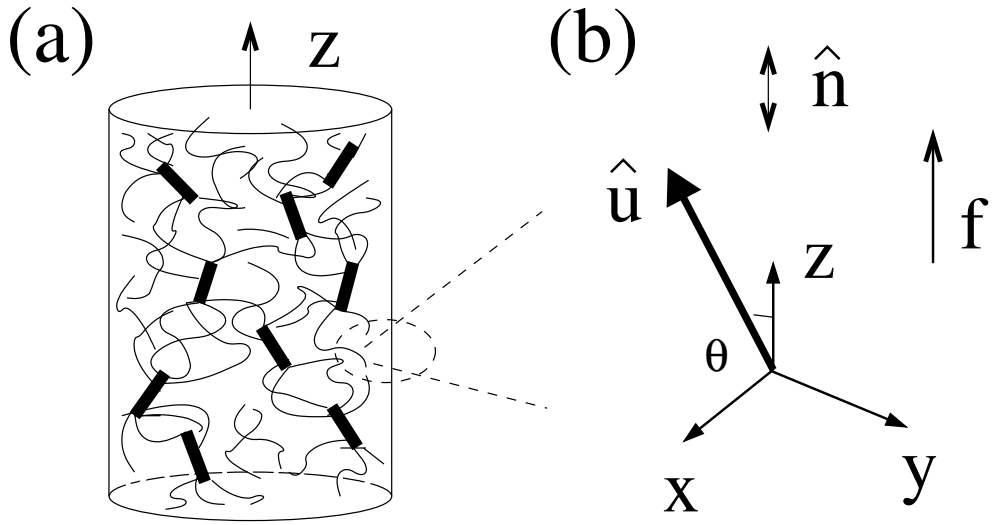

Fig. 2. (a). A schematic diagram of the structure of the dragline silk. The bold lines represent the β-sheet crystals, and the thin lines represent the polypeptide chains in the amorphous region. The z-axis is along the silk axis. (b). The coordinate system of the nematics. $\hat{\mathbf{n}}$ is the director of the nematics, $\hat{\mathbf{u}}$ is the director of the mesogenic molecule, and θ is the angle between the long axis of the molecule and the silk axis z.

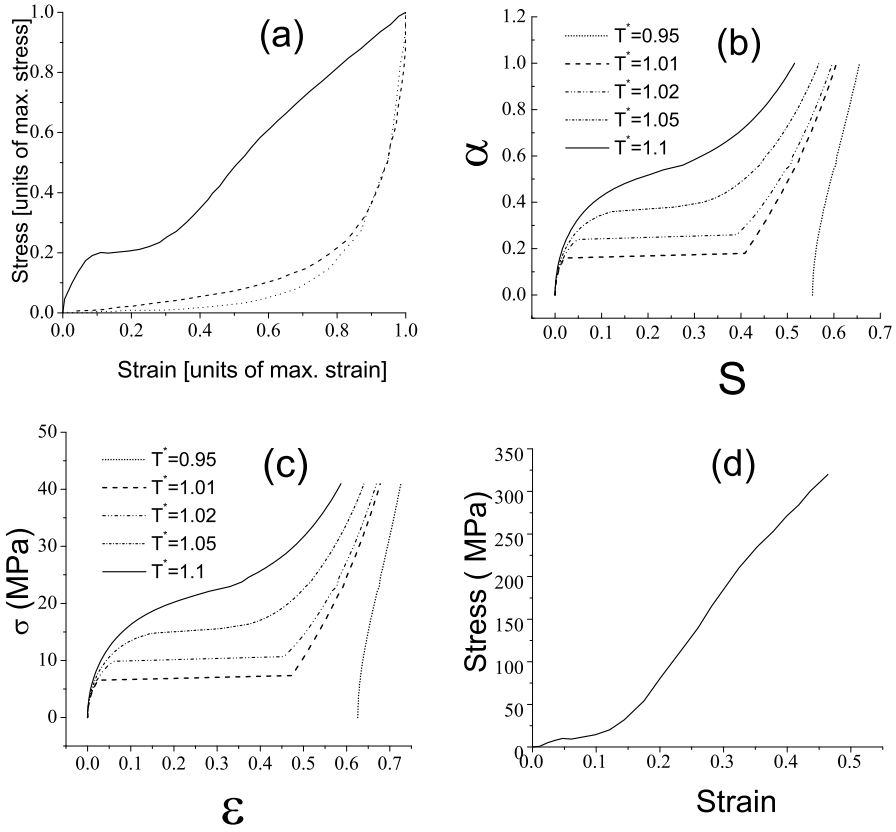

Fig. 3. (Color online.) (a) Comparison of a typical measured dragline silk's stress-strain curve (black solid line) with theoretical curves evaluated by the freely jointed chain (red dash dot line) and the hierarchical chain model (olive dash line) [After T. Vehoff *et al.*]. (b) The orientation order parameter S as a function of $\alpha(= fl/\mathrm{k_B}T)$. (c) The stress-strain curves at different temperatures $T^*(= T/T_{\mathrm{ni}})$. Calculated with $N/l \sim 10\mathrm{nm}^{-3}$, and $\mathrm{k_B}T_r \sim 4.1\mathrm{pNnm}$. (d) The stress-strain curve of the SDS spinned with the speed of $1\mathrm{mms}^{-1}$ (19).

4. Conclusion

In conclusion, we investigate the mechanical properties of SDS from the view point of LC continuum theory. This LC approach is justified by the following considerations: 1) Solid SDS is spined from a polypeptide LC solution and has well aligned beta-sheet nanocrystals as a frozen-in LC phase (36). 2) A large part of the amorphous region (the polypeptide chain network) of the solid SDS has alpha-helix and beta-coils secondary structures, which tend to form LC phase due to their elongated shape (41). 3) By solving a self-consistent equation, both the stress-strain relation and the orientation-reduced temperature relation are obtained from the LC model. These curves agree well with the experimental curves quantitatively and especially help to interpret the high extensibility behavior of SDS at the yield point. 4) The LC model can also describe the shape memory and the supercontraction properties of SDS. 5) The major energy term, the Maier-Saupe potential (41), in the LC model shares the same physical background with the essential energy contributor, the cohesive energy, in polymer theory (31; 49). They both origin from van der Waals forces, although with different emphasis: The LC model focuses on understanding the orientation change and the contribution of LC phase transition to the high extensibility of SDS; while the conventional polymer theories emphasize on either phenomenological descriptions (18) or molecular modelings with high computation requirements (31).
Ongoing work is to develop the model to understand more of the fascinating properties of SDS. More experimental work is highly needed as well to further verify the LC model.

5. References

[1] J. M. Gosline, M. W. Denny, and M. E. Demont, Nature **309**, 551 (1984).
[2] I. Agnarsson, M. Kuntner, T. A. Blackledge, PLoS ONE**5**, e11234 (2010).
[3] O. Emile, A. L. Floch, and F. Vollrath, Nature **440**, 621 (2006).
[4] F. Vollrath and D. P. Knight, Nature **410**, 541 (2001).
[5] M. Kang M, and H. J. Jin, Colloid. Polym. Sci.**285**, 1163 (2007).
[6] J. G. Hardy, and T. R. Scheibel, Prog. Polym. Sci.**35**, 1093 (2010).
[7] C. Fu, Z. Shao, F. Vollrath, Chem. Mater., 6515 (2009).
[8] H. Kim *et al.*, J. Nanosci. Nanotechnol.**8**, 5543 (2008).
[9] A. J. Mieszawska *et al.*, Chem. Mater.**22**, 5780 (2010).
[10] A. W. Morgan *et al.*, Biomaterials**29**, 2556 (2008).
[11] M. Kang *et al.*, J. Nanosci. Nanotechnol.**7**, 3888 (2007).
[12] Y. Xia, G. Gao, and Y. Li, J. Biomed. Mater. Res. Part B**90**, 653 (2009).
[13] A. Singh, S. Hede, and M. Sastry, Small**3**, 466 (2007).
[14] Y. Zhou *et al.*, Chem. Commun.**23**, 2518 (2001).
[15] N. Kukreja *et al.*, Pharmacol Res**57**, 171 (2008).
[16] H. S. Yin, S. Y. Ai, W. J. Shi, and L. S. Zhu, Sens. Actuators B**137**, 747 (2009).
[17] A. Glisąęovic, T. Vehoff, R. J. Davies, and T. Salditt, Macromolecules **41**, 390 (2008).
[18] I. Krasnov *et al.*, Phys. Rev. Lett. **100**, 048104 (2008).
[19] N. Du *et al.*, Biophys. J. **91**, 4528 (2006).
[20] C. Y. Hayashi and R. V. Lewis, J. Mol. Biol. **275**, 773 (1998).
[21] E. Oroudjev *et al.*, Proc. Natl. Acad. Sci. USA **99**, 6460 (2002).
[22] A. H. Simmons, C. A. Michal, and L. W. Jelinski, Science **271**, 84 (1996).
[23] Y. Termonia, Macromolecules **27**, 7378 (1994).

[24] T. Lefevre, M. E. Rousseau, and M. Pezolet, Biophys. J. **92**, 2885 (2007).
[25] P. Papadopoulos, J. Solter, and F. Kremer, Eur. Phys. J. E **24**, 193 (2007).
[26] J. Kummerlen *et al.*, Macromolecules **29**, 2920 (1996).
[27] J. Beek *et al.*, Proc. Natl. Acad. Sci. USA **99**, 10266 (2002).
[28] P. T. Eles and C. A. Michal, Biomacromolecules **5**, 661 (2004).
[29] M. Xu, and R. V. Lewis, Proc. Natl. Acad. Sci. USA **87**, 7120 (1990).
[30] F. Vollrath and D. Porter, Soft Matter **2**, 377 (2006).
[31] D. Porter, F. Vollrath, and Z. Shao, Eur. Phys. J. E **16**, 199 (2005).
[32] T. Vehoff, A. Gliąęsoviąäc, H. Schollmeyer, A. Zippelius, and T. Salditt, Biophys. J. **93**, 4425 (2007).
[33] H. J. Zhou and Y. Zhang, Phys. Rev. Lett. **94**, 028104 (2005).
[34] K. Kerkam, C. Viney, D. Kaplan, and S. Lombardi, Nature **349**, 596 (1991).
[35] P. J. Willcox, S. P. Gido, W. Muller, and D. L. Kaplan, Macromolecules **29**, 5106 (1996).
[36] E. T. Samulski, Liquid Crystalline Order in Polymers, edited by A. Blumstein, (Academic Press, New York, 1978), Chap. 5, p. 186.
[37] D. P. Knight and F. Vollrath, Phil. Trans. R. Soc. Lond. B **357**, 155 (2002).
[38] D. Knight and F. Vollrath, Proc. R. Soc. Lond. B **266**, 519 (1996).
[39] K. Kerkam *et al.*, Nature **349**, 596 (1991).
[40] P. J. Wilcox *et al.*, Macromolecules **29**, 5106 (1996).
[41] P. G. de Gennes, J. Prost, The Physics of Liquid Crystals(2nd edt), (Clarendon Press, Oxford, 1993).
[42] W. Maier and A. Saupe, Z. Naturforsch. A., 14, 882 (1959).
[43] F. I. Bell, I. J. McEwen, and C. Viney, Nature **416**, 37 (2002).
[44] P. Pincus and P. G. de Gennes, J. Polymer Sciences: Polymer Symposium **65**, 85 (1978).
[45] M. Warner, E. M. Terentjev, Liquid Crystal Elastomers, (Clarendon Press, Oxford, 2003).
[46] R. W. Work, J. exp. Biol. **118**, 379 (1985).
[47] R. W. Work, Textile Res. J. **47**, 650 (1977).
[48] R. W. Work, J. Arachnol. **9**, 299 (1981).
[49] D. Porter, Group Interaction Modelling og Polymer Properties, (Marcel Dekker, New York, 1995).

6

Application of Low-Temperature Plasma Processes for Biomaterials

Uwe Walschus[1], Karsten Schröder[2], Birgit Finke[2], Barbara Nebe[3], Jürgen Meichsner[1], Rainer Hippler[1], Rainer Bader[3], Andreas Podbielski[3] and Michael Schlosser[1]
[1]*University of Greifswald, Greifswald*
[2]*Leibniz Institute for Plasma Science and Technology, Greifswald*
[3]*University of Rostock, Rostock*
Germany

1. Introduction

Physical plasma is defined as a gas in which part of the particles that make up the matter are present in ionized form. This is achieved by heating a gas leading to dissociation of the molecular bonds and subsequently ionization of the free atoms. Thereby, plasma consists of positively and negatively charged ions and negatively charged electrons as well as radicals, neutral and excited atoms and molecules (Raizer, 1997; Conrads and Schmidt, 2000). On the one hand, plasma is a natural phenomenon as more than 90 % of the universe is in the plasma state, for example in fire, in the polar aurora borealis and perhaps most importantly in the nuclear fusion reactions of the sun. On the other hand, plasma can be created artificially and has found applications in technology like plasma screens or light sources. The use of high temperature plasma for energy production is still the focus of ongoing research.

For the modification of biomaterial surfaces, low temperature plasma which is sometimes also called cold plasma is used. It is characterized by a low degree of ionization at low or atmospheric pressure (Roth, 1995; Roth 2001; Hippler et al., 2008). To create low temperature plasmas, a compound is first transformed into a gas and then ionized by applying energy in the form of heat, direct or alternating electric current, radiation or laser light. Commonly used plasma gas sources are oxygen, nitrogen, hydrogen or argon. Two typical research plasma reactors for different applications are shown in Fig. 1. Depending on the nature and amount of energy, low temperature plasmas are characterized by a non-equilibrium between electron temperature and gas temperature. Thus the main parameters which define the characteristics of a plasma and thereby its applicability are its temperatures, types and densities of radicals and its level of ionization. In material science, possible applications of low-temperature plasmas include the modification of surface properties like electrochemical charge or amount of oxidation as well as attachment or modification of surface-bound chemical groups. Consequently, properties like hardness, resistance to chemical corrosion or physical abrasion, wettability, the water absorption capacity as well as the affinity toward

specific molecules can be modulated specifically and precisely by the use of low-temperature plasmas (Meichsner et al., 2011).

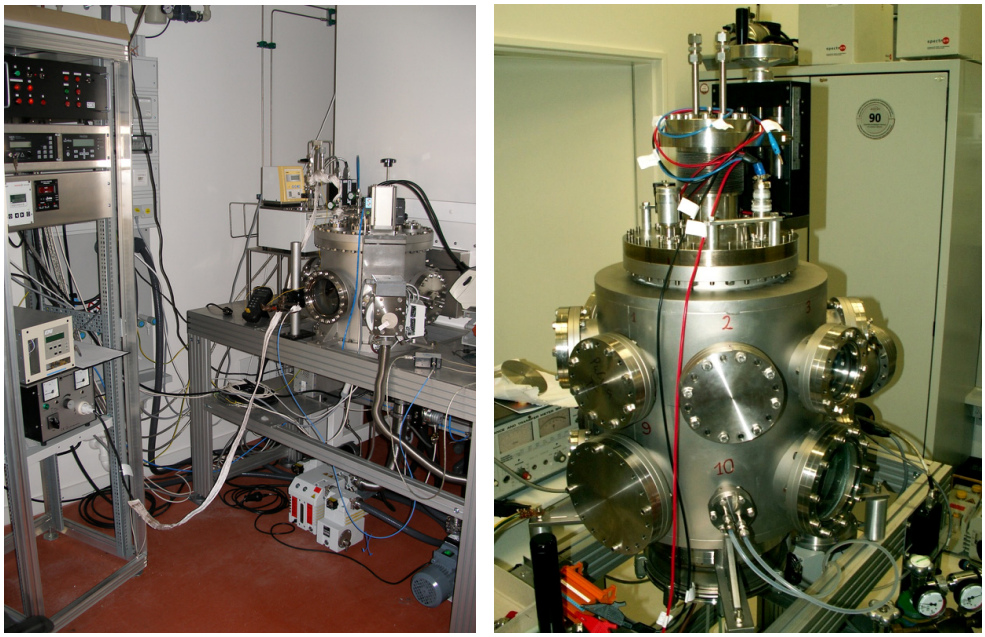

Fig. 1. Laboratory-size low-temperature plasma reactors for argon / ethylenediamine plasma (left) and pulsed magnetron sputtering (right)

Plasma treatments can be used to improve different aspects of the therapeutic characteristics of medical implants (Ohl & Schröder, 2008; Schröder et al., 2011). Possible applications include the incorporation of therapeutic agents into implants or the attachment of drug molecules onto the material surface. This includes for example plasma processes used for surface coupling of antibiotic substances or for integration of metal ions into biomaterial surfaces to create implants which exhibit long-lasting antibacterial properties after implantation. By creating such implants with antibacterial properties, the often devastating effects of implant-related infections could be markedly reduced. Therapeutic agents for other applications can be loaded onto implant surfaces via plasma treatment as well to achieve their controlled release over time. Possible applications are drug-eluting stents and vascular prostheses which release drugs to reduce blood coagulation and thombosis as well as to prevent intima hyperplasia and restenosis.

Low-temperature plasma-modified surfaces were furthermore found to possess specific bioactive properties in vitro and in vivo. For example, such surfaces influence the attachment and growth of osteoblasts, fibroblasts and inflammatory cells which provides the possibility to enhance implant ingrowth and tissue regeneration as well as to reduce implant-related inflammation, thereby improving the biocompatibility. Another field of application is plasma sterilization of prosthetic materials which is a gentle approach that can be adapted for many different materials and which is especially advantageous over

conventional methods regarding the required time. From a process technology point of view, sterilization would also be a beneficial concomitant effect of other plasma treatments aimed at modulating specific material properties. The range of materials which can be treated with low-temperature plasma processes includes many materials with an established track record in regenerative medicine, for example ceramics like hydroxyapatite, polymeric materials like polyester, polypropylene, silicone and polytetrafluoroethylene, and metals like titanium, titanium-based alloys and steel. Consequently, the possible utilization of plasma treatments in the field of biomaterials includes a wide range of applications in cardiovascular and reconstructive surgery, orthopaedics and dentistry. Therefore, low-temperature plasma processes have great potential for improvement of medical implants. In the following, a concise overview of the respective applications and the underlying plasma processes is presented, putting an emphasis on recent developments. The main directions of research in this developing field are reviewed in terms of the respective aims, the relevant materials and the potential clinical applications.

2. Plasma-assisted creation of implants containing therapeutic compounds

The coating of implant surfaces with therapeutic agents is an interesting approach to improve the clinical outcome of implantation. In this field, the treatment with plasma can be used to either facilitate the surface attachment of the respective drug itself or to create a layer on top of a coating with a therapeutic compound to modulate the kinetics of its release. Among the multitude of possible applications, recent research activities are focused on two main directions: the equipment of implants with antibiotics and other compounds with antibacterial properties to prevent implant-related infections and the coating with anti-thrombogenic agents to prevent the formation of blood clots and thrombosis for implants with blood contact like vascular prostheses and stents. In principle, most of the plasma-based approaches used in these areas could also be applied with other drugs which have already been examined for drug-eluting implants, for example paclitaxel and everolimus (Butt et al., 2009), dexamethasone (Radke et al., 2004) or trapidil, probucol and cilostazol (Douglas, 2007) all aimed at reducing restenosis after implantation of vascular stents which is an emerging and clinically promising field for controlled drug release in biomaterials research.

2.1 Implant surfaces with antibacterial properties

The equipment of implants with antibacterial properties can be achieved either by attaching antibiotic substances or by creating surfaces which release metal ions which are known to have anti-infective effects. Polyvinylchloride, a polymer which is used for endotracheal tubes and catheters, was equipped with triclosan and bronopol, compounds with immediate and persistent broad-spectrum antimicrobial effects, after the surface was activated with oxygen plasma to produce more hydrophilic groups for effective coating (Zhang et al., 2006). Experiments using *Staphylococcus aureus* and *Escherichia coli* demonstrated the effectiveness of these surfaces. Similarly, polyvinylidenfluoride used for hernia meshes was modified by plasma-induced graft polymerization of acrylic acid with subsequent binding of the antibiotic gentamycin (Junge et al., 2005). In addition to the microbiological examination of the gentamycin-releasing material, the in vitro and in vivo biocompatibility was examined by cytotoxicity testing and implantation into Sprague-Dawley rats for up to 90 days, and no side effects on biocompatibility were observed. The fact that an implant

coating with a sustained release of gentamycin is effective against bacteria with no adverse effects on cellular proliferation was also confirmed by the evaluation of titanium implants with gentamycin grafted onto the surface of a plasma sprayed wollastonite coating (Li et al., 2008). Wollastonite was previously found to be a promising material for bone tissue repair due to its high bonding strength to titanium substrates, its mechanical properties and its bioactivity and biocompatibility (Liu et al., 2008).

Due to their well-known antibacterial effects, metals like silver, copper or tin are possible alternatives to classical antibiotic compounds as an effective and sustained release from coatings is possibly easier to achieve due to their small size. Similarly to gentamycin as mentioned before, silver has been used as a powder added to a plasma-sprayed wollastonite coating on titanium implants (Li et al., 2009). In comparison to a coating without silver, tests with *Escherichia coli* confirmed the antibacterial activity of the silver while an examination of osteoblast morphology revealed no obvious difference between both coatings. Furthermore, the release of silver was also examined for amino-hydrocarbon plasma polymer coatings (Lischer et al., 2011), after plasma immersion ion implantation into polyethylene (Zhang et al., 2008) and for silver nanoparticles bound to an allylamine plasma polymer thin film (Vasilev et al., 2010b). Similarly, the use of copper for antibacterial implant coatings has also been studied by plasma implantation into polyethylene (Zhang et al., 2007). The use of plasma immersion ion implantation is however not restricted to polymer materials as demonstrated by recent work on the application of this process for equipment of titantium surfaces with copper ions (Polak el al., 2010). Compared to controls, the implants created by this Plasma immersion ion implantation of copper reduced the number of methicillin-resistant *Staphylococcus aureus* cultivated on the respective surfaces (Schröder et al., 2010a). Ion implantation can also be used for non-metals like fluorine which is of particular relevance for dental applications. This was examined with titanium, stainless steel and polymethyl methacrylate for fluorine alone (Nurhaerani et al., 2006) or with stainless steel for a combination of fluorine with silver (Shinonaga & Arita, 2009).

2.2 Implant surfaces with reduced thrombogenicity

Another field of interest for plasma applications is the coating of implants with anti-thrombogenic agents. This is of special importance for vascular prostheses and stents which are in constant contact with blood. For these implants, thrombosis and blood clot formation are severe and potentially life-threatening complications. Classical anti-coagulants used for thrombosis prophylaxis and treatment include coumarin derivates like phenprocoumon for oral application as well as heparin which is physiologically found in the body and extracted for medicinal use from mucosal tissues of slaughtered meat animals and hirudin, originally from the European medical leech *Hirudo medicinalis*, for parenteral use. The Plasma-based attachment of heparin has for example been examined for stainless steel which is used in stents (Yang et al., 2010). For this application, a pulsed-plasma polymeric allylamine film with a high amino group density was created to subsequently immobilize heparin via its carboxylic groups and established coupling chemistry using 1-Ethyl-3-(3-dimethylaminopropyl) carbodiimide and N-Hydroxysuccinimide. In a similar way, a heparin coating of polystyrene surfaces was achieved by preadsorption with undecylenic acid, a FDA-approved natural fungicide for skin disorders, followed by treatment with argon plasma and covalent immobilization of an albumin-heparin conjugate (van Delden et

al., 1997). Another example is the heparinization of polyurethane by low temperature plasma and grafting of poly(acrylic acid), water-soluble chitosan and heparin (Lin et al., 2005). In addition to well-established anti-coagulants, the endothelial membrane protein thrombomodulin, a co-factor in the thrombin-activated anticoagulant pathway, has also been examined regarding plasma-based attachment on biomaterial surfaces. This application was studied for polytetrafluoroethylene, a common material for vascular prostheses, via CO_2 plasma activation and subsequent vapour phase graft polymerization of acrylic acid (Vasilets et al., 1997; Sperling et al., 1997). Another surface modification which was examined for reduced thrombogenicity was plasma-induced graft polymerization of 2-methacryloyloxyethyl phosphorylcholine on titanium alloy surfaces which resulted in reduced deposition and activation of platelets in subsequent in vitro experiments with ovine blood (Ye et al., 2009).

2.3 Regulation of drug release by barrier layers

In addition to plasma-assisted surface attachment of therapeutic compounds, plasma processes can also be used to create an over-coating which acts as a barrier to regulate the drug release. This application has for example been examined using daunomycin, an antibiotic substance, and rapamycin, a compound with immunosuppressive and anti-proliferative effects which is used for example in stents to prevent excessive tissue growth, in combination with a plasma polymerized tetramethylcyclo-tetrasiloxane coating (Osaki et al., 2011). Changing the deposition time length resulted in different coating thickness which, like the molecular weight of the drug, was found to influence the drug-release rate. A comparable approach was used on polyetherurethane onto which a plasma-deposited poly(butyl methyacrylate) membrane with controlled porosity was applied to control the release of ciprofloxacin (Hendricks et al., 2000). Adhesion and colonization of *Pseudomonas aeruginosa* was evaluated to assess the antimicriobial effectiveness.

Furthermore, an over-coating can also be applied to surfaces which release metal ions. For instance, the antibacterial surfaces created by plasma immersion ion implantation of copper as mentioned before were also treated with an additional layer of plasma-polymerized allylamine to regulate the Cu release and to modulate cellular adhesion and spreading. This combination reduced the antibacterial effects of the surface to some extent but did not completely disable it (Schröder et al., 2010a). On the other hand, the combined treatment also led to lower local inflammatory reactions after implantation into rats (Schlosser, unpublished data), highlighting the need to find an optimal balance between in vivo biocompatibility and sufficient antibacterial effects. Another study demonstrated that creation of thin films by plasma polymerization for controlled release of silver ions and traditional antibiotics is applicable to the surface of many different medical devices (Vasilev et al., 2010a).

The use of an over-coating to regulate the release rate is not only possible for antibiotics but also for antithrombogenic agents. This has for example been studied for hirudin for which an additional layer of 2-hydroxyethyl methacrylate created by glow discharge plasma deposition on drug-loaded polyurethane matrices served as a diffusional barrier controlling the hirudin release kinetics depending on the plasma coating conditions (Kim et al., 1998).

Of more general interest for the field of drug-releasing implants is a recent study which describes the use of liposomes, artificial vesicles enclosed by a lipid bilayer. Liposomes can

be used as drug containers by encapsulation of therapeutic compounds, in some cases additionally targeted to their site of action by antibodies, and potentially offer a wide range of applications. Covalent coating of liposomes onto stainless steel was achieved via radiofrequency glow plasma assisted creation of a thin film of acrylic acid characterized by surface carboxylic groups to which the liposomes were attached via formation of amide bonds (Mourtas et al., 2011). While the study was considered by the authors to be a proof of principle, the presented method seems to be a versatile approach due to possible changes of process parameters for the liposome immobilization procedure as well as regarding the choice of different drugs for encapsulation.

3. Plasma-based surface functionalization

Medical implants interact with their surrounding tissue in a complex manner. For example, a so called neointima layer is formed over time at the inner surface of vascular prostheses. Bone implants based on calcium phosphate possess osteoconductive and osteoinductive properties. Most importantly, all biomaterials are foreign to the body and the aim of acute and chronic inflammatory reactions which can persist for as long as the implant remains in the body. While short-term temporary implants which are removed some time after implantation should rather be inert, long-term implants intended for permanent presence in the recipient's body should ideally possess bioactive properties to facilitate proper tissue integration. A multitude of different approaches has been examined with the aim to influence the interactions between biomaterials and the host tissue, for example by regulation of protein and cell attachment to improve the implant ingrowth and to reduce implant-related inflammation. Possible methods include for example the coating with different proteins, with biomembrane-derived phospholipids, with diamond-like carbon or ceramics or the attachment of chemical groups to create surfaces with a specific electric charge. Low-temperature plasmas have extensively been examined in vitro and in vivo for these applications.

3.1 Creation of bioactive surfaces

The cell-material and tissue-material interactions can be influenced by modifying the surface charge via chemical groups. For example, an enhanced osteoblast growth in vitro was observed for surfaces modified with plasma-polymerized 1-aminoheptane (Zhao et al., 2011). The plasma-based deposition of acetaldehyde and allylamine polymer coatings on silicon and perfluorinated poly(ethylene-co-propylene) was found to influence the outgrowth of bovine corneal epithelial tissue for up to 21 days (Thissen et al., 2006). A treatment of Titanium samples with a comparable process called plasma-polymerized allylamine, based on the polymerization of allylamine after activation with a continuous wave oxygen-plasma, creates a positively charged amino group rich surface aimed at improving attachment of the negatively charged matrix substance hyaluronan. This coating was found to be advantageous concerning initial osteoblast adhesion and spreading (Nebe et al., 2007) and to have beneficial effects in vitro on the formation of focal adhesions as well as on cell morphology and spreading (Finke et al., 2007) and vinculin mobility (Rebl et al., 2010) of osteoblasts. An in vivo examination in rats revealed no negative influence on the number of total and tissue macrophages, T cells and MHC class II antigen-presenting cells in the peri-implant tissue (Hoene et al., 2010). Furtheremore, it was demonstrated that the

plasma parameters influence the surface properties and thereby the host response. Samples with a lower plasma duty cycle (ratio of plasma on-time t_{on} divided by the overall pulse duration $t_{on} + t_{off}$) resulted in a higher layer thickness and protein absorption as well as a lower oxygen uptake due to sonication in distilled water. Consequently, the hydrogel-like character of the plasma-polymerized allylamine films was probably more developed for the high duty cycle samples, resulting in an overall lower inflammatory response in vivo than for the implants created with a low duty cycle (Hoene et al., 2010). Similar results regarding enhanced cell adhesion were also obtained for a plasma consisting of a mixture of argon and ethylenediamine (Finke et al., 2011). A treatment of a hip prosthesis with this plasma process is exemplarily shown in Fig. 2.

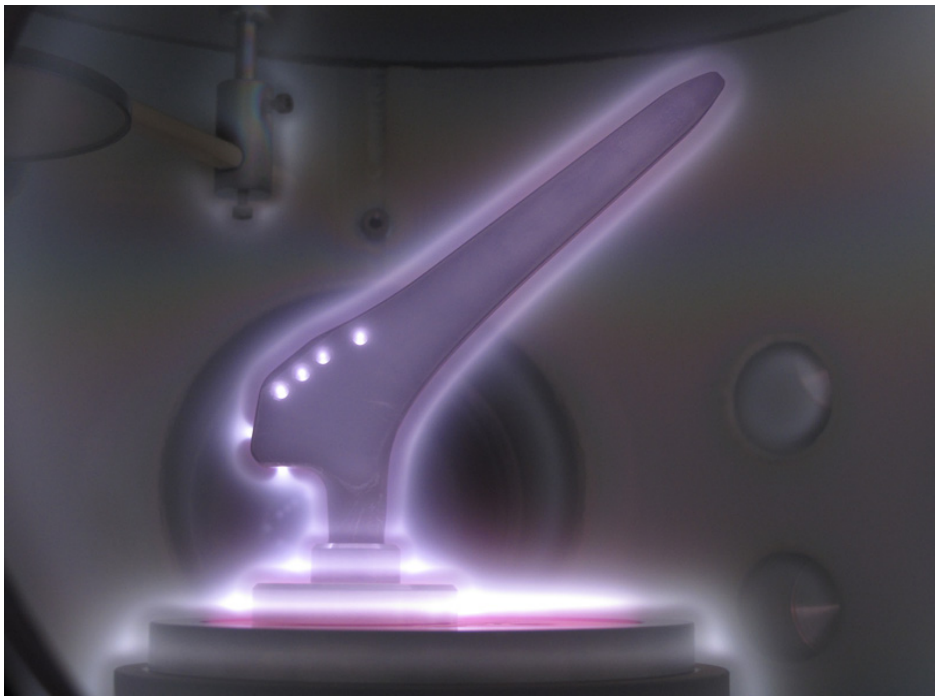

Fig. 2. Hip joint implant in low pressure plasma using a mixture of argon and ethylenediamine for cell adhesive coating

In contrast to these positively charged NH_2 films, a coating of Titanium implants with acrylic acid after similar plasma activation, called plasma-polymerized acrylic acid, results in a negatively charged COOH-group rich surface which was found to facilitate osteogenic differentiation by stimulation of mRNA expression of early (ALP, COL, Runx2) as well as late (BSP, OCN) bone differentiation markers (Schröder et al., 2010b). However, the long-term inflammatory response in vivo caused by this coating were increased compared to uncoated controls (Schröder et al., 2010b), highlighting the difficult balance that improving one specific aspect of implant characteristics is often accompanied by adverse changes in other parameters. Furthermore, it illustrates the problem that the results of in vitro experiments on the one hand and in vivo studies on the other are often inconsistent due to

the complex nature of reactions in a living organism which can only partially and often inadequately be modelled using in vitro approaches.
Similar to metals and metal alloys, cell attachment on polymers can also be modulated by plasma treatment. The application of glow-discharge plasma of mixed ammonia and oxygen on polytetrafluoroethylene surfaces reduced the hydrophobicity and increased the attachment of aorta endothelial cells (Chen et al., 2003). Furthermore, an oxygen plasma has been shown to improve surface attachment of mouse fibroblasts L-929 on thermoplastic polyetherurethane used for gastric implants (Schlicht et al., 2010).
Low-temperature plasma can also be used to achieve immobilization of bioactive molecules. This was demonstrated for example by an oxygen plasma treatment to enhance the immobilization of simvastatin, which stimulates bone formation, onto Ti surfaces (Yoshinari et al., 2006). The deposition of thin film from ethylene plasma on Ti surfaces allows the chemical attachment of hydroxyethylmethacrylate onto Ti to improve the in vitro adhesion of mouse fibroblasts L-929 (Morra & Cassinelli, 1997). Albumin nanoparticles conjugated with a truncated fragment of fibronectin were directly patterned onto polymers to elicit adhesion and spreading of human mesenchymal stem cells and fibroblasts (Rossi et al., 2010). Stable coating of collagen type I onto two different metal alloys (Ti6Al4V, X2CrNiMo18) was achieved using a argon-hydrogen plasma and found to increase the viability and attachment of human osteoblast-like osteosarcoma cells SAOS-2 (Hauser et al., 2010), and coating of collagen onto silicone performed with an argon-oxygen plasma led to increased adhesion and viability of mouse fibroblasts 3T3 (Hauser et al., 2009). Poly(lactide-co-glycolide), a biodegradable polymer widely used as scaffold material for tissue engineering, was modified by oxygen plasma treatment followed by anchorage of cationized gelatine for improved attachment and growth of mouse fibroblasts 3T3 (Shen et al, 2007).
A popular material for bioactive coatings on implants for bone replacement is calcium phosphate which is the main natural component in the bone matrix where it accounts for more than half of the bone weight. It exists in a variety of different chemical preparations differing in their atomic and ionic lattice configuration, their Ca:P ratio, the number and size of pores, and their surface area. One calcium phosphate preparation commonly used for biomaterials is hydroxyapatite ($Ca_{10}(PO_4)_6(OH)_2$) which is generally considered to be osteoconductive and osteoinductive (Walschus et al., 2009). Using a process called plasma spraying, it is possible to deposit thin and dense layers of hydroxyapatite onto metal implant surfaces (de Groot et al., 1987). Due to the well-established bioactive properties and good biocompatibility of hydroxyapatite, these coatings have been clinically used in dentistry and orthopedics since the mid 1980s (Tang et al., 2010). Furthermore, plasma spraying can also be used to create other layers like Ca-Si-Ti-based sphene ceramics (Wu et al., 2009), hydroxyapatite/ silica ceramics (Morks 2008), zirconia (Morks & Kobayashi 2008; Wang et al., 2010), yttria-stabilized zirconia (Wang et al., 2009) or hydroxyapatite/ yttria/ zirconia composites (Chang et al., 1997; Gu et al., 2004). One important advantage of plasma-sprayed coatings for biomaterials is the ability to precisely modify the microstructure by modulating the parameters of the plasma process (Khor et al., 2004; Huang et al., 2010) to study and improve microstructure-related tissue growth stimulation.

3.2 Plasma-assisted vapour deposition of inert diamond-like carbon layers

Another field of increasing interest which should be mentioned briefly in this chapter is the plasma-based coating of implants with diamond-like carbon for which plasma-assisted chemical vapour deposition is the most commonly used deposition method. Diamond-like

carbon layers can exhibit the typical diamond crystalline structure, an amorphous structure or a mixture of both (Schlosser & Ziegler, 1997). Furthermore, depending on the coating procedure, they can consist of pure carbon or contain other elements. Overall, diamond-like carbon films are characterized by an excellent mechanical stability and hardness, a high corrosion resistance as well as reduced tissue-material interactions and no detectable cytotoxicity (Schlosser & Ziegler, 1997). Particularly for implants where inertness of the surface is required, they are therefore an attractive option for coating of medical implants in a number of applications in reconstructive surgery and dentistry (Roy & Lee, 2007). Diamond-like carbon coatings have for example been examined for ureteral stents (Laube et al., 2007), orthodontic archwires (Kobayashi et al., 2007), joint implants (Thorwarth et al., 2010) or cardiovascular stents (De Scheerder et al., 2000).

4. Plasma sterilization

Sterilization as the elimination of living microorganisms like bacteria, viruses and fungi, especially pathogenic agents, is an important aspect in biomaterials applications to prevent implant-related infections. Commonly used methods to achieve sterility include the treatment with heat, chemicals and irradiation. Each of those methods has its specific disadvantages and not all are equally usable for the sterilization of medical implants. For example, a heat treatment can lead to irreversible modifications of heat-labile materials and to denaturation of protein coatings. Irradiation with UV or gamma rays requires cost-intensive equipment with high safety requirements and can also cause irreversible modifications of proteins such as albumin and collagen used as sealing impregnation of vascular prostheses, as well as biomaterials like polymers. Chemical sterilization using for example ethylene oxide could result in residuals on the treated surface. Therefore, the application of low-temperature plasma processes as an alternative sterilization technique which is a gentle process from a physico-chemical point of view has been the focus of ongoing research since several years. It is known that exposure to plasma effectively and irreversibly damages cells from different bacteria species like for example *Escherichia coli, Staphylococcus aureus*, *Pseudomonas aeruginosa*, *Bacillus cereus* or *Bacillus subtilis* (Bazaka et al., 2011). Especially for modified or functionalized biomaterials, sterilization with low-temperature plasma would therefore be an attractive option as it could be achieved as a secondary effect of plasma treatment aimed at other surface modification purposes (Bazaka et al., 2011).

The application of plasma sterilization of heat-sensitive silicone implants has recently been demonstrated (Hauser et al., 2011). Similarly, sterilization of poly-L-lactide electrospun microfibers which can be used to repair tissue defects can effectively be achieved by hydrogen peroxide gas plasma which ensures sterility of the scaffolds and does not affect their chemical and morphological features (Rainer et al., 2010). Biodegradable polyester three-dimensional tissue engineering scaffolds which are particularly prone to morphological degeneration by high temperature and pressure were successfully sterilized with an argon-based radio-frequency glow discharge plasma (Holy et al., 2001), demonstrating the usefulness of plasma sterilization for damageable materials. Similar results were also obtained for starch based biomaterials for which a recent study found that treatment with oxygen plasma resulted in more hydrophilic surfaces compared to UV-irradiation (Pashkuleva et al., 2010). Furthermore, both methods gave comparable results regarding osteoblast adherence, from which the authors concluded that plasma sterilization

as well as UV-irradiation improved the biocompatibility and can be used as cost-effective methods for sterilization.
For metal implants, it was found that rapid and efficient sterilization of different alloys like X2CrNiMo18-15-3, Ti6Al7Nb und Ti6Al4V is possible with plasmas based on different gas mixtures such as argon/oxygen, argon/hydrogen and argon/nitrogen (Hauser et al., 2008). Sterilization of non-woven polyethylene terephthalate fiber structures for vascular grafts with either ethylene oxide or low temperature plasma resulted in comparable fibroblastic viability but a significantly higher TNF-α release, indicating activation of macrophages, for macrophages incubated on the fibres which were treated with ethylene oxide (Dimitrievska et al., 2011). Subcutaneous implantation into mice demonstrated inflammation accompanied by a foreign body reaction with no difference after 30 days between the samples treated with the two sterilization methods. A comparison of the effects of sterilization with gamma irradiation, ethylene oxide treatment, electron beam irradiation and plasma sterilization on the in vitro behaviour of polylactide fibres revealed that sterilization with both gamma and electron beam irradiation caused a decrease of the intrinsic viscosity while treatment with ethylene oxide and plasma sterilization had no pronounced effects on the sample properties (Nuutinen et al., 2002). These results also highlight the potential of plasma sterilization as a gentle alternative to other commonly used sterilization methods. However, it is not equally suitable for all materials as it might have adverse effects on relevant material properties. For example, demineralized bone matrix which was sterilized with low-temperature gas-plasma sterilization lost its osteoinductive capacity (Ferreira et al., 2001).
Another application related to sterilization is the removal of surface contaminations. This is particularly important for residues like prion proteins which have contagious and pathogenic properties. The usefulness of plasma treatment for molecular-level removal of proteinaceous contamination was recently demonstrated for silicon and surgical stainless steel surfaces (Banerjee et al., 2010).

5. Conclusions and outlook

Low temperature plasmas offer a wide range of applications in biomaterials research to improve the clinical performance of medical implants by modifying their surface characteristics. In many cases, the use of plasmas facilitates modifications which are difficult or unable to achieve by conventional physical or chemical methods, like for example the stable attachment of molecules onto noble metal surfaces. The concise overview presented in this chapter demonstrates the potential of low temperature plasma processes for the precise modification of specific implant surface properties while retaining the overall characteristics of the material. The main aims of research in this field are to reduce implant-related complications like infections, thrombus formation and inflammation as well as to modulate the cell-material and tissue-material interactions for improved implant ingrowth. Another equally important area of research is the use of plasmas for sterilization. The studies which were presented here indicate that plasma processes are applicable for practically all commonly used biomaterials including metals, polymers, ceramics and composites, offering a wide range of clinical applications in all fields of reconstructive medicine.
Given the versatility of low temperature plasma processes and the diverse nature of materials and clinical applications, it is difficult to predict future developments in this field. If there is any specific trend, then it is an increase in the number of studies which deal with biodegradable materials, reflecting an overall surge of interest in biomaterials research for this kind of materials. Another development is the use of increasingly sophisticated methods for surface analysis, making it possible to draw precise conclusions regarding relationships

between process parameters, surface characteristics and the biological response. Two important aspects in need of more research are on the one hand the aging-related surface changes of plasma-modified biomaterials and on the other hand their in vivo behaviour. Most of the studies discussed here used only in vitro methods to assess the biocompatibility. However, for the step from the lab into clinical practice it is essential to examine the in vivo biocompatibility by using appropriate animal models. There are several aspects of biocompatibility, both short- and long-term, which can not be adequately examined with in vitro methods like cell culture techniques. More detailed in vivo testing together with a better understanding of the influence of the plasma parameters on the physico-chemical material properties and on the response of cells, tissues and living organisms will ultimately turn currently promising research projects into clinical applications for improved implants. The increasing interest in the application of low-temperature plasmas in biomaterials science is illustrated by the formation of long-term and large-scale research projects, scientific centers and institutional networks in recent years, for example the Plasma Physics and Radiation Technology Cluster at the Eindhoven University of Technology in the Netherlands, the Center for Advanced Plasma Surface Technology (CAPST) in Korea, and the Campus PlasmaMed at the Leibniz Institute of Plasma Science and Technology Greifswald, the University of Greifswald and the University of Rostock in Germany.

6. References

Banerjee K.K., Kumar S., Bremmell K.E. & Griesser H.J. (2010). Molecular-level removal of proteinaceous contamination from model surfaces and biomedical device materials by air plasma treatment. *Journal of Hospital Infection*, Vol. 76, No. 3, pp. 234-242.

Bazaka K., Jacob M.V., Crawford R.J. & Ivanova E.P. (2011). Plasma-assisted surface modification of organic biopolymers to prevent bacterial attachment. *Acta Biomaterialia*, Vol. 7, No. 5, pp. 2015-2028.

Butt M., Connolly D. & Lip G.Y. (2009). Drug-eluting stents: a comprehensive appraisal. *Future Cardiology*, Vol. 5, No. 2, pp. 141-157.

Chang E., Chang W.J., Wang B.C. & Yang C.Y. (1997). Plasma spraying of zirconia-reinforced hydroxyapatite composite coatings on titanium. Part I: phase, microstructure and bonding strength. *Journal of Materials Science: Materials in Medicine*, Vol. 8, No. 4, pp. 193-200.

Chen M., Zamora P.O., Som P., Peña L.A. & Osaki S. (2003). Cell attachment and biocompatibility of polytetrafluoroethylene (PTFE) treated with glow-discharge plasma of mixed ammonia and oxygen. *Journal of Biomaterials Science: Polymer Edition*, Vol. 14, No. 9, pp. 917-935.

Conrads H. & Schmidt M. (2000). Plasma generation and plasma sources. *Plasma Sources Science and Technology*, Vol. 9, No. 4, pp. 441-454.

de Groot K., Geesink R., Klein C.P. & Serekian P. (1987). Plasma sprayed coatings of hydroxylapatite. *Journal of Biomedical Materials Research*, Vol. 21, No. 12, pp. 1375-1381.

De Scheerder I., Szilard M., Yanming H., Ping X.B., Verbeken E., Neerinck D., Demeyere E., Coppens W. & Van de Werf F. (2000). Evaluation of the biocompatibility of two new diamond-like stent coatings (Dylyn) in a porcine coronary stent model. *Journal of Invasive Cardiology*, Vol. 12, No. 8, pp. 389-394.

Dimitrievska S., Petit A., Doillon C.J., Epure L., Ajji A., Yahia L. & Bureau M.N. (2011). Effect of sterilization on non-woven polyethylene terephthalate fiber structures for vascular grafts. *Macromolecular Bioscience*, Vol. 11, No. 1, pp. 13-21.

Douglas J.S. Jr. (2007). Pharmacologic approaches to restenosis prevention. *American Journal of Cardiology*, Vol. 100, No. 5 Suppl. 1, pp. S10-S16.

Ferreira S.D., Dernell W.S., Powers B.E., Schochet R.A., Kuntz C.A., Withrow S.J. & Wilkins R.M. (2001). Effect of gas-plasma sterilization on the osteoinductive capacity of demineralized bone matrix. *Clinical Orthopaedics and Related Research*, Vol. 388, pp. 233-239.

Finke B., Lüthen F., Schröder K, Mueller P.D., Bergemann C., Frant M., Ohl A. & Nebe B.J. (2007). The effect of positively charged plasma polymerization on initial osteoblastic focal adhesion on titanium surfaces. *Biomaterials*, Vol. 28, No. 30, pp. 4521-4534.

Finke B., Hempel F., Testrich H., Artemenko A., Rebl H., Kylián O., Meichsner J., Biederman H., Nebe B., Weltmann K.-D., Schröder K. (2011). Plasma processes for cell-adhesive titanium surfaces based on nitrogen-containing coatings. *Surface & Coatings Technology*, Vol. 205, Suppl. 2, pp. S520-S524

Gu Y.W., Khor K.A., Pan D. & Cheang P. (2004). Activity of plasma sprayed yttria stabilized zirconia reinforced hydroxyapatite/Ti-6Al-4V composite coatings in simulated body fluid. *Biomaterials*, Vol. 25, No. 16, pp. 3177-3185.

Hauser J., Halfmann H., Awakowicz P., Köller M. & Esenwein S.A. (2008). A double inductively coupled low-pressure plasma for sterilization of medical implant materials. *Biomedical Engineering*, Vol. 53, No. 4, pp. 199-203.

Hauser J., Zietlow J., Köller M., Esenwein S.A., Halfmann H., Awakowicz P. & Steinau H.U. (2009). Enhanced cell adhesion to silicone implant material through plasma surface modification. *Journal of Materials Science: Materials in Medicine*, Vol. 20, No. 12, pp. 2541-2548.

Hauser J., Köller M., Bensch S., Halfmann H., Awakowicz P., Steinau H.U. & Esenwein S. (2010). Plasma mediated collagen-I-coating of metal implant materials to improve biocompatibility. *Journal of Biomedical Materials Research Part A*, Vol. 94, No. 1, pp. 19-26.

Hauser J., Esenwein S.A., Awakowicz P., Steinau H.U., Köller M. & Halfmann H. (2011). Sterilization of heat-sensitive silicone implant material by low-pressure gas plasma. *Biomedical Instrumentation & Technology*, Vol. 45, No. 1, pp. 75-79.

Hendricks S.K., Kwok C., Shen M., Horbett T.A., Ratner B.D. & Bryers J.D. (2000). Plasma-deposited membranes for controlled release of antibiotic to prevent bacterial adhesion and biofilm formation. *Journal of Biomedical Materials Research*, Vol. 50, No. 2, pp. 160-170.

Hippler R., Kersten H., Schmidt M. & Schoenbach K.H. (2008). Low temperature plasma physics: Fundamental aspects and applications. Wiley-VCH, Weinheim, Germany.

Hoene A., Walschus U., Patrzyk M., Finke B., Lucke S., Nebe B., Schröder K., Ohl A. & Schlosser M. (2010). In vivo investigation of the inflammatory response against allylamine plasma polymer coated titanium implants in a rat model. *Acta Biomaterialia*, Vol. 6, No. 2, pp. 676-683.

Holy C.E., Cheng C., Davies J.E. & Shoichet M.S. (2001). Optimizing the sterilization of PLGA scaffolds for use in tissue engineering. *Biomaterials*, Vol. 22, No. 1, pp. 25-31.

Huang Y., Song L., Liu X., Xiao Y., Wu Y., Chen J., Wu F. & Gu Z. (2010). Hydroxyapatite coatings deposited by liquid precursor plasma spraying: controlled dense and porous microstructures and osteoblastic cell responses. *Biofabrication*, Vol. 2, No. 2, paper 045003.

Junge K., Rosch R., Klinge U., Krones C., Klosterhalfen B., Mertens P.R., Lynen P., Kunz D., Preiss A., Peltroche-Llacsahuanga H. & Schumpelick V. (2005). Gentamicin supplementation of polyvinylidenfluoride mesh materials for infection prophylaxis. *Biomaterials*, Vol. 26, No. 7, pp. 787-793.

Khor K.A., Gu Y.W., Pan D. & Cheang P. (2004). Microstructure and mechanical properties of plasma sprayed HA/YSZ/Ti-6Al-4V composite coatings. *Biomaterials*, Vol. 25, No. 18, pp. 4009-4017.

Kim D.D., Takeno M.M., Ratner B.D. & Horbett T.A. (1998). Glow discharge plasma deposition (GDPD) technique for the local controlled delivery of hirudin from biomaterials. *Pharmaceutical Research*, Vol. 15, No. 5, pp. 783-786.

Kobayashi S., Ohgoe Y., Ozeki K., Hirakuri K. & Aoki H. (2007). Dissolution effect and cytotoxicity of diamond-like carbon coatings on orthodontic archwires. *Journal of Materials Science: Materials in Medicine*, Vol. 18, No. 12, pp. 2263-2268.

Laube N., Kleinen L., Bradenahl J. & Meissner A. (2007). Diamond-like carbon coatings on ureteral stents--a new strategy for decreasing the formation of crystalline bacterial biofilms? *Journal of Urology*, Vol. 177, No. 5, pp. 1923-1927.

Li B., Liu X., Cao C., Dong Y., Wang Z. & Ding C. (2008). Biological and antibacterial properties of plasma sprayed wollastonite coatings grafting gentamicin loaded collagen. *Journal of Biomedical Materials Research Part A*, Vol. 87, No. 1, pp. 84-90.

Li B., Liu X., Cao C., Dong Y. & Ding C. (2009). Biological and antibacterial properties of plasma sprayed wollastonite/silver coatings. *Journal of Biomedical Materials Research Part B: Applied Biomaterials*, Vol. 91, No. 2, pp. 596-603.

Lin W.C., Tseng C.H. & Yang M.C. (2005). In-vitro hemocompatibility evaluation of a thermoplastic polyurethane membrane with surface-immobilized water-soluble chitosan and heparin. *Macromolecular Bioscience*, Vol. 5, No. 10, pp. 1013-1021.

Lischer S., Körner E., Balazs D.J., Shen D., Wick P., Grieder K., Haas D., Heuberger M. & Hegemann D. (2011). Antibacterial burst-release from minimal Ag-containing plasma polymer coatings. *Journal of the Royal Society Interface*, Vol. 8, No. 60, pp. 1019-1030.

Liu X., Morra M., Carpi A. & Li B. (2008). Bioactive calcium silicate ceramics and coatings. *Biomedicine & Pharmacotherapy*, Vol. 62, No. 8, pp. 526-529.

Meichsner J., Schmidt M., Wagner H.E. (2011). Non-thermal Plasma Chemistry and Physics. Taylor & Francis, London, UK.

Morks M.F. (2008). Fabrication and characterization of plasma-sprayed HA/SiO(2) coatings for biomedical application. *Journal of the Mechanical Behavior of Biomedical Materials*, Vol. 1, No. 1, pp. 105-111.

Morks M.F. & Kobayashi A. (2008). Development of ZrO2/SiO2 bioinert ceramic coatings for biomedical application. *Journal of the Mechanical Behavior of Biomedical Materials*, Vol. 1, No. 2, pp. 165-171.

Morra M. & Cassinelli C. (1997). Organic surface chemistry on titanium surfaces via thin film deposition. *Journal of Biomedical Materials Research*, Vol. 37, No. 2, pp. 198-206.

Mourtas S., Kastellorizios M., Klepetsanis P., Farsari E., Amanatides E., Mataras D., Pistillo B.R., Favia P., Sardella E., d'Agostino R. & Antimisiaris S.G. (2011). Covalent immobilization of liposomes on plasma functionalized metallic surfaces. *Colloids and Surfaces B: Biointerfaces*, Vol. 84, No. 1, pp. 214-220.

Nebe B., Finke B., Lüthen F., Bergemann C., Schröder K., Rychly J., Liefeith K. & Ohl A. (2007). Improved initial osteoblast functions on amino-functionalized titanium surfaces. *Biomolecular Engineering*, Vol. 24, No. 5, pp. 447-54.

Nurhaerani, Arita K., Shinonaga Y. & Nishino M. (2006). Plasma-based fluorine ion implantation into dental materials for inhibition of bacterial adhesion. *Dental Materials Journal*, Vol. 25, No. 4, pp. 684-692.

Nuutinen J.P., Clerc C., Virta T. & Törmälä P. (2002). Effect of gamma, ethylene oxide, electron beam, and plasma sterilization on the behaviour of SR-PLLA fibres in vitro. *Journal of Biomaterials Science: Polymer Edition*, Vol. 13, No. 12, pp. 1325-1336.

Ohl A., Schröder K. (2008). Plasma assisted surface modification of biointerfaces. In: Hippler R., Kersten H., Schmidt M. & Schoenbach K.H. Low temperature plasma physics: Fundamental aspects and applications. Wiley-VCH, Weinheim, Germany, pp. 803-819.

Osaki S.G., Chen M. & Zamora P.O. (2011). Controlled Drug Release through a Plasma Polymerized Tetramethylcyclo-tetrasiloxane Coating Barrier. *Journal of Biomaterials Science: Polymer Edition*, published online before print January 28, 2011, doi: 10.1163/092050610X552753.

Pashkuleva I., Marques A.P., Vaz F. & Reis R.L. (2010). Surface modification of starch based biomaterials by oxygen plasma or UV-irradiation. *Journal of Materials Science: Materials in Medicine*, Vol. 21, No. 1, pp. 21-32.

Polak M., Ohl A., Quaas M., Lukowski G., Lüthen F., Weltmann K.-D. & Schröder K. (2010). Oxygen and Water Plasma-Immersion Ion Implantation of Copper into Titanium for Antibacterial Surfaces of Medical Implants. *Advanced Engineering Materials*, Vol. 12, No. 9, pp. B511-B518.

Radke P.W., Weber C., Kaiser A., Schober A. & Hoffmann R. (2004). Dexamethasone and restenosis after coronary stent implantation: new indication for an old drug? *Current Pharmaceutical Design*, Vol. 10, No. 4, pp. 349-355.

Rainer A., Centola M., Spadaccio C., Gherardi G., Genovese J.A., Licoccia S. & Trombetta M. (2010). Comparative study of different techniques for the sterilization of poly-L-lactide electrospun microfibers: effectiveness vs. material degradation. *International Journal of Artificial Organs*, Vol. 33, No. 2, pp. 76-85.

Raizer Y.P. (1997). Gas Discharge Physics. Springer, Berlin, Germany.

Rebl H., Finke B., Ihrke R., Rothe H., Rychly J., Schröder K. & Nebe B.J. (2010). Positively Charged Material Surfaces Generated by Plasma Polymerized Allylamine Enhance Vinculin Mobility in Vital Human Osteoblasts. *Advanced Engineering Materials*, Vol. 12, No. 8, pp. B356-B364.

Rossi M.P., Xu J., Schwarzbauer J. & Moghe P.V. (2010). Plasma-micropatterning of albumin nanoparticles: Substrates for enhanced cell-interactive display of ligands. *Biointerphases*, Vol. 5, No. 4, pp. 105-113.

Roth J.R. (1995). Industrial Plasma Engineering. Volume 1: Principles. Institute of Physics Publishing, Bristol, UK.

Roth J.R. (2001). Industrial Plasma Engineering. Volume 2: Applications to Nonthermal Plasma Processing. Institute of Physics Publishing, Bristol, UK.

Roy R.K. & Lee K.R. (2007). Biomedical applications of diamond-like carbon coatings: a review. *Journal of Biomedical Materials Research Part B: Applied Biomaterials*, Vol. 83, No. 1, pp. 72-84.

Schlicht H., Haugen H.J., Sabetrasekh R. & Wintermantel E. (2010). Fibroblastic response and surface characterization of O(2)-plasma-treated thermoplastic polyetherurethane. *Biomedical Materials*, Vol. 5, No. 2, paper 25002

Schlosser M. & Ziegler M. (1997). Biocompatibility of Active Implantable Devices. In: Fraser, D.M. (Ed.). Biosensors in the Body. Continuous In Vivo Monitoring. John Wiley & Sons, Chicester, UK, pp. 140-170.

Schröder K., Finke B., Polak M., Lüthen F., Nebe J.B., Rychly J., Bader R., Lukowski G., Walschus U., Schlosser M., Ohl A. & Weltmann K.-D. (2010a). Gas-Discharge Plasma-Assisted Functionalization of Titanium Implant Surfaces. *Materials Science Forum*, Vols. 638-642, pp. 700-705.

Schröder K., Finke B., Ohl A., Lüthen F., Bergemann C., Nebe B., Rychly J., Walschus U., Schlosser M. Liefeith K., Neumann H.-G. & Weltmann K.-D. (2010b). Capability of Differently Charged Plasma Polymer Coatings for Control of Tissue Interactions with Titanium Surfaces. *Journal of Adhesion Science and Technology*, Vol. 24, No. 7, pp. 1191-1205.

Schröder K., Foest R., Ohl A. (2011). Biomedical applications of plasmachemical surface functionalization. In: Meichsner J., Schmidt M., Wagner H.E. Non-thermal Plasma Chemistry and Physics. Taylor & Francis, London, UK, in press

Shen H., Hu X., Yang F., Bei J. & Wang S. (2007). Combining oxygen plasma treatment with anchorage of cationized gelatin for enhancing cell affinity of poly(lactide-co-glycolide). *Biomaterials*, Vol. 28, No. 29, pp. 4219-4230.

Shinonaga Y. & Arita K. (2009). Surface modification of stainless steel by plasma-based fluorine and silver dual ion implantation and deposition. *Dental Materials Journal*, Vol. 28, No. 6, pp. 735-742.

Sperling C., König U., Hermel G., Werner C., Müller M., Simon F., Grundke K., Jacobasch H.J., Vasilets V.N. & Ikada Y. (1997). Immobilization of human thrombomodulin onto PTFE. *Journal of Materials Science: Materials in Medicine*, Vol. 8, No. 12, pp. 789-791.

Tang Q., Brooks R., Rushton N. & Best S. (2010). Production and characterization of HA and SiHA coatings. *Journal of Materials Science: Materials in Medicine*, Vol. 21, No. 1, pp. 173-181.

Thissen H., Johnson G., Hartley P.G., Kingshott P. & Griesser H.J. (2006). Two-dimensional patterning of thin coatings for the control of tissue outgrowth. *Biomaterials*, Vol. 27, No. 1, pp. 35-43.

Thorwarth G., Falub C.V., Müller U., Weisse B., Voisard C., Tobler M. & Hauert R. (2010). Tribological behavior of DLC-coated articulating joint implants. *Acta Biomaterialia*, Vol. 6, No. 6, pp. 2335-2341.

van Delden C.J., Lens J.P., Kooyman R.P., Engbers G.H. & Feijen J. (1997). Heparinization of gas plasma-modified polystyrene surfaces and the interactions of these surfaces with proteins studied with surface plasmon resonance. *Biomaterials*, Vol. 18, No. 12, pp. 845-852.

Vasilets V.N., Hermel G., König U., Werner C., Müller M., Simon F., Grundke K., Ikada Y. & Jacobasch H.J. (1997). Microwave CO2 plasma-initiated vapour phase graft

polymerization of acrylic acid onto polytetrafluoroethylene for immobilization of human thrombomodulin. *Biomaterials*, Vol. 18, No. 17, pp. 1139-1145.

Vasilev K., Simovic S., Losic D., Griesser H.J., Griesser S., Anselme K. & Ploux L. (2010a). Platforms for controlled release of antibacterial agents facilitated by plasma polymerization. *Conference Proceedings of the IEEE Engineering in Medicine and Biology Society*, pp. 811-814.

Vasilev K., Sah V.R., Goreham R.V., Ndi C., Short R.D. & Griesser H.J. (2010). Antibacterial surfaces by adsorptive binding of polyvinyl-sulphonate-stabilized silver nanoparticles. *Nanotechnology*, Vol. 21, No. 21, paper 215102.

Walschus U., Hoene A., Neumann H.-G., Wilhelm L., Lucke S., Lüthen F., Rychly J. & Schlosser M. (2009). Morphometric immunohistochemical examination of the inflammatory tissue reaction after implantation of calcium phosphate-coated titanium plates in rats. *Acta Biomaterialia*, Vol. 5, No. 2, pp. 776-784.

Wang G., Liu X., Gao J. & Ding C. (2009). In vitro bioactivity and phase stability of plasma-sprayed nanostructured 3Y-TZP coatings. *Acta Biomaterialia*, Vol. 5, No. 6, pp. 2270-2278.

Wang G., Meng F., Ding C., Chu P.K. & Liu X. (2010). Microstructure, bioactivity and osteoblast behavior of monoclinic zirconia coating with nanostructured surface. *Acta Biomaterialia*, Vol. 6, No. 3, pp. 990-1000.

Wu C., Ramaswamy Y., Liu X., Wang G. & Zreiqat H. (2009). Plasma-sprayed CaTiSiO5 ceramic coating on Ti-6Al-4V with excellent bonding strength, stability and cellular bioactivity. *Journal of the Royal Society Interface*, Vol. 6, No. 31, pp. 159-168.

Yang Z., Wang J., Luo R., Maitz M.F., Jing F., Sun H. & Huang N. (2010). The covalent immobilization of heparin to pulsed-plasma polymeric allylamine films on 316L stainless steel and the resulting effects on hemocompatibility. *Biomaterials*, Vol. 31, No. 8, pp. 2072-2083.

Ye S.H., Johnson C.A. Jr., Woolley J.R., Oh H.I., Gamble L.J., Ishihara K. & Wagner W.R. (2009). Surface modification of a titanium alloy with a phospholipid polymer prepared by a plasma-induced grafting technique to improve surface thromboresistance. *Colloids and Surfaces B: Biointerfaces*, Vol. 74, No. 1, pp. 96-102.

Yoshinari M., Hayakawa T., Matsuzaka K., Inoue T., Oda Y., Shimono M., Ide T. & Tanaka T. (2006). Oxygen plasma surface modification enhances immobilization of simvastatin acid. *Biomedical Research*, Vol. 27, No. 1, pp. 29-36.

Zhang W., Chu P.K., Ji J., Zhang Y., Liu X., Fu R.K., Ha P.C. & Yan Q. (2006). Plasma surface modification of poly vinyl chloride for improvement of antibacterial properties. *Biomaterials*, Vol. 27, No. 1, pp. 44-51.

Zhang W., Zhang Y., Ji J., Yan Q., Huang A. & Chu PK. (2007). Antimicrobial polyethylene with controlled copper release. *Journal of Biomedical Materials Research Part A*, Vol. 83, No. 3, pp. 838-844.

Zhang W., Luo Y., Wang H., Jiang J., Pu S. & Chu PK. (2008). Ag and Ag/N2 plasma modification of polyethylene for the enhancement of antibacterial properties and cell growth/proliferation. *Acta Biomaterialia*, Vol. 4, No. 6, pp. 2028-2036.

Zhao J.H., Michalski W.P., Williams C., Li L., Xu H.S., Lamb P.R., Jones S., Zhou Y.M. & Dai X.J. (2011). Controlling cell growth on titanium by surface functionalization of heptylamine using a novel combined plasma polymerization mode. *Journal of Biomedical Materials Research Part A*, Vol. 87, No. 2, pp. 127-134.

Part 2

Polymer-Based Nanomedicine for Targeted Therapy

7

δ-Free F_oF_1-ATPase, Nanomachine and Biosensor

Jia-Chang Yue[1], Yao-Gen Shu[2], Pei-Rong Wang[1] and Xu Zhang[1]
[1]*Institute of Biophysics, Chinese Academy of Sciences*
[2]*Institute of Theoretical Physics, Chinese Academy of Sciences*
China

1. Introduction

F_oF_1-ATPase is an exquisite nanomachines self-assembled by eight kinds of subunits, and is ubiquitous in the plasma membrane of bacteria, chloroplasts and mitochondria as well as uses the transmembrane electrochemical potential to synthesize ATP. The holoenzyme is a complex of two opposing rotary motors, F_o and F_1, which are mechanically coupled by a common central stalk ("rotor"), $c_n\epsilon\gamma$, and δb_2 subunits connecting two "stator", $\alpha_3\beta_3$ crown in F_1 and a in F_o. The membrane embedded F_o unit converts the proton motive force (p.m.f.) into mechanical rotation of the "rotor", thereby causing cyclic conformational change of $\alpha_3\beta_3$ crown ("stator") in F_1 and driving ATP synthesis. A striking characteristic of this motor is its reversibility. It may rotate in the reverse direction for ATP hydrolysis and utilize the excess energy to pump protons across the membrane(Ballmoos et al., 2009; Boyer, 1997; Feniouk & Yoshida, 2008; Junge, 2004; Saraste, 1999; Weber & Senior, 2003).
The basic hypothesis, "binding change mechanism"(Boyer et al., 1973), however, had not been confirmed until the direct observation of the rotation of F_1-ATPase at single molecule level in 1997(Noji et al., 1997), although it was partly proven by the eccentric structure of γ subunit in 1994(Abrahams et al., 1994). Single molecule technologies have contributed very much to the motor. For example, fluorescence imaging and spectroscopy revealed the physical rotation of isolated F_1(Adachi et al., 2007; Nishizaka et al., 2004; Noji et al., 1997; Yasuda et al., 1998) and F_o(Düser et al., 2009; Zhang et al., 2005), or F_1F_o holoenzyme(Diez et al., 2004; Kaim et al., 2002; Ueno et al., 2005). Magnetic tweezers also be employed to manipulate the ATP synthesis/hydrolysis in F_1(Itoh et al., 2004; Rondelez et al., 2005), and proton translation in F_o(Liu et al., 2006a). Recently, a membrane scaffold protein has been applied to observe the stepping rotation of proton channels (c_n)(Ishmukhametov et al., 2010).
There are three catalytic sites localized three identical β subunits in F_1 respectively. However, the three sites have different affinities for substrate at any given moment in time during catalysis. On the other hand, with different technologies such as AFM, Electron density, and laser-induced liquid bead ion desorption-MS(LILBID-MS) etc., the number of proton channels have been revealed ranging from 10 to 15 for different species(Jiang et al., 2001; Meier et al., 2007; Mitome et al., 2004; Pogoryelov et al., 2005; Seelert et al., 2000; Stock et al., 1999). Thus, it seems reasonable that three ATP molecules will be generated/consumed in F_1 for every cycle, at the same time $n(10 \sim 15)$ protons will be translated transmembrane in F_o because of the tight coupling between the two motors. That is, the H^+/ATP ratio should be $3/n$.
With the development of gene engineering, all subunits of the motor can be expressed in *E. Coli*. such that the motor can be self-assembled *in vitro* into a nanodevice for different

application(Choi & Montemagno, 2005; Liu et al., 2002; Luo et al., 2005; Martin et al, 2007; Soong et al., 2000). For example, if the δ subunit is removed from the motor, the two stators are structurally uncoupled, thereby the F_1 stator only contact with the common rotor. This is named δ-free F_oF_1 motor. Its stator is the a and b_2 subunits, while the rotor is built by c_n, ϵ, γ and $\alpha_3\beta_3$ subunits. Furthermore, this motor can be embedded in a chromatophore which functions as a battery recharged by illumination. Thus, the motor has been reconstructed into a self-driven nanomachine in which the only power is the transmembrane p.m.f. Here, we briefly review our works on the δ-free F_oF_1 motor including reconstituting, direct observation of its rotation, developing as a biosensor and a activator, and so on. However, we begin with the enzymatics of the holoenzyme to investigate the relation between the rotation speed and substrate/product concentrations, transmembrane p.m.f. and damping coefficient etc. which is of benefit to the quantitative analysis.

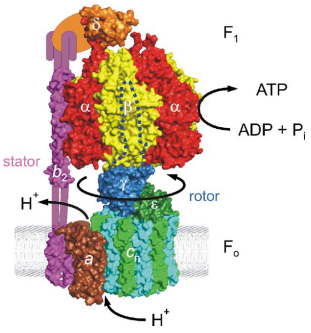

(a) Structure of F_oF_1-ATPase

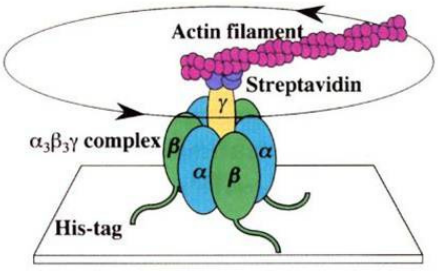

(b) Single-molecule experiment of isolated F_1

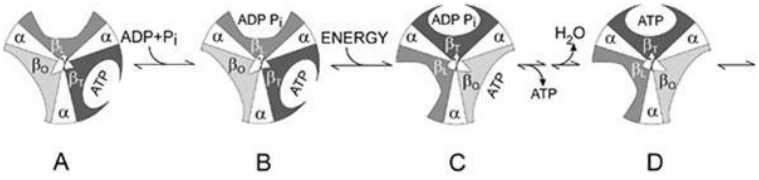

(c) Binding Change Mechanism of ATP synthase

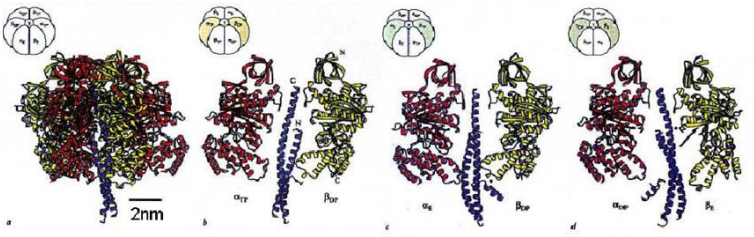

(d) The crystal structure of F_1

Fig. 1. The full-atom structure of the F_oF_1-ATPase(a)(Weber, 2006) and three main breakthroughs including direct observation of rotation of F_1(b)(Noji et al., 1997), basic hypothesis of "binding change mechanism" for ATP synthase(c)(Boyer, 1997) and crystal structure proving of the eccentric rotation of γ subunit(d)(Abrahams et al., 1994).

2. Enzymatics of the holoenzyme

From the viewpoint of enzymatics, conventional theory generally concerned with irreversible reaction on a single substrate which can be described by the Michaelis-Menten kinetics. But ATP can be reversibly synthesized and hydrolyzed in F_oF_1-ATPase, and the reaction involves several substrates/products. In particular, ATP hydrolysis does spontaneously occur in F_1, whereas the thermodynamically unfavorable reaction, ATP synthesis, has to be driven by harnessing the transmembrane proton flow in F_o. If it functions as a synthase, the two substrates, ADP and P_i, are recombined into one product, ATP. Though it is well established that the mechanical process, chemical reactions in F_1 and transmembrane proton transport in F_o are tightly coupled, that is, three ATP molecules will be generated in F_1 for every cycle with n protons transmembrane translation in F_o, the fundamental relation between the rotation speed and substrate/product concentrations, transmembrane p.m.f. and damping coefficient is still challenging.

2.1 Systematic kinetics of the holoenzyme

A few of theoretical approaches have been proposed aiming for a better understanding of the operating mechanism of this reversible motor. Some work focused on the hydrolysis or synthesis of F_1. For example, Oster *et al.* constructed a 4^3 states model for the couplings among three catalytic sites and provided a physical view of the dynamics(Sun et al., 2004; Wang & Oster, 1998; Xing et al., 2005). However, the model is too sophisticated to be investigated analytically. Some other models studied the mechanism of torque generation of F_o with a turbine or all-atom model(Aksimentiev et al., 2004; Elston et al., 1998; Oster et al., 2000). On the other hand, the kinetics of this motor has been investigated by Pänke *et al.* with simulations or storage of elastic energy model(Pänke & Rumberg, 1996; 1999). Here, we focus on analytical investigation of the systematic kinetics of the holoenzyme. Furthermore, presumably analytical results could allow for a deeper insight for the working principles of the motor.

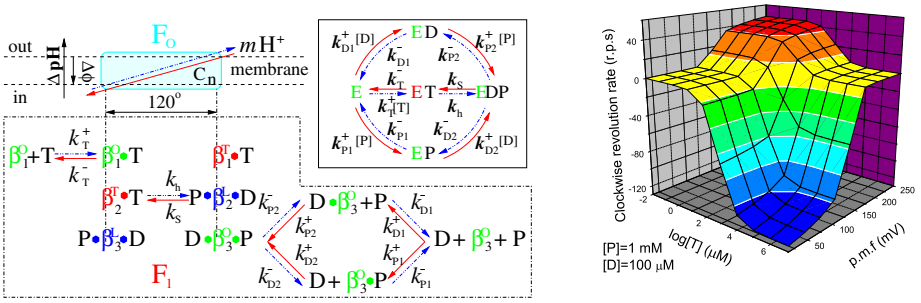

(a) Tri-site filled with random order binding model. (b) Speed versus ATP concentration and p.m.f.

Fig. 2. (a) Tri-site filled with random order binding model. Synthesis pathway runs from right to left (red solid), whereas hydrolysis one runs from left to right (blue dash dots). (b) Rotational speed of motor versus ATP concentration and p.m.f. Red or blue means that motor works in synthesis or hydrolysis respectively, and yellow represents that motor is near equilibrium(Shu & Lai, 2008).

It is well established that the mechanical process in F_o and the chemical reactions in F_1 are tightly coupled. Therefore, it is possible to construct a theory which can systematically describe the whole machine. Here, we propose a tri-site filled with random order of ADP and P_i binding model (shown in Fig.2(a)). The kinetics of this reversible reaction may be described by the equations governing the probabilities(denoted by P_E, P_{ET}, P_{EDP}, P_{ED}, and P_{EP}) of these five states:

$$\left.\begin{array}{ll}
\dot{P}_{E} &= k_{T}^{-}P_{ET} + k_{D1}^{-}P_{ED} + k_{P1}^{-}P_{EP} - (k_{D1}^{+}[D] + k_{P1}^{+}[P] + k_{T}^{+}[T])P_{E} \\
\dot{P}_{ET} &= k_{T}^{+}[T]P_{E} + k_{s}P_{EDP} - (k_{T}^{-} + k_{h})P_{ET} \\
\dot{P}_{EDP} &= k_{h}P_{ET} + k_{P2}^{+}[P]P_{ED} + k_{D2}^{+}[D]P_{EP} - (k_{D2}^{-} + k_{P2}^{-} + k_{s})P_{EDP} \\
\dot{P}_{ED} &= k_{P2}^{-}P_{EDP} + k_{D1}^{+}[D]P_{E} - (k_{D1}^{-} + k_{P2}^{+}[P])P_{ED} \\
P_{EP} &= 1 - (P_{E} + P_{ET} + P_{EDP} + P_{ED})
\end{array}\right\}, \tag{1}$$

where the square bracket [ ] denotes the concentration, T, D and P represent ATP, ADP and P_i respectively, and $k^+(k^-)$ is the binding(unbinding) constant. The steady-state reaction rate has been derived to be of second degree in ADP and P_i concentrations, and cannot be treated in terms of a Michaelis-Menten form. However, if the bindings and unbindings of ADP and P_i are completely independent and there is no mutual interaction, i.e. $k_{D1}^{\pm} = k_{D2}^{\pm} \equiv k_{D}^{\pm}$ and $k_{P1}^{\pm} = k_{P2}^{\pm} \equiv k_{P}^{\pm}$, it can be put into an apparent Michaelis-Menten equation. In addition, clamped ΔpH experiment(Kothen et al., 1995) has shown that binding and unbinding of a substrate (at cosubstrate saturation) are rapid processes as compared to the synthesis/hydrolysis step (mechanical rotation), which means that $k_{s/h} \ll k_L \equiv k_P^+[P] + k_D^+[D] + k_P^- + k_D^-$. Within the framework of steady-state conditions, the clockwise revolution rate of the motor at steady state is given by $\frac{1}{3}(k_s P_{EDP} - k_h P_{ET})$ and can be computed to be

$$r_c = \frac{\frac{1}{3}v_M^s v_M^h \left\{[D][P] - \frac{[T]}{K_e}\right\}}{(K_M^P[D] + K_M^D[P] + [D][P])\, v_M^h + \frac{K_M^T + \sigma[T]}{K_e} v_M^s}. \tag{2}$$

The definition and meaning of various quantities in the above equation are given below: v_M^s and v_M^h are the saturated rates of synthesis and hydrolysis and are given by

$$v_M^s \equiv \frac{v_{max}^s k_s}{k_s + k_h + v_{max}^s(1 - k_s/k_L)} \approx \frac{v_{max}^s k_s}{k_s + v_{max}^s + k_h}, \tag{3}$$

$$v_M^h \equiv \frac{v_{max}^h k_h}{k_h + v_{max}^h[1 - (k_h - k_s)/k_L]} \approx \frac{v_{max}^h k_h}{k_h + v_{max}^h} \tag{4}$$

respectively, where the maximum rates are $v_{max}^s \equiv k_T^-$ and $v_{max}^h \equiv k_P^- k_D^- / (k_P^- + k_D^-)$. The corresponding Michaelis constants are given by

$$K_M^T \equiv v_M^h \left[\frac{1}{k_T^-} + \frac{1}{k_h}\left(1 + \frac{k_s}{k_L}\right)\right] K_d^T \approx \left[1 - v_M^h\left(\frac{1}{v_{max}^h} - \frac{1}{k_T^-}\right)\right] K_d^T, \tag{5}$$

$$K_M^P \equiv v_M^s \left[\frac{1}{k_P^-} + \frac{1}{k_s}\left(1 + \frac{k_h}{k_T^-}\right)\right] K_d^P \approx \left[1 - v_M^s\left(\frac{1}{v_{max}^s} - \frac{1}{k_P^-}\right)\right] K_d^P, \tag{6}$$

$$K_M^D \equiv v_M^s \left[\frac{1}{k_D^-} + \frac{1}{k_s}\left(1 + \frac{k_h}{k_T^-}\right)\right] K_d^D \approx \left[1 - v_M^s\left(\frac{1}{v_{max}^s} - \frac{1}{k_D^-}\right)\right] K_d^D. \tag{7}$$

The equilibrium constant is given by $K_e \equiv K_e^b e^{-\Delta G/k_B T}$, where $K_e^b \equiv K_d^T/(K_d^D K_d^P)$ and the dissociations constant are $K_d^I = k_I^-/k_I^+$ with the subscript I=T, D, P respectively. The equilibrium constant varies exponentially with p.m.f.

The inhibitions between substrates and products are complicated because ATP or ADP/P_i binds competitively to the same "open" site no matter the motor functions as a synthase or hydrolase. For convenience, we express the inhibitions in an uncompetitive hydrolysis form with the parameter: $\sigma \equiv 1 + [P]/K_I^{TP} + [D]/K_I^{TD} + [D][P]/K_I^{TDP}$, where $K_I^{TP} \equiv K_d^P \chi k_D^-/k_P^-$, $K_I^{TD} \equiv K_d^D \chi k_P^-/k_D^-$, $K_I^{TDP} \equiv K_d^D K_d^P \chi/[1 + e^{\Delta G/k_B T}]$, and $\chi = e^{\Delta G/k_B T} k_L/v_M^h$.

Eq.(2) implies that the motor is a synthase if $r_c > 0$, a hydrolase if $r_c < 0$, and at equilibrium if $r_c = 0$. Fig.2(b) shows the reversible rotational speed of the motor versus ATP concentration and p.m.f. The motor functions as a synthase only if the ATP concentration is lower than a critical value such as 100μM and p.m.f is higher than 175mV. On the other hand, it becomes a hydrolase when [T]$>$ 100μM and p.m.f$<$ 175mV. The surface in Fig.2(b) also shows the sigmoid kinetics with respect to ΔpH at different Q(Junesch & Gräber, 1987; 1991). The relation between k_h/k_s and ΔpH and damping coefficient of "rotor" can be determined by a stochastic mechanochemical coupling model(Li et al., 2009; Shu & Shi, 2004; Shu & Lai, 2008; Shu et al., 2010)

2.2 Dynamics of system with rotary motor and battery

Recently, F_oF_1 motor is usually reconstituted in liposomes to investigate the H^+/ATP with pH clamp(Steigmiller et al., 2008; Toei et al., 2007; Turina et al., 2003). The dynamics of the system composed of motor and vesicle is urgent. Here we propose a possible experimental situation to study the dynamics of the F_oF_1 motor and vesicle system. In CF_oF_1-liposome experiments, a single purified H^+-translocating ATP synthase from chloroplast can be reconstituted on a vesicle. If the F_1 is extended inside and the vesicle is impermeable except for the proton channel in F_o, how long does the system take to achieve equilibrium once the outside pH is disturbed? This question involves the dynamics of the system and seems too complicated to be solved. However, if the diffusions of the substrates and proton in buffer are rapid enough, i.e., the time that the system takes to achieve steady concentrations of substrates and proton inside is much less than the rate-limiting rotational step, the dynamics of this system can be directly derived form Eqs.1 with different initial conditions as shown in Fig.3. Here, we assumed that the rate-limiting rotational step is equal to the rate of ATP hydrolysis/synthesis and may approximately be calculated from Refs(Shu & Lai, 2008; Shu et al., 2010)

Here, we only need to estimate the upper limit of the ATP diffusion time since ATP is the biggest molecule involved with radius $\sim$ 0.7 nm(Ravshan & Yasunobu, 2004). The distance to be covered is, therefore, at most, the radius of the vesicle which has been taken to be $R_v = 350$ nm. With a free diffusion coefficient of $D_A = 0.3 \times 10^9$ nm^2/s, The most diffusion time of ATP may be estimated as $t_A = R_v^2/(6D_A) = 0.06$ ms. This is two orders of magnitude shorter than the time spent for one ATP synthase even at maximum rate. Although this analysis describes a three-dimensional free diffusion, it gives a reasonable estimate for the particular confined geometry when ATP has explored the whole inside of the vesicle and found the corresponding binding site.

Fig.3 shows the dynamics of F_oF_1 in such a vesicle system calculated from our model. The synthesis/hydrolysis rate achieves a maximum value at 0.1 ms for initial conditions of $P_{EDP} = 1.0$ or $P_{ET} = 1.0$ respectively. After 10 ms, the system enters the steady state. The dynamics is constant with the kinetics values (symbols) and is independent of initial conditions. The rotational rate and inside pH decrease with time, while the ATP concentration

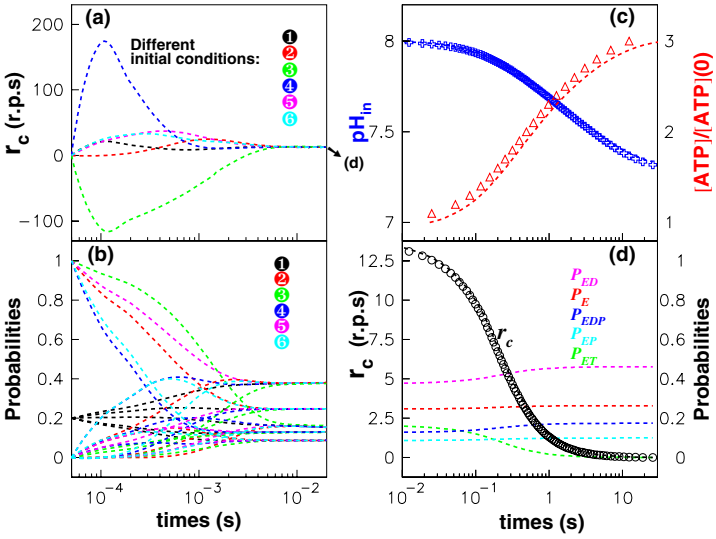

Fig. 3. Dynamics of F_oF_1 motor embedded in a vesicle system. (a) and (b): Evolutions of rotational rates and probabilities with six different initial conditions before 0.02 seconds. (c) Evolutions of pH and ATP concentrations inside. (d) Evolutions of rotational rates and probabilities after 0.01 seconds. The outside pH is constant (=6), while initial inside pH=8, [T]=100 nM, [D]=100 μM, and [P]=1 mM. The diameter of vesicle is 700 nm(Shu & Lai, 2008).

increases monotonically as expected. Here, we do not consider the influence of pH on the activity of F_1. These dynamical predictions can be tested in future experiments.

3. δ-free F_oF_1 rotary motor

An important feature of the two coupled rotary motors is that their stators are rigidly united by b_2 and δ subunits, in which δ subunit connects b_2 and $\alpha_3\beta_3$ crown. Once the δ subunit is deleted, the $\alpha_3\beta_3$ crown stators is no longer constrained, while another stator is still fixed in membrane. Therefore, the $\alpha_3\beta_3$ crown will accompany the "rotor" on rotation, and the transmembrane electrochemical energy is the only power. This is named δ free F_oF_1 rotary motor. On the other hand, chromatophore vesicles are small lipid vesicles that are differentiated to host only the photosynthetic apparatus. These vesicles are closed units, separated from their environment. The the photosynthetic apparatus convert light energy into transmembrane electrochemical energy. The chromatophore vesicle, thus, functions as a rechargeable battery.

We had developed a method to reconstitute the δ free F_oF_1 rotary motor into chromatophore vesicle so that the motor is an ideal self-driven nano-machine(Moriyama et al., 1991; Zhang et al., 2005). Employing a fluorescent actin filament attached to the β-subunits, we have directly observed the light-driven rotation of δ free F_oF_1 rotary motor at single molecule level(Zhang et al., 2005). If the fluorescent actin filament is replaced by a propeller, the motor becomes a self-propelled nano-machine and can serves for nano-submarine in artery to promote thrombolysis. Furthermore, if we exchange an antibody for the fluorescent actin

filament, the self-driven nano-machine can detect antigen because it will slowdown due to damp increasing caused by antigen binding. The speed decreasing can be detected by measuring the rate varying of inside pH of chromatophore. Thus, δ free F_oF_1 rotary motor has a great potential to be developed into a biosensor and activator for different applications.

3.1 Reconstitution of δ-free F_oF_1 motor

Purification of the β-subunit, F_1 ($\alpha_3\beta_{(10\times his\text{-}tag)3}\gamma$), and F_oF_1-ATPase: The F_1-ATPase coding sequence was isolated from thermophilic bacterium PS3, site-directed mutations of a cys193ser and gamaser107cys were introduced, and a 10 *histidine* tag was inserted downstream of the initiation codon. The mutated construct, pGEMMH, was then cloned into the expression plasmid pQE-30, and the expression plasmid pQE-MH was inserted into *E. coli* JM103(*uncB-UncD*) in which a majority of F_1-ATPase genes have been eliminated. Thermophilic bacterium, *Bacillus* PS3$\beta_{10\times his\text{-}tag}$ subunit ($TF_1\beta$), and F_1-ATPase ($\alpha_3\beta_{(10\times his\text{-}tag)3}\gamma$) were expressed and purified as Ref.(Yang et al., 1998), in which the JM103 strain expressing F_1-ATPase was cultured in 2× YT medium (AMP^+) for 3-4 h at 37°C. When the A_{660} increased to 0.6-0.8, the expression of the F_1-ATPase was induced by addition of 1 mmol/L isopropylthio-β-D-galactoside for 3 h. Cells were harvested by centrifuging for 15 min at 4000g and cell extractions were prepared using lysozyme (1 mg/mL)/sonication (5 min) in 50 mmol/L Tris-HCl (pH 8.0) buffer containing 0.5 mol/L NaCl and 1 mmol/L phenylmethane sulfonyl fluoride. The extracts were incubated at 60 °C for 30 min, and $TF_1\beta$ was purified using Ni^{2+}-NTA affinity chromatography at 4 °C. F_1-ATPase ($\alpha_3\beta_{(10\times his\text{-}tag)3}\gamma$) was purified as Ref.(Montemagno & Bachand, 1999) at 25 °C. The F_oF_1-ATP synthase from the *E. coli* JM103(*uncB-UncD*) was purified as Ref.(Yang et al., 1998). The mutant ATP synthase containing the His-tag could be isolated with Ni-NTA column. F_oF_1-ATPase was eluted with buffer B containing 0.05% lysolecithin and 250 mM imidazole at 4 °C, and then further purified by a gel filtration column (Superdex 200 HR 10/30 Pharmacia). The purified protein was analyzed by SDS-PAGE.

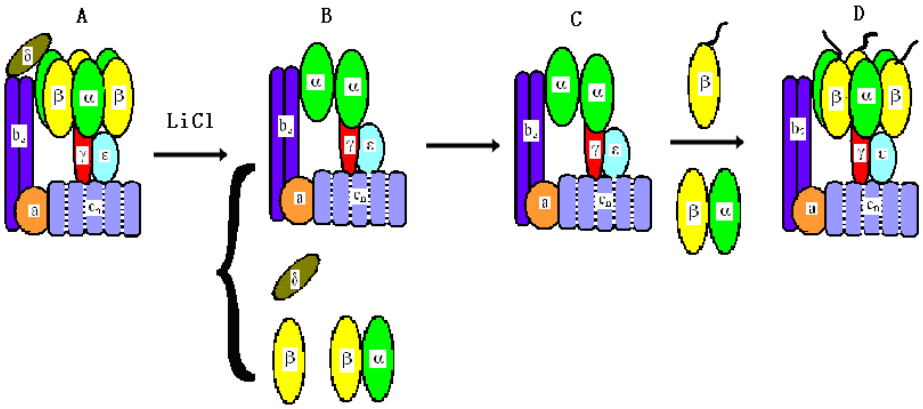

Fig. 4. The procedure of reconstitution of δ-free F_oF_1-ATPase motor. (A) F_oF_1-ATPase; (B) F_oF_1-ATPase is treated by LiCl to remove δ subunit; (C) Rebinding of purified β and α subunits; (D) The reconstituted δ-free F_oF_1-ATPase motor(Zhang et al., 2005).

The procedure of δ-subunit deletion of F_oF_1-ATPase is briefly shown in Fig.4. The proteoliposome containing F_oF_1-ATPase and bacteriorhodopsins (BRs) was incubated with 2 M LiCl, 0.1 mM Tricine-NaOH, 10 mM $MgCl_2$, and 1 mM ATP for 20 min at 4 °C. Then the proteoliposome was washed and isolated by centrifuging. Because some α and β subunits may be removed during δ delation, the LiCl-treated proteoliposome needs incubating with purified $\alpha_3\beta_3\gamma$(or β) subunits at 4 °C for 60 min (for each divided subunit of F_1 with buffer 0.1 mM Tricine-NaOH, 10 mM $MgCl_2$, 50 mM KCl, 0.5 mM NaCl, and 1 mM ATP), and then is cultured at 37 °C for 60 min (for reconstituting of δ-free F_oF_1-ATPase). The proteoliposome needs to be isolated to obtain the reconstituted δ-free F_oF_1-ATPase(Liao et al., 2009; Su et al., 2006; Tao et al., 2008).

3.2 Direct observation of the light-driven rotation of the δ-free F_oF_1 motor

Preparation of motor and liposome: F_oF_1-ATPase from the *E. coli* JM103(*uncB-UncD*) was purified as Ref.(Yang et al., 1998). The purified BR and F_oF_1-ATPase were co-reconstituted into a liposome. The liposome was prepared by reverse-phase evaporation with the mixture of soybean lipid and 1,2-dipalmitoyl-sn-glycero-3 phosphoethanolamine-N-biotinyl (molar ratio: 7:0.001)(Matsui & Yoshida, 1995). The molar ratio of BR and F_oF_1-ATPase was about 100:1, and that of lipids and protein was 30:1(w/w), so that it is possible for one proteoliposome to contain one F_oF_1-ATPase and more than 20 BR molecules.

Preparation of fluorescent actin filaments: The G-actin was co-labeled with FITC and Maleimido-C3-NTA-Ni^{2+} in buffer (50 mM Hepes-KOH, pH 7.6, 4 mM $MgCl_2$, and 0.2 mM ATP) for one night at 4 °C. The free FITC and Maleimido-C3-NTA (Ni-NTA) were removed by a desalting column. Then the labeled G-actin was polymerized in buffer containing 50 mmol/L Hepes-KOH (pH 7.6), 50 mmol/L KCl, 4 mmol/L $MgCl_2$, and 2 mmol/L ATP.

Preparation for immobilization of proteoliposomes in the experimental system for observation. Biotin-AC5-Sulfo-OSu was linked to the polylysine which had previously coated on the bottom of the dishes, and then 100 μl of 10 nM streptavidin was added into the dish bottom. After 5 min, the free streptavidin was washed. The proteoliposomes were conjugated by lipid-biotin-streptavidin-biotin-polylysine to the glass surface. And then the FITC-labeled F-actin filaments were attached to theβ-subunit of F_1 part through the His-tag with Maleimido-C3-NTA, as a marker of orientation for observation under an Olympus IX71 fluorescent microscope equipped with an ICCD camera.

To visualize the rotation of F_o in proteoliposome, a fluorescent actin filament was attached to β subunits through His-tag, while the proteoliposome was immobilized onto the glass surface through the biotin- streptavidin-biotin complexes(Fig.5A). The sample was exposed under the 570 nm cool light for 30 min to initiate the rotation of the F_o motor. Before illumination, the buffer containing 2 mM NaN_3 and 2 mM ADP was infused into the chamber. The clockwise rotation of actin filament was traced directly by an Olympus IX71 fluorescent microscope equipped with an ICCD camera (Roper Scientific, Pentamax EEV 512×512 FT) viewing from F_o side to F_1. Fig.5B shows an example of the sequential clockwise rotation images with 100 ms interval. We have selected six rotational data with different length filaments to show in Fig.5C. The rotation displays occasional pause or even backwards due to Brownian fluctuation. The rotation speed decreases with the length of filament increasing, which is in agreement with the results of single molecule experiments of F_1Noji et al. (1997); Yasuda et al. (1998) as expected. In addition, several control experiments were performed to confirm that the observed rotation is driven by transmembrane proton flow. As shown in Fig.5D, the rotation stopped immediately once 5 μl of 10 μM CCCP was added. It was also found that if the

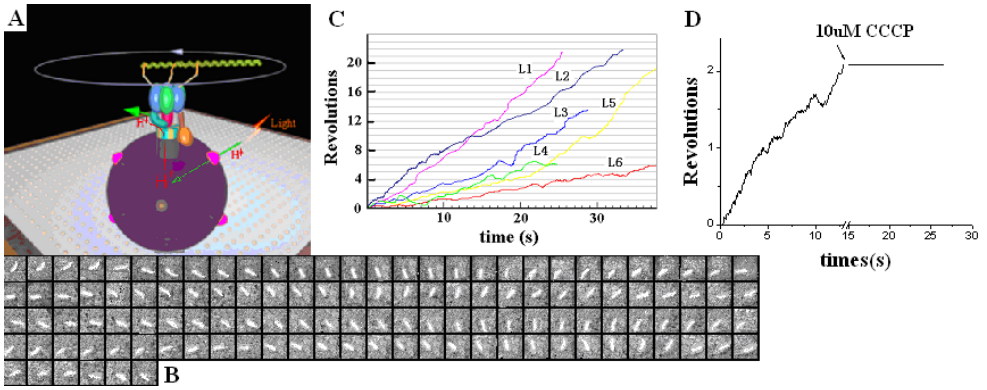

Fig. 5. (A)The system used for observation of the F_o rotation in the proteoliposome which was immobilized on the cover glass with biotin-streptavidin-biotin. (B)The sequential images of a clockwise rotating fluorescent actin filament. Time interval is 100 ms. (C)Time courses of the actin filament rotation with different length. The fluorescent filament was attached to the β subunits through His-tag. The length of filaments denoted L1,L2,L3,L4,L5 and L6 are 1.7, 1.9, 2.0, 2.3, 2.8 and 3.3 μm respectively. (D)The rotation was inhibited by adding CCCP, which verified the motor was indeed driven by transmembrane ΔpH(Zhang et al., 2005).

sample is in dark or is incubated with DCCD before illumination, no rotation has been observed (data are not shown) because CCCP destroyed the transmembrane p.m.f and DCCD blocked the proton channels. Furthermore, if NaN_3 and ADP disappeared in the buffer, no rotation of filament was found because NaN_3 and ADP prevented the $\alpha_3\beta_3$ crown from sliding to γ subunit(Muneyuki et al., 1993). These results demonstrated that the rotation of filaments depended on the p.m.f produced in proteoliposome. It is interesting that the ΔpH transmembrane of proteoliposome can persist for a long time. After the illumination, some filaments rotated continuously more than 20 min. The proteoliposome function as a recharge battery to supply energy to the rotary motor.

4. Biosensor developed by δ-free F_oF_1 motor

Light-driven electron transfer causes the proton gradient across the membrane and leads the proton flux through n channels(c_n) in F_o. The interaction between a subunit and proton flux generates the relative movement between a subunit and c ring. Proton flux will simultaneously alter the inside and outside pH of chromatophore. It is well established that the rotational speed of motor is tightly coupled to the rate of proton transmembrane transport, that is, the changing of speed is equivalent to the altering of proton transfer rate. On the other hand, motor speed can be regulated by changing the load, while the pH altering can be detected by pH-sensitive fluorescent probes such as QDs (quantum dots)(Deng et al., 2007). Thus, the nanomachine can be developed as a sensitive biosensor if the rotor is linked antibody/complementary strand and pH-sensitive probes are labeled outside (or inside) chromatophore.

5. Protein or virus detector

The first type of rotary biosensor was based on the antibody-antigen reaction to capture virus or specific protein. The nanomachine was constructed as shown in Figure6(a): β subunit(1) was linked by its antibody(2), while the antibody(4) of H9 avian influenza virus was connected to β antibody(2) in series by biotin-streptavidin-biotin (3). The chromatophore(6) with F_oF_1 -ATPase was hold on glass surface(7) coated with chitosan. If H9 avian influenza virus(5) exist, they will load to the motor through antibody-antigen reactions. Virus or protein loading, therefore, change motor speed. The speed changing can be detected by monitoring the fluorescent intensity indicated by pH-sensitive dye (or QDs). That is, the fluorescent intensity altering can be used to indirectly detect virus or protein. Its signal-to-noise ratio can be distinguished at single molecular level. Thus, this nanomachine may be a convenient, rapid, and even super-sensitive for detecting virus/protein particles.

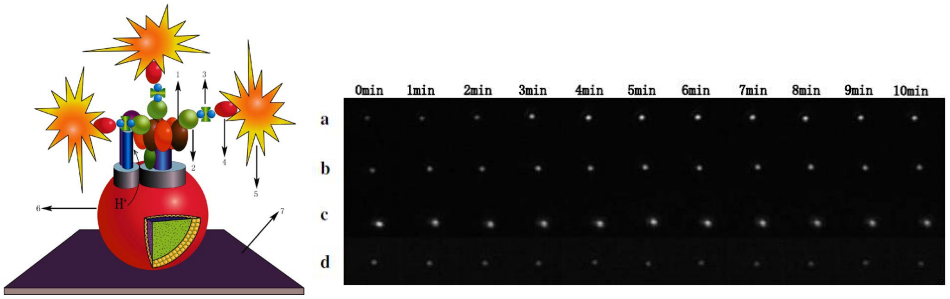

(a) Cartoon of detector (b) The course of fluorescence intensity

Fig. 6. (a) Basic design of biosensor based on δ-free F_oF_1. The fluorescence probe F1300 labeled inside of chromatophores was used as a proton flux indicator. **1** β subunit; **2** antibody of β subunit; **3** the complex of biotin-streptavidin-biotin; **4** the antibody of H9 avian influenza virus; **5** H9 avian influenza virus; **6** chromatophore; **7** glass surface coated with chitosan. (b) Images of intensity change of fluorescence dots caused by pH changing inside chromatophore in the course of 10 min. **a** with virus; **b** without virus; **c** with two antibodies; **d** without ADP(Liu et al., 2006b).

Preparation of H9 avian influenza virus: The avian H9 influenza were propagated in the allantoic cavities of 11-day-old embryonated chicken eggs at 37 °C for 3 days. The allantoic cavities were collected and centrifuged at 4000 rpm for 40 min and then the supernatant was centrifuged again at 100,000g for 2 h. The viruses were resuspended in PBS buffer and used in the experiments.

Labeling of fluorescence probe: The fluorescence probe F1300 was labeled into chromatophore as follows: 3 μl F1300 (0.0015 mol/L, dissolved in ethanol) was added to 150μl chromatophores and then was ultrasonicated in ice for 3 min to make the probe into inner chromatophores. The free fraction was washed by centrifugation at 12,000 rpm for 30 min at 4 °C three times. The precipitate was resuspended in tricine-NaOH buffer.

6. DNA or RNA detector

The second type of rotary biosensor was based on base-pair reaction to capture nucleic acid sequences such as DNA or RNA. Specific RNA/DNA probes, which are the complementary

strand of target RNA/DNA, were linked to each β subunits of nanomachine. Once base-pair reaction take places between two strands, the flexible probes will transform into a rigid rods so that motor will slowdown because the damp of rigid rod is much larger than that of flexible single chain. Detection of RNA/DNA was based on the proton flux altering induced by light-driven rotation of δ-free F_oF_1 motor. The base-pair reaction was indicated by changing in the fluorescent intensity of pH-sensitive CdTe quantum dots. Our results showed that the assay was so sensitive (1.2×10^{-18}M) that it can distinguish the target miRNA family members. Moreover, the method could be used to monitor real-time base-pair reaction without any complicated fabrication. The nanomachine has a great potential of clinical application of RNA/DNA.

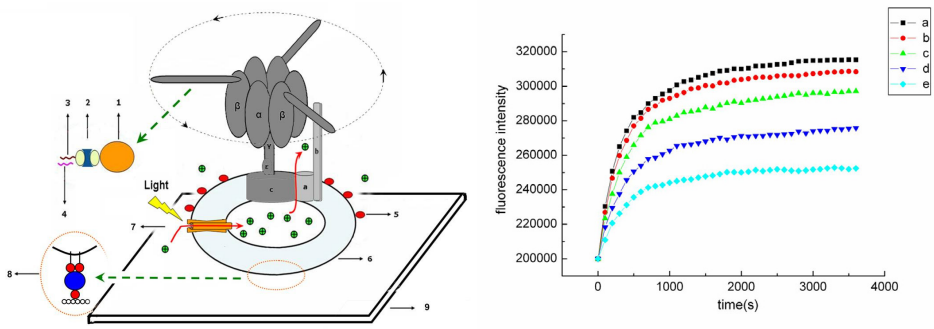

(a) Cartoon of detector. (b) Results of different concentration of miRNA.

Fig. 7. (a)Schematic diagram of the biosensor based on δ-free F_oF_1-ATPase embedded chromatophore. 1, 2, 3, 4, 5, 6, 7, 8, and 9 represent the antibody against β subunit, the linking complex composed of [biotin-AC5-sulfo-OSu]-streptavidin-[biotin-AC5-sulfo- OSu], miRNA probe, target miRNA, 535nm QDs, chromatophore, bacteriorhodopsins (BRs), the linking system of lipid-biotin-streptavidin-[biotin-AC5-sulfo-OSu]-Polylysine, and the glass surface, respectively. (b)Results of different concentration of miRNA. RNA was extracted from MCF-7 cells. **a** without RNA; from **b** to **e** the amounts of miRNA was summed from $10, 10^2, 10^4$ and 10^6 cells respectively. Base-pair reaction was hold at 37°C(Liao et al., 2009).

The chromatophores (100 μL) were resuspended in buffer A (50mM tricine-NaOH, 5mM $MgCl_2$, 10mM KCl, pH 6.5) and incubated for 3 h at room temperature with 100 μL CdTe QDs ($1\times10^{15}/\mu$L, dissolved in water)(Zhang et al., 2007). Free QDs were washed away by centrifuging at 13 000 rpm for 30 min at 4 °C in three times. The precipitate (QD-labeled chromatophores) was resuspended in 100 μL of 50mM tricine buffer (pH 6.5). Meanwhile, 2 μL of 2 μM biotin was added in 20 μL β subunit antibody at room temperature for 30 min, followed by adding 2 μL of 2 μM streptavidin at room temperature for 30 min. The streptavidin-biotinlabeled β-subunit antibody was incubated with 5 μL QDs labeled chromatophores fixed on the glass slips at 37°C for 1 h. Redundant free biotin-streptavidin-labeled β-subunit antibody was rinsed with 50mM TSM buffer (50mM Tricine-NaOH pH 7.0, 0.25M sucrose, and 4mM $MgCl_2$). Then 100 μL 10μM miRNA probe labeled with biotin was added and incubated at room temperature for 30 min. Free probes were washed out by 50mM TSM buffer. The δ-free F_oF_1-ATPase with chromatophore was immobilized on the glass surface through the biotin-streptavdin-biotin. miRNA probe system was hybridized with miRNA target in 100μL formamide hybridization solution at 37°C.

Before the detection, the sample was exposed under the 570 nm cool light for one hour to initiate the rotation of the F_oF_1-ATPase. During illumination, the buffer containing 2mM NaN_3 and 2 mM ATP was infused into the chamber to inhibit the hydrolysis activity of the F_oF_1-ATPase and prevent relative sliding between $\alpha_3\beta_3$ crown and γ subunit.

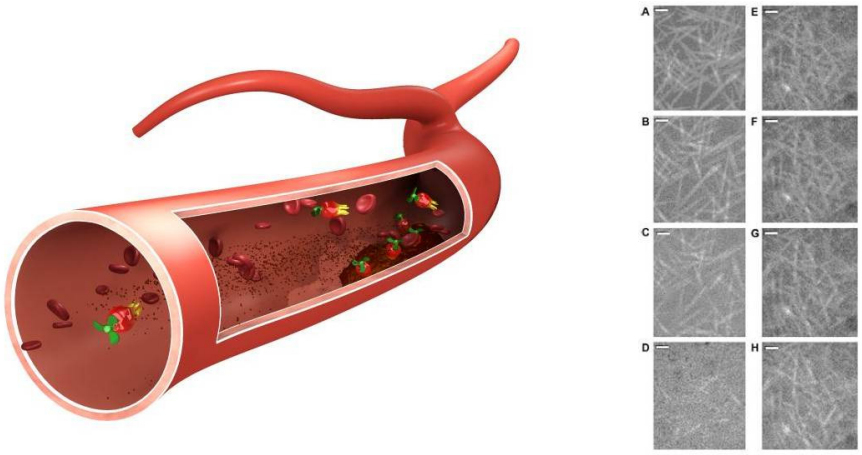

(a) Cartoon of submarine cruising in artery to promote thrombolysis. (b) Results of experiment *in vitro*.

Fig. 8. (a) Cartoon of submarine cruising in artery to promote thrombolysis. (b) Results of experiments *in vitro*. Left row (A-D) represents the course of fibrinolysis in 30 min with lumbrokinase and δ-free F_oF_1 motor, while right row (E-H) does that of fibrinolysis in 30 min only with lumbrokinase(Tao et al., 2008).

7. A potential activator to promote thrombolysis

Cardiovascular disease such as ischemic stroke is a substantial cause of morbidity and mortality. The primary aim of thrombolysis in acute ischemic stroke is recanalization of an occluded intracranial artery. Recanalization is an important predictor of stroke outcome as timely restoration of regional cerebral perfusion helps salvage threatened ischemic tissue. At present, intravenously administered tissue plasminogen activator (IV-TPA) remains the only FDA-approved therapeutic agent for the treatment of ischemic stroke within 3 hours of symptom onset. Recent studies have demonstrated safety as well as efficacy of IV-TPA even in an extended therapeutic window. However, the short therapeutic window, low rates of recanalization, and only modest benefits with IV-TPA have prompted a quest for alternative approaches to restore blood flow in an occluded artery in acute ischemic stroke. Although intra-arterial delivery of the thrombolytic agent seems effective, various logistic constraints limit its routine use and as yet no lytic agent have not received full regulatory approval for intra-arterial therapy. Mechanical devices and approaches can achieve higher rates of recanalization but their safety and efficacy still need to be established in larger clinical trials(Sharma et al., 2010). The δ-free F_oF_1 motor has a potential to be designed a self-driven nanomachine, which serve as a submarine cruising in artery to promote thrombolysis. Our

experiment *in vitro* has demonstrated that the motor may be one of alternative approaches to restore blood flow in an occluded artery in acute ischemic stroke. However, the mechanism of promoting thrombolysis has not been uncovered.

FITC Labeling on fibrinogen and fibrin formation: Fibrinogen (1 ml, 0.03 mM) was dissolved in PBS buffered saline containing 137 mM NaCl, 3 mM KCl, 8 mM Na_2HPO_4, 1 mM KH_2PO_4, pH 8.5. FITC was added to the fibrinogen solution under intensive stirring to a final concentration of 50 mg/ml(Sakharov et al., 1996). The fibrin fiber obtained from fibrinogen was polymerized with thrombin (0.5 U/μl) and fixed on the glass surface. After incubation at 37 °C for 30 min, a fibrin network with an approximate length of 200 μm was formed.

Fig.8(b) shows the morphological features of the fibrinolysis process observed directly under a fluorescence microscope. At the outset, two fibrin networks A and E, including fiber size, density, and branch point density, were similar. However, promotion of the fibrinolysis by δ-free F_oF_1 motor can be observed by comparing left and right rows. After 30 min, the fibrin almost disappear due to δ-free F_oF_1 motor (D), while the control one (H) still partly exist. It can be imaged that the many self-driven nanomachines will specially bind to fibrin and promote thrombolysis because of cooperative effect of collective propellers.

8. Self-assembly of ghost with the nanomachine

Nanotechnology aims to construct materials and operative systems at nanoscale dimensions. Several potential applications can be envisioned: targeted drug delivery systems, tissue engineering scaffolds, photonic crystals, and micro/nano fluidic and computational devices. The fundamental challenge in nanotechnology is to construct systems with varied functional features and predictably manipulate processes at the nanometer length scale. Conventional construction methods based on photolithography can successfully generate two-dimensional structures using a "top-down" approach, in which patterned surfaces are prepared by etching with light. Feature sizes on the order of 50 nm are easily achieved with commonly available technologies. Advances in specialized lithographic techniques (e.g. scanning probe lithography) have extended the resolution to below 20 nm. Molecular self-assembly serves as an alternative paradigm for preparing functional nanostructures, is perhaps one of the most intriguing phenomena in the fields of chemistry, materials, and bioscience, as well as is characterized by spontaneous diffusion and specific association of molecules dictated by non-covalent interactions. There are numerous recent examples involving different molecular entities: organic molecules, proteins, peptides, DNA and molecular motors(Kumar et al., 2011; Lo et al., 2010; Rajagopal & Schneider, 2004; Tao et al., 2009; Yin et al., 2008; Zhao et al., 2010).

A current challenge in molecular self-assembly is to achieve controlled organization in three-dimensions, to provide tools for biophysics, molecular sensors, enzymatic cascades, drug delivery, tissue engineering, and device fabrication. Ghosts (Erythrocyte membranes) are promising bioactive materials and have a great potential of application in drug delivery. The ghost is a kind of flexile membrane, composed of a lipid bilayer and cytoskeleton. One of special shapes is concave disk with the diameter about 8 μm and the thickness about 1.7μm respectively. Ghosts loaded with drugs or other therapeutic agents have been exploited extensively, owing to their remarkable degree of bio-compatibility, biodegradability, and a series of other potential advantages. We have been motivated to design a novel self-organized material using ghosts with δ-free F_oF_1 motor. A lot of interesting phenomena appear: Most chromatophores combined with δ-free F_oF_1 motor arrayed in a filament-like fashion through biotin-streptavidin-biotin interaction. The filament-like nanomachines were able to stick

around the surface of the ghost with the F_1 part against the ghost. Moreover, many ghosts, which were stuck around by filament-like nanomachines, assembled spontaneously to a larger scale complex with two or three layers. This sandwich structure may be useful for the self-driven delivery of drugs or other therapeutic agents.

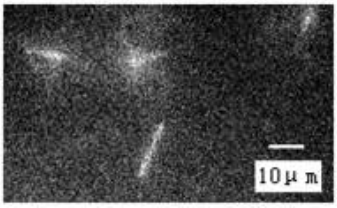

(a) Micrograph of chromatophore-filaments.

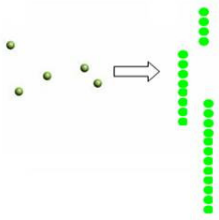

(b) Possible mechanism of self-assembly of filament.

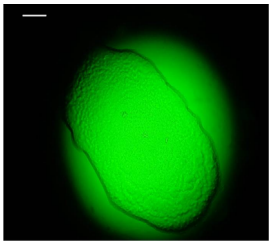

(c) Micrograph of larger scale assembly structure.

Fig. 9. (a) Self-assembled filaments of δ-free F_oF_1 motors observed by fluorescence microscopy. (b) Possible mechanism of self-assembly of filament. Green ball represents individual δ-free F_oF_1 motor with chromatophore. Green lines represent chromatophores linked through biotin-streptavidin-biotin into filament structures. Scale bar represents 10 μm. (c) Micrograph of larger scale assembly structure. Ghosts with fluorescence-labeled δ-free F_oF_1 motors aggregate together and self-assemble into a large structure about 0.6 mm $\times$ 1.2 mm in size, which is stable for more than one week.(Tao et al., 2009).

Here, we present a novel type of self-assembled complex consisting of filaments of chromatophores with δ-free F_oF_1-ATPases and ghost, the detailed structure of which was observed by fluorescence microscopy and confocal microscopy. In the absence of light, biotin-labeled chromatophores embedded F_oF_1-ATPase are joined together by streptavidin to form filaments. These filaments can attach to ghost surface, such that the ghosts will aggregate into a larger scale self-assembled complexes with two or three layers, held together in head to head fashion between the rotary F_1's. However, if the complex is illuminated, it will disassemble due to rotation of F_1 caused by light energy. The diameter of these macroscopic complexes is more than 1 mm. δ-free F_oF_1-ATPase act as a switch to control the ghosts' self-assembly and self-disassembly, while the remote control signal (power) is light. This system, thus, has a great potential to be developed into a controllable micronmachine of drug delivery.

Ghost Preparation: Fresh blood of pig was washed three times with cold 0.15 M NaCl buffer, pH 8.0, and plasma and leukocytes were discarded. Ghosts were obtained by hypotonic lysis. Red blood cells were obtained from fresh blood and washed three times with PBS buffer (isotonic phosphate-buffered saline, pH 8.0). The washed cells were added to 40 volumes of ice-cold 5P8 buffer (5 mM sodium phosphate, pH 8.0) and left at room temperature for 20 min before centrifuging at 20 000g for 1 h at 4 °C. The pale ghost layer was collected and washed three more times with lysis solution(Steck et al., 1970).

Observation of Self-Assembly: Ghosts attached chromatophore-filaments were resuspended in 40 volumes of ice-cold buffer (0.5 mM sodium phosphate, pH 7.6) for 1 h. Addition of 5 mM NaN_3, 2 mM $MgCl_2$, 50 mM KCl, and 2 mM adenosine 50-diphosphate (ADP) to the buffer created conditions for light driven rotation of δ-free ATPase within the ghosts. The complexes were put into a cell, in which the chromatophores were illuminated by 570 nm

light for 30 min at 4 °C. This illumination initiated proton transfer across the membrane of the chromatophores, and the rotation of δ-free F_oF_1-ATPase was then driven by the p.m.f. Once proton transfer was initiated, the cell was incubated at 37 °C throughout the whole experiment. The self-assembly and self-disassembly process was observed with an Olympus IX71 fluorescence microscope and recorded with a digital CCD camera (iXon CCD, ANDOR Technology). Confocal microscopy (Olympus FV500, optical scanning confocal microscope) was used during the scanning process of multiple layers of self-assembled complexes. FV1000 software was used to reconstruct the three-dimensional images.

9. Conclusion

In contrast to human-made machines, protein motors are self-assembled by natural biomaterial or elements, and operate in a world where Brownian motion and viscous forces dominate. The relevant energy scale is k_BT, which amounts to 4 pN·nm. This may be compared to the $\sim$ 80 pN·nm of energy derived from hydrolysis of a single ATP molecule at physiological conditions. Thermal, nondeterministic motion is thus an important aspect of the dynamics of molecular motors.

ATP hydrolysis does spontaneously occur in F_1, whereas the thermodynamically unfavorable reaction, ATP synthesis, has to be driven by harnessing the transmembrane proton flow in F_o. The mechanism of ATP formation in the F_1 part is well described by the "binding change mechanism". This has been developed in great detail by many techniques, and understanding of the mechanism has been claimed to be "almost complete". However, if the motor functions as a synthase, the two substrates, ADP and P_i, are recombined into one product, ATP. The binding order of the two substrates is still unclear(Watanabe et al., 2010). Another challenging question is whether the main kinetic enhancement occurs upon filling the second or the third site(Boyer, 2000; Milgrom & Cross, 2005; Senior et al., 2002). For F_o, the torque generation between a and c_n in F_o is still covered(Pogoryelov et al., 2010). In addition, it has remained unsettled whether the entropic (chemical) component of $\Delta\tilde{\mu}_{H^+}$ relates to the difference in the proton activity between two bulk water phases (ΔpH^B) or between two membrane surfaces (ΔpH^S)(Cherepanov et al., 2003).

It is of interest to ponder whether we can employ F_oF_1-ATPase nanomachine in artificial environments outside the cell to perform tasks that we design to our benefit(Martin et al, 2007)? One striking demonstration is the construction of a nickel nanopropeller that rotates through the action of an engineered F_1-ATPase motor(Soong et al., 2000). A metal-binding site was engineered into the motor and acted as a reversible on-off switch by obstructing the rotation upon binding of a zinc ion(Liu et al., 2002), similar to the action of putting a stick between two cogwheels. The other high light examples are the sol-gel packaging of vesicles containing bacteriorhodopsin, a light driven proton pump, and F_oF_1-ATP synthase(Choi & Montemagno, 2005; Luo et al., 2005), or F_oF_1-ATPase embedded chromatophore(Cui et al., 2005). Upon illumination, protons are pumped into the vesicles and ATP is created outside the vesicle by the ATP synthase. Besides the excellent stability of these gels (bacteriorhodopsin continued functioning for a few months), this technology provides a convenient packaging method and a way to use light energy for fueling devices. Therefore, these nanodevices with a battery can be employed to design a rapid, no labeled, sensitive and selective biosensor(Cheng et al., 2010; Deng et al., 2007; Liu et al., 2006b; Zhang et al., 2007), or construct a self-propelled nano-machine which can serves for nano-submarine in artery to promote thrombolysis(Tao et al., 2008). With ghost, the motor also has a great potential for drug delivery(Tao et al., 2009). Of course, all of these application tries are very coarse,

and little more than proof-of-principle examples. Thus, there are many questions to be investigated for application.

10. Acknowledgements

This work was supported by the National Basic Research Program of China (973 Program) under the grant No. 2007CB935903 and No. 2007CB935901, the National Natural Science Foundation of China (90923009 and 20873176), Knowledge Innovation Program of the Chinese Academy of Sciences (YYYJ-0907), Instrument Program of Chinese Academy of Sciences (07CZ203100), and Starting Mérieux Research Grants 2011-Institute of Biophysics-Prof. JiachangYue.

11. References

Abrahams, J. P.; Leslie, A. G. W.; Lutter, R.; Walker, J. E. (1994). Structure at 2.8 Å resolution of F_1-ATPase from bovine heart mitochondria. *Nature*. 370., 621-628

Adachi, K.; Oiwa, K.; Nishizaka, T.; Furuike, S.; Noji, H.; Itoh, H.; Yoshida, M. & Kinosita, K. Jr. (2007). Coupling of rotation and catalysis in F_1-ATPase revealed by single-molecule imaging and manipulation. *Cell.* 130., 309-321

Aksimentiev, A.; Balabin, I. A.; Fillingame, R. H. & Schulten, K. (2004).Insights into the molecular mechanism of rotation in the F_o sector of ATP synthase. *Biophys. J.* 86., 1332-1344

Ballmoos, C. von; Wiedenmann, A. & Dimroth, P. (2009). Essentials for ATP synthesis by F_1F_o ATP synthase. *Annu. Rev. Biochem.* 78., 649-672

Boyer, P. D.; Cross, R. L. & Momsen, W. (1973). A new concept for energy coupling in oxidative phosphorylation based on a molecular explanation of the oxygen exchange reactions . *Proc. Natl. Acad. Sci. USA*. 70., 2837-2839

Boyer, P. D. (1997). The ATP synthase-A splendid molecular machine. *Annu. Rev. Biochem.* 66.,717-749

Boyer, P. D. (2000). Catalytic site forms and controls in ATP synthase catalysis. *Biochim. Biophys. Acta*. 1458., 252-262

Cheng, J.; Zhang, X. A.; Shu, Y. G. & Yue, J. C. (2010). F_oF_1-ATPase activity regulated by external links on β subunits. *Biochem. Biophys. Res. Commun.* 391., 182-186

Cherepanov, D. A.; Feniouk, B. A.; Junge, W. & Mulkidjanian, A. Y. (2003). Low dielectric permittivity of water at the membrane interface: effect on the energy coupling mechanism in biological membranes. *Biophys. J.* 85., 1307-1316

Choi, H. J. & Montemagno, C. D. (2005). Artificial Organelle: ATP Synthesis from cellular mimetic polymersomes. *Nano. Lett*. 5., 1538-1542

Cui, Y. B.; Fan, Z. & Yue, J. C. (2005). Detecting proton flux across chromatophores driven by F_oF_1-ATPase using *N*-(fluorescein-5-thiocarbamoyl)-1,2-dihexadecanoyl-*sn*-glycero-3-phosphoethanolamine, triethylammonium salt. *Anal. Biochem*. 344., 102-107

Deng, Z. T.; Zhang, Y.; Yue, J. C.; Tang, F. Q. & Weil, Q. (2007). Green and Orange CdTe Quantum Dots as Effective pH-Sensitive Fluorescent Probes for Dual Simultaneous and Independent Detection of Viruses. *J. Phys. Chem. B*. 111., 12024-12031

Diez, M.; Zimmermann, B.; Börsch, M.; König, M.; Schweinberger, E.; Steigmiller, S.; Reuter, R.; Felekyan, S.; Kudryavtsev, V.; Seidel, C. A. M. & Gräber, P. (2004). Proton-powered

subunit rotation in single membrane-bound F_1F_o-ATP synthase. *Nat. Struct. Mol. Biol.* 11., 135-141

Düser, M. G.; Zarrabi, N.; Cipriano, D. J.; Ernst, S.; Glick, G. D.; Dunn, S. D. & Börsch, M. (2009). 36° step size of proton-driven *c*-ring rotation in F_1F_o-ATP synthase. *EMBO J.* 28., 2689-2696

Elston, T.; Wang, H. & Oster, G. (1998). Energy transduction in ATP synthase. *Nature*. 391., 510-513

Feniouk, B. A. & Yoshida, M. (2008). Regulatory mechanisms of proton-translocating F_1F_o-ATP synthase. *Results Probl. Cell Differ.* 45.,279-308

Ishmukhametov, R.; Hornung, T.; Spetzler, D. & Frasch, W. D. (2010). Direct observation of stepped proteolipid ring rotation in *E. coli* F_oF_1-ATP synthase. *EMBO J.* 29.,3911-3923

Itoh, H.; Takahashi, A.; Adachi, K.; Noji, H.; Yasuda, R.; Yoshida, M. & Kinosita, K. (2004). Mechanically driven ATP synthesis by F_1-ATPase. *Nature*. 427., 465-468

Jiang, W. P.; Hermolin, J. & Fillingame, R. H. (2001). The preferred stoichiometry of c subunits in the rotary motor sector of *E. coli* ATP synthase is 10. *Proc. Natl. Acad. Sci. USA*. 98., 4966-4971

Junesch, U. & Gräber, P. (1987). Influence of the redox state and the activation of the chloroplast ATP synthase on proton-transport-coupled ATP synthesis/hydrolysis. *Biochim. Biophys. Acta*. 893., 275-288

Junesch, U. & Gräber, P. (1991). The rate of ATP-synthesis as a function of ΔpH and $\Delta\psi$ catalyzed by the active, reduced H^+-ATPase from chloroplasts. *FEBS. Lett.* 294., 275-278

Junge, W. (2004). Protons, Proteins and ATP. *Photosynthesis Res.* 80.,197-221

Kaim, G.; Prummer, M.; Sick, B.; Zumofen, G.; Renn, A.; Wild, U. P. & Dimroth, P. (2002). Coupled rotation within single F_1F_o enzyme complexes during ATP synthesis or hydrolysis. *FEBS Lett*. 525., 156-163

Kothen, G.; Schwarz, O. & Strotmann, H. (1995). The kinetics of photophosphorylation at clamped ΔpH indicate a random order of substrate binding. *Biochim. Biophys. Acta.* 1229., 208-214

Kumar, P.; Pillay, V.; Modi, G.; Choonara, Y. E.; du Toit, L. C.& Naidoo, D. (2011). Self-assembling peptides: implications for patenting in drug delivery and tissue engineering. *Recent Pat Drug Deliv. Formul.* 5., 24-51

Li, M.; Shu, Y. G. & Ou-Yang, Z. C. (2009). Mechanochemical Coupling of Kinesin Studied with a Neck-Linker Swing Model. *Commun. Theor. Phys.* 51., 1143-1148

Liao, J. Y.; Yin, J. Q. & Yue, J. C. (2009). A novel biosensor to detect microRNAs rapidly. *Journal of Sensors*. 2009., 671896

Liu, H. Q.; Schmidt, J. J.; Bachand, G. D.; Rizk, S. S.; Looger, L. L.; Hellinga, H. W. & Montemagno, C. D. (2002). Control of a biomolecular motorpowered nanodevice with an engineered chemical switch. *Nat. Mater*. 1., 173-177

Liu, X. L.; Zhang, X. A.; Cui, Y. B.; Yue, J. C.; Luo, Z. Y. & Jiang, P. D. (2006a). Mechanically driven proton conduction in single δ-free F_oF_1-ATPase. *Biochem. Biophys. Res. Commun.* 347., 752-757

Liu, X. L; Zhang, Y.; Yue, J. C.; Jiang, P. D. & Zhang, Z. X. (2006b). F_oF_1-ATPase as biosensor to detect single virus. *Biochem. Biophys. Res. Commun.* 342., 1319-1322

Lo, P. K.; Metera, K. L. & Sleiman, H. F. (2010). Self-assembly of three-dimensional DNA nanostructures and potential biological applications. *Curr Opin Chem Biol*. 14., 597-607

Luo, T. J. M.; Soong, R.; Lan, E.; Dunn, B. & Montemagno, C. D. (2005). Photo-induced proton gradients and ATP biosynthesis produced by vesicles encapsulated in a silica matrix. *Nat. Mater*. 4., 220-224

Martin, G. L.; Heuvel, V. D. & Dekker, C. (2007). Motor proteins at work for nanotechnology. *Science*. 317., 333-336

Matsui, T. & Yoshida, M. (1995). Expression of the wild-type and the Cys-/Trp-less $\alpha_3\beta_3\gamma$ complex of thermophilic F_1-ATPase in *E. coli*. *Biochim. Biophys. Acta.* 1231., 139-146

Meier, T.; Morgner, N.; Matthies, D.; Pogoryelov, D.; Keis, S.; Cook, G. M.; Dimroth, P. & Brutschy, B. (2007). A tridecameric c ring of the adenosine triphosphate (ATP) synthase from the thermoalkaliphilic *Bacillus* sp. strain TA2.A1 facilitates ATP synthesis at low electrochemical proton potential. *Mol. Microbiol*. 65., 1181-192

Milgrom, Y. M. & Cross, R. L. (2005). Rapid hydrolysis of ATP by mitochondrial F_1-ATPase correlates with the filling of the second of three catalytic sites. *Proc. Natl. Acad. Sci. USA*. 102., 13831-13836

Mitome, N.; Suzuki, T.; Hayashi, S. & Yoshida, M. (2004). Thermophilic ATP synthase has a decamer c-ring: Indication of noninteger 10:3 H^+/ATP ratio and permissive elastic coupling. *Proc. Natl. Acad. Sci. USA*. 101., 12159-12164

Montemagno, C. & Bachand, G. (1999). Constructing nanomechanical devices powered by biomolecular motors. *Nanotechnology*. 10., 225-231

Moriyama, Y.; Iwamoto, A.; Hanada, H.; Maeda, M. & Futai, M. (1991). One-step purification of *E. coli* H^+-ATPase (F_1F_o) and its reconstitution into liposomes with neurotransmitter transporters. *J. Biol. Chem*. 266., 22141-22146

Muneyuki, E.; Makino, M.; Kamata, H.; Kagawa, Y.; Yoshida, M. & Hirata, H. (1993). Inhibitory effect of NaN_3 on the F_oF_1 ATPase of submitochondrial particles as related to nucleotide binding. *Biochim. Biophys. Acta*. 1144., 62-68

Nishizaka, T.; Oiwa,K.; Noji, H.; Kimura, S.; Muneyuki, E.; Yoshida, M. & Kinosita, K. (2004). Chemomechanical coupling in F_1-ATPase revealed by simultaneous observation of nucleotide kinetics and rotation. *Nat. Struct. Mol. Biol*. 11., 142-148

Noji, H.; Yasuda, R.; Yoshida, M.; Kinosita, K. Jr. (1997). Direct observation of the rotation of F_1-ATPase.*Nature*. 386., 299-302

Oster, G.; Wang, H. & Grabe, M. (2000). How F_o-ATPase generates rotary torque. *Phil. Trans. R. Soc. Lond. B*. 355., 523-528

Pänke, O. & Rumberg, B. (1996). Kinetic modelling of the proton translocating CF_oCF_1-ATP synthase from spinach. *FEBS Lett*. 383., 196-200

Pänke, O. & Rumberg, B. Kinetic modeling of rotary CF_oF_1-ATP synthase: storage of elastic energy during energy transduction. *Biochim. Biophys. Acta.* 1412., 118-128

Pogoryelov, D.; Yu, J. S.; Meier, T.; Vonck, J.; Dimroth, P. & Müller, D. J. (2005). The c_{15} ring of the Spirulina platensis F-ATP synthase: F_1/F_o symmetry mismatch is not obligatory. *EMBO rep*. 6., 1040-1044

Pogoryelov, D.; Krah, A.; Langer, J. D.;, Yildiz, Ö.; Faraldo-Góez, J. D. & Meier, T. (2010). Microscopic rotary mechanism of ion translocation in the F_o complex of ATP synthases. *Nat. Chem. Biol*. 6., 891-899

Rajagopal, K & Schneider, J. P. (2004). Self-assembling peptides and proteins for nanotechnological applications. *Curr Opin Struct Biol*. 14., 480-486

Ravshan, Z. S. & Yasunobu, O. (2004). Wide Nanoscopic Pore of Maxi-Anion Channel Suits its Function as an ATP-Conductive Pathway. *Biophys. J*. 87., 1672-1685

Rondelez, Y.; Tresset, G.; Nakashima, T.; Kato-Yamada, Y.; Fujita, H.; Takeuchi, S. & Noji, H. (2005). Highly coupled ATP synthesis by F_1-ATPase single molecules. *Nature*. 433., 773-777

Sakharov, D. V.; Nagelkerke, J. F. & Rijken, D. C. (1996). Rearrangements of the fibrin network and spatial distribution of fibrinolytic components during plasma clot lysis. *J. Biol. Chem.* 271., 2133-2138.

Saraste, M. (1999). Oxidative phosphorylation at the *fin desiécle*. *Science*. 283., 1488-1493

Seelert, H.; Poetsch, A.; Dencher, N. A.; Engel, A.; Stahlberg, H. & Müller, D. J. (2000). Structural biology: Proton-powered turbine of a plant motor. *Nature*. 405., 418-419

Senior, A. E.; Nadanaciva, S.; Weber, J. (2002). The molecular mechanism of ATP synthesis by F_1F_o-ATP synthase. *Biochim. Biophys. Acta*. 1553., 188-211

Sharma, V. K.; Teoh, H. T.; Wong, L. Y. H.; Su, J.; Ong, B. K. C. & Chan, B. P. L. (2010). Recanalization Therapies in Acute Ischemic Stroke: Pharmacological Agents, Devices, and Combinations. *Stroke Research and Treatment.* 2010., 672064

Shu, Y. G. & Shi, H. L. (2004). Cooperative effects on the kinetics of ATP hydrolysis in collective molecular motors. *Phys. Rev. E*. 69., 021912

Shu, Y. G. & Lai, P. Y. (2008). Systematic kinetics study of F_1F_o-ATPase: Analytic results and comparison with experiments. *J. Phys. Chem. B*. 112., 13453-13459

Shu, Y. G.; Yue, J. C. & Ou-Yang, Z. C. (2010). F_1F_o-ATPase, rotary motor and biosensor. *Nanoscale*. 2., 1284-1293

Soong, R. K.; Bachand, G. D.; Neves, H. P.; Olkhovets, A. G.; Craighead, H. G. & Montemagno, C. D. (2000).Powering an inorganic nanodevice with a biomolecular motor. *Science*. 290., 1555-1558

Steck, T. L.; Weinstein, R. S.; Straus, J. H.& Wallach, D. F. (1970). Inside-Out Red Cell Membrane Vesicles: Preparation and Puirification. *Science* 168.; 255-257

Steigmiller, S.; Turina, P. & Gräber, P. (2008). The thermodynamic H^+/ATP ratios of the H^+-ATP synthases from chloroplasts and *E. coli*. *Proc. Natl. Acad. Sci. USA*. 105., 3745-3750

Stock, D.; Leslie, A. G. W. & Walker, J. E. (1999). Molecular Architecture of the Rotary Motor in ATP Synthase. *Science.* 286., 1700-1705

Su, T.; Cui, Y. B.; Zhang, X. A.; Liu, X. L.; Yue, J. C.; Liu, N. & Jiang, P. D. (2006). Constructing a novel Nanodevice powered by δ-free F_1F_o-ATPase. *Biochem. Biophys. Res. Commun.* 350., 1013-1018

Sun, S. X.; Wang, H. & Oster, G. (2004). Asymmetry in the F_1-ATPase and its implications for the rotational cycle. *Biophys. J.* 86., 1373-1384

Tao, N.; Cheng, J. & Yue, J. C. (2008). Using F_1F_o-ATPase motors as micro-mixers accelerates thrombolysis. *Biochem. Biophys. Res. Commun.* 377., 191-194

Tao, N.; Cheng, J.; Wei, L. & Yue, J. C. (2009). Self-Assembly of F0F1-ATPase Motors and Ghost. *Langmuir*. 25., 5747-5752

Toei, M.; Gerle, C,; Nakano, M.; Tani, K,; Gyobu, N.; Tamakoshi, M.; Sone, N.; Yoshida, M.; Fujiyoshi, Y.; Mitsuoka, K. & Yokoyama, K. (2007). Dodecamer rotor ring defines H^+/ATP ratio for ATP synthesis of prokaryotic V-ATPase from *Thermus thermophilus*. *Proc. Natl. Acad. Sci. USA*. 104., 20256-20261

Turina, P.; Samoray, D. & Gräber, P. (2003). H^+/ATP ratio of proton transport-coupled ATP synthesis and hydrolysis catalysed by CF_oF_1-liposomes. *EMBO J.* 22., 418-426

Ueno, H.; Suzuki, T.; Kinosita, K. Jr. & Yoshida, M. (2005). ATP-driven stepwise rotation of F_oF_1-ATP synthase. *Proc. Natl. Acad. Sci. USA*. 102., 1333-1338

Wang, H. & Oster, G. (1998). Energy transduction in the F_1 motor of ATP synthase. *Nature*. 396., 279-282

Watanabe, R.; Iino, R. & Noji, H. (2010). Phosphate release in F_1-ATPase catalytic cycle follows ADP release. *Nat. Chem. Biol*. 6., 814-820

Weber, J. & Senior, A. E. (2003). ATP synthesis driven by proton transport in F_1F_o-ATP synthase. *FEBS Lett.* 545., 61-70

Weber, J. (2006). ATP synthase: Subunit-subunit interactions in the stator stalk. *Biochim. Biophys. Acta*. 1757., 1162-1170

Xing, J.; J. C. Liao, J. C. & Oster, G. (2005). Making ATP. *Proc. Natl. Acad. Sci. USA*. 102., 16539-16546

Yang, Q.; Liu, X. Y.; Miyake, J. & Toyotama, H. (1998). Self-assembly and immobilization of liposomes in fused-silica capillary by avidin-biotin binding. *Supramol. Sci*. 5., 769-772.

Yasuda, Y.; Noji, H.; Kinosita, K. Jr.; Yoshida, M. (1998). F_1-ATPase is a highly efficient molecular motor that rotates with discrete 120° steps. *Cell.* 93., 1117-1124

Yin, P.; Choi, H. M. T.; Calvert, C. R. & Pierce, N. A. (2008). Programming biomolecular self-assembly pathways. *Nature*. 451., 318-322

Zhang, Y. H.; Wang, J.; Cui, Y. B.; Yue, J. C. & Fang, X. H. (2005). Rotary torque produced by proton motive force in F_1F_o motor. *Biochem. Biophys. Res. Commun*. 331., 370-374

Zhang, Y.; Deng, Z. T.; Yue, J. C.; Tang, F. Q. & Wei, Q. (2007). Using cadmium telluride quantum dots as a proton flux sensor and applying to detect H9 avian influenza virus. *Anal. Biochem.* 364., 122-127

Zhao, X.; Pan, F.; Xu, H. Yaseen, M.; Shan, H.; Hauser, C. A.; Zhang, S.; Lu, J. R. (2010). Molecular self-assembly and applications of designer peptide amphiphiles. *Chem. Soc. Rev.* 39., 3480-98

8

PLGA-Alendronate Conjugate as a New Biomaterial to Produce Osteotropic Drug Nanocarriers

Rosario Pignatello
Department of Pharmaceutical Sciences
Faculty of Pharmacy, University of Catania
Italy

1. Introduction

Targeting bone tissue to treat specific diseases, such as primary tumour or bone metastases from peripheral malignancies is a current and pressing research field for modern pharmaceutical technology, and nanomedicine in particular. Bone is the third most common site of metastasis and the incidence of bone metastases in patients died of cancer is reported to be around 70% [1,2]. Primary carcinomas of the lung, breast, prostate, kidney, and thyroid may develop skeletal metastases. In children affected by disseminated neuroblastoma bone metastases are also highly frequent.

Tumour osteolysis is responsible for pathologic fractures, intractable pain, nerve compression syndrome, and severe hypercalcemia. In addition, patients with bone metastases may have neurologic impairment from spinal lesions, anaemia, and complications exacerbated by immobilization. Bone matrix resorption is minimally due to direct cancer cell activity. In fact, bone-colonizing tumour cells also stimulate osteoclast-mediated bone resorption via the secretion of potent osteolytic agents [3]. The increased bone resorption that follows releases bone-derived growth factors into the extracellular milieu and systemic circulation, thereby further enhancing bone resorption, promoting tumour growth, and altering the tumour microenvironment. Vice versa, metastatic cancer cells are largely influenced by messages embedded within the bone matrix [4]. Under the influence of bone microenvironment, tumour cells proliferate and interact with osteoblasts and osteoclasts leading to lytic or sclerotic lesions.

Clinical management of metastatic bone disease is really hard. The probability of long-term survival decreases dramatically in patients with skeletal metastases. Current treatments are based both on systemic therapy (chemotherapy, immunotherapy, hormone therapy) [5,6] and local therapy (surgery and radiotherapy) [7,8].

The restoration of functionality and mobility, along with pain relief can improve patients' quality of life, but is unable to affect the negative progression of the disease. Because of the unique characteristics of tumours growth within bone tissues, conventional therapeutic strategies often lack efficiency in cure bone metastases. Moreover, most of the drugs used for the adjuvant therapy of osteolytic metastases interfere with signalling that induce osteoclast differentiation and osteoclast-mediated bone resorption, but they are not effective on tumour growth in the bone and their use is obviously associated with heavy side effects.

A number of drugs are effective for the treatment of bone tumours, but their systemic delivery is inevitably associated with significant side effects and lack of targeting. Thereby, targeting specific biochemical patterns inside bone cancer areas may theoretically provide a mean to improve the efficacy and reduce the required dose of anticancer drugs.

1.1 Bone targeting strategies

Development of osteotropic drug delivery systems (ODDS) is therefore an appealing issue in the wide field of innovative pharmaceutical technology. To realize an effective system, many obstacles must be overcome. Bones are covered with lining cells acting as a marrow-blood barrier; therefore, the contact of exogenous compounds to the bone surface is restricted. Furthermore, the expression of biomolecules having a specific targets, like enzymes or antigens is relatively low in mineralized tissues, thus restraining the chances for an active drug targeting.

The strategies proposed for targeting drugs to the bone can essentially be condensed in two fields: the passive targeting approach, realised by the encapsulation in or association of drugs to colloidal carriers, such as polymeric or lipid nanoparticles (NP), liposomes or dendrimers (strategy 1, **Figure 1**). Drug-loaded nanocarriers allow to achieve a selective release to some tissues, like tumours, by means of the well-known phenomenon called 'EPR effect' [9], due to the fact that all cancers are characterized by permeable (leaky) blood neovessels and an impaired lymphatic outflow. Because of their multifunctional properties, nanosized systems can carry both targeting molecules and drugs, and deliver the latter in very specific sites within the body. Another advantage of NPs is the possibility of carrying in the bloodstream poorly soluble or unstable compounds, such as peptides and proteins, preventing their premature inactivation by circulating enzymes.

However, active targeting should be in some case more useful to reach effective drug concentrations in specific tissues and organs. Thus, other approaches have also been explored in which a drug is covalently linked to a targetor moiety able to recognize the bone tissues, and selectively convey the whole compound (e.g., a prodrug or a polymeric conjugate) to the site of action (strategy 2, **Figure 1**) [10].

Since bones are made of a mineralized matrix, a logical solution to the problem of bone targeting would be the development of delivery systems that possess affinity for hydroxyapatite (HA) via osteotropic molecules, such as bisphosphonates (BP) [11,12]. BP are synthetic, non-hydrolysable compounds structurally related to pyrophosphate. The P-C-P structure of BP is responsible for the ability of binding divalent ions, such as Ca^{++}, and thereby for the high affinity to HA [13]. Upon administration, BP are hence rapidly cleared from the bloodstream and bind to bone mineral surfaces at sites of active bone remodelling, like the areas undergoing osteoclast resorption [13].

BP are the most effective antiresorptive agents for the treatment of bone diseases associated to an increase in the number or activity of osteoclasts, including tumour-related osteolysis and hypercalcemia [14]. Moreover, BP are also able to reduce the survival, proliferation, adhesion, migration, and invasion of tumour cells [15, 16] and to inhibit angiogenesis in experimental and animal tumour models [17]. Since HA crystals are only present in 'hard' tissues, like teeth and bones, conjugation to BP can represent a valid strategy for selectively deliver bioactives to the bones.

The scientific literature presents many papers and patents exploring such approach, sometimes carrying original ideas or integrating together different chemical and technological pathways. In particular, osteotropic drug delivery systems (ODDS) have been proposed some years ago as a possible mean to impart to drugs an affinity to bone tissues

[11, 12, 18, 19]. Bisphosphonates (BP) have been for instance conjugated to small drugs [20, 21], and proteins [22] with the aim at optimizing the treatment of osteoporosis, osteoarthritis, and bone cancer, and to radiopharmaceuticals to obtain novel agents for bone scintigraphy [23]. The conjugation of bisphosphonates to polymer backbones has been studied as a mean for bone targeting [24,25]. Recently, cholesteryl-trisoxyethylene-bisphosphonic acid (CHOL-TOE-BP), a new tailor-made BP derivative, has been used as a bone targeting moiety for liposomes [26]. In other works, the amino-bisphosphonate drug alendronate (ALE; Fosamax®) was co-conjugated to HPMA polymer backbones together with an anticancer agent. Thereby, passive targeting was achieved by extravasation of the nanoconjugates from the tumour vessels via the EPR effect, while active targeting to the calcified tissues was achieved by ALE affinity to HA [27].

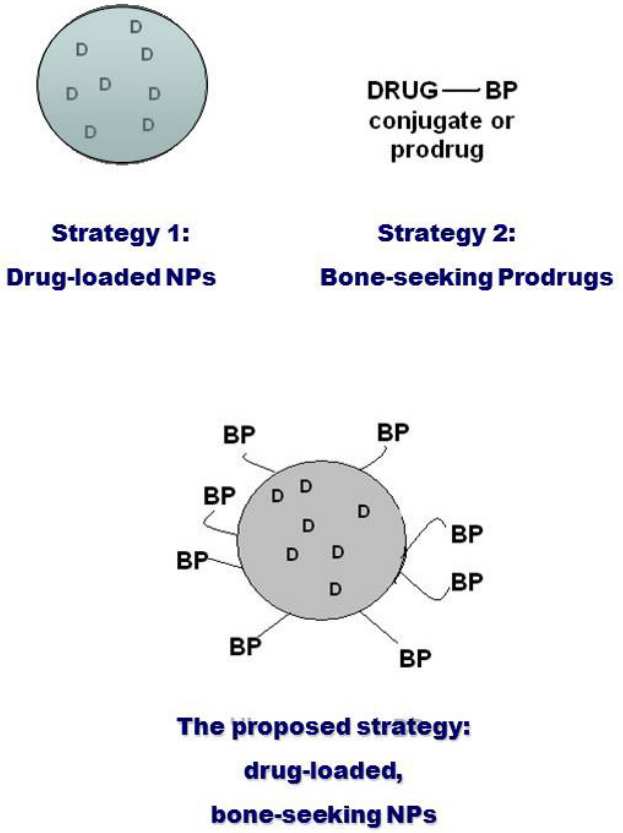

Fig. 1. The strategies described in the literature to achieve targeting to bone tumours: 1) an anticancer drug (D) is encapsulated/loaded into a nanocarrier (e.g., polymeric or lipid nanoparticles, liposomes, micelles, etc.) and passive targeting is expected (EPR effect); 2) a biologically active molecule is covalently linked to an osteotropic targetor moiety (e.g., a bisphosphonate, BP); 3) nanoparticles are made by an osteotropic polymer (e.g., a polymer-BP conjugate) and then loaded with a bioactive agent: in this way, both passive and active targeting possibilities can be achieved.

1.2 The scientific and technical rationale for a new targeting strategy

Targeted DDS should be preferable over drug-BP conjugates due to different factors, such as drug protection from biodegradation in the bloodstream, transport duration, and drug-payload. Thereby, in a recent and partially still on-going research, the two strategies depicted in **Figure 1** have been merged, leading to an innovative solution for active targeting of drugs to the bone. The working hypothesis was to realize a biocompatible nanocarrier showing high affinity to bone (i.e., an osteotropic nanocarrier), which can be loaded with different classes of drugs active against bone diseases, such as anticancer, anti-angiogenic, antibiotics, or anti-osteolytic agents.

To this aim, in a first step a new polymeric biomaterial showing osteotropic properties was produced through the conjugation of a poly(lactide-*co*-glycolide) (PLGA) to the BP agent alendronate (ALE). PLGA copolymers are diffusely used biocompatible and biodegradable materials for controlled drug release systems [28], including anticancer agents, and they have also been recognized as GRAS by US FDA. In this study, a copolymer made of 50:50 polylactic-*co*-glycolic acid was used (Resomer® RG 502 H; **Figure 2**) because of the presence of free carboxyl end groups susceptible to chemical derivatisation. The typical weight composition of this copolymer allows it to remain in the human body enough to let the bound BP moiety to recognize the bone proteins.

ALE (4-amino-1-hydroxybutyldiene-1,1-phosphoric acid, **Figure 2**) is an amino-BP, approved for the treatment and prevention of osteoporosis, treatment of glucocorticoid-induced osteoporosis in men and women, and therapy of Paget's disease of bone [29]. ALE was selected among BP agents because of some peculiar properties: a) the presence of a free amine group, able to create a stable covalent link with the carboxyl group present in the used PLGA; b) such amine group is not essential for the interaction of ALE with HA, and thus for its pharmacological effects, but exerts only a supportive role [30]; c) the possibility of easily converting the commercial sodium salt of ALE into its free acid form. The choice of an amide bond between the targeting BP and the polymer was also driven by the known relatively high resistance to enzymatic hydrolysis in plasma of this linkage, that should ensure the intact conjugate to reach the target (bone) tissues.

The haemo- and cytocompatibility of the PLGA-ALE conjugate was confirmed *in vitro*. Therefore, a nanoparticle system (NP) was produced starting from this new biomaterial. The NP were studied for their technological properties, as well as for their biocompatibility. Finally, PLGA-ALE NP were then loaded with a model cytotoxic drug, doxorubicin (DOX) and tested *in vitro* and *in vivo*.

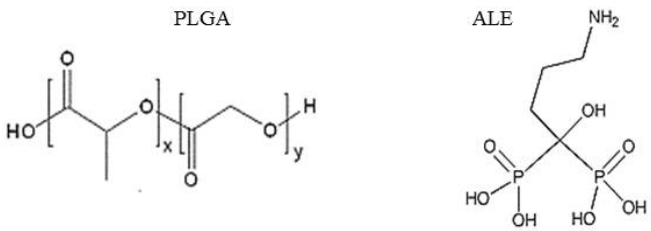

Fig. 2. Schematic structure of Resomer® RG 502 H (PLGA) and alendronic acid (ALE).

2. Synthesis and characterization of the PLGA-ALE conjugate

Polyl(D,L-lactic-*co*-glycolic acid) (50:50) containing a free carboxylic acid end group [Resomer® RG 502 H; inherent viscosity: 0.16-0.24 dl/g (0.1% in chloroform, 25°C)] was used (Boehringer Ingelheim, Ingelheim am Rhein, Germany). Sodium alendronate was converted into the acid form by treatment with aqueous acetic acid and lyophilisation. The conjugate was synthesized by two alternative methods, i.e., carbodiimide-assisted direct conjugation or preparation of an activated intermediate through N-hydroxysuccinimide [31]. In the first case, a solution of Resomer® RG 502 H in DMSO and dichloromethane (DCM) (1:1) was activated at 0°C for 2 h by N'-(3-dimethylaminopropyl)-N-ethyl carbodiimide hydrochloride (EDAC), in the presence of 1-hydroxy-benzotriazole (HOBt) and triethylamine. Alendronic acid was dissolved in DMSO and added to the reaction mixture, which was stirred for 2 h at 2°C and then at r.t. for 8 h. The solvent was partially removed under vacuum and the remaining solution was purified by dialysis water (CelluSep H1 MWCO 2000; M-Medical s.r.l., Cornaredo, Italy). In the alternative procedure, the PLGA was previously activated with N-hydroxysuccinimide (NHS) and dicyclohexylcarbodiimide in anhydrous dioxane at 15°C under stirring for 3 h [32]. The formed dicyclohexylurea was filtered off and the solution was poured in anhydrous diethyl ether. The solvent was decanted and the oily residue was purified by dissolution in anhydrous dioxane and precipitation with anhydrous diethyl ether (3 times), and finally dried in vacuo. A solution of NHS-PLGA in anhydrous DMSO was treated with triethylamine and sodium alendronate under stirring at r.t. for 12 h. At the end of the reaction the solvent was partially removed under vacuum and the remaining solution was purified by dialysis. The dialysed samples were frozen into using liquid nitrogen and lyophilised. Both methods resulted in similar production yields (70-75%) and purity of the final conjugate, therefore the first method could be better proposed as more direct and simple. The chemical structure of the PLGA-ALE conjugate was confirmed by MALDI-TOF MS and ^{1}H-NMR; analytical details are available [31].

In the view of using the PLGA-ALE copolymer to prepare bone-targeted NPs, the conjugate was evaluated for blood and cyto-compatibility, to individuate any negative effect which might have precluded any further biological investigation. Haemolysis was evaluated because erythrocytes are among the first cell lines that come into contact with injected materials. Experimental results did not show haemolytic effects of the conjugate; the plasmatic phase of coagulation was measured by the activated partial thromboplastin time (APTT) and prothrombin activity; they respectively evaluate the intrinsic and extrinsic phases of coagulation. In basal conditions, prothrombin activity was 140.2 ± 2.5 and APTT was 35.6 ± 0.3. In plasma incubated with PLGA-ALE at different dilutions, prothrombin activity and APTT were not significantly different from the plasma incubated with PBS (**Figure 3A** and **3B**). DMSO at the same dilutions did not affected either prothrombin activity or APTT.

In the bloodstream, nanoparticles come in contact with endothelium before passing through the vessel wall and reaching tissues. Therefore, the effect of PLGA-ALE on endothelial cells was tested to verify the lack of cytotoxicity. As expected, PLGA-ALE was not cytotoxic for human umbilical vein endothelial cells (HUVEC), as proven by the neutral red test (**Figure 3C**). Absence of cytotoxicity was also shown in cultures of human primary trabecular osteoblasts (BMSC) (**Figure 3D**).

In conclusion, PLGA-ALE conjugate did not cause either haemolysis on human erythrocytes, or alterations of the plasmatic phase of coagulation or cytotoxic effects on endothelial cells and trabecular osteoblasts [31].

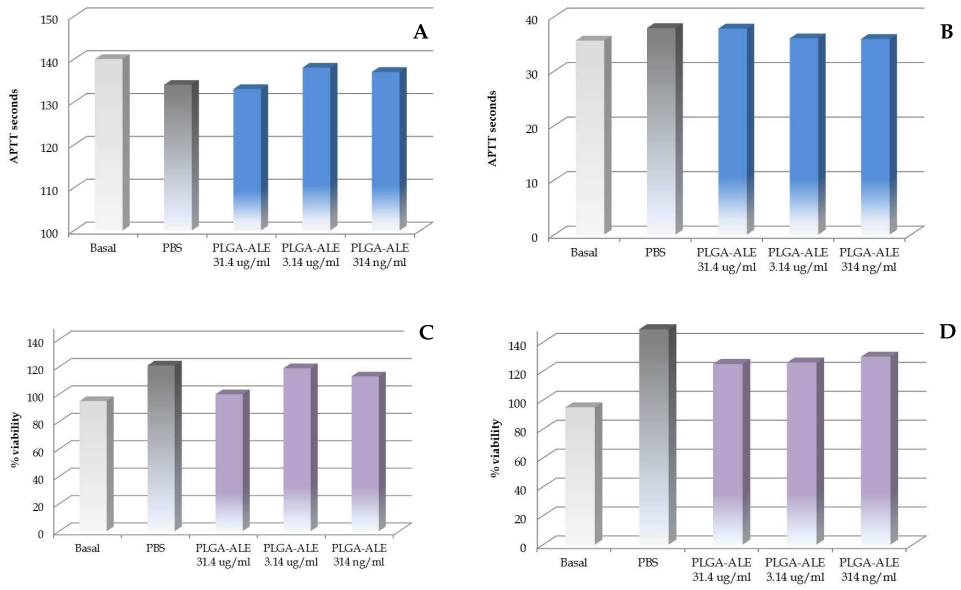

Fig. 3. Biocompatibility results of the PLGA-ALE conjugate: (A) mean prothrombin activity and (B) APTT of human plasma incubated with different concentrations of the conjugate; (C) viability of human umbilical vein endothelial cells (HUVEC) and (D) human primary osteoblasts from trabecular bone, respectively, after incubation with the conjugate. No haemolytic activity was given by the tested compound (not shown) (adapted from ref. [31]).

3. PLGA-ALE nanoparticles

NP were produced by the PLGA-ALE conjugate by a nanoprecipitation method, using an opportunely adapted emulsion/solvent evaporation technique [33]. The conjugate was dissolved in acetone, DMSO or their 1:1 mixture (*v:v*). The organic solution was added drop wise into phosphate buffered saline (PBS), pH=7.4, containing Pluronic F68. After stirring at r.t. for 10 min, the solvent was partially removed at 30 °C under reduced pressure and the concentrated suspension was purified by dialysis against water.

In **Figure 4** the size analysis of the formed systems, obtained by photon correlation spectroscopy is illustrated. DMSO was used in the NP production due to the low solubility of the conjugate in acetone (from which low production yields were achieved), but it did not appear to be an ideal solvent; in fact, NP obtained from pure DMSO solution showed a higher mean size with respect to those obtained using an acetone/DMSO mixture. These NP showed a homogeneous distribution, with an average size of 198.7 nm and a polidispersity index of about 0.3. However, in all cases mean sizes between 200-300 nm were obtained, an interesting feature for a further development of these systems as injectable drug carriers.

Also a dialysis method using a DMSO solution of the conjugate was attempted to prepare the NP [34], but it resulted in much larger particles (around 400 nm) (not shown).

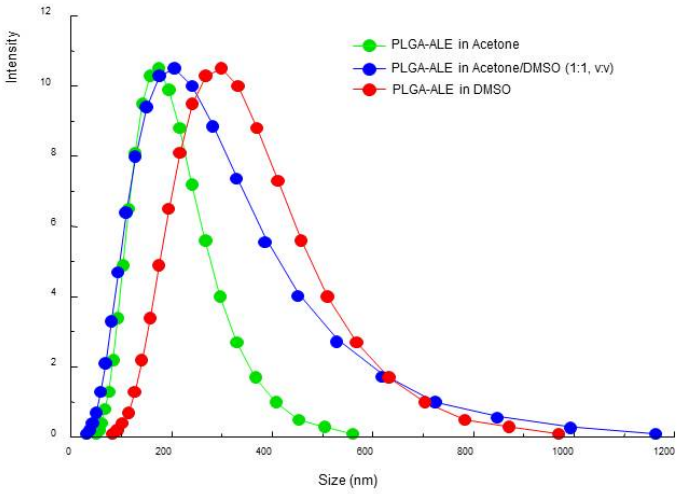

Fig. 4. Size distribution patterns of PLGA-ALE NP prepared using different organic phases (adapted from [31].

The PLGA-ALE NPs showed a net negative surface charge (ζ-potential of –38 mV), close to the value given by the NPs obtained from pure PLGA (-41.8 mV). SEM analysis revealed spherical particles with a smooth surface (**Figure 5**). The system was also shown to be sterilisable by gamma irradiation at 10 kGy, showing only minimal particle size changes [33]. This finding prospects the possibility of using sterilized NPs for further *in vivo* studies of the system.

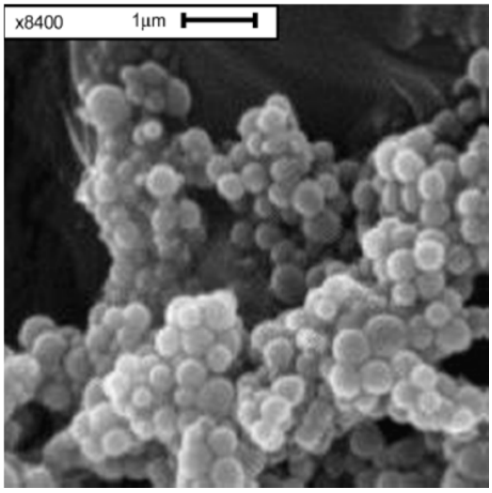

Fig. 5. SEM picture of PLGA-ALE NPs produced in 1:1 acetone/DMSO.

To assess the affinity for HA, PLGA-ALE and PLGA NPs were loaded with a lipophilic probe (Red Oil O) and incubated with two different HA concentrations (1 and 5 mg/ml) for 15 or 30 min. PLGA-ALE NPs showed a relative increase of affinity towards the phosphate salt compared to pure PLGA NPs (**Figure 6**). The affinity increased with the incubation time and was proportional to the concentration of HA in the suspension. This latter observation would suggest that some form of chemical interaction occurred between PLGA-ALE and HA, reinforcing the mere physical absorption of the phosphate on NP surface, which justifies the affinity already measured for pure PLGA NPs.
The biocompatibility profile of PLGA-ALE NPs was assessed by means of several *in vitro* assays, able to demonstrate their effects on biological systems which use to come in contact with a material injected into the body [33, 35, 36]. The use of NPs for drug delivery necessitates an accurate assessment of their biocompatibility [37, 38]. For their nanoscale size, NPs may have a reduced blood compatibility in comparison with the starting material: even if the biocompatibility of a macromolecule is well-established, the enormous increase of its surface when in the form of NPs may bring on negative effects that are not given by the bulk material.

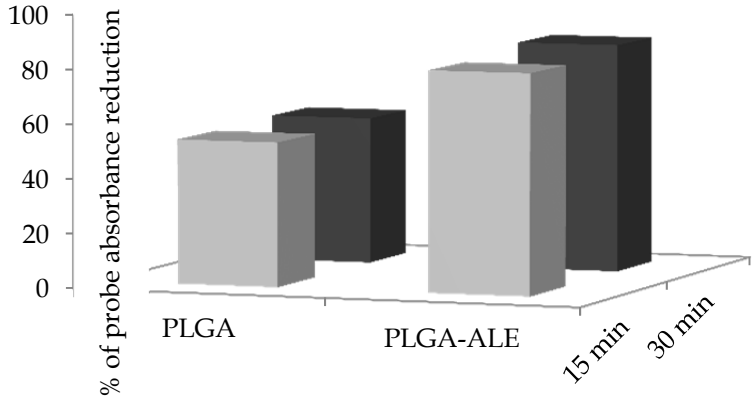

Fig. 6. Affinity of PLGA-ALE and PLGA NPs for hydroxyapatite (HA). Oil Red O-loaded NP suspensions were incubated at r.t. for either 15 or 30 min with an aqueous suspension containing 5 mg/ml of the phosphate salt. Results are expressed as the percentage decrease of light absorbance at 523 nm with respect to the corresponding NPs incubated without HA [*cf*. ref. 33].

3.1 Biocompatibility studies

Blood-biomaterial interactions are complex events that involve erythrocyte and leukocyte damage, and activation of platelet, coagulation, and complement. Damage of red blood cells, as well as complement activation may favour haemolysis and other forms of general toxicity. Analogously, NPs should not activate platelets and the plasmatic phase of coagulation, nor damage endothelial cells to avoid thrombogenesis [39, 40]. In the meantime, they should not reduce the levels of the plasmatic factors of coagulation, to prevent haemorrhagic accidents. Finally, with the aim of bone targeting, when NP will

reach bone tissues they should inhibit osteoclast activity without altering osteoblasts. Therefore, a preliminary evaluation of NP biocompatibility has been necessary before their loading with actives.
The PLGA-ALE NP at different concentrations did not show any haemolytic effects towards a suspension of human erythrocytes. The percentage of haemolysis was in fact similar to the erythrocytes incubated with PBS (Table 1).

Sample	NP concentration	% of haemolysis
PLGA-ALE NP	56 μg/ml	0.001±0.165
	5.6 μg/ml	0.289±0.320
	560 ng/ml	0±0.272
	56 ng/ml	0.356±0.309
	5.6 ng/ml	0.167±0.191
	0.56 ng/ml	0±0.155
PBS	-	0
Saponin	-	132.72±2.74
Distilled water	-	100

Table 1. Hemolytic activity (arithmetic mean ± S.E. of 6 experiments) of PLGA-ALE NPs. Their concentration was expressed as the amount of ALE in each sample.

As a further proof of their compatibility with blood components, at all the tested concentrations PLGA-ALE NPs did not induce any significant effect either on the total leukocyte number or on their subpopulations percentage. Analogously, the NPs did not cause platelet adhesion or activation (release reaction), as assessed by the platelet factor 4 measurement (**Figure 7**), all process that may induce thrombotic phenomena after NP injection [33].

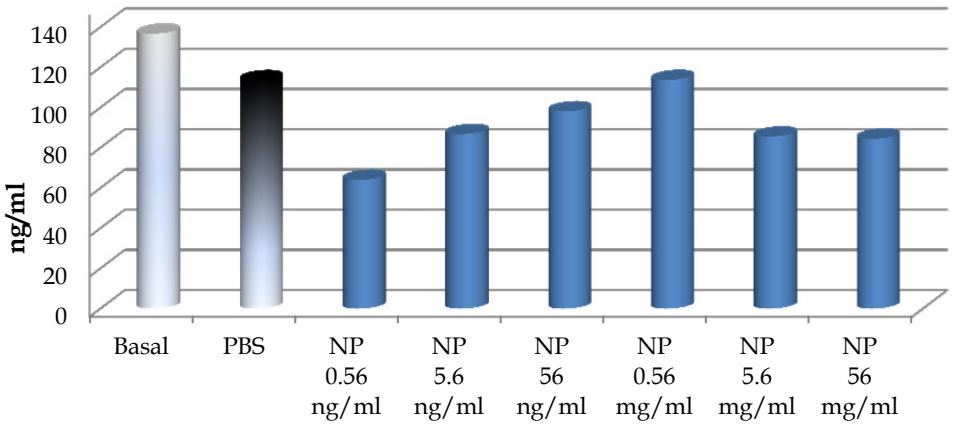

Fig. 7. Platelet factor 4 concentration after incubation with PLGA-ALE NP.

To assess the lack of alterations of blood proteins, we evaluated the effects of PLGA-ALE NPs on the plasmatic phase of coagulation and on complement. A decrease of the coagulation factors levels favours haemorrhage, while an increase of their activity may induce thrombotic phenomena. In our experiments, only the highest tested concentration of NPs caused a decrease of the prothrombin activity, while all the lower concentrations increased it, with changes however always ranging within normal physiological values (**Figure 8**). Since APTT (i.e., the intrinsic and the common phase of coagulation) was also not significantly affected by the NPs (not shown), the observed changes could be due to an alteration of Factor VII of the extrinsic pathway of coagulation. Probably, Factor VII was adsorbed on the NPs surface at high concentration and was less available for coagulation; conversely, lower concentrations of PLGA-ALE NPs could activate factor VII, in a way similar to the effect of tissue factor. Another hypothesis could involve the activation of Factors XII and XI by the NPs, similarly to silica gel or glass (*cf.* [33] for more details).

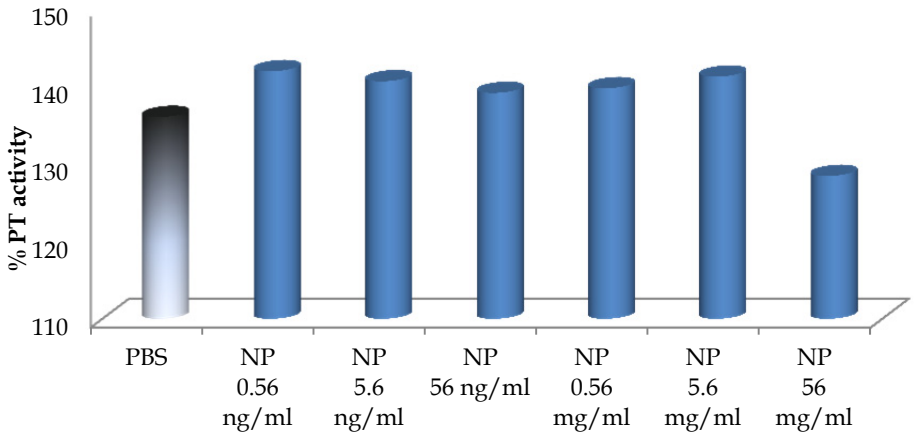

Fig. 8. Protrombin activity induced by different PLGA-ALE NP concentrations.

Activation of complement induces the production and release of small biologically active peptides. C3a and C5a are chemo-attractive for leukocytes and favour their aggregation. Furthermore, C5a induces the adhesion of granulocytes and monocytes to the endothelium, their migration into the external tissues, enzyme release and production of pro-coagulant or platelet aggregating compounds. C3a and the C5b-9 complex can directly activate platelets. Therefore, complement activation should not be considered as a strictly local phenomenon, but results also in systemic effects. Complement activation may occur by the classical and the alternative pathways. In the classical pathway, the protein C1q recognises activators (usually immune complexes) and binds to them. The activation via the alternative pathway starts by the binding of C3b to the activator surface (such as microbial polysaccharides or lipids or surface antigens present on some viruses, parasites and cancer cells) and then follow the same events of the classical pathway. NPs predominantly activate the complement through the alternative pathway.

In our experiments PLGA-ALE NPs did not activate complement by none of the two pathways, as shown by a non-significant different complement consumption from PBS (**Figures 9A** and **9B)**. Conversely, the positive control zymosan induced a 70% complement consumption, twice the amount consumed by PBS. Also the Bb fragment, which is produced during the complement activation by the alternative pathway, was not significantly affected by the PLGA-ALE NPs (not shown).

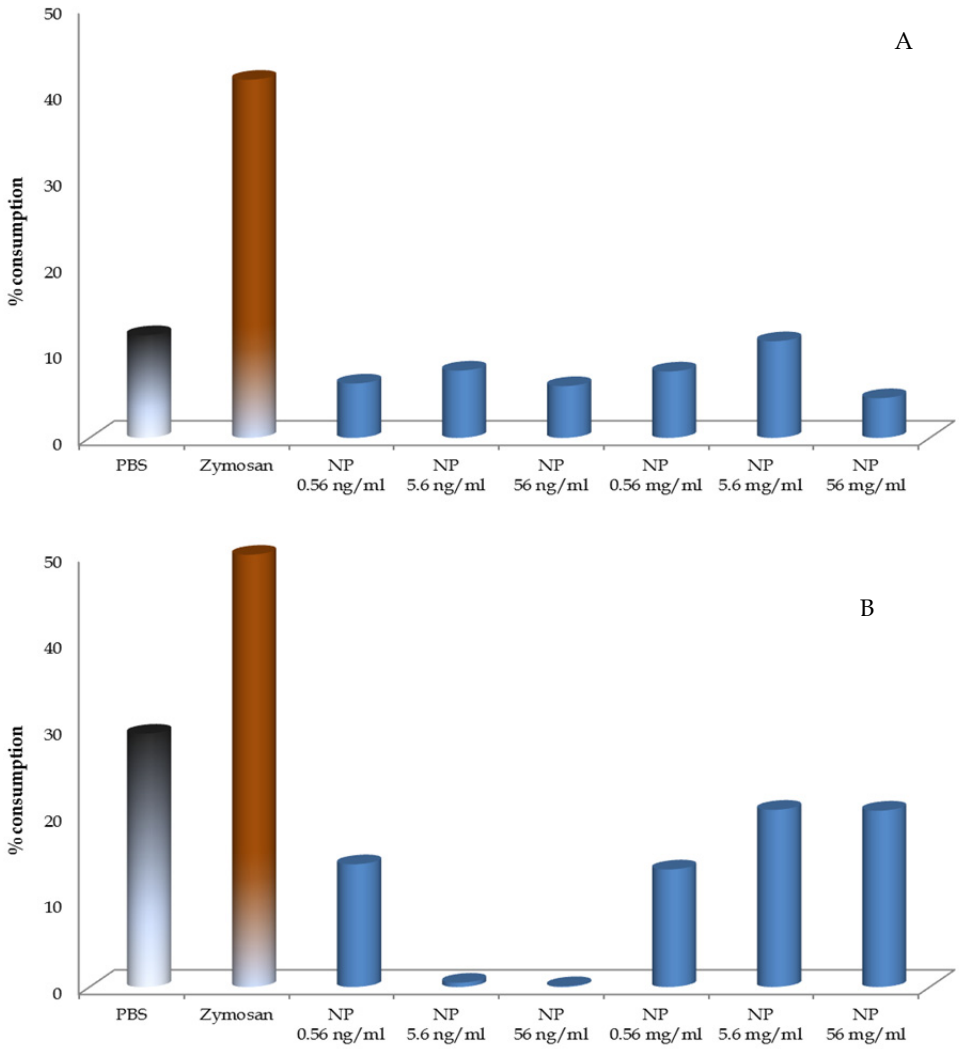

Fig. 9. Percentage consumption of human serum complement activity via the classical pathway (A) or the alternative pathway (B), after incubation with the PLGA-ALE NPs (adapted from ref. [33]).

In the bloodstream, NP come rapidly in contact with vessel endothelium before passing to the outer tissues; therefore, absence of damage to endothelial cells must be ensured. Moreover, bone oriented NPs should not affect the vitality and function of normal osteoblasts. The cytotoxicity of the prepared PLGA-ALE NPs was excluded on both endothelial (HUVEC) cells and osteoblasts derived by bone marrow stromal cells (BMSC). Cell viability was always higher than 80% upon 24 h-exposure to the various concentrations of NPs or to PBS. Phenol, used as a positive control, reduced the cell viability to 19.0% (HUVEC) and to 27.5% (BMSC) (**Figure 10)**.

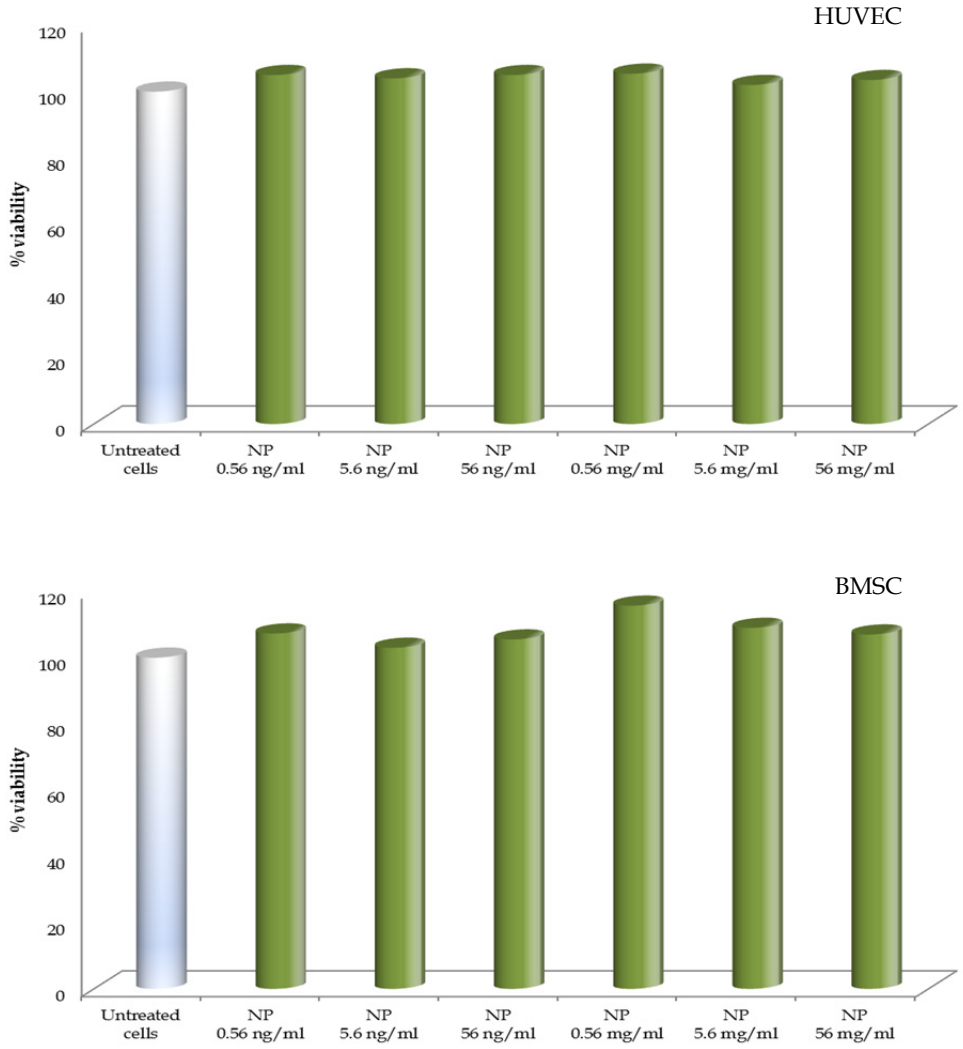

Fig. 10. Viability of endothelial (HUVEC) cells and osteoblasts (BMSC) exposed to various concentrations of PLGA-ALE NPs (adapted from ref. [33]).

In conclusion, PLGA-ALE NPs did not affect platelets, leukocytes and complement, did not induce haemolysis and did not exert cytotoxic effects on endothelial cells and osteoblasts [33].
To assess if the PLGA-ALE NPs are able to retain the antiosteoclastic properties of the bisphosphonate, osteoclast cultures obtained from human peripheral blood mononuclear cells (PBMC) were incubated with either PLGA-ALE or pure PLGA NPs, at an equivalent concentration of 0.64 μM or 6.4 μM of ALE; free ALE was tested as a positive control. Experiments showed that ALE retained the ability of inhibiting the osteoclast-mediated degradation of type I human bone collagen, determined a dose-dependent reduction of osteoclast number, and induced apoptosis in osteoclast cultures, also when conjugated with the copolymer PLGA and in the form of NPs [41]. Interestingly, pure PLGA NPs also showed similar effects, and this can be considered an useful phenomenon in the view of the overall aim of this study: since the conjugation of ALE to PLGA, and the resulting NP formation was aimed at targeting antitumor drugs to osteolytic bone metastases, the additional antiosteoclastic effect observed for polymer-bound ALE and also of PLGA could even contribute to the inhibition of the associated osteolysis.

4. Drug-loaded nanoparticles

Doxorubicin (DOX) is an anticancer agent of wide clinical use, from leukaemia and Hodgkin's lymphoma to symptomatic metastatic breast cancer, from neuroblastoma to many other cancers (prostate, thyroid, bladder, stomach, lung, ovary). Its therapeutic applications are nevertheless limited by the strong cardiac and bone marrow toxicity. DOX effectiveness has been greatly improved when specific targeting at the tumour sites has been achieved, for instance by loading the drug into liposomes (e.g., Caelyx®/Doxil®) [42, 43].
DOX was loaded in the previously described PLGA-ALE NPs and the anti-tumour effect of the carrier was assessed *in vitro* and *in vivo* [44]. In a first instance, the intracellular accumulation and distribution of DOX-loaded NPs was assessed by fluorescence and confocal microscopy, in comparison with free DOX. A panel of potential target cells was used in these experiments: MDA-MB-231 and MCF7 breast adenocarcinoma cell lines, Saos-2 and U-2 OS osteosarcoma cell lines, SH-SY5Y neuroblastoma cell line, and ACHN renal adenocarcinoma cell line. The above tumour histotypes were chosen because all originate from or can metastasize to the bone.
The final localization of DOX in cell nucleus is important because of it mechanism of action [45]. We observed that the incubation of free DOX with cells resulted in its accumulation in the nuclei, while it was absent in the cytoplasm (**Figure 11**). Conversely, cells treated with DOX-loaded NPs showed also fluorescent spots localized in the cytoplasmic vacuoles. Polymeric NPs typically accumulate in lysosomal vesicles, from which the drug is released into the cytoplasm [46, 47]. Therefore, it is likely that the observed cytoplasmic fluorescence was due to the same phenomenon, and that the DOX-loaded NPs were trafficked through the endo-lysosomal compartment.
The incubation of the above cell lines with DOX-loaded PLGA-ALE NPs (48 and 72 h) gave a cell growth inhibition profile very similar to that one of the free drug [44]. To evaluate the *in vivo* activity, DOX-loaded NPs were injected into a mouse model of breast cancer bone metastases: osteolytic lesions were induced by intratibial inoculation of the human breast carcinoma cells MDA-MB-231 that can induce prominent bone metastases. Histological analysis confirmed that the NP did not cause any organ abnormality, hence they should not exert any systemic cytotoxic effect. Control mice treated with PBS developed pronounced

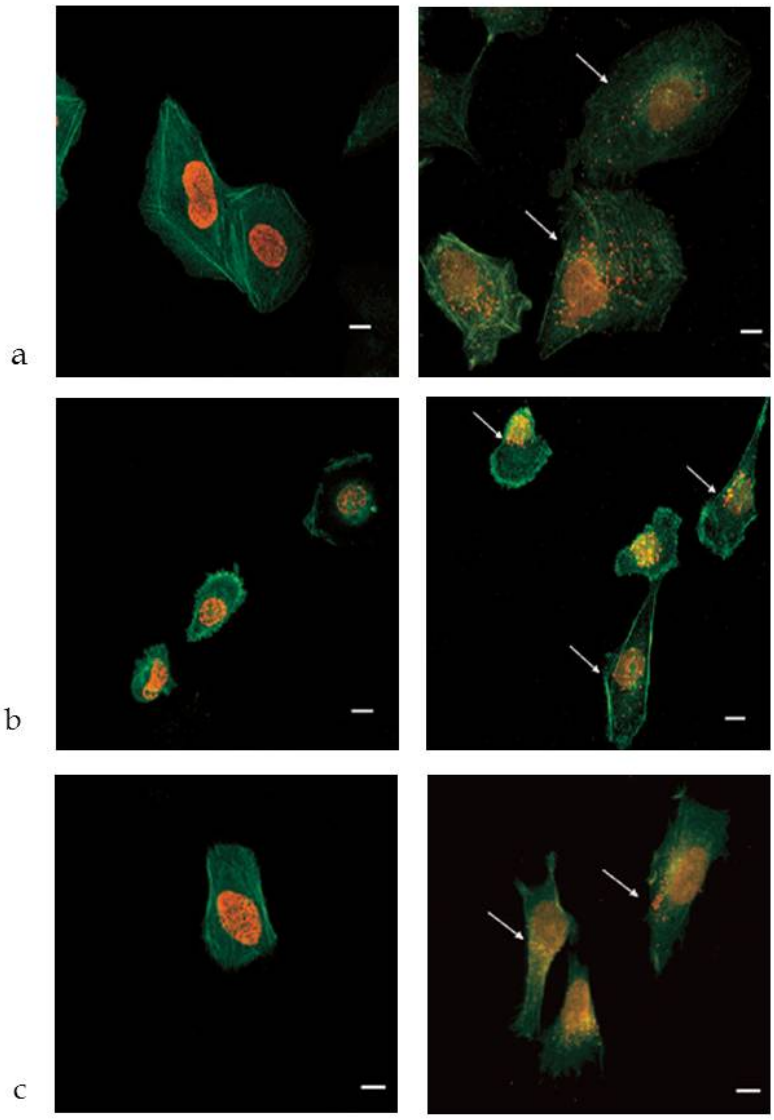

Fig. 11. Confocal analysis of cellular uptake of DOX-loaded PLGA-ALE NPs. Free DOX (left) or NP samples (right) were incubated for 24 h with U-2 OS (a), MDA-MB-231 (b), or SH-SY5Y cells (c). Cytoplasm fluorescence (red spots) was evidenced by arrows. Bars, 10 μm; magnification, 60X (adapted from ref. [44]).

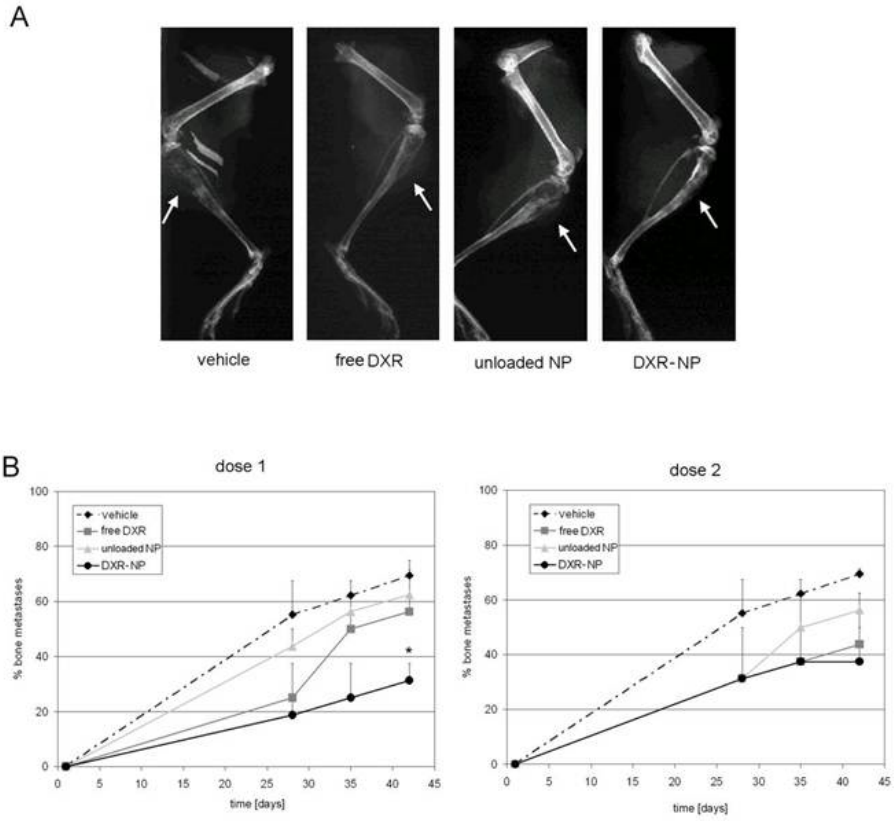

Fig. 12. Effect of DOX-loaded NPs on the incidence of osteolytic bone metastases *in vivo*. BALB/c-nu/nu mice were injected intratibially with a suspension of MDA-MB-231 cells. Mice were weekly treated for six weeks with PBS, free DOX, unloaded NPs, or drug-loaded NPs (DOX-NP) at the dose of 0.2 or 1 mg/kg. *A*, X-ray of hind limbs at day 42 of MDA-MB-231-injected mice and treated with PBS, free DOX, unloaded NPs or DOX-NP at an equivalent drug dose of 0.2 mg/kg (arrows: osteolytic areas). *B*, incidence of osteolytic bone metastases after the same treatments at the lower (left panel) and higher dose (right panel). Means ± SE, n = 8 (modified from ref. [44]).

osteolytic lesions detectable by X-ray analysis starting from the 28th day after the tumour cell inoculation (**Figure 12A**). The free drug was effective in retarding the onset of metastases and reducing their incidence compared to the animals treated with PBS or blank NPs (**Figure 12B**). However, a significant effect was observed only in the DOX-loaded NP-treated group at the dose of 0.2 mg/kg (**Figure 12B**, left panel; P= 0.028 vs. vehicle).
The extension of tumour size was significantly smaller in animal groups which received both the free drug and DOX-loaded NPs at a drug concentration of 0.2 mg/kg or 1 mg/kd (**Figure 13A**), whereas unloaded NPs were ineffective. A trend of reduction of the osteolytic areas was measured in mice treated with either free DOX, DOX-loaded NPs or unloaded NPs. However, DOX-loaded NPs induced a higher inhibition of osteolysis than unloaded

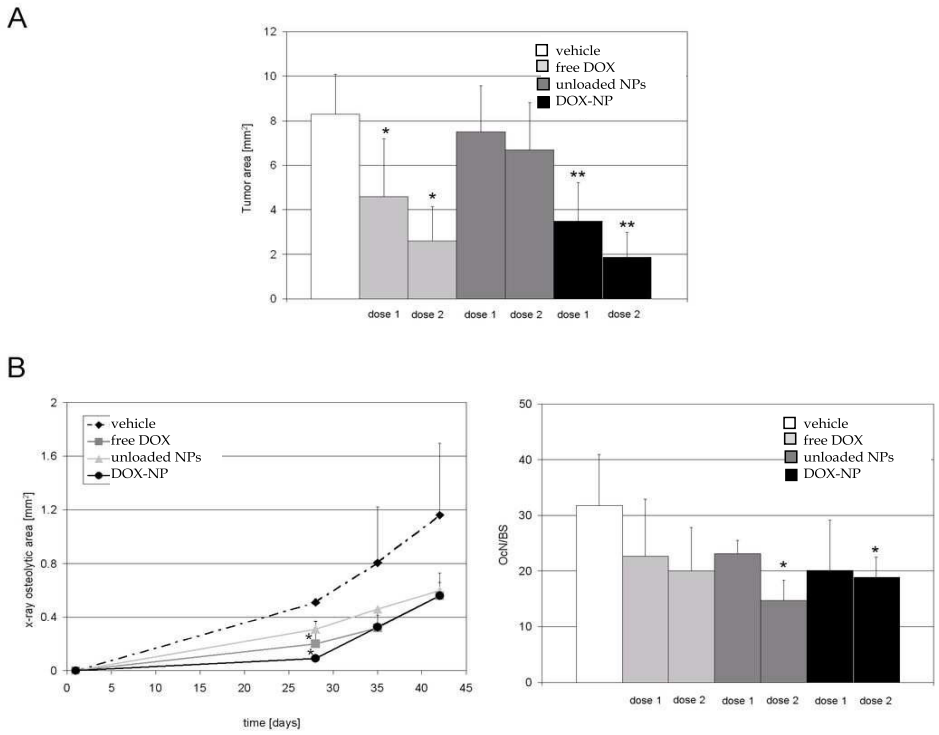

Fig. 13. Effects of DOX-loaded NPs on tumour area and osteolysis. Mice were treated with either PBS, free DOX, unloaded NPs, or DOX-loaded NPs (DOX-NP) at 0.2 mg/kg (dose 1) or 1 mg/kg (dose 2). At the end point, the extension of the osteolytic area was determined by X-ray analysis; sections of the tibiae were histologically examined to evaluate tumour area and the number of osteoclasts on the bone surface. *A*, tumour area (mean ± SD); *B*, osteolytic areas quantified on X-ray images of mice treated with dose 1 (mean± SD); *C*, number of osteoclasts found on the bone surface (OcN/BS) in TRAP stained sections of the tibiae (mean ± SD). * $P < 0.05$, ** $P < 0.005$ (modified from ref. [44]).

NPs (0.090±0.009 *vs*. 0.310±0.040 mm², $P = 0.033$); both free and NP-loaded DOX reached a similar effect at the end of the experiment (day 42) (**Figure 13B**). Similarly, the histomorphometric analysis of sections stained for TRAP activity showed a trend of reduction for the number of osteoclasts found at the bone surface by either free DOX, unloaded NPs, and DOX-loaded NPs (**Figure 13C**). However there was a significant inhibition only for unloaded NPs and DOX-loaded NPs at the highest dose (P= 0.04 and P = 0.014 *vs.* vehicle, respectively).

In conclusion, loading of DOX in the osteotropic PLGA-ALE did not affect the drug efficacy on bone metastases formation; the reduction of the incidence of metastases induced by DOX-loaded NPs was significantly higher than that allowed by the free drug. The enhanced efficacy of the drug when loaded in these NPs can be used as an indirect demonstration of

the successful delivery of DOX to the bones. The modest activity registered with unloaded PLGA-ALE NPs could be related to the inhibitory effect of ALE conjugated to PLGA on osteoclast activity, that indirectly reduced tumour expansion, and of a direct effect exerted by ALE on tumour cells [48]. Treatment of mice with both free or NP-loaded DOX significantly reduced also the tumour area.

All the above experimental findings provide *in vitro* and *in vivo* evidences of the effectiveness of a new osteotropic delivery system for DOX, and possibly other antitumour agents, in which a synergism between the antineoplastic activity of the drugs and the antiosteolytic activity of ALE can afford a better inhibition of tumour development and progression. In the meantime, loading of DOX in biodegradable and biocompatible NPs, made from a conjugate between PLGA and ALE, can allow a site-specific delivery of the drug to osteolytic areas, possibly reducing its systemic side effects. A potential tool for the development of innovative regimens for metastatic bone diseases can thus be exploited by this novel nanocarrier.

5. Acknowledgments

The wide research project described in this chapter was originally supported by a grant from the Associazione Italiana per la Ricerca sul Cancro (AIRC): "Targeting skeletal metastases by nanoscale multifunctional bone-seeking agents". Thanks are due to all the researchers from the Istituto Ortopedico Rizzoli of Bologna (N. Baldini, E. Cenni and co-workers), the University of L'Aquila (A. Teti and co-workers), and the University of Catania (Italy) (F. Castelli and co-workers), who have actively contributed to the project.

6. References

[1] Hanahan D, Weinberg RA. The hallmark of cancer. Cell. 2000;100:57.
[2] Mundy GR, Yoneda T. Facilitation and suppression of bone metastasis. Clin. Orthop. 1995;312:34.
[3] Guise TA, Mohammad KS, Clines G, Stebbins EG, Wong DH, Higgins LS, et al. Basic mechanisms responsible for osteolytic and osteoblastic bone metastases. Clin. Cancer. Res. 2006;12:6213s.
[4] Couzin J. Tracing the steps of metastases, cancer's menacing ballet. Science. 2003;299:1002.
[5] Houston SJ, Rubens RD. The systemic treatment of bone metastases. Clin. Orthop. 1995;312:95.
[6] Pritchard KI. The best use of adjuvant endocrine treatments. Breast. 2003;12:497.
[7] Lin A, Ray ME. Targeted and systemic radiotherapy in the treatment of bone metastasis. Cancer Metastasis Rev. 2006;25:669.
[8] Sim FH, et al. Orthopaedic management using new devices and prostheses. Clin. Orthop. 1995;312:160.
[9] Torchilin VP. Passive and active drug targeting: drug delivery to tumours as an example. Handb. Exp. Pharmacol. 2010;(197):3-53.
[10] Hirsjärvi S, Passirani C, Benoit JP. Passive and active tumour targeting with nanocarriers. Curr. Drug Discov. Technol. 2011 (in press)
[11] Hirabayashi H, Fujisaki J. Bone-specific drug delivery systems: approaches via chemical modification of bone-seeking agents. Clin. Pharmacokinet. 2003;42:1319.

[12] Wang D, Miller SC, Kopeckova P, Kopecek J. Bone-targeting macromolecular therapeutics. Adv. Drug Del. Rev. 2005;57:1049-1076.
[13] Masarachia P, et al. Comparison of the distribution of 3H-alendronate and 3H-etidronate in rat and mouse bones. Bone. 1996;19:281.
[14] Coleman RE. Metastatic bone disease: clinical features, pathophysiology, and treatment strategies. Cancer Treat. Rev. 2001;27:165.
[15] Clezardin P, Ebetino FH, Fournier PGJ. Bisphosphonates and cancer-induced bone disease: beyond their antiresorptive activity. Cancer Res. 2005;65:4971.
[16] Hashimoto K, Morishige K, Sawada K, Tahara M, Kawagishi R, Ikebuchi Y. et al. Alendronate inhibits intraperitoneal dissemination in in vivo ovarian cancer model. Cancer Res. 2005;65:540.
[17] Giraudo E, Inoue M, HanahanD. An amino-bisphosphonate targets MMP-9-expressing macrophages and angiogenesis to impair cervical carcinogenesis. J. Clin. Invest. 2004;114:623.
[18] Fujisaki J, Tokunaga Y, Takahashi T, Hirose T, Shimojo F, Kagayama A, et al. Osteotropic drug delivery system (ODDS) based on bisphosphonic prodrug. I: synthesis and in vivo characterization of osteotropic carboxyfluorescein.. J. Drug Target. 1995;3:273-282.
[19] Hirabayashi H, Sawamoto T, Fujisaki J, Tokunaga Y, Kimura S, Hata T. Relationship between physicochemical and osteotropic properties of bisphosphonic derivatives: rational design for osteotropic drug delivery system (ODDS). Pharm. Res. 2001;18:646-651.
[20] Niemi R, Vepsalainen J, Taipale H, Jairvinen T. Bisphosphonate prodrugs: synthesis and in vitro evaluation of novel acyloxyalkyl esters of clodronic acid. J. Med. Chem. 1999;2:5053-5058
[21] Ezra A, Hoffman A, Breuer E, Alferiev S, Monkkonen, El Hanany- Rozen N, et al. A peptide prodrug approach for improving bisphosphonate oral absorption. J. Med. Chem. 2000;43:3641-3652
[22] Wright JE, Gittens SA, Bansal G, Kitov PI, Sindrey D, Kucharski C, et al. A comparison of mineral affinity of bisphosphonate-protein conjugates constructed with disulfide and thioether linkages. Biomaterials. 2006; 27(5):769-784.
[23] Ogawa K, Mukai T, Inoue Y, Ono M, Saji H. Development of a novel 99mTc-chelate conjugated bisphosphonate with high affinity for bone as a bone scintigraphic agent. J. Nucl. Med. 2006;47:2042-2047.
[24] Uludag H, Yang J, Targeting systemically administered proteins to bone by bisphosphonate conjugation. Biotechnol. Prog. 2002;18:604-611.
[25] Wang D, Miller S, Sima M, Kopeckova P, Kopecek J. Synthesis and evaluation of water-soluble polymeric bone-targeted drug delivery systems. Bioconj. Chem. 2003;14:853-859.
[26] Hengst V, Oussoren C, Kissel T, Storm G. Bone targeting potential of bisphosphonate-targeted liposomes. Preparation, characterization and hydroxyapatite binding in vitro. Int. J. Pharm. 2007;331:224-227.
[27] Miller K, Erez R, Segal E, Shabat D, Satchi-Fainaro R. Targeting bone metastases with a bispecific anticancer and antiangiogenic polymer-alendronate-taxane conjugate. Angew Chem. Int. Ed. Engl. 2009;48:2949-2954.

[28] Bala I, Hariharan S, Kumar MN. PLGA nanoparticles in drug delivery: the state of the art. Crit. Rev. Ther. Drug Carrier Syst. 2004;21:387-422.

[29] http://www.drugs.com/pro/alendronate.html; revision May, 2011 (last visit: July 2011).

[30] De Ruiter J, Clark R. Bisphosphonates: calcium antiresorptive agents. http://www.duc.auburn.edu/~deruija/endo_bisphos.pdf; revision Spring 2002 (last visit: July 2011).

[31] Pignatello R, Cenni E, Miceli D, Fotia C, Salerno M, Granchi D, et al. A novel biomaterial for osteotropic drug nanocarriers. Synthesis and biocompatibility evaluation of a PLGA-alendronate conjugate. Nanomed. 2009;4:161-175.

[32] Tosi G, Rivasi F, Gandolfi F, Costantino L, Vandelli MA, Forni F. Conjugated poly(D,L-lactide-co-glycolide) for the preparation of in vivo detectable nanoparticles. Biomaterials 2005;26:4189-4195.

[33] Cenni E, Granchi D, Avnet S, Fotia C, Salerno M, Micieli D, et al. Biocompatibility of poly(D,L-lactide-co-glycolide) nanoparticles conjugated with alendronate. Biomaterials. 2008;29:1400-1411.

[34] Choi SW, Kim JH. Design of surface-modified poly(D,L-lactide-co-glycolide) nanoparticles for targeted drug delivery to bone. J. Control. Release. 2007;122:24-30.

[35] Salerno M, Fotia C, Avnet S, Cenni E, Granchi D, Castelli F, et al. Effects of bone-targeted nanoparticles on bone metastasis. Calcified Tissue Int. 2008;82(Suppl. 1):S91.

[36] Cenni E, Salerno M, Fotia C, Avnet S, Granchi D, Castelli F, et al. Osteotropic poly(D,L-lactide-co-glycolide)-alendronate nanoparticles for the treatment of bone cancer. Cancer Treat. Rev. 2008;34(Suppl. 1):S74.

[37] Oberdorster G, Maynard A, Donaldson K, Castranova V, Fitzpatrick J, Ausman K, et al. Principles for characterizing the potential human health effects from exposure to nanomaterials: elements for a screening strategy. Particle Fibre Toxicol. 2005;2:8.

[38] Borm PJA, Robbins D, Haubold S, Kuhlbusch T, Fissan H, Donaldson K, et al. The potential risk of nanomaterials: a review carried out for ECETOC. Particle Fibre Toxicol. 2006;3:11.

[39] Radomski A, Jurasz P, Alonso-Escolano D, Drews M, Morandi M, Malinski T, et al. Nanoparticle-induced platelet aggregation and vascular thrombosis. Br. J. Pharmacol. 2005;146:882.

[40] Salvador-Morales C, Flahaut E, Sim E, Sloan J, Green MLH, Sim RB. Complement activation and protein adsorption by carbon nanotubes. Mol. Immunol.2006;43:193.

[41] Cenni E, Avnet S, Granchi D, Fotia C, Salerno M, Micieli D, et al. The effect of poly(D,L-lactide-co-glycolide) nanoparticles conjugated with alendronate on human osteoclast precursors. J. Mat. Sci. Polym. Med. 2011 (in press)

[42] http://www.drugs.com/pro/doxil.html (last visit: July 2011).

[43] Andreopoulou E, Gaiotti D, Kim E, Downey A, Mirchandani D, Hamilton A, et al. Pegylated liposomal doxorubicin HCL (PLD; Caelyx/Doxil®): Experience with long-term maintenance in responding patients with recurrent epithelial ovarian cancer. Ann. Oncol. 2007;18:716-721.

[44] Salerno M, Cenni E, Fotia C, Avnet S, Granchi D, Castelli F, et al. Bone-targeted doxorubicin-loaded nanoparticles as a tool for the treatment of skeletal metastases. Curr. Cancer Drug Targets. 2010;10:649-659.

[45] Calabresi P, Chabner A. In Goodman and Gilman's the pharmacological basis of therapeutics. Goodman Gilman A, Rall TW, Nies AS, Taylor P., eds. Chemotherapy of neoplastic diseases. The McGraw-Hill Companies: New York, 1991, pp. 1202-1263.

[46] Panyam J, Zhou WZ, Prabha S, Sahoo SK, Labhasetwar V. Rapid endo-lysosomal escape of poly(D,L-lactide-co-glycolide) nanoparticles: implications for drug and gene delivery. FASEB J. 2002;16:1217-1226.

[47] Vasir JK, Labhasetwar V. Biodegradable nanoparticles for cytosolic delivery of therapeutics. Adv. Drug. Deliv. Rev. 2007;59: 718-728.

[48] Clézardin P, Ebetino FH, Fournier PGJ. Bisphosphonates and cancer-induced bone disease: beyond their antiresorptive activity. Cancer Res. 2005;65:4971-4974.

9

Complete Healing of Severe Experimental Osseous Infections Using a Calcium-Deficient Apatite as a Drug-Delivery System

G. Amador Del Valle, H. Gautier et al.*
University of Nantes, Teaching Hospital of Nantes
France

1. Introduction

1.1 Classifications

Osteomyelitis represents the majority of severe bone infections. The localization of osteomyelitis originating in the bloodstream is most often the metaphysis of long bones [femur (36%), tibia (33%), and humerus (10%)] in children and vertebral bodies in adults (Lazzarini et al., 2004; Calhoun & Manring, 2005) (Figure 1).

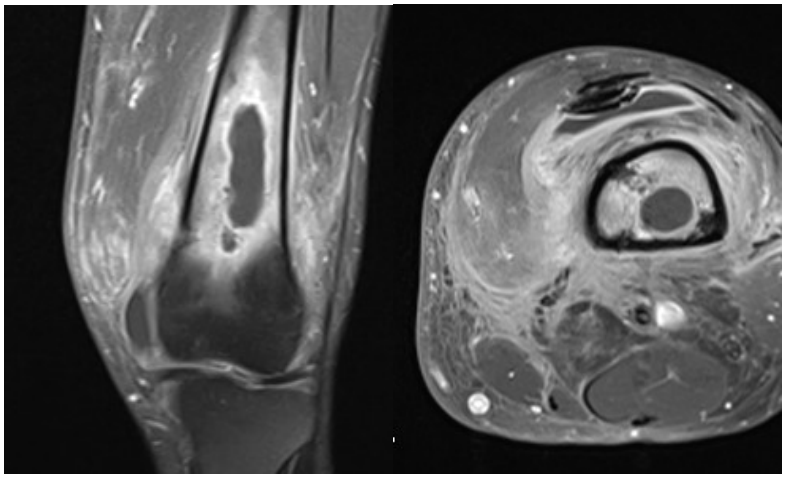

Fig. 1. Magnetic resonance tomography showing an osteolysis of the distal epiphysis of the left femur in an osteomyelitis case in a 40-year-old male patient.

Contiguous-focus bone infections from infected prosthetic devices are more frequently observed in adult males, who are more exposed to trauma (Jorge et al., 2009). Three

*A. Gaudin, V. Le Mabecque, A.F. Miegeville, J.M. Bouler, J. Caillon, P. Weiss, G. Potel and C. Jacqueline
University of Nantes, Teaching Hospital of Nantes, France

classifications are widely used in clinical practice. Waldvogel et al. (1970) described osteomyelitis according to duration, either acute or chronic. The disease is also classified according to the source of infection (i.e., hematogenous or contiguous focus). A third category defines osteomyelitis in terms of vascular insufficiency (Table 1).

Duration	Origin	Sub-divisions
Acute	Hematogenous	
	Contiguous focus	No generalized vascular disease
		Generalized vascular disease
Chronic	Necrotic bone	

Table 1. Osteomyelitis staging system (adapted from Waldvogel et al., 1970)

Nosocomial or traumatic transmissions are not considered in this classification system. Cunha (2002) suggested a simple classification based on acuteness (acute, subacute, or chronic) and microorganisms present for the elderly. The most recent classification system, based on anatomical, clinical, and radiologic features, was described by Cierny et al. (1985) (Table 2). Osteomyelitis is first defined by four stages, depending on the degree of extension: confined (medullary bone), superficial (cortical bone), localized (both), and diffuse. Second, the status of the patient (host) is considered, from A (healthy) to C (severely compromised).

Stages	Anatomical type	Description
1	Medullar	Endosteal focus
2	Superficial	Limited to the surface of the bone
3	Localized	Full thickness of the cortical bone
4	Diffused	Entire cortical bone is involved
Host	Description	Equivalent ASA status
A	Normal	ASA 1
B	Bs: systemic compromise	ASA 2 - 4
	Bl: local compromise	
	Bsl: local and systemic compromise	
C	Major comorbidities	ASA 5 -6

Table 2. Adult osteomyelitis staging system (adapted from Cierny et al., 1985)

1.2 Microbiology

In the case of acute osteomyelitis (AHO), the infection is caused by a hematogenous pathogen and is often located at a metaphysis (Table 3). *Staphylococcus aureus* is isolated in 60-80% of cases (Gafur et al., 2008) with an increasing minimal inhibitory concentration (MIC) to methicillin, followed by other Gram-positive cocci (i.e., coagulase-negative staphylococci, *Streptococcus* spp.), *Pseudomonas aeruginosa*, and *Escherichia coli* (Lew & Waldvogel, 1997; Gutierrez, 2005; Saavedra-Lozano et al., 2008) (Table 4). Bacteria are isolated from blood cultures or tissue biopsy in only 45% in children. Incidence of osteomyelitis was found to reach one in 808 to more than 2,000 admissions (Georgens et al., 2004; Weichert et al., 2008). Methicillin-resistant *S. aureus* (MRSA) represents approximately 10% of the causative bacteria, except in the USA (40-50%) (Weichert et al., 2008). The

presence of Panton-Valentine leukocidin could explain the persistence and rapid local extension of AHO in humans (Crémieux et al., 2009; Labbé et al., 2010).

< 1 year	1 to 16 years	More than 16 years
Group B streptococci *Staphylococcus aureus* *Escherichia coli*	*Staphylococcus aureus* *Streptococcus pyogenes* *Haemophilus influenzae*	*Staphylococcus epidermidis* *Staphylococcus aureus* *Pseudomonas aeruginosa* *Serratia marcescens* *Escherichia coli*

Table 3. Organisms commonly isolated in osteomyelitis based on patient age (adapted from Dirschl et al., 1993)

Bacteria	Circumstances
Staphylococcus aureus	All types of osteomyelitis
Coagulase-negative staphylococci or *Propionibacterium* species	Foreign-body–associated infection
Enterobacteriaceae sp or *Pseudomonas aeruginosa*	Nosocomial infections
Streptococci or anaerobic bacteria	Wounds infected by saliva, diabetic foot lesions, decubitus ulcers
Salmonella species or *Streptococcus pneumoniae*	Sickle cell disease
Bartonella henselae, *Aspergillus* sp, *Mycobacterium avium*-intracellulare or *Candida albicans*	Immunocompromised patients
Pasteurella multocida or *Eikenella corrodens*	Bites

Table 4. Main bacteria isolated in bacterial osteomyelitis (adapted from Lew et al., 1997)

1.3 Diagnosis and treatment

The clinical picture of AHO is often classic: it is commonly a child from 6 to 12 years of age who suddenly presents with a disability absolved from the affected limb and associated with a 39-40°C fever. After clinical investigation, the pain is extremely intense, and the preferential location is the lower extremity of the thighbone or the superior extremity of the shin. Emergency treatment must be initiated, associated with fixed immobilization in plaster and intravenous antibiotic therapy. If the treatment is administrated early, cure is most often achieved within 3 weeks. If a delay in diagnosis is made or the treatment is inadequate, chronic osteomyelitis associated with a 38°C fever can develop and the affected limb aches, is red and warm, and sometimes abscesses. Radiography shows osteolysis at the metaphysis, with thickening or detachment of the periostium with ossification and appearance of a sequestrum. The treatment of these forms, which can become subacute or chronic, is complex and is often associated with 6 months to 1 year of medical treatment and repeated surgical procedures to remove intra-osseous or under-periostium abscesses and sequestra. The after-effects are important: osseous fragility with risk of fracture and disorders of healing and growth in length or with deviation. The osteitis is usually subacute with *S. aureus* and more or less painful. When osteitis affects a lower limb, patients have a

limp, and clinical examination shows amyotrophy regarding the skeletal area of interest. The biology shows all the signs of infection (leucocytosis, erythrocyte sedimentation rate, C-reactive protein); radiology reveals evidence of uni- or polycyclic osteolysis that is finely encircled by dense bone (Brodie's abscess). Surgical treatment is necessary, and osseous trepanning is performed to decompress this internal infection, administering antibiotics intravenously first and then orally. The duration of treatment is at least 3 weeks. If everything does not quickly normalize, oral antibiotics are necessary for several months. Osteomyelitis is an infective process that may also require numerous surgical interventions and leads to bone sclerosis and deformity, and even to a loss of limb.

2. Animal experimental models

Clinical trials for antibiotic treatment of osteomyelitis are rare and difficult to perform for many reasons. First, the anatomical localization of the lesions varies. Moreover, the treatment of patients suffering from severe bacterial infection with new drugs raises complicated ethical concerns that must be addressed. In vitro alternatives to replace animal tests, specifically to study osteomyelitis due to MRSA, are unrealistic and do not allow for surgical procedures. For these reasons, animal studies are the most appropriate and feasible way to assess the impact of antibiotic therapy on the outcome of osteomyelitis. Several different models exist and were developed to study hematogenous (or post-traumatic) osteomyelitis or osteomyelitis related to orthopedic implants and prosthetic joint infections. The features and history of these osteomyelitis models have been summarized by several authors (Mader, 1985; Norden, 1988; Rissing, 1990; Patel et al. 2009). Further, osteomyelitis studies have been conducted using various species, including rats (Power et al. 1990), rabbits (Andriole et al., 1973; Norden 1988), dogs (Deysine et al., 1976; Fitzgerald, 1983), and guinea pigs (Passl et al., 1984)., each with advantages and limitations.

2.1 Limitations and failures

The osteomyelitis experimental model is demanding but critical for testing new antibiotics because eradication of bacteria from bone represents a very difficult challenge (Yin et al., 2005). In experimental studies, viable bacteria can be retrieved from the bone despite prolonged antibiotic treatment (i.e., up to 4 weeks). The development and maturation of bacterial biofilms could explain the failure of antibiotic treatments and subsequent relapses (Brady et al. 2008). However, current animal models of osteomyelitis have a number of limitations, including low success rates for the induction of osteomyelitis, the elimination of causative bacteria by the host immune system, and the need for administration of sclerosing agents (SAs) in most cases (Patel et al., 2009). These SAs, as morrhuate sodium or its derivative arachidonic acid, are thought to induce varying degrees of aseptic bone necrosis, providing ideal conditions for bacterial proliferation and likely facilitating bone infection by occluding the microvasculature. In most animal models of osteomyelitis, SAs are usually injected prior to bacterial injection (Yoshii et al., 2001; Fukushima et al., 2005).

2.2 The acute rabbit model

In the acute model developed by Gaudin et al. (2011), devascularized bone made from a surgically induced bone defect provided a site in which to establish a productive infection.

Femoral trepanation using a biopsy needle was followed by injection of 1 mL of 10^9 colony-forming units (CFU)/mL *S. aureus* suspension directly into the knee cavity. Using this protocol, bacterial densities approached 9-$\log_{10}$ CFU/g infected tissue 3 days post-infection that persisted at least 14 days without treatment. Unlike chronic models of osteomyelitis, no spontaneous recovery of the bacterial infection was observed. Moreover, the rabbit long bone model is appropriate for the study of osteomyelitis because rabbits are more prone to infection than other animals, such as rats. The size of New Zealand white rabbits makes it possible to more closely mimic human surgical procedures such as bone debridement and computer-controlled pharmacokinetic .

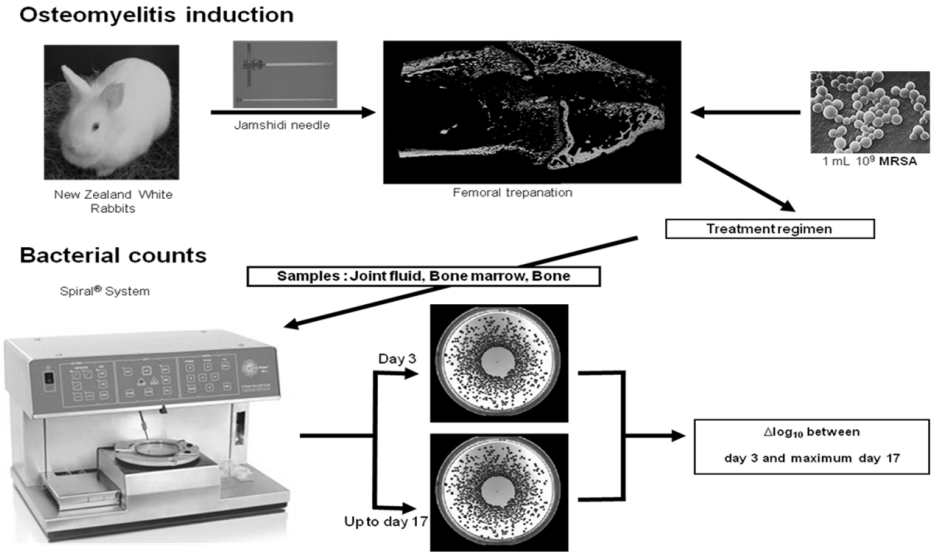

Fig. 2. The acute experimental osteomyelitis rabbit model (Gaudin et al., 2011)

3. Calcium phosphate as a matrix of antibiotic release

The term "biomaterial" has recently been defined as "a substance that has been engineered to take a form that, alone or as part of a complex system, is used to direct…the course of any therapeutic or diagnostic procedure" (Williams, 2009). Implantable biomaterials are inert or can promote biological activities, such as bone regeneration, or minimize undesirable activities, such as infection or blood clotting (Williams, 2008, 2009).
In the osseous and dental fields, biomaterials are often necessary to fill or treat different pathological situations, such as bone trauma, infections, irradiations, or various diseases such as osteoporosis and tumor resection (Campoccia et al., 2010). As alternatives to bone grafts, different biomaterials have been developed.

3.1 Biomaterials

Inorganic materials are frequently used as bone matrixes and are divided into three chemical families that represent current alternatives to biological bone grafts: calcium

phosphate (CaP), calcium sulphate, and calcium carbonate. These materials can be shaped into different forms such as powders, granules, ceramics, cements, and coating, depending on the site, and the size and shape of the bone defect. Granules are more convenient than blocks, allowing the replacement of a large bone volume. As blocks are difficult to fit into cavities, vacant areas are often observed between blocks and bone. Vertebrate bone tissue is primarily composed of CaP, which explains why CaP materials are excellent candidates for bone reconstruction (Rush, 2005; Vallet-Regi, 2006: LeGeros, 1991). CaP materials are also interesting because of their cell resorption and osteoconductive properties. Calcium sulphate and calcium carbonate are less frequently used because they promote poor osseous formation because of their higher solubilities.

Based on composition, currently used synthetic CaP matrixes are classified as hydroxyapatite [HA: $Ca_{10}(PO_4)_6(OH)_2$], alpha- or beta-tricalcium phosphate [α or β-TCP : $Ca_3(PO_4)_2$], mixtures of these compounds, biphasic CaP (BCP), or unsintered apatites called calcium-deficient apatite (CDA).

HA and ß-TCP ceramics can be prepared by grinding CaO and P_2O_5 powders with Ca/P equal to 1.67 and 1.5, respectively. These mixtures must be sintered at more than 1100°C. These CaP biomaterials differ in their extent of dissolution (Chow, 2009):

$$\alpha\text{-TCP} >> \text{CDA} > \beta\text{-TCP} >> \text{HA}$$

CDAs can be prepared either by aqueous precipitation from calcium and phosphate salts or alkaline hydrolysis of acidic CaP (Jarcho, 1981; Gauthier et al., 1998; Venesmaa et al., 2001; Nehme et al., 2003). For BCPs, the dissolution rate depends on the HA/TCP ratio: the higher the ratio, the higher the dissolution (LeGeros, 1991; Daculsi et al., 1997). HA, TCP, BCPs, and CDA are frequently described in the literature as excellent candidates for bone substitution because of their similarity to bone structures (Figures 3 and 4).

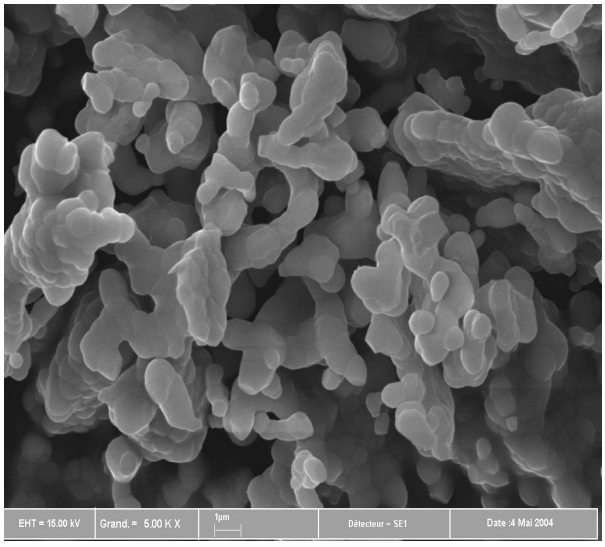

Fig. 3. Scanning electron micrograph picture of BCP at a magnification of 5000.

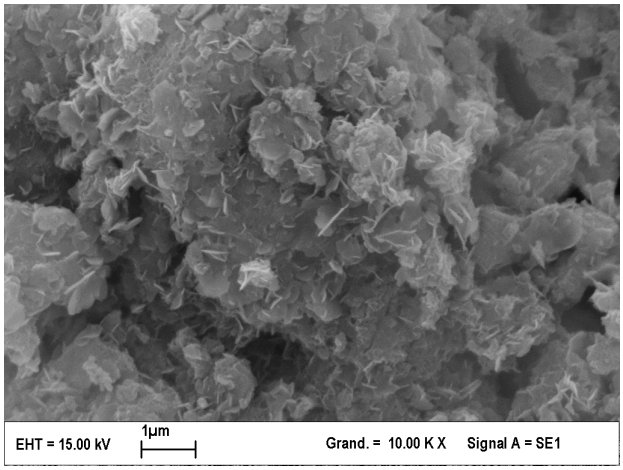

Fig. 4. Scanning electron microscopy picture of CDA at a magnification of x10 000.

These materials have all the necessary properties required for a graft: biocompatibility, bioactivity, biofunctionality, and osteoconductivity. Because of CDA's better solubility than BCP, bone colonization with CDA will be quicker and more significant and will thus provide a better reconstitution of the bone.

Others matrix properties are also very important. Macroporosity, which corresponds to pores larger than 100 µm, defines its capacity to be colonized by cells. Different agents can be associated with the matrix during the preparation process (naphthalene or sucrose particles and granules) and then calcinated or sublimated at high temperature (Lecomte et al., 2008; Le Ray et al.; 2010). Microporosity, corresponding to pores smaller than 10 µm, defines the matrix capacity to be impregnated by biological fluids. These micropores depend on the sintering process, and the microporosity depends mainly on the material composition and the used thermal cycle. Solubility and biological properties of these CaP materials depend on crystal size, ionic impurities, specific surface area, and porosity. The control of the macro- and micropore size and distribution of CaP bone substitutes represent the most important parameters to promote or induce bone formation. All these parameters have a specific influence on the final mechanical properties of the bioceramics (Bouler et al., 1996).

CaP biomaterials possess three fundamental properties that govern potential bone substitution:

- Biocompatibility: CaP ceramics are perfectly tolerated by the host organism, as described by numerous studies (Deligianni et al., 2001; Ooms et al., 2003; Julien et al., 2007; Williams, 2008),
- Bioactivity: After implantation, the biological fluids interact with the CaP ceramics and initiate the dissolution of the material. Depending on the chemical composition of the CaP ceramics, a precipitation of a layer of biological apatite can be obtained on their surfaces. The continuity thus obtained between the host bone tissue and the biomaterial promotes cellular colonization and the formation of bone tissue. The cellular resorption and degradation of the bone substitute results from the concomitant action of osteoclasts and macrophages, respectively **(**Anderson & Miller, 1984; Minkin & Marinho, 1999; Detsch et al., 2008). The resorption rate of the material and the *de novo*

bone tissue rate ideally must be similar to ensure stability of the interface (Zerbo et al., 2005). The biological, chemical, and mechanical properties at the bone/material interface are therefore essential to ensure good osteointegration of the implant (Ducheyne & Cuckler, 1992).

- Biofunctionality (Daculsi et al., 1999; Parikh, 2002; LeGeros, 2002): The material mechanical properties of CaP ceramics are limited by low initial mechanical properties compared to host bone mechanical properties. However if osteoconduction and resorption are favored (e.g., by a convenient porous structure), the fragility of the CaP ceramic implant is going to decrease, and an optimal final biofunctionality will be achieved with the total resorption/substitution process. Therefore, intrinsic material parameters [e.g., rate of porosity and solubility (Ca/P ratio)] and extrinsic parameters (e.g., primary stability, instrumentation) must be adapted to promote both complete implant resorption and tissue regeneration. Then, the three functions (mechanic, metabolic, and hematopoietic) of bone can be fully restored.

3.2 Biomaterials as drug delivery systems

The "fill-in" properties are interesting but rapidly it became necessary to not only fill in osseous or dental defects (Navarro et al., 2008) but to treat locally different pathologies. Thus, several combinations of biomaterial matrices and therapeutic agents were prepared. Such biomaterials are called drug delivery systems (DDS). First, polymethylmethacrylate cements were tried as innovative drug delivery systems, but these materials were progressively replaced by resorbable materials whose major advantage is to be left *in situ* in the bone defect and do not require surgical removal. These materials are numerous, ranging from inorganic to organic and from natural to semi-synthetic or synthetic.

Therapeutic agent-CaP biomaterial combinations prepared to produce an *in situ* DDS with a sustained release profile were numerous; a large panel of therapeutic agents loaded onto biomaterials was used, including growth factors (Verron et al. 2010) such as bone morphogenetic proteins (Ripamonti et al., 1992; Deckers et al., 2002), human growth hormone (Goodwin et al., 1995; Downes et al., 1995; Guicheux et al., 1998), transforming growth factor-beta (Kim et al., 2005), insulin-like growth factor (Matsuda et al., 1992); antiosteoporotics (Denissen et al., 1994, 1997; Golomb et al.,1992); anticancer drugs (Otsuka et al., 1995; Itokazu et al., 1998); insulin (Otsuka et al., 1994); steroid hormones (Bajpai & Benghuzzi, 1988); analgesic drugs (morphine and lidocaine (Gautier et al., 2010), and antibiotics (Penner et al., 1996; Suzuki et al., 1998).

Concerning antibiotics, the incorporation of antibacterial therapeutic agents in biomaterials dates back to the 1950s with the association of dental cements and resins with antibiotic drugs. The idea was to release locally therapeutic agent at the infection site. As cements and resins are not bioresorbable, other biomaterials that are resorbable and soluble were developed. Therapeutic agent release must be controlled to ensure adequate tissue concentrations several times higher than the MIC and maintained sufficiently to entirely cover the difficult post-surgery period, avoiding the systemic administration of intravenous or oral antibiotics and their subsequent side effects. Among the antibiotics (Sudo et al., 2008), gentamicin sulphate (Specht & Kühn, 1998) and crobefat (Joschek et al., 1998), cephalexin (Yu et al., 1992), tobramycin (Nijhof et al., 1997; Anaja et al., 2008), arbekacin (Itokazu et al., 1997), ciprofloxacin ((Wu et al., 1997), isepamicin sulphate (Itokazu et al., 1998; Kawanabe et al., 1998), gentamicin (Randelli et al., 2010), and vancomycin (Hamanishi et al., 1996) are commonly used for these associations. Recently, a new DDS using linezolid

was developed (Gautier et al., 2010). Tetracyclines cannot be used with CaPs because their fixation to the matrix is irreversible (Misra, 1991). Tetracycline is moreover used as a tracer for forehead mineralization in histology studies but is not used for the treatment of children.

3.3 Associating therapeutic agents with biomaterials

Various techniques associating a therapeutic agent with a CaP biomaterial have been reported in the literature: powder-powder mixing (Yu et al., 1992; Dacquet et al., 1992; Hamanishi et al., 1996; Trécant et al., 1997); soaking of beads (Thomazeau & Langlais, 1996; Brouard et al., 1997), granules (Joschek et al., 1998), or blocks (Prat-Poiret et al., 1996) in a therapeutic agent solution; packing the therapeutic agent in a central, cylindrical cavity in porous blocks (Shinto et al., 1992) or in the central cavity of TCP capsules to maintain high-level, long-term release of the therapeutic agent (Wu et al., 1997); adsorption of the therapeutic agent in solution on the biomaterial (Guicheux et al., 1997; Trécant et al., 1997; Gautier et al., 1998); centrifugation (Itokazu et al., 1995; Nijhof et al., 1997; Itokazu et al., 1994a, 1998d, 1998e, 1998f); or immersion of a biomaterial block in a therapeutic agent solution followed by vacuum (Itokazu et al., 1998f; Kawanabe et al., 1998). Adsorption and soaking both allow the therapeutic agent to be incorporated at the surface of the biomaterial, whereas centrifugation and vacuum enable the therapeutic agent to enter the pores of the biomaterial. These different processes of therapeutic agent–matrix association are chosen to either facilitate contacts between the biomaterial and the therapeutic agent or achieve compaction. At the same time, our laboratory has dismissed the use of wet granulation and developed two compaction techniques: dynamic compaction and isostatic compression for the successful preparation of sustained-release forms.

The technique of wet granulation, a densification technique widely used in the pharmaceutical industry for the manufacture of granules and pellets, is commonly used for the association of CaP (CDA or BCP) with the therapeutic agent, making it possible to acquire a homogeneous distribution of the constituents of the granules and create close links between CDA and the therapeutic agent (Ormos, 1994). In addition, the acquired granules have a spherical form that is suitable for filling bone defects. This technique has already been used for bone substitute formulations with vancomycin and linezolid (Gautier H et al., 2000). A particle size analysis by laser light diffraction can be performed on acquired granules after sieving of the fraction (40- to 80-µm fraction, 80- to 200-µm fraction, 200- to 500-µm fraction, depending on the defect size). The results show that a large majority of the granules belong to the required fraction. If necessary, and to select more precisely the fraction desired, aspiration with an air jet sieving machine can be performed.

Dynamic compaction is a powder compaction technique developed in 1995 to consolidate CaP powders (Trécant et al., 1997). During this process, particle surfaces are highly deformed, producing interparticulate bonding in a one-step procedure. This process occurs during the passage of a shock wave through the powder. As this technique requires no external heat and allows the compaction to be formed without a sintering step, a heat-sensitive therapeutic agent can be associated with a CaP powder without denaturing the active element. The agent and powder can be melted and associated before compaction, and the pressure can vary between 0.5 and 2 MPa. Different studies showed the advantage of dynamic compaction to obtain compact CaP biomaterials (Trécant et al., 1995) and to associate therapeutic agents with those materials (Guicheux et al., 1997; Trécant et al., 1997). These studies investigated the association of growth factors (e.g., human growth hormone) and antibiotics, such as vancomycin and polymyxin B, with the CaP matrix (CDA and BCP).

The physicochemical characterization of CaP granules by X-ray diffraction, infrared spectroscopy, and nuclear magnetic resonance showed that the structures of BCP and vancomycin were unchanged by dynamic compaction at 1.9 MPa. This finding was concordant with another study (Trécant et al., 1995), showing that the structures of powders such as hydroxyapatite, β-CaP, BCP, and octacalcium phosphate were conserved after a 2-MPa dynamic compaction. Scanning electron microscopy showed that granule porosity depends on the manufacturing process, ranging between 37.7 ± 6.8 and 9.9 ± 4.7%. Granule porosity with dynamic compaction was 3-to 4-fold lower than with wet granulation. In fact, the wet granulation process is performed during a single step in which densification occurs, whereas granule preparation is done in two steps with the dynamic compaction process: densification by powder volume reduction (which gives a compact with lower density) followed by crushing. This volume reduction is correlated with the pressure applied (porosity is reduced when compaction pressure is high). As bone ingrowth correlates with material porosity (Lu et al., 1999), the choice of preparation process allows various granules to be obtained.

Polymyxin B, a polypeptidic antibiotic that undergoes thermodamage above 60°C, was also studied and associated with CaP by dynamic compaction (Kimakhe et al., 1999). The biological activity of polymyxin B-loaded CaP was determined by the effect of the antibiotic and monocyte/macrophage degradation on compact surfaces. The biological activities (i.e., antibacterial activity and inhibited lipopolysaccharide effects on monocyte/macrophage CaP degradation) of polymyxin B released from compacted calcium-deficient apatite were unaltered. Thus, dynamic compaction allows polymyxin B to be used with CaP ceramics without any loss in integrity or biological effects.

Isostatic compression is a technique based on the transmission of an isostatic omni-directionnal hydraulic pressure to powder, thus making the materials denser within a few minutes at room temperature. This cold technique allows the association of drugs without any degradation and allows the direct preparation of a correctly and directly molded implant. Compression pressure is applied uniformly and from all directions to consolidate the material (Gautier et al., 2000a, 2000b).

Physicochemical characterization of BCP granules by X-ray diffraction, infrared spectroscopy, and nuclear magnetic resonance showed that BCP, linezolid, and vancomycin structures remained the same. After association, release profiles must be determined to characterize the biomaterials. To establish the granule release profiles of the therapeutic agents, different tests can be used: culture chamber dissolution tests (Guicheux et al., 1997) or paddle apparatus dissolution tests (European Pharmacopoeia 7.1). Proportions of therapeutic agents released daily from a CaP matrix must be measured by an UV–visible spectrophotometric or high-pressure liquid chromatography (HPLC) assay.

Generally, using the culture chamber dissolution test, independent of the therapeutic agent (e.g., vancomycin or linezolid), after a waiting time of approximately 6 hours, the kinetics were observed to be order 0 up to a complete release in 3 to 26 days, depending on the amount of therapeutic agent loaded, its solubility, and the process of association. The waiting time of 6 hours, noticed before the beginning of the release of the antibiotic, corresponds to the time of the anchoring of grains, necessary at the beginning of the dissolution of the antibiotic in the medium.

For example, in wet granulation, the process allows a faster delivery, releasing the associated vancomycin in a maximum of 3 days. Dynamic compaction increases the period of vancomycin release to 4 to 6 days. Granules obtained by this process form a matrix that releases the therapeutic agent slowly, depending on the binding force (not yet determined)

of vancomycin to CaP. The pressure of dynamic compaction has no significant influence on release time, and there was no significant difference in the vancomycin adsorbed on granules prepared by dynamic compaction or compacted with BCP granules. In the first case, the water of the dissolution medium penetrates into the pores to release the therapeutic agent; in the second case, a vancomycin dissolution-diffusion process operates from the periphery toward the center of the granule.

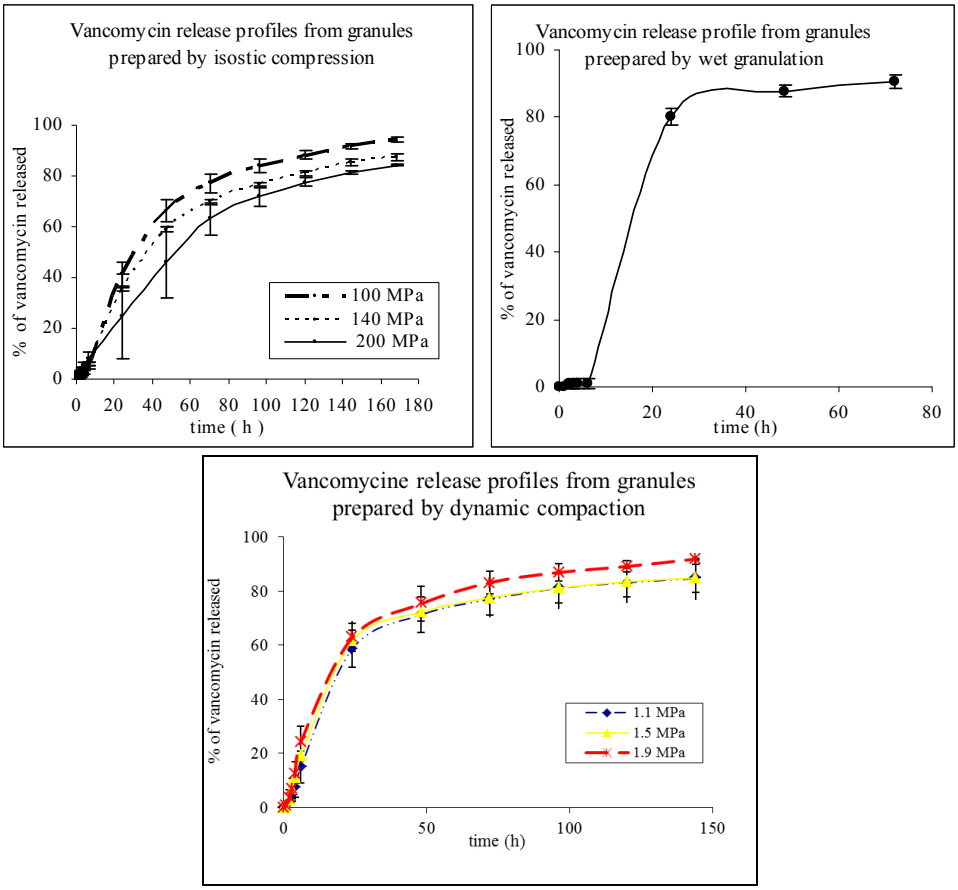

Fig. 5. Vancomycin release profiles from BCP granules prepared by different techniques.

Another study compared wet granulation and isostatic compression (Gautier et al., 2000b). Release was faster for granules prepared by wet granulation than for those prepared by isostatic compression. Moreover, vancomycin release time was prolonged as compression increased: an increase in isostatic compression from 100 to 200 MPa allowed a doubling of 75% vancomycin release. The use of isostatic compression allowed a 3- to 5-fold increase in the period of vancomycin release compared to granules prepared by wet granulation. These differences in the rate of vancomycin release may have been due to the nature of BCP-vancomycin binding strength. Vancomycin is always released faster when associated by

adsorption at the surface of the granule compared to direct incorporation into the granule mass, regardless of the manufacturing process used. Release is also faster for wet granulation than for isostatic compression. Moreover, therapeutic agent release slows as isostatic pressure increases. Figure 5 shows different vancomycin release profiles from 200- to 500-µm BCP granules prepared by isostatic compression, wet granulation, and dynamic compaction.

Scanning electron micrographs show that granules prepared by wet granulation have a greater number of macropores and those prepared by isostatic compression possess a greater number of micropores (Figure 6). Image analysis also indicates that porosity is greater for granules prepared by isostatic compression. Pores of granules prepared by wet granulation appear to be more accessible to the release medium, thereby increasing the rate of vancomycin release. Moreover, the porosity percentage for granules prepared by isostatic compression is greater as isostatic pressure increases.

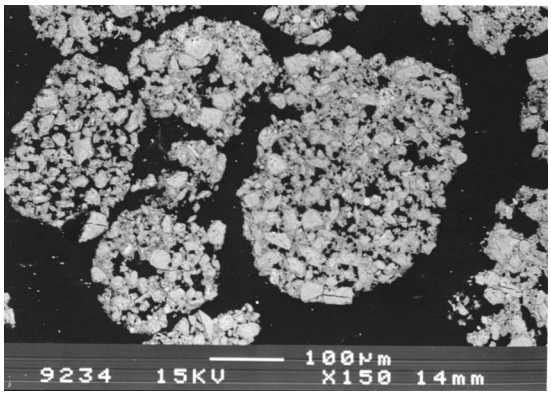

6a: porosity = 33.93 ± 4.29 %

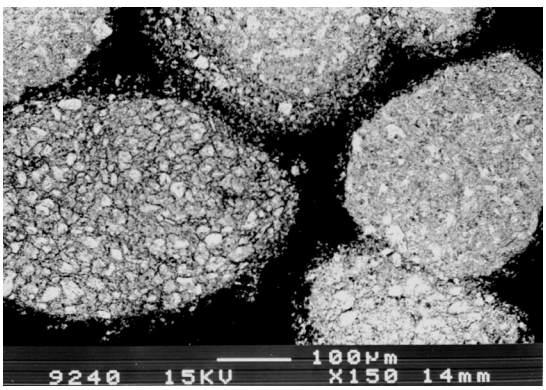

6c: porosity = 47.92 ± 5.94 %

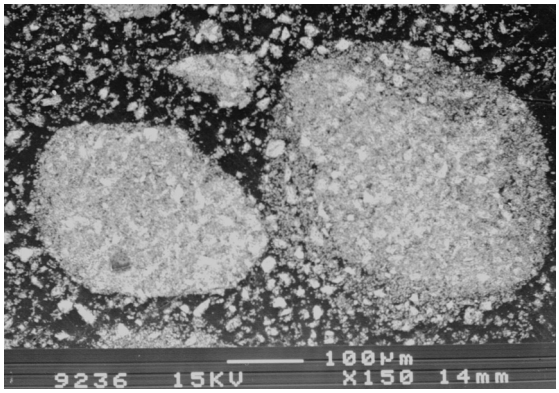

6b

porosity = 63.4 ± 14.30 %

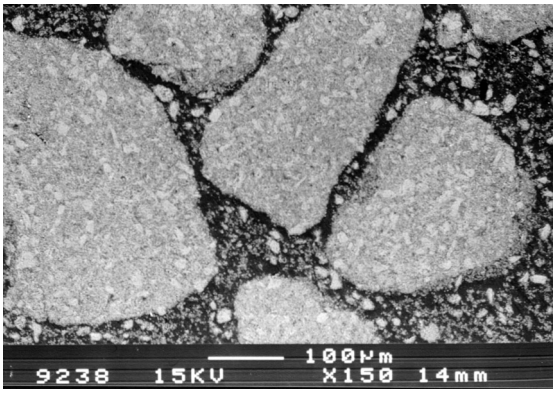

6d

porosity = 42.71 ± 7.48 %

Fig. 6. Scanning electron micrographs of BCP granules. BCP granules (200- to 500-µm) were prepared by wet granulation (a) and isostatic compression at 100 MPa (b), 140 MPa (c), and 200 MPa (d). Porosity percentages are expressed as the mean ± SD (Gautier et al., 2000b)

Another study was performed on CDA granules containing linezolid associated by a wet granulation process (Gautier H, Biomaterials 2010). Figure 5 shows images of CDA containing 10% linezolid (a) and 50% linezolid (b) acquired by scanning electronic microscopy. A comparison of the slope of the linear regression was made. For 10% linezolid-loaded granules, the slope (p) was equal to 17.068 with correlation coefficient $r^2 = 0.994$; for 50% linezolid-loaded granules, p = 5.11 and $r^2 = 0.9969$. For granules containing 10% linezolid, the release was rather quick (3.3 times more important for 10%-loaded granules than for 50%-loaded granules). After a waiting time of approximately 6 hours, the kinetics observed were order 0 up to a complete release in 9 days. The results of the release kinetics for CDA loaded with 10% linezolid were similar to those observed for vancomycin integrated into BCP, although with a slightly longer release time. For the release kinetics of CDA containing 50% linezolid, the release kinetics were similar, with a waiting time from

approximately 6 hours, and kinetics of order 0. The release was complete after 26 days, which is three times greater than for grains loaded with 10% linezolid.

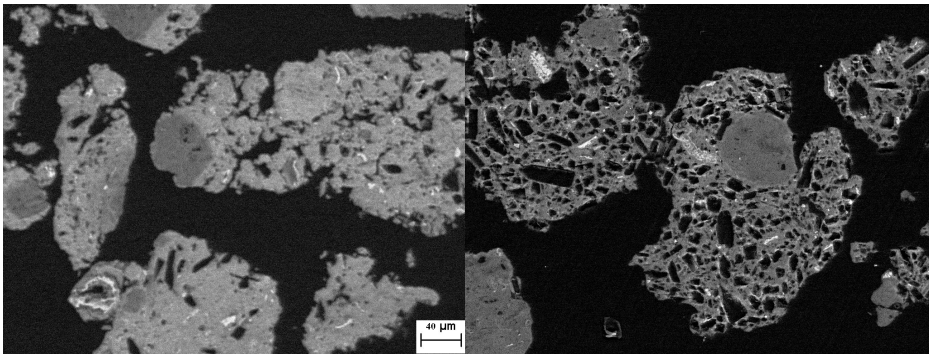

7a) 7b)

Fig. 7. CDA containing 10% linezolid (a) and 50% linezolid (b) acquired by scanning electronic microscopy at a magnification of ×250 (Gautier et al., 2010a)

Another laboratory (Kundu et al., 2010) developed HA-based porous scaffolds loaded with ceftriaxone-sulbactam (i.e., a drug combination consisting of an irreversible β-lactamase inhibitor and a β-lactam antibiotic) and presented that results of in vitro and in vivo drug elution after 41 days showed release rates higher than minimum inhibitory concentration of ceftriaxone-sulbactam against *S. aureus* in a chronic osteomyelitis model.

Additionally, there is no correlation between these in vitro release results, the release test used, and the in vivo therapeutic agent released. It appears to be important to choose the fabrication process in terms of the needed release time: a flash release of just a few days to avoid infections after surgical intervention or long-term release at high concentrations after bone infection.

It is important to demonstrate the effectiveness of the antibiotic released from the granules. This can be performed by nuclear magnetic resonance-mediated structural identification as well as by antibacterial assay. The analysis by ^{1}H- nuclear magnetic resonance (^{1}H-NMR) must be performed on samples of CaP granules to verify that the association process does not modify the CaP structure. ^{1}H-NMR analysis must also be performed on samples of CaP granules loaded with therapeutic agent to identify the structure of the therapeutic agent molecule in the different samples regardless of the percentage of therapeutic agent associated. Analysis performed on BCP and CDA showed that wet granulation, isostatic compression, and dynamic compaction processes did not affect the structure of the CaP matrices. Analysis performed either on vancomycin or linezolid showed that the incorporation of pharmacological agents into CDA and BCP by wet granulation and isostatic compression did not affect the structure of the antibiotic. The chemical structure of the vancomycin and linezolid remained identical in granules even during release. In fact, no significant spectral differences were noticed during the NMR analyses of the therapeutic agent molecule released and extracted from the release profiles from 24 hours to 7 days.

The bacteriological test consists of measuring the amount of therapeutic agent still active in samples after its release. Bacterial strains must be shown to be sensitive to the therapeutic

agent, and the matrices (i.e., CDA and BCP) do not inhibit the bacterial growth of the bacterial strain. The ratio of the therapeutic agent (i.e., vancomycin or linezolid) quantities calculated by bacteriological and assay measurements, derived from release kinetics of the granules after 24 hours, 5 days, or 7 days of release are determined and correlated to the NMR analyses, showing that the chemical structures of the released vancomycin and linezolid were maintained. It can be concluded that the manufacture of granules by wet granulation and isostatic compression, as well as the tests of release, changes neither the structure nor the activity of the vancomycin or linezolid, and thus, the antibiotics might be able to treat bone infection. However, a comparison of the amounts of activity detected by spectrophotometry and microbiological assay shows that only 28% of the vancomycin released from biomaterials prepared by dynamic compaction was active. This compaction technique is known to cause large but brief local temperature increases in compact materials, which are not quantifiable but high enough to induce grain joint formation. This process could denature vancomycin activity, which remains stable for 6 h at 80°C. As dynamic compaction reduces the microbiological activity of vancomycin, wet granulation and isostatic compression processes are preferred.
As a result, according to the nature of the implant and the release profiles of the different therapeutic agents, surgeons will be able to choose the most appropriate biomaterial (blocks, grains, or powders) for their patients.

4. CDA as a vancomycin delivery system: results

4.1 Rationale

In this study, we evaluated whether CDA could be used as a local DDS for vancomycin. The antibacterial activities of CDA loaded with 10% vancomycin over 14 days, in the presence or absence of a standard systemic treatment of vancomycin, were assessed using an in vivo model of acute MRSA osteomyelitis (Amador et al., 2010; Gaudin et al., 2011).

4.2 Materials and methods

4.2.1 Animals

Female New Zealand rabbits (2.0 to 2.5 kg) used in this study were individually caged and had free access to water and food. Experiments were performed according to the Committee of Animal Ethics of the University of Nantes, France. Animals soon to be moribund (i.e., having difficulty accessing water and food associated with 10% weight loss per day for 2 days) were euthanatized by lethal injection of thiopental under general anesthesia. A fentanyl patch (Durogesic®, Janssen-Cilag Lab.) was used for pain management. Due to the delay of action (approximately 12 hours), the patch was placed on the animals the night before beginning the experiment (induction) and changed every 72 hours.

4.2.2 Bacterial strain

The MRSA strain used in this study was isolated from a blood culture and exhibited heterogeneous, low-level methicillin resistance (methicillin MIC=16 µg/mL). Molecular characterization showed this strain has a cassette chromosome *SCCmec* type IVa and agr-1 and was Panton-Valentine leukocidin toxin- and toxic shock syndrome toxin-negative. The MRSA vancomycin MIC was 2 µg/mL. Inocula (CFU per mL) were adjusted to 10^9 CFU/mL.

4.2.3 Bacterial counts

Bacterial counts were determined after 48 hours of incubation at 37°C on tryptic soy agar plates. To evaluate whether vancomycin treatment induced the selection of in vivo-resistant variants, undiluted sample homogenates were spread on agar plates containing 8 µg/mL vancomycin, 4-fold greater than the MIC.

4.2.4 DDS synthesis

The most efficient concentrations of antibiotics were previously determined by in vitro and in vivo analyses (Amador et al., 2010). Granules containing 10% vancomycin were prepared by wet granulation. The size of the granules was determined to be 200-500 µm, compatible with common handling human practice.

4.2.5 Vancomycin tissue measurements

Dosages of vancomycin in joint fluid, bone marrow, and spongy bone were realized at λ=214 nm by HPLC (ThermoFisher Spectra System SCM1000/P1000XR, with automatic syringe AS3000 and UV6000LP detectors and FL3000). The column was a C18RP (Hypersil GOLD, 150-mm length, 5 µm × 4.6 mm, ThermoFisher). The isocratic mobile phase was 12% acetonitrile in an ammonium acetate buffer adjusted to pH 6 by phosphoric acid. Experiments with every range and dosage were performed in triplicate.

4.2.6 Experimental design

Animals were randomly assigned to six groups: (1) vancomycin group $V_{(IV)}$ [vancomycin constant intravenous infusion to reach a 20× MIC serum steady-state concentration (CIV)] for 4 days; (2) $V_{(CDA10\%)}$ (CDA loaded with 100 µg/mg vancomycin) for 4 days or (3) for 14 days; (4) $V_{(IV)}$ for 4 days + $V_{(CDA10\%)}$ (CDA loaded with 100 µg/mg) for 4 days (5) or 14 days (6) for vancomycin tissue measurement.

We used a percutaneous, transarticular route to perform femoral trepanation using a Jamshidi bone marrow biopsy needle under general anesthesia. The Jamshidi needle was inserted between the two femoral condyles and through the epiphysis, physis, and metaphysis to reach the medullar canal. After the needle was removed, the skin incision was closed. Subsequently a 1-mL suspension containing 10^9 CFU MRSA was injected parapatellarly into the knee cavity. At day 3, osteomyelitis was induced, causing unbridling, and the infected site was washed as recommended in human practice. Samples of joint fluid, bone marrow, and spongy bone were removed for bacterial counts. At day 7 or 17 post-inoculation, animals were euthanized to measure the bacterial load in the joint fluid, bone marrow, and bone. Results were expressed as the bacterial counts (log_{10}/g of tissue) at day 3 (reference level) and either day 7 or 17. The lower limit of detection for this method was 1 CFU/50 µl undiluted tissue homogenate. Infusions of antibiotics began at day 3 and continued for only 4 days due to ethical reasons.

4.2.7 Statistical analysis

Statistical analyses were performed using Graphpad Prism® 4 for Windows (Graphpad Software, San Diego, CA, USA). Results were expressed as the means ± standard deviation. Regimens were compared using one-way analysis of variance. This analysis was performed using a post-hoc Student-Newman-Keuls test. Time-dependant efficacy was tested by a non-

parametric *t* test associated with a Wilcoxon post-test. *P* less than 0.05 was considered statistically significant.

4.3 Results and discussion

4.3.1 Vancomycin tissue measurements

Wysocki et al. (2001) demonstrate that CIV patients (targeted plateau drug serum concentrations of 20 to 25 mg/L) reached the targeted concentrations faster, and fewer samples were required for treatment monitoring than with intermittent infusion patients (IIV). For comparable efficacy and tolerance, CIV may be a cost-effective alternative to IIV. Samples of plasma, spongy bone, and bone marrow were analyzed for vancomycin by HPLC in healthy and infected femurs. Vancomycin concentrations were 7.50 ± 2.48 μg/g in bone marrow and 6.11 ± 3.18 μg/g in spongy bone in healthy tissues, associated with a vancomycin plasma level of 19.09 ± 3.79 μg/mL. For infected bone tissues, vancomycin concentrations were 6.70 ± 2.23 μg/g, 12.63 ± 5.16, and 22.63 ± 8.53 for bone marrow, spongy bone, and plasma, respectively, related to the vancomycin MCIs of the causative MRSA (2 μg/mL). The constant infusion of vancomycin exhibits more than three times the MICs of the studied strain in any compartment.

For the CDA loaded with 10% vancomycin group (without a systemic approach), samples were taken at the maximum local delivering time (24 hours): plasma for vancomycin dosage and bone marrow and spongy bone, near the CDA implants, to assess local tissue delivery. Vancomycin plasma levels were 3.36 ± 0.81 μg/mL, corresponding to a very weak elevation. Local bone tissue concentrations were more than 100 times and 150 times the vancomycin MICs for the MRSA strain for bone marrow and spongy bone, respectively. Surprisingly, the introduction of CDA loaded with 10% vancomycin did not significantly increase the plasma concentration obtained at steady-state by continuous infusion of vancomycin, reducing the risk of general toxicity. In contrast, the contribution of local antibiotic-loaded material appeared to be considerable.

4.3.2 Bacterial counts

No vancomycin-resistant mutants were detected after either 4 or 14 days of treatment in any group and in any compartment.

Data from the in vivo experiments are summarized in Table 5. Because infusion caused major venous time-dependent impairment, the efficacy of $V_{(IV)}$ could not be assessed over the full 14-day treatment period. Moreover, $V_{(IV)}$ did not demonstrate significant antibacterial activity in any of the three tissues (joint fluid, bone marrow, and spongy bone) after the 4-day treatment. Of the different treatments [$V_{(CDA10\%)}$ and $V_{(CDA10\%)}$ + $V_{(IV)}$], only treatment with CDA-vancomycin plus constant infusion of vancomycin [$V_{(CDA10\%)}$ + $V_{(IV)}$] showed a significant inhibitory effect in joint fluid, with $P<0.05$ after 14 days of treatment.

Treatment with 10% vancomycin-loaded CDA alone exhibited a greater activity than $V_{(IV)}$ alone ($P<0.01$), but combining these treatments significantly enhanced treatment efficacy ($P<0.001$). $V_{(CDA10\%)}$ did not exhibit greater efficacy after 14 days compared with 4 days. In spongy bone and bone marrow, most samples were sterile after 14 days of treatment with CDA-vancomycin plus intravenous vancomycin [$V_{(CDA10\%)}$ + $V_{(IV)}$], but none after $V_{(CDA10\%)}$.

Furthermore, the combined $V_{(CDA10\%)}$ + $V_{(IV)}$ treatment seemed to be the most effective. These data indicate the addition of a local delivery system enhanced the antibacterial effects of these drugs in a tissue-specific manner. One possible mechanism for the enhanced efficacy of the combined treatment is that the release of vancomycin loaded onto CDA is limited to the site of infection, with cortical bone acting as a semi-permeable membrane and preventing the elimination of vancomycin through the bloodstream.

		Means ±SD log10 CFU/g tissue								
Treatment regimens	n	day 3			day 7			day 17		
		JF	BM	Bo	JF	BM	Bo	JF	BM	Bo
$V_{(IV)}$	10	7.88 0.62	6.97 1.15	7.86 0.44	7.78 ± 0.75	6.38 ± 1.89	7.29 ± 0.80	ND	ND	ND
$V_{(CDA10\%)}$	21	7.86 0.55	8.47 0.80	8.11 0.05	7.81± 1.03	5.06 ± 1.43	5.76 ± 1.45	6.27 ± 2	4.80 ± 1.56 [a]	6.16 ± 1.36 [a]
$V_{(CDA10\%)}$ + $V_{(IV)}$	15	7.53 0.69	8.58 1.32	8.41 1.36	6.63 ± 0.39	4.55 ± 1.33 [a]	3.78 ± 1.28 [a]	2.52 ± 0.97* [a,b]	2.33 ± 0.34 * [a,b]	2.30 ± 0.09 * [a,b]

ND: not done n: number of animals [a] $P<0.05$ *vs* day 3 [b] $P<0.05$ *vs* $V_{(CDA10\%)}$ and $V_{(IV)}$
*under the lower limit of detection

Table 5. Bacterial counts in joint fluid (JF), bone marrow (BM), and spongy bone (Bo) at day 3 (post-inoculation) and 4 and 14 days after the beginning of the treatment.

5. Conclusion

Biomaterials as local DDS could reduce or eliminate the toxic side effects and complications of systemic antibiotic treatments, enhancing patient safety. From this perspective, the reference antibiotic against MRSA, vancomycin, was selected, and optimized concentrations were loaded into a CaP matrix (CDA) by wet granulation. The in vitro antibacterial activity of eluents from the DDS showed that the nature of the antibiotics was not altered either as a result of CDA loading or after sustained release from the granules. After a 14-day in vitro release, the CDA matrix was still able to deliver antibiotics at a concentration 50 times greater than the MIC of the MRSA strain used, providing local effective bactericidal concentrations of antibiotic and not inducing the development of antibiotic resistance from a slow residual release at suboptimal antibiotic concentrations. While more traditional antibiotic carrier systems are available, CDA has both desirable antibiotic release kinetics and a high osteogenic-promoting activity, including degradation of the apatite, obviating the need for a second surgery to remove the implanted material.

6. References

Amador, G., Gautier, H., Le Mabecque, V., Miegeville, A.F., Potel, G., Bouler, J.M., Weiss, P., Caillon, J. & Jacqueline, C. (2010). In vivo assessment of the antimicrobial activity of a calcium-deficient apatite vancomycin drug delivery system in a methicillin-resistant Staphylococcus aureus rabbit osteomyelitis experimental model. *Antimicrob Agents Chemother,* 54(2), pp. 950-952.

Anderson, J.M. & Miller K.M. (1984). Biomaterial biocompatibility and the macrophage. *Biomaterials*, 26, pp.1445-1451.

Andriole, V.T., Nagel, D.A. & Southwick, W.O. (1973). A paradigm for human chronic osteomyelitis. *J Bone Joint Surg Am*, 55, pp.1511-1515.

Aneja, A., Woodall, J., Wingerter, S., Tucci, M. &, Benghuzzi, H. (2008). Analysis of tobramycin release from beta tricalcium phosphate drug delivery system. *Biomed Sci Instrum*, 44, pp.88-93.

Bajpai, P.K. & Benghuzzi, H.A. (1988). Ceramic systems for long delivery of chemicals and biologicals. *J Biomed Mater Res*, 22, pp.1245-1266.

Bouler, J.M., Trecant, M., Delecrin, J., Royer, J., Passuti N. & Daculsi, G. (1996). Macroporous biphasic calcium phosphate ceramics: influence of five synthesis parameters on compressive strength. *J Biomed Mater Res*, 32, pp.603-609.

Brady, R.A., Leid, J.G., Calhoun, J.H., Costerton, J.W. & Shirtliff, M.E. (2008). Osteomyelitis and the role of biofilms in chronic infection. *FEMS Immunol Med Microbiol*, 52, pp.13-22.

Brouard, S., Lelan, J., Lancien, G., Bonnaure, M., Cormier, M. & Langlais, F. (1997). Phosphate tricalcique, vecteur d'antibiotiques : gentamicine et vancomycine. Caractérisation physicochimique *in vitro*, étude de la porosité du matériau et du relargage de la gentamicine et de la vancomycine. *Chirurgie*, 122, pp.397-403.

Calhoun, J.H. & Manring, M.M. (2005). Adult osteomyelitis. *Infect Dis Clin North Am.* 19(4), pp.765-786.

Calhoun, J.H., Manring, M.M. & Shirtliff, M. (2009). Osteomyelitis of the long bones. *Semin Plast Surg,*23(2), pp.59-72.

Campoccia, D., Montanaro, L., Speziale, P. & Arciola, C.R. (2010). Antibiotic-loaded biomaterials and the risks for the spread of antibiotic resistance following their prophylactic and therapeutic clinical use. *Biomaterials*, 25, pp.6363-6377.

Chow, L.C. (2009). Next generation calcium phosphate-based biomaterials. *Dent Mater J*, 1, pp. 1–10.

Cierny, G., Mader, J.T. & Pennick J.J. (1985). A clinical staging system for adult osteomyelitis. *Contemp Orthop,* 10, pp.17–37.

Crémieux, A.C., Dumitrescu, O., Lina, G., Vallee, C., Côté, J.F., Muffat-Joly, M., Lilin, T., Etienne, J., Vandenesch, F. & Saleh-Mghir, A. (2009). Panton-valentine leukocidin enhances the severity of community-associated methicillin-resistant *Staphylococcus aureus* rabbit osteomyelitis. *PLoS One*, 25, 4(9):e7204.

Cunha, B.A. (2002) Osteomyelitis in elderly patients. *Clin Infect Dis*, 35(3), pp.287-293.

Dacquet, V., Varlet, A., Tandogan, R.N., Tahon, M.M., Fournier, L., Jehl, F., Monteil, H. &, Bascoulergue, G. (1992). Antibiotic impregnated plaster of Paris beads - Trials with teicoplanin. *Clin Orthop*, 282, pp.241-249.

Daculsi, G., Bouler, J.M., LeGeros, R.Z. (1997). Adaptive crystal formation in normal and pathological calcifications in synthetic calcium phosphate and related biomaterials. *Int Rev Cytol*, 172, pp.129-191.

Daculsi, G., Weiss, P., Bouler, J.M., Gauthier, O., Millot, F. & Aguado E. (1999). Biphasic calcium phosphate/hydrosoluble polymer composites: a new concept for bone and dental substitution biomaterials. *Bone*, 25(2 Suppl), pp.59S-61S.

Deckers, M., van Bezooijen, R.L., van der Horst, G., Hoogendam, J., van Der Bent, C., Papapoulos, S.E. & Löwik, C.W. (2002). Bone morphogenetic proteins stimulate angiogenesis through osteoblast-derived vascular endothelial growth factor A. *Endocrinology*, 143(4), pp.1545-1553.

Deligianni, D.D., Katsala, N.D., Koutsoukos, P.G. & Missirlis, Y.F. (2001). Effect of surface roughness of hydroxyapatite on human bone marrow cell adhesion, proliferation, differentiation and detachment strength. *Biomaterials*, 22, pp.87-96.

Denissen, H., Van Beek, E., Löwik, C., Papapoulos, S. & van den Hooff, A. (1994). Ceramic hydroxyapatite implants for the release of bisphosphonate. *Bone Miner*, 25, pp.123-134.

Denissen, H., Van Beek, E., Martinetti, R., Klein, C., van der Zee, E. & Ravaglioli, A. (1997). Net-shaped hydroxyapatite implants for release of agents modulating periodontal-like tissues. *J Periodontal Res*, 32, pp.40-46.

Detsch, R., Mayr, H. & Ziegler, G. (2008). Formation of osteoclast-like cells on HA and TCP ceramics. Acta Biomater, 4, pp.139-148.

Deysine, M., Rosario, E. & Isenberg, H.D. (1976). Acute hematogenous osteomyelitis: an experimental model. *Surgery*, 79, pp.97-99.

Dirschl, D.R. & Almekinders, L.C. (1993). Osteomyelitis. Common causes and treatment recommendations. *Drugs*, 45, pp.29–43.

Downes, S., Clifford, C.J., Scotchford, C. & Klein C.P. (1995). Comparison of the release of growth hormone from hydroxyapatite, heat-treated hydroxyapatite, and fluorapatite coatings on titanium. *J Biomed Mater Res*, 29, pp.1053-1060.

Ducheyne, P. & Cuckler, J.M. (1992). Bioactive ceramic prosthetic coatings. *Clin Orthop Relat Res*, 276, pp.102-114.

European Pharmacopoea 7.1, Consil of Europe 2011.

Fitzgerald, R.H. (1983). Experimental osteomyelitis: description of a canine model and the role of depot administration of antibiotics in the prevention and treatment of sepsis. *J Bone Joint Surg Am*, 65, pp.371-380.

Fukushima, N., Yokoyama, K., Sasahara, T., Dobashi, Y. & Itoman, M. (2005). Establishment of rat model of acute staphylococcal osteomyelitis: relationship between inoculation dose and development of osteomyelitis. *Arch Orthop Trauma Surg*, 125, pp.169-176.

Gafur, O.A., Copley, L.A., Hollmig, S.T., Browne, R.H., Thornton, L.A. & Crawford, S.E. (2008). The impact of the current epidemiology of pediatric musculoskeletal infection on evaluation and treatment guidelines. *J Pediatr Orthop*, 28(7), pp.777-785.

Gaudin, A., Amador Del Valle, G., Hamel, A., Le Mabecque, V., Miegeville, A.F., Potel, G., Caillon, J. & Jacqueline, C. (2011). A new experimental model of acute osteomyelitis due to methicillin-resistant *Staphylococcus aureus* in rabbit. *Lett Appl Microbiol*, 52(3), pp.253-257.

Gautier, H., Guicheux, J., Grimandi, G., Faivre, A., Daculsi, G. & Merle, C. (1998). *In vitro* influence of apatite-granule-specific area on human growth hormone loading and release. *J Biomed Mater Res*, 40, pp.606-613.

Gautier, H., Caillon, J., Le Ray, A.M., Daculsi, G. & Merle, C. (2000a). Influence of isostatic compression on the stability of vancomycin loaded with a calcium-phosphate implantable drug-delivery device. *J Biomed Mater Res*, 52(2), pp.308-314.

Gautier, H., Merle, C., Auget, J.L. & Daculsi, G. (2000b). Isostatic compression, a new process for incorporating vancomycin into biphasic calcium phosphate: comparison with a classical method. *Biomaterials*, 21, pp.243-249.

Gautier, H., Plumecocq, A., Amador, G., Weiss, P., Merle, C. & Bouler J.M. (2010a). In vitro characterization of calcium phosphate biomaterial loaded with linezolid for osseous bone defect implantation. *J Biomater Appl*. Sep 28.

Gautier, H., Chamblain, V., Weiss, P., Merle, C. & Bouler, J.M. (2010b). In vitro characterisation of calcium phosphate biomaterials loaded with lidocaine hydrochloride and morphine hydrochloride. *J Mater Sci: Mater Med*, 21(12), pp. 3141-3150.

Gauthier, O., Bouler, J.M., Aguado, E., Pilet P. & Daculsi G. (1998). Macroporous biphasic calcium phosphate ceramics: influence of macropore diameter and macroporosity percentage on bone ingrowth. *Biomaterials*, 19: pp.133-139.

Goergens, E.D., McEvoy, A., Watson, M. &, Barrett, I.R. (2005). Acute osteomyelitis and septic arthritis in children. *J Paediatr Child Health*,41(1-2), pp.59-62.

Golomb, G., Levi, M., van Gelder, J.M. (1992). Controlled release of bisphosphonate from a biodegradable implant: evaluation of release kinetics and anticalcification effect. *J Appl Biomater*, 3, pp.23-28.

Goodwin, C.J., Braden, M., Downes, .S & Marshall, N.J. (1995). A comparison between two methacrylate cements as delivery system for bioactive human growth hormone. *J Mater Sci: Mater Med*, 6, pp.590-596.

Guicheux, J., Grimandi, G., Trécant, M., Faivre, A., Takahashi, S. & Daculsi, G. (1997). Apatite as carrier for growth hormone: i*n vitro* characterization of loading and release. *J Biomed Mater Res*, 34, pp.165-170.

Guicheux, J., Heymann, D., Rousselle, A.V.,, Gouin, F., Pilet, P., Yamada, S. & Daculsi, G. (1998). Growth hormone stimulatory effects on osteoclastic resorption are partly mediated by insulin-like growth factor I: an in vitro study. *Bone*, 22(1), pp.25-31.

Gutierrez, K. (2005). Bone and joint infections in children. *Pediatr Clin North Am,*52(3), pp.779-794.

Hamanishi, C., Kitamoto, K., Tanaka, S., Otsuka, M., Doi, Y. & Kitahashi, T. (1996). A self-setting TTCP-DCPD apatite cement for release of vancomycin. *J Biomed Mater Res A*, 33, pp.139-143.

Itokazu, M., Matsunaga, T., Kumazawa, S. & Oka, M. (1994a). Treatment of osteomyelitis by antibiotic impregnated porous hydroxyapatite block. *Clin Mater*, 17, pp.173-179.

Itokazu, M., Matsunaga, T., Kumazawa, S. & Wenyi, Y. (1995b). A novel drug delivery system for osteomyelitis using porous hydroxyapatite blocks loaded by centrifugation. *J Appl Biomater*, 6, pp.167-169.

Itokazu, M., Ohno, T., Tanemori, T., Wada, E., Kato, N. & Watanabe, K. (1997c). Antibiotic-loaded hydroxyapatite blocks in the treatment of experimental osteomyelitis in rats. *J Med Microbiol*, 46, pp.779-783.

Itokazu, M., Aoki, T., Nonomura, H., Nishimoto, Y. & Itoh, Y. (1998d). Antibiotic-loaded porous hydroxyapatite blocks for the treatment of osteomyelitis and postoperative infection. A preliminary report. *Bull Hosp Joint Dis*, 57(3), pp.125-129.

Itokazu, M., Sugiyama, T., Ohno, T., Wada, E. & Katagiri, Y. (1998e). Development of porous apatite ceramic for local delivery of chemotherapeutic agents. *J Biomed Mater Res*, 39, pp.536-538.

Itokazu, M., Yang, W., Aoki, T., Ohara, A. & Kato, N. (1998f). Synthesis of antiobiotic-loaded interporous hydroxyapatite blocks by vacuum method and *in vitro* drug release testing. *Biomaterials*, 19, pp.817-819.

Jarcho, M. (1981). Calcium phosphate ceramics as hard tissue prosthetics. *Clin Orthop Relat Res.* 157, pp.259-278.

Jorge, L.S., Chueire, A.G. & Rossit, A.R. (2010). Osteomyelitis: a current challenge. *Braz J Infect Dis,* 14(3), pp.310-315.

Joschek. S., Krote, R., Nies, B. & Göpferich, A. (1998). Porous ceramics for local drug delivery. *Proc 2nd World Meeting APGI/APV*, Paris:353-354.

Julien, M., Khairoun, I., LeGeros, R.Z., Delplace, S., Pilet, P., Weiss, P., Daculsi, G., Bouler, J.M. & Guicheux, J. (2007). Physico-chemical-mechanical and in vitro biological properties of calcium phosphate cements with doped amorphous calcium phosphates. *Biomaterials*, 28, pp.956-965.

Kaplan, S.L. (2009). Challenges in the evaluation and management of bone and joint infections and the role of new antibiotics for gram positive infections. *Adv Exp Med Biol*, 634, pp.111-120.

Kawanabe, K., Okada, Y., Matsusue, Y., Ida, H. & Nakamura, T. (1998). Treatment of osteomyelitis with antibiotic-soaked porous glass ceramic. *J Bone Joint Surg*, 80-B, pp.527-530.

Kim, I.Y., Kim, M.M. & Kim, S.J. (2005). Transforming growth factor-beta : biology and clinical relevance. *J Biochem Mol Biol*, 38(1), pp.1-8.

Kimakhe, S., Bohic, S., Larrose, C., Reynaud, A., Pilet, P., Giumelli, B., Heymann, D. & Daculsi, G. (1999). Biological activities of sustained polymyxin B release from calcium phosphate biomaterial prepared by dynamic compaction: An *in vitro* study. *J Biomed Mater Res*, 47, pp.18-27.

Kundu, B., Soundrapandian, C., Nandi, S.K., Mukherjee, P., Dandapat, N., Roy, S., Datta, B.K., Mandal, T.K., Basu, D. & Bhattacharya, R.N. (2010). Development of new localized drug delivery system based on ceftriaxone-sulbactam composite drug impregnated porous hydroxyapatite: a systematic approach for in vitro and in vivo animal trial. *Pharm Res,*27(8), pp.1659-1676.

Labbé, J.L., Peres, O., Leclair, O., Goulon, R., Scemama, P., Jourdel, F., Menager, C., Duparc, B. & Lacassin, F. (2010). Acute osteomyelitis in children: the pathogenesis revisited? *Orthop Traumatol Surg Res,* 96(3), pp.268-275.

Lazzarini, L., De Lalla, F. & Mader, J.T. (2002). Long bone osteomyelitis. *Curr Infect Dis Rep,* 4(5), pp.439–445.

Le Ray, A.M., Gautier, H., Bouler, J.M., Weiss, P. & Merle, C. (2010). A new technological procedure using sucrose as porogen compound to manufacture porous biphasic calcium phosphate ceramics of appropriate micro- and macrostructure. Ceramics International. 36(1), pp.93-101.

Lecomte, A., Gautier, H., Bouler, J.M., Gouyette, A., Pegon, Y., Daculsi, G. & Merle, C. (2008). Biphasic calcium phosphate: a comparative study of interconnected porosity in two ceramics. *J Biomed Mater Res B Appl Biomater*. 84(1), pp.1-6.

LeGeros, R.Z. (1991). Calcium phosphate in oral biology and medicine. *Monogr Oral Sci*, 15 pp.1-201.

LeGeros, R.Z.. (2002). Properties of osteoconductive biomaterials: calcium phosphates. *Clin Orthop*, 395, pp. 81-98.

Lew, D.P & Waldvogel, F.A. (1997). Osteomyelitis. *N Engl J Med,* 336, pp.999–1007.

Lu, J.X., Flautre, B., Anselme, K. & Hardouin, P. (1999). Role of interconnections in porous bioceramics on bone recolonization in vitro and in vivo. *J Mater Sci: Mater Med*, 10, pp.111-120.

Mader, J.T. (1985). Animal models of osteomyelitis. *Am J Med,* 78, pp.213-217.

Mader, J.T., Shirtliff, M. & Calhoun, J.H. (1997). Staging and staging application in osteomyelitis. *Clin Infect Dis*, 25(6), pp.1303-1309.

Matsuda, N., Lin, W.L., Kumar, N.M., Cho, M.I. & Genco, R.J. (1992). Mitogenic, chemotactic, and synthetic responses of rat periodontal ligament fibroblastic cells to polypeptide growth factors in vitro. *J Periodontol,* 63(6), pp.515-525.

Minkin, C. & Marinho, V.C. (1999). Role of the osteoclast at the bone-implant interface. *Adv Dent Res*,13, pp.49-56.

Misra, D.N. (1991). Adsorption and orientation of tetracycline on hydroxyapatite. *Calcif Tissue Int,* 48(5), pp.362-367.

Navarro, M., Michiardi, A., Castaño, O. & Planell, J.A. (2008). Biomaterials in orthopaedics. *J R Soc Interface*, 5(27), pp.1137-1158.

Nehme, A., Maalouf, G., Tricoire, J.L., Giordano, G., Chiron, P. & Puget, J. (2003). Effect of alendronate on periprosthetic bone loss after cemented primary total hip arthroplasty: a prospective randomized study. *Rev Chir Orthop Reparatrice Appar Mot*, 89(7), pp.593-8.

Nijhof, M.W., Dhert, W.J.A., Tilman, P.B.J., Verbaut, A.J. &, Fleer, A. (1997). Release of tobramycin from tobramycin-containing bone cement in bone and serum of rabbits. *J Mat Sci: Mater Med*, 8, pp.799-802.

Norden, C.W. (1988). Lessons learned from animal models of osteomyelitis. *Rev Infect Dis*,10, pp.103-110.

Ooms, E.M., Wolke, J.G., van de Heuvel, M.T., Jeschke, B. & Jansen J.A. (2003). Histological evaluation of the bone response to calcium phosphate cement implanted in cortical bone. *Biomaterials*, 24, pp.989-1000.

Ormos, Z.D. (1994). Granulation and coating. In: Williams JC, Allen T, advisory editors. Handbook of powder technology, volume 9, Powder technology and pharmaceutical processes. London, New York, Tokyo: Elsevier, pp.359-376.

Otsuka, M., Matsuda, Y., Suwa, Y., Fox, J.L. & Higuchi, W. (1994). A novel skeletal drug delivery system using self-setting calcium phosphate cement. 3: Physicochemical properties and drug release of bovin insulin and bovin albumin. *J Pharm Sci*, 83(2), pp.255-258.

Otsuka, M., Matsuda, Y., Fox, J.L. & Higuchi, W. (1995). A novel skeletal drug delivery system using self-setting calcium phosphate cement. 9: effects of the mixing solution volume on anticancer drug release from homogeneous drug-loaded cement. *J Pharm Sci*, 6, pp.733-736.

Parikh, S. (2002). Bone graft substitutes in modern orthopedics. *Orthopedics*, 2, pp. 1301-1310.

Passl, R., Muller, C., Zielinski, C.C. & Eibl, M.M. (1984). A model of experimental post-traumatic osteomyelitis in guinea pigs. *J Trauma*, 24, pp.323-326.

Patel, M., Rojavin, Y., Jamali, A.A., Wasielewski, S.J. & Salgado, C.J. (2009). Animal models for the study of osteomyelitis. *Semin Plast Surg,*23, pp.148-154.

Penner, M.J., Masri, B.A. & Ducan, C.P. (1996). Elution characteristics of vancomycin and tobramycin combined in acrylic bone cement. *J Arthroplasty*, 11(8), pp.939-944.

Prat-Poiret, N., Langlais, F., Bonnaure, M., Cormier, M. & Lancien, G. (1996). Phosphate tricalcique et gentamicine. Diffusion de l'antibiotique *in vitro* et *in vivo*, réhabitation en site osseux chez le mouton. *Chirurgie*, 121, pp.298-308.

Randelli, P., Evola, F.R., Cabitza, P., Polli, L., Denti, M. & Vlenti, L. (2010). Prophyllactic use of antibiotic-loaded bone cement in primary total knee replacement. *Knee Surg Sports Traumatol Arthrosc*, 18(2), pp. 181-186.

Ripamonti, U., Ma, S. & Reddi, A.H. (1992). The critical role of geometry of porous hydroxyapatite delivery system in induction of bone by osteogenin, a bone morphogenetic protein. *Matrix*, 12, pp.202-212.

Rissing, J.P. (1990). Animal models of osteomyelitis. Knowledge, hypothesis, and speculation. *Infect Dis Clin North Am,* 4, pp.377-390.

Rush SM. (2005). Bone graft substitute: osteologics. *Clin Podiatr Med Surg*, 22, pp.619-630.

Saavedra-Lozano, J., Mejías, A., Ahmad, N., Peromingo, E., Ardura, M.I., Guillen, S., Syed, A., Cavuoti, D. & Ramilo, O. (2008). Changing trends in acute osteomyelitis in children: impact of methicillin-resistant *Staphylococcus aureus* infections. *J Pediatr Orthop,* 28(5), pp.569-575.

Shinto, Y., Uchida, A., Korkusuz, F., Araki, N. & Ono, K. (1992). Calcium hydroxyapatite ceramic used as a delivery system for antibiotics. *J Bone Joint Surg*, 74-B, pp.600-604.

Specht, R. & Kühn, K. Palamed® and Palamed® G: new bone cements. *Proc 14th ESB Conference*, The Hague, The Netherlands 1998:169.

Sudo, A., Hasegawa, M., Fukuda, A. & Uchida, A. (2008). Treatment of infected hip arthroplasty with antibioticimpregnated calcium hydroxyapatite, *J Arthroplasty*, 23(1), pp.145-150.

Suzuki, Y., Tanihara, M., Nishimura, Y., Suzuki, K., Kakimaru, Y. & Shimizu, Y. (1998). A new drug delivery system with controlled release of antibiotic only in the presence of infection. *J Biomed Mater Res*, 42, pp.112-116.

Thomazeau, H. & Langlais, F. (1996). Relargage d'antibiotiques par implantation osseuse de phosphate tricalcique. *Chirurgie*, 121, pp.663-666.

Trécant, M., Daculsi, G. & Leroy, M. (1995). Dynamic compaction of calcium phosphate biomaterials. *J Mater Sci*, 6, pp.545-551.

Trécant, M., Guicheux, J., Grimandi, G., Leroy, M. & Daculsi, G. (1997). Dynamic compaction: a new process to compact therapeutic agent-loaded calcium phosphate. *Biomaterials*, 18, pp.141-145.

Vallet-Regi, M. (2006). Revisting ceramics form medical appilications. *Dalton Trans*, 28, pp.5211-5220.

Venesmaa, P.K., Kroger, H.P., Miettinen, H.J., Jurvelin, J.S., Suomalainen O.T. & Alhav, E.M. (2001). Alendronate reduces periprosthetic bone loss after uncemented primary total hip arthroplasty: a prospective randomized study. *J Bone Miner Res*, 11, pp.2126-2131.

Verron, E., Khairoun, I., Guicheux, J. & Bouler J.M. (2010). Calcium phosphate biomaterials as bone drug delivery systems: a review. *Drug Discov Today.* 15(13-14, pp.547-52.

Waldvogel, F.A, Medoff, G. & Swartz, M.N. (1970). Osteomyelitis: a review of clinical features, therapeutic considerations and unusual aspects. 3. Osteomyelitis associated with vascular insufficiency. *N Engl J Med,*282(6), pp.316-322.

Weichert, S., Sharland, M., Clarke, N.M. & Faust, S.N. (2008). Acute haematogenous osteomyelitis in children: is there any evidence for how long we should treat? *Curr Opin Infect Dis,*21(3), pp.258-262.

Williams, D.F. (2008). On the mechanisms of biocompatibility. *Biomaterials*, 29(20), pp.2941-2953.

Williams, D.F. (2009). On the nature of biomaterials. *Biomaterials*, 30(30), pp. 5897-5909.

Wu, H., Zheng, O., Du, J., Yan, Y. & Liu, C. (1997). A new drug delivery system-ciprofloxacine/tricalcium phosphate delivery capsule (CTDC) and its in vitro drug release patern. *J Tongji Med Univ*, 17(3), pp.160-164.

Wysocki, M., Delatour, F., Faurisson, F., Rauss, A., Pean, Y., Misset, B., Thomas, F., Timsit, J.F., Similowski, T., Mentec, H., Mier, L. & Dreyfuss, D. (2001). Continuous versus intermittent infusion of vancomycin in severe Staphylococcal infections: prospective multicenter randomized study. *Antimicrob Agents Chemother*, 45(9), pp. 2460-2467.

Yin, L.Y., Lazzarini, L., Li, F., Stevens, C.M. & Calhoun, J.H. (2005). Comparative evaluation of tigecycline and vancomycin, with and without rifampicin, in the treatment of methicillin-resistant *Staphylococcus aureus* experimental osteomyelitis in a rabbit model. *J Antimicrob Chemother,*55, pp.995-1002.

Yoshii, T., Nishimura, H., Yoshikawa, T., Furudoi, S., Yoshioka, A., Takenono, I., Ohtsuka, Y. & Komori, T. (2001). Therapeutic possibilities of long-term roxithromycin treatment for chronic diffuse sclerosing osteomyelitis of the mandible. *J Antimicrob Chemother*, 47, pp.631-637.

Yu, D., Wong, J., Matsuda, Y., Fox, J.L., Higuchi, W. & Otsuka, M. (1992). Self-setting hydroxyapatite cement: a novel skeletal drug delivery system for antibiotics. *J Pharm Sci*, 81(6), pp. 529-531.

Zerbo, R., Bronckers, A.L., de Lange G. & Burger, E.H. (2005). Localisation of osteogenic and osteoclastic cells in porous beta-tricalcium phosphate particles used for human maxillary sinus floor elevation. *Biomaterials*, 26, pp.1445-1451.

10

Nanocrystalline Diamond Films: Applications and Advances in Nanomedicine

Ying-Chieh Chen[1,2], Don-Ching Lee[1] and Ing-Ming Chiu[1,3,4*]
[1]*Institute of Cellular and System Medicine, National Health Research Institutes, Miaoli,*
[2]*Center for Biomedical Engineering, Department of Medicine,*
Brigham and Women's Hospital, Harvard Medical School, Boston,
[3]*Department of Life Sciences, National Chung Hsing University, Taichung*
[4]*Department of Internal Medicine, The Ohio State University, Columbus*
[1,3]*Taiwan*
[2,4]*USA*

1. Introduction

Biomaterials play essential roles in modern strategies in regenerative medicine and tissue engineering by designable biophysical and biochemical cues that direct cellular behavior and function [1-4]. The guidance provided by biomaterials may improve restoration and function of damaged or nonfunctional tissues both in cell-based therapies, such as those where carriers deliver transplanted cells or matrices induce morphogenesis in bioengineered tissues constructed *ex vivo*, and in cellular therapies, such as those where materials induce growth and differentiation of cells from healthy residual tissues *in situ* [3, 5-7].

Stem cells are defined by their ability to self-renew and produce specialized progeny [8, 9]. Consequently, they are the most versatile and promising cell source for the regeneration of aged, injured and diseased tissues. According to their developmental status, stem cells can be classified into two categories: embryonic stem cells and adult stem cells. However, despite the remarkable potential clinical applications of each of these stem-cell populations, their use is currently limited. Thus, a major goal is to develop new culture based approaches, using advanced biomaterials, that more closely mimic what the body already does so well, to promote differentiation of pluripotent cells [3].

Nanomedicine, the application of nanotechnology for medical purpose, is emerging as a new interdisciplinary research field, cutting across biology, chemistry, engineering and medicine. It is expected to lead major advances in disease detection, diagnosis, treatment and further to replacement of damaged tissues and organs. Over the past two decades, there have been significant advances in disease diagnostics, drug delivery, stem cell therapy and tissue engineering. In parallel, nanotechnology has shown great potential for the creation of the next generation of new biomaterials.

Biomaterials that promote regeneration are important in both research and clinical applications [10]. However, current implants have a limited life-expectancy, and younger patients who receive them generally expect to endure revision surgeries to replace worn components. A primary problem with current designs is the generation of wear debris

particles at the articulating surface that causes local pain and inflammation. Large debris are normally sequestered by fibrous tissue, while small debris are taken up by macrophages and multinucleated giant cells which may release cytokines that result in inflammation. Thus, the proposed solution for the problem caused by wear debris is to develop durable materials for the articulating surfaces that are more wear resistant, which would reduce the generation of debris particles.

Recently, it was shown that diamond particles (NDs), the diamond structure at a nanometer scale (4-5 nm in size), appear to possess high bioactivity at the molecular level, presenting antioxidant and anticarcinogenic properties. Functionalization of NDs with biological molecules, such as peptides, proteins and nucleic acid, has led to practical significance for biomedical applications, covering their use for single particle imaging in cells, drug delivery and protein separation. For instance, carboxylated nanodiamond has been shown as a useful probe for detecting and labeling the interaction of nanoparticles and bio-objects such as cells and bacteria [11], because NDs can be easily functionalized to conjugate with bio-molecules and can emit bright fluorescence without photobleaching [12-15]. Moreover, the ND particles were phagocytosed into cells by macropinocytosis and clathrin-mediated endocytosis pathways during tracking of cells. However, cell growth ability such as cell division and differentiation were not altered after long-term cell culture for 10 days. Together, NDs are non-cytotoxic and with bright fluorescence, thus has served as a versatile tool in biosensing and bioimaging applications [12, 16].

Diamond has been one of the most desired and investigated materials in the past years. From an extensive list of superlative properties, the ultra-hardness, the chemical inertness, the high thermal conductivity, and the high optical transparency are just a few examples of its remarkable nature. Applications such as cutting tools, abrasives, structural components, heat sinks, bearings, and optical windows (X-ray, IR, and laser windows) are examples that diamond has a wide-ranging impact in many fields.

2. Nanodiamond films

In the late 1980s, polycrystalline diamond films with fine grains were grown for optical coatings [17, 18], wear resistant coatings [19], high-pressure synchrotron X-ray windows [20] and X-ray lithography masks [21]. The first reference to these materials as 'nanocrystalline' was at the Workshop on the Science and Technology of Diamond Films in 1990 [17]. Most of these materials would now be classified as forms of nanocrystalline diamond (NCD) and further characterized the presence of large intrinsic stress and non-diamond phases in these material [22-25]. These NCD materials were all grown in hydrogen-rich chemical vapour deposition (CVD) environments, with typically less than 2% methane (or hydrocarbon) in hydrogen as reactants, exhibiting clusters (cauliflower morphologies), limited surface smoothness, high compressive stress, delamination, and high content of non-diamond phase. NCD was deposited on Si or other substrates which had been 'treated' or 'seeded' to increase the diamond nucleation density [26, 27]. This wet seeding process was in solution containing diamond powder for ultrasonication to create necessary nucleation sites and the process was varied among labs and individuals [28, 29]. By controlling nucleation density and growth conditions, grain sizes were usually 5–150 nm for films less than several μm thick. In 1994, Gruen and coworkers [30-32] developed the growth of nanocrystalline diamond films by CVD under hydrogen-poor and carbon-containing argon gas plasmas conditions. In 1999 [33], this new material was reviewed under the label of 'Nanocrystalline

Diamond Films'. In 2001 [34], the label ultra-nanocrystalline diamond films (UNCD) came to be applied to these materials in order to distinguish them from the more traditional NCD films discussed above [35]. The nanocrystallinity is the result of new growth and nucleation mechanisms, which involve the insertion of C_2, carbon dimer, into carbon-carbon and carbon-hydrogen bonds, resulting in heterogeneous nucleation rates on the order 10^{10} cm^2 s^{-1} [26, 29]. Detailed investigations using synchrotron-based, near-edge X-ray absorption fine-structure spectroscopy (NEXAFS) showed that UNCD films grown using this seeding approach and growth chemistry are of very high quality, with greater than 99% sp^3 bonding [33]. The UNCD films, a form of NCD, has led to applications in micro-electromechanical systems (MEMS) and nano-electromechanical systems (NEMS) [36-38], corrosion resistance [39], biocompatible coatings [40-42], and biosensors [16, 43, 44].

Diamond coatings with nanosized crystallites, NCD, present a great potential in biomedicine and biotechnology. NCD combines surface smoothness with high corrosion resistance and biotolerance, which are ideal features for applications in medicine onto surgical tools and medical implants. For example, joint implants coated with NCD can take benefit of its protective character. The NCD coating acts as a selective protective barrier between the implant and the human environment, preventing the release of metallic ions into the body. NCD presents the highest resistance to bacterial colonization when compared to medical steel and titanium [45]. This property is very important since infection due to microbial colonization of the implant surface may lead to implant rejection. In addition, the high wear resistance and the low coefficient of friction of NCD allow the reduction of the amount of wear debris generated during the joint functioning, thus increasing the life of the prosthesis [46]. Further, the residues formed due to wear in this case are diamond particles, which are completely harmless, initiating little or no adverse reactions from human monocytes and polymorphonuclear leukocytes [47-49]. NCD is also included in this recent group of materials and can be used as a template for the immobilization of active molecules for biological applications or for biosensor applications [44, 50-52]. One example is the functionalization of NCD surface with bone morphogenetic protein-2 (BMP-2) creating a biomimetic coating that results in improved osseointegration, which is a powerful strategy in tissue engineering as well as in bone tissue regeneration [53]. The NCD surface can also be modified with the linking of antibody, human IgG, which provide biomolecular recognition capability and specificity characteristics, proving a biologically sensitive field-effect transistor (Bio-FET) [44].

This paper offers a review of present knowledge of the synthesis and characterization, cell behavior, focused on *in vitro* adhesion, proliferation and differentiation on nanodiamond films. The aim is to highlight nanodiamond films as new generation biomaterials for improving the future development on clinical transplantation and tissue engineering.

3. Surface modifications

Cellular adhesion is of fundamental importance in many biological processes as the adhered cells will sense, interpret, integrate, and then respond to the extracellular signals. Chemical and physical signals from the substrate such as surface energy, topography, electrostatic charge, and wettability play a vital role in stimulating cell adhesion and influencing cell growth behavior. The cellular adhesion properties of as-grown diamond surfaces or functionalized diamond surfaces have been studied recently. The as-grown diamond films were characterized as hydrophobic surfaces with abundance of C-C and C-H bonds [54].

The functionalized surface properties of diamond can be made hydrophobic or hydrophilic with hydrogen or oxygen termination, respectively, which have implications for cellular adhesion. The methods of surface modifications are summarized as following:

1. Hydrogen termination (hydrophobic surface):
2. Diamond films were treated in pure hydrogen plasma treatment at 300-800 W in the microwave plasma CVD system at 5 mTorr for 2-15 min. All freshly prepared hydrogen-terminated diamond samples were used immediately for cell culture.[55-58]
3. Oxygen termination (hydrophilic surface):
    a. Diamond samples were exposed to UV irradiation (18 W, 254 nm) for 18 h in air. After UV functionalization, the samples were rinsed with ultrapure water, tetrahydrofuran, and finally with hexane.[55]
    b. Diamond films were exposed to pure oxygen plasma CVD system at 800 W at 5 mTorr for 10-15 min.[56, 58]
    c. Diamond films were oxidized in concentrated HNO_3 at 60-70° C for 24 hours. This oxidation reaction transformed the face of the film from hydrophobic to hydrophilic surface by adding carboxylate groups to the films. [59, 60]
4. Bio-molecular conjugation [61-64]

4. Nanodiamond-cell interaction: biological performance and response

Cell adhesion is involved in various natural phenomena such as embryogenesis, maintenance of tissue structure, wound healing, immune response, and tissue integration of biomaterial. The biocompatibility of biomaterials is very closely related to cell behavior on contact with them and particularly to cell adhesion to their surface. Surface characteristics of materials, such as their topography, chemistry, or surface energy, play an essential part in cell adhesion on biomaterials. Thus attachment, adhesion and spreading belong to the first phase of cell/material interactions and the quality of this phase will influence the cell's capacity to proliferate or to differentiate itself on contact with the implant. Material/cell interaction depends on the surface aspects of materials which may be described according to their wettability, topography, chemistry and surface energy. These surface characteristics determine how and what kinds of biological molecules will adhere to the surface and more particularly determine the orientation of adhered molecules, and also finally determine the cell behavior while in contact [3, 8, 65]. As previously shown, cells in contact with a surface will firstly attach, adhere and then spread. This first phase depends on specific adhesion proteins such as integrin and cadherin as demonstrated by Chen et al [66]. Thereafter, the quality of this adhesion will influence their morphology, and their capacity for proliferation and differentiation. Early *in vitro* biocompatibility and cytocompatibility studies focused on the morphology and growth capacity of cells on nanodiamond films with various chemical compositions and topographies [15, 53, 56, 58, 67, 68]. Recently, it was found that nanodiamond films further determine the differentiating stage in stem cells, which expands other possibilities for nanodiamond films into organ repair and tissue engineering.

4.1 Biocompatibility tests: morphological aspect and growth capacity of cells on nanodiamond films

NCD films possess numerous valuable physical, chemical and mechanical properties, making NCD an excellent material for implantable biomedical devices. There is still one

very important property required for biomaterials, i.e., biocompatibility. The biocompatibility of a material is determined by *in vitro* and *in vivo* tests, involving the interaction of the material with cells.

In vitro studies of biocompatibility of UNCD coatings, produced by MPECVD using Ar/CH_4 as reactive gas, were carried out by Shi et al. [69]. They grew mouse embryonic fibroblasts (MEFs) on UNCD films up to 4 days and found that UNCD film coated substrates can dramatically promote the growth of MEFs, while the quartz substrates inhibit cell attachment. On growing human cervical carcinoma cell line (HeLa), neuronal cell line (PC12) and osteoblastic cells (MC3T3) on UNCD films, no toxicological effects on the cells in culture were observed. It was noted that maximum cell attachment, cell spreading and nuclear coverage were observed on UNCD films compared to two commonly used materials in MEMS platinum and silicon substrates [70]. Amaral et al performed bone marrow cell culture tests on NCD films, prepared by using a hot-filament chemical vapor deposition (HFCVD) technique in $Ar\text{-}CH_4\text{-}H_2$ gas mixtures, to observe its effects on cellular reaction, osteoblast, and osteoblast activity [71]. The nanometric feature of NCD resulted in increased bone cell proliferation and minimized activity of osteoclast-like cells. Following previous study, Amaral and coworkers cultured primary human gingival fibroblast cell cultures on NCD films for 21 days and no damage to the cells was observed. On performing the cytotoxicity tests using a standard cell line, it was found out that NCD films promotes cell attachment and normal cell growth rates [72]. Several other studies were made on the morphological behavior of mesenchymal stem cells on NCD coating prepared by MPECVD method in hydrogen-rich gas mixtures, which revealed good surface biocompatibility of the coatings [58] . Their investigations indicated that NCD coatings were biocompatible to not only cell lines, but also primary stem cells.

All these *in vitro* studies showed that NCD films tended to promote the growth and adhesion of cells without any toxicological effect. There are other applications where it is desirable that there should not be any cell attachment to a surface, for example, in case of catheters and temporary implants. After getting a primary indication of the biocompatibility of NCD films through *in vitro* tests, several *in vivo* studies were initiated by implants with NCD coating in laboratory animals. An attempt was made to study the osseous healing at the implant sites by inserting implants into 4-year-old female sheep calvaria for 3 days, 1 week and 4 weeks intervals. It was observed that implant surfaces coating with NCD films and then conjugating with BMP-2 enhanced osseointegration *in vivo*. After implanting NCD coated implants in transplantation sites of sheep for different time periods, it has been observed that the NCD-coated implants did not show any significant toxicological effect and are well tolerated in the sheep body. Results further suggest that this technical advancement can be readily applied in clinical therapies with regard to bone healing, since primary human mesenchymal stromal cells strongly activated the expression of osteogenic markers when being cultivated on NCD absorbed with physiological amounts of BMP-2 [73].

The above *in vitro* and *in vivo* studies indicated the biocompatibility of NCD films prepared by a variety of techniques. The general finding so far is that control of cell adhesion and proliferation on NCD can be achieved by altering NCD surface chemistry and surface topography and wettability, probably due to the correlation between these surface properties and the adsorption of endogenous proteins that regulate cell behavior. Adsorbed proteins can be detected on biomaterials within seconds of exposure to the blood, and a monolayer of adsorbed proteins forms in seconds to minutes. Fibronectin, vitronectin and laminin are pro-adhesive proteins, with relatively high concentration in blood, that are

recognized by various cellular integrin receptors [74]. It has been observed that fibronectin governs the adhesion and spreading of cells on a material surface [75]. These plasma proteins play an important role in the initial recruitment of cells to the biomaterial surface. The glycoprotein fibronectin consists of multiple specific binding sites and is capable of interacting with a wide variety of other biomaterials, through the formation of fibrilar extracellular matrix or fibrils. So, the specific surface of a biomaterial plays a key role in adsorption of fibronectin or other pro-adhesive proteins and hence better proliferation of cells. The interaction of neural stem cells with UNCD films and the consequent cellular signaling processes are schematized in Figure 1. Some studies revealed that the adhesion and spreading of cells on NCD surfaces is related to the bonding structure present on the surface and the ratio of sp^2/sp^3 [76]. It has also been observed that the microstructure of the NCD films and the kind of treatments seemed to influence the biological effects of cells. However, the correlation between these surface properties (chemistry, topography and wettability) and cell responses is complicated and not clearly understood.

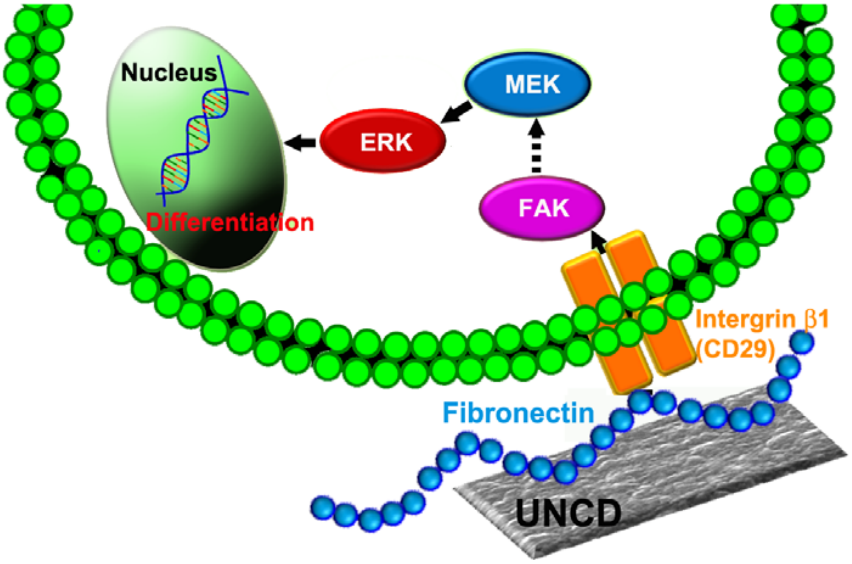

Fig. 1. Schematic drawing summarizes the role of H-UNCD films in mediating differentiation from neural stem cells. Absorbed fibronectin on H-UNCD surface activates integrin β1 (CD29), focal adhesion kinase (FAK) and (extracellular signaling kinase) ERK1/2 pathways and, in turn, leads to an ultimate and specification of neuronal differentiation from NSC.

4.2 Topography effects of nanodiamond films on cells

The comparison of the behavior of different cell types on nanodiamond films shows that they react differently according to surface smoothness [55, 57, 60, 68, 77, 78]. Scanning electron microscopy (SEM) and immunofluorescence staining examinations of osteoblast on nanodiamond films with various surface roughness (nanometer and micrometer) generally demonstrated that enhanced osteoblast functions (including adhesion, proliferation,

intracellular protein synthesis, alkaline phosphatase activity and extracellular calcium deposition) on nanocrystalline diamond (RMS~20 nm) compared to submicron diamond grain size films and control for all time periods tested up to 21 days [57, 60]. In addition, an SEM study of osteoblast attachment on NCD films explains the topographical impact diamond had on osteoblast functions by showing complex and longer filopodia extensions.
To investigate the adhesion of normal human dermal fibroblast cells grown on NCD films with various surface smoothnesses, atomic force microscopy were performed. The examination demonstrated that cell viability and adhesion force was better on smooth surfaces (UNCD films) compared to micron diamond grain size films, no matter the terminations of diamond films [55]. Although mesenchymal stem cells and non-differentiated cells adhere similarly on all NCD surfaces with different roughness (20, 270, and 500 nm) and control polystyrene, their metabolic activity on NCD surfaces is increased. On the other hand, osteoblasts adhere on NCD significantly more than on polystyrene, and their metabolic activity is decreased on nano/microrough NCD surfaces in contrast to mesenchymal stem cells. These differences could be attributed to the distinct properties of the two cell types in the human body. Alternatively, the different response of osteoblasts could be attributed to the specific surface topography as well as to the biocompatible properties of diamond. [79]. Hence the controlled topographically structured NCD coatings on various substrates is promising for preparation of better implants, which offer faster colonization by specific cells as well as longer-term stability.

4.3 Surface chemistry effects of nanodiamond films on cells

The bio-compatibility and resistance to chemical corrosion of diamond may increase lifetime of stents, joints, and other implants in the human body. It is also possible to make a chemical functionalization of diamond surface and create bio-passive or bio-active patterns. Kalbacova et al [80] showed that viability and adhesion of human osteoblasts (SAOS-2) cultured on NCD films are predominantly determined by NCD surface termination. Increasing surface nano-roughness plays a secondary yet positive role. Hydrophilic surface of NCD films (O-terminated surface) provides good conditions for osteoblast adhesion and spreading and consequently on their viability (metabolic activity and proliferation). It was shown that hydrophobic H-terminated diamond surfaces are less favorable for osteoblast-like cell adhesion and growth than hydrophilic O-terminated surfaces [80, 81]. This is in agreement with observations on other materials and cells, such as Ti6Al4V titanium alloy [82, 83] and human dermal fibroblast [55]. In addition to cells lines, different kinds of stem cells have also been studied and the results show difference on cell lines and stem cells. Chen et al [56] cultured neural stem cells on different functionalized diamond films in low serum and without any differentiation factors to investigate the biological effects on NSCs. We found that H-terminated UNCD films spontaneously induced cell proliferation and neuronal differentiation and O-terminated UNCD films were also shown to further improve neural differentiation, with a preference to differentiate into oligodendrocytes. Clem [58] reported that H-terminated ultra-smooth nanostructured diamond surfaces supported robust adhesion and survival of mesenchymal stem cells, while oxygen (O)- and fluorine (F)-terminated surfaces resisted cell adhesion. Thalhammer [84] used four different materials (glass, PCD, NCD and Si) coated with monolayers nanodiamonds and displayed promising similarity to the protein-coated materials regarding neuronal cell attachment,

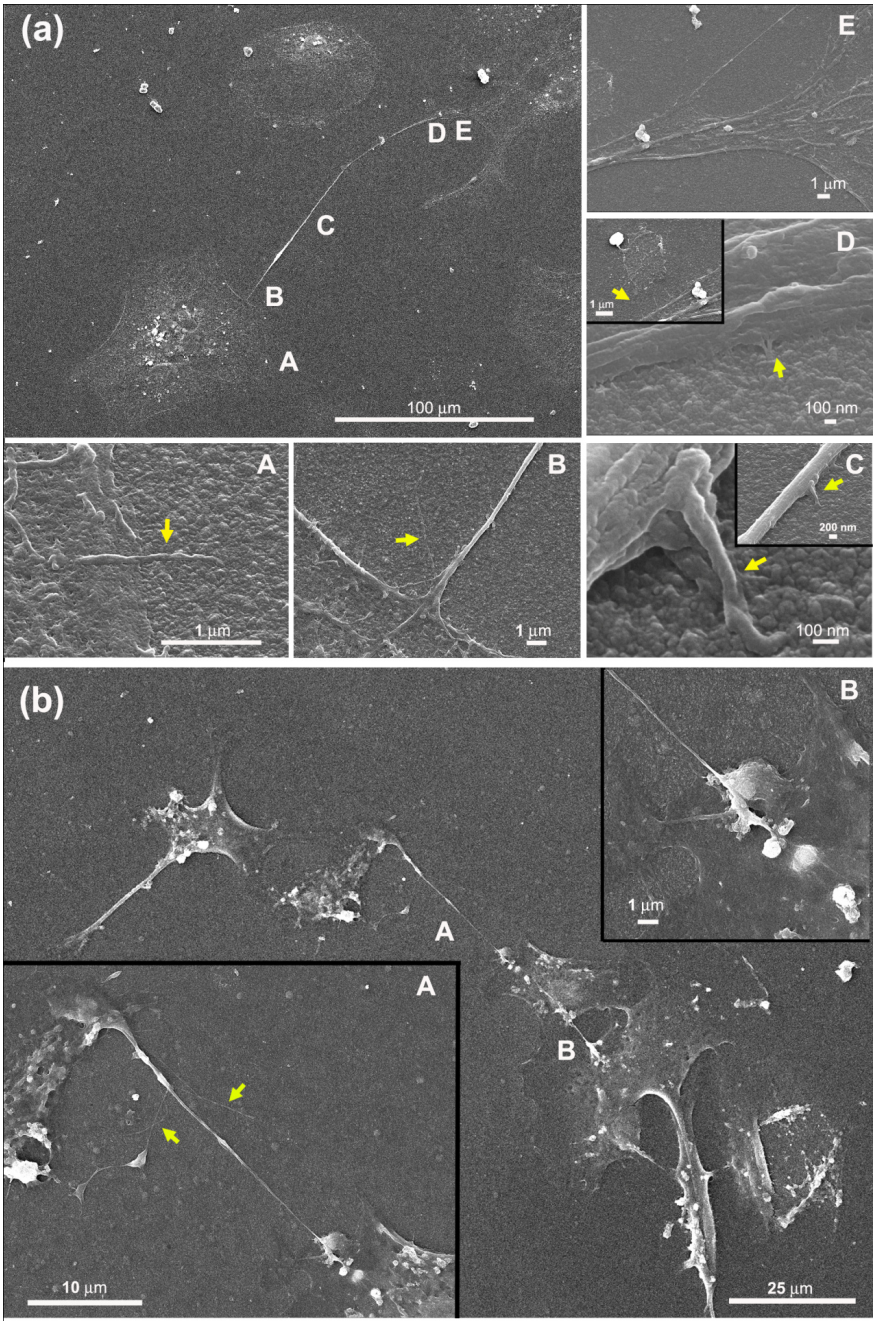

Fig. 2. Scanning electron photomicrographs of neural stem cells cultured on H-UNCD films in regular medium without any differentiating reagents for seven days. Higher

magnification scanning electron microscopy was performed to enlarge different areas (A-E) in graph (a) and (A-B) in graph (b). Yellow arrows show the filopodia at higher magnifications.

neurite outgrowth and functional network formation. Importantly, the neurons were able to grow in direct contact with the NCD-coated material and could be easily maintained in culture for an extended period, equal to those on protein-coated substrates. To further investigate the interaction of cell to NCD film, Chen et al observed the morphology of cells cultured in H-terminated UNCD films and revealed that there were filopodia/nano-diamond interactions (Figure 2). Thus, NCD layering might prove a valuable material for implants on a wide range of substrates. These indicate that diamond films can be easily modified to either promote or prevent cell/biomaterial interactions. This is an interesting feature for tissue engineering and bio-electronics. A question remained though to what kinds of mechanism and key points to affect the degree of the cell adhesion and selectivity.

5. Molecular mechanisms of signaling transduction from UNCD films to nuclei

Cells do not interact with a naked material either *in vitro* or *in vivo*. At the beginning step, the material is conditioned by the biological fluid components. This is a complex process strongly dependent on the cell culture conditions including the underlying substrate and mediating medium/proteins. Surface energy may influence protein adsorption and the structural rearrangement of the proteins on positively and negatively charged substrates (hydrophilic/hydrophobic surface). Protein from serum containing media adsorbed on surfaces forming multiple molecular layers. Hydrophobic H-terminated surfaces were found less favorable for osteoblastic cell adhesion, spreading and viability than hydrophilic O-terminated surfaces [5]. Recently, it was shown that microscopic (30–200 μm) patterns of H- and O-terminated surface can lead to a selective adhesion and arrangement of osteoblasts [85]. This effect also works on human periodontal ligament fibroblast and human cervical carcinoma (HeLa) cells [85-87]. The differential adsorption of "serum proteins" on the negative or positive charged regions from medium with fetal bovine serum (FBS) was studied. It was proposed that the selectivity is due to the serum proteins, which are adsorbed in about the same monolayer thickness (2–4 nm) on both H and O-diamond surfaces, but in different composition and conformations of proteins [88]. When osteoblasts were placed on the diamond surface in McCoy's 5A medium without FBS, cell attachment on H/O-patterned diamond surfaces was not selective [85, 89]. This excluded a direct effect of diamond C-H and C-O surface dipoles on the cell selectivity. FBS adsorption to diamond proceeds in two stages. Formation of monolayer thickness (2-4 nm) FBS layer on both H- and O-diamond was observed within short period of time (<18 h) [86, 88]. AFM nanoshaving showed that this primary FBS layer is less adhesive to H-diamond than to O-diamond. After long time adsorption (6 days), formation of a thick FBS layer was observed on H-diamond (~35 nm) than on O-diamond (~17 nm) [86]. Moreover, it is clear that not only the nature of adsorbed biological molecules but also their conformation and composition will influence consequent cell adhesion. Changes in conformation of pre-adsorbed specific proteins, fibronectin, (not bovine serum albumin or vitronectin, which is abundant in FBS) were observed. These would affected cell binding domain conformations and then affect the affinity with its cell surface receptor [58, 86].

Osteoblast adhesion on materials may also be considered in relation to the expression of the various adhesion proteins and cell receptors. Numerous studies using immunefluorescent staining have shown the presence of vinculin and pY397 focal adhesion kinase (FAK) in cultured human osteoblasts on nanostructured diamond films [60, 78, 79]. The osteoblasts adhered on ultra nano-cones and nano-cones, showing large focal adhesions and relatively strong activation of FAK, are thus more predestined for successful colonization of the entire environment [60, 78]. Hamilton [90] suggested that osteoblast response to substrates with specific topographical features requires FAK-Y397-Src-Y416 complexes for ERK1/2 phosphorylation. Yet on smooth surfaces, Src-independent routes of ERK1/2 activation are present, which finally induce the differentiation of osteoblast further to promote bone formation. The same cell signaling pathway has been studied on other materials, such as titanium alloys [83]. According to published data, the contact of cell to fibronectin could be

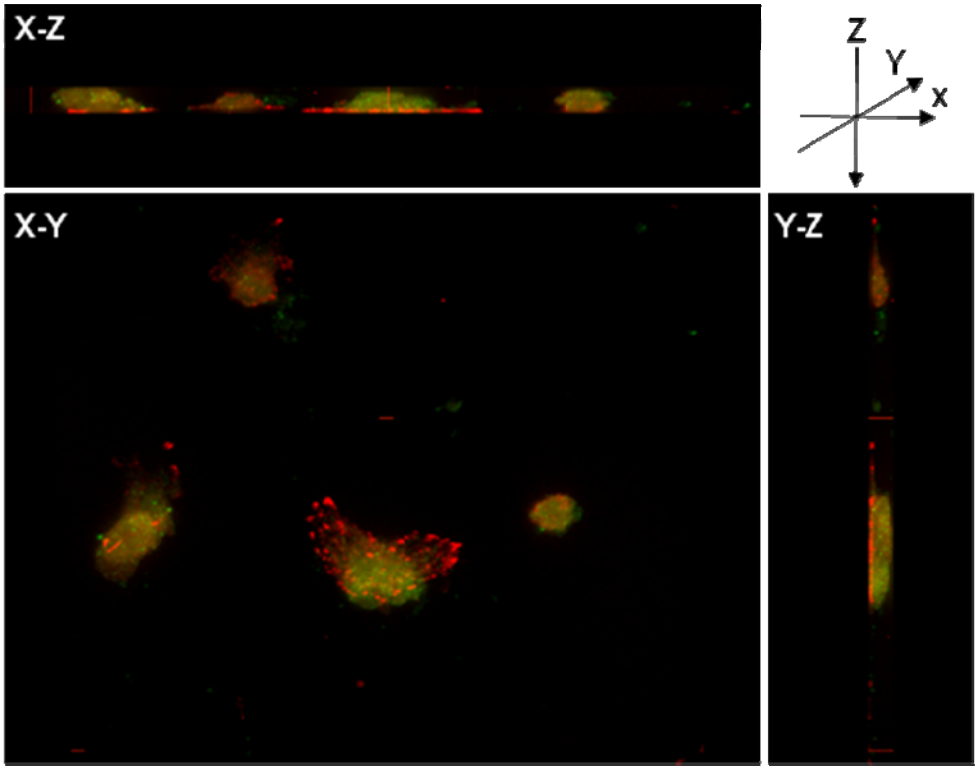

Fig. 3. The confocal immunofluorescence image of neural stem cells grown on the H-UNCD film in the regular medium without any differentiating reagents for 8 hours of culture. Alexafluor 594 labeled phospho-FAK (Red) and DyLight 488 labeled phospho-ERK (Green). The phospho-FAK and phospho-ERK were detected in the cells simultaneously and localized to their proper subcellular positions. In the quadrant of X-Z and Y-Z stacking images, phospho-FAK was observed in basal cell membrane adherent to H-UNCD films, while phosphor-ERK was shown assembled in the cell body.

mediated by integrin β1 [91, 92]. Integrins are transmembrane protein family and composed of α and β subunits as heterodimer. Functions of integrins were involved in the regulation of proliferation, survival, migration and differentiation. The high level of integrin β1 expression has been used to enrich human epidermal and rodent neural stem cells from more restricted progenitor populations [58, 92]. Moreover, Chen et al [66] showed that increased levels of neuronal differentiation in neural stem cells grown on H-UNCD surfaces are due to absorbance of fibronectin from medium to H-terminated UNCD films, resulting in integrin β1-FAK-ERK1/2 signaling (Figure 3) in conditions of low serum-growth factors and free of differentiating reagents.

Number	Function	gi number	Name
1	Extracellular matrix	224863	Fibronectin
2	Blood	78099200	Hemoglobin subunit epsilon
3		126022898	Hemoglobin alpha subunit 1
4		203283896	Apolipoprotein A-I preproprotein
5		3915607	Apolipoprotein A-I
6		77735387	Fetuin B
7		166159174	Angiotensinogen (serpin peptidase inhibitor, clade A, member 8)
8		95147674	Complement factor B
9		2501351	Transferrin
10		27807209	Alpha-2-macroglobulin
11		78369364	Group-specific component (vitamin D binding protein)
12	Epithelium	16303309	Type II keratin 5
13		148747492	Keratin 2
14		73996312	Similar to Keratin, type II cytoskeletal 5 (Cytokeratin 5) (58 kDa cytokeratin) isoform 3
15		9910294	Keratin 71
16		4159806	Type II keratin subunit protein
17	Cytoskeleton	28336	Mutant beta-actin
18	Others	27806907	Clusterin
19		2232299	IgM heavy chain constant region
20		27806809	Regucalcin

Table 1. Differential protein expression profile identified by LC-MS/MS, showing proteins preferentially absorbed on H-UNCD films, but not on Petri dish polystyrene surface.

6. Proteomic analysis of proteins that are adsorbed to UNCD films by using LC-MS/MS

We showed that the abundant fibronectin adsorbed onto the H-UNCD film formed locally dense and conformed layer that allows for the pro-adhesive motifs to be accessible by integrins and further activates the whole signaling pathway [66]. To further investigate what other serum proteins might be bound to UNCD films, we performed proteomic analysis,

using LC-MS/MS on serum proteins that are adsorbed to H-UNCD films. We demonstrated that H-UNCD films could adsorb proteins from culture medium more efficient than Petri dish's polystyrene surface could (Table 1). These proteins included not only fibronectin but also proteins that are known to be present in blood, epithelium, cytoskeleton, and others. It would be of interest to further explore the roles of these proteins in shaping the UNCD-cell interaction and the ultimate differentiation into desired cell types.

7. Conclusion

Highly intense research on biocompatibility of NCD films showed that it is a promising material for biomedical applications. NCD films possess easy surface functionalization and nano-topography, offering favorable condition for the growth of fibroblasts, osteoblasts and stem cells without inflammatory response and cytotoxicity. From published *in vitro* studies, NCD films elicited an improved proliferation and differentiation capacity for human osteoblasts and neural stem cells, compared to conventional polystyrene Petri dishes. The relevant mechanism of cellular signaling transduction has been investigated and shown to act through fibronectin-integrin-FAK-ERK pathway. These results suggest the potential usage of NCD films as novel medical devices and implants such as a coating for joint implant and nerve repair in tissue engineering. The delamination and corrosion of the NCD films during its long-term use in medical implants are to be carefully considered for its future biomedical applications. We performed proteomic analysis, using LC-MS/MS, to identify proteins that are adsorbed to UNCD films. We demonstrated proteins such as fibronectin, transferrin, and several keratin proteins that could be adsorbed more efficiently onto UNCD films than to Petri dish's polystyrene surface. It would be of interest to further explore the roles of these proteins in shaping the UNCD-cell interaction and the subsequent differentiation into desired cell types. Finally, more systematic studies *in vivo* are now warranted to confirm its use in biomedical devices for commercial applications.

8. References

[1] Peppas NA, Langer R. New Challenges in Biomaterials. Science 1994 Mar;263(5154):1715-1720.
[2] Hubbell JA. Biomaterials in Tissue Engineering. Bio-Technology 1995 Jun;13(6):565-576.
[3] Lutolf MP, Hubbell JA. Synthetic biomaterials as instructive extracellular microenvironments for morphogenesis in tissue engineering. Nat Biotechnol 2005 Jan;23(1):47-55.
[4] Langer R, Tirrell DA. Designing materials for biology and medicine. Nature 2004 Apr;428(6982):487-492.
[5] Discher DE, Mooney DJ, Zandstra PW. Growth Factors, Matrices, and Forces Combine and Control Stem Cells. Science 2009 Jun;324(5935):1673-1677.
[6] Chai C, Leong KW. Biomaterials approach to expand and direct differentiation of stem cells. Mol Ther 2007 Mar;15(3):467-480.
[7] Hwang NS, Varghese S, Elisseeff J. Controlled differentiation of stem cells. Adv Drug Deliv Rev 2008 Jan;60(2):199-214.
[8] Lutolf MP, Gilbert PM, Blau HM. Designing materials to direct stem-cell fate. Nature 2009 Nov;462(7272):433-441.

[9] Morrison SJ, Spradling AC. Stem cells and niches: Mechanisms that promote stem cell maintenance throughout life. Cell 2008 Feb;132(4):598-611.
[10] Guilak F, Cohen DM, Estes BT, Gimble JM, Liedtke W, Chen CS. Control of Stem Cell Fate by Physical Interactions with the Extracellular Matrix. Cell Stem Cell 2009 Jul;5(1):17-26.
[11] Chao JI, Perevedentseva E, Chung PH, Liu KK, Cheng CY, Chang CC, et al. Nanometer-sized diamond particle as a probe for biolabeling. Biophysical Journal 2007 Sep;93(6):2199-2208.
[12] Liu KK, Wang CC, Cheng CL, Chao JI. Endocytic carboxylated nanodiamond for the labeling and tracking of cell division and differentiation in cancer and stem cells. Biomaterials 2009 Sep;30(26):4249-4259.
[13] Vaijayanthimala V, Tzeng YK, Chang HC, Li CL. The biocompatibility of fluorescent nanodiamonds and their mechanism of cellular uptake. Nanotechnology 2009 Oct;20(42):9.
[14] Ho DA. Beyond the Sparkle: The Impact of Nanodiamonds as Biolabeling and Therapeutic Agents. Acs Nano 2009 Dec;3(12):3825-3829.
[15] Schrand AM, Hens SAC, Shenderova OA. Nanodiamond Particles: Properties and Perspectives for Bioapplications. Critical Reviews in Solid State and Materials Sciences 2009;34(1-2):18-74.
[16] Chan HY, Aslam DM, Wiler JA, Casey B. A Novel Diamond Microprobe for Neuro-Chemical and -Electrical Recording in Neural Prosthesis. Journal of Microelectromechanical Systems 2009 Jun;18(3):511-521.
[17] Ong TP, Chiou WA, Chen FR, Chang RPH. Preparation of Nanocrystalline Diamond Films for Optical Coating Applications Using a Pulsed Microwave Plasma Cvd Method. Carbon 1990;28(6):799-799.
[18] Ong TP, Chang RPH. Low-Temperature Deposition of Diamond Films for Optical Coatings. Applied Physics Letters 1989 Nov;55(20):2063-2065.
[19] Fan WD, Wu H, Jagannadham K, Goral BC. Wear-Resistant Diamond Coatings on Alumina. Surface & Coatings Technology 1995 May;72(1-2):78-87.
[20] Kato M, Fujisawa T. High-pressure solution X-ray scattering of protein using a hydrostatic cell with diamond windows. Journal of Synchrotron Radiation 1998 Sep;5:1282-1286.
[21] Ravet MF, Rousseaux F. Status of diamond as membrane material for X-ray lithography masks. Diamond and Related Materials 1996 May;5(6-8):812-818.
[22] Sharda T, Umeno M, Soga T, Jimbo T. Strong adhesion in nanocrystalline diamond films on silicon substrates. Journal of Applied Physics 2001 May;89(9):4874-4878.
[23] Lifshitz Y, Meng XM, Lee ST, Akhveldiany R, Hoffman A. Visualization of diamond nucleation and growth from energetic species. Physical Review Letters 2004 Jul;93(5):4.
[24] Lee YC, Lin SJ, Chia CT, Cheng HF, Lin IN. Effect of processing parameters on the nucleation behavior of nano-crystalline diamond film. Diamond and Related Materials 2005 Mar-Jul;14(3-7):296-301.
[25] Berry BS, Pritchet WC, Cuomo JJ, Guarnieri CR, Whitehair SJ. INTERNAL-STRESS AND ELASTICITY OF SYNTHETIC DIAMOND FILMS. Applied Physics Letters 1990 Jul;57(3):302-303.

[26] Liu YK, Tso PL, Lin IN, Tzeng Y, Chen YC. Comparative study of nucleation processes for the growth of nanocrystalline diamond. Diamond and Related Materials 2006 Feb-Mar;15(2-3):234-238.
[27] Lee ST, Lin ZD, Jiang X. CVD diamond films: nucleation and growth. Mater Sci Eng R-Rep 1999 Jul;25(4):123-154.
[28] Sumant AV, Gilbert P, Grierson DS, Konicek AR, Abrecht M, Butler JE, et al. Surface composition, bonding, and morphology in the nucleation and growth of ultra-thin, high quality nanocrystalline diamond films. Diam Relat Mat 2007 Apr-Jul;16(4-7):718-724.
[29] Naguib NN, Elam JW, Birrell J, Wang J, Grierson DS, Kabius B, et al. Enhanced nucleation, smoothness and conformality of ultrananocrystalline diamond (UNCD) ultrathin films via tungsten interlayers. Chem Phys Lett 2006 Oct;430(4-6):345-350.
[30] Gruen D, Krauss A. Buckyball precursors produce ultra-smooth diamond films. R&D Magazine 1997 Apr;39(5):57-&.
[31] Gruen DM, Liu SZ, Krauss AR, Luo JS, Pan XZ. FULLERENES AS PRECURSORS FOR DIAMOND FILM GROWTH WITHOUT HYDROGEN OR OXYGEN ADDITIONS. Applied Physics Letters 1994 Mar;64(12):1502-1504.
[32] Gruen DM, Pan XZ, Krauss AR, Liu SZ, Luo JS, Foster CM. DEPOSITION AND CHARACTERIZATION OF NANOCRYSTALLINE DIAMOND FILMS. Journal of Vacuum Science & Technology a-Vacuum Surfaces and Films 1994 Jul-Aug;12(4):1491-1495.
[33] Gruen DM. Nanocrystalline diamond films. Annual Review of Materials Science 1999;29:211-259.
[34] Gruen DM. Ultrananocrystalline diamond in the laboratory and the cosmos. Mrs Bulletin 2001 Oct;26(10):771-776.
[35] Butler JE, Sumant AV. The CVD of nanodiamond materials. Chem Vapor Depos 2008 Jul-Aug;14(7-8):145-160.
[36] Hutchinson AB, Truitt PA, Schwab KC, Sekaric L, Parpia JM, Craighead HG, et al. Dissipation in nanocrystalline-diamond nanomechanical resonators. Applied Physics Letters 2004 Feb;84(6):972-974.
[37] Sekaric L, Parpia JM, Craighead HG, Feygelson T, Houston BH, Butler JE. Nanomechanical resonant structures in nanocrystalline diamond. Applied Physics Letters 2002 Dec;81(23):4455-4457.
[38] Zhang JC, Zimmer JW, Howe RT, Maboudian R. Characterization of boron-doped micro- and nanocrystalline diamond films deposited by wafer-scale hot filament chemical vapor deposition for MEMS applications. Diamond and Related Materials 2008 Jan;17(1):23-28.
[39] Lee CK. Effects of hydrogen and oxygen on the electrochemical corrosion and wear-corrosion behavior of diamond films deposited by hot filament chemical vapor deposition. Applied Surface Science 2008 Apr;254(13):4111-4117.
[40] Yang WS, Auciello O, Butler JE, Cai W, Carlisle JA, Gerbi J, et al. DNA-modified nanocrystalline diamond thin-films as stable, biologically active substrates. Nature Materials 2002 Dec;1(4):253-257.
[41] Yang WS, Auciello O, Butler JE, Cai W, Carlisle JA, Gerbi J, et al. DNA-modified nanocrystalline diamond thin-films as stable, biologically active substrates (vol 1, pg 253, 2002). Nature Materials 2003 Jan;2(1):63-63.

[42] Yang WS, Butler JE, Russell JN, Hamers RJ. Interfacial electrical properties of DNA-modified diamond thin films: Intrinsic response and hybridization-induced field effects. Langmuir 2004 Aug;20(16):6778-6787.
[43] Ariano P, Lo Giudice A, Marcantoni A, Vittone E, Carbone E, Lovisolo D. A diamond-based biosensor for the recording of neuronal activity. Biosensors & Bioelectronics 2009 Mar;24(7):2046-2050.
[44] Yang WS, Hamers RJ. Fabrication and characterization of a biologically sensitive field-effect transistor using a nanocrystalline diamond thin film. Applied Physics Letters 2004 Oct;85(16):3626-3628.
[45] Jakubowski W, Bartosz G, Niedzielski P, Szymanski W, Walkowiak B. Nanocrystalline diamond surface is resistant to bacterial colonization. Diamond and Related Materials 2004 Oct;13(10):1761-1763.
[46] Papo MJ, Catledge SA, Vohra YK. Mechanical wear behavior of nanocrystalline and multilayer diamond coatings on temporomandibular joint implants. J Mater Sci-Mater Med 2004 Jul;15(7):773-777.
[47] Nordsletten L, Hogasen AKM, Konttinen YT, Santavirta S, Aspenberg P, Aasen AO. Human monocytes stimulation by particles of hydroxyapatite, silicon carbide and diamond: In vitro studies of new prosthesis coatings. Biomaterials 1996 Aug;17(15):1521-1527.
[48] Aspenberg P, Anttila A, Konttinen YT, Lappalainen R, Goodman SB, Nordsletten L, et al. Benign response to particles of diamond and SiC: Bone chamber studies of new joint replacement coating materials in rabbits. Biomaterials 1996 Apr;17(8):807-812.
[49] Tang L, Tsai C, Gerberich WW, Kruckeberg L, Kania DR. Biocompatibility of Chemical-Vapor-Deposited Diamond. Biomaterials 1995 Apr;16(6):483-488.
[50] Kulisch W, Popov C, Bliznakov S, Ceccone G, Gilliland D, Sirghi L, et al. Surface and bioproperties of nanocrystalline diamond/amorphous carbon nanocomposite films. Thin Solid Films 2007 Sep;515(23):8407-8411.
[51] Popov C, Kulisch W, Reithmaier JP, Dostalova T, Jelinek M, Anspach N, et al. Bioproperties of nanocrystalline diamond/amorphous carbon composite films. Diamond and Related Materials 2007 Apr-Jul;16(4-7):735-739.
[52] Rubio-Retama J, Hernando J, Lopez-Ruiz B, Hartl A, Steinmuller D, Stutzmann M, et al. Synthetic nanocrystalline diamond as a third-generation biosensor support. Langmuir 2006 Jun;22(13):5837-5842.
[53] Steinmuller-Nethl D, Kloss FR, Najam-U-Haq M, Rainer M, Larsson K, Linsmeier C, et al. Strong binding of bioactive BMP-2 to nanocrystalline diamond by physisorption. Biomaterials 2006 Sep;27(26):4547-4556.
[54] Haensel T, Uhlig J, Koch RJ, Ahmed SIU, Garrido JA, Steinmuller-Nethl D, et al. Influence of hydrogen on nanocrystalline diamond surfaces investigated with HREELS and XPS. Physica Status Solidi a-Applications and Materials Science 2009 Sep;206(9):2022-2027.
[55] Chong KF, Loh KP, Vedula SRK, Lim CT, Sternschulte H, Steinmuller D, et al. Cell adhesion properties on photochemically functionalized diamond. Langmuir 2007 May;23(10):5615-5621.
[56] Chen YC, Lee DC, Hsiao CY, Chung YF, Chen HC, Thomas JP, et al. The effect of ultra-nanocrystalline diamond films on the proliferation and differentiation of neural stem cells. Biomaterials 2009 Jul;30(20):3428-3435.

[57] Yang L, Sheldon BW, Webster TJ. The impact of diamond nanocrystallinity on osteoblast functions. Biomaterials 2009 Jul;30(20):3458-3465.
[58] Clem WC, Chowdhury S, Catledge SA, Weimer JJ, Shaikh FM, Hennessy KM, et al. Mesenchymal stem cell interaction with ultra-smooth nanostructured diamond for wear-resistant orthopaedic implants. Biomaterials 2008 Aug-Sep;29(24-25):3461-3468.
[59] Huang HJ, Chen M, Bruno P, Lam R, Robinson E, Gruen D, et al. Ultrananocrystalline Diamond Thin Films Functionalized with Therapeutically Active Collagen Networks. Journal of Physical Chemistry B 2009 Mar;113(10):2966-2971.
[60] Kalbacova M, Rezek B, Baresova V, Wolf-Brandstetter C, Kromka A. Nanoscale topography of nanocrystalline diamonds promotes differentiation of osteoblasts. Acta Biomaterialia 2009 Oct;5(8):3076-3085.
[61] Popov C, Bliznakov S, Boycheva S, Milinovik N, Apostolova MD, Anspach N, et al. Nanocrystalline diamond/amorphous carbon composite coatings for biomedical applications. Diamond and Related Materials 2008 Apr-May;17(4-5):882-887.
[62] Huang HJ, Pierstorff E, Osawa E, Ho D. Protein-mediated assembly of nanodiamond hydrogels into a biocompatible and biofunctional multilayer nanofilm. Acs Nano 2008 Feb;2(2):203-212.
[63] Jian W, Firestone MA, Auciello O, Carlisle JA. Surface functionalization of ultrananocrystalline diamond films by electrochemical reduction of aryldiazonium salts. Langmuir 2004 Dec;20(26):11450-11456.
[64] Wang J, Carlisle JA. Covalent immobilization of glucose oxidase on conducting ultrananocrystalline diamond thin films. Diamond and Related Materials 2006 Feb-Mar;15(2-3):279-284.
[65] Williams DF. On the nature of biomaterials. Biomaterials 2009 Oct;30(30):5897-5909.
[66] Chen YC, Lee DC, Tsai TY, Hsiao CY, Liu JW, Kao CY, et al. Induction and regulation of differentiation in neural stem cells on ultra-nanocrystalline diamond films. Biomaterials 2010:In press.
[67] Kromka A, Grausova L, Bacakova L, Vacik J, Rezek B, Vanecek M, et al. Semiconducting to metallic-like boron doping of nanocrystalline diamond films and its effect on osteoblastic cells. Diamond and Related Materials Feb-Mar;19(2-3):190-195.
[68] Ariano P, Budnyk O, Dalmazzo S, Lovisolo D, Manfredotti C, Rivolo P, et al. On diamond surface properties and interactions with neurons. European Physical Journal E 2009 Oct;30(2):149-156.
[69] Shi B, Jin QL, Chen LH, Auciello O. Fundamentals of ultrananocrystalline diamond (UNCD) thin films as biomaterials for developmental biology: Embryonic fibroblasts growth on the surface of (UNCD) films. Diamond and Related Materials 2009 Feb-Mar;18(2-3):596-600.
[70] Bajaj P, Akin D, Gupta A, Sherman D, Shi B, Auciello O, et al. Ultrananocrystalline diamond film as an optimal cell interface for biomedical applications. Biomedical Microdevices 2007 Dec;9(6):787-794.
[71] Amaral M, Dias AG, Gomes PS, Lopes MA, Silva RF, Santos JD, et al. Nanocrystalline diamond: In vitro biocompatibility assessment by MG63 and human bone marrow cells cultures. Journal of Biomedical Materials Research Part A 2008 Oct;87A(1):91-99.

[72] Amaral M, Gomes PS, Lopes MA, Santos JD, Silva RF, Fernandes MH. Nanocrystalline diamond as a coating for joint implants: Cytotoxicity and biocompatibility assessment. Journal of Nanomaterials 2008:9.

[73] Kloss FR, Gassner R, Preiner J, Ebner A, Larsson K, Hachl O, et al. The role of oxygen termination of nanocrystalline diamond on immobilisation of BMP-2 and subsequent bone formation. Biomaterials 2008 Jun;29(16):2433-2442.

[74] Tate MC, Garcia AJ, Keselowsky BG, Schumm MA, Archer DR, LaPlaca MC. Specific beta(1) integrins mediate adhesion, migration, and differentiation of neural progenitors derived from the embryonic striatum. Molecular and Cellular Neuroscience 2004 Sep;27(1):22-31.

[75] Hynes RO, Yamada KM. Fibronectins - Multifunctional Modular Glycoproteins. Journal of Cell Biology 1982;95(2):369-377.

[76] Cui FZ, Li DJ. A review of investigations on biocompatibility of diamond-like carbon and carbon nitride films. Surface & Coatings Technology 2000 Sep;131(1-3):481-487.

[77] Yang L, Sheldon BW, Webster TJ. Orthopedic nano diamond coatings: Control of surface properties and their impact on osteoblast adhesion and proliferation. Journal of Biomedical Materials Research Part A 2009 Nov;91A(2):548-556.

[78] Kalbacova M, Broz A, Babchenko O, Kromka A. Study on cellular adhesion of human osteoblasts on nano-structured diamond films. Physica Status Solidi B-Basic Solid State Physics 2009 Dec;246(11-12):2774-2777.

[79] Broz A, Baresova V, Kromka A, Rezek B, Kalbacova M. Strong influence of hierarchically structured diamond nanotopography on adhesion of human osteoblasts and mesenchymal cells. Phys Status Solidi A-Appl Mat 2009 Sep;206(9):2038-2041.

[80] Kalbacova M, Kalbac M, Dunsch L, Kromka A, Vanecek M, Rezek B, et al. The effect of SWCNT and nano-diamond films on human osteoblast cells. Physica Status Solidi B-Basic Solid State Physics 2007 Nov;244(11):4356-4359.

[81] Kalbacova M, Michalikova L, Baresova V, Kromka A, Rezek B, Kmoch S. Adhesion of osteoblasts on chemically patterned nanocrystalline diamonds. Physica Status Solidi B-Basic Solid State Physics 2008 Oct;245(10):2124-2127.

[82] Anselme K, Linez P, Bigerelle M, Le Maguer D, Le Maguer A, Hardouin P, et al. The relative influence of the topography and chemistry of TiAl6V4 surfaces on osteoblastic cell behaviour. Biomaterials 2000 Aug;21(15):1567-1577.

[83] Anselme K. Osteoblast adhesion on biomaterials. Biomaterials 2000 Apr;21(7):667-681.

[84] Thalhammer A, Edgington RJ, Cingolani LA, Schoepfer R, Jackman RB. The use of nanodiamond monolayer coatings to promote the formation of functional neuronal networks. Biomaterials Mar;31(8):2097-2104.

[85] Rezek B, Michalikova L, Ukraintsev E, Kromka A, Kalbacova M. Micro-Pattern Guided Adhesion of Osteoblasts on Diamond Surfaces. Sensors 2009 May;9(5):3549-3562.

[86] Ukraintsev E, Rezek B, Kromka A, Broz A, Kalbacova M. Long-term adsorption of fetal bovine serum on H/O-terminated diamond studied in situ by atomic force microscopy. Physica Status Solidi B-Basic Solid State Physics 2009 Dec;246(11-12):2832-2835.

[87] Michalikova L, Rezek B, Kromka A, Kalbacova M. CVD diamond films with hydrophilic micro-patterns for self-organisation of human osteoblasts. Vacuum 2009 Aug;84(1):61-64.

[88] Rezek B, Ukraintsev E, Michalikova L, Kromka A, Zemek J, Kalbacova M. Adsorption of fetal bovine serum on H/O-terminated diamond studied by atomic force microscopy. Diamond and Related Materials 2009 May-Aug;18(5-8):918-922.

[89] Rezek B, Ukraintsev E, Kromka A, Ledinsky M, Broz A, Noskova L, et al. Assembly of osteoblastic cell micro-arrays on diamond guided by protein pre-adsorption. Diamond and Related Materials Feb-Mar;19(2-3):153-157.

[90] Hamilton DW, Brunette DM. The effect of substratum topography on osteoblast adhesion mediated signal transduction and phosphorylation. Biomaterials 2007 Apr;28(10):1806-1819.

[91] Ivankovic-Dikic I, Gronroos E, Blaukat A, Barth BU, Dikic I. Pyk2 and FAK regulate neurite outgrowth induced by growth factors and integrins. Nature Cell Biology 2000 Sep;2(9):574-581.

[92] Mruthyunjaya S, Manchanda R, Godbole R, Pujari R, Shiras A, Shastry P. Laminin-1 induces neurite outgrowth in human mesenchymal stem cells in serum/differentiation factors-free conditions through activation of FAK-MEK/ERK signaling pathways. Biochemical and Biophysical Research Communications Jan;391(1):43-48.

11

Transfection of Bone Cells *In Vivo* Using HA-Ceramic Particles - Histological Study

Patrick Frayssinet and Nicole Rouquet
Urodelia, Rte de St Thomas,
France

1. Introduction

The non-viral introduction of genes into mammalian cells (transfection) is of growing interest for tissue engineering and used as an alternative to viral transfer of recombinant genes. The introduction of a foreign gene into cells *in vivo* is often limited to the use of viral vectors such as adeno or retroviruses (Rochliz, C.F., 2001, Kahn, A., 2000). Viral vectors may present several disadvantages or side effects, which can be disastrous. Adenoviruses produce proteins, which can trigger immune reactions. Furthermore, the expression of a gene transduced with a viral vector is transient and can be shortened when an immune reaction occurs against the viral proteins. It must also be noted that the selection of cells, which are transduced by the virus is very poor and its efficiency is dependent on the stage the cell is in.

A number of non-viral vectors have been explored and used to date i.e. lipid-based carriers, hydrogel polymers, polycationic lipids, polylysine, polyornithine, histones and other chromosomal proteins, hydrogen polymers, precipitated calcium phosphate (Maurer, N., et al., 1999; Cullis, P.R., Chonn, A., 1998; Zauner, W., 1998; Ramsay, E., et al., 2000 ; Schwartz, B, 1999; Leong, W., 1998; Perez, C., et al., 2001; Graham, F.J. et al, 1973). Most of these vectors are usable *in vitro* but are difficult to apply *in vivo*, especially when a local transfection to a specific cell line must be achieved.

Transfection using polymer matrices i.e. gel, foams or bulk material have recently been developed to overcome these difficulties (Lauffenburger, D.A., and Schaffer, D.V., 1999). They are polycationic and are able to adsorb the negatively charged DNA molecules on their surfaces (Bonadio et al.). This concept is also extended to calcium phosphate ceramics which are widely used in human surgery as bone substitutes, cell carriers, or even thin layers at the surface of metal alloys to improve their integration by bones (Frayssinet, P., et al., 1998; Frayssinet, P., et al., 1992). The use of calcium phosphate ceramics for gene delivery presents several advantages. These matrices are biocompatible and are totally degradable by the cells of the monocyte lineage (Frayssinet, P., et al., 1994). Their behaviour in the organism is well known.

This matrix was tested in jaw bones in order to transfect bone and dental ligament cells to increase bone formation during parodontal disease. We adsorbed a plasmid DNA containing an *Escherichia coli* galactosidase gene (Lac-Z) at the surface of hydroxyapatite ceramic particles which were implanted at the junction between the incisor dental ligament and bone of rabbit jaws.

2. Materials and methods

2.1 Surgical implantation

Four white New Zealand rabbits were used for each implantation period (21 and 90 days). A pouch was created at the junction between the right incisors and the bone. 0.5 mg of HA-powder (Urodelia, St Lys, France) was introduced in the pouch using a curette. The powder was aggregated in the curette using PBS and the implanted particles were covered with a mucosal flap.

Control animals: in one animal the HA-particles were implanted without any contact with plasmid and in another one, the same amount of plasmid solution as used for particle adsorption was injected at the implantation location. The histological sections were done at 21 days and 90 days.

2.2 Particle characteristics

The hydroxylapatite particle characteristics are given in table 1.

Form :	irregularly shaped micro-particles
Colour :	White
Molecular formula :	$Ca_{10}(OH)_2(PO_4)_6$
Molecular weight :	1004.6
Solubility :	Stable at neutral and basic pH, soluble in acidic pH.
Granulometry range :	45 - 80 µm
Apparent density :	1.4 ± 0.2 g/ml
Composition	HA ≥ 97%
Ca/P :	1.663 ≤ Ca/P ≤ 1.728
Surface area :	0.7 m²/g
Surface potential :	- 35 mV
Surface pH :	7,8
BSA binding capacity :	> 22 mg/g
DNA binding capacity :	> 0.1 mg/ml (pCMV□ plasmid – Contech)
Dry weight/volume :	2 g/ml

Table 1. Characteristics of the implanted powder

2.3 Plasmid adsorption

10 mg of powder was soaked in 0.5 ml of a 0.1 M phosphate buffer pH 7 at 60°C for 4-8 hours. The buffer was removed and the powder was washed with new phosphate buffer. The excess buffer was removed and the powder was introduced in 1 ml of a phosphate buffer solution (0.1 M phosphate buffer pH 7) containing 25 µg of plasmid DNA (Clontech, Palo Alto, California) and incubated 2 hours at 37°C. The excess solution was then removed and the powder was dried at room temperature.

2.4 Bone histology

The jaw was fixed in a mixture ethanol/acetone (50/50 V/V) at room temperature and partially decalcified in a 4% solution of diNa-EDTA for 6 days. The jaw fragments were then embedded inside hydroxyl-ethylmethacrylate. 5 µm thick sections were then performed using a microtome for calcified tissues (Reicher-Jung type K). The galactosidase activity was

evidenced using a X-gal solution at 37°C for two hours (100 mM sodium phosphate pH 7.3, 1.3 mM $MgCl_2$, 3 mM $K_3Fe(CN)_6$, 3mM $K_4Fe(CN)_6$ and 1mg/ml X-Gal). The sections were observed under a light microscope, and then counterstained by a Giemsa solution. The cells expressing the LacZ gene were stained in blue. The sections were done through the implanted particles and the same zone in the controlateral region.

3. Results

Macroscopically, the particles can be seen at the basis of the incisors at the first implantation time and they were stained in blue (fig. 1).

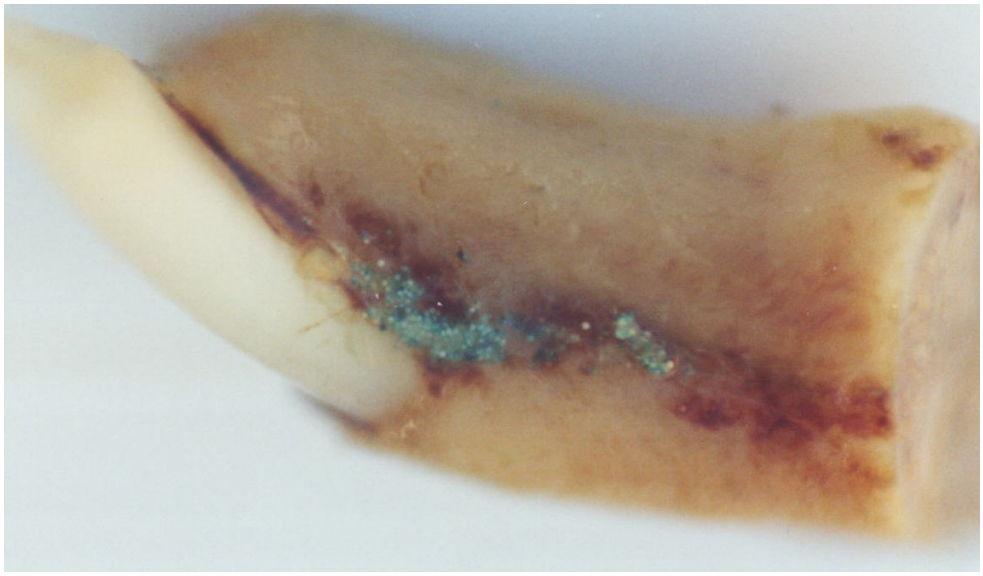

Fig. 1. Photograph of the implantation site at 21 days. The particles were visible at the junction between the incisor and the bone. The particles are stained in blue indicating that the cells having ingrown the material express the Lac-Z gene.

At 21 days, the particles were surrounded by a mild foreign body reaction constituted by mono and plurinucleated cells (fig. 2). These cells contained fragments of calcium phosphate ceramics.

The monocytes and multinucleated cells located around the particles were stained in blue (fig. 3). In the controlateral site, blue stained cells were dispersed in the stromal tissue evidenced in the bone pores. They were circulating cells such as monocytes and multinucleated cells (fig. 4). These late cells were often evidenced at the bone surface and sometimes in Howship's lacunae (fig. 4).

Some other cells expressing the galactosidase gene were found inside stromal tissue and showed a fibroblastic aspect (fig. 5). Some of these cells were identified as pericytes as they were evidenced in the immediate proximity to the capillaries.

Blue stained cells were also evidenced in the dental ligament (fig. 6). Some of them have the morphology of circulating cells as others are ligament fibroblasts.

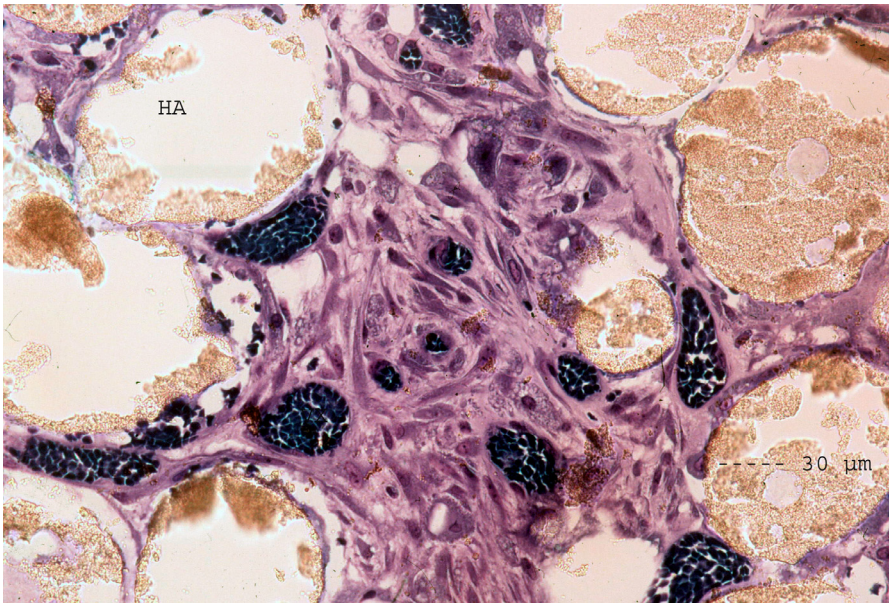

Fig. 2. Microphotograph of the implantation zone at 21 days showing that at an early implantation time, the microparticles (HA) were embedded in a mild foreign body reaction made of monocytes and multinucleated cells. Giemsa staining.

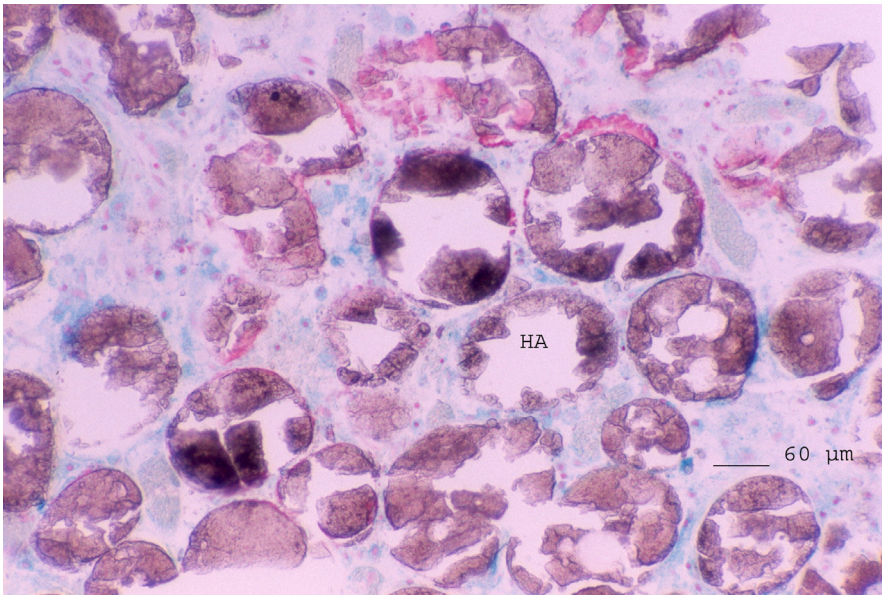

Fig. 3. Section of the implantation zone at 21 days after X-Gal staining showing that almost all the foreign body reaction cells were stained in blue. X-Gal and neutral red staining.

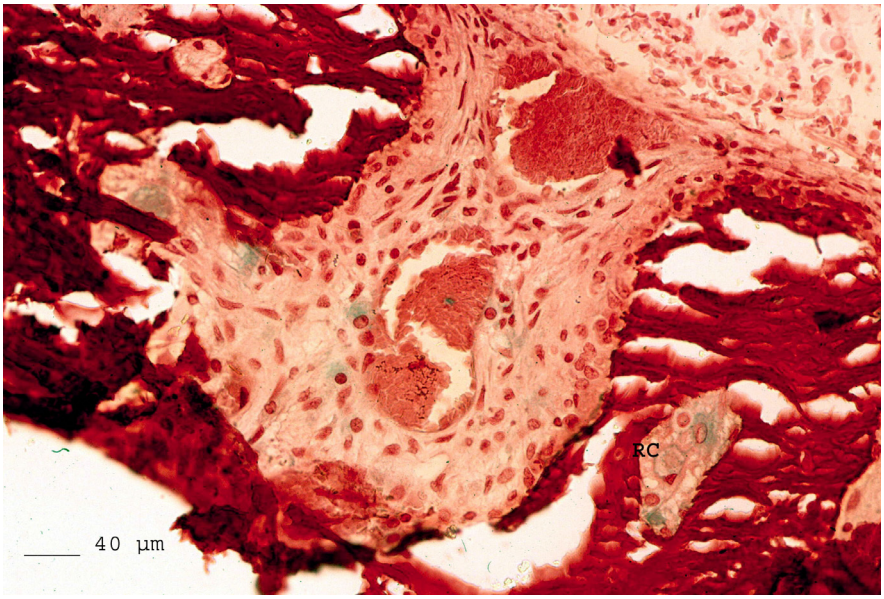

Fig. 4. Section of bone at remote distance from the implantation zone at 21 days. There were monocytes stained in blue in the pores of the bone tissue. Cells expressing the galactosidase gene were evidenced in Howship's lacunae or resorption cavities (RC). X-Gal and neutral red staining.

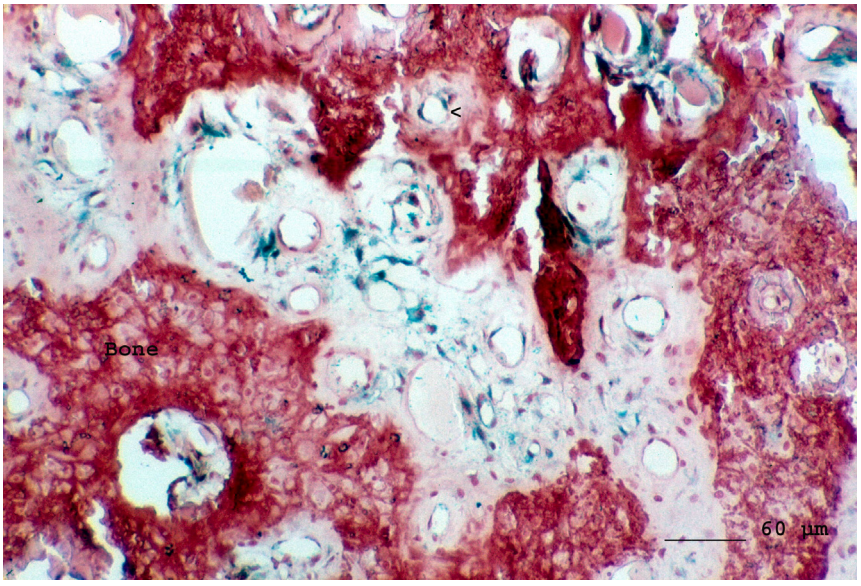

Fig. 5. At 21 days, the bone stromal tissue contained blue stained cells which were stellar shaped. Some of these cells were perivascular (<). X-Gal and neutral red staining.

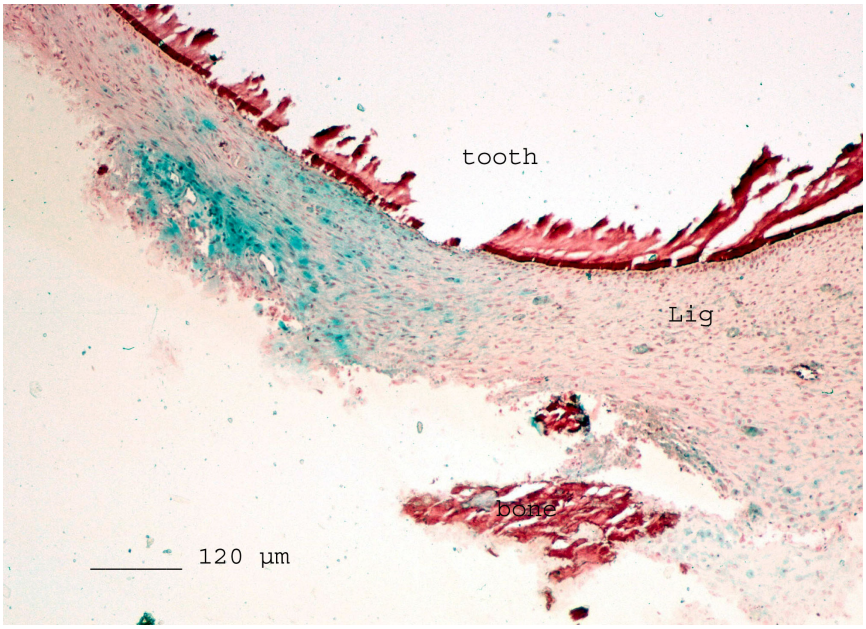

Fig. 6. At 21 days, section of the dental ligament (lig) of the implanted incisor. Some ligament cells were stained in blue. X-Gal and neutral red staining

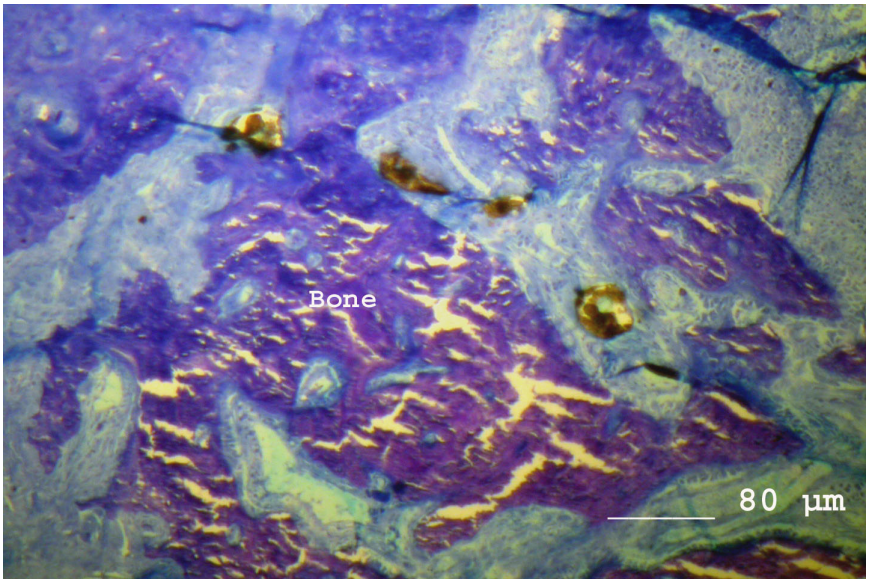

Fig. 7. At 3 months after implantation, the histological sections showed that the HA-particles (grey) were dispersed and integrated in the bone tissue without sign of foreign body reaction. Giemsa staining.

At 90 days (fig. 7), the particles were degrading and some of them were integrated inside bone trabeculae.
There were almost no circulating cells around the microparticles. The cells expressing the lac-Z gene were dispersed in the connective tissue. Some other cells showed a blue staining. Odontoblasts and fibroblasts were among these cells (fig. 8). The percentage of the labelled cells was low.
Sections of the control animals did not show any staining at any time.

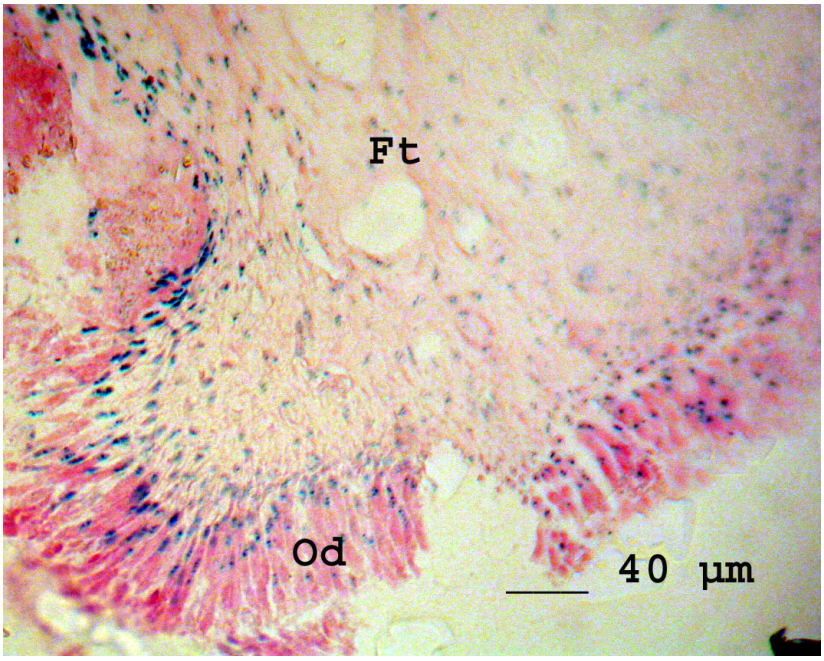

Fig. 8. Histological section of the incisor connective tissue of a three month implanted site. There were still some cells like odontoblasts showing a galactosidase gene expression. Numerous other cells mainly fibroblasts were also expressing the gene. X-Gal staining.

4. Discussion

This experiment showed that a transient transfection can be obtained using calcium phosphate ceramics with some level of specificity limited to the cells being in contact with the ceramic or located to its proximity. This "geo-specificity" allows to transfect the circulating cells i.e. monocytes, macrophages, multinucleated cells which are the first cells to come in contact with the material.
The transfection does not seem to interfere with the differentiation of the cells, as the monocytes transfected at the ceramic contact are found in Howship's lacunae and identified as osteoclasts. Furthermore, they are also found in various locations of bone indicating that the cells of the foreign body reaction are still able to circulate and differentiate from macrophages into osteoclasts. Thus, it indicates that contact with the ceramic and the phagocytosis of the ceramic particles would not impair the migration of cells toward the

lymph node and their role of antigen presenting cells. It is also indicated that the degradation of the ceramic does not release toxic particles or products responsible for a cell death or apoptosis in the site of implantation.

The cell transfection with calcium phosphate/DNA coprecipitates has been used for decades *in vitro* (Schenborn, E.T., and Goiffon, V., 2000), it is almost impossible to obtain *in vivo* in an open medium. The use of nanoparticles which are already precipitated are also difficult to use *in vivo* because it is not possible to maintain them in a particular location.

It has been reported that a direct injection of a plasmid suspension in rodent muscles could trigger a significant transfection of the muscle cells (Danko, I., et al., 1997). However, it is not known what are the other cells transfected and what is the transfection kinetic and yield. It is also difficult to ensure any specificity of the transfected cells by this way. In this study, plasmid injection did not bring a significant transfection in the injection site, probably because the injected solution did not stay in the site.

Macrophages have the reputation of being difficult to transfect. This material can thus be of interest to target these cells. During the first time, only the circulating cells are labelled, while at three months, some other cells could be evidenced such as odontoblasts or fibroblasts of the connective tissue.

The mechanism of transfection is not clear and cannot totally be dissociated from that of the co-precipitate. Furthermore, the degradation of the ceramic takes place at the grain boundaries of the ceramic particles. A release of particle grains occurs in the proximity of the implantation zone explaining the localisation of the transfected cells (Frayssinet, P., and Guilhem, A., 2004; Frayssinet, P., et al., 2006).

The material degradation leads to the release of several particle sizes and shapes depending on the degradation stage. The ceramic grains after the dissolution of the grain boundaries, can be released alone or aggregated. At this stage, they are micronic in size. Then the particles are degraded inside the low pH compartments of the cells and their size decreases and they become nanosized (Frayssinet, P., et al., 1999; Jallot, E., et al., 1999). During this time, the shape becomes round with a disappearance of the particle angles. The dissolution/precipitation process occurring at the particle surface is very complex as there is a carbonated apatite epitaxial growth at neutral pH and finally a dissolution at low pH.

The physical interaction with between the HA and the hydroxylapatite chemically stabilizes the DNA molecules increasing the denaturation temperature (Martinoson, H.G., 1978). This stabilization can partly explain the transfection mechanism as the complex DNA/calcium phosphate could impair or slow the DNA destruction in the cytoplasm (Orrantia, E., Chang, P.L., 1990).

The adsorption mechanism at the HA surface is not clear. The DNA molecule is negatively charged as is the ceramic surface. Thus the adsorption is not driven by electrostatic forces. The surface modifications occurring during the culture or implantation make it difficult for the elucidation of the adsorption mechanism.

These results have to be compared to those obtained *in vitro* with isolated cells or tissue culture. It was shown that the percentage of transfected cells was time dependent and could be very high after a few days of contact. It was also shown that, regarding bone tissue, all the cell types could be transfected by this way.

5. Conclusions

Hydroxyapatite ceramics have numerous applications relating to the field of human and animal health. Their surface properties can explain the molecule adsorption and the ability

of these materials for transient cell transfection both *in vitro* and *in vivo*. Applications for cell transfection could be numerous as the material is safe, degradable, and shows a good transfection yield. Furthermore, this material demonstrates interesting properties allowing to target antigen presenting cells. These cells can show some deficiencies in their role of antigen presentation which is essential in very different pathology such as cancers, infectiology or autoimmune diseases. It could be particularly appropriate as a DNA vaccine vector in order to bring the antigen presenting cells the properties they would need to overcome the immune evasion strategies of cancer cells.

6. References

Bonadio, J., Smiley, E., Patil, S., Goldstein. S., (1999) , Localized, direct plasmid gene delivery *in vivo*: prolonged therapy results in reproducible tissue regeneration. Nature Medicine 5 (7):753-759.

Cullis, P.R., Chonn, A. (1998) Recent advances in liposome technologies and their applications for systemic gene delivery. Adv Drug Deliv Rev, 30: 73-83

Danko,I., Williams, P., Herweijer, H., Zhang, G., Latendresse, J.S., Bock, I., Wolff, J.A., (1997) High expression of naked plasmid DNA in muscles of young rodents. Human Molecular Genetics 6 (9):1435-1443.

Frayssinet,P., Fages, J., Bonel,G., Rouquet,N., (1998) Biotechnology, material sciences and bone repair. European Journal of Orthopaedic Surgery & Traumatology 8: 17-25.

Frayssinet, P., Guilhem, A., (2004) Cell transfection using HA-ceramics. Bioprocessing Journal, 3, 4

Frayssinet, P., Hardy, D., Rouquet, N., Giammara, B., Guilhem, A., Hanker, J.S., (1992) New observations on middle term hydroxylapatite-coated titanium alloy hip prostheses. Biomaterials , 13, 10: 668-673.

Frayssinet, P., Rouquet, N., Mathon, D., (2006) Bone cell transfection in tissue culture using hydroxyapatite microparticles. Journal of Biomedical Material Research. 79: 225-8

Frayssinet, P., Rouquet, N., Tourenne, F., Fages, J., Bonel, G. (1994) *In vivo* degradation of calcium phosphate ceramics.Cells and materials 4: 383-394.

Frayssinet, P., Schwartz, C., Beya, B., Lecestre, P., (1999) Biology of the calcium phosphate integration in human long bones. European Journal of Orthopaedic Surgery & Traumatology 9: 167-170

Graham, F.L., van der Eb, A.J., A new technique for the assay of infectivity of human adenovirus 5 DNA. 1973, Virology 52, 456-467.

Jallot, E., Irigaray,J.L., Oudadesse, H., Brun,V., Weber,G., Frayssinet,P. (1999) Resorption kinetics of four hydroxyapatite-based ceramics by particle induced X-ray emission and neutron activation analysis. The European Physical Journal-Applied Physics 6, 205-215.

Kahn, A., (2000) Dix ans de thérapie génique: déceptions et espoirs. Biofutur 202:16-21

Lauffenburger, D.A., Schaffer, D.V., (1999). The matrix delivers. Nature Medicine 7 (5):733-734

Leong, W. (1998) DNA-polycation nanospheres as non-viral gene delivery vehicles. J Contr Rel 53: 183-193

Martinoson, H.G., (1973) The nucleic acid-hydroxyapatite interaction. I. Stabilization of native double-stranded deoxyribonucleic acid by hydroxylapatite. Biochemistry, 12, 139-143

Maurer, N., Mori, A., Palmer, L., Monck, M.A., Mok, K.W., Mui, B., Akhong, Q.F., Cullis, P.R., (1999) Lipid-based systems for the intracellular delivery of genetic drugs. Mol Membr Biol 16, 129-140

Orrantia, E., Chang, P.L., (1990). Intracellular distribution of DNA internalized through calcium phosphate precipitation. Experimental Cell Research 190 (2):170-174.

Perez, C., Sanchez, A., Putnam, D., Ting, D., Langer, R., Alonso, M.J. , (2001) Poly(lactic acid)-poly(ethylene glycol) nanoparticles as new carriers for the delivery of plasmid DNA. J Contr Rel 75: 211-224

Ramsay, E., Headgraft, J., Birchall, J., Gumbleton, M., (2000). Examination of the biophysical interaction between plasmid DNA and the polycations, polylysine, and polyornithine, as a basis for their differential gene transfection *in vitro*. Int J Pharm 210: 97-107

Rochliz C. F. (2001) Gene therapy of cancer. Swiss Med Wkly 131:4-9,.

Schenborn, E.T., Goiffon, V., (2000) Calcium phosphate transfection of mammalian cultured cells. Tymms, M.J.,Totowa NJ, (eds) Humana Press Inc, p. 135-144.

Schwartz, B., (1999) Synthetic DNA-compacting peptides derived from human sequence enhanced cationic lipid-mediated gene transfer *in vitro* and *in vivo*. Gene Ther 6, 282-292

Zauner, W., Ogris, M., Wagner, E., (1998). Polylysine-based transfection system using receptor-mediated delivery. Adv Drug Del Rev 30: 97-113

12

Magnetite Nanoparticles for Cell Lysis Implanted Into Bone - Histological and TEM Study

Patrick Frayssinet[1], Didier Mathon[2],
Marylène Combacau[1] and Nicole Rouquet[1]
[1]*Urodelia, Rte de St Thomas, St Lys,*
[2]*Ecole Nationale Vétérinaire, Toulouse,*
France

1. Introduction

Magnetite nanoparticles are frequently used to eliminate by heating in a high frequence oscillating magnetic field the tumor cells into which they are introduced in order to directly kill the cells or to make them more sensitive to radiotherapy (Ito, A., et al., 2005; Jordan, A., et al., 2001).

The appearance of bone metastases is a sign of a dissemination of primitive cancers. They rapidly become resistant to chemotherapy and radiotherapy and are often very painful necessitating local and/or alternative treatments in order to reduce the osteolysis triggered by the cancerous cells. The osteolysis is due to local activation of the osteoclasts and macrophages by factors synthesized by the tumor cells (Shimamura, T., et al., 2005). It is the osteolysis that is very often responsible for the pain.

We have developed a biomaterial containing magnetite nanoparticles which can be introduced into bone metastases in order to release naked nanoparticles in the contact with both the cancerous and the osteolytic cells. The material is made of a calcium sulphate paste containing a small percentage of nanoparticles which can be injected inside the metastasis (fig. 1). It sets within a few minutes *in situ*. The degradation of the calcium sulphate matrix within a few days releases the nanoparticles which are then available for cell internalisation. *In vitro*, these particles can be internalised in high amounts by metastatic cells from adenocarcinoma. The number of nanoparticles found inside the cells depends on the nanoparticle size, however the mass internalized seems to be almost independent of their size (Frayssinet, P., et al., 2005).

The nanoparticles did not show *in vitro* any signs of cell toxicity. This is consistent with previous reports which showed that cytotoxicity of magnetite nanoparticles could be due to several factors such as coating (Häfeli & Pauer, 1999). Furthermore, they are intented for use in very low doses (a few mgs). The degradation products of iron oxide are well known. They do not have a reported toxicity and are easily eliminated from the organism (Schoepf, U., et al. 1998, Okon, E.E., et al. 2000, Okon, F., et al. 1994).

Migration of the nanoparticles can however be a cause of concern due to the possible unwanted heating of other regions of the organism when submitted to a magnetic field.

When injected as a suspension in the blood, they were shown to be mostly taken up by the spleen and liver in the days following injection (Magin, R.L. et al., 1991). They can also migrate into the lymph nodes when directly injected into tissues.

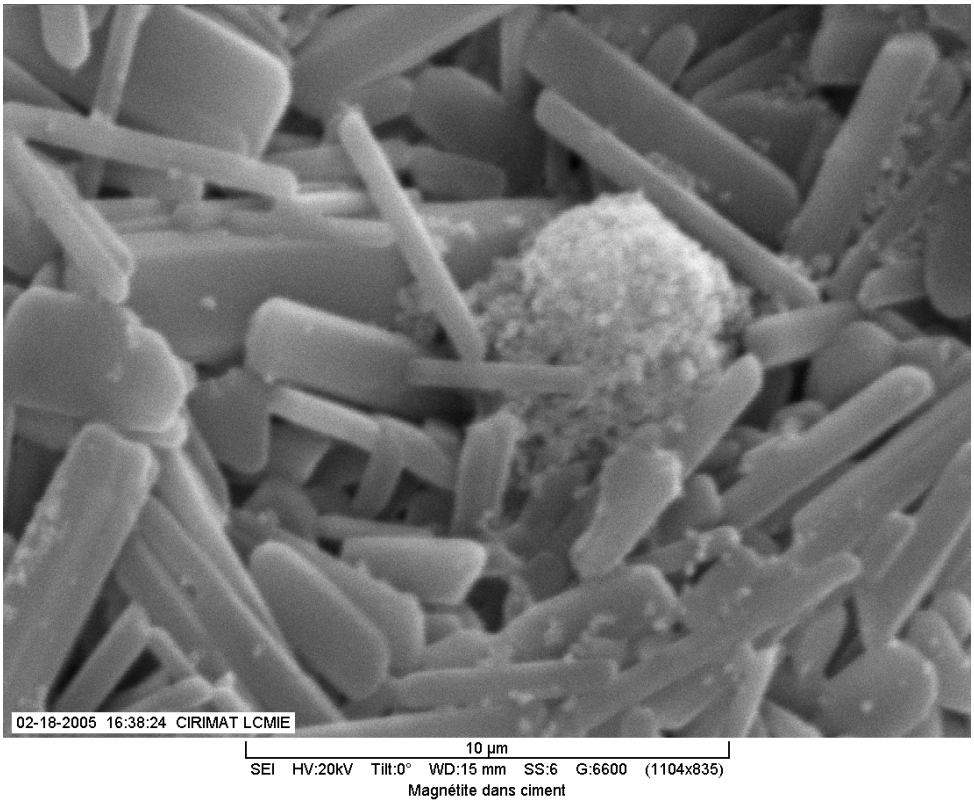

Fig. 1. SEM of calcium sulphate (flat crystals) matrix containing nanoparticles of magnetite. Isolated nanoparticles can be evidenced at the surface of the calcium sulphate crystals or as agregates between the crystals.

We have demonstrated that the nanoparticles used in this device penetrate adenocarcinoma cells by endocytosis *in vitro* (Frayssinet et al. 2004). The aim of this experiment was to check the uptake of these nanoparticles by the various types of bone tissue cells *in vivo,* their migration in the lymphatic tissue and the time *needed* for their *elimination*.
Thus, the nanoparticles were introduced through a bone defect drilled into the cancellous bone while the implantation zone and lymph nodes draining the region were examined by light and transmission electron microscopy.

2. Materials and methods

2.1 animal model

In order not to lose the nanoparticles, they were placed inside an open titanium alloy chamber implanted inside the cancellous bone of external condyles in the sheep. A titanium

alloy was used because it was demonstrated that there was no or a very limited foreign body reaction against this kind of alloy and device implanted inside the bone (Aspenberg et al., 1996). The chamber in which the particles were inserted was tunnel shaped and open at the ends communicating with the bone allowing tissue at all stages of bone regeneration to cross the tunnel and come in contact with the nanoparticles . Using this device it is straight forward to locate the nanoparticles for histological and TEM sections.
The device containing the chamber can be screwed into the cancellous bone to avoid any micromovement between the bone and the chamber which would shear the regenerating tissue. It can also be opened to facilitate the collection of the tissue to analyse (fig. 2).
Two sheep were used for each sample implanted for a 3 weeks. 0.1 mg of sterile nanoparticles were placed inside the chambers which were then implanted in the external condyle by a lateral approach.
After the three-week exposure the animals were killed by a Nembutal injection and the chambers the inguinal and aortic lymph nodes draining the implantation zone retrieved. The operation and the care of the animals followed the European commission guidelines concerning animal experimentation.

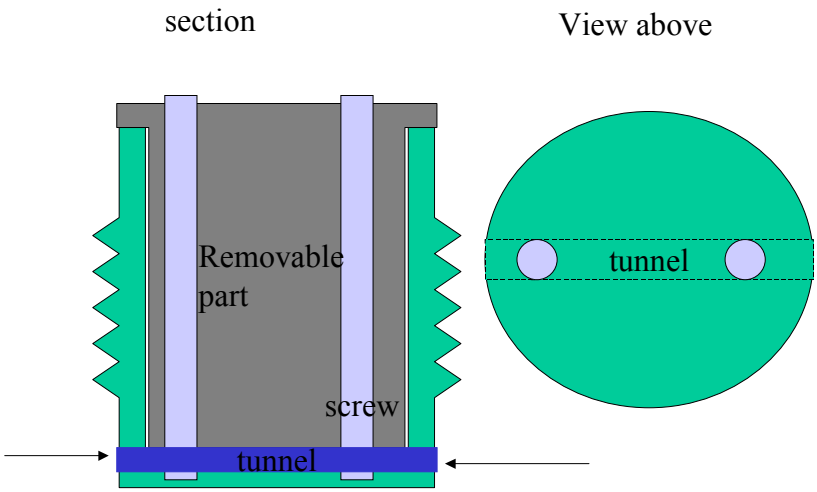

Fig. 2. The titanium device containing the tunnel in which the nanoparticles were introduced was screwed in the cancellous bone of the condyles. The healing tissue ingrews the tunnel according to the arrows. After the implantation period, the removable part was extracted to open the tunnel and the tissue containing the nanoparticles was available for histology.

2.2 Magnetite powder characteristics

The powders were constituted by Fe_3O_4 (99%). Their shape was polyhedral. Three different particle size groups were used: 70 nm, 150 nm, 500nm.

2.3 Histological methods

The retrieved tissues were immediately immersed in isotonic phosphate buffer containing 2% glutaraldehyde for 2 days at 4°C. All the samples were then cut and either processed for light microscopy or TEM.

For light microscopy, the samples were dehydrated in increasingly concentrated ethanol solutions and embedded in hydroxyethyl methacrylate. 5 µm thick sections were cut and coloured with Perl's stain to reveal the nanoparticles in the sections. The tartrate resistant acid phosphatase activity (TRAP) of the cells was evidenced using a commercial leukocyte acid phosphatase kit (Sigma, St Louis, MO).

For TEM, the sections were dehydrated in increasingly concentrated ethanol solution and embedded in an epoxy polymer before ultrathin sections were performed and stained with uranyl acetate. Observations were made at 20 kV.

3. Results

3.1 Bone healing in the titanium tunnels

After the three-week experimental period, the tunnel was filled by loose connective tissue which did not show any signs of ossification.

Under light microscopy, the tissue in the tunnels showed that numerous cells contained nanoparticles. Some of the cells showed a black tattoo while in others the nanoparticles were not visible but were revealed by the blue-grey color of the cell after Perl's staining (fig. 3). The nanoparticles were either contained inside $TRAP^+$ or TRAP- cells. These $TRAP^+$ cells were uniformly dispersed inside the tunnel volume and were not aggregated around the foreign material as is usual for a foreign body reaction (fig. 4). The tissue appearance was the same for the three size of nanoparticles.

Under TEM, all tissues present in the tunnels contained cells loaded with the nanoparticles. It seemed that the smallest particles (70nm) penetrated the cells in larger numbers than the biggest ones (500 nm); at least their density was more uniform inside the cells. The 500 nm sized particles formed smaller aggregates in the cells than the 70 nm ones. These late particles could constitute large aggregates at the contact of which multinucleated cells were found. The cells dissociated or fragmented the aggregates before internalising the nanoparticules (fig. 5).

Inside the cells, the nanoparticles were found inside lysosomes, or phagolysosomes depending on the size of the particle aggregates. There were almost no particles alone inside cell vesicles (fig. 6). They occurred in groups of a few units to several dozen.

3.2 Lymph nodes

Using light microscopy, it appeared in most sections that nanoparticles had migrated to the lymph nodes after the three-week contact. Their number was very low, as only a few cells on each section were blue from Perl's stain. The nanoparticles were not found in the lymphoid follicles but in the capsule and subcapsular sinus. The migration was identical for the three types of nanoparticles.

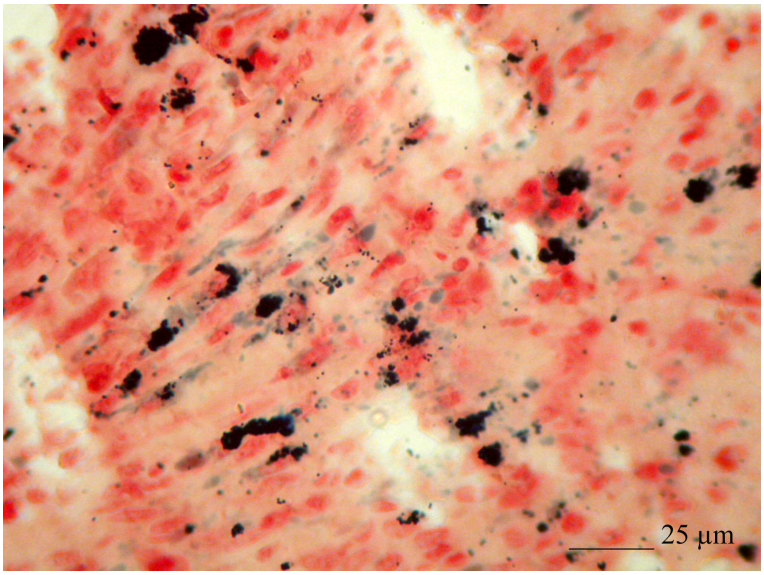

Fig. 3. The particles (70 nm) under light microscopy appear uniformly dispersed in the ingrown tissue in the titanium chambers. They can form aggregates inside the cells which are visible under the microscope or with Perl'staining a kind of blue grey tattoo

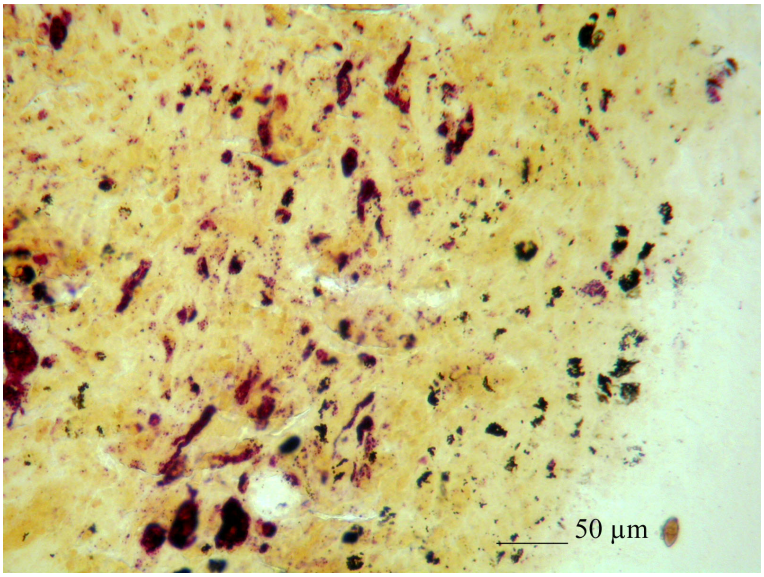

Fig. 4. Section of a Ti chamber containing 70 nm particles showing the TRAP+ cells in red. The particles are not necessarily internalised within the TRAP+ cells.

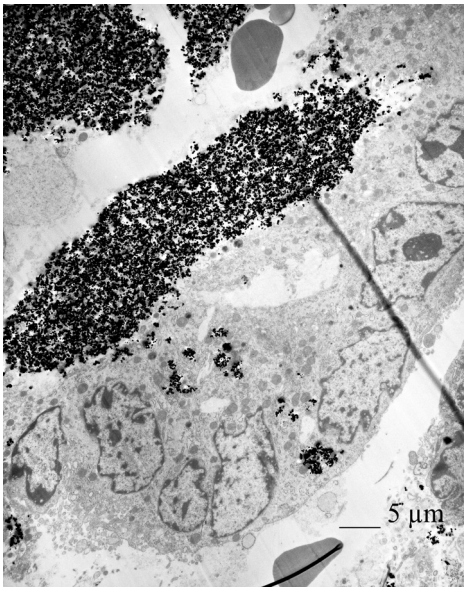

Fig. 5. When aggregates of 70 nm sized nanoparticles are formed, there can be multinucleated cells in contact with the material. The aggregate is dissociated by the cells which internalize the nanoparticles under the form of much smaller groups of particles.

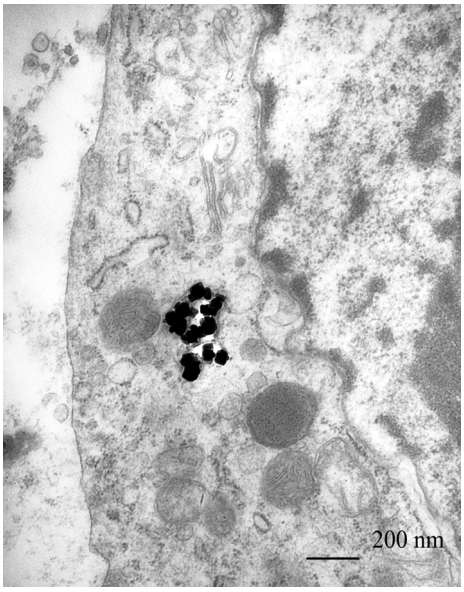

Fig. 6. Inside the cells the magnetite particles are found inside cell vesicles such as endosomes, lysosomes or phago- lysosomes.

By TEM, the nanoparticles were observed in the vesicles of macrophages and lymphocytes (fig. 7, 8,9, 10). All the particles seen in the lymph nodes showed one or several degradation signs. Nanoparticles of all three sizes were found in the lymph nodes, however in very low number.

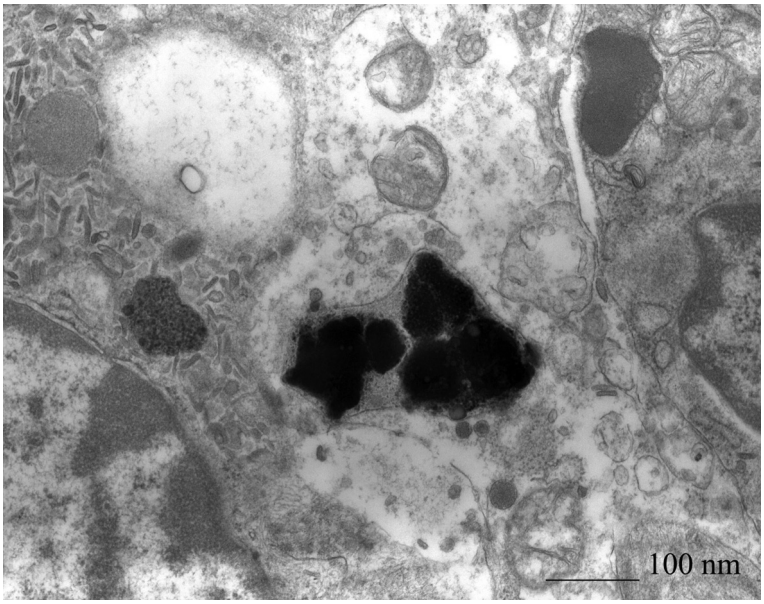

Fig. 7. TEM of 70 nm particles observed inside the lysosome of a lymph node macrophage. The particles show fuzzy edges, a modified shape and some have merged.

3.3 Degradation

Signs of nanoparticle degradation were evidenced both in the bone tissue and the lymph nodes (fig. 7, 8, 9, 10). The degradation took place in the cell vesicles. The big particles were sometimes fragmented. The small ones became fuzzy and lost their shape suggesting that material had dissolved. Very fine and needle like particles were sometimes observed in the periphery of the nanoparticles suggesting precipitation. Most of the particles, whatever their size, showed a modification of the shape and some particles fused together.

4. Discussion

Direct implantation of magnetite nanoparticles into the tumor instead of injection into bloodstream avoids their concentration inside liver, lung or spleen. It allows the use of lower doses of magnetite limiting its toxicity, if any, and side effects such as heating of the reticulo endothelial cells in these organs.

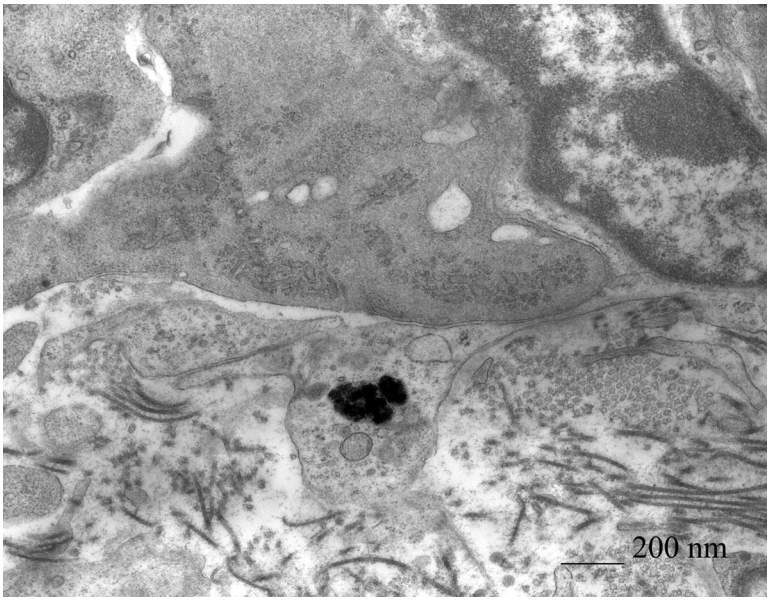

Fig. 8. TEM of 70 nm nanoparticles showing a precipitate formed in the lysosome around the nanoparticles.

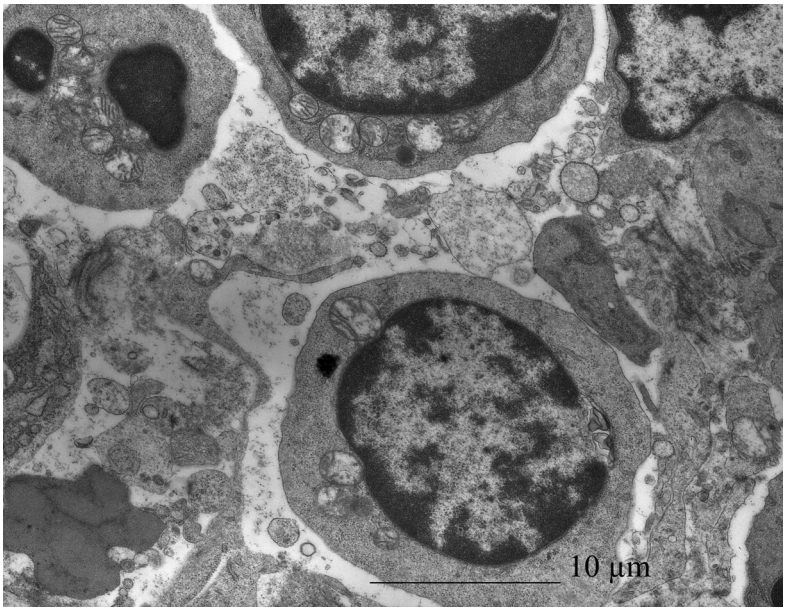

Fig. 9. 70 nm nanoparticles showing degradation signs in vesicles located inside a lymphocyte from a lymph node.

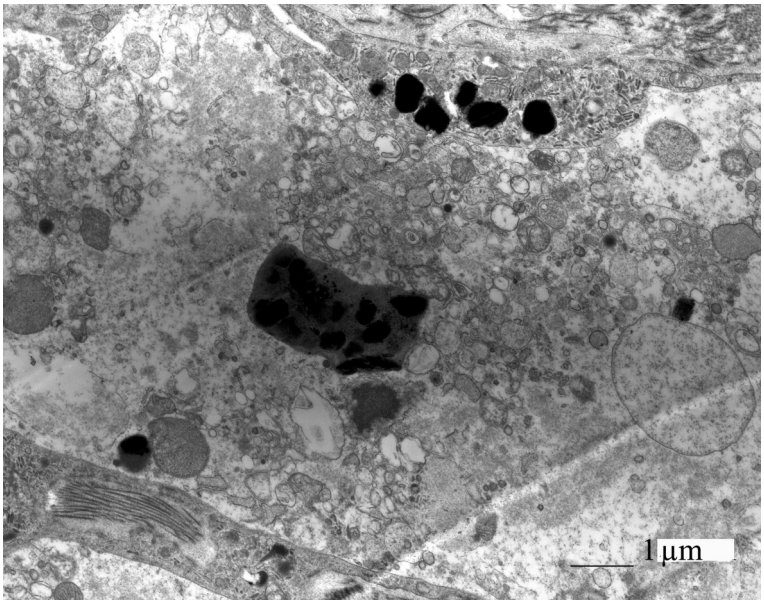

Fig. 10. 500 nm sized particles inside the vesicles of a cell going into apoptosis inside a lymph node. The nanoparticles have lost their shape and show a core surrounded by a fuzzy zone.

This experimentation shows that when implanted into bones the magnetite nanoparticles can migrate within the cells having internalised them. At this time however, the nanoparticles did not seem to be present in sufficient amounts to induce secondary heating as only a few particles appeared in each section of the lymph nodes.

The particles were found inside lysosomes or phagolysosomes. The physico-chemical environment in these vesicles is very aggressive with a low pH and many hydrolytic enzymes (Dell'Angelica et al., 2001). These conditions could explain the degradation of the material which was seen to occur in some of them. It must be noted that magnetite degradation at a low pH has already been demonstrated (Florindo et al., 2003, Gruendle et al., 2002). The rate depends on the pH and the type of acid present.

It is not clear how the endocytosis takes place. There is no indication of specific endocytosis. The amount of nanoparticles endocytosed by non- transformed cells is lower than the amount endocytosed by cancer cells. It is suggested that fast dividing cells show a large particle uptake (Jordan et al., 1999). This means that, in this case, the cells of the regenerating tissue would internalise fewer nanoparticles than bone metastasis cells.

From the TEM pictures it seemed that, when the nanoparticles formed aggregates in the implantation zone, isolated nanoparticles or small groups were able to penetrate inside the cells in contact with the aggregates. This suggests that the cells are able to separate the nanoparticles which are internalized from the aggregates.

There was no true foreign body reaction against this material even when large aggregates formed as TRAP+ cells were uniformly dispersed in the tunnel volume and not aggregated in contact with the material. Furthermore, the internalisation of the particles was not limited

to the TRAP+ cells which are known to be among professional macrophages. This suggests that in bone metastasis these particles can potentially penetrate both the cancer cells and the cells of the monocyte lineage involved in osteolysis.
After three weeks of implantation, the healing tissue was similar to that occurring when there are no particles (Frayssinet, unpublished results). This result must be compared to *in vitro* experiments showing that when grown with a primary line of monocytes the small particles do not trigger the synthesis of cytokines or TGF and so do not activate these cells (Frayssinet, unpublished results) suggesting that the cells do not recognize the magnetite nanoparticle having this range of size as a foreign body.
Breakdown of iron oxides in the organism can form several kinds of degradation products: fragments of the material; salts such as iron chloride or hydroxide; complexes of the salts with organic molecules (Michel, A., Bénard, J., 1964). It was demonstrated that the iron released from magnetite can be incorporated into haemoglobin, erythrocytes or feritin (Weissleder et al., 1989). It is important to know the degradation rate of these nanoparticles and the location of the degradation because the degradation products show altered magnetic properties. Thus, knowing the migration and degradation rates of the material will help avoid heating unwanted zones.
All three types of particles tested migrated from the bone into the lymph nodes, however, the proportion of particles found in the lymph nodes was very low and the percentage of the lymph node cells containing nanoparticles was also very low.
It must also be pointed out that the nanoparticles were not found only in the macrophages of the lymph nodes but also in the lymphocytes.
This has direct consequences on the functionality of the biomaterials using iron oxide as seen to heat tissues under oscillating magnetic fields. The heating ability (SAR) of the nanoparticles decreases within weeks after implantation. Thus, the heating protocol must be performed in a window of time to be specified.
It is also probable that the material does not persist in the organism for a very long time. However, as long as a magnetic core persists in the particles it is possible to follow the migration of the cells containing the particles by MRI; It could be very useful to follow the migration of metastatic cells before they can form a visible tumor by MRI.

5. Conclusions

Magnetite nanoparticles can easily penetrate the cells with which they are in contact whether or not they are professional phagocytes. This property is particularly useful and is the essential rationale for injecting a medical device releasing iron oxide nanoparticles inside a bone metastasis. The aggregation of the magnetic nanoparticles outside the cells does not seem to impair their endo or phagocytosis inside the cells as isolated nanoparticles.
Magnetite nanoparticles able to be used for heating bone tumors can migrate with the cells in which they are internalised. They are degradable in the cell vesicles indicating that they will lose their magnetic properties in a few weeks to months depending on the structural modifications they undergo during their migration through the different cell compartments and the different cells of the site. During this time, their heating properties will decrease but as long as they have some magnetic properties they will be able to serve as a probe to follow the cells migrating from the tumor.

6. References

Aspenberg, P., Tägil, M., Kristensson, C., Lidin, S., (1996) Bone graft proteins influence osteoconduction : A titanium chamber study in rats, Acta orthopaedica Scandinavica, 67: 377-382

Dell'Angelica, E.C., Mullins, C., Caplan, S., Bonifacino, J.S., (2001) Lysosome-related organelles. FASEB J, 14: 1265-78

Florindo, F., Roberts, A.P., Palmer, M.R., Magnetite dissolution in siliceous sediments, (2003) Geochem Geophys Geosyst, 7: 1053

Frayssinet, P., Combacau, M., Gougeon, M., Mathon, D., RouquetN., (2005) Migration and degradation of magnetite nanoparticles in lymph nodes. Society for Thermal Medicine. Annual Meeting, Bethesda. Maryland.

Frayssinet, P., Goujeon, M., Lebugle, A., Boetto, S., Rousset, A., Rouquet, N., (2004) Magnetite nanoparticles for thermal therapy. Influence of the particle size for their uptake in cells of breast carcinoma metastasis. 9th International Congress on Hyperthermic Oncology. April 20-24, 2004, St Louis, Missouri, USA

Gruendle, K.V., Noll, M.R., Magnetite dissolution rates in acidic solutions, The Geological Society of America 2002 Annual Meeting, Denver Colorado, October 2002

Häfeli, U.O., Pauer, G.J., In vitro and in vivo toxicity of magnetic microspheres. Journal of Magnetism and Magnetic Materials, 1999, 194: 76-82.

Ito, A., Shinkai, M., Honda, H., Kobayashi, T., (2005) Medical application of functionalized magnetic nanoparticles, Journal of Bioscience and Bioengineering, 100: 1-11

Jordan, A., Scholz, R., Maier-Hauff, K., Johansen, M., Wust, P., Nadobny, J., Schirra, H., Schmidt, H., Deger, S., Loening, S., Lanksch, W., Felix, R.,(2001) Presentation of a new magnetic field therapy system for the treatment of human solid tumors with magnetic fluid hyperthermia. Journal of Magnetism and Magnetic Materials, 225: 118-126

Jordan, A., Scholz, R., Wust, P., Schirra, H., Schiestel, T., Schmidt, H., Felix, R., (1999) Endocytosis of dextran and silan-coated magnetite nanoparticles and the effect of intracellular hyperthermia on human mammary carcinoma cells in vitro. Journal of Magnetism and Magnetic Materials, 194: 185-196.

Magin, R.L., Bacic, G., Niesman, R.L., Alameda, J.C., Wright, S.M., Swartz, S.W., (1991). Dextran magnetite as a liver contrast agent. Magnetic Resonance in Medicine, 20: 1-16.

Michel, A., Bénard, J., in: Chimie Minérale. Généralités et Etude Particulière des Eléments. Masson et Cie eds. Paris 1964 : 646-49

Okon, F., Pouliquen, D., Okon, F., Kovaleva, Z.V., Stepanova, T.P., Lavit, S.G., Kudryavtsev, B.N., Jallet, P., Biodegradation of magnetite dextran nanoparticles in the rat. A histologic and biophysical study, Lab Invest, 1994, 71: 895-903.

Okon, E.E., Pulikan, D., Pereverzev, A.E., Kudriavtsev, B.N., Zhale, P., Toxicity of magnetite-dextran particles: morphological study. Tsitologia, 2000, 42: 358-366

Schoepf, U., Marecos, E.M., Melder, R.J., Jain, R.K., Weissleder, R., Intracellular magnetic labelling of lymphocytes for in vivo trafficking studies, Biotechniques, 1998, 24 : 642-646.

Shimamura, T., Amizuka, N., Li, M., Freitas, P.H.L., White, J.H., Henderson, J.E., Shingaki, S., Nakajima, T., (2005) histological observations on the microenvironment of

osteolytic bone metastasis by breast carcinoma cell line. Biomedical Research, 26, 159-172

Weissleder, R., Stark, D.D., Engelstad, B.L., Bacon, B.R., Compton, C.C., White, D.L., Jacobs, P., Lewis, J., (1989) Superparamagnatic iron oxide: pharmacokinetics and toxicity. AJR, 152: 167-173

Part 3

New and Classical Materials for Biomedical Use

13

Polysaccharides as Excipients for Ocular Topical Formulations

Ylenia Zambito and Giacomo Di Colo
University of Pisa
Italy

1. Introduction

The topical treatment of extraocular or intraocular diseases, especially by eye drops, is the best accepted by patients. Treatment with eye drops, however, poses the issue of a poor drug bioavailability because the precorneal area, i. e., the site of drug action/absorption, is rapidly cleared of drugs by protective mechanisms of the eye, such as blinking, basal and reflex tearing, and nasolachrymal drainage. This implies the need of frequent instillations, and hence, the risk of side effects. Increasing ocular bioavailability remains a stimulating challenge for the formulators of topical systems. An approach to the task has been the reduction of drainage rate by increasing the viscosity of liquid preparations (Lee & Robinson, 1986) or resorting to mucoadhesive polymers (Hui & Robinson, 1985). The ability of a polymer to improve the ocular bioavailability of drugs by adhering to the ocular surface and binding the drug to it is a more promising property than the polymer viscosifying power (Di Colo et al., 2009), so far as fluid solutions are better tolerated than viscous ones (Winfield et al., 1990). The ocular retention of drugs administered by eye drops is also potentially improved by colloidal drug carriers, such as liposomes, submicron emulsions, nanoparticles and nanocapsules. The drugs are incorporated into these submicron particles which can be internalized into the corneal and/or conjunctival cells of the ocular epithelium (Alonso & Sanchez, 2009; Nagarwal et al., 2009). Prolonging the residence of drugs in the precorneal area serves either the extra- or intraocular therapy. In those cases where a well tolerated topical treatment is desired to implement an intraocular therapy, the ocular formulation can be made to contain an effective, biocompatible, non-irritant polymeric corneal permeability enhancer.

A description of the structures of the eye that come into contact with topical drug delivery systems has been reported recently (Ludwig, 2005). A summary is given in the next section, followed by an outline of the routes of intraocular drug penetration. Polysaccharides such as chitosan, xyloglucan, arabinogalactan, cellulose derivatives (methylcellulose, hydroxyethylcellulose, hydroxypropylmethylcellulose, sodium carboxymethylcellulose), hyaluronic acid, alginic acid, gellan gum, have been studied extensively as excipients for ocular formulations. In the present survey of the literature the relevant properties of polysaccharides will be presented and discussed, with emphasis on the functions of polymers in the ophthalmic formulations where they have been used. Only polysaccharides the ocular tolerability of which has been ascertained will be dealt with.

2. Anatomy and physiology of the eye

2.1 Structure of the ocular globe

The human eye is schematically shown in Fig.1. The wall of the eyeball consists of an outer coat (sclera and cornea), a middle layer (uveal coat) and an inner coat (retina). The eyelids spread the tear fluid over the eye. The rate of shear during blinking (about 20,000 s^{-1}) influences the rheological properties of instilled ophthalmic formulations and hence, drug bioavailability.

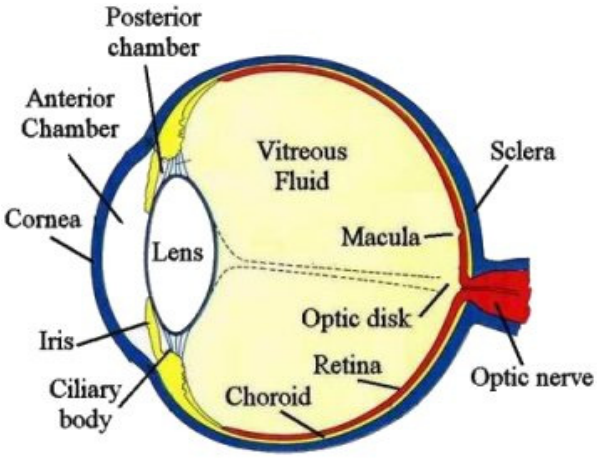

Fig. 1. Schematic view of the human eye

The cornea is a clear, avascular tissue composed of five layers: epithelium, Bowman's layer, stroma, Descemet's membrane and endothelium. The epithelium consists of 5-6 cell layers. The corneal epithelium is little permeable due to the presence of tight junctions connecting cells. High extracellular and low intracellular calcium levels are required for the low permeability of tight junctions. On the surface of the epithelium flattened cells are found microvilli which enhance the stability of the tear film.

The conjunctiva is a clear membrane, lining the inner surface of the eyelids, adjoining the corneal epithelium. The conjunctiva is vascularized and moistened by the tear film. Its epithelium is composed of 5-7 cell layers. The cells are connected by tight junctions, therefore the conjunctiva is impermeable to molecules larger than 20,000 Da, whereas the cornea is permeable up to 5000 Da.

A volume of about 2-3 μL of mucus is secreted daily whereby foreign particles and bacteria are entrapped and swept by blinking to the drainage system for discharge. The turnover of the mucous layer (15-20 h) is much slower than that of the tear fluid.

2.2 Nasolachrymal drainage system

The tear fluid is spread on the ocular surface by blinking and collected by the canaliculi, the lachrymal sac and the nasolachrymal duct which opens into the inferior nasal passage. The tear fluid produced by the lachrymal gland is composed of the following:

1. Basic tearing (0.5-2.2 μL/min), needed to maintain a tear film on the corneal surface, corresponding to a turnover rate of 16%/min while awake.

2. Reflex tearing, caused by such stimuli as emotional, chemical or mechanical ones, cold temperature, light, which can raise lachrymation up to 300 μL/min, thus clearing drugs away.

Undesired drug absorption through nasal mucosa can occur during drainage.

2.3 Tear film

The precorneal tear film (thickness 3-10 μm; volume ~10 μL) is composed of the following layers:

The superficial lipid layer (thickness 100 nm), which spreads over the aqueous layer during eye opening. It contains such lipids as triglycerides, phospholipids, sterols, sterol esters, fatty acids, and helps tear fluid to maintain its normal osmolality by limiting evaporation.

The aqueous layer, which contains inorganic salts, glucose, urea, retinol, ascorbic acid, proteins, lipocalins, immunoglobulins, lysozyme, lactoferrin and glycoproteins. The tear fluid has an osmolality of 310-350 mOsm/kg and a mean pH of 7.4. Its buffering ability is determined by bicarbonate ions, proteins and mucins. The viscosity is ~3 mPas, with a non-Newtonian rheological behaviour. The surface tension is ~44 mN/m.

The mucus layer, which forms a gel with viscoelastic properties. Mucins improve the spreading of the tear film and enhance its stability and cohesion. The mucus gel entraps bacteria, cell debris and foreign bodies forming bundles of thick fibers, which are conveyed by blinking to the inner canthus and expelled onto the skin. Mucus, which is charged negatively, can bind positively charged substances.

More recent studies have somewhat revised the above "three layers theory", proposing a 40-μm thick film essentially made of mucus with an external lipid layer, but without a distinct thin aqueous layer. Mucus is made of glycoproteins (mucins), proteins, lipids, electrolytes, enzymes, mucopolysaccharides and water. As the polysaccharide side chains of mucins usually terminate in sialic acid (pKa 2.6) the mucins are negatively charged in physiological conditions. A combination of cross-linking via disulfide bridges and hydrophobic bonds and also through entanglements of randomly coiled macromolecules determines the tertiary structure of mucin.

Various factors influence the mucoadhesion of polymeric ocular delivery systems, linked to the composition, physicochemical properties and structure of the tear film. The polymer must come into intimate contact with the mucus layer. The polymer chains must be mobile and flexible enough to interpenetrate into the mucus to a depth sufficient to create a strong entangled network with mucin. The polymer and mucin should interact by hydrogen bonding, electrostatic and hydrophobic interactions which depend on the ionic strength and pH of the applied vehicle. Decreasing the pH enhances the mucoadhesion of polymers containing carboxyls because these groups preferentially interact with mucins in the unionized form via hydrogen bonding. On the other hand, the repulsion of carboxylate anions which form at higher pH values causes extension of polymer chains and decrease in density of such chains, which result in enhancement of chain mobility, interdiffusion and physical entanglement. Depending on the pKa of the functional groups of the polymer, either hydrogen bonding or entanglement prevails. Then, the precorneal residence of mucoadhesive polymers varies from a few hours to one day.

The tear film is not quite stable. In the short interval between blinks it ruptures with formation of dry spots on the cornea, which induces blinking and spreading of a new tear film. The breakup time of the tear film depends on dispersion forces, interfacial tension and

viscous resistance of the mucus layer. These factors should be taken into account when developing mucoadhesive pharmaceutical systems.

3. Routes of intraocular penetration

Drugs penetrate across the epithelium into the eye *via* the transcellular (lipophilic drugs) or paracellular (hydrophilic drugs) route (Nanjawade et al., 2007). The main mechanism of transepithelial either transcellular or paracellular intraocular penetration of topically applied drugs is passive diffusion along their concentration gradients. The cornea provides the rate-limiting resistance against penetration of hydrophilic drugs, whereas partitioning from the epithelium into the hydrophilic stroma is the rate-liming factor for lipophilic drugs (Nanjawade et al., 2007). Permeation of ionizable drugs depends on the chemical equilibrium between ionized and unionized species in the tear fluid. The unionized species usually penetrates more easily than the ionized species. In the latter instance the type of charge affects transcorneal penetration. Indeed, the corneal epithelium is negatively charged, in physiological conditions (pH 7.4), hence cationic drugs permeate more easily than anionic ones (Nanjawade et al., 2007). In addition to the corneal route, topically applied drugs may be absorbed *via* non-corneal routes. Hydrophilic and large molecules, showing poor corneal permeability, can penetrate across the bulbar conjunctiva and underlying sclera into the uveal tract and vitreous humor (Nanjawade et al., 2007). Tight junctions of the superficial conjunctival epithelium are wider than those in the cornea, therefore, the conjunctival permeability of hydrophilic drugs is generally significantly higher than their corneal permeability (Nanjawade et al., 2007). However, the conjunctiva is vascularized, therefore it is generally considered a site for systemic, hence, unproductive absorption.

4. Polysaccharides in ocular formulations

The use of natural polysaccharides in ocular formulations is attractive as these products are economical, readily available, non-toxic, potentially biodegradable, generally biocompatible and capable of chemical modifications. Such modifications have recently led to derivatives with improved biopharmaceutical performances, e.g. rhelogical behavior, mucoadhesivity, ability to enhance corneal permeability, easy solubilization.

4.1 Chitosan and its derivatives

Chitosan (Ch) is a linear polysaccharide composed of randomly distributed β-(1-4)-linked D-glucosamine (deacetylated unit) and N-acetyl-D-glucosamine (acetylated unit) (Fig.2).

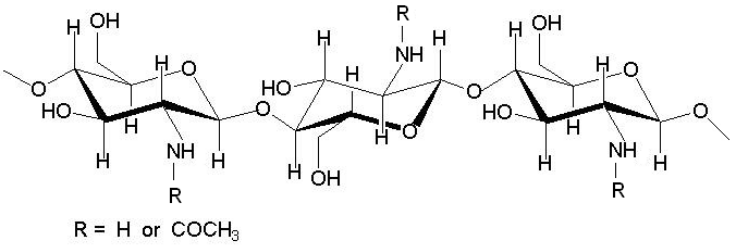

Fig. 2. Chitosan structure

Ch is produced commercially by deacetylation of chitin, which is the structural element in the exoskeleton of crustaceans (crabs, shrimps, etc.) and cell walls of fungi. The degree of deacetylation in commercial Chs is in the range of 60-100 %. The tremendous potential of Ch in the pharmaceutical area is illustrated in several review articles (Alonso & Sanchez, 2009; Nagarwal et al., 2009; Dodane & Vilivalam, 1998; Felt et al., 1998; Paul & Sharma, 2000; Singla & Chawla, 2001, Di Colo et al., 2008). These point out that Ch is biodegradable, has low toxicity and good ocular tolerability, exhibits bioadhesion and permeability-enhancing properties and also physico-chemical characteristics that make it suitable for the design of ocular drug delivery vehicles. The Ch repeating unit bears a primary amino group bestowing a reactivity on the polymer that allows its transformation into derivatives of interest as biocompatible and bioactive excipients for ophthalmic drug delivery systems (Di Colo et al., 2004a; Zambito et al., 2006a; Zambito et al., 2007). Over the last decade efforts have been made to put into evidence the ability of Ch to safely promote intraocular drug penetration by enhancing corneal permeability, and to synthesize Ch derivatives with improved such bioactivity. The significant results of these efforts will be discussed in the next subsections.

4.1.1 Eye drops

The main role of Ch in ocular solutions was to improve ocular drug bioavailability by prolonging drug residence in precorneal area in virtue of polymer mucoadhesivity and effect on viscosity (Alonso & Sancez, 2009). More recently Ch solutions have been investigated for their ability to improve intraocular drug bioavailability, following topical administration, by enhancing corneal permeability. Although the ability of Ch to permeabilize nasal mucosa and intestinal epithelium has been known since 1994 (Illum et al., 1994; Artursson et al., 1994) the permeabilizing effect of this polymer applied via eye drops on the cornea was demonstrated for the first time ten years later (Di Colo et al., 2004b). Unlike the intestinal and nasal epithelia, both made of a single layer of cells joined by tight junctions, the cornea is a stratified epithelium the cells of which also are joined by tight junctions. Therefore, the ability of Ch to enhance the permeability of intestinal and nasal epithelia would not necessarily imply a similar effectiveness on the corneal epithelium.

Instead of using the excised cornea, as in previous studies of the enhancement of corneal permeability to drugs, the permeabilizing effect of Ch was investigated *in vivo* (Di Colo et al., 2004b) . To this purpose, ofloxacin was instilled into the eyes of albino rabbits via isoviscous eye drops containing Ch hydrochloride (Ch-HCl), or *N*-carboxymethyl Ch (CMCh) (Muzzarelli et al., 1982), or poly(vinyl alcohol) (PVA), and the resulting pharmacokinetics in tear fluid and aqueous humor were determined (Di Colo et al., 2004b). CMCh, a polyanion at the physiological pH of the tear fluid (Fig.3), was tested to ascertain the relevance of the polycationic nature of Ch-HCl and because CMCh was claimed to behave as an intestinal absorption enhancer (Thanou et al., 2001).

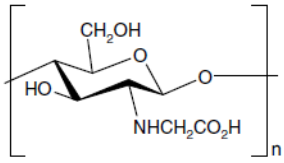

Fig. 3. Structure of *N*-carboxymethyl chitosan.

Only small differences among the rates of drug disappearance from tear fluid were measured for the three solutions, reflecting the small differences among the respective viscosity values. Such values were high enough to ensure the presence of drug in tear fluid at measurable concentrations after about 1.5 h of instillation. Although the time of drug residence in the precorneal area was almost the same for the three solutions containing Ch-HCl, CMCh or PVA, the respective pharmacokinetic data for the aqueous humor were neatly distinct. This was taken as a sign of different effects of polymers on the corneal permeability. PVA produced an increase of t_{max} with respect to the reference Exocin®, which was ascribed to the increased viscosity of the PVA solution with respect to the commercial eye drops, causing a reduction of tear fluid drainage, and hence, of the precorneal elimination rate. This polymer, however, produced no permeabilization of the cornea, indeed, there was no significant increase of neither concentration peak (C_{max}) nor bioavailability (AUC) in the aqueous. On the other hand, Ch-HCl produced C_{max} and AUC values remarkably higher than the respective values for the reference, at the same t_{max}. Then unlike the case of PVA, with Ch-HCl the increased viscosity of the solution was found to cause no prolongation of t_{max}. These pharmacokinetic data were taken as indicative of an increase of the corneal absorption rate constant, due to an enhancement of corneal permeability by Ch-HCl.

More recently the effects of Ch and other non-polymeric permeabilizers on the permeation of acyclovir across excised rabbit cornea have been studied (Majumdar et al., 2008). Ch was solubilized at the concentration of 0.1 or 0.2% by 2% acetic acid added to Dulbecco's phosphate buffered saline. The apparent corneal permeability (P_{app}) was determined by normalizing the permeant flux to the permeant concentration in the donor. In the presence of 0.2 and 0.1% Ch the transcorneal acyclovir permeability was enhanced almost 5.8-fold (7.61×10^{-6} cm/s) and 3.1-fold (4.1×10^{-6} cm/s), respectively, over that of acyclovir alone (1.32×10^{-6} cm/s).

The use of unmodified Ch in eye drops as a cornea-permeabilizing agent is not quite rational because of problems with its solubility in tear fluid at the physiological pH of 7.4. Although Ch-HCl is in the dissolved, and hence, bioactive state just as applied, yet its permeability-enhancing effect is presumably temporary. Indeed Ch requires $pH \leq 5$ for dissolution, hence it is expected to precipitate as the free base some time after instillation, as soon as the physiological pH of the tear fluid is restored. For this reason the effect of CMCh, a polyanionic Ch derivative soluble at this pH (Fig.3), on transcorneal drug absorption is of particular relevance. Although CMCh was found to behave as an intestinal absorption enhancer (Thanou et al., 2001) , it failed to significantly enhance corneal permeability, in fact, the drug levels produced in the aqueous by CMCh never exceeded the C_{max} for the reference Exocin® (Di Colo et al., 2004b). Then it appears that the polycationic nature of Ch is essential to its permeabilizing effect on the cornea. Interestingly, however, the drug concentration in the aqueous *vs.* time data relative to CMCh pointed to zero-order transcorneal absorption kinetics. This observation prompted the hypothesis that CMCh might mediate a pseudo-steady-state transcorneal transport, via polymer interactions with the drug and polymer adhesion to the corneal mucus (Di Colo et al., 2004b). Such a mucoadhesion could prolong the drug residence at the absorption site. Despite the different effects of Ch-HCl and CMCh on ofloxacin ocular pharmacokinetics, these polymers increased the drug intraocular bioavailability with respect to the reference by about the same factor, as shown by the relevant AUC values. CMCh, being a polyanion, is potentially able to bind cationic drugs. Then it can prolong the precorneal residence of, e.g., aminoglucoside antibiotics at effective antimicrobial concentrations, thus allowing reduction of the frequency of instillations.

Polycationic derivatives of Ch, soluble in tear fluid at the physiological pH of 7.4, can have an increased potential for enhancing the corneal permeability (Di Colo et al., 2004a). A similar derivative, i.e., *N*-trimethylchitosan (TMC), has been obtained by quaternizing the primary amino group of Ch with methyl iodide, thus bestowing fixed, pH-independent positive charges on the polymer (Fig.4). The complete quaternization is unnecessary to make the polymer soluble at neutral or alkaline pH, in fact, a quaternization degree (QD) of around 40% is sufficient for this purpose (Snyman et al., 2002; Di Colo et al., 2004a). TMC has proved a potent permeation enhancer of hydrophilic molecules and macromolecules across the intestinal epithelium in neutral environments (Kotzé et al., 1997; Kotzé et al., 1998; Thanou et al., 2000). A study of the enhancing effects of TMC polymers having varying QD on the permeation of the hydrophilic mannitol or PEG 4000 across epithelial cell monolayers (Caco-2) demonstrated the existence of an optimum QD, beyond which the permeability was no further increased (Hamman et al., 2003).

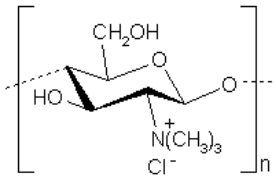

Fig. 4. Structure of *N*- trimethylchitosan.

It has been shown that TMC is able to enhance the permeability of the rabbit corneal epithelium reconstituted *in vitro* (RRCE) to ofloxacin. A dependence of such a permeabilizing ability on the QD of TMC, similar to that found previously with the Caco-2 intestinal epithelium model (Hamman et al., 2003), has been evidenced (Di Colo et al., 2004a). The steady-state flux of ofloxacin across the RRCE in the presence of TMCs having different QDs was measured and P_{app} values were calculated by dividing such a flux by the drug concentration in the applied solution (0.001% w/v, not cytotoxic to the RRCE cells). The P_{app} enhancement was calculated as the ratio of the P_{app} value in the presence to that in the absence of polymer (enhancement ratio, ER). TMC polymers having low QD (3-4%) were barely soluble and ineffective, whereas those having intermediate QD (35-45%) were soluble and significantly bioactive (ER 1.5-1.6). TMC polymers having high QD (80-90%) showed no further increase of permeability (ER 1.5) (Di Colo et al., 2004a). To explain these findings the following hypotheses may be put forward (Di Colo et al., 2004a; Hamman et al., 2003). At intermediate QD TMC has favorable chain flexibility and conformation whereas at higher QD the TMC electrostatic interactions with the epithelial cell membrane may be hindered by steric effects of the attached methyl groups. Another explanation may be the saturation of the interaction sites on the membrane. A polycationic polysaccharide, i.e., the fully quaternized N-methyl-diethylaminoethyl dextran (MeDEAED) was tested for its ability to permeabilize the RRCE. Although MeDEAED has similar charge density and molecular weight as the TMC having QD 80%, yet only the latter produced a significant P_{app} increase on the RRCE (Di Colo et al., 2004a). This means that charge density and MW are not the sole properties of Chs that concur to determine the ability of these polysaccharides to promote transcorneal drug absorption.

The TMC polymers with intermediate QD, which had proven effective on the RRCE, were also tested *in vivo*, in the eyes of albino rabbits. The polymers were synthesized from Chs of MW 580 kDa (TMCL) and 1460 kDa (TMCH), respectively, in order to investigate the relevance of MW to the polymer bioactivity. The pharmacokinetic data for ofloxacin obtained in the presence of these derivatives were compared with those obtained with Ch-HCl (Di Colo et al., 2004a; Di Colo et al., 2004b). For making these comparisons indicative of the relative bioactivity of polymers all solutions were made isoviscous using PVA, which had been shown to be inert on the cornea (Di Colo et al., 2004b). A significant enhancement of transcorneal absorption rate was produced by TMCH, i.e., the Ch derivative with higher MW, through an increase of corneal permeability, as could be deduced from increases of drug bioavailability and peak concentration in the aqueous (AUC and C_{max}, respectively) by 283 % and 318 %, respectively, over the control. Such an enhancement was also indicated by a shortening of the time to peak (t_{max}). In the presence of TMCH the C_{max} exceeded 4 μg/ml, which is the $MIC_{90\%}$ for the more resistant ocular pathogens (Taravella et al., 1999). On the basis of this consideration, TMCH can be regarded as a potential absorption enhancer to be formulated into ophthalmic ofloxacin solutions for the topical treatment of endophthalmitis. A comparison of the data for TMCH with those for Ch-HCl showed that the permeabilizing effect of the partially quaternized derivative is stronger that that of the hydrochloride of unmodified Ch. This was indeed predicted in the foregoing discussion on the basis of considerations about polymer solubility. Data for TMCL showed that for this derivative C_{max} was significantly lower and t_{max} longer than the corresponding values for TMCH, which points to a weaker enhancing effect of TMCL. The stronger effect of the derivative having the higher MW was ascribed to its stronger adhesion to the corneal mucus (Di Colo et al., 2004a). Indeed it was reported that mucoadhesion, along with the opening of tight junctions, is a key element of TMC polymers for being effective as absorption enhancers at mucosal surfaces (Snyman et al., 2003).

The absorption-enhancing efficacy of TMC was thought to depend on its charge density which, in neutral or alkaline environments, is determined by its quaternization degree (Hamman et al., 2003). In the light of this consideration, novel chitosan derivatives with pendant quaternary ammonium groups were prepared by reacting Ch with 2-diethylaminoethyl chloride (DEAE-Cl) under different conditions (Zambito et al., 2006b). The general structure of these derivatives, assessed by NMR analysis, is depicted in Fig.5.

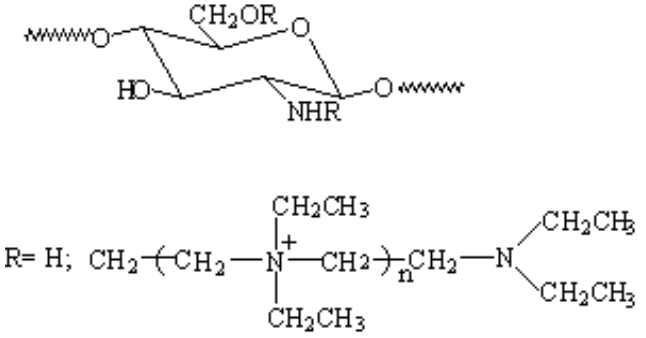

Fig. 5. Structure of N,O-[N,N-diethylaminomethyl(diethyldimethylene ammonium)$_n$methyl] chitosans.

They are assigned the general code, N^+-Ch, referring to their nature of quaternary ammonium (N^+)-chitosan (Ch) conjugates. The degree of substitution by the pendant chain (DS) and the mean number of quaternary ammonium groups in the chain (n) depend on the MW of the starting Ch and on the molar ratio between reactant (DEAE-Cl) and Ch repeating unit, used in the synthesis. A Ch from shrimp shell (MW=590 kDa), with a reagent excess of 4:1 yielded a derivative, N^+-Ch-4, with values of the parameters, DS and n, higher than those of N^+-Ch-2, obtained with a reagent excess of 2:1 (DS=132, n= 2.5 *vs.* DS=40, n=1.6). The transcorneal penetration-enhancing properties of N^+-Ch-2 and N^+-Ch-4 were tested *ex vivo* on the excised rabbit cornea, using the lipophilic dexamethasone and the hydrophilic fluorescein sodium as permeabilization probes (Zambito et al., 2007). The results were compared with corresponding data obtained with a TMC having a QD of 46%, synthesized from the same Ch as that used to prepare the N^+-Ch conjugates. Dexamethasone was applied on the cornea as a suspension, hence the relevant P_{app} values were calculated by dividing the steady-state flux by the drug aqueous solubility. A significant binding of fluorescein to the Ch derivatives was measured by a dynamic dialysis technique, so the concentration of free fluorescein applied to the cornea was used to calculate the relevant P_{app}.

TMC and the N^+-Ch derivatives of whichever DS and n, each at the concentration of 1% w/v, enhanced the P_{app} of the hydrophobic dexamethasone across the excised cornea to about the same extent. On the other hand the *ER* value for the hydrophilic probe fluorescein sodium was the lowest with N^+-Ch-2 (the less substituted), intermediate with TMC, and the highest with N^+-Ch-4 (the more substituted). The apparent difference between the polymer effects on the corneal permeability of dexamethasone and fluorescein reflects the difference in the corneal structures on which the effects were probably exerted, that is, the membrane of the corneal cells, in the case of dexamethasone, and the tight junctions connecting the corneal cells, in the case of fluorescein (Zambito et al., 2007).

N^+-Ch-4 has been tested for its ability to promote the intraocular penetration of dexamethasone or fluorescein *in vivo*, in rabbit eyes (Zambito et al., 2007). The intraocular availability of dexamethasone was much higher than that of fluorescein in the reference eye drops. This reflected a much better partitioning of the lipophilic dexamethasone in the corneal cell membrane. In fact, fluorescein transcorneal penetration from the reference eye drops was almost insignificant essentially because of a poor partitioning of the permeant in the cornea. N^+-Ch-4 significantly enhanced intraocular absorption of fluorescein. In fact the results of the *ex vivo* and *in vivo* experiments agree in indicating a much stronger enhancement effect of this polymer on fluorescein than on dexamethasone. Yet the enhanced P_{app}, AUC and C_{max} values for fluorescein, which reflect the enhanced availability of this highly polar drug model in the aqueous humor, remained lower than the respective values for the non-polar dexamethasone. This means that the paracellular route across the cornea, which is the more likely for very polar molecules, such as fluorescein sodium, remains difficult to penetrate despite the permeabilizing action of the Ch derivatives. On the other hand the use of such enhancers as TMC and N^+-Ch conjugates may turn profitable for improving the effectiveness of existing commercial ophthalmic formulations of such drugs as dexamethasone and ofloxacin.

As in the cases of protonated or quaternized Chs, the activity of which as epithelial permeability enhancers is now well documented (see, e.g., Di Colo et al., 2008), an electrostatic interaction with negatively charged sites in the mucus, on the cell membranes, or in the tight junctions joining epithelial cells is supposed to be at the basis of the bioactivity of the N^+-Ch conjugates. The more significant representatives of these derivatives

are characterized by degrees of substitution of 40-60% (Zambito et al., 2008). The comparatively high fraction of free, unsubstituted primary amino groups still available on the polymer backbone has been used for covalent attachment of thiol-bearing compounds, via formation of 3-mercaptopropionamide moieties. This has led to water-soluble thiolated quaternary ammonium-Ch conjugates (N^+-Ch-SH) the epithelial permeability-enhancing potential of which was tested using the Caco-2 cell monolayer and the excised rat jejunum as substrates (Zambito et al., 2009). On the basis of the obtained results the quaternary ammonium groups of these derivatives were ascribed the ability to reversibly open the epithelial tight junctions and also perturb the plasma membrane of the epithelial cells. On their part the thiol groups were believed to keep the polymer adherent to the epithelium by reacting with the thiols of the epithelial mucus to form disulphide bonds thus favouring the permeability-enhancing action of the positive ions. An N^+-Ch conjugate with DS=60% and n=1.7 was used to synthesize a multifunctional non-cytotoxic thiomer carrying 4.5% thiol-bearing 3-mercaptopropionamide besides quaternary ammonium groups (Fig.6).

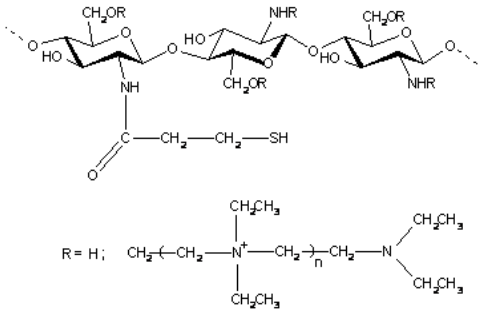

Fig. 6. Strcture of thiolated quaternary ammonium-Ch conjugates

The potential of this N^+-Ch-SH thiomer and the parent N^+-Ch as bioactive excipients for dexamethasone eye drops was evaluated. The drug permeability across excised rabbit cornea was enhanced over the control value by the thiomer and the parent polymer to about the same extent (3.8 vs. 4.1 times). The mean precorneal retention time (MRT) and AUC in the aqueous of dexamethasone instilled in rabbit eyes *via* eye drops were enhanced by the thiomer (MRT=77.96±3.57 min, AUC=33.19±6.96 μg ml^{-1} min) more than the parent polymer (MRT=65.74±4.91 min, AUC=21.48±3.81 μg ml^{-1} min) over the control (MRT=5.07±0.25 min, AUC=6.25±0.65 μg ml^{-1} min). The quaternary ammonium ions were responsible for both permeabilization of corneal epithelium and polymer adhesion to precorneal mucus, while the thiols increased the latter. This synergistic action is the basis of the higher thiomer bioactivity *in vivo* (Zambito & Di Colo, 2010).

4.1.2 In situ-gelling systems

It is now known that prolonged-release ocular inserts, though causing some discomfort to patients, can remarkably increase the drug ocular bioavailability with respect to the traditional eye drops (Saettone & Salminen, 1995; Di Colo et al., 2001a; Di Colo et al., 2001b). It was found that ocular inserts based on poly(ethylene oxide) (PEO) immediately after application in the lower conjunctival sac of the rabbit eye formed mucoadhesive gels, well

tolerated by the animals; then the gels spread over the corneal surface and eroded (Di Colo et al., 2001a; Di Colo et al., 2001b). In order to evaluate the potential of Ch as an intraocular drug absorption promoter ofloxacin was selected as a drug of practical interest and Ch-HCl microspheres medicated with this drug were dispersed into PEO (MW 900 kDa) in the PEO-Ch-HCl (9:1) wt proportion. Erodible ocular inserts, each containing a dose of 0.3 mg ofloxacin, were obtained by compression of the mixture. They were fairly tolerable in the precorneal area of rabbits. The ofloxacin concentration profiles in the aqueous, following administration of a 0.3 mg dose by the PEO-Ch-HCl (9:1) insert, or a medicated PEO insert not containing Ch-HCl, or commercial Exocin eye drops were obtained along with the relevant pharmacokinetic data ($C_{max,}$ t_{max}, AUC) (Di Colo et al., 2002).
As expected, the inserts produced remarkable (one order of magnitude) increases of the AUC values, hence of intraocular bioavailability, over the commercial eye drops. The medicated Ch-HCl microspheres dispersed in the PEO insert produced no substantial bioavailability change with respect to the plain PEO insert. However, with the PEO-Ch-HCl (9:1) insert the C_{max} value was significantly increased over that produced by the Ch-HCl-free PEO insert (7.16±0.77 *vs.* 4.39±0.58 μg ml^{-1}), while the t_{max} was reduced (150 *vs.* 300 min). It was reasoned that Ch-HCl, once in contact with the cornea, could exert a gradual enhancing effect on the corneal permeability which could explain the above data (Di Colo et al., 2002).
Microspheres of TMC, medicated with dexamethasone or tobramycin sulfate, were dispersed into PEO (MW 900 kDa) inserts with the aim of both maximizing the intraocular bioavailability of the drugs and studying the permeabilizing effects of TMC on the cornea (Zambito et al., 2006a). Introduction of 10% TMC microspheres into PEO inserts did not substantially affect the drug release pattern and rate from vehicle, nor the vehicle residence time in the precorneal area of rabbits. This allowed assessing the TMC effect on corneal permeability simply by comparing the concentration *vs.* time profiles in the aqueous obtained with the TMC-containing and the TMC-free inserts. The presence of TMC in the insert significantly increased C_{max} (5.69±0.49 *vs.* 3.07±0.31 μg ml^{-1}) and AUC (619.3±32.5 *vs.* 380.5±32.0 μg ml^{-1}min) for a dose of 0.3 mg of the lipophilic dexamethasone, indicating an enhancement effect of TMC on the transcellular penetration pathway. This effect could be exerted through an interaction with the glycoproteins of the mucous layer covering the cornea and/or with the lipid bilayer of the corneal cell membrane (Zambito et al., 2006a). In fact, interactions of protonated chitosan with model phospholipid membranes have been reported (Chan et al., 2001; Fang et al., 2001). A comparison of pharmacokinetic data for an equal dose of the dexamethasone administered as eye drops (C_{max}=0.21±0.02μg ml^{-1}; AUC=17.1±0.1 μg ml^{-1}min) with those obtained with the inserts shows a tremendous potential of inserts for maximizing intraocular drug availability. This compensates for the moderate discomfort *in situ* gel-forming inserts may cause to patients. On the other hand, the tobramycin concentration in the aqueous was below the limit of detection, even with the TMC-containing insert. It is known that TMC is able to enhance the paracellular penetration of hydrophilic molecules or macromolecules across cell monolayers, such as the intestinal epithelium, by opening the tight junctions between cells (Kotzé et al., 1997; Kotzé et al., 1998; Thanou et al., 2000). The results obtained with tobramycin (Zambito et al., 2006a) demonstrate that the tight junctions of such a stratified epithelium as the cornea are not effectively opened by TMC, at least to such an extent as to allow therapeutically effective penetration of hydrophilic drugs of the tobramycin molecular size. If the cornea is virtually impermeable to tobramycin, although the external cell layer might be affected by TMC the

deeper layers could remain impervious to this drug. On the other hand, dexamethasone could effectively permeate the cornea, hence the TMC action, although exerted on the corneal surface, could significantly enhance the apparent permeability of this drug.
In the foregoing discussion it was shown that the transcorneal penetration of a paracellular marker, such as fluorescein sodium, was significantly promoted by the polycationic Ch derivatives TMC and N^+-Ch, although the enhanced flux remained comparatively low. These results can be reconciled with those currently discussed concerning tobramycin by considering that the enhancing effect could be measured in the case of fluorescein, but not in that of tobramycin, because the detection limit of the analytical method for the former was much lower than for the latter ($8x10^{-3}$ vs. 0.5 μg/ml). In the light of the discussion so far, the remarkable promotion of the transcorneal absorption of ofloxacin by TMC (Di Colo et al., 2004a) is ascribable to a polymer action on the mucous layer covering the cornea and/or on the corneal cell membrane, rather than to an effective opening of the tight junctions in all layers of corneal cells.
To overcome the bioavailability problems associated with the administration of conventional eye drops the use of *in situ* gel-forming systems that are instilled as drops into the eye and undergo a sol-gel transition in the cul-de-sac has been proposed (Gupta et al., 2007). Different combinations of Ch (MW 150 kDa, 75-85% deacetylated) and poloxamer (Pluronic F-127) were evaluated for gelling ability and viscosity. The selected formulation (0.25% chitosan, 9.0% Pluronic F-127) had a viscosity that could allow easy instillation into the eye as drops and rapid sol-to-gel transition in the precorneal area triggered by a rise in pH from 6.0 to 7.4 and in temperature from ambient to 35-37 °C. A 0.25% timolol concentration usually prescribed for the therapy of glaucoma was added to the formulation. This was a clear, isotonic solution having pH 6.0-6.2. The formulation was converted into a stiff gel during autoclaving but recovered its original properties after cooling. Transcorneal permeation was studied *ex vivo* using excised goat corneas. The authors report a larger drug amount permeated after 4 h with the *in situ* gelling system (63.41±2.6%) as compared with the plain drug solution (42.11±2.1%) (Gupta et al., 2007) . They ascribe this difference to a permeabilizing action of Ch on the cornea, on the basis of the renown of Ch as a transmucosal permeation enhancer. It should be considered, however that the comparison between gelling system and control is based on the cumulative permeation and not on the P_{app} value. Then factors other than corneal permeability might contribute to the difference. Ocular irritation was tested by the chick embryo chorioallantoic membrane test (Gupta et al., 2007). It was found that the *in situ* gel formulation is nonirritant to mildly irritant and is well tolerated. *In vivo* precorneal drainage of the formulation was assessed by gamma scintigraphy, using albino rabbits for the study. The observation of the acquired gamma camera images showed good spreading of the *in situ*-gelling system over the entire precorneal area immediately after administration. The curve of the remaining activity on the corneal surface as a function of time showed that the plain drug solution cleared very rapidly from the corneal region. The drug passed into the systemic circulation, as significant activity was recorded in kidney and bladder 2 h after ocular administration. On the other hand the *in situ* gel formulation cleared slowly and no radioactivity was observed in kidney and bladder. This behaviour was ascribed to the known bioadhesivity of Ch and to the gelation that was induced by Ch and Pluronic F-127 (Gupta et al., 2007).
Another *in situ* gel-forming solution was obtained by coupling poly(*N*-isopropylacrylamide) (PNIPAAm), a well-known thermosensitive polymer having a thermoreversible phase

transition temperature close to human body surface (Maeda et al., 2006; Taylor & Ceranaowski, 1975; Hsiue et al., 2002; Hsiue et al., 2003), with Ch with the hope that this novel polymer (PNIPAAm-Ch) might couple the advantages of Ch and PNIPAAm (Cao et al., 2007). The ocular pharmacokinetics of timolol maleate, applied by this thermosensitive gel-forming system, were measured by microdialysis, a technique for continuously monitoring the drug in the rabbit aqueous (Wei et al., 2006; Macha & Mitra, 2001; Rittenhouse et al., 2000). By means of the sampling technique the behaviour of the drug was studied after the gel-forming solution and the conventional eye drops, both at the concentration of 0.5%, were administered in the *cul-de-sac*. The peak concentrations of 5.58 and 11.2 ng/ml were reached in the aqueous 15 and 30 min after instillation of the conventional eye drops and the thermosensitive gel-forming solution, respectively. It was also noted that the AUC for the latter was two-fold greater than that for the former. These data suggested that the gel-forming system improved the intraocular bioavailability and effectiveness of timolol maleate, which was embedded in the gel and therefore retained in the pre-corneal area for a prolonged period. As a hypothesis from the authors, however not substantiated by further data, PNIPAAm-Ch might enhance the corneal permeability and absorption of timolol maleate due to its positive charge and adhesive characteristics. The MTT assay showed little cytotoxicity of PNIPAAm-Ch at concentrations in the 0.5-400 μg/ml range (Cao et al., 2007).

4.1.3 Ch-based colloidal drug carriers

The potential of colloidal drug carriers, such as liposomes, submicron emulsions, nanocapsules and nanoparticles in ocular delivery has been put into evidence by a review article in 2009 (Alonso et al., 2009). It has been shown that the action of Ch-based nanoparticle systems relies on particle interactivity with the corneal or conjunctival epithelium cells. The nanoparticles can be uptaken within the epithelial cells without causing any damage to them. In this way these nanosystems, once loaded with drugs, might make the conjunctival and corneal epithelia reservoirs for drug delivery to the exterior or interior of the eye. The interaction between Ch nanoparticles and the corneal and conjunctival epithelial surfaces have been investigated (Lehr et al, 1992). The nanoparticles were usually obtained by adding a solution of tripolyphosphate to a Ch solution in acetic acid. To study the interaction of Ch nanoparticles with ocular structures by spectrofluorimetry and confocal fluorescence microscopy, Ch was converted into a fluorescent derivative by the reaction between the fluorescein acid group and the Ch amino group. The stability of nanoparticles in the presence of proteins and enzymes was deemed a crucial issue. The presence of lysozyme was found not to significantly compromise the integrity of Ch nanoparticles since only a slight particle size reduction and no surface charge modification were observed (Lehr et al, 1992). Fluorescence microscopy of eyeball and lid sections confirmed the *in vivo* uptake of Ch nanoparticles by conjunctival and corneal epithelia. *In vivo* studies in rabbits showed that the nanoparticles were well tolerated by the ocular surface structures, which showed no histologic alterations nor abnormal inflammatory cells in cornea, conjunctiva and lids, in full consistency with the lack of clinical signs (de Salamanca et al., 2006).

Another potential colloidal drug carrier has been studied, which combines liposomes and Ch nanoparticles (Diebold et al. , 2007). The rehydration at 60 °C of a lyophilized mixture of Ch nanoparticles, loaded with FITC-BSA, and liposomes led to the coating of nanoparticles

with a phospholipid shell. The resulting nanosystem was characterized for size and zeta potential (407.8±9.6 nm and +5.8±1.3 mV to 755.3±30.0 nm and +14.7±0.4 mV, depending on composition) while its structure was assumed theoretically on the basis of an interaction between the positively charged nanoparticles and the negatively charged lipid vesicles, and a reorganization of the membranes to cover the nanoparticle surface. All nanosystems, namely, Ch nanoparticles, liposomes, and liposome-Ch nanoparticle complexes showed physical stability so far as no significant change in particle size was observed by photon-correlation spectroscopy after 2 h in simulated lachrymal fluid. The underlying hypothesis of the authors was that an appropriate combination of liposomes and Ch nanoparticles could increase the ability of the resulting system to interact with biological surfaces and cell membranes and potentially deliver drugs to target tissues.

Studies of Ch-coated colloidal systems loaded with tetanus toxoid, indomethacin or diazepam, or Ch-based nanoparticles loaded with cyclosporin have been reviewed (Alonso & Sanchez, 2009). It was concluded that a Ch coating could add a clear benefit to the potential of colloidal systems as ocular drug carriers, and that Ch nanoparticles might represent an interesting vehicle for drugs the target of which is the ocular mucosa.

The preparation of Ch/Cabopol nanoparticles loaded with pilocarpine, a drug used for the treatment of glaucoma, has been reported (Huei-Jen et al., 2006). A solution of Ch in 1% w/v acetic acid was dropped into a Carbopol dispersion under stirring by a homogenizer to form an opalescent suspension of Ch/Carbopol nanoparticles. The pilocarpine-loaded nanoparticles were prepared by dissolving the drug in a measured volume of Ch/Carbopol nanoparticle suspension and stirring for 48 h. The drug-loaded nanoparticles were isolated by ultracentrifugation and dried by lyophilization. The nanoparticles were assumed to be formed by ionic interaction between the polycationic Ch and the polyanionic Carbopol. A particle size of 294±30 nm, a zeta potential of +55.78±3.41 mV and a pilocarpine encapsulation efficiency of 77±4% were reported (Huei-Jen et al., 2006). After pilocarpine in various formulations, i.e., eye drops, liposomes, gel and nanoparticles, had been applied in the eyes of rabbits, the resulting miotic responses were compared. The decrease in pupil diameter was in the rank order of nanoparticles>liposomes>gel>eyedrops. With nanoparticles and liposomes the miosis effect lasted up to 24 h. The AUC for the curve of decrease in pupil diameter *vs.* time was the largest for the nanoparticle formulation, indicating that this formulation was the most efficient system of the four tested for the topical delivery of pilocarpine (Huei-Jen et al., 2006).

Lipophilic nanoparticles for the delivery of the macrolide rapamycin for immunosuppression in corneal transplantation have recently been described (Xu-Bo et al., 2008). In brief, the preparation of rapamycin-loaded nanoparticles is described by the authors as follows. Poly(lactic acid) (PLA) and rapamycin, dissolved in acetone, are added under ultrasonication to an aqueous solution containing a Ch-cholesterol conjugate (Ch-Chol), after which the solvent is removed by evaporation under stirring. The resulting nanoparticle suspension is centrifuged to remove the drug not entrapped within the particles, and then lyophilized. It is claimed that the amphiphilic Ch-Chol self-aggregates into nanoparticles, with hydrophobic microenvironment inside. When PLA was added to the aqueous Ch-Chol under ultrasonication the size of the nanoparticles slightly increased to about 300 nm, with a zeta potential of +30.3 mV. The presence of PLA favoured the entrapment of the hydrophobic drug into the particles. The drug-loaded Ch-Chol/PLA nanoparticles and a rapamycin suspension were radiolabeled and the ocular distribution of

either system was assessed by scintillation counter and single photon emission computed tomography (SPECT) image analysis. The rabbits treated with Ch-Chol/PLA nanoparticles showed radioactivity fractions remaining on cornea and conjunctiva significantly higher than those treated with the suspension of rapamycin. This behaviour is ascribed to the mucoadhesive character of the Ch nanoparticles (Xu-Bo et al., 2008), while disregarding the possibility of particle internalization by corneal and/or conjunctival cells. The radioactivity levels in the aqueous and iris/ciliary body were close to background level. This is taken as an indication that the corneal barrier hindered transport of either the drug or the nanoparticles. Nevertheless the prolonged residence of nanoparticles on the ocular surface is expected to promote drug absorption by the external ocular tissues. The rapamycin-loaded Ch-Chol/PLA were used to treat corneal allografts in comparison with the drug-free nanoparticles and the rapamycin suspension eyedrops. All of 10 grafts in the untreated control group were rejected within 13 days (median survival time, 10.6±1.26 days). Rabbits treated with empty nanoparticles rejected the corneal allografts in a median time of 10.9±1.45 days and none of these grafts survived beyond 13 days. In the group treated with the rapamycin suspension, grafts were rejected between 19 and 27 days with a median survival time of 23.7±3.20 days, while in the group treated with the rapamycin-loaded nanoparticles the median survival time of grafts was 27.2±1.03 days and 50% grafts were still surviving by the end of the observation (4 weeks). These results indicated an improved immunosuppressive effect compared with rapamycin eye drops (Xu-Bo et al., 2008).
A very recent report describes the potential use in ocular drug delivery of liposomes coated with low molecular weight (8 kDa) Ch (LCh) (Li et al., 2009). LCh was prepared by degradation of Ch with H_2O_2. Liposomes loaded with diclofenac sodium were coated with LCh (LChL). These systems, containing 0.1% diclofenac sodium, were compared with a 0.1% aqueous solution of the drug (control) for their effects on drug retention in precorneal area of rabbits. The LChL formulations produced significantly higher AUC (area under concentration in tear fluid vs. time curve) and longer MRT than either non-coated liposomes or the control solution, indicating that the LCh coating was essential to prolong the retention of liposome-encapsulated drug. No irritation or toxicity, caused by continual administration of LChL in a period of 7 days, resulted from an ocular tolerance study. The effect of LChL on drug corneal penetration was studied (Li et al., 2009) using excised rabbit cornea and a diffusion apparatus (Camber, 1985). The apparent corneal permeability was determined by normalizing the permeant steady-state flux to the permeant concentration in the donor (1.0 mg/ml). The P_{app} produced by LChL was significantly higher than that relative to non-coated liposomes, while the latter was not higher than that produced by the aqueous solution. According to the authors (Li et al., 2009) the LCh coating could intensify liposome binding to the corneal surface, thus facilitating drug absorption into the cornea. In addition, the polycationic LCh could enhance the corneal permeability as in the case of the Ch of much higher molecular weight, described earlier (Di Colo et al., 2004b). These results are interesting in that they show that a Ch of as low a molecular weight as 8 kDa can act as a corneal permeabilizer. However, the effect of this Ch on precorneal retention and corneal drug permeability is not reported for the case where drug and Ch are applied in solution, so the advantages of using a liposome formulation instead of a solution are not neatly highlighted by data.

4.2 Xyloglucan

Xyloglucan is a polysaccharide derived from tamarind seeds, therefore it is often coded TSP (tamarind seed polysaccharide). It has a backbone of β(1→4)-linked glucose residues. Three

out of four glucose units are substituted with α(1→6) xylose residues, which are partially substituted by β(1→2)-linked galactose, as shown in Fig.7. Some of the galactose residues can be further substituted with α(1→2) fucose. TSP is highly water-soluble.

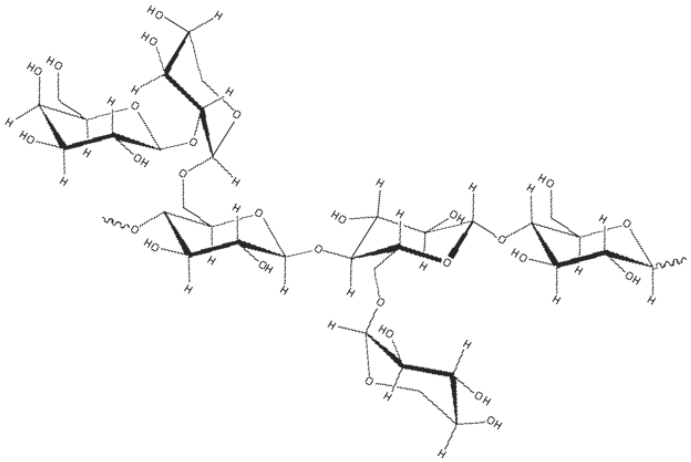

Fig. 7. Structure of the polysaccharide derived from tamarind seeds.

4.2.1 Eye drops

TSP has been described as a viscosity enhancer with mucomimetic activity. Therefore it is currently used in commercial artificial tears for the treatment of dry eye syndrome (DES) (Saettone et al., 1997). Concentrations of such antibiotics as gentamicin and ofloxacin in the rabbit aqueous humor depended on whether rabbit eyes were topically treated with antibiotics alone or drug formulations viscosified with TSP. In the latter instance significantly higher intraocular drug levels were observed. Also, the drugs delivered with TSP produced significantly higher intra-corneal levels than those attained with the corresponding TSP-free formulations. This suggested that TSP enhances corneal drug accumulation by reducing the wash-out of drugs (Ghelardi et al., 2000).

Eye drops containing 3 mg/ml rufloxacin and 10 mg/ml TSP, along with other excipients were topically applied to rabbits for the treatment of experimental *Pseudomonas aeruginosa* and *Staphylococcus aureus* keratitis. Rufloxacin delivered by the polysaccharide reduced *P. aeruginosa* and *S. aureus* in the cornea at a higher rate than that obtained with rufloxacin alone. These results suggested that TSP is able to prolong the precorneal residence time of the antibiotic and enhance drug accumulation in the cornea, thereby increasing the intra-aqueous antibiotic penetration. (Ghelardi et al., 2004).

4.2.2 In situ-gelling systems

When xyloglucan is partially degraded by β-galactosidase the resultant product exhibits thermally reversible gelation in dilute aqueous solutions, which does not occur with native xyloglucan. Gelation is only possible when the galactose removal exceeds 35%. The sol-gel

transition temperature was shown to decrease from 40 to 5 °C when the galactose removal ratio increased from 35 to 58% (Nanjawade et al., 2007). Xyloglucan formulations have been studied for ocular delivery of pilocarpine, using Poloxamer 407 as a positive thermosensitive control. The 1.5 wt.% xyloglucan formulation enhanced the miotic response to a degree similar to a 25 wt.% Poloxamer 407 gel (Nanjawade et al., 2007).

4.3 Arabinogalactan

Arabinogalactan (AG), a natural polysaccharide contained in *Larix Occidentalis* (Western Larch), has been found to be biocompatible in the eye, mucomimetic and mucoadhesive (Burgalassi et al., 2007). It is a non-ionic highly branched polysaccharide of the 3,6-β-D-galactan type, the side chains of which consist of β-galactose and β arabinose residues (Gregory & Kelly, 1999).

4.3.1 Eye drops

AG dispersions showed a Newtonian non-viscous behaviour (η=1.6 mPas at 10% w/w concentration) along with good mucoadhesive properties, useful for retention on the eye surface. In fact, a prolonged time of residence in rabbit eyes was ascertained using fluorescein-labeled AG. Five percent w/w AG exerted a good protective effect against the appearance of corneal dry spots. It also reduced significantly the healing time of an experimental corneal lesion. These findings suggested that AG is potentially effective for dry eye protection and in the treatment of corneal wounds (Burgalassi et al., 2007).

4.4 Cellulose derivatives

Cellulose is a polysaccharide consisting of a linear chain of several hundred to over ten thousand β(1→4) linked D-glucose units. The chemical structures of cellulose derivatives used in topical ocular formulations (methyl cellulose, hydroxyethyl cellulose, hydroxypropylmethyl cellulose, sodium carboxymethyl cellulose) are shown in Fig.8.

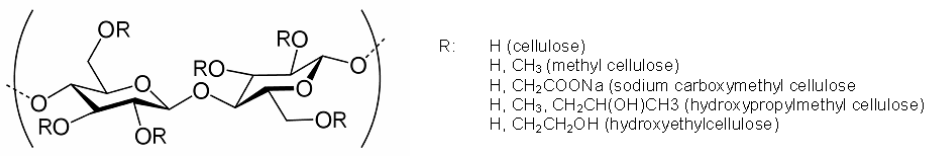

Fig. 8. Structure of cellulose and its derivatives.

4.4.1 Eye drops

Eye drops containing cellulose derivatives, such as methyl cellulose (MC), hydroxypropylmethyl cellulose (HPMC) or sodium carboxymethyl cellulose (NaCMC), have largely been used as eye lubricants for the treatment of DES. This is characterized by a set of alterations of the eye surface which could relate to tear quality, normal makeup of tear film and alterations in blinking or regular closing of eyelids which entail a reduction of the stability of the tear film and the alteration of the eye surface. HPMC solutions were patented as a semisynthetic substitute for tear-film (Hahnenberger, 1997). When applied, an HPMC solution acts to absorb water, thereby expanding the thickness of the tear film and resulting in extended time of lubricant presence on the cornea and decreased eye irritation (Koroloff

et al., 2004). Aside from its widespread commercial and retail availability in a variety of products, HPMC has been used as a 2% solution during surgery to aid in corneal protection and during orbital surgery. Treatment with an isotonic 0.5%solution of NaCMC found in the market (Cellufresh®, Allergan SA, Madrid) produced a significant decrease in the frequency of subjective DES symptoms and improvement of tear film interface stability and corneal surface wettability compared to controls (Bruix et al., 2006).
Hydroxyethyl cellulose (HEC) is used as a viscosity-enhancing agent in ophthalmic formulations to prolong corneal contact time and increase intraocular drug levels.

4.4.2 In situ-gelling systems

Aqueous solutions of MC or HPMC at concentrations in the 1-10 wt.% range are liquid at low temperatures, but form gels upon heating. The transition temperature is between 40 and 50 °C for MC and between 75 and 90 °C for HPMC. Sodium chloride lowers the sol-gel transition temperature of MC to 32-34 °C, while the transition temperature of HPMC can be lowered to about 40 °C by reducing the hydroxypropyl molar substitution (Nanjawade et al., 2007).
Gelation of MC or HPMC solutions is produced by the hydrophobic interaction between methoxy-substituted residues. At low temperatures the macromolecules are hydrated and interact by simple entanglement. At higher temperatures the hydration of polymer chains tends to decrease, chain-chain associations take place, and the system approaches a network structure, corresponding to a sharp rise in viscosity. This sol-gel transition has been exploited to design *in situ* gelling systems having low viscosity at 23 °C and forming soft gels at 37 °C (Nanjawade et al., 2007).

4.5 Hyaluronic acid

Hyaluronic acid (HA) is a high molecular weight, natural and linear polysaccharide composed of β-1,3-N-acetyl glucosamine and β-1,4-glucuronic acid repeating disaccharide units (Fig.9). This biocompatible, nonimmunogenic and biodegradable polymer is one of the most hygroscopic molecules in nature, in fact, HA can hydrate up to 1000 times its dry weight. This property is responsible for enhanced hydration of the corneal surface. Moreover, ocular topical application of formulations based on hyaluronic acid reduces the elimination rate of tear fluid and stabilizes the tear film. This is useful for the treatment of DES (Guillaumie et al., 2010).

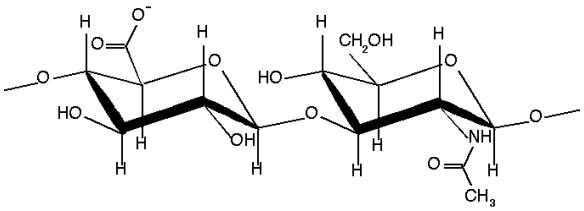

Fig. 9. Structure of hyaluronic acid.

4.5.1 Eye drops

Non-Newtonian and shear thinning properties grant HA solutions a high viscosity at low shear rate (when the eye is open) and a low viscosity at high shear rate (during blinking) thus allowing an even distribution of the solution, improving lubrication of the ocular

surface, retarding drainage, improving bioavailability, and reducing discomfort. Another important feature of this high molecular weight, anionic biopolymer is its mucoadhesivity, which provides effective coating and long-lasting protection of the cornea as well as extended residence times on the ocular surface (Guillaumie et al., 2010). Finally, when topically instilled on the eye, hyaluronic acid has been shown to promote physiological wound healing by stimulating corneal epithelial migration and proliferation of keratocytes and to reduce the healing time of corneal epithelium. Topical ophthalmic solutions should exhibit a certain degree of viscosity to prevent immediate drainage from the ocular surface and provide there high efficacy and long residence time. However, the solutions should not be too viscous to avoid blurred vision and to ease their manufacturing process including their sterile filtration (Guillaumie et al., 2010).

4.6 Alginic acid/sodium alginate

Alginic acid (AA) is a natural hydrophilic polysaccharide distributed widely in the cell walls of brown algae. It contains the monomers β-D-mannuronic acid (M) and α-L-guluronic acid (G), arranged as homopolymeric blocks of M-M blocks or G-G blocks together with blocks of alternating sequence (M-G). The polymer forms 3-dimensional ionotropic hydrogel matrices, generally by the preferential interaction of calcium ions with the G moieties resulting in the formation of inhomogeneous gels (Grant et al., 1973 via Cohen et al., 1997).

4.6.1 In situ-gelling systems

An aqueous solution of sodium alginate (NaAA) can gel in the eye. Alginates with G contents of more than 65% instantaneously formed gels upon addition to simulated tear fluid, due to ionotropic gelation by Ca^{++} ions. In contrast, alginates having low G contents formed weak gels at a comparatively low rate (Cohen et al., 1997). Pilocarpine was released slowly from alginate gels *in vitro* over a period of 24 h, and the release occurred mostly via diffusion from the gels. In agreement with the *in vitro* results, intraocular pressure (IOP) measurements of rabbit eyes treated with 2% w/v pilocarpine nitrate in solution or in the *in situ* gel-forming formulation containing high G-content NaAA indicated that the latter significantly extended the duration of the IOP-reducing effect compared to the former (10 h vs. 3 h). On the other hand, the effect of low G-content NaAA on the duration and extent of IOP reduction was insignificant (Cohen et al., 1997).

AA has been evaluated as a potential vehicle in ophthalmic *in situ*-gelling solutions for prolonging the IOP-reducing effect of carteolol. *In vitro* studies indicated that carteolol is released slowly from mucoadhesive AA formulations, suggesting an ionic interaction between the basic drug and AA. IOP measurements of rabbit eyes treated with a 1% carteolol formulation with or without AA showed that this polymer significantly extended the duration of the IOP-reducing effect to 8 h. AA produced an ocular bioavailability increase of a carteolol formulation, as indicated by a drug concentration in the target tissue, following a once-daily administration, equivalent to a twice-daily administration of the AA-free carteolol solution (Sechoy et al., 2000).

4.7 Gellan gum

Gellan gum (GG), commercial name Gelrite®, is a water-soluble polysaccharide produced by the bacterium *Pseudomonas elodea*. The repeating unit of the polymer is a tetrasaccharide

consisting of two residues of D-glucose and one of each L-rhamnose and D-glucuronic acid, in the following sequence: $[D\text{-}Glc(\beta1\rightarrow4)D\text{-}GlcA(\beta1\rightarrow4)D\text{-}Glc(\beta1\rightarrow4)L\text{-}Rha(\alpha1\rightarrow3)]_n$.

4.7.1 In situ-gelling systems

GG solutions form gels in the presence of mono- or divalent cations, therefore a 0.6% GG solution containing 0.34% timolol maleate underwent a sol-gel transition in the rabbit eye due to the presence of sodium and calcium ions in tear fluid. *In vitro* release of timolol from GG gelled solutions was retarded and controlled by drug diffusion in the gel. Accordingly, i*n vivo* the formation of the gel prolonged the precorneal residence time, and therefore, it increased the ocular bioavailability of timolol in the cornea, aqueous humor and iris+ciliary body of rabbits (Rozier et al., 1989). A similar *in situ*-gelling behaviour and *in vitro* release of the antibacterial agent pefloxacin was reported of a 0.6% GG solution. This allowed attainment of the minimum inhibitory concentration of antibacterial in the aqueous of rabbits, and maintained it for 12 h, while with the conventional eye drops the drug concentration in the aqueous after the same time interval dropped to negligible values (Sultana et al., 2006).

4.8 Polysaccharide mixtures

Mixtures of polysaccharides have been investigated considering that possible interpolimer non-covalent interaction might generate excipients for eye drops, having synergistically improved properties over those of the separate polymers. Ascertaining the above possibility and evaluating the composition of the mixture corresponding to the strongest interaction and optimal biopharmaceutical properties have been the fundamental purposes of these studies.

4.8.1 Eye drops

An interaction between TSP and HA in aqueous solution was ascertained. Various TSP/HA mixtures were studied, among which the 3/2 ratio showed the strongest interaction. The properties of this mixture as a potential excipient for eye drops were synergistically improved over those of the separate polymers. Information about the nature of interpolymer interactions and their dependence on TSP/HA ratio was obtained by nuclear magnetic resonance (NMR) spectroscopy. The affinity of the TSP/HA (3/2) mixture for mucin, assessed by NMR, is higher than that of the single polysaccharides. The mucoadhesivity of this mixture, evaluated *in vitro* by NMR or viscometry, and *in vivo* by its mean and maximum residence time in rabbit precorneal area, is stronger than that of the component polysaccharides or the TSP/HA mixtures of different composition. TSP/HA (3/2) is little viscous and well tolerated by rabbit eyes, so it shows a considerable potential for the treatment of DES. This mixture stabilizes the tear film, hence it has been shown to prolong the residence of drugs, such as ketotifen fumarate and diclofenac sodium, in tear fluid. It is unable to permeabilize the cornea, therefore mucoadhesivity is responsible for the TSP/HA (3/2) synergistic enhancement of either extra- or intra-ocular drug bioavailability (Uccello-Barretta et al., 2010).

4.8.2 In situ-gelling systems

The rheological properties of GG, NaAA and GG/NaAA solutions were evaluated. It was found that the optimum concentration of GG solution for *in situ* gel-forming delivery

systems was 0.3% w/w and that of NaAA solution was 1.4% w/w. The mixture of 0.2% GG and 0.6% NaAA, when gelled by simulated tear fluid, showed a significant enhancement in gel strength in physiological conditions. Such a gelled mixture released *in vitro* the anticancer drug matrine most slowly. When the solution of this mixture was instilled in rabbit eyes the *in situ* gelling significantly prolonged drug residence in the precorneal area over the time allowed by the GG or NaAA solution alone (Liu et al., 2010).
A further *in situ* gel-forming polysaccharide mixture is composed of Ch and GG. Both polysaccharides form gels in the physiological conditions of the eye, gelation of Ch being activated by the neutral pH of tear fluid, that of GG by the cations of the electrolytes contained in such a fluid. The *in situ*-gelling system composed of 0.25% w/v Ch and 0.50% w/v GG was prepared by mixing solutions of Ch and GG in acetate buffer pH 5.5-6.0 and ultrapure water, respectively. The system was medicated with 0.25% w/v timolol maleate. *In vitro* transcorneal permeation studies on the formulation showed a significant increase of the drug amount permeated across goat cornea in 4 h compared to plain drug solution and the *in situ*-gelling system based on GG alone. This effect was ascribed to the permeation-enhancing ability of Ch. *In vivo* precorneal drainage of the formulation was studied in rabbits by gamma scintigraphy. Radio-labelled timolol maleate applied as plain solution cleared very rapidly from the corneal region, whereas the drug applied by the Ch/GG *in situ*-gel forming formulation was retained on the corneal surface for a remarkably longer time (Gupta et al., 2010).

4.9 Comparison of polysaccharide mucoadhesivity

Different polysaccharides, i.e., AG, TSP, HA, HEC, have been compared for their ability to resist removal from tear fluid. Their mucoadhesivity was compared *in vitro*, by the polymer-induced viscosity increase of a mucin dispersion, and *in vivo*, by the polymer residence time in rabbit tear fluid (Di Colo et al., 2009).
The optimal polymer to be used as an additive in ophthalmic drops should be mucoadhesive without increasing the viscosity of the solution to an excessive extent. A solution of TSP 0.7% w/v was shown to possess more of these properties than the other polymers at comparison, in fact, it exhibited the highest MRT in the rabbit precorneal area. HA and HEC, although mucoadhesive, increased the solution viscosity to an excessive degree, and this, in addition to worsening the patient compliance, could induce an anomalous reflex tearing with consequent acceleration of precorneal clearance. AG, at the concentrations at which TSP, HA and HEC were tested, exhibited no significant mucoadhesive properties. This polysaccharide, nevertheless, did not increase the solution viscosity, so it showed the potential for being used at much higher concentrations, e.g., 5-10% w/w, at which its mucoadhesivity is significant (Burgalassi et al., 2007). In virtue of its mucoadhesivity, TSP 0.7% w/v is supposed to stabilize the tear film. For this reason the residence of two different drugs, i.e., ketotifen fumarate and diclofenac sodium, in the precorneal area of rabbit eyes was significantly prolonged by this excipient (Di Colo et al., 2009).

5. Conclusion

The polysaccharides, either natural or semi-synthetic, described in the present survey are non-irritant to the eye and show an ample array of possible solutions to formulation issues

in ophthalmology. The polysaccharides introduced in eye drops are mucoadhesive and mucomimetic at comparatively low viscosities. Hence they have been used as lubricants of the eye surface to treat DES. In virtue of their mucoadhesivity they stabilize the tear film and prolong the residence of ophthalmic drugs on the eye surface thereby increasing their extra- and intra-ocular bioavailability. Ch and some of its polycationic derivatives, when topically applied *via* eye drops, have shown the additional ability to promote intra-ocular drug absorption by reversibly permeabilizing the cornea. It is in virtue of this peculiar ability and of mucoadhesivity that Ch has been used to prepare nanoparticles for ocular topical application, or added to ophthalmic *in situ*-gelling systems, based on PEO, poloxamer, or PNIPAAm, intended to improve the ocular drug bioavailability. When the basic excipients of *in situ*-gelling systems were polysaccharides, such as AA/NaAA or GG, the basic principles of the drug bioavailability increase were the prolonged retention of gel in precorneal area and the slow drug release from gel.

Most of the *in vivo* studies of ocular formulations employing polysaccharides have used rabbits as the animal model. It must be recognized, however, that the precorneal clearance determined in rabbits is not representative of that in humans, mainly due to differences in blinking frequency. Such differences may be reflected in differences in shear-thinning of tear film, mucoadhesion of polymer and ultimately in drainage of drugs. Nevertheless, the inaccuracies due to blinking differences can be considered to be similar for the different preparations tested, then the rabbit model is deemed robust for those studies where it has been used for comparative purposes.

6. Abbreviation

AA	alginic acid
AG	arabinogalactan
AUC	area under curve
Ch	chitosan
Ch-Chol	chitosan-cholesterol conjugate
Ch-HCl	chitosan hydrochloride
CMCh	*N*-carboxymethyl chitosan
DEAE-Cl	2-diethylaminoethyl chloride
DES	dry eye syndrome
DS	degree of substitution
ER	enhancement ratio
FITC	fluorescein-isothiocyanate
G	guluronic acid unit in AA
GG	gellan gum
HA	hyaluronic acid
HEC	hydroxyethyl cellulose
HPMC	hydroxypropylmethyl cellulose
IOP	intra ocular pressure
LCh	low molecular weight chitosan
LChL	liposomes coated with LCh
M	mannuronic acid unit in AA
MC	methyl cellulose
MeDEAED	*N*- methyl-diethylaminoethyl dextran

MRT	mean precorneal retention time
n	mean number of quaternary ammonium groups in the pendant chains of N^+-Ch
NaAA	sodium alginate
NaCMC	sodium carboxymethyl cellulose
N^+-Ch	*N,O*-[*N,N*-diethylaminomethyl(diethyldimethylene ammonium)$_n$methyl] chitosan
N^+-Ch-SH	thiolated quaternary ammonium-chitosan conjugate
P_{app}	apparent permeability
PEO	poly(ethylene oxide)
PLA	poly(lactic acid)
PNIPAAm	poly(*N*-isopropylacrylamide)
PVA	poly(vinyl alcohol)
QD	quaternization degree
RRCE	rabbit reconstituted corneal epithelium
SPECT	single photon emission computed tomography
TMC	*N*-trimethyl chitosan
TMCL	TMC synthesized from a Ch of MW 580 kDa
TMCH	TMC synthesized from a Ch of MW 1460 kDa
TSP	tamarind seed polysaccharide

7. References

Alonso, M. J. & Sánchez, A. (2009). The potential of chitosan in ocular drug delivery. *J. Pharm. Pharmacol.*, Vol. 55, pp. 1451-1463.

Artursson, P.; Lindmark, T.; Davis, S.S. & Illum, L. (1994). Effect of chitosan on the permeability of monolayers of intestinal epithelial cells (Caco-2). *Pharm. Res.*, Vol. 11, pp. 1358-1361.

Bruix, A; Adan, A. & Casaroli-Marano, R.P. (2006). Efficacy of sodium carboxymethylcellulose in the treatment of dry eye syndrome. *Arch. Soc. Esp. Oftalmol.*, Vol. 81, pp. 85-92.

Burgalassi, S.; Nicosia, N.; Monti, D.; Falcone, G.; Boldrini, E. & Chetoni, P. (2007). Larch arabinogalactan for dry eye protection and treatment of corneal lesions: Investigation on rabbits. *J. Ocul Pharmacol. Ther.*, Vol. 23, pp. 541-549.

Camber, O. (1985). An *in vitro* model for determination of drug permeability through the cornea. *Acta Pharm. Suec.*, Vol. 22, pp. 335-342.

Cao, Y.; Zhang, C.; Shen, W.; Cheng, Z.; Yu, L.L. & Ping, Q. (2007). Poly(*N*-isopropylacrylamide)—chitosan as thermosensitive *in situ* gel-forming system for ocular drug delivery. *J.Control. Rel.*, Vol. 120, pp. 186-194.

Chan, V.; Mao, H.Q. & Leong, K.W. (2001). Chitosan-induced perturbation of dipalmitoyl-*sn*-glycero-3-phosphocholine membrane bilayer. *Langmuir*, Vol. 44, pp. 201-208.

Cohen, S.; Lobel, E.; Trevgoda, A.; Peled, Y. (1997). A novel in situ-forming ophthalmic drug delivery system from alginates undergoing gelation in the eye. *J. Control. Rel.*; Vol. 44, pp. 201-208.

de Salamanca, A.E.; Diebold, Y.; Calonge, M.; García-Vazquez, C.; Callejo S.; Vila, A. & Alonso, M.J. (2006). Chitosan nanoparticles as a potential drug delivery system for

the ocular surface: toxicity, uptake mechanism and *in vivo* tolerance. *Invest. Ophthalmol. Vis. Sci.*, Vol. 47, pp. 1416-1425.

Diebold, Y.; Jarrín, M.; Sáez, V.; Carvalho, E.L.S.; Orea, M.; Calonge, M.; Seijo, B. & Alonso, M. J. (2007). Ocular drug delivery by liposome-chitosan nanoparticle complexes (LCS-NP). *Biomaterials*, Vol. 28, pp. 1553-1564.

Di Colo, G.; Burgalassi, S.; Chetoni, P.; Fiaschi, M.P.; Zambito, Y. & Saettone, M.F. (2001a). Gel-forming erodible inserts for ocular controlled delivery of ofloxacin. *Int. J. Pharm.*, Vol. 215, pp. 101-111.

Di Colo, G.; Burgalassi, S.; Chetoni, P.; Fiaschi, M. P.; Zambito, Y. & Saettone, M.F. (2001b). Relevance of polymer molecular weight to the *in vitro/in vivo* performances of ocular inserts based on poly(ethylene oxide). *Int. J. Pharm.*, Vol. 220, pp. 169-177.

Di Colo, G.; Zambito, Y.; Burgalassi, S.; Serafini, A. & Saettone, M.F. (2002). Effect of chitosan on in vitro release and ocular delivery of ofloxacin from erodible inserts based on poly(ethylene oxide). *Int. J. Pharm.*, Vol. 248, pp. 115-122.

Di Colo, G.; Burgalassi, S.; Zambito, Y.; Monti, D. & Chetoni, P. (2004a). Effects of different N-trimethylchitosans on *in vitro/in vivo* ofloxacin transcorneal permeation. *J. Pharm. Sci.*, Vol. 93, pp. 2851-2862.

Di Colo, G.; Zambito, Y.; Burgalassi, S.; Nardini, I. & Saettone, M.F. (2004b). Effect of chitosan and of N-carboximethylchitosan on intraocular penetration of topically applied ofloxacin. *Int. J. Pharm.*, Vol. 273, pp. 37-44.

Di Colo, G.; Zambito, Y. & Zaino, C. (2008). Polymeric enhancers of mucosal epithelia permeability: synthesis, transepithelial penetration-enhancing properties, mechanism of action, safety issues. *J. Pharm. Sci.*, Vol. 97, pp. 1652-1680.

Di Colo, G.; Zambito, Y.; Zaino, C. & Sansò, M. (2009). Selected polysaccharides at comparison for their mucoadhesiveness and effect on precorneal residence of different drugs in the rabbit model. *Drug Dev. Ind. Pharm.*, Vol. 35, pp. 941-949.

Dodane, V. & Vilivalam, V.D. (1998). Pharmaceutical applications of chitosan. *Pharma Sci. Technol. Today*, Vol. 1, pp. 246-253.

Fang, N.; Chan, V.; Mao, H. Q. & Leong, K. W. (2001). Interactions of phospholipid bilayer with chitosan: effect of molecular weight and pH. *Biomacromolecules*, Vol. 2, pp. 1161-1168.

Felt, O.; Buri, P. & Gurny, R. (1998). Chitosan: a unique polysaccharide for drug delivery. *Drug Dev. Ind. Pharm.*, Vol. 24, pp. 979-993.

Ghelardi, E.; Tavanti, A.; Pelandroni, F.; Lupetti, A.; Blandizzi, C.; Boldrini, E.; Campa, M. & Senesi M. (2000). Effect of a novel mucoadhesive polysaccharide obtained from tamarind seeds on the intraocular penetration of gentamicin and ofloxacin in rabbits. *J. Antimicrob. Chemother.*, Vol. 48, pp. 3396-3401.

Ghelardi, E.; Tavanti, A.; Davini, P.; Pelandroni, F.; Solvetti, S.; Parisio, E.; Boldrini, E.; Senesi, S. & Campa, M. (2004). A mucoadhesive polymer extracted from tamarind seed improves the intraocular penetration and efficacy of rufloxacin in topical treatment of experimental bacterial keratitis. *Antimicrob. Agents Chemother.*, Vol. 48, pp. 3396-3401.

Grant, G.T.; Morris, E.R.; Rees, D.A.; Smith, P.J.C. & Thom, D. (1973). Biological interactions between polysaccharides and divalent cations: The egg box model. *FEBS Lett.*, Vol. 32, pp. 195-198.

Gregory, S. & Kelly, N.D. (1999). Larch arabinogalactan: Clinical relevance of a novel immune-enhancing polysaccharide. *Altern. Med. Rev.*, Vol. 4, pp. 96-103.

Guillaumie, F.; Furrer, P.; Felt-Baeyens, O.; Fuhlendorff, B.L.; Nymand, S.; Westh, P.; Gurny, R. & Schwach-Abdellaoui, K. (2010). Comparative studies of various hyaluronic acids produced by microbial fermentation for potential topical ophthalmic applications. *J. Biomed. Mater. Res. Part A*, Vol. 92, No. 4, pp. 1421-1430.

Gupta, H.; Jain, S.; Mathur, R.; Mishra, P. & Mishra, A. K. (2007). Sustained ocular drug delivery from a temperature and pH triggered *in situ* gel system. *Drug Deliv.*, Vol. 14, pp. 507-515.

Gupta, H.; Velpandian, T. & Jain, S. (2010). Ion- and pH-activated novel *in-situ* gel system for sustained ocular drug delivery. *J. Drug Targeting*, Vol. 18, pp. 499-505.

Hahnenberger, R.W. (1997). Pharmaceutical composition containing carbachol and other cholinergic substances. United States Patent 5,679,713.

Hamman, J.H.; Schultz, C. M. & Kotzé, A.F. (2003). N-trimethyl chitosan chloride: optimum degree of quaternization for drug absorption enhancement across epithelial cells. *Drug Dev. Ind. Pharm.*, Vol. 29, pp. 161-172.

Huei-Jen, K.; Hong-Ru, L.; Yu-Li, L. & Shi-Ping Y. (2006). Characterization of pilocarpine-loaded chitosan/Carbopol nanoparticles. *J. Pharm. Pharmacol.*, Vol. 58, pp. 79-186.

Hui H.W. & Robinson, J. R.(1985). Ocular drug delivery of progesterone using a bioadhesive polymer. *Int. J. Pharm.*, Vol. 26,pp. 203-213.

Illum, L. (1998). Chitosan and its use as a pharmaceutical excipient. *Pharm. Res.*, Vol. 15, pp. 1326-1331.

Illum, L.; Farraj, N. F. & Davis, S.S. (1994). Chitosan as a novel nasal delivery system for peptide drugs. *Pharm. Res.*, Vol. 11, pp. 1186-1189.

Janes, K.A.; Calvo, P. & Alonso, M.J. (2001). Polysaccharide colloidal particles as delivery systems for macromolecules. *Adv. Drug Deliv. Rev.*, Vol. 47, pp. 83-97.

Koroloff, N.; Boots, R.; Lipman, J.; Thomas, P.; Rickard, C. & Coyer, F. (2004). A randomised controlled study of the efficacy of hypromellose and Lacri-Lube combination versus polyethylene/Cling wrap to prevent corneal epithelial breakdown in the semiconscious intensive care patien". *Intensive Care Med*, Vol. 30, No. 6, pp. 1122–1126.

Kotzé, A.F.; Lueßen, H.L.; De Leeuw, B.J.; De Boer, A.G.; Verhoef, J.C. & Junginger, H.E. (1997). N-trimethyl chitosan chloride as a potential absorption enhancer across mucosal surfaces: *in vitro* evaluation in intestinal epithelial cells (Caco-2). *Pharm. Res.*, Vol. 14, pp. 1197-1202.

Kotzé, A.F.; Lueßen, H.L.; De Leeuw, B.J.; De Boer, A.G.; Verhoef, J.C. & Junginger, H.E. (1998). Comparison of the effect of different chitosan salts and N-trimethyl chitosan chloride on the permeability of intestinal epithelial cells (Caco-2). *J. Control. Rel.*, Vol. 51, pp. 35-46.

Lee, V.H.L. & Robinson, J.R. (1986). Review: topical ocular drug delivery: recent developments and future challenges. *J. Ocul. Pharmacol.*, Vol. 2, pp. 67-108.

Lehr, C.M.; Bowstra, J.A.; Schacht, E.H. & Junginger, H.E. (1992). *In vitro* evaluation of mucoadhesive properties of chitosan and some other natural polymers. *Int. J. Pharm.*, Vol. 78, pp. 43-48.

Li, N.; Zhuang, C.; Wang, M.; Sun, X.; Nie, S. & Pan, W. (2009). Liposome coated with low molecular weight chitosan and its potential use in ocular drug delivery. *Int. J. Pharm.*, Vol. 379, pp. 131-138.

Liu, Y.; Liu, J.; Zhang, X.; Huang, Y. & Wu, C. (2010). *In situ* gelling gelrite/alginate formulations as vehicles for ophthalmic drug delivery. *AAPS Pharm. Sci. Technol.*, Vol. 11, pp. 610-620.

Ludwig, A. (2005). The use of mucoadhesive polymers in ocular drug delivery. *Adv. Drug Del. Rev.*, Vol. 57, pp. 1595-1639.

Macha, S. & Mitra, A. K. (2001). Ocular pharmacokinetics of cephalosporins using microdialysis. *J. Ocular Pharmacol. Ther.*, Vol. 17, pp. 485-498.

Maeda, T.; Kanda, T.; Yonekura, Y.; Yamamoto, K. & Aoyagi, T. (2006). Hydroxylated poly(*N*-isopropylacrylamide) as functional thermoresponsive materials. *Biomacromolecules*, Vol. 7, pp. 545-549.

Majumdar, S.; Hippalgaonkar, K. & Repka, M.A. (2008). Effect of chitosan, benzalkonium chloride and ethylenediaminotetraacetic acid on permeation of acyclovir across isolated rabbit cornea. *Int. J. Pharm.*, Vol. 348, pp. 175-178.

Muzzarelli, R.A.A.; Tanfani, F.; Emmanueli, M. & Mariotti, S. (1982). N-(carboxymethylidene)-chitosans and N-(carboxymethyl)-chitosans: novel chelating polyampholytes obtained from chitosan glyoxylate. *Carbohydr. Res.*, Vol. 107, pp. 199-214.

Nagarwal, R. C.; Kant, S.; Singh, P.N.; Maiti, P. & Pandit, J.K. (2009). Polymeric nanoparticulate system: A potential approach for ocular drug delivery. *J. Control. Rel.*, Vol. 136, pp. 2-13.

Nanjawade, B.V.; Manvi, F.V. & Manjappa, A.S. (2007). In situ-forming hydrogels for sustained ophthalmic drug delivery. *J. Control. Rel.*, Vol. 122, pp. 119-134.

Paul, W. & Sharma, C. (2000). Chitosan, a drug carrier for the 21st century. *STP Pharma Sci.*, Vol. 10, pp. 5-22.

Rittenhouse, K.D.; Peiffer, R.L. Jr. & Pollack, G.M. (1999). Microdialysis evaluation of the ocular pharmacokinetics of propanolol in the conscious rabbit. *Pharm. Res.*, Vol. 16, pp. 736-742.

Rittenhouse, K.D. & Pollack, G.M. (2000). Microdialysis and drug delivery to the eye. *Adv. Drug Deliv. Rev.*, Vol. 45, pp. 229-241.

Rozier, A.; Mazuel, C.; Grove, J. & Plazonnet, B. (1989). Gelrite®: A novel, ion-activated, in-situ gelling polymer for ophthalmic vehicles. Effect on bioavailability of timolol. *Int. J. Pharm.*, Vol. 57, pp. 163-168

Saettone, M. F. & Salminen, L. (1995). Ocular Inserts for topical delivery. *Adv. Drug Deliv. Rev.*, Vol. 16, pp. 95-106.

Saettone, M.F.; Burgalassi, S.; Boldrini, E.; Bianchini, P. & Luciani, G. (1997). Ophthalmic solutions viscosified with tamarind seed polysaccharide. International patent application. PCT/IT97/00026.

Sechoy, O.; Tissie, G.; Sebastian, C.; Maurin, F.; Driot, J.Y. & Trinquand, C. (2000). A new long acting ophthalmic formulation of carteolol containing alginic acid. *Int. J. Pharm.*, Vol. 207, pp. 109-116.

Singla, A. K. & Chawla, M. (2001). Chitosan: some pharmaceutical and biological aspects – an update. *J. Pharm. Pharmacol.*, Vol. 53, pp. 1047-1067.

Snyman, D.; Hamman, J.H.; Kotzé, J.S.; Rollings, J.E. & Kotzé, A.F. (2002). The relationship between the absolute molecular weight and the degree of quaternisation of N-trimethyl chitosan chloride. *Carbohydrate Polym.*, Vol. 50, pp. 145-150.

Snyman, D.; Hamman, J.H. & Kotzé, A.F. (2003). Evaluation of the mucoadhesive properties of N-trimethyl chitosan chloride. *Drug Dev. Ind. Pharm.*, Vol. 29, pp. 61-69.

Sultana, Y.; Aquil, M. & Ali, A. (2006). Ion-activated Gelrite®-based in situ ophthalmic gels of pefloxacin mesylate: Comparison with conventional eye drops. *Drug Delivery*, Vol. 13, pp. 215-219.

Taravella, M.J.; Balentine, J.; Young, D.A. & Stepp, P. (1999). Collagen shield delivery of ofloxacin to the human eye. *Cataract Refract. Surg.*, Vol. 25, pp. 562-565.

Taylor, L.D. & Ceranaowski, L.D. (1975). Preparation of film exhibiting a balanced temperature dependence to permeation by aqueous solutions-A study of lower consolute behavior. *J. Polym. Sci., Polym. Chem. Ed.*, Vol. 13, pp. 2551-2570.

Thanou, M.; Florea, B.I.; Langemeyer, M.W.E.; Verhoef, J.C. & Junginger, H.E. (2000). N-trimethyl chitosan chloride (TMC) improves the intestinal permeation of the peptide drug buserelin *in vitro* (Caco-2 cells) and *in vivo* (rats). *Pharm. Res.*, Vol. 17, pp. 27-31.

Thanou, M.; Nihot, M.T.; Jansen, M.; Verhoef, J.C. & Junginger, H.E. (2001). Mono-N-carboxymethyl chitosan (MCC), a polyampholytic chitosan derivative, enhances the intestinal absorption of low molecular weight heparin across intestinal epithelia *in vitro* and *in vivo*. *J. Pharm. Sci.*, Vol. 90, pp. 38-46.

Uccello-Barretta, G.; Nazzi, S.; Zambito, Y.; Di Colo, G.; Balzano, F. & Sansò, M. (2010). Synergistic interaction between TS-polysaccharide and hyaluronic acid: Implications in the formulation of eye drops. *Int. J. Pharm*, Vol. 395, pp. 122-131.

Xu-Bo, Y.; Yan-Bo, Y.; Wei, J.; Jie, L.; En-Jiang, T.; Hui-Ming, S.; Ding-Hai, H.; Xiao-Yan, Y.; Hong, L. S. & Jing., S. (2008). Preparation of rapamycin-loaded chitosan/PLA nanoparticles for immunosuppression in corneal transplantation. *Int. J. Pharm.*, Vol. 349, pp. 241-248.

Wei, G.; Ding, P.T.; Zheng, J.M. & Lu, W.Y. (2006). Pharmacokinetics of timolol maleate in aqueous humor sampled by microdialysis after topical administration of thermosetting gels. *Biomed. Chromatogr.*, Vol. 20, pp. 67-71.

Winfield, A.J.; Jessiman, D.; Williams, A. & Esakowitz, L. (1990). A study of the causes of non-compliance by patients prescribed eyedrops. *Br. J. Ophthalmol.*, Vol. 74, pp. 477-480.

Zambito, Y.; Zaino, C. & Di Colo, G. (2006a). Effects of N-trimethylchitosan on transcellular and paracellular transcorneal drug transport. *Eur. J. Pharm. Biopharm.*, Vol. 64, pp. 16-25.

Zambito, Y.; Uccello-Barretta, G.; Zaino, C.; Balzano, F. & Di Colo, G.(2006b). Novel transmucosal absorption enhancers obtained by aminoalkylation of chitosan. *Eur. J. Pharm. Sci.*, Vol. 29, pp. 460-469.

Zambito, Y.; Zaino, C.; Burchielli, S.; Carelli, V.; Serafini, M. F. & Di Colo, G. (2007). Novel quaternary ammonium chitosan derivatives for the promotion of intraocular drug absorption. *J. Drug Deliv. Sci. Technol.*, Vol. 17, pp. 19-24.

Zambito, Y.; Zaino, C.; Uccello-Barretta, G.; Balzano, F. & Di Colo, G. (2008). Improved synthesis of quaternary ammonium-chitosan conjugates (N^+-Ch) for enhanced intestinal drug permeation. *Eur. J. Pharm. Sci.*, Vol. 33, pp. 343-350.

Zambito, Y.; Fogli, S.; Zaino, C.; Stefanelli, F.; Breschi, M.C. & Di Colo, G. (2009). Synthesis, characterization and evaluation of thiolated quaternary ammonium-chitosan conjugates for enhanced intestinal drug permeation. *Eur. J. Pharm. Sci.*, Vol. 38, pp. 112-120.

Zambito, Y. & Di Colo, G. (2010). Thiolated quaternary ammonium-chitosan conjugates for enhanced precorneal retention, transcorneal permeation and intraocular absorption of dexamethasone. *Eur. J. Pharm. Biopharm.*, Vol. 75, pp. 194-199.

14

Nacre, a Natural Biomaterial

Marthe Rousseau
Henri Poincaré University, Nancy I
France

1. Introduction

Nacre, or mother-of-pearl, is a calcium carbonate structure produced by bivalves, gastropods, and cephalopods as an internal shell coating. Because of its highly organized internal structure, chemical complexity, mechanical properties and optical effects, which create a characteristic and beautiful lustre, the formation of nacre is among the best-studied examples of calcium carbonate biomineralization. In this chapter we will detail the structure of nacre and its growth mechanism. We will summarize the several results obtained on the *in vivo* and *in vitro* biological activity of nacre and its organic molecules.

2. Nacre structure

The interdigitating brickwork array of nacre tablets (Fig.1), specific, in bivalves ("sheet nacre") is not the only interesting aspect of nacre structure. Nacre is an organo-mineral composite at micro- and nano-scale. The bio-crystal itself is a composite. It has not only the mineral structure of aragonite but possesses intracrystalline organic material (Watabe, 1965). The primary structural component is a pseudohexagonal tablet, about 0.5 μm thick and about 5 to 10 μm in width, consisting primarily (97%) of aragonite, a polymorph of $CaCO_3$, and of organics (3%). Nacre can be worked as pieces and powder.

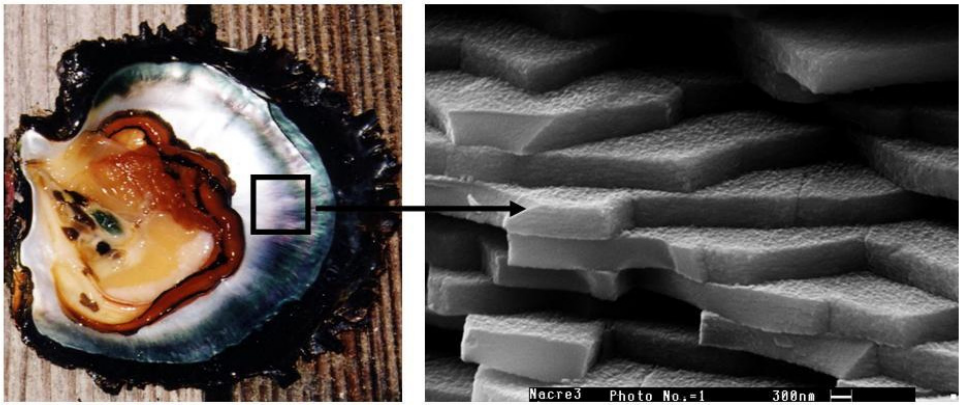

Fig. 1. Characteristic brick and mortar structure of the nacreous layer of *Pinctada*.

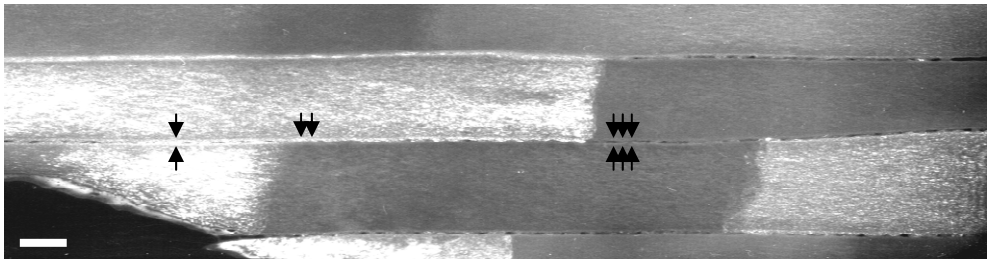

Fig. 2. Darkfield TEM image of nacre evidencing the crystalline structure of the organic matrix (bar is 100nm). Organic matter is in contrast when under Bragg conditions whilst the mineral phase remains systematically extinguished.

Transmission electron microscopy performed in the darkfield mode evidences (Fig.2) that intracrystalline matrix is highly crystallised and responds like a 'single crystal'. The organic matrix is continuous inside the tablet, mineral phase is thus finely divided but behaves in the same time as a single crystal.

The tablet of nacre, the biocrystal, does diffract as a single crystal but is made up of a continuous organic matrix (intracrystalline organic matrix) which breaks the mineral up into coherent nanograins (~45 nm mean size, flat-on) which share the same crystallographic orientation. The single crystal-like mineral orientation of the tablet is supposedly created by the heteroepitaxy of the intracrystalline organic matrix. This is a strong hypothesis because this work demonstrates at the same time that this intracrystalline matrix is well crystallized (i.e. periodic) and diffracts as a "single crystal" too (darkfield TEM mode, Fig. 2). However these "organic crystals" do not show the same orientation in adjacent tablets.

Neighbouring tablets above and below can maintain a common orientation, which again raises the issue of the transmission of mineral orientation from one row to the next. Bridges are well identified in *Pinctada* between successive rows in the pile. This implies that an organic template is controlling the orientation of the aragonite.

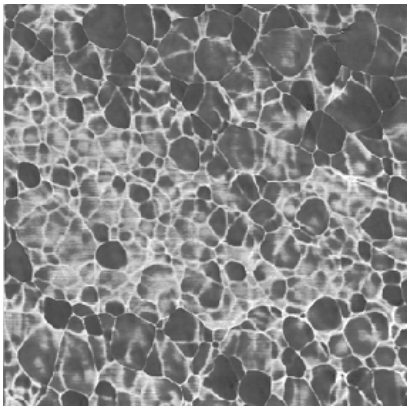

Fig. 3. AFM picture in Phase Contrast (1x1µm²) at the nanometer (nm) length scale, the aragonite component inside individual tablets is embedded in a crystallographically oriented foam-like structure of intra-crystalline organic materials in which the mean size of individual aragonite domains is around 50 nm.

Intermittent-Contact Atomic Force Microscopy with phase detection imaging reveals a nanostructure within the tablet (Fig.3). A continuous organic framework divides each tablet into nanograins. Their mean extension is 45nm. It is proposed that each tablet results from the coherent aggregation of nanograins keeping strictly the same crystallographic orientation thanks to a hetero-epitaxy mechanism (Rousseau et al., 2005a).

3. Nacre growth mechanism

Formation of nacre (*mother-of-pearl*) is a biomineralization process of fundamental scientific as well as industrial importance. However, the dynamics of the formation process is still not all understood. Scanning electron microscopy and high spatial resolution ion-microprobe depth-profiling have been used to image the full three-dimensional distribution of organic materials around individual tablets in the top-most layer of forming nacre in bivalves. Nacre formation proceeds by lateral, symmetric growth of individual tablets mediated by a growth-ring rich in organics, in which aragonite crystallizes from amorphous precursors (Fig.4). The pivotal role in nacre formation played by the growth-ring structure documented in this study adds further complexity to a highly dynamical biomineralization process.

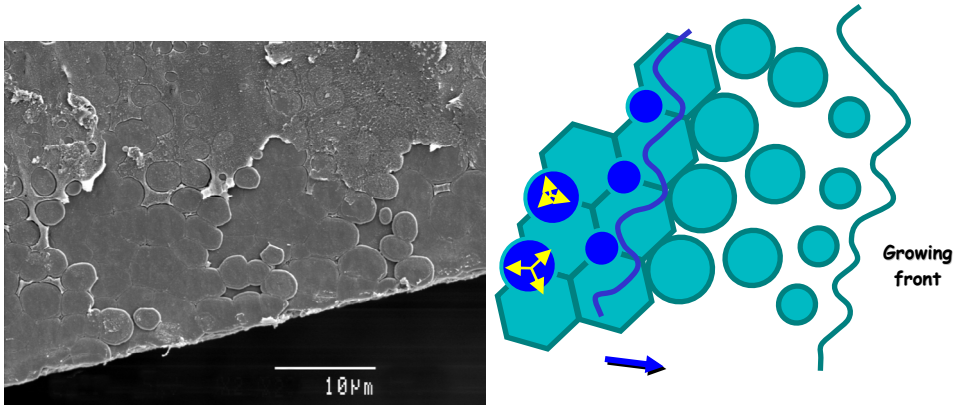

Fig. 4. Nuclei (future nacre tablets) grow circularly in a film, get in contact and form polygons.

Figure 5 shows the surface membrane, observed from the point of view of the nacre layer, and corresponding features in the growing nacre surface, respectively. Several important observations can be made. i) For each nacre tablet, there exists in the membrane a circular structure (Fig. 5a, c). The circular membrane structure displays higher topography than the adjacent surface membrane. We refer to this circular structure as the 'ring'. ii) This ring makes direct physical contact with the growing nacre tablets. Each nacre tablet features a similar ring, several hundred nm wide, with a complementary (i.e. lower) topography (Fig. 5b, d). iii) Neighbouring tablets can merge during growth by lateral expansion that leads to a 'collision'. In this process, ring structures surrounding each tablet first merge together, then disappear (Fig. 5d).

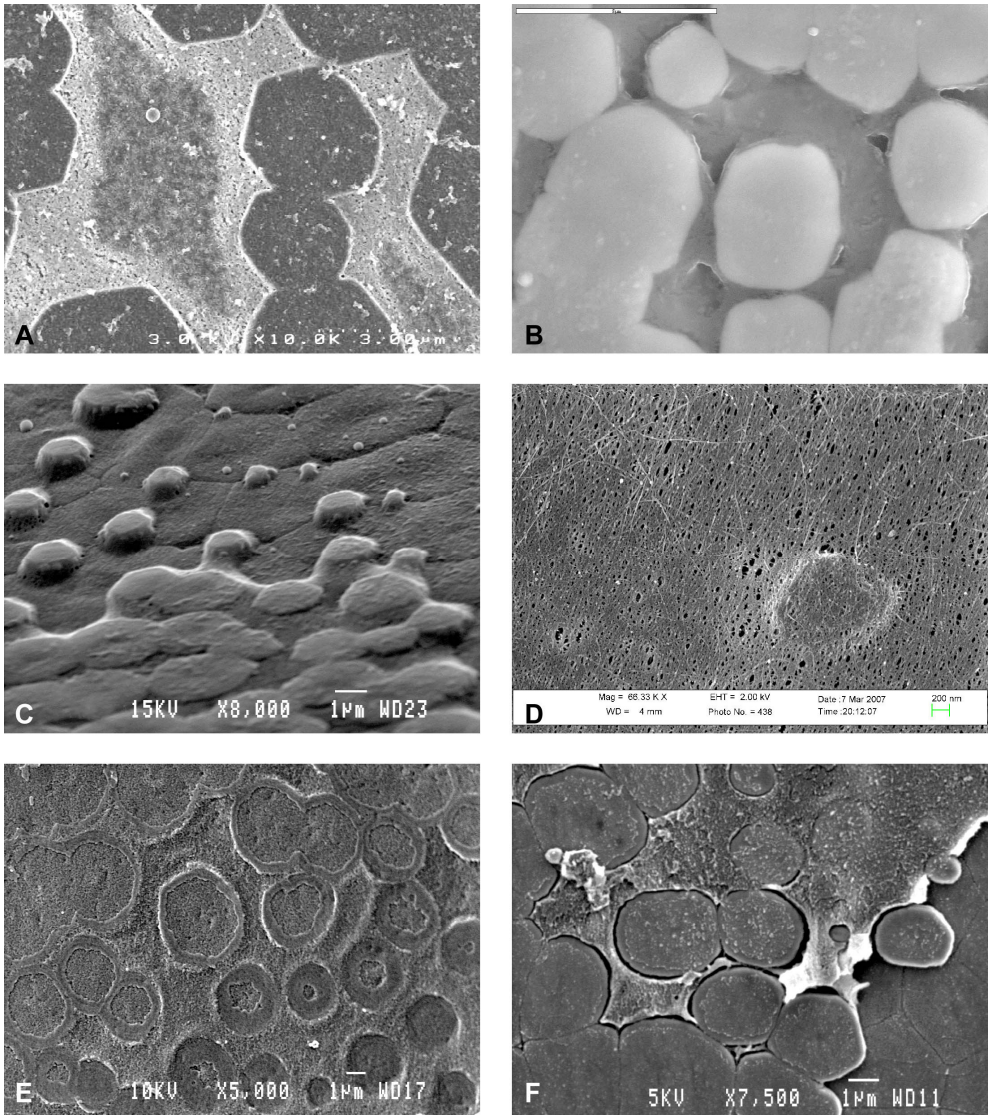

Fig. 5. Direct observation of the nacre surface of the same sample series with different SEM secondary electron detectors : A: in-lens detector at 3kV, B: same but at 15kV both with an Hitachi 4500-FEG microscope, C, E, F: lower detector of the JEOL JSM-840A at 15, 10 and 5kV, D: with a high-resolution Ultra 55 Zeiss using an in-lens secondary electron detector at 2kV.

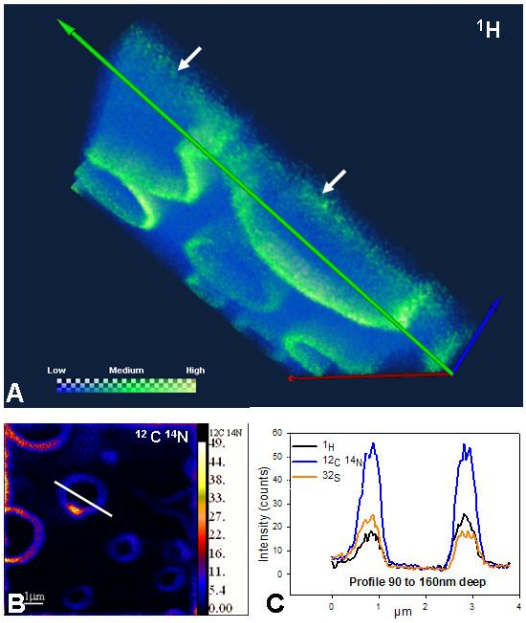

Fig. 6. Distribution of organics around nacre tablets. a) A 3-dimensional reconstruction of the H distribution at different depths in the surface layers of the forming nacre. The data were obtained with the NanoSIMS ion microprobe. The direction of sputtering is indicated by a white arrow. The sputtered volume is about 10µmx10µmx0.2µm. For greater clarity, the thickness of this volume (blue axis) has been expanded by a factor of 6. The surface membrane is visible in the first images (white arrow) but deeper in the structure organics are concentrated only in the growth-rings surrounding each nacre tablet. (Full 3-D reconstructions of the H, N and S distributions are available in SD as movies) b) NanoSIMS image showing the distribution of N, which is also preferentially concentrated in the growth-ring around each nacre tablet. c) Line-profile (track indicated in b) showing the enhanced concentrations of H, N, and S in the growth-ring. See text for discussion.

The NanoSIMS allows chemical composition to be imaged with extremely high spatial resolution (on the order of 100 nm), while depth-profiling through the inter-lamellar matrix and into the nacreous structure with a depth resolution of about 10 nm per image (Meibom et al., 2004, 2007). The 3-dimensional distribution of H, N and S are diagnostic of organic compounds in which their concentration is greatly increased over that in the aragonitic nacre tablets. Figure 6a shows the 3D reconstruction of a depth-sequence of H images from the top-most layers (in the membrane), via intermediate levels to an estimated depth of around 0.2 µm in the tablet structure, where the overlying membrane has been sputtered away completely and the distribution of organics around individual tablets becomes visible. The distribution of organics in the ring surrounding each nacre tablet corresponds to the characteristic ring in the overlying mantle; see Fig. 5d. Figure 6c shows in greater detail the distribution of organics around individual tablets. Importantly, concentrations of H, N and S

are clearly confined to the rim around each tablet. In the ring, the signal from N is almost two orders of magnitude higher than in the surrounding aragonitic tablets. Sulfur and Hydrogen are enriched by factors of about 10 and 7, respectively over the signal observed from inside the tablet. We proposed a model illustrated in Fig. 7. A growth-ring structure, rich in organic materials, surrounds each growing nacre tablet during formation of sheet nacre in *Pinctada margaritifera* bivalves. This structure disappears as nacre tablets grow laterally and collide with adjacent tablets. It is conceivable that this organic ring structure acts to nucleate aragonite into the highly oriented nano-crystals (~50 nm in size) that make up the meso-crystal (i.e. µm sized) nacre tablets (Wohlrab et al., 2005; Kulak et al., 2007). This adds support for a highly dynamic biomineralization process during which organic materials and carbonate precursor phases (likely amorphous) are delivered to the site of nacre tablet formation from the overlying mantle with a high degree of spatial control.

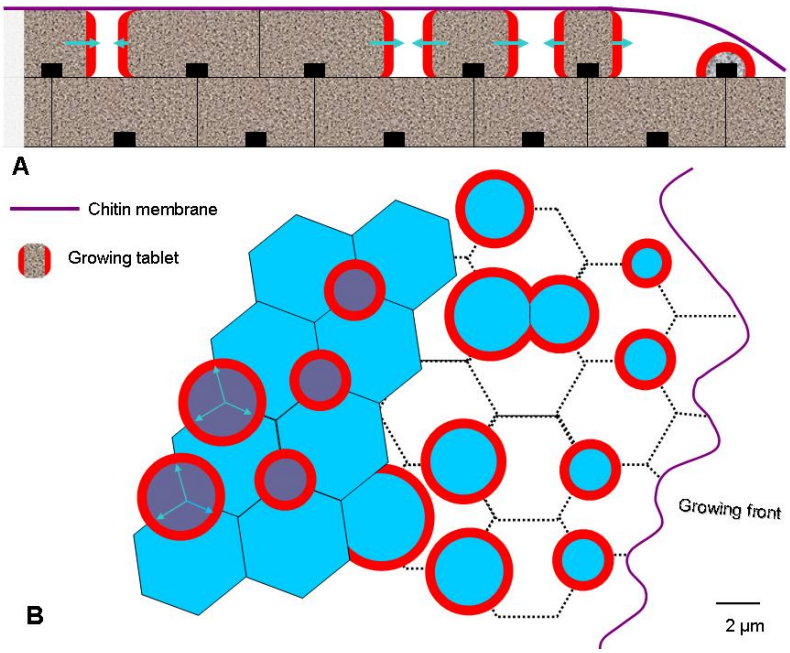

Fig. 7. Schematic representation of the nacre tablet growth-model. a) Side-view of the top-most tablet-layers. Underneath the top membrane, which is in direct contact with the overlying mantle of the animal, individual tablets grow laterally from a carbonate-charged silk-phase through crystallization mediated by organics in the nucleation sites (black rectangles) and in the growth-rings (shown in red). The nucleation sites are generally placed above the junctions of three tablets in the underlying layer of tablets. When two tablets collide during growth, the growth-rings first merge and subsequently disappear, allowing adjacent tablets to make physical contact. b) Top view of the nacre growth front. Individual tablets nucleate and grow concentrically reflecting the shape of the surrounding organic growth-ring. Only after collision and disappearance of the growth-rings do individual tablets take the form of hexagons. The hexagonal geometry of individual tablets is therefore the result of the distribution of nucleation sites, which inherit their distribution from the underlying layer.

4. Biological action of raw nacre

Nacre biological action. A major breakthrough was done in 1992, when E. Lopez et al. discovered that natural nacre from the pearl oyster *Pinctada maxima* is simultaneously biocompatible and osteoinductive. Nacre shows osteogenic activity after implantation in human bone environment (Silve et al., 1992). Raw nacre pieces designed for large bone defects were used as replacement bone devices in the femur of sheep. Over a period of 12 months, the nacre blocks show persistence without alteration of the implant shape. A complete sequence of osteogenesis resulted from direct contact between newly formed bone and the nacre, anchoring the nacre implant (Atlan et al., 1997). Furthermore, when nacre is implanted in bone, new bone formation occurs, without any inflammatory reaction and fibrous formation. We observed an osteoprogenitor cellular layer lining the implant, resulting in a complete sequence of new bone formation (Fig.8). Results showed calcium and phosphate ions lining the nacre within the osteoprogenitor tissue (Atlan et al, 1999).

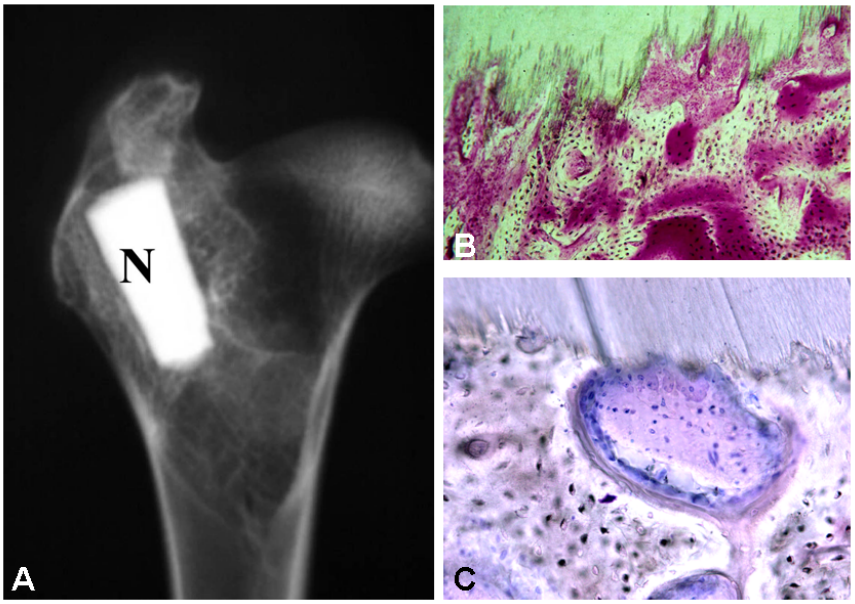

Fig. 8. Radiographic image of the femur epiphysis harvested 10 months after implantation of a block of nacre (N) showing the preserved size and shape of the implant and the close contact between the implant and surrounding cancellous bone (A). After erosion of the implant surface nacre is in direct contact with the new formed bone (B). At the interface bone forming cells are stimulated (C) (Atlan et al, 1999).

Osteogenesis thought to begin with the recruitment of mesenchymal stem cells, which differentiate to form osteoblasts in response to one or more osteogenic factors. In previous studies (Atlan et al., 1997; Silve et al., 1992), as reviewed in Westbroek and Marin (1998), it has been shown by means of *in vivo* and *in vitro* experiments that nacre can attract and activate bone marrow stem cells and osteoblasts.

Other authors have demonstrated the same activity of nacre. Liao et al., in 2000 have published results about the implantation in back muscles and femurs of rats of nacre pieces coming from the shell of the freshwater *Margaritifera*. They concluded that their nacre was biocompatible, biodegradable and osteoconductive material. They confirmed the results obtained with *Pinctada* nacre. More recently Shen et al. (2006) have demonstrated the *in vitro* osteogenic activity of pearl. Hydroxyapatite can be formed on pearl surface in Simulated Body Fluid based on a dissolution-binding-precipitation mechanism. Cell culture shows that pearl has the same osteogenic activity as shell nacre.

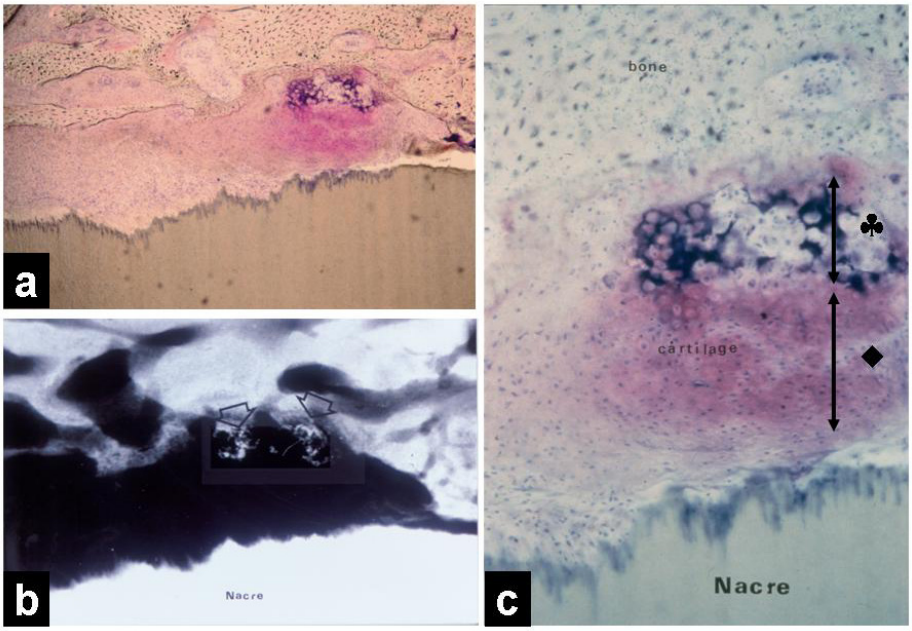

Fig. 9. Histological study of the nacre/ bone interface, lateral to the nacre trochlea, after 6 months of implantation: longitudinal section of nacre subchondral implant, islets of ossification at the interface between nacre and bone (a: x8; b: microradiography of the same area), showing the sequence of cell differentiation from nacre to spongy host bone, chondrocytes (♦) and hypertrophic chondrocytes (♣), after basic fuchsin and toludine bleu staining (c: x 16).

Nacre has also been implanted in the subchondral bone area in the sheep knee. We implanted nacre blocks in sheep trochlea by replacing the half of the femoral trochlea (nacre group). For comparison we used complete cartilage resection (resection group) down to the subchondral bone. In the "nacre group", implants were well tolerated without any synovial inflammation (Fig.9). This complementary study was the first one designed to analyze the behaviour of nacre *in vivo*, in the intra articular cavity after implantation into the subchondral bone in the sheep's knee (Delattre, 2000). After 6 months of implantation, a new tissue was formed on the articular surface of nacre. This tissue is composed of new formed bone and articular cartilage, partially covering the

subchondral implant placed in the defect. The presence of nacre can progressively stimulate the regrowth of a tissue, reproducing the functional osteochondral structure in which the subchondral bone sends stimulating messages to the cartilage layer. The regrowth reaction seems to be a well regulated physiological process, demonstrating the efficacy and good tolerance to nacre. Laterally to the nacre implant we observed islets of endochondral ossification. Endochondral ossification is initiated by the formation of cartilage templates of future bones, built by mesenchymal progenitor cells, which condensate and differentiate into chondrocytes. During the repair process the events of endochondral ossification are recapitulated (Fig.9).

A process of nacre powder preparation has been patented (Lopez et al., 1995). The obtained nacre powder has been experimented in injectable form in vertebral and maxillar sites of sheep (Lamghari et al., 1999a, 1999b). This work has demonstrated that nacre powder is resorbable and that this resorption induced the formation of normal bone. The nacre powder filled the whole experimental cavity after 1 week post-surgery. There was no inflammatory or foreign body reaction in the cavity area. Samples taken at 8 weeks after injection showed dissolution of the nacre within the cavity. Angiogenesis had began by that time and the cavity was invaded by a network of capillaries. The cavity contained newly formed woven bone (Fig.10). The vertebral bone adjacent to the cavities contained interconnected bone lamellae. They were also bone remodelling units with central lacunae rich in bone marrow. This new formed Bone was functional as normal bone.

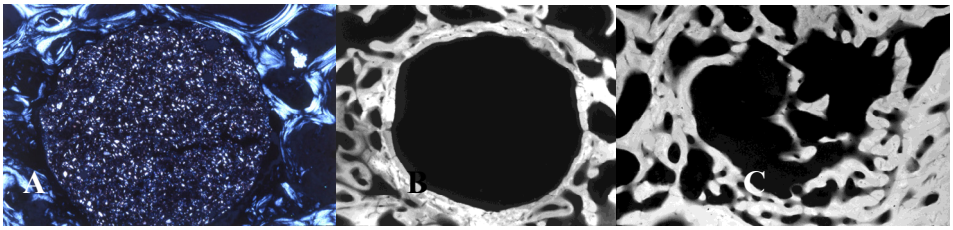

Fig. 10. Nacre injected into the sheep vertebrae. Polarized light image showing transverse section throught a bone defect. The cavity is filled with nacre (A, x25). In the empty cavity after 8 weeks, the bone was organised into concentric rings (B). 8 weeks after injection the nacre powdered has disappeared and been replaced by new formed bone (C) (Lamghari et al, 2001).

In the *in vivo* studies nacre has been shown to be resorbable. Osteoclast activity was therefore studied *in vitro* on nacre (Fig.11). The idea was to assess the plasticity of bone resorbing cells and their capacity to adapt to a biomineralized material with a different organic and mineral composition. Osteoclast stem cells and mature osteoblasts were cultured on nacre substrate and osteoclast precursor were shown to differentiate into osteoclasts capable of resorbing nacre (Duplat et al, 2007).

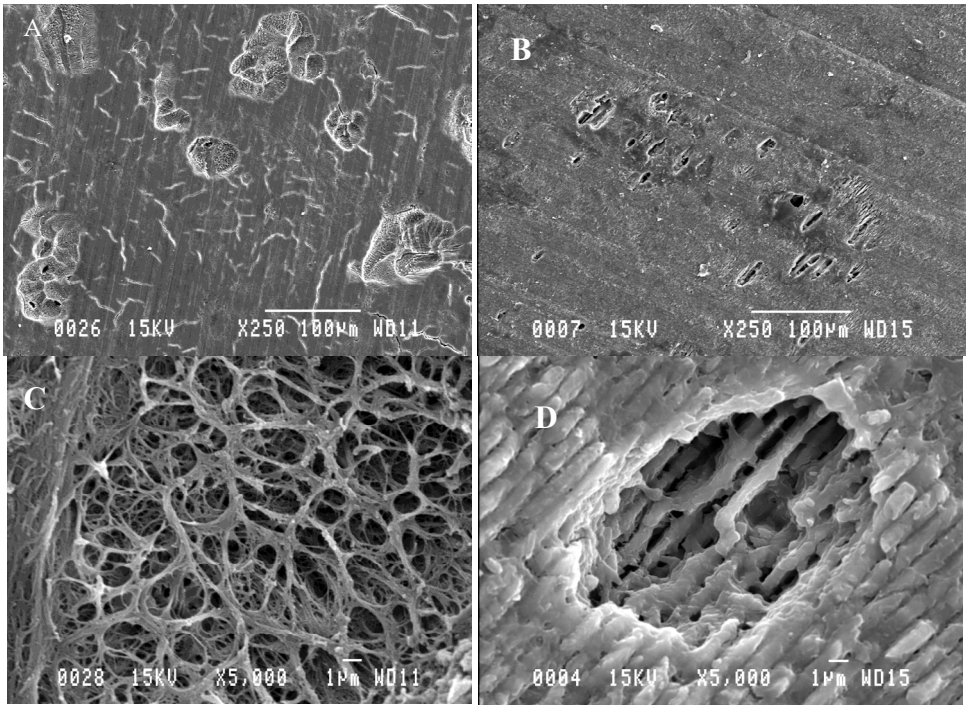

Fig. 11. Resorption process of osteoclasts differentiated from human CD14+ monocytes on bone (A, C) and on nacre (B, D). SEM examination of resorption lacunae. The form of the lacunae is quite different and can be explained by the different organic and mineral compositions as well as by the mineral density of bone and nacre.

5. Biological action of nacre extracts

Nacre is composed of aragonite crystal tablets covered by an organic matrix (3%) (Bevelander & Nakahara, 1969). This organic phase is composed of chitine, polysaccharides, proteins, peptides, lipids and other small molecules lower than 1000 Da. The organic molecules can be extracted with aqueous and organic solvents. The water-soluble organic matrix dictates which calcium carbonate crystal structure is formed and when it is deposited (Cariolou & Morse, 1988). The bulk of the watersoluble biopolymer is thought to consist of a complex mixture of proteins and peptides (Kono et al., 2000; Weiss et al., 2000**).** Nacre possess in its organic matrix molecular signals that have the ability to trigger bone cell commitment. Efforts were undertaken in order to identify these active molecules and to determine their mode of action on mammalian bone cells. A particular attention was paid to the water-soluble matrix (WSM) molecules of nacre. We supposed that this fraction contains molecules which are released when the nacre implants are placed in living systems. Molecules extracted from nacre of the pearl oyster *P. maxima* with water have been shown to have a biological activity on various mammalian pre-osteogenic cell types (Rousseau et al., 2003).

The activity of the nacre water-soluble matrix (WSM) from *P. maxima* was measured on the clonal osteogenic cell-line MC3T3-E1 established from newborn mouse calvaria. These cells have the capacity to differentiate into osteoblasts, and form calcified bone tissue *in vitro*. The WSM increased alkaline phosphatase activity (Pereira-Mouriès et al., 2002b) and induced the formation of bone nodules (Rousseau et al., 2003). On bone marrow stromal cells, WSM stimulated the proliferation, the differentiation and the early mineralization of osteoprogenitor cells (Lamghari et al., 1999a).

Recently, a great number of low molecular weight molecules was identified in WSM as main components, whereas proteins are minor (15 % w/w). It was supposed that the signal-molecules of nacre might to be low molecular weight molecules. This feature may facilitate their diffusion in the host tissues from nacre implants. The hypothesis that nacre low MW molecules are active in bone cell differentiation was evaluated. Water-soluble molecules from nacre were fractionated according to dialysis, solvent extraction and reversed-phase HPLC. The two sub-fractions ESM and F1 were tested on MC3T3-E1 cell culture. Mass spectrometry analysis showed that the F1 sub-fraction contains around 30 polar molecules ranging from 50 to 300 Da (Fig.12). Peptides were not identified in this fraction. However, the aggregative property of these molecules during chromatography precludes the obtaining of a more purified active fraction.

The presence of BMP-like molecules in WSM was supposed but not demonstrated (Rousseau et al., 2007). Molecules isolated from nacre induced mineralization of the preosteoblasts extracellular matrix after 16 days of culture that was analyzed as hydroxyapatite by Raman spectroscopy. This study indicated that the nacre molecules efficient in bone cell differentiation are certainly different from proteins, and probably more related to peptides (Rousseau et al., 2003, 2007). Molecules isolated from nacre, ranging from 50 to 235 Da, in induced red alizarin staining of the preosteoblasts extracellular matrix after 16 days of culture. The treatment of cells with nacre molecules accelerated expression of collagen I and increased mRNA expression of Runx2 and osteopontin (Fig.13). Raman spectroscopy demonstrated the presence of hydroxyapatite in samples treated with this molecules. Scanning electron microscopy pictures showed at the surface of the treated cells the occurrence of clusters of spherical particles resembling to hydroxyapatite (Fig. 14). Nacre low molecular weight molecules stimulate the early stages of bone differentiation and the formation of an extracellular matrix able to initiate hydroxyapatite nucleation.

The water-soluble matrix of nacre is composed of at least 110 molecules ranging from 100 to 700 Da, with a low content (10 %) of peptides (Bédouet et al., 2006). On the other hand, the protein content of the WSM represents 15 % (w/w) of the extract (Pereira-Mouriès et al., 2002a). Dialysis fractionation of the water-soluble matrix of nacre indicated that low molecular mass molecules lower than 1kDa were important components. They represents 0.14% of the nacre weight, i.e. 60% of the water soluble matrix itself, and contained a huge chemical diversity, since 100 molecules with close molecular weight were gathered after MS analyses of only half of the recovered fractions lower than 1kDa. Some of the low molecular weight molecules were glycine-rich pepetides (9%) whereas the chemical nature of the others remains unidentified. These molecules could correspond either to degradation product of biopolymers or to metabolites accumulated in nacre during the growth of the oyster shell.

The low molecular weight fraction contained specific inhibitors of cysteine protease in addition to proteinase K inhibitors (Bédouet et al., 2007). The specificity of the proteinase

inhibitors Found in the nacre water-soluble fraction is quite interesting. Indeed, the cysteine proteinases, particularly cathepsin B and L, are involved in different pathologies, such as arhtrosis and cartilage degradation. The organic matrix of nacre contains both general and more specific inhibitors of cysteins protease in addition to proteinase K inhibitors. The mollusc shell may be used as a new source of natural inhibitors, particularly for the cystein proteinases. The proteinase inhibitors present in the shell may play a major role in the regulation of biomineralization, and they may protect the nacre layer against proteolytic digestion during the perforation of the shell by worms.

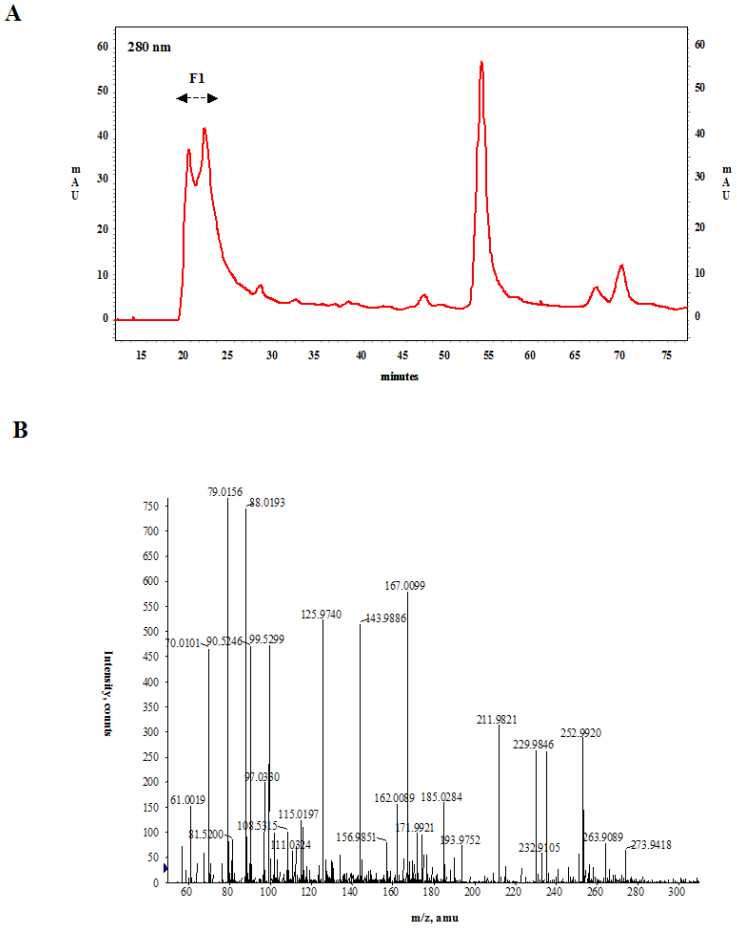

Fig. 12. Isolation of active fraction F1 from the nacre low molecular weight molecules using reversed-phase chromatography. The ESM fraction (75 mg) was loaded onto a C_4 column (2.2 x 25 cm) before elution with a linear acetonitrile-0.1 % TFA gradient. The flow rate was 3 mL/min and fractions (5 mL) eluted between 16 and 25 min were pooled giving the fraction F1 (A). Analysis using electrospray mass spectrometry (ion-positive mode) of the fraction F1. Labels indicate $[M+H^+]^+$ ion species (B).

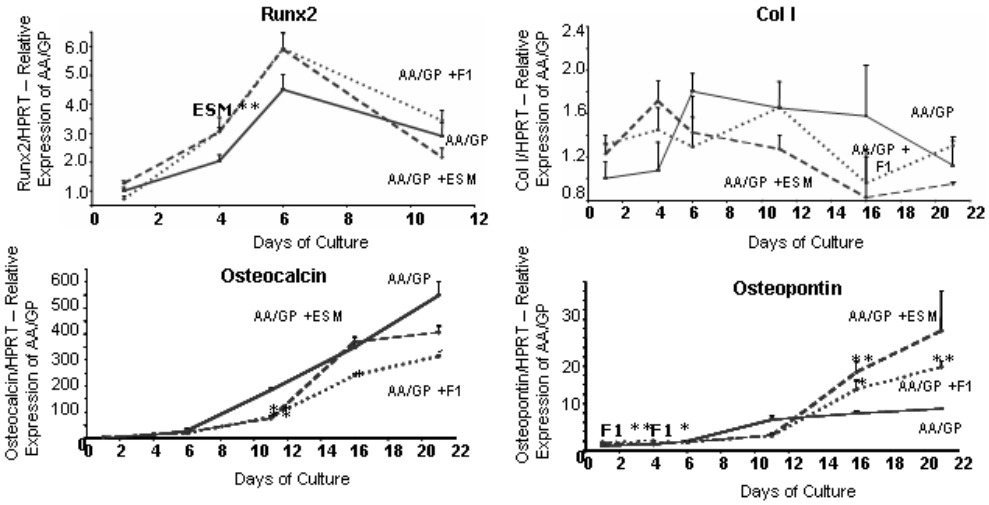

Fig. 13. Effects of ESM and F1 fractions on Runx2, type I collagen, osteopontin and osteocalcin gene expression in MC3T3-E1 cells analyzed by quantitative RT-PCR. The MC3T3-E1 cells were cultured during 1, 4, 6, 11, 16 and 21 days in the absence or presence of ESM and F1 fraction (200 µg/mL) in α-MEM medium supplemented with 10 mM GP (β-glycerophosphate) and 50µg/µL AA (ascorbic acid). Total cellular RNA was isolated and expression of Runx2, type I collagen, osteopontin and osteocalcin were determined by quantitative RT-PCR relative to the HPRT expression. Results are the means + SEM of 5 experiments for Runx2 and 3 experiments for col I, osteopontin and osteocalcin. The reference is day 1 from AA/GP samples. Data were corrected for initial template quantity variations by normalizing values by HPRT. A minimum significant difference (* $p<0.05$, ** $p<0.01$) between control and the samples ESM and F1 was determined.

Lipids presence was discovered in the so-called "ethanol soluble matrix" (ESM). The extract contains fatty acids, triglycerides, cholesterol and ceramides in low abundance (Fig.15). Application of ESM on human skin explants previously partially dehydrated induced an overexpression of filaggrin (responsible for hydration of stratum corneum) and a decrease of transglutaminase expression (overexpressed in inflammatory skin diseases). We also showed that ESM extracted from the mother of pearl of *P. margaritifera* induced a reconstitution of the intercellular cement of the *Stratum corneum* (Fig.16) (Rousseau et al., 2006). If the physiological and structural functions of the lipids in the nacre remain elusive, their biological activity on delipidated human skin explants is more accurate. Two lipids preparations containing respectively 0.5 and 1% of nacre lipids in weight were prepared with an excipient. According to the immunolabelling of filaggrin in skin explants, it has been showed that the nacre lipids induced on the delipidated skin an expression of filaggrin higher to the the level found in untreated skin. On the other hand, the lipid formulation reduced the expression of TGase 1 in the cornified envelope in a dose dependent manner. It seemed that the lipids extracted from nacre had brought to the stratum corneum the elements necessary to a rapid reconstruction of the intercellular cement, by acting on the expression levels of transglutaminase and filaggrin.

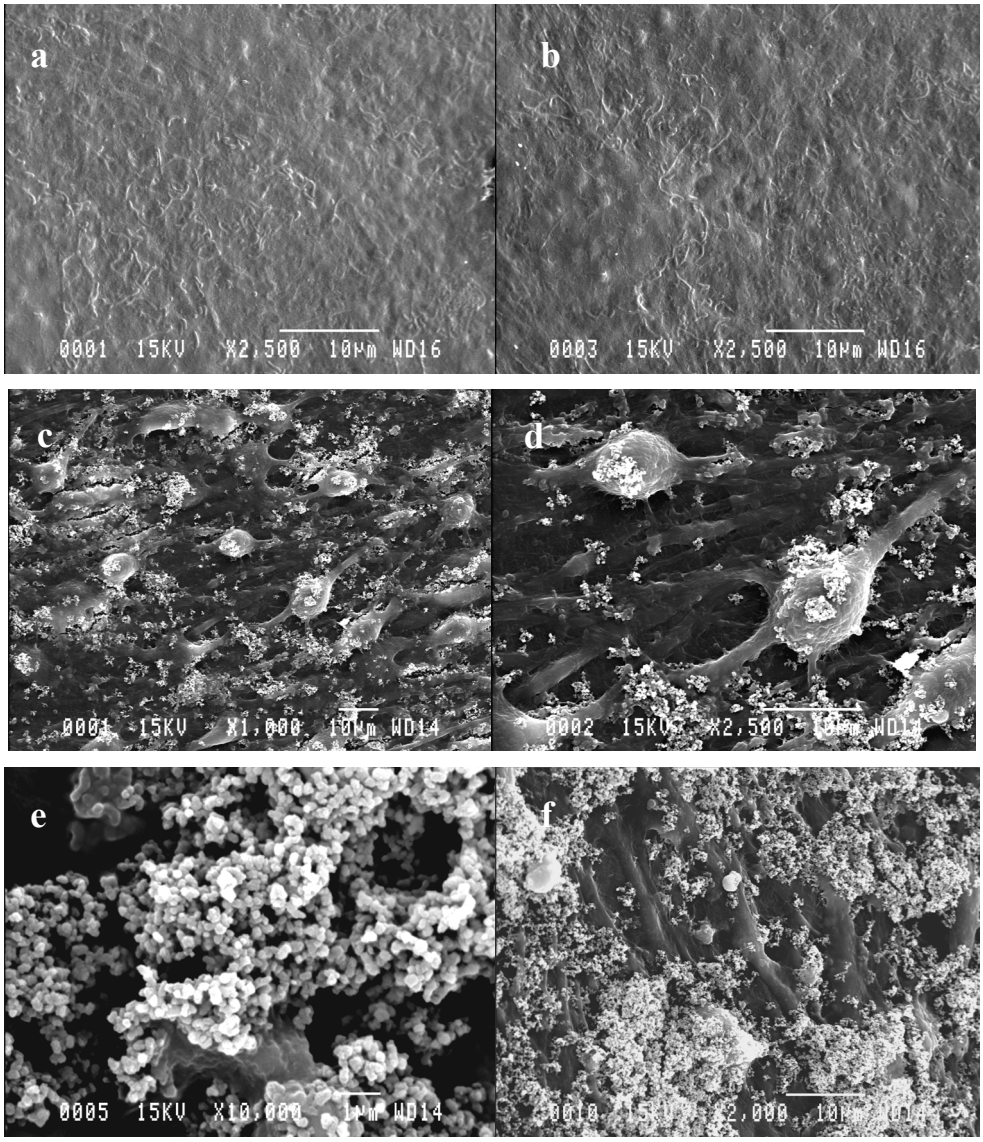

Fig. 14. Scanning electron microscopy observation of the MC3T3-E1 cells extracellular matrix treated with ESM for 16 days. Control cell (a), cells treated with AA/GP (b), cells treated with ESM (200 μg/mL) in presence of AA/GP (c, d, e, f) at different magnifications.

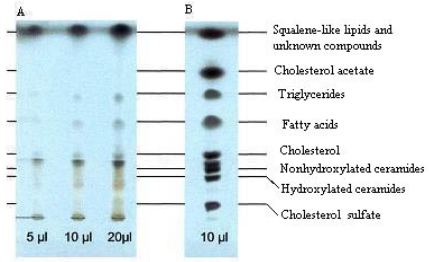

Fig. 15. TLC analysis of lipids extracted from the nacre of *P. margaritifera* with hexane/diethylether/acetic acid (60,25,15, v/v/v) as a mobile phase. Samples of 5, 10 and 20 µl of the lipid extracts at 20 mg/ml and a standard lipid mixture loaded and stained with copper sulfate reagent.

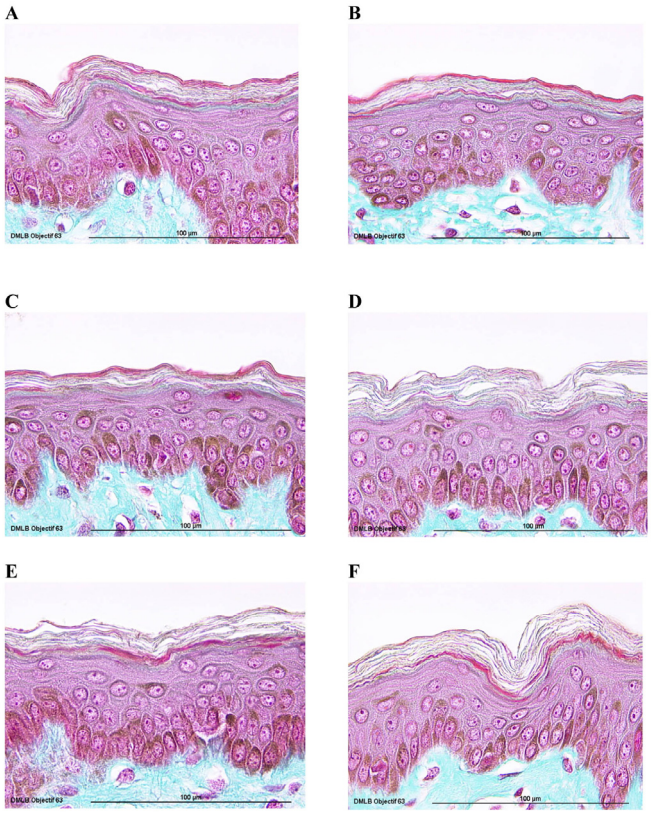

Fig. 16. Histological observation of the skin explants morphology. Control at To (A), in dehydrated skin at To (B), in dehydrated skin at T + 3 h (C), in dehydrated skin at T + 3 h treated with excipient (D) and in dehydrated skin treated with 0.5 % (E) and 1 % (F) of nacre lipids at T + 3 h. Staining was performed according to the Masson's Trichrom.

6. Conclusion

Nacre, or mother-of-pearl, is a calcium carbonate structure produced by bivalves, gastropods, and cephalopods as an internal shell coating. Because of its highly organized internal structure, chemical complexity, mechanical properties and optical effects, which create a characteristic and beautiful lustre, the formation of nacre is among the best-studied examples of calcium carbonate biomineralization. A major breakthrough was done in 1992, when E. Lopez et al. discovered that natural nacre from the pearl oyster *Pinctada* is simultaneously biocompatible and osteoinductive. A complete sequence of osteogenesis resulted from direct contact between newly formed bone and the nacre, anchoring the nacre implant. Furthermore, when nacre is implanted in bone, new bone formation occurs, without any inflammatory reaction and fibrous formation. In previous studies as reviewed in Westbroek and Marin, it has been shown by means of *in vivo* and *in vitro* experiments that nacre can attract and activate osteoblasts. Nacre has been implanted in the subchondral bone area in the sheep knee. A process of nacre powder preparation has been patented. The obtained nacre powder has been experimented in injectable form in vertebral and maxillar sites by sheep. Nacre implant induced no inflammatory reaction. Nacre is biocompatible, osteogenic and osteoinductor.

Nacre is composed of aragonite crystal tablets covered by an organic matrix. The water-soluble organic matrix dictates which calcium carbonate crystal structure is formed and when it is deposited. The bulk of the watersoluble fraction is thought to consist of a complex mixture of proteins and peptides.

The water soluble matrix (WSM) increases alkaline phosphatase activity and induces formation of bone nodules of the clonal osteogenic cell-line MC3T3-E1. WSM, Dexamethasone and BMP-2 all stimulate alkaline phosphatase activity in a manner corresponding to a differentiation into an osteoblast phenotype. On bone marrow stromal cells, WSM stimulates the proliferation, the differentiation and the early mineralization of osteoprogenitor cells. Small molecules isolated from nacre induce mineralization of the preosteoblast extracellular matrix after 16 days of culture. Raman spectroscopy revealed as hydroxyapatite the crystals formed extracellularly. We also extracted proteinase inhibitors from the nacre of *Pinctada*. The low molecular weight fraction contained specific inhibitors of cysteine protease in addition to proteinase K inhibitors. We also discovered the presence of lipids in nacre and we showed that their lipids induced a reconstitution of the intercellular cement of the human *Stratum corneum*.

Nacre has been mostly studied the last two decades for its action on bone and skin (Table 1).

Biocompatiblity

- Nacre is not toxic for the human body after maxillary implantation
- When nacre is implanted in bone, no inflammatory reaction nor fibrous formation was observed.

Effects on Bone

- Osteogenic activity was observed in sheep after implantation in bone environment
- Nacre powder is resorbable and this resorption induced the formation of normal bone *in vivo*
- Nacre can attract and stimulate osteoblasts activity *in vitro*
- The nacre molecules involved in bone cell differentiation are small, certainly different from proteins, and probably peptides

Effects on Cartilage
- Nacreous trochlea is covered with new non fibrous cartilage after implantation in sheep

Anti-proteases effect
- Presence of cysteine proteases and proteinase K inhibitors in nacre organics

Effect on Skin
- Nacre lipids are able to reconstitute the epiderm intercellular cement

Table 1. Summary of the biological actions of nacre

7. Acknowledgement

We would like to thank all the investigators and co-investigators involved in the research on nacre: particularly Professor Evelyne Lopez for the discovery of the biological activity on nacre, Dr Xavier Bourrat for his help on the structure study and the growth mechanism of nacre, Dr Philippe Stempflé for the nanostructure and the mechanical study on nacre, Meriem Lamghari for her nice work with nacre powder injection, Dr Olivier Delattre for the nacre implantation, Professor Anders Meibom for giving me the opportunity to put nacre samples in the NanoSIMS machine, Dr Denis Duplat for his work on nacre degradation and Dr Laurent Bedouet for his important work on nacre molecules. The authors would like to thank Dr. Bernus, veterinary surgeon, for his kind help with the animal surgery. We would particularly thank Mr. G. Mascarel and Prof A. Couté of the Common Service of Electron microscopy of the National Museum of Natural History (Paris, France) for their exceptional scanning electron microscopy artwork of a great part of the studies on nacre.

8. References

Atlan G, *et al*. Interface between bone and nacre implants in sheep. Biomaterials; 20, 1017-1022, 1999.

Atlan G, *et al.* Reconstruction of human maxillary defects with nacre powder: histological evidence for bone regeneration. C R Acad Sci Paris, Life Sci; 320, pp.253-258, 1997.

Bédouet L., *et al*. Low molecular weight molecules as new components of the nacre organic matrix. Comp Biochem Physiol B; 144:532-543, 2006.

Bédouet L., et al. Heterogeneity of proteinase inhibitors in the water-soluble organic matrix from the oyster nacre. Marine Biotechnology; 9, 437-449, 2007.

Bevelander G, Nakahara H. An electron microscope study of the formation of nacreous layer in the shell of certain bivalve molluscs. Calc Tiss Res; 3:84-92, 1969.

Cariolou M, Morse D. Purification and characterization of calcium-binding conchiolin shell peptides from mollusc, *Haliotis rufescens*, as a function of development. J Comp Physiol B; 157:717-729, 1988.

Delattre O., PhD thesis, La nacre de *Pinctada maxima,* biomatériau de substitution et de réparation dans les pertes de substances osseuses et cartilagineuses chez le mouton. Applications potentielles en chirurgie orthopédique, 2000.

Duplat D., *et al*. The in vitro osteoclastic degradation of nacre. Biomaterials; 28, 2155-2162, 2007.

Kono M, *et al*. Molecular mechanism of the nacreous layer formation in *Pinctada maxima*. Biochem Biophys Res Commun; 269:213-218, 2000.

Kulak, A.N., Iddon, P., Li, Y., Armes, S.P., Cölfen, H., Paris, O., Wilson, R.M., Meldrum, F.C., 2007. Continuous structural evolution of calcium carbonate particles: a unifying model of copolymer-mediated crystallization. J. Am. Chem. Soc. 129, 3729-3736.

Lamghari M, *et al*. Stimulation of bone marrow cells and bone formation by nacre: *In vivo and in vitro* studies. Bone; 25(2), Suppl.:91S-94S, 1999.

Lamghari M., et al. Bone reactions to nacre injected percutaneously into the vertebrae of sheep. Biomaterials; 22, 555-562, 2001.

Lamghari M., *et al*., A model for evaluating injectable bone replacements in the vertebrae of sheep: radiological and histological study. Biomaterials, 20, 2107-2114, 1999.

Liao H., *et al*. Tissue responses to natural aragonite (Margaritifera shell) implants in vivo. Biomaterials; 21, pp.457-468, 2000.

Lopez E, *et al*. Demonstration of the capacity of nacre to induce bone formation by human osteoblasts maintained *in vitro*. Tissue Cell; 24, pp.667-679, 1992.

Lopez E., et al. Procédé de preparation de substances actives à partir de la nacre, produits obtenus, utiles notamment comme médicaments, Patent FR9515650, 1995.

Meibom, A., Cuif, J.P., Hillion, F., Constantz, B.R., Juillet-Leclerc, A., Dauphin, Y., Watanabe, T., Dunbar, R.B., 2004. Distribution of magnesium in coral skeleton. Geophys. Res. Lett. 31, L23306.

Meibom, A., Mostefaoui, S., Cuif, J.-P., Dauphin, Y., Houlbreque, F., Dunbar, R.G., Constanz, B., 2007. Biological forcing controls the chemistry of reef-building coral skeleton. Geophys. Res. Lett. 34, L02601.

Pereira-Mouries L, *et al*. Soluble silk-like organic matrix in the nacreous layer of the bivalve *Pinctada maxima*. Eur J Biochem; 269:4994-5003, 2002a.

Rousseau M., *et al*. The water-soluble matrix fraction extracted from the nacre of *Pinctada maxima* produces earlier mineralization of MC3T3-E1 mouse pre-osteoblasts. Comp Biochem Physiol A; 135:271-278, 2003.

Rousseau M., *et al*., Low molecular weight molecules of oyster nacre induce mineralization of the MC3T3-E1 cells, J. Biomed. Mater. Res., 85A (2), 487-497, 2007.

Rousseau M., et al., Multi-scale structure of sheet nacre, Biomaterials, 26, 6254-6262, 2005a.

Rousseau M., *et al*., Restauration of *Stratum corneum* with nacre lipids, Comp. Biochem. Physiol. Part B, 145, 1-9, 2006.

Shen Y., *et al*., In vitro osteogenetic activity of pearl. Biomaterials 27, 281-287, 2006.

Silve C., *et al*., Nacre initiates biomineralization by human osteoblasts maintained *in vitro*, Calcif. Tissue Int., 51, pp. 363-369, 1992.

Watabe N., J Ultrastructure Research 12: 351-370, 1965.

Weiss IM, *et al*., Purification and characterization of perlucin and perlustrin, two proteins from the shell of the mollusc *Haliotis laevigata*. Biochem Biophys Res Commun; 267:17-21, 2000.

Westbroek P, Marin F. A marriage of bone and nacre. Nature; 392:861-862, 1998.

Wohlrab, S., Cölfen, H., Antonietti, M., 2005. Crystalline, porous microspheres made from amino acids by using polymer-induced liquid precursor phases. Angew. Chem. Int. Ed. 44, 4087-4092.

15

Alumina and Zirconia Ceramic for Orthopaedic and Dental Devices

Giulio Maccauro, Pierfrancesco Rossi Iommetti,
Luca Raffaelli and Paolo Francesco Manicone
Catholic University of the Sacred Hearth Rome
Italy

1. Introduction

Ceramic materials are made of an inorganic non-metallic oxide. Usually ceramics are divided into two groups: silicon ceramics and aluminous ceramics. Ceramics are also divided into crystalline and non-crystalline depending on inner molecular organization. Depending on their *in vivo* behaviour, ceramics are classified as bioresorbable, bioreactive or bioinert. Alumina and zirconia are bioinert ceramics; their low reactivity togheter with their good mechanical features (low wear and high stability) led to use them in many biomedical restorative devices. Their most popular application is in arthroprosthetic joints where they have proven to be very effective, that make their use suitable especially in younger, more active patients. Also dental use of these materials was proposed to achieve aesthetic and reliability of dental restorations.

2. Mechanical and chemical features of bioceramics

2.1 Alumina

Corundum known as α-alumina is the alumina ceramic used for biomedical application,. In nature single crystals of this material are known as ruby if containing Cr2O3 impurities, or as sapphire if containing titanium impurities which give them blue colour. Al_2O_3 molecule is one of the most stable oxides because of high energetic ionic and covalent bonds between Al and O atoms. These strong bonds (Alumina DG(298K) =1580 KJ/mol) leave the ceramic unaffected by galvanic reactions (absence of corrosion, e.g. absence of ion release from bulk materials and from wear debris). Adverse conditions such as strong acidic or alkaline environment at high temperatures didn't corrupt allumina properties. Under compression allumina showed good resistance but under tensile strength shows its brittleness. at room temperature alumina does not show plastic deformation before fracture (e.g. no yield point in stress-strain curve before fracture), and once started fractures progress very rapidly (low toughness K_{IC}).

Tensile strength of alumina improves with higher density and smaller grain size. A careful selection of raw materials and a strict control of production process are performed by manufacturers to optimize allumina mechanical properties. Introduction of low melting MgO in the ceramic process enhanced mass transport during solid state sintering so that

ceramic reached full density at lower temperature. Moreover decreasing grain growth a stronger ceramic was obtained.
Additions of small amounts of Chromia (Cr_2O_3) compensated the reduction of hardness subsequent to the introduction of MgO. CaO content in medical grade alumina devices must be reduced since in wet environment it can compromise its mechanical properties. NaOH impurities in powders obtained by the Bayer process makes allumina unsuitable for the hi-tech biomedical application. Continuous efforts to improve the properties of alumina bioceramics are being made, e.g. by the introduction of high purity raw materials, hot isostatic pressing, proof testing on 100% of manufactured components. The use of hot isostatic pressing (HIP) in bioceramics production minimizes the residual stresses within ceramic pieces and gives ceramics with density close to the theoretical one, improving the strength and reliability of the product. Proof testing of Allumina components consists in the application of internal pressure inducing a stress close to the maximum load bearing capability; when applied to 100% of the parts manufactured, defective products can be eliminated before final inspection. The introduction of laser marking contributed to components traceability due improving the overall quality of the manufacturing process
In 1930 for the first time allumina was used as a biomaterial with the first patent applied by Rock in Germany. Sandhaus in 1965 patented a screw-shaped dental implant made of high alumina powder Degussit AL23. This was the first step in a new era in ceramic engineering. A new dental implant , step-shaped, followed the screw shaped, and was named Tübingen type. But only with the use in orthopaedic purpose in 1970 by Boutin, Allumina was worldwide diffused. He implanted successfully first allumina joints since 1970. Nowadays more than 3 million alumina ball heads have been implanted worldwide. Today, almost 50% of hip arthroplasties performed in Central Europe make use of ceramic ball heads.

2.2 Zirconia

Zirconia, the metal dioxide of zirconium (ZrO_2), was used for a long time as pigment for ceramics; it was identified in 1789 by the German chemist Martin Heinrich Klaproth.
To stabilize zirconium oxide a little amount of non-metallic oxide were added (such as MgO, CaO and Y_2O_3); at a first time magnesia- partially stabilized zirconia (MgPSZ) was the most studied ones, in which a tetragonal phase is present as small acicular precipitates within large cubic grains (Ø40÷50 μm) forming the matrix. But wear properties were badly influenced by this feature; most of the developments were focused on yttria stabilized tetragonal zirconia polycrystal (Y-TZP), a ceramic completely formed by submicron-sized grains, which is today the standard material for clinical applications. Tetragonal grains in Y-TZP ale smaller than 0.5 μm. Tetragonal phase rate retained at room temperature is influenced by: - grains size and on its homogeneous distribution; - the concentration of the yttria stabilizing oxide; - the constraint exerted by the matrix onto grains. The equilibrium among such microstructural parameters influences mechanical features of Y-TZP ceramics. Tetragonal grains can transform in monoclinic, with a 3-4% volume growth of grains: this is the origin of the toughness of the material, e.g. of its ability to dissipate fracture energy. When the pressure on the grains is relieved, i.e. by a crack advancing in the material, the grains near the crack tip shift into monoclinic phase. This gives origin to increased toughness, because the energy of the advancing crack is dissipated at the crack tip in two ways, the first one due to the T-M transformation, the second one due to the need of the crack as it advances to overcome the compression due to the volume expansion of the grains.

In wet environments, over 100°C, tetragonal phase of zirconia ceramics can spontaneously transform into monoclinic. Because this phenomenon starts from the surface of the material, it is possible to report a loss of material density and a reduction in strength and toughness of zirconia. This degradation goes under the name of "ageing" and is due to the progressive spontaneous transformation of the metastable tetragonal phase into the monoclinic phase. Spontaneous T-M transformation in TZP is probably due to the formation of zirconium hydroxides or yttrium hydroxides that promoted phase transition for local stress concentration or variation of the yttrium/zirconium ratio

Swab summarized main steps of TZP ageing in the following way:

The most critical temperature range is 200-300°C.

The effects of ageing are the reduction in strength, toughness and density, and an increase in monoclinic phase content.

Degradation of mechanical properties is due to the T-M transition, taking place with micro and macro-cracking of the material.

T-M transition starts on the surface and progresses into the material bulk.

Reduction in grain size and/or increase in concentration of stabilising oxide reduce the transformation rate.

T-M transformation is enhanced in water or in vapour.

Strength degradation rate is not the same for all TZP ceramics. Swab described that in ten materials tested in presence of water vapour at low temperature, different levels of strength degradation occurred in all the materials but one, where strength remained the same after the treatment. The differences in equilibrium of microstructural parameters like yttria concentration and distribution, grain size, flaw population and distribution in the samples tested caused this variability in ageing behaviour. Strength degradation rate can be controlled by having a high density, small and uniform grain size, a spatial gradient of yttria concentration within grains, introduction of alumina into the matrix. All the above parameters are controlled by the manufacturing process and by the chemical-physic behaviour of the precursors selected for the production of the ceramic. These facts make stability a characteristic of each Y-TZP material and of each manufacturing process.

Hydrothermal treatment has an high risk of phase transition: steam sterilization of zirconia ball heads is not recommended. These process may change the surface finish, reducing wear resistance. Nevertheless, mechanical properties of the material are not altered by these process. Gamma rays or ethylene oxide sterilization are the best choice to manage zirconia biomedical devices. Rare hearth impurities that may be present at part per million (ppm) level within the structure can interact with ionising radiation inducing some changes in colour in ceramic materials. Praseodymium impurities cause a shift to violet of zirconia after irradiation, but the material can return to its ivory colour with heating and putting it under an intense light source; its mechanical properties weren't unaffected by this treatment.

At room temperature Y-TZP ceramic is formed by submicron size grain. during sintering the grains will grow and it is necessary to start from submicron grain size powders and to introduce some sintering aid to limit the phenomenon. The introduction of the stabilizing oxide (yttria Y2O3) is a key component in TZP structure at room temperature. hydrothermal stability of the ceramic is enhanced by enriching grain boundaries in yttria: ZrO2 grains may be yttria coated as in plasma, an alternative to obtain Y-TZP powders by co-precipitation. silica impurities must be avoided because the dissolution of glassy phases at the grain boundaries in wet environment causes the spontaneous transformation of the grains from tetragonal to monoclinic with a loss of mechanical properties. To achieve an

equilibrium a higher toughness and hydrothermal stability must be balanced by a lower bending strength

2.3 Zirconia toughened alumina

Zirconia toughened alumina (ZTA) is obtained adding zirconia up to 25% wt into an alumina matrix. This allow to obtain a class of ceramic materials with increased toughness. These materials, developed in the second half of the seventies are featured by toughness (KIC) up to 12 MPam-1/2 and bending strength up to 700 MPa. Alumina matrix exerts a constraint on the metastable tetragonal zirconia particles maintaining them in the tetragonal state. T-M transformation of the zirconia particles give toughness to this ceramic. Because of different elastic modulus between alumina matrix and the zirconia particles cracks are propagated along zirconia crystals inducing their T-M phase transformation thus dissipating the crack energy. Microcracking of the matrix due to the expansion of the dispersed particles is a further dissipative effect. To ensure the better mechanical performances to this material is mandatory to control the high density of the matrix and the optimisation of the microstructure of the zirconia particles. In this way the maximum amount of metastable phase is retained assuring the transformation of the maximum volume. When hardness is of paramount importance ZTA have some drawbacks: zirconia into the hard alumina matrix results in a decrease in hardness of the ceramic Extensive research has been focussed on ZTA in France and in Italy on ceramics containing up to 80% zirconia, without leading to clinical applications. Allumina can also be toughened by addition of whiskers; but concerns about carcinogenicity of whiskers, and limits in adhesion of the whiskers to the matrix decreased the interest for the biomedical applications of these materials. Elongated grains (platelets), acting as whiskers, can be nucleated within the structure of a ZTA ceramic. This can be obtained by adding e.g. strontium oxide (SrO) to ZTA obtaining SrAl12O19platelets by in situ solid state reaction during sintering. Chromia (Cr2O3), introduced to save the alumina hardness and of Yttria (Y2O3) that acts as stabilizer of the T phase of zirconia in ZTA, leads to a material known as ZPTA(Zirconia Platelet Toughened Alumina) The resulting mechanical properties are very interesting, as wear rates were very low in the laboratory tests, even lower than the ones of alumina and zirconia both on hip and knee simulator studies

ZPTA is a great innovation in ceramic for biomedical devices. Mechanical properties of this new ceramic, allow to develop many innovative ceramic devices.

Property	Unit	Allumina	Y-TZP	ZTA	ZPTA
Density	g/cm²	3.98	6.08	5.00	4.36
Average grain size	μm	≤1.8	0.3÷0.5	-	-
Bending strength	MPa	>550	1200	900	1150
Compression strenght	MPa	5000	2200	2900	4700
Young modulus	GPa	380	200	285	350
Fracture toughness K_{IC}	$M_{pam}^{-1/2}$	4-5	9	6.9	8.5
Microhardness	HV	2200	1000-1300	1500	1975

Table 1. Selected Properties of load bearing bioceramics for medical devices

3. Biocompatibility

Biocompatibility has been defined as "the ability of a material to perform with an appropriate host response in a specific application". Reaction of bone, soft collagenous tissues and blood are involved in the host response to ceramic implants. Interfacial reaction between these materials and body tissues both *in vitro* and *in vivo* must be considered evaluating biocompatibility of bioinert ceramics. Low rate of tissue reactions towards Alumina are the reason because it is often considered reference in testing orthopaedic ceramic biomaterials. The first experimental data of dense ceramics (ZrO2) *in vivo* biocompatibility in orthopaedic surgery were published 1969 by Helmer and Driskell while the first clinical cases on alumina were described later by Boutin shortly followed by Griss. *In vitro* biocompatibility evaluation of Alumina and Zirconia were performed later than their clinical use. As biocompatibility tests often are reporting the comparison of alumina and zirconia biocompatibility, in the following the results are reviewed in the same manner.

3.1 In vitro tests

Ceramic materials in different physical forms (powders and dense ceramics) were used to perform *in vitro* tests on cell cultures. Absence of acute toxic effects of ceramic in powder and disk form on the different cell lines used in tests both towards allumina both toward zirconia was reported by many studies. *In vitro* assays are influenced by material characteristics, such as the physical form, reactive surface, chemical composition, impurity content etc, as well as by the cell conditions during the tests. Alumina and zirconia disks with 30% of porosity allow adhesion and spreading of 3T3 fibroblasts as observed using SEM. HUVEC and 3T3 fibroblasts osteoblast didn't show any toxic reaction toward Al2O3 or ZrO2 samples (MTT test on cells direct in contact with ceramic particles); the same effects were also observed on ceramic extracts cocultured with fibroblasts. Li, et al demonstrated that powders were more toxic than dense ceramics, using direct contact tests and MTT test with human oral fibroblasts. Ceramic powders can induce apoptosis in macrophages depending on materials concentration as observed by Catelas. Mebouta, et al reported for the first time a different toxic effect between alumina and zirconia: in particular a higher cytotoxicity of alumina particles in comparison to the zirconia ones was measured as human monocytes differentiation; this is probably due to the higher reactive surface of the alumina particles, that were significantly smaller than the zirconia ones

Degidi compared soft tissues reactions to ZrO_2 and titanium; he reported that inflammatory infiltrate, microvessel density and vascular endothelial growth factor expression appeared higher around titanium samples than around ZrO_2 ones. Moreover cellular proliferation on zirconia surface is higher than on titanium ones. Furthermore Warashima reported less proinflammatory mediators(IL-1β, IL-6 and TNF−α) generated by ZrO_2 than titanium or polyethylene.

3.2 In vivo tests

Different physical forms and in different sites of implantation were evaluated in order to analyzing systemic toxicity, adverse reactions of ceramics in soft tissue and/or bone The work of Helmer and Driskell already cited is the first report of implant in bone of zirconia. Pellets were implanted into the monkey's femur, the Authors observed an apparent bone

ingrowth without any adverse tissue reaction. Hulbert, et al implantated of porous and non porous disks and tubes in the paraspinal muscles of different ceramics Authors observed ingrowth depending on porous size, and no signs of systemic toxicity. After subcutis, intramuscular or intraperitoneal and intraarticular introduction of alumina and zirconia powders in rats and/or mice mant authors reported the absence of acute systemic adverse tissue reactions to ceramics; similar results were reported after implantation of bars or pins to paraspinal muscles of rabbits or rats and after insertion in bone. bone ceramic interface showed connective tissue presence, progressively transformed in bone direct contact with ceramic. Bortz reported adverse tissue reaction: fibrous tissue in the lumen of zirconia cylinders implanted in dogs and rabbits trachea, and an inflammatory reaction against ceramic powders inserted on PMMA grooves implanted in rabbits femur. In any case this inflammatory reaction was lower than the one observed against CoCr and UHMWPE.

3.3 Carcinogenicity

Griss, et al. in 1973 reported that Alumina and zirconia powders did not induce tumours. They analyzed the long term in vivo reactions to ceramics.

Ames test, and carcinogenicic or mutagenic tests used to study zirconia dishes confirmed that this bioceramic did not elicit any mutagenic effect in vitro. Moreover zirconia radioactivity and its possible carcinogenic effect was also evaluated: radioactivity of the powder is depending on the source of ores used in the production of the chemical precursor of the zirconia powders. Only Ryu RK, et al reported a possible carcinogenic effect of ceramic. They observed association between ceramic and soft tissue sarcoma. Some recent studies have been performed about carcinogenicity of Zirconia Toughened Alumina. Maccauro et al. showed that ZPTA as well as Alumina and Zirconia ceramics did not elicit any in vitro carcinogenic effects; the same group are going to demonstrate the possible carcinogenic in vivo effects of ZPTA.

4. Biomedical applications of zirconia

Several comprehensive reviews on the clinical outcomes of ceramic ball heads for orthopaedical devices are aviable. Jenny, Caton, Oonishi, Hamadouche, demonstrate the favourable behaviour of ceramic biomaterials in reducing the wear of arthroprostheses joints.

THR ball heads
THR acetabular inlays
THR condyles
Finger joints
Spinal spacers
Humeral epiphysis
Hip endoprostheses

Table 2. Orthopaedic medical devices made of bioinert ceramics

Clinical trials demonstrated that ceramic-on-ceramic coupling decreased significantly the amount of wear debris (Boeler,). Nevertheless Wroblesky demonstrated that ceramic in couple with new generation polyethylene may constitute a significant evolution in

arthroplasty. This makes ceramics in joints suitable especially in younger patients. The matching of surface roughness, roundness and linearity in the coupling of ceramic tapers with the metallic trunnion plays a relevant role on stresses distribution and intensity, depending also on cone angle, extent of the contact, friction coefficient among the two surfaces Mismatch in female- to-male taper, e.g. due to the many angles in clinical use, roundness, roughness or linearity errors in the taper, are among the most likely "technologic" initiators of ceramic ball head failures. It must be remarked that the mechanical behaviour of ceramic ball heads once installed on the metallic taper depend not only on the ceramic but also on material and design of the taper. Besides the "technologic" failure initiators, several other precautions are necessary when using ceramic ball heads: avoid third body interposition to the ceramic metal, or ceramic/ceramic interface during surgery (e.g.blood clots, bone chips, PMMA cement debris); avoid use of metallic mallets when positioning ball heads on metallic taper (or of alumina inlay into the metal back): use plastic tools provided by the manufacturer or gently push rotate by hand; avoid thermal shocks to ball heads (e.g. dip the ceramic in saline to cool it after autoclave sterilization); avoid application of new ceramic ball heads onto stems damaged during revision surgery. A third important aspect to achieve good arthroprostheses results is surgical technique: both perfect THR component adaptation and orientation, together with soft tissue tension are required. Special care must be taken with orientation, as edge loading of the socket and impingement on components depend on this parameter.

In the past zirconia was highly used in orthopedics; about 900000 zirconia ball heads have been implanted in total hip arthroplasties, even if a debate arose regarding the potential radioactivity and carcinogenicity of zirconia source. But, after the observation of some ball head fractures, zirconia has no longer been used for total hip arthroplasties.

Zirconium oxide is also used as a dental restorative material. Inlays, onlays, single crowns, fixed partial dentures, can be realized using a ZrO_2 core. Moreover, also implant abutment and osteointegrated implant for tooth replacement are available in zirconia.

Realization of dental products requires a preventive project and successive manufacturing in order to satisfy clinical requirement. But, not only individualization is needed: accuracy is absolutely mandatory. Misfits greater than 50 μm are considered unacceptable for dental restorations. Mechanical resistance must be also considered. Frameworks with minimal thickness, often less than 1mm, must be able to sustain chewing stresses. Masticatory load on posterior teeth range from 50N to 250N, while parafunctional behavior such as clenching and bruxism can create loads about 500 and 800N. Zirconia frameworks can bear load between 800 and 3450N. These values are compatible with restorations on posterior teeth if parafunctional loads are not present and a correct framework design is performed .

In order to avoid misfit due to shrinkage during sintering, it is possible to obtain zirconia frameworks by milling full-sintered ZrO_2 samples. This technique is not influenced by sintering problems because zirconia is already sintered, but, anyway, it is influenced by operator accuracy in probe use. CAD/CAM technique is the ultimate opportunity in managing zirconia dental devices production. CAD/CAM is acronym of Computer Aided Design and of Computer Assisted Manufacturing. This system is composed by a digitizing machine to collect information about teeth position and shape, appropriate software for design zirconia restoration and a computer assisted milling machine that cut from a zirconia

sample the desidered framework. This technique reduces human influences allowing obtaining greater accuracy in zirconia core production.
Fully sintered zirconia blocks are very difficult to be grinded. Milling procedures are very slow and requires very effective burs to perform cut in the optimal way. Dimensional stability is granted because there aren't any procedures that can influence volume of framework after milling. On the other hand, grinding reduces significatively toughness of zirconia. This can be due to surfacial stresses during milling. Crystals were induced to transform from tetragonal into monocline reducing T-M phases ratio and consequently toughness. Lutardth measured flexural strength and fracture toughness of zirconia before and after grinding and concluded that mechanical resistance was reduced of about 50% after machining. Also Kosmac studying surface grinding effects on ZrO_2 confirmed these results.
Machining partially sintered zirconia (or green zirconia) presents, on the other hand, different problematics. Green zirconia has a very soft consistency resulting very easy to be milled. Grinding procedures are easy, faster and cheaper. But, after grinding, frameworks must be sintered. This procedure presents some technical problems that require accurate managing to grant a reliable outcome. During Sintering time (about 11 hours) an accurate control of temperature and pressure, especially during cooling phase, is needed to obtain the correct T-M crystals ratio. Moreover, sintering lead to a 20% volumetric shrinkage that must be foresight in advance during designing and milling. For these reasons use of green zirconia results more difficult and expensive: complex designing software and sintering machine are required to obtain accuracy and correct crystal composition. On the other side, if procedures are preformed correctly mechanical resistance results greater than ZrO_2 frameworks milled after sintering]. Moreover sinterization after grinding allows technician also to pigment frameworks helping achieving a satisfying aesthetical outcome.
Ceramic restorations allow an aesthetical outcome more similar to teeth than conventional metal-ceramic ones. Also gingival aesthetic is improved by colour of restoration similar to teeth, that is, together with mucosal thickness the basic parameter for an optimal soft tissue colour outcome. Toughness and colour similar to teeth of zirconia, lead to use this material for different purpose. Zirconiun oxide is used as a reinforce for endocanalar fiber-glass post. Also orthodontic brackets were proposed in ZrO_2. But the most interesting application of this material is nowadays for fixed partial dentures. Single crowns and 3-5 units FPD are described and studied in literature. The continuative search for an optimal metal-free material for prosthetical use found in zirconia an answer for many problems still not solved with other ceramic restorations. Also small dental restorations, like inlays and onlays were proposed with this material. Implanto-prothesical components, such as implant abutment are available with zirconia. Osteointegrated implants for tooth replacement are proposed by some manufacturers, but at the present time there aren't enough studies about behaviour of zirconia implants.
Zirconia restorations have found their indications for FPDs supported by teeth or implants. Single tooth restorations are possible on both anterior and posterior elements because of the mechanical reliability of this material. Mechanical resistance of zirconia FPD was studied on single tooth restorations and on partial dentures. Luthy asserted that Zirconia core could fracture with a 706N load Tinshert reported a fracture loading for ZrO_2 over 2000N, Sundh measured fracture load between 2700-4100N. Zirconia restorations can reach best results as fracture resistance if compared with alumina or lithium disilicate ceramic restorations.

Ageing of Zirconia can have detrimental effects on its mechanical properties. To accelerate this process mechanical stresses and wetness exposure are critical. Ageing on zirconium oxide used for oral rehabilitation is not completely understood. However, an in vitro simulation reported that, although ageing the loss of mechanical features does not influence resistance under clinical acceptable values. Further evaluations are needed because zirconia behavior in long time period is not yet investigated.

On these basis a new family of ceramic material that would complement alumina ceramic where needed. It had to posses the highest possible toughness, the smallest matrix grain size all leading towards improved mechanical reliability but this had to be accomplished without sacrificing the wear resistance and chemical stability of current day alumina ceramics. Alumina Matrix Composites were selected as the best new family of ceramics to provide the foundation for an expanded use of ceramics in orthopaedics. The main characteristics of this Alumina Matrix Composite are its two toughening mechanisms. One is given by in-situ grown platelets which have a hexagonal structure and are homogeneously dispersed in the microstructure. Their task is to deflect any sub-critical cracks created during the lifetime of the ceramic and to give the entire composite stability. The other important characteristic is related to the addition of 17 vol.-% zirconia nano-particles that are dispersed homogeneously and individually in the alumina matrix. This increases strength and toughness of the material to levels equal and in some cases above those seen in pure zirconia. Here, the effect of tetragonal to monoclinic phase transformation is used as a toughening mechanism. In the case of micro-crack initiation the local stress triggers phase transformation at an individual zirconia grain which acts then as an obstacle to further crack propagation. It is a desired behaviour which uses the volume expansion in an attempt to prevent further crack propagation. These two well known effects in material science, crack deflection and transformation toughening give Alumina Matrix Composite a unique strength and toughness unattained by any other ceramic material used in a structural application in the human body.

5. References

Carinci, F.; Pezzetti, F.; Volinia, S.; Francioso, F.; Arcelli, D.; Farina, E. & Piattelli, A. (2004) Zirconium Oxide: Analysis Of Mg63 Osteoblast-Like Cell Response By Means Of A Microarray Technology. *Biomaterials* Vol.25 p.215.

Christel, P.; Meunier, A.; Dorlot, J-M. (1988) Biomechanical Compatibility And Design Of Ceramic Implants For Orthopedic Surgery, In: *Bioceramics: Material Characteristics Versus In Vivo Behavior*. Ducheyne, P. & Lemons, J. E. Annals Of New York Academy Of Sciences,Vol. 523 pp. 234-256.

Covacci, V.; Bruzzese, N. & Maccauro, G. (1999) In Vitro evaluation Of The Mutagenic and carcinogenic power of high purity zirconia ceramics. *Biomaterials* Vol. 20 pp.371-376

Dion, I.; Bordenave, L. & Lefebvre, F. (1994) Physico-Chemistry And Cytotoxicity Of Ceramics, Part 2 *J. Mater. Sci. Mater. Med.* Vol. 5 pp. 18-24

Fenollosa, J.; Seminario, P. & Montijano C. (2000) Ceramic Hip Prostheses In Young Patients - A Retrospective Study. *Clin Orthop*; Vol.379 pp. 55-67

Heimke, G.; Leyen, S. & Willmann, G. (2002) Knee Arthroplasty: Recently Developed Ceramics Offer New Solutions. *Biomaterials* Vol.23 pp.1539-51

Helmer, J.D. & Driskell, T.D, (1969) *Research On Bioceramics.* Symp. On Use Of Ceramics As Surgical Implants. South Carolina (Usa): Clemson University.

Kingery, W.D.; Bowen, H.K. & Uhlmann, D.R. (1960) *Introduction To Ceramics*. John Wiley & Sons Publ. USA

Maccauro, G.; Cittadini, A.; Magnani, G.; Sangiorgi, S.; Muratori, F.; Manicone, P.F.; Rossi Iommetti, P.; Marotta, D.; Chierichini, A.; Raffaelli, L. & Sgambato, A. (2010) In Vivo Characterization Of Zirconia Toughened Alumina Material: A Comparative Animal Study. *Int J Immunopathol Pharmacol*. Vol. 23 pp.841-6.

Maccauro, G.; Piconi, C. & Burger, W. (2004) Fracture Of A Y-Tzpceramic Femoral Head. Analysis Of A Fault. *J Bone Joint Surg Br* Vol. 86 pp.1192-6.

Maccauro, G.; Bianchino, G.; Sangiorgi, S.; Magnani, G.; Marotta, D.; Manicone, P.F.; Raffaelli, L.; Rossi Iommetti, P.; Stewart, A.; Cittadini, A. & Sgambato, A. (2009) Development Of A New Zirconia-Toughened Alumina: Promising Mechanical Properties And Absence Of In Vitro Carcinogenicity. *Int J Immunopathol Pharmacol*. Vol. 22 pp.773-9.

Manicone, P.F.; Rossi Iommetti, P. & Raffaelli, L. (2007) An Overview Of Zirconia Ceramics: Basic Properties And Clinical Applications. *J Dent.* Vol. 35 pp. 819-26.

Mendes, D.G.; Said, M. & Zukerman, V. (2000) Ten Rules Of Technique For Ceramic Bearing Surfaces In Total Hip Arthroplasty. In: *Bioceramics In Total Hip Joint Replacement.* Willman, G. & Zweymüller, K. Stuttgart: Thieme Publ pp.9-11.

Oonishi, H.; Amino, H.; Ueno, M. & Yunoki, K. (1999) Concepts And Design With Ceramics For Total Hip And Knee Replacement. In: *Reliability And Long Term Results Of Ceramics In Orthopedics.* Sedel, L. Willmann, G. Stuttgart, Germany: Thieme Publ pp. 7-28.

Piconi, C.; Burger,W. & Richter, H.G. (1998) Y-Tzp Ceramics For Artificial Joint Replacements. *Biomaterials* Vol. 19 pp.1489-1494

Piconi, C. & Maccauro, G. (1999) Zirconia As A Ceramic Biomaterial. *Biomaterials* Vol. 20 pp. 1-25.

Raffaelli, L.; Rossi Iommetti, P.; Piccioni, E.; Toesca, A.; Serini, S., Resci, F.; Missori, M.; De Spirito, M.; Manicone, P.F. & Calviello, G. (2008) Growth, Viability, Adhesion Potential, And Fibronectin Expression In Fibroblasts Cultured On Zirconia Or Feldspatic Ceramics In Vitro. *J Biomed Mater Res A.* Vol.86 pp.959-68.

Rieger, W. (2001) Ceramics In Orthopaedics – 30 Years Of Evolution And Experience. In: *World Tribology Forum In Arthroplasty* Rieker , C.; Oberholtzer, S. & Wyss, U. Hans Huber Publ, Bern, Ch, pp.309-318.

Salomoni, A.; Tucci, A.; Esposito, L. & Stamenkovich, I. (1994) Forming And Sintering Of Multiphase Bioceramics, *J Mater Sci Mater Med* Vol. 5 pp. 651-653.

Sato, T. & Shimada, M. (1985) Control Of The Tetragonal-To-Monoclinic Phase Transformation Of Yttria Partially Stabilized Zirconia In Hot Water. *J Mater Sci.* Vol. 20 pp. 3899-992.

Swab, J.J.(1991) Low Temperature Degradation Of Y-Tzp Materials. *J Mater Sci* Vol.26 pp.6706-14.

Vigolo, P.; Fonzi, F.; Majzoub, Z. & Cordioli, G. (2006) An In Vitro Evaluation Of Titanium, Zirconia, And Alumina Procera Abutments With Hexagonal Connection. *International Journal Of Oral Maxillofacial Implants* Vol. 21 pp.575-80.

16

Natural-Based Polyurethane Biomaterials for Medical Applications

Doina Macocinschi, Daniela Filip and Stelian Vlad
Institute of Macromolecular Chemistry "Petru Poni" Iasi
Romania

1. Introduction

Biomaterials are biologically inert or compatible materials placed inside a patient on a long-term or permanent basis. Advances in engineering and a greater availability of synthetic materials triggered the development of engineered polymers for use in biomaterials medical devices. As for other biomaterials, the basic design criteria for polymers used in the body call for compounds that are biocompatible, processable, sterilizable and capable of controlled stability or degradation in response to biological conditions.
The interdisciplinary field of biomaterials and tissue engineering has been one of the most dynamic disciplines during the last decades (Durairaj, 2001; Grundke, 2005; Norde, 2006; Ohya, 2002; Pilkey, 2005; Thomson, 2005; Vermette et al., 2001). The selection of the materials used in the construction of prostheses and implants is basically focused on their ability to maintain mechanical, chemical and structural integrity and on various characteristics which allow this function to substitute any organ or tissue properly and exhibit safe, effective performance within the body. Biocompatibility has been defined as the ability of a material to perform with an appropriate host response in a specific application. Any material used satisfactorily in orthopedic surgery may be inappropriate for cardiovascular applications because of its thrombogenic properties. Any deleterious effects may be encountered if used under stress-strain conditions. Biocompatibility of a material can be simulated by comparing its behaviour to reference materials in standardized experimental condition. Biocompatibility is in fact, complex being interpreted as a series of events of interactions happening at the tissue/material interface, allowing the identification of those materials with surface characteristics and/or polymer chemistry more biocompatible; these interactions are influenced by intrinsic characteristics of the material, the confrontational circumstances related to the bioactive and biocooperative responses.
Blood contact assays have been developed and include tests investigating the adhesion or activation of blood cells, proteins, and macromolecules such as those found in the complement or coagulation cascade. Other biocompatibility tests have been tentatively proposed and involve analytical testing or observations of physiological phenomena, reactions or surface properties attributable to a specific application such as protein adsorption characteristics.
Polyurethanes are one of the most popular groups of biomaterials applied for medical devices. Their segmented block copolymeric character endows them a wide range of versatility in terms of tailoring their physical properties, blood and tissue compatibility.

Polymers from natural sources are particularly useful as biomaterials and in regenerative medicine, given their similarly to the extracellular matrix and other polymers in the human body. Polyester- and polyether-urethanes have been modified with hydroxypropyl cellulose aiming the change of their surface and bulk characteristics to confer them biomaterial qualities (Macocinschi et al., 2008; Macocinschi et al., 2009a; Macocinschi et al., 2009b). In this respect, dynamic contact angle measurements, dynamic mechanical analyses accompanied by mechanical testing have been done. Platelet adhesion test has been carried out *in vitro* and the use of hydroxypropyl cellulose in the polyurethane matrix reduces the platelet adhesion and therefore recommends them as candidates for biocompatible materials. Polymeric composites prepared by mixing polyurethanes and natural polymers offer improved mechanical properties and biocompatibility for functional tissue replacements *in vivo*. The biological characteristics in contact with blood and tissues for long periods, in particular good antithrombogenic properties, recommend the use of extracellular matrix components such as collagen, elastin and glycosaminoglycans (GAG) for obtaining biomaterials (Macocinschi et al., 2010a; Macocinschi et al., 2011; Moldovan et al., 2008; Musteata et al., 2010; Raschip et al., 2009). The introduction of biodegradable polymers into a synthetic polymer matrix restricts the action of a fungal, microbial or enzymatic attack (Macocinschi et al., 2010b). Such limitations appear even when the biodegradable component occurs as a continuous phase in the composite material.

Our previous publications presented the synthesis and some properties of new polyurethane-cellulose, (Macocinschi et al., 2008).

Herein the effects of the chemical structure of polyurethanes-cellulose on their surface properties are discussed. Investigations are based on the geometric mean approach of Kälble, Owens and Wendt, Rabel (Kälble, 1969; Owens & Wendt, 1969; Rabel, 1977), on the Lifshitz-van der Waals acid/base approach of Van Oss and co-workers (Van Oss et al., 1988a; Van Oss et al., 1988b; Van Oss, 1994) and on the theoretical methods involving quantitative structure-property relationship (Bicerano, 1996). By scanning electron microscopy surface morphology was investigated. For estimation of the haemocompatibility properties of the obtained materials, water sorption was determined as well as the amount of fibrinogen adsorbed from solution, the amount of fibrinogen adsorbed from blood plasma, and the time of prothrombin consumption.

2. Surface, mechanical and biological characterizations of polyurethane biomaterials

An ideal polymer for medical applications would have adequate surface and mechanical properties to match the application, would not induce inflammation or other toxic response, and would be sterilizable and easily processed into a final end product with an acceptable shelf life. Polyurethanes are good biomaterials due to their high biocompatibility having chemical structure similar to that of proteins and elastomer characteristics.

2.1 Surface properties

Segmented polyurethanes have gained considerable position as useful biomaterials for implants or biomedical devices, (Baumgartner et al., 1997; Hung et al., 2009; Reddy et al., 2008; Wu et al., 2009). Polyurethanes have been widely used for various commercial and experimental blood contacting and tissue-contacting application, such as vascular prostheses, blood pumps end tracheal tubes, mammary prostheses, heart valves, pacemaker

lead wire insulations, intra-aortic balloons, catheters and artificial hearts, because of their generally favorable surface physical properties, together with their fairly good biocompatibility and haemocompatibility characteristics, (Lamba et al., 1997; Lelah & Cooper, 1986; Plank et al., 1987). The balance between the surface hydrophilic and hydrophobic properties is important for achieving an enhanced biocompatibility of polyurethanes. Plasma treatments or other types of stimuli may alter the surface energy of most polymers, thus changing their surface polarity, hydrophilicity and adhesiveness, (Desai et al., 2000; Ozdemir et al., 2002; Ramis et al., 2001).
In Table 1 are provided the compositional parameters and the average molecular weights values, polydispersity indices (GPC).

Sample code	Composition macrodiol/MDI/EG/HPC, wt %	M_n	M_w/M_n
PEA-PU	55.56/37.50/6.94/0.0	109613	1.287
PEA-HPC	52.24/36.57/7.27 /3.92	134522	1.865
PTHF-HPC	52.24/36.57/7.27 /3.92	70291	1.590
PPG-HPC	52.24/36.57/7.27 /3.92	72951	1.669

Table 1. Compositional parameters, number-average molecular weights, polydispersity indices

The measurement methods used for determination of surface tension are based on contact angles between the liquid meniscus and the polyurethane surface. The contact angle is a measure of the ability of a liquid to spread on a surface. The contact angle is linked to the surface energy and so one can calculate the surface energy and discriminate between polar and apolar interactions. Table 2 lists the contact angles between double distilled water, ethylene glycol, or CH_2I_2 and polyurethane samples, before and after effecting of high frequency cold plasma treatment.

Polymer code	Untreated samples/ Plasma –treated samples		
	Water	Ethylene glycol	CH_2I_2
PEA-HPC	45/60	40/35	40/29
PTHF-HPC	45/52	36/29	33/29
PPG-HPC	60/50	45/30	32/27

Table 2. Contact angle degrees of different liquids and polyurethane samples before and after plasma treatment

For the calculation of the surface tension parameters, the geometric mean method (Eqns. (1) and (2)), (Kälble, 1969; Owens & Wendt, 1969; Rabel, 1977) the acid/base method (LW/AB) (Eqns. (3)-(5)), (Van Oss et al., 1988a; Van Oss et al., 1988b; Van Oss, 1994), and theoretical method based on the structure-property relationship considering the group contribution techniques (Eqn. (6)), (Bicerano, 1996) , were used.

$$\frac{1+\cos\theta}{2}\frac{\gamma_{lv}}{\sqrt{\gamma_{lv}^{d}}} = \sqrt{\gamma_{sv}^{p}}\cdot\sqrt{\frac{\gamma_{lv}^{p}}{\gamma_{lv}^{d}}} + \sqrt{\gamma_{sv}^{d}} \tag{1}$$

$$\gamma_{sv} = \gamma_{sv}^{d} + \gamma_{sv}^{p} \tag{2}$$

where θ is the contact angle determined for water, ethylene glycol and CH_2I_2, subscripts 'lv' and 'sv' denote the interfacial liquid-vapour and surface-vapour tensions, respectively, while superscripts 'p' and 'd' denote the polar and disperse components, respectively, of total surface tension, γ_{sv}.

$$1+\cos\theta=\frac{2}{\gamma_{lv}}(\sqrt{\gamma_{sv}^{LW}.\gamma_{lv}^{LW}}+\sqrt{\gamma_{sv}^{+}.\gamma_{lv}^{-}}+\sqrt{\gamma_{sv}^{-}.\gamma_{lv}^{+}} \tag{3}$$

$$\gamma_{sv}^{AB}=2\sqrt{\gamma_{sv}^{+}.\gamma_{sv}^{-}} \tag{4}$$

$$\gamma_{sv}^{LW/AB}=\gamma_{sv}^{LW}+\gamma_{sv}^{AB} \tag{5}$$

where superscripts 'LW' and 'AB' indicate the disperse and the polar component obtained from the γ_{sv}^{-} electron donor and the γ_{sv}^{+} electron acceptor interactions, while superscript 'LW/AB' indicates the total surface tension.

$$\gamma\,(298\text{ K})\approx 0.75\cdot[E_{coh}/\,V(298\text{ K})]^{2/3} \tag{6}$$

where γ is the total surface tension, E_{coh} the cohesive energy and V the molar volume.
According to the geometric mean method, the solid surface tension components were evaluated with Eqn. (1), (Van Oss et al., 1989) using the known surface tension components, (Erbil, 1997; Rankl et al., 2003; Strom et al., 1987) of different liquids from Table 3 and the contact angles from Table 2. The total surface tension was calculated with Eqn. (2).

Test liquids	γ_{lv}	γ_{lv}^{d}	γ_{lv}^{p}	γ_{lv}^{-}	γ_{lv}^{+}
Water	72.8	21.8	51.0	25.5	25.50
Ethylene glycol	48.0	29.0	19.0	47.0	1.92
Methylene Iodide	50.8	50.8	0.0	0.0	0.72

Table 3. Surface tension parameters (mN/m) of the liquids used for contact angle measurements

Table 4 shows the surface tension parameters for both untreated and plasma-treated polyurethane samples, according to the geometric mean method and to the acid/base method. In this table it was considered that γ_{sv}^{LW} is equivalent to γ_{sv}^{d} of the geometric mean method, the mean values of γ_{sv}^{-} and γ_{sv}^{+} were calculated with Eqn. (3). Also, the total surface tension was calculated with Eqn. (2). Following the plasma treatment the disperse component of surface tension, γ_{sv}^{d}, increases in absolute value, while the polar component surface tension γ_{sv}^{p}, decreases except PPG-HPC sample for which these dependences varies in a less extent (γ_{sv}^{p} increases from 32.2 to 38.9 mN/m, and γ_{sv}^{d} increases from 9.1 to 10.7 mN/m).
Table 5 shows the contribution of the polar component to the total surface tension obtained from the geometric mean method GM for untreated and plasma treated polyurethanes. Table 5 shows that the polar term γ_{sv}^{p} in general gives a large contribution to γ_{sv}, due to the large electron donor γ_{sv}^{-} interactions. Before and after plasma treatment all samples exhibits predominant electron donor properties. Table 5 shows that the contribution of the polar component decreases after plasma treatment, except the same PPG-HPC sample. The total, disperse and polar surface tension parameters are influenced by the matrix structure of

polyurethanes possessing various soft segments. Generally, all samples possess high polar surface tension parameters, which decrease after low-pressure plasma treatment, except the PPG-HPC sample.

Polymer code	Untreated samples/ Plasma treated samples				
	γ_{sv}^{p}	γ_{sv}^{d}	γ_{sv}^{-}	γ_{sv}^{+}	γ_{sv}
PEA-HPC	57.0/24.8	2.1/16.6	55.2/23.6	12.5/4.7	59.1/41.4
PTHF-HPC	53.1/34.7	4.7/12.9	50.7/33.2	10.2/6.6	57.8/47.6
PPG-HPC	32.2/38.9	9.1/10.7	30.7/37.2	6.2/7.4	41.3/49.6

Table 4. Surface tension parameters (mN/m) for untreated and plasma treated HPC-polyurethanes according to the geometric mean method and to the acid/base method

The studied segmented cellulose polyurethanes manifest a hydrophilic character, due to cellulosic component. After HF plasma treatment the hydrophile-hydrophobe balance is changed in the sense of decreasing their hydrophilicity. This can be explained through cross-linking chemical network and by the etching effect, which modifies the rugousity and chemical composition of the surface. The exception is given by the PPG-HPC sample, which is less hydrophilic due to $-CH_3$ substituent in the soft macromolecular chain that is not favourable for polar interactions. It appears in our case that plasma induces competitive hydrophilic and hydrophobic effects and in the case of PPG-HPC sample these effects are equilibrated, such as the polar component is not changed after plasma treatment.

Polymer code	Untreated samples	Plasma treated samples
	$\gamma_{sv}^{p} / \gamma_{sv} \cdot 100$ (%)	$\gamma_{sv}^{p} / \gamma_{sv} \cdot 100$ (%)
PEA-HPC	96.5	60.0
PTHF-HPC	91.9	73.0
PPG-HPC	78.0	78.5

Table 5. Contribution of the polar component to the total surface tension obtained from the geometric mean method for untreated and plasma treated polyurethanes

The total surface tension was estimated from the structure-property relationship, according to Eqn. (6) in the following steps, (Bicerano, 1996):

1. Calculation of the zeroth-order connectivity indices ${}^{o}\chi$ and ${}^{o}\chi^{v}$ and of the first-order connectivity indices ${}^{1}\chi$ and ${}^{1}\chi^{v}$, according the values of the atomic simple connectivity indices and of the valence connectivity indices (Table 6).
2. Calculation of cohesive energy, by two methods, by applying the group contributions of Fedors, (Bicerano, 1996; Van Krevelen, 1990) and those of Van Krevelen and Hoftyzer, (Bicerano, 1996; Van Krevelen, 1990), (Table 7).
3. Calculation of the molar volume at room temperature (298 K), (Table 7).

Polymer code	${}^{o}\chi$	${}^{o}\chi^{v}$	${}^{1}\chi$	${}^{1}\chi^{v}$
PEA-HPC	179.93	139.56	121.34	32.17
PTHF-HPC	175.56	149.16	123.36	90.33
PPG-HPC	180.31	140.74	119.24	84.74

Table 6. Zeroth-order connectivity indices ${}^{o}\chi$ and ${}^{o}\chi^{v}$ and first-order connectivity indices ${}^{1}\chi$ and ${}^{1}\chi^{v}$

Polymer code	$E_{coh(1)}$, (10^{-5} J/mol)	$E_{coh(2)}$, (10^{-5} J/mol)	V (298 K), mL/mol	$\gamma_{(1)}$, mN/m	$\gamma_{(2)}$, mN/m
PEA-HPC	13.88	15.28	2812	46.89	49.95
PTHF-HPC	12.77	16.39	2613	46.61	54.76
PPG-HPC	12.25	14.75	2560	45.98	51.87

Table 7. Total surface tensions, $\gamma_{(1)}$ and $\gamma_{(2)}$, from the theoretical data calculated for cohesive energies, $E_{coh(1)}$ and $E_{coh(2)}$, and molar volume, V, for studied polyurethanes

The theoretical results are closed to the experimental values, derived from the contact angle measurements.
The hydrophobe-hydrophile balance of untreated and plasma treated polyurethanes has been evaluated by calculation of free energy of hydration, ΔG_w. The ΔG_w values were obtained from Eqn.(7), (Faibish, 2002):

$$\Delta G_w = -\gamma_{lv}(1+\cos\theta_{water}) \quad (7)$$

where γ_{lv} is the total surface tension of water from Table 3 and θ_{water} is contact angle of water with polyurethanes. The results are presented in Table 8.

Polymer code	Untreated samples/ plasma treated samples	
	ΔG_w (mJ/m^2)	γ_{sl} (mN/m)
PEA-HPC	-124.28/-109.2	10.6/5.0
PTHF-HPC	-124.28/-117.62	6.3/2.7
PPG-HPC	-109.2/-119.59	4.9/2.8

Table 8. Surface free energy between polyurethane and water and interfacial tensions for untreated and plasma treated samples

Generally, the literature (Faibish, 2002; Van Oss, 1994) of the field mentions that for ΔG_w < -113 mJm^{-2} the polymer can be considered more hydrophilic while when ΔG_w > -113 mJm^{-2} it should be considered more hydrophobic. High frequency cold plasma treatment modifies ΔG_w indicating that the surface becomes more hydrophilic in the case of PPG-HPC sample and less hydrophilic in the case of PEA-HPC and PTHF-HPC samples.
Solid-liquid interfacial tension is defined with the following relation:

$$\gamma_{sl} = (\sqrt{\gamma_{lv}^{p}} - \sqrt{\gamma_{sv}^{p}})^2 + (\sqrt{\gamma_{lv}^{d}} - \sqrt{\gamma_{sv}^{d}})^2 \quad (8)$$

Free energy of hydration and interfacial tension are very important in that they determines the interactional force between two different media and controls the different processes: stability of the colloidal aqueous suspensions, dynamic of the molecular self-assembling, wetability of the surface, space distribution and adhesiveness. The biological and chemical processes, which take place at the level of the surface of the implant, depend on the interfacial interactions between solid and liquid (water).
(1)When the blood-biomaterial interfacial tension is high, the blood proteins will be anchored on many points on the surface, they strongly interact with the surface and thus the solid-liquid interfacial tension decreases. Consequently, the proteins change their conformation. A new interface is formed, between the protein surface and sanguine plasma.

(2)When the blood-biomaterial tension is relatively low, the force, which determines the protein adsorption, will be smaller. Conformation of the proteins initially adsorbed is similar to that found for the proteins in solution. Therefore, the interfacial tension between the protein surface and the sanguine plasma will not be high, not being an appreciable force able to determine the adsorption of sanguine components. This corresponds to a better compatibility of the biomaterial surface with blood comparing with the case (1). The surface of the biomaterial must reduce to minimum the blood-biomaterial interfacial tension such as the modification of the initially adsorbed proteins to be little. Although, apparently an interfacial tension equal to zero would be ideal for realization of the blood compatibility, however this is not desirable in view of the mechanical stability of the blood-biomaterial interface. It is generally considered that the blood-biomaterial interfacial tension should be 1-3 mN/m for a good blood - biomaterial compatibility, as well as a good mechanical stability of the interface.

The values for solid-liquid interfacial tensions are given in Table 8 for untreated and plasma treated samples. It can be observed that the interfacial tensions are in general low, and after plasma treatment become even lower. Moreover, 1 mN/m < γ_{sl} for PTHF-HPC and PPG-HPC samples treated in plasma < 3 mN/m which is required for a good biomaterial.

An important goal in material science, biochemistry, cell biology and bioanalytics is to establish a relationship between surface morphology and surface properties of a polyurethane composite on one hand and on the other hand the interconnective interactions synthetic polymer matrix-extracellular matrix natural polymer components (Macocinschi et al., 2010a). The polyurethane was modified with natural polymers aiming the improvement of the surface and bulk properties, to confer good biomaterial qualities. The added natural extracellular matrix polymers determine an increase of the surface tension value for all the biocomposite samples in comparison with starting polyurethane. The fact that the total surface tension values experimentally evaluated for starting polyurethane (untreated and treated in plasma) are less than the theoretical one calculated on the basis of quantitative structure-properties relationships (Bicerano), which can be explained by the complex morphology of polyurethanes with microdomain segregation and network. The complex network morphology gives stability against plasma action. For all the tested biocomposites the values of the total surface tension after plasma treatment are higher, therefore the samples become more hydrophilic except one sample containing chondroitin sulfate, which suggests that chondroitin sulfate component induces further crosslinks and network formation and hence a reducing of hydrophilicity. The evaluated surface tension parameters show that the biocomposites have biomaterial qualities through their increased hydrophilicity. Moreover, plasma treatment decreases the hydration energy while the interfacial tensions fall within 1-3 mN/m, interval required for a good biomaterial. Biocompatible interfaces were constructed based on non-toxic, hydrophilic assembled macromolecular networks, as viable platforms for the affinity of biomolecules. The mechanical strength of the biocomposites decreases in comparison with starting polyurethane but it is higher than that of carotid porcine arteries.

2.2 Scanning electron microscopy

In Fig 1 are illustrated the SEM micrographs corresponding to the treated and untreated polyurethane samples. It is obvious that plasma caused a change in the surface morphology and etching effects are observed.

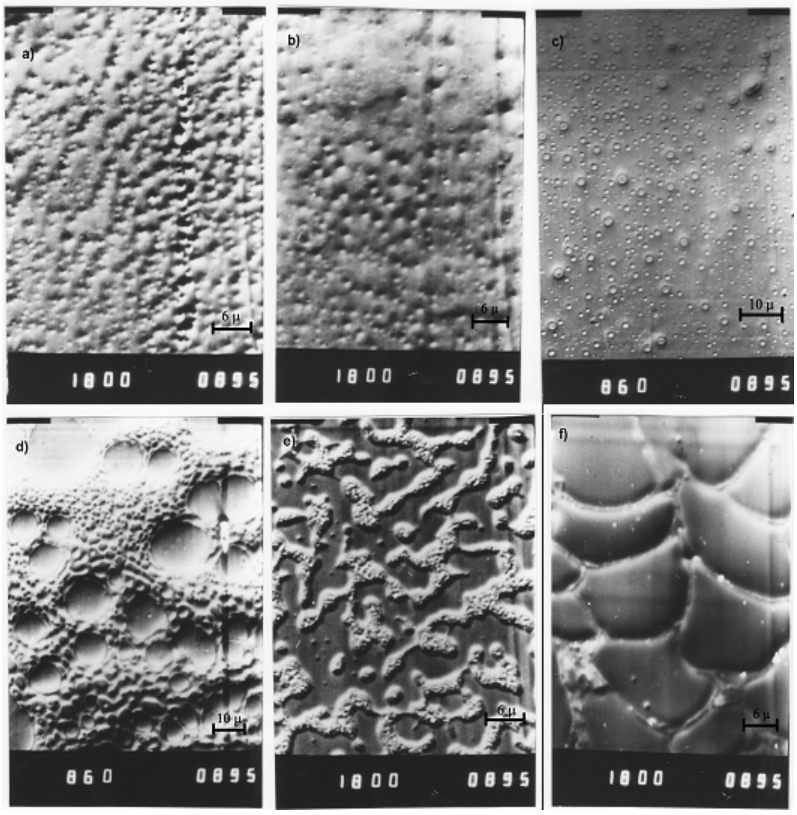

Fig. 1. SEM images of the polyurethane samples untreated and treated in HF cold plasma (PEA-HPC (a,b); PTHF-HPC (c,d); PPG-HPC (e,f))

2.3 Water sorption

The biocompatibility of the materials depend on their ability to swell in aqueous media. A high water level on the surface of the biomaterial provides a low interfacial tension with blood, thus reducing fibrinogen adsorption, cell adhesion and clot formation, (Abraham, 2002; Faibish, 2002; Van Krevelen, 1990; Wang, 2004). The results are presented in Fig 2. It is observed that the water uptake is given by the PEA-PU sample (reference polyurethane sample without hydroxypropylcellulose, PEA/MDI/EG, M_n=109.613, M_w/M_n=1.3), PEA-HPC and PTHF-HPC samples (151 %, 140 % and 167 %, respectively) and in a less extent by the PPG-HPC (92 %) due to its less polar soft segment having the lateral –CH_3 substituent which confer a different geometry to the polyurethane internal microporous structure, unfavorable for water uptake.

2.4 Fibrinogen adsorption

The experimental data related to the amount of adsorbed fibrinogen before and after incubating of polymers with a physiological solution of fibrinogen (3.00 mg/mL) and sanguine plasma (2.98 mg/mL) are presented in Fig 3.

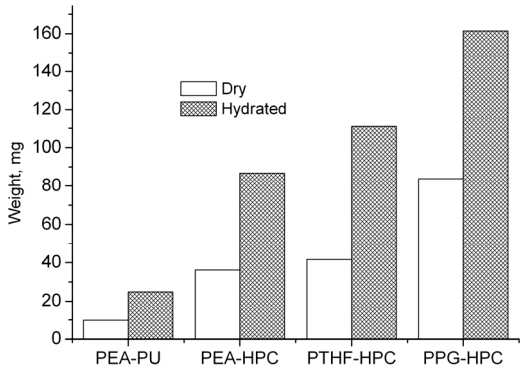

Fig. 2. Weight of polymer sample in dry and maximum hydrated state

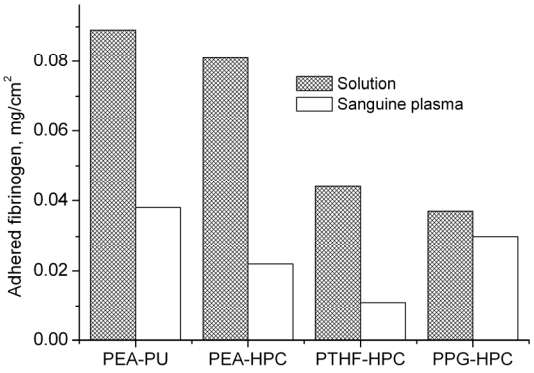

Fig. 3. Amount of adsorbed fibrinogen from physiological solution and sanguine plasma

It is observed that after incubation for 1 h at 37°C of the tested materials, no significant fluctuations of the fibrinogen concentration were recorded in comparison with the reference solution. Incubation of the samples with sanguine plasma realized in the same conditions of the incubation in solution and leaded to the results from Fig 3. Determination of the adhered fibrinogen from sanguine plasma was coupled with the determination of the prothrombin time, i.e. the time of transformation of the prothrombin in thrombin, followed by transformation of the fibrinogen in fibrin and clot formation. It is observed that the amount of fibrinogen adsorbed from sanguine plasma is less in comparison with that in solution, for all the materials except PPG-HPC, for which the differences are not significant. Also, it is remarked that prothrombin time stand in physiological normal limits (Table 9) so studied polyurethane samples did not affect the clot formation mechanisms.

The significant differences between adsorptions of the fibrinogen solution and sanguine plasma, suggest that the fibrinogen adsorption properties of the polyurethane samples, under physiological condition are affected by the concurrent affinities for other plasma proteins, which do not disturb the haemostatic mechanisms. Probably among the plasma proteins that can concur with fibrinogen is albumin, which was investigated in (Lupu et al., 2007a), and it was found that the adsorption value of a sub-physiological solution of serum albumin, (3 mg/ml) to PEA-PU materials was 0.3±0.06 mg/cm^2.

Parameter	Physiological normal limits, mg/ml	Reference sample (sanguine plasma)	PEA-PU	PEA-HPC	PTHF-HPC	PPG-HPC
Prothrombin time	8.3-11.3	10.43±0.04	11.06±0.4	10.9±0.09	10.9±0.09	10.9±0.07

Table 9. Prothrombin time before and after the contact sanguine plasma with polyurethane samples

2.5 Dynamic contact angle

In Table 10 are presented the dynamic contact angle values (advancing $\theta_{adv,}^{o}$ receding $\theta_{rec,}^{o}$ and hysteresis H, %) of the film samples in contact with water.

Polymer code		$\theta_{adv,}^{o}$	$\theta_{rec,}^{o}$	H, %
First immersion	PEA-PU	85.31±1.11	44.21±0.53	36.31
	PEA-HPC	84.85±1.09	54.33±0.59	47.89
	PTHF-HPC	77.40±1.12	42.91±0.49	44.56
	PPG-HPC	85.63±1.08	44.81±0.51	47.67
Second immersion	PEA-PU	51.01±0.55	54.06±0.56	5.64
	PEA-HPC	52.57±0.49	43.67±0.49	16.93
	PTHF-HPC	31.61±0.41	42.26±0.45	25.20
	PPG-HPC	60.33±0.59	44.07±0.52	26.95

Table 10. Dynamic contact angles values of the film samples in contact with water

From Table 10 it is observed that at first immersion θ_{adv} are less than 90^{o} which concludes that the polyurethane materials show hydrophilicity. These film samples have been prepared through precipitating in water making them microporous and enough hydrophile at surface through orientation of the hydrophile groups towards surface. The evaluated receding contact angles are 44-48 % less, except PEA-PU which is the polyurethane without HPC in its composition. Thus, HPC reduces the $\theta_{rec.}$ At the second immersion the hysteresis for PEA-PU is significantly less comparing with all samples having HPC. It appears that a polar material induces a low hysteresis, and the polarity of the soft segment in the polyurethane influences the results, considering additionally at second immersion the water up-take within the microporous layer disposed at surface. Advancing contact angles at second immersion are less than at first immersion, thus the material is better wet. Of all the polyurethane samples, PTHF-HPC evidences the lowest dynamic contact angles, both advancing and receding angles, at first and second immersion, which recommends it for biomedical applications.

In Table 11 are given the experimental values of the surface tension for the polyurethane solutions in DMF and DMF as solvent, by using Wilhelmy plate method. Solutions of the polyurethane sample 4g/dL in DMF were employed and DMF as a starting solvent.

Polymer solution	γ, mN/m	γ_{DMF}, mN/m	Δ γ, %
PEA-PU	33.44±0.045	36.19±0.038	7.62
PEA-HPC	33.19±0.042	36.45±0.051	8.96
PTHF-HPC	29.26±0.035	37.36±0.044	21.69
PPG-HPC	29.51±0.031	37.34±0.041	20.96

Table 11. The experimental values of the surface tension for the polyurethane solutions in DMF and DMF as solvent

It is obvious in Table 11 that γ_{DMF} decreases only with 7.62 % by solving the PEA-PU polymer. When PEA-HPC is solved, due to cellulose derivative, OH groups and hydrogen bonding, the decrease is found to be somewhat higher. For polyether-urethanes, PTHF-HPC and PPG-HPC, there is found a much more significant Δ γ (21.69 %, respectively 20.96 %), and this is due to the polyether nature of the soft segment. This can be explained by the fact that when polar polymers like poly(ester urethane)s are solved in a polar solvent like DMF reduces in some extent the surface tension, while a somewhat less polar polymer like poly(ether urethane)s in the same solvent reduces more.

2.6 Dynamic mechanical thermal analysis (DMTA)

Polyurethanes are characterized by their high and heterogeneous morphology and by important intermolecular forces that determine their mechanical behavior. In such way that the forces applied to polymers in general and the deformations produced by those are not thoroughly local. Consequently the response of the polymer to the foreign solicitations is extended in a wide time interval (relaxation time), originating its peculiar viscoelastic behavior. While energy supplied to a perfectly elastic material is stored and a purely liquid dissipates it, polymeric materials dissipate a part of energy that excites to them. DMTA is a sensitive technique used to study and characterize macroscopic responses of the materials as well local internal motions. By monitoring property changes with respect to the temperature and/or frequency of oscillation, the mechanical dynamic response of the material is referred to two distinct parts: an elastic part (E′, storage modulus) and a viscous component (E″, loss modulus). The damping is called tan delta, loss factor or loss tangent, tan δ =E″/E′. With increasing temperature different physical states are revealed: glass, leathery, rubbery and elastic of rubbery flow, viscous flow. The glass transition is easily identified from dynamical mechanical data because of the sharp drop in storage modulus, peaks of loss dispersion modulus or tan δ. Tan δ peak may occur at higher temperatures than those given by E′ drop or E″ peak, because it responds to the volume fraction of the relaxing phase, its shape and height depends on the amorphous phase, being a good measure of the 'leather like' midpoint between glassy and rubbery state, (Sirear, 1997). The glass transition temperature (Tg) is often measured by DSC (Differential Scanning Calorimetry), but the DMTA technique is more sensitive and yields more easily interpreted data. This is usual as the degree of dependence is specific to the transition type. DMTA can also resolve sub-Tg transitions, like beta, gamma, and delta transitions, in many materials that the DSC technique is not sensitive enough to pick up. The magnitude of the low temperature relaxations is much smaller than that of α-relaxation considered as the glass transition. These relaxations are due to local mode (main chain) relaxations of polymer chains and rotations of terminal groups or side chains, or crankshaft motion of a few segments of the main chain.

In literature for polyurethanes based on poly(epsilon caprolactone) and 1,4-butane diisocyanate with different soft segment lengths and constant hard segment length it was evidenced by DMTA additional transitions at room temperature due to crystalline fraction of PCL while the hard segment crystallinity influence the rubber plateau, (Heijkants et al., 2005). For poly(ether urethane) networks prepared from renewable resources: epoxidized methyl-oleate polyether polyol and 1,3-propandiol by using L-lysine diisocyanate, it was found very well differentiated both from DSC and DMTA, two glass transitions for the soft segment (-17-1^{o}C; 9-22^{o}C) and respectively hard segment (35, 44^{o}C; 45, 58^{o}C) explainable through phase segregated morphology, (Lligadas et al., 2007). Three kinds of polyurethane mixed blocks (polycaprolactone glycol, polypropylene glycol, polytetramethylene glycol) and 4,4′-diphenylmethane diisocyanate extended with 1,4-butane diol were studied by DMTA and it was revealed that soft chain mobility affects the glassy state modulus. From E′ and tan δ graphs the T_g values are less than -50^{o}C, (Mondal, 2006). Gao and Zhang, (Gao & Zang, 2001) found IPNs as a novel kind of material with complex internal friction behavior and thermal dynamic incompatibility: for their semiinterpenetrating networks of castor oil polyurethane and nitrokonjac glucomannan, glass transition temperatures ($T_g \leq 50^{o}$C) increased with molecular weight of the latter component which affects the storage modulus and shape and position of tan δ by changing the degree of order and motion of molecules through concentration fluctuations of molecular structural units. For graft-interpenetrating polyurethane networks and natural polymers such as nitrolignin, (Huang & Zhang, 2002), the influence of the NCO/OH molar ratio was studied by DSC and DMTA revealing T_g = -4.09-23.97^{o}C (DSC) and respectively (T_g= 6.3-31.1^{o}C) which increase with NCO/OH molar ratio through formation of three-dimensional allophanate or biuret networks. DMTA and DSC investigations on new blends of hydroxypropylcellulose and polyurethane (poly (ethylene glycol) adipate -4,4′-diphenylmethane diisocyanate-ethylene glycol) reveals glass transitions ranging between (-17-11.8^{o}C) by DMTA and T_m for soft segments (41.6-49.7)^{o}C by DSC, (Raschip et al., 2009).

Characteristic temperatures for the studied samples determined from DMTA curves (Figs. 4, 5, 6) are listed in Table 12.

Storage modulus E′ is a measure of the stiffness of the material, (Zlatanic et al., 2002). It appears from the Fig. 4 that the following order of E′ values at its drop (at the glass transition from glassy to leathery state) can be stated: $E'_{PEA\text{-}HPC} > E'_{PPG\text{-}HPC} > E'_{PEA\text{-}PU} > E'_{PTHF\text{-}HPC}$. This is related to the crystalline domains or physical/chemical network/entanglements which constraint molecular motions in amorphous state. For all the samples E′ is less than 10^9 Pa, being generally known that when $E' > 10^9$ Pa the material is glassy. In addition we recall that for an amorphous linear polymer the decline of E′ in the glass transition range amounts three orders of magnitude in a narrow temperature span. In particular for our samples the decline found for E′ is about two orders of magnitude, polyester urethanes are expected to be stiffer, than polyether, cellulose derivative induces also stiffness to the material, while lateral methyl groups in amorphous atactic PPG provokes constraints in the mobility of the soft segment. PTHF macromolecular chain is more mobile with a low stiffness and low tan δ. The glass transition of the soft segment (SS) was determined from DMTA curves as follows: from the intersection of tangents to the E′ (log E′) curves from the glassy region and the transition "leathery" region, from E″ (log E″) peaks and tan δ peaks. T_g of the soft segment from DSC was evaluated from the second heating scan. It can be noticed that T_g from DSC are close to those from DMTA, for poly(ester urethanes) while for

poly(ether urethanes) are different and this can be explained by the sensitivity of DMTA technique to the mobility of the macromolecular segment. And we referred here to the T_g values evaluated from E′ (log E′) graphs. The log E′ or log E″ vs. E′ or E″ evidence better the biphasic behaviour of the samples by revealing the melting phenomena related to the soft and hard segment. We remark slope changes on log E′ descent and the right edge of the E″ peak has a descent trend which indicate a possible overlapping of the melting of the soft phase with a glass transition of the hard phase. The broadening of the glass transition reveals large distribution of the relaxation times that implies a heterogeneous structure with a soft phase constraint by a hard phase which reduces its mobility. Poly(ether urethanes) samples evidence secondary relaxations of the soft segment, attributed to local relaxations in glassy state, which may imply few methylene groups or the motion of $-CH_3$ attached to the backbone or crankshaft motion: for PTHF-HPC sample below glass transition of the soft segment β relaxation is evidenced by tan δ graph (T_β= -51.4°C) while for PPG-HPC sample β and γ relaxations arised probably at the level of the main chain and lateral $-CH_3$ groups (E″ graph T_γ = -128°C and T_β=-81.1°C; log E″ graph T_γ = -131.6°C and T_β=-82.5°C; tan δ graph T_γ = -129.1°C and T_β= -84.4°C

Sample	Testing method	Analyzed curve	Temperature transformation, °C			
			T_g(SS)/T_α	T_m(SS)	T_m(HC)	T_β
PEA-PU	DSC		-27.0	52.8	180	-
	DMTA f=1 Hz	log E′	-23.5	65.8	157	-
		log E″	-13.4	63.6	169	-
		tan δ	15.0	78.5	-	-
PEA-HPC	DSC		-23.0	58.7	189.2	-
	DMTA f=1 Hz	log E′	-17.7	62.3	172	-
		log E″	-9.6	51.7	181	-
		tan δ	11.7	102.5	-	-
PTHF-HPC	DSC		-41.0	52.6	189.6	-
	DMTA f=1 Hz	log E′	-68.3	52.3	180	-
		log E″	-61.4	62.6	176	-
		tan δ	16	113.3	-	-51.4
PPG-HPC	DSC		-74	59.5	196	-
	DMTA f=1 Hz	log E′	-37.1	93	-	-
		log E″	-29.3	93.3	-	-82.5
		tan δ	-8.9	82.2	-	-84.4

T_m(SS) –melting point of soft segment; T_m(HS)dec. -melting point of hard segment accompanied by decomposition; T_β -secondary transitions below glass transition considered as α-transition (T_α).

Table 12. Characteristic temperatures for the studied samples determined from DMTA and DSC curves

From Fig. 6 tan δ values at glass transition peaks show that E′ is almost 5E″ for all the samples, except PTHF-HPC for which E′ is almost 10 E″. This result evidences that for all the samples the elastic modulus component is more important than the viscous modulus one.

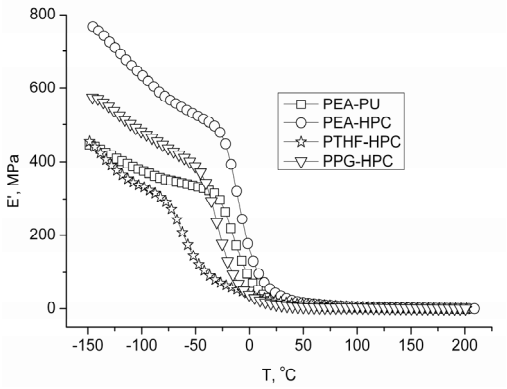

Fig. 4. Storage modulus as a function of temperature for the studied samples

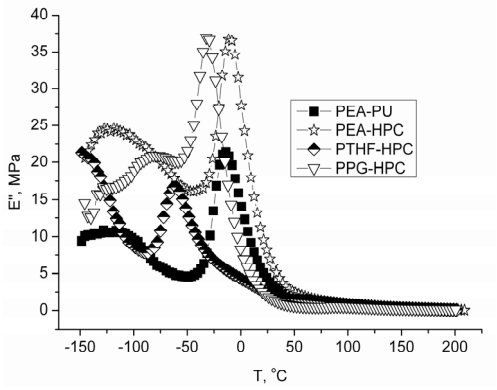

Fig. 5. Loss modulus as a function of temperature for the studied samples

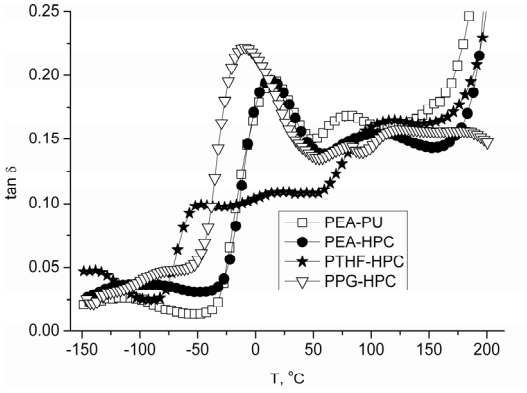

Fig. 6. Tan δ as a function of temperature for the studied samples

2.7 Mechanical properties

Biological materials have a wide range of mechanical properties matching their biological function. This is achieved via assembly of different size building block segments (soft and hard) spanning many length scales. Due to specific chemical versatility of polyurethanes, different morphologies at different length scales can be obtained and thus different physical properties which satisfy diverse clinical needs have been achieved. The modulability of mechanical properties make polyurethanes excellent candidates for applications in soft tissue engineering. Because of the strong tendency of rigid aromatic moieties to pack efficiently and the presence of hydrogen bonding between urethane and urea groups they tend to self-organize to form semi-crystalline phases within the polymer macromolecular assembly. As the elasticity of the polymers depends on their degree of crystallinity and the degree of hard segment segregation, it is clear that the selection of the diisocyanate monomer will be one of the key parameters that influence polyurethane mechanical characteristics.
The resulted tensile properties are tabulated in Table 13.

Sample	Young modulus, MPa	Elongation at break, %	Tensile strength at break, MPa	Toughness, MJ/m^3	C_1, MPa	C_2/C_1
PEA-PU	166/186	47/66	11/18	4.0/9.4	9.2/7.3	2.3/3.2
PEA-HPC	90/113	71/84	19/22	9.3/13.1	2/0.64	7.3/18.83
PTHF-HPC	70/30	72/159	14/10	7.7/11.8	3.7/0.91	4.7/3.28
PPG-HPC	75/39	53/56	15/9	5.6/3.5	4.3/0.42	4/16.03

'/ ' means dry/conditioned (37°C, saline water 0.9 % w/v, 24 h)

Table 13. Mechanical testing results

The stress-strain curves of the studied polyurethanes are plotted in Fig. 7 for dry film samples and in Fig. 8 the stress-strain curves of the film samples previously conditioned in warm (37 °C) saline water (NaCl, 0.9 % w/v, pH=7.4) for 24 h, then blotted with absorbent filter paper, are presented. We compare in this way, the mechanical properties of the films in dry state vs. physiological condition.

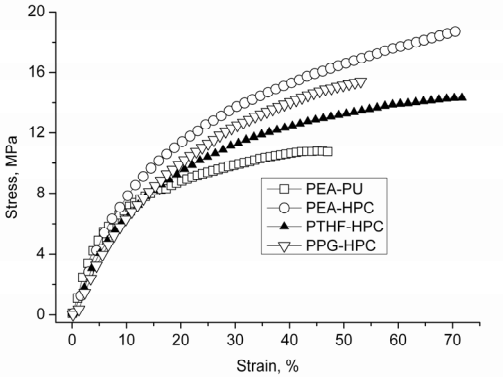

Fig. 7. Stress-strain curves of the dry polyurethanes samples

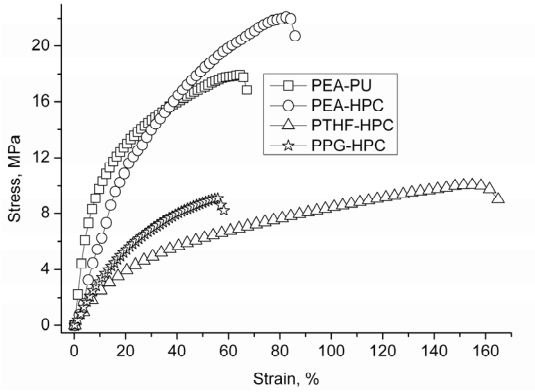

Fig. 8. Stress-strain curves of the polyurethane samples conditioned in saline water

The influence of the physical and chemical cross-links on the elastic behaviour of the polyurethanes is investigated by using Mooney-Rivlin equation, (9), for rubbers, (Sekkar et al., 2000; Spathis, 29) :

$$\sigma / (\lambda - \frac{1}{\lambda^2}) = 2C_2\lambda^{-1} + 2C_1 \tag{9}$$

where σ is the stress, λ is the extension ratio (L/L_0) and C_1, C_2 are the Mooney-Rivlin constants.

From the stress-strain experimental data, the Mooney-Rivlin curves are plotted (Fig. 9 and Fig. 10) and the values of C_1 and C_2 are obtained (see Table 13). C_1 can be obtained by extrapolating the linear portion of the curve to $\lambda^{-1} = 0$, and C_2 from the slope of the linear portion. The elastic behaviour depends on the size and the distribution of the hard domains into the soft matrix and is more or less reflected in the deviation from the Mooney-Rivlin equation.

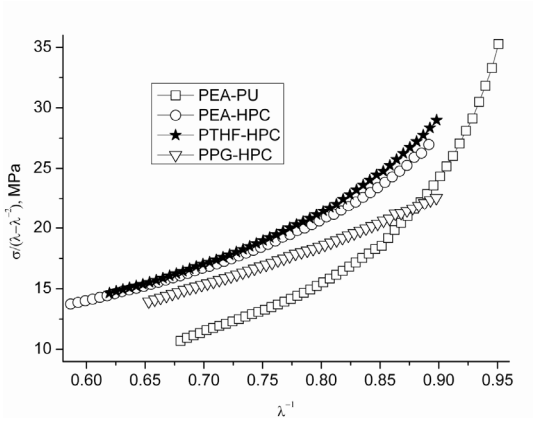

Fig. 9. Mooney-Rivlin plots of the dry polyurethanes samples

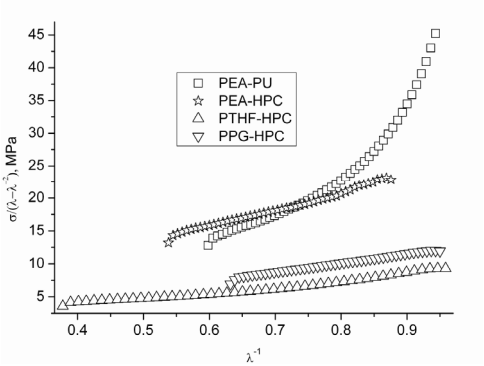

Fig. 10. Mooney-Rivlin plots of the conditioned in saline water polyurethanes samples

Moreover, the Eqn. (9) has been used to analyze the effects of different environments on the tensile behaviour of the polyurethane film samples. It has been suggested that the Mooney-Rivlin constants C_1 and C_2 are respectively associated with the network structure and the flexibility of the network. In case of dry biopolyurethanes samples it appears that polyurethane PPG-HPC shows an almost linear behaviour when comparing with PEA-PU, PEA-HPC and PTHF-HPC samples. In these block-copolymers the number of physical and chemical cross-links depends on the nature of the macrodiol used, the hydroxypropyl cellulose which generates chemical cross-links in the matrix and on the feed ratio. In the case of polyester-based matrix, PEA-HPC dry sample, the low value of C_1 evidences clearly that the more polar ester groups lead to a matrix dominated by physical cross-links. Therefore, C_1 is different for HPC polyether- and polyester-urethanes (C_1 is lower for polyester- than polyether-urethanes). At higher strains a disrupting of the physical cross-links is taking place and C_1 becomes lower. C_2 is not so sensitive relative to the nature of soft segment but shows the presence of both physical and chemical cross-links specific to a polyurethane network. The effect of conditioning in saline water (0.9 % w/v, 24 h, 37°C) is clearly revealed by C_1 which is found lower for all the samples evidencing that after conditioning the physical network is affected as well as its flexibility.

The toughness representing the energy absorbed before the sample breaks is higher as expected for PEA-HPC sample than for the PPG-HPC and PTHF-HPC samples, both for dry and conditioned samples. Moreover it can be noticed that the cellulose derivative makes that this absorbed energy to be much higher in case of dry samples. Hydration of samples leads to the increase of toughness except PPG-HPC sample due to amorphous and atactic soft segment structure.

Hydration of the semicrystalline, more or less ordered structures like polyurethanes, have as main result the disrupting of the physical bonding, and the plasticizing of the biopolyurethane matrix, affecting strain behaviour. Water may penetrate within interstitials of the microporous structure favoring biological interactions. The heat is also important in softening the material acting upon the soft segment and physical hydrogen bonding. From Table 13 one can notice that for polyether-urethanes (PTHF-HPC, PPG-HPC), Young modulus decreases after conditioning in saline water at 37°C for 24 h, the material achieve more flexibility, which may bring as advantage for realization of biopolyurethane tissular structures, such heart valves and leather grafts.

Hydrogen bonding is known as an important driving force for the phase separation of a hard segment from a soft-segment matrix consisting of polyether or polyester polyol. The separated

hard segment acts as physical cross-links and filler particles for the soft-segment matrix. Microphase separation of segmented polyurethanes is probably the single most influential characteristic of these materials. The degree of phase separation plays a key role in determining mechanical properties and blood compatibility, (Yoon et al., 2005). The heterogeneous morphology of polyurethanes will determine the surface composition exposed to a polar environment (water or blood) or to a nonpolar environment (air or vacuum). The surface segregation phenomenon reflects the difference in surface energy between the polar and nonpolar components, (Lupu et al., 2007b). The surface composition constitutes a crucial parameter for a biomedical material in contact with blood. The mobility of polymer chains coupled with environmental changes can lead to surface composition and properties that are time-dependent and dependent on the contacting medium, temperature, that the polymer experiences. It is, however, an unresolved question as to whether an air-stored polyurethane surface indeed adapts to the aqueous environment on biomedical usage. As the polyurethane biomaterial is placed into contact with a physiological medium, such as blood or tissue, its surface layers will undergo motions in order to accommodate the new interfacial situation. In contact with aqueous environments, it is obviously favorable for hydrophilic constituents of the polymer to become enriched at the interface, (Vermette & Griesser, 2001).
For crosslinked blends of Pellethene and multiblock polyurethanes containing phospholipids, (Yoo & Kim, 2005), it was found for elastic modulus values ranged between 21-47 MPa, whereas for biomaterials based on cross-linked blends of Pellethene and multiblock polyurethanes containing poly(ethylene oxide) it was found for elastic modulus values ranged between 85-246 MPa, (Yoo & Kim, 2004).

2.8 Platelet adhesion

In vitro platelet adhesion experiments were conducted to evaluate the preliminary blood compatibility. It is very well known that the surface properties particularly platelet adhesion of the biomaterials is very important with respect to their haemocompatibility, especially when they are used as cardiovascular devices, (Park et al., 1998).
It is well known that when blood is in contact with a synthetic material, firstly the latter one adsorbs onto its surface blood plasma proteins, and secondly attract and activate the thrombocytes. In function of the type of the adsorbed plasma proteins (fibrinogen or albumins) this phenomenon can exert in a more or less extent. In case of the preferentially fibrinogen adsorption (important protein in endogenous haemostasis), platelet adhesion is increased followed by thrombus activation and clot formation. In case of albumin absorbtion platelet adhesion is diminished which confer to the surface a thromboresistant character, (Bajpai, 2005; Wang et al., 2004).

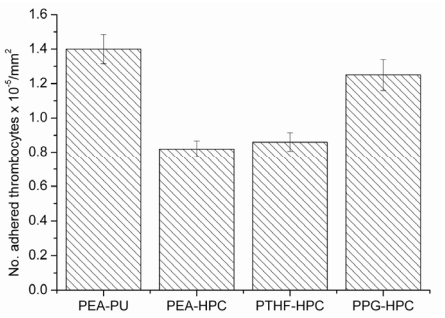

Fig. 11. Platelet adhesion on the studied biopolyurethanes film surfaces

In Fig. 11 platelet adhesion corresponding to the studied polyurethane samples is given. It can be noticed that when comparing PEA-PU with PEA-HPC the no. of adhered thrombocytes is much lower for PEA-HPC and this is due to the cellulose derivative which confers improved biomaterial qualities. Among the PPG-HPC, PTHF-HPC and PEA-HPC samples the most promising thromboresistant ones are PTHF-HPC and PEA-HPC. In our previous paper, the fibrinogen adsorption tests, (Macocinschi et al., 2009a), revealed that PTHF-HPC and PEA-HPC polyurethanes proved to be indicated for thromboresistant devices, and the polyether-urethane PTHF-HPC proved to have more relevant haemocompatible material qualities.
From literature for Biospan polyurethane, (Korematsu et al., 1999), the values for adhered thrombocytes found are 101500 adhered thrombocytes per mm^2. The number of adhered platelet is sensitive also to the soft segment length in the case of fluorinated polyurethanes, (Wang & Wei, 2005). The presence of cellulose in segmented polyurethane matrix indeed inhibits platelet adhesion, (Hanada et al., 2001). For PU/hydrophilic poly(ethylene glycol)diacrylate IPNs, platelet adhesion is suppressed by microseparated IPN structure, (Yoon et al., 2005). For poly(carbonate urethane)s with various degree of nanophase segregation the number of platelet adhered found was 5.33×10^6 up to 10.67×10^6 (for Pellethane is $8x10^6$), (Hsu & Kao, 2005).

3. Conclusion

The effect of the chemical structure of some cellulose derivative based segmented biopolyurethanes and polyurethane biocomposites containing extracellular matrix components on surface properties (static and dynamic contact angle measurements), on dynamical mechanical thermal analysis, mechanical properties was investigated. Specific biological tests were performed (platelet adhesion, protein adsorption tests of fibrinogen) and the results obtained recommend them as biomaterials with enhanced biocompatibility for biomedical applications. Thus, the proper understanding of blood compatibility and the development of prosthetic materials require the investigations of both natural and synthetic materials. Extensive in vitro, ex vivo, and in vivo testing in suitable animals and related differences between the properties of blood components of animals and humans are essential. Future research should be directed in order to clarify the influence of anatomical site of implantation on the behaviour of the implant, with a goal towards the development of site specific implants.

4. Acknowledgment

This work was supported by CNCS-UEFISCDI, Research Projects, Code: PN-II-ID-PCE-988/2008, contract no. 751/2009.

5. References

Abraham, G.A., De Queiroz, A.A.A. & Roman, J.S. (2002). Immobilization of a Nonsteroidal Antiinflammatory Drug onto Commercial Segmented Polyurethane Surface to Improve Haemocompatibility Properties. *Biomaterials*, Vol. 23, No. 7, (April 2002), pp. 1625-1638, ISSN 0142-9612

Bajpai, A.K. (2005). Blood Protein Adsorption onto a Polymeric Biomaterial of Polyethylene glycol and Poly[(2-hydroxyethylmethacrylate)-co-acrylonitrile] and Evaluation of In Vitro Blood Compatibility. *Polymer International*, Vol. 54, No. 2, (February 2005), pp. 304-315, ISSN 1097-0126

Baumgartner, J.N., Yang, C.Z. & Cooper, S.L. (1997). Physical Property Analysis and Bacterial Addhesion on a Series of Phosphonated Polyurethanes. *Biomaterials*, Vol. 18, No. 12, (May 1998), pp. 831-837, ISSN 0142-9612

Bicerano, J. (1996). Prediction of the Properties of Polymers from Their Structures. *Journal of Macromolecular Science-Reviews in Macromolecular Chemistry and Physics*, Vol. 36, No. 1, (February 1996), pp. 161-196, ISSN 0736-6574

Desai, S., Thakore, I.M., Sarawade, B.D. & Dewi, S. (2000). Effect of polyols and diisocyanates on thermo-mechanical and morphological properties of polyurethanes. *European Polymer Journal*, Vol. 36, No. 4, (April 2000), pp. 711-725, ISSN 0014-3057

Durairaj, R.B. (2001). HER Materials for Polyurethane Applications, In: *Advances in Urethane Science and Technology*, Klempner, D. & Frisch, K.C. (Eds.), pp. 369-419, Rapra Technology Ltd., ISBN 1-85957-275-8, Shawbury, UK

Erbil, H.Y. (1997). Surface Tension of Polymers, In: *Handbook of Surface and Colloid Chemistry*, Birdi, K.S. (Ed.), pp. 265-312, CRC Press, ISBN 0-8493-9459-7, Boca Raton, USA

Faibish, R.S., Yoshida, W. & Cohen, Y. (2002). Contact Angle Study on Polymer-Grafted Silicon Wafers. *Journal of Colloid and Interface Science*, Vol. 256, No. 2, (December 2002), pp. 341-350, ISSN 0021-9797

Gao, S. & Zhang, L. (2001). Molecular Weight Effects on Properties of Polyurethane/Nitrokonjac Glucomannan Semiinterpenetrating Polymer Netwoks. *Macromolecules*, Vol. 34, No. 7, (March 2001), pp. 2202-2207, ISSN 0024-9297

Grundke, K. (2005). Surface-energetic Properties of Polymers in Controlled Architecture, In: *Molecular Interfacial Phenomena of Polymers and Biopolymers*, Chen, P. (Ed.), pp. 323-374, Woodhead Publishing Ltd., ISBN-13 978-1-85573-928-4, Cambridge, England

Hanada, T., Li, Y.J. & Nakaya, T. (2001). Synthesis and Haemocompatibilities of Cellulose-Containing Segmented Polyurethanes. *Macromolecular Chemistry and Physics*, Vol. 202, No. 1, (January 2001), pp. 97-104, ISSN 1022-1352

Heijkants, R.G.J.C., Van Calck, R.V., Van Tienen, T.G., De Groot, J.H., Buma, P., Pennings, A.J., Veth, R.P.H. & Schouten, A.J. (2005). Uncatalyzed Synthesis, Thermal and Mechanical Properties of Polyurethanes based on Poly(epsilon-caprolactone) and 1,4-Butane Diisocyanate with Uniform Hard Segment. *Biomaterials*, Vol. 26, No. 20, (July 2005), pp. 4219-4228, ISSN 0142-9612

Hsu, S. & Kao, Y.C. (2005). Biocompatibility of Poly(carbonate urethane)s with Various Degrees of Nanophase Separation. *Macromolecular Bioscience*, Vol. 5, No. 3, (March 2005), pp. 246-253, ISSN 1616-5187

Huang, J. & Zhang, L. (2002). Effect of NCO/OH Molar Ratio on Structure and Properties of Graft-Interpenetrating Polymer Networks from Polyurethane and Nitrolignin. *Polymer*, Vol. 43, No. 8, (April 2002), pp. 2287-2294, ISSN 0032-3861

Hung, H.S., Wu, C.C., Chien, S. & Hsu, S.H. (2009). The Behavior of Endothelial Cells on Polyurethane Nanocomposite and the Associated Signaling Pathways. *Biomaterials*,Vol. 30, No. 8, (March 2009), pp. 1502-1511, ISSN 0142-9612

Kalble, D.H. (1969). Peel Adhesion: Influence of Surface Energies and Adhesive Rheology. *The Journal of Adhesion*, Vol. 1, No. 2, (February 1969), pp. 102-123, ISSN 0021-8464

Korematsu, A., Tomita, T., Kuriyama, S., Hanada, T., Sakamoto, S. & Nakaya, T. (1999). Synthesis and Blood Compatibilities of Novel Segmented Polyurethanes Grafted Phospholipids Analogous Vinyl Monomers and Polyfunctional Monomers. *Acta Polymerica*, Vol. 50, No. 10, (October 1999), pp. 363-372, ISSN 0323-7648

Lamba, N.M.K., Woodhouse, K.A. & Cooper, S.L. (1997). *Polyurethanes in Biomedical Applications*, CRC Press, ISBN-10 0849345170, New York

Lelah, M.D. & Cooper, S.L. (1986). *Polyurethanes in medicine*, CRC Press, ISBN-10 0849363071, Boca Raton, FL

Lligadas, G., Ronda, J.C, Galia, M. & Cadiz, V. (2007). Poly(ether urethane) Networks from Renewable Resources as Candidate Biomaterials: Synthesis and Characterization. *Biomacromolecules*, Vol. 8, No. 2, (February 2007), pp. 686-692, ISSN 1525-7797

Lupu, M., Butnaru, M., Macocinschi, D., Oprean, O.Z., Dimitriu, C., Bredetean, O., Zagnat, M. & Ioan, S. (2007a). Surface Properties of Segmented Poly(ester urethane)s and Evaluation of In Vitro Blood Compatibility and In Vivo Biocompatibility. *Journal of Optoelectronics and Advanced Materials*, Vol. 9, No. 11, (November 2007), pp. 3474-3478, ISSN 1454-4164

Lupu, M., Macocinschi, D., Ioanid, G., Butnaru, M. & Ioan, S. (2007b). Surface Tension of Poly(ester urethane)s and Poly(ether urethane)s. *Polymer International*, Vol. 56, No. 3, (March 2007), pp. 389-398, ISSN 1097-0126

Macocinschi, D., Filip, D. & Vlad, S. (2008). New Polyurethane Materials from Renewable Resources: Synthesis and Characterization. *e-Polymers*, no.062, (May 2008), ISSN 1618-7229

Macocinschi, D., Filip, D., Butnaru, M. & Dimitriu, C.D. (2009a). Surface Characterization of Biopolyurethanes Based on Cellulose Derivatives. *Journal of Materials Science: Materials in Medicine*, Vol. 20, No. 3 (March 2009), pp. 775-783, ISSN 0957-4530

Macocinschi, D., Filip, D., Vlad, S., Cristea, M. & Butnaru, M. (2009b). Segmented Biopolyurethanes for Medical Applications. *Journal of Materials Science: Materials in Medicine*, Vol. 20, No. 8, (August, 2009), pp. 1659-1668, ISSN 0957-4530

Macocinschi, D., Filip, D. & Vlad, S. (2010a). Surface and Mechanical Properties of Some New Biopolyurethane Composites. *Polymer Composites*, Vol. 31, No. 11, (November 2010), pp. 1956-1964, ISSN 1548-0569

Macocinschi, D., Tanase, C., Filip, D., Vlad, S. & Oprea, A. (2010b). Study of the Relationship Between New Polyurethane Composites for Biomedical Applications and Fungal Contamination. *Materiale Plastice*, Vol. 47, No. 3, (September 2010), pp. 286-291, ISSN 0025-5289

Macocinschi, D., Filip, D., Vlad, S., Cristea, M., Musteata, V.E. & Ibanescu, S. (2011). Thermal, Dynamic Mechanical, and Dielectric Analyses of Some Polyurethane Biocomposites. *Journal of Biomaterials Applications*, DOI 10.1177/0885328210394468, ISSN 0885-3282

Moldovan, L., Craciunescu, O., Zarnescu, O., Macocinschi, D. & Bojin, D. (2008). Preparation and Characterization of New Biocompatibilized Polymeric Materials for Medical Use. *Journal of Optoelectronics and Advanced Materials*, Vol. 10, No. 4, (April 2008), pp. 942-947, ISSN 1454-4164

Mondal, S. & Hu, J.L. (2006). Structural Characterization and Mass Transfer Properties of Polyurethane Block Copolymer: Influence of Mixed Soft Segment Block and Crystal Melting Temperature. *Polymer International*, Vol. 55, No. 9, (September 2006), pp. 1013-1020, ISSN 1097-0126

Musteata, V.E., Filip, D., Vlad, S. & Macocinschi, D (2010). Dielectric Relaxation of Polyurethane Biocomposites. *Optoelectronics and Advanced Materials-Rapid Communications*, Vol. 4, No. 8, (August 2010), pp. 1187-1192, ISSN 1842-6573

Norde, W. (2006). Surface Modifications to Influence Adhesion of Biological Cells and Adsorption of Globular Proteins, In: *Surface Chemistry in Biomedical and Environmental Science*, Blitz, J.P. & Gun'Ko, V.M. (Eds.), pp. 159-176, Springer, ISBN-10 1-4020-4740-1, Dordrecht, Netherlands

Ohya, Y. (2002). Hydrogen Bonds, In: *Supramolecular Design for Biological Applications*, Yui, N. (Ed.), pp. 33-72, CRC Press, ISBN 0-8493-0965-4, Boca Raton, Florida

Owens, D.K. & Wendt, R.C. (1969). Estimation of Surface Free Energy of Polymers. *Journal of Applied Polymer Science*, Vol. 13, No. 8, (March 2003), pp. 1741-1747, ISSN 1097-4628

Ozdemir, Y., Hasirici, N. & Serbetci, K. (2002). Oxygen Plasma Modification of Polyurethane Membranes. *Journal of Materials Science: Materials in Medicine*, Vol. 13, No. 12, (December 2002), pp. 1147-1152, ISSN 0957-4530.

Park, K.D., Okano, T., Nojiri, C. & Kim, S.W. (1988). Heparin Immobilization onto Segmented Polyurethaneurea Surfaces-Effect of Hydrophilic Spacers. *Journal of Biomedical Materials Research*, Vol. 22, No. 11, (November 1988), pp. 977-992, ISSN 1549-3296

Pilkey, W.D. (2005). *Formulas for Stress, Strain, and Structural Matrices*, Second edition, Wiley & sons. Inc., ISBN 0-471-03221-2, Hoboken, New Jersey

Plank, H., Syre, I., Dauner, M. & Egberg, G. (Eds.). (1987). *Polyurethane in Biomedical Engineering: II. Progess in Biomedical Engineering 3*, Elsevier Science, ISBN 0-44-442759-7, Amsterdam

Rabel, W. (1977). Flussigkeitsgrenzflachen in Theorie und Anwendungstechnik. *Physicalische Blatter*, Vol. 33, pp. 151-161, ISSN 0031-9279

Ramis, X., Cadenato, A., Morancho, J.M. & Salla, J.M. (2001). Polyurethane-Unsaturated Polyester Interpenetrating Polymer Networks: Thermal and Dynamic Mechanical Thermal Behaviour. *Polymer*, Vol. 42, No. 23, (November 2001), pp. 9469-9479, ISSN 0032-3861

Rankl, M., Laib, S. & Seeger, S. (2003). Surface Tension Properties of Surface-Coatings for Application in Biodiagnostics Determined by Contact Angle Measurements. *Colloids and Surfaces B: Biointerfaces*, Vol. 30, No. 3, (July 2003), pp. 177-186, ISSN 0927-7765

Raschip, I.E., Vasile, C. & Macocinschi, D. (2009). Compatibility and Biocompatibility Study of New HPC/PU Blends. *Polymer International*, Vol. 58, No. 1, (January 2009), pp. 4-16, ISSN 1097-0126

Reddy, T.T., Kano,A., Maruyama, A., Hadano, M. & Takahara, A. (2008). Thermosensitive Transparent Semi-Interpenetrating Polymer Networks for Wound Dressing and Cell Adhesion Control. *Biomacromolecules,* Vol. 9, No. 4, (April 2008), pp. 1313-1321, ISSN 1525-7797

Sekkar, V., Bhagawan, S.S., Prabhakaran, N., Rama, R.M. & Ninan, K.N.(2000). Polyurethanes Based on Hydroxyl Terminated Polybutadiene: Modeling of

Network Parameters and Correlation with Mechanical Properties. *Polymer*, Vol. 41, No. 18, (August 2000), pp. 6773-6786, ISSN 0032-3861

Siegwart, R. (2001). Indirect Manipulation of a Sphere on a Flat Disk Using Force Information. *International Journal of Advanced Robotic Systems,* Vol. 6, No. 4, (December 2009), pp. 12-16, ISSN 1729-8806

Sirear, A.K. (1997). Elastomers. In: *Thermal Characterization of Polymeric Materials*. Turi, E.A. (Ed.), Vol. 1, Academic Press, pp. 970-1025, ISBN 0-12-703782-9

Spathis, G.D. (1991). Polyurethane Elastomers Studied by the Mooney Rivlin Equation for Rubbers. *Journal of Applied Polymer Science*, Vol. 43, No. 3, (August 1991), pp. 613-620, ISSN 1097-4628

Strom, G., Fredriksson, M. & Stenius, P. (1987). Contact Angles, Work of adhesion, and Interfacial Tensions at a Dissolving Hydrocarbon Surface. *Journal of Colloid and Interface Science*, Vol. 119, No. 2, (October 1987), pp. 352-361, ISSN 0021-9797

Thomson, T. (2005). *Polyurethanes as Specialty Chemicals. Principles and Applications*, CRC Press, ISBN 0-8493-1857-2, Boca Raton, Florida

Van Krevelen, D.W. (1990). *Properties of Polymers; Their Correlation with Chemical Structure, their Numerical Estimation and Prediction from Additive Group Contributions*, Elsevier, ISBN 0-444-88160-3, Amsterdam

Van Oss, C.J., Good, R.J. & Chaudhury, M.K. (1988a). Additive and Nonadditive Surface Tension Components and the Interpretation of Contact Angles. *Langmuir*, Vol. 4, No. 4, (July 1988), pp. 884-891, ISSN 0743-7463

Van Oss, C.J., Ju, M.K., Chaudhury, M.K. & Good, R.J. (1988b), Interfacial Lifshitz-van der Waals and Polar Interactions in Macroscopic Systems. *Chemical Reviews*, Vol. 88, No. 6, (September 1988), pp. 927-941, ISSN 0009-2665

Van Oss, C.J., Ju, L., Chaudhury, M.K. & Good, R.J. (1989). Estimation of the Polar Parameters of the Surface Tension of Liquids by Contact Angle Measurements on Gels. *Journal of Colloid and Interface Science*, Vol. 128, No. 2, (March 1989), pp. 313-319, ISSN 0021-9797

Van Oss, C.J. (1994). *Interfacial Forces in Aqueous Media*, Marcel Dekker, ISBN 0-8274-9168-1, New York

Vermette, P., Griesser, H.J., Laroche, G. & Guidoin, R. (2001). *Biomedical Applications of Polyurethanes. Tissue Engineering Intelligence Unit 6,* Eurekah.com, ISBN 1-58706-023-X, Texas, USA

Wang, L.F. & Wei, Y.H. (2005). Effect of Soft Segment Length on Properties of Fluorinated Polyurethanes. *Colloids and Surfaces B: Biointerfaces*, Vol. 41, No. 4, (April 2005), pp. 249-255, ISSN 0927-7765

Wang, Y.X., Robertson, J.L., Spillman Jr., W.B. & Claus, R.O. (2004). Effects of the Chemical Structure and the Surface Properties of Polymeric Biomaterials on Their Biocompatibility. *Pharmaceutical Research*, Vol. 21, No. 8, (August 2004), pp. 1362-1373, ISSN 0724-8741

Wu, Z.Q., Chen, H., Huang, H., Zhao, T., Liu, X., Li, D. & Yu, Q. (2009). A Facile Approach to Modify Polyurethane Surfaces for Biomaterial Applications. *Macromolecular Bioscience,* Vol. 9, No. 12, (December 2009), pp. 1165-1168, ISSN 1616-5195

Yoo, H.J. & Kim, H.D. (2004). Properties of Crosslinked Blends of Pellethene and Multiblock Polyurethane Containing Poly(ethylene oxide) for Biomaterials. *Journal of Applied Polymer Science*, Vol. 91, No. 4, (February 2004), pp. 2348-2357, ISSN 1097-4628

Yoo, H.J. & Kim, H.D. (2005). Characteristics of Crosslinked Blends of Pellethene and Multiblock Polyurethanes Containing Phospholipids. *Biomaterials*, Vol. 26, No. 16, (June 2005), pp. 2877-2886, ISSN 0142-9612

Yoon, S.S., Kim, J.H. & Kim, S.C. (2005). Synthesis of Biodegradable PU/PEGDA IPNs Having Micro-Separated Morphology for Enhanced Blood Compatibility. *Polymer Bulletin*, Vol. 53, No. 5-6, (March 2005), pp. 339-347, ISSN 0170-0839

Zlatanic, A., Petrovic, Z.S. & Dusek, K. (2002). Structure and Properties of Triolein-Based Polyurethane Networks. *Biomacromolecules*, Vol. 3, No. 5, (September 2002), pp. 1048-1056, ISSN 1525-7797

17

Collagen-Based Drug Delivery Systems for Tissue Engineering

Mădălina Georgiana Albu[1], Irina Titorencu[2] and Mihaela Violeta Ghica[3]
[1]*INCDTP – Leather and Footwear Research Institute, Bucharest*
[2]*Institute of Cellular Biology and Pathology "Nicolae Simionescu", Bucharest*
[3]*Carol Davila University of Medicine and Pharmacy, Faculty of Pharmacy, Bucharest*
Romania

1. Introduction

Biomaterials are considered those natural or artificial materials that can be used for any period of time, as a whole or as part of a system which treats, augments or replaces a tissue, organ or function of the human or animal body (Williams, 1999). In medicine a wide range of biomaterials based on metals, ceramics, synthetic polymers, biopolymers, etc. is used. Among biopolymers, collagen represents one of the most used biomaterials due to its excellent biocompatibility, biodegradability and weak antigenecity, well-established structure, biologic characteristics and to the way it interacts with the body, the latter recognizing it as one of its constituents and not as an unknown material (Friess, 1998; Lee et al., 2001). Irrespective of the progress in the field of biomaterials based on synthetic polymers, collagen remains one of the most important natural biomaterials for connective tissue prosthetic in which it is the main protein. Due to its excellent properties collagen can be processed in different biomaterials used as burn/wound dressings, osteogenic and bone filling materials, antithrombogenic surfaces, collagen shields in ophthalmology, being also used for tissue engineering including skin replacement, bone substitutes, and artificial blood vessels and valves. Biomaterials based on type I fibrillar collagen such as medical devices, artificial implants, drug carriers for controlled release and scaffolds for tissue regeneration have an important role in medicine, being widely used at present (Healy et al., 1999; Hubell, 1999; Wang et al., 2004). In this chapter, we attempted to summarize some of the recent developments in the application of collagen as biomaterial in drug delivery systems and tissue engineering field.

2. Collagen-based biomaterials

Collagen is the main fibrous protein constituent in skin, tendons, ligaments, cornea etc. It has been extensively isolated from various animals, including bovine (Renou et al., 2004; Doillon, 1992), porcine (Smith et al., 2000; Lin et al., 2011; Parker et al., 2006), equine (Angele et al., 2004), ovine (Edwards et al., 1992), shark, frog, bird (Limpisophon et al., 2009) and from marine origin such as: catfish (Singh et al., 2011), silver carp (Rodziewicz-Motowidło et al., 2008), marine sponge (Swatschek et al., 2002), jumbo squid (Uriarte-Montoya et al., 2010),

paper nautilus (Nagai & Suzuki, 2002), tilapia fish-scale (Chen et al., 2011), red fish (Wang et al., 2008). Among these types of sources the most used has been bovine hide. Although to date 29 different types of collagen have been identified (Albu, 2011), type I collagen is the most abundant and still the best studied. This work is focused on biomaterials based on type I collagen of bovine origin. Type I collagen consists of 20 amino acids, arranged in characteristic sequences which form a unique conformational structure of triple helix (Trandafir et al., 2007). Hydroxyproline is characteristic only for collagen and it confers stability for collagen, especially by intramolecular hydrogen bonds. The collagen structure is very complex, being organised in four levels, named primary, secondary, tertiary and quaternary structure. Depending on the process of collagen extraction, the basic forms of collagen are organized on structural level.

2.1 Process of collagen extraction

To obtain extracts of type I fibrillar collagen, fresh skin or skin technological waste from leather industry can be used as raw materials (Trandafir et al., 2007), extraction being performed from dermis. To minimize the exogenous degradation the skin has to be ready for immediate extraction. Yield of good extraction is obtained from skin of young animals (preferably younger than two years) due to weaker crosslinked collagen.

Figure 1 schematically shows the obtaining of collagen in different forms by the currently used technologies at Collagen Department of Leather and Footwear Research Institute, Bucharest, Romania.

As figure 1 shows, the bovine hide was used as raw material. After removal of hair and fat by chemical, enzymatic or mechanical process, the obtained dermis could undergo different treatment and *soluble* or *insoluble collagen* is obtained.

2.1.1 Process of extraction for soluble collagen

Depending on structural level the solubilised collagen extracts can be denatured (when 90% of molecules are in denatured state) or un-denatured (when 70% of molecules keep their triple helical structure) (Trandafir et al., 2007).

The process for obtaining of *denatured collagen* took place at high temperature, pressure or concentrated chemical (acid or alkali) or enzymatic agents. Following these critical conditions the collagen is solubilised until secondary or primary level of structure and *gelatine* or *partial* (polypeptide) and *total* (amino acids) *hydrolisates* are obtained.

The *undenatured collagen* can be isolated and purified by two technologies, depending on the desired structural level (Li, 2003): molecular and fibrillar. They allow the extraction of type I collagen from bovine hide in aqueous medium while maintaining the triple helical structure of molecules, of microfibrils and fibres respectively (Wallace & Rosenblatt, 2003).

Isolation and purification of collagen molecules from collagenic tissues can be performed using a proteolytic enzyme such as pepsin, which produces cleavage of telopeptides - places responsible for collagen crosslinking. Removing them makes the collagen molecules and small aggregates (protofibrils) soluble in aqueous solutions of weak acid or neutral salts.

Extraction of collagen soluble in neutral salts. Studies on the extraction of soluble collagen with neutral salt solutions were performed with 0.15 to 0.20 M sodium chloride at 5^0C for 1-2 days (Fielding, 1976). Yield of this technology is low and the most collagenic tissues extracted with salts contain small quantities of collagen or no collagen at all.

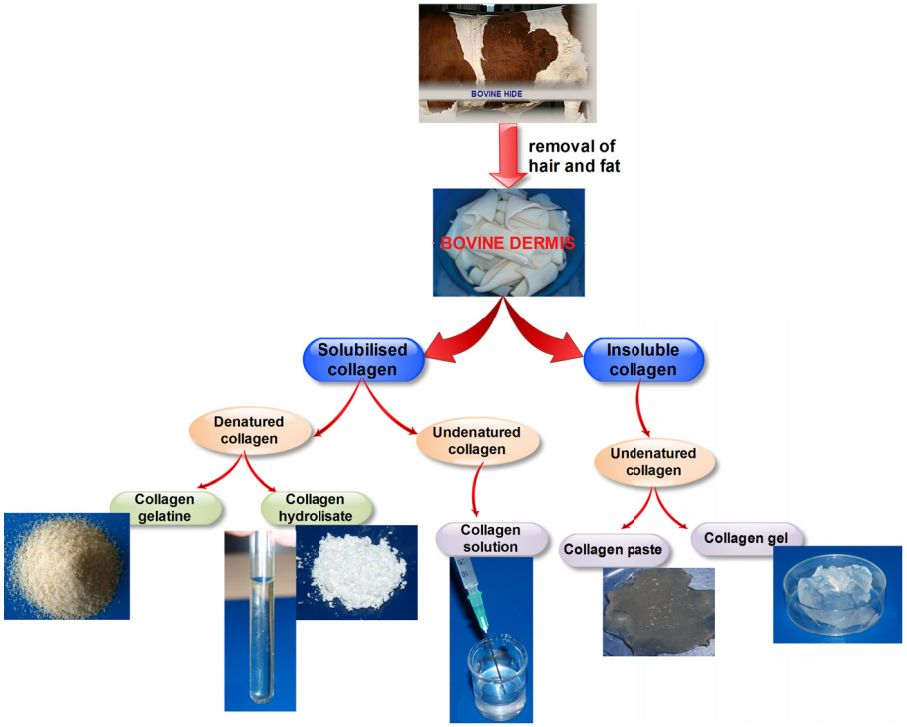

Fig. 1. Basic forms of collagen

Extraction of acid soluble collagen. Dilute acids as acetic, hydrochloric or citrate buffer solution with pH 2-3 are more effective for extraction of molecular collagen than neutral salt solutions. Type aldiminic intermolecular bonds are disassociated from dilute acids and by exerting forces of repulsion that occur between the same charges on the triple helix, causing swelling of fibril structure (Trelstad, 1982). The diluted acids do not dissociate keto-imine intermolecular bonds. For this reason collagen from tissues with high percentage of such bonds, such as bone, cartilage or tissue of aged animals is extracted in smaller quantities in dilute acids.

To obtain soluble collagen with diluted acids tissue is ground cold, wash with neutral salt to remove soluble proteins and polysaccharides, then collagen is extracted with acid solutions (Bazin & Delaumay, 1976). Thus about 2% of collagen can be extracted with salts or diluted acid solutions.

Enzymatic extraction is more advantageous, collagen triple helix being relatively resistant to proteases such as pronase, ficin, pepsin or chemotripsin at about 20^{o}C (Piez, 1984). The efficacy of enzymatic treatment arises from selective cleavage in the terminal non-helical regions monomer and higher molecular weight covalently linked aggregates, depending on the source and method of preparation. Thus, telopeptidic ends are removed, but in appropriate conditions the triple helices remain intact. Solubilised collagen is purified by salt precipitation, adjusting pH at the isoelectric value or at temperature of 37^{0}C (Bazin & Delaumay, 1976). Collagen extracted with pepsin generally contains higher proportions of intact molecules extracted with salts or acids.

2.1.2 Process of extraction for insoluble collagen

Collagen extraction by alkaline and enzymatic treatments. Alkaline pretreatment destroys covalent bonds resistant to acids. Collagen interaction with alkali shows the presence of certain specificities, hydrogen bonds being more sensitive to alkali. Degradation of the structure is more intense and irreversible if treatment is progressing on helicoidal structure (collagen → gelatin transition, alkaline hydrolysis).

Breaking of hydrogen bonds occurs by replacing the hydrogen atom from carboxyl groups with metal which is unable to form hydrogen bonds. Collagen can be extracted by treating the dermis with 5-10% sodium hydroxide and 1 M sodium sulphate at 20-25^{o}C for 48 hours (Cioca, 1981; Trandafir et al., 2007). Thus, fats associated with insoluble collagen are saponified, the telopeptidic non-helical regions are removed, collagen fibers and fibrils are peptized. Size of resulted fragments of collagen depends on the time and concentration of alkali treatment (Roreger, 1995). The presence of sodium sulfate solution controlled the swelling of collagen structure, protecting the triple-helical native conformation. Alkaline treatment is followed by an acid one, which leads to total solubilization of collagen in undenatured state from the dermis of mature animals.

Thus technologies of molecular and fibrilar extraction are enabled to extract type I collagen from bovine hide in an aqueous medium keeping triple helical structure of molecules, microfibrils and fibrils (Wallace & Rosenblatt, 2003).

2.2 Obtaining of collagen-based biomaterials

Obtaining of collagen-based biomaterials starts from undenatured collagen extracts – gels and solutions – which are processed by cross-linking, free drying, lyophilization, elecrospinning, mineralisation or their combinations. To maintain the triple helix conformation of molecules the conditioning processes must use temperatures not higher than 30^{0}C (Albu et al., 2010a). Extracted as aqueous solution or gel, type I collagen can be processed in different forms such as hydrogels, membranes, matrices (spongious), fibers, tubes (Fig. 2) that have an important role in medicine today. Figure 2 shows some collagen-based biomaterials obtained at our Collagen Department.

Among the variety of collagen-based biomaterials, only the basic morphostructural ones will be presented: hydrogels, membranes, matrices, and composites obtained from undenatured collagen.

Collagen hydrogels are biomaterials in the form of tridimensional networks of hydrofil polymeric chains obtained by physical or chemical cross-linking of gels. Chemical cross-linking consists in collagen reaction with aldehydes, diisocyanates, carboimides, acyl-azide, polyepoxydes and polyphenolic compounds which lead to the formation of ionic or covalent bonds between molecules and fibrils (Albu, 2011). Physical cross-linking includes the drying by heating or exposure at UV, gamma or beta irradiations. Their mechanical and biological properties are controllable and superior to the gels from which they were obtained.

The hydrogels have the capacity of hydration through soaking or swelling with water or biological fluids; hydrogels with a solid laminar colloidal or solid sphero-colloidal colloidal frame are formed, linked by means of secondary valences, where water is included by swelling. One of the exclusive properties of hydrogels is their ability to maintain the shape during and after soaking, due to the isotropic soaking. Also the mechanical properties of the collagen hydrogels are very important for the pharmaceutical applications, the modification of the cross-linking degree leading to the desired mechanical properties. The spreading

ability of the different size molecules in and from hydrogels serves for their utilization as drug release systems. The development and utilization of collagen hydrogels in therapeutics is supported by some advantages contributing to patients compliance and product efficiency. Thus, the hydrogels are easy to apply, have high bioadhesion, acceptable viscosity, compatibility with numerous drugs (Albu & Leca, 2005; Satish et al., 2006; Raub et al., 2007).

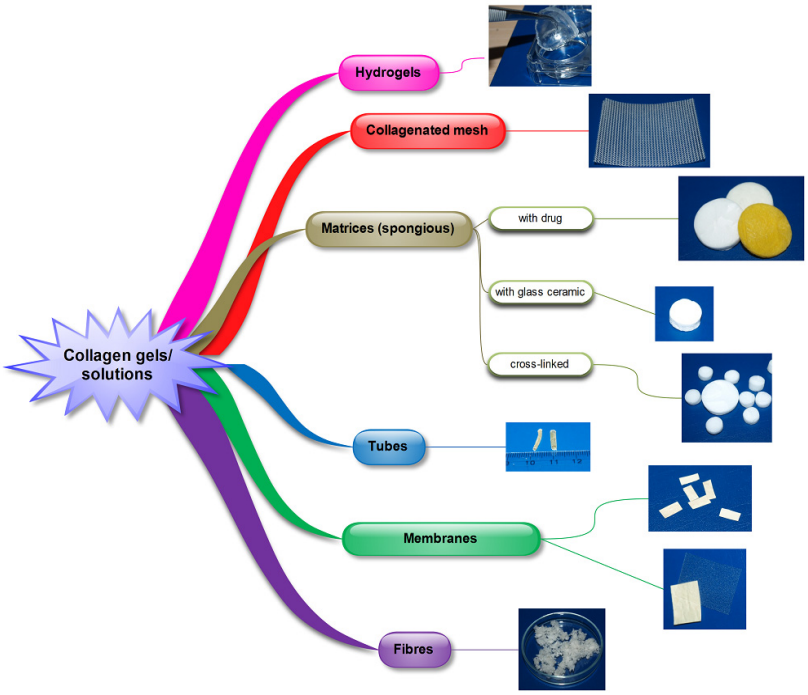

Fig. 2. Collagen-based biomaterials

Collagen membranes/films are obtained by free drying of collagen solution/gel in special oven with controllable humidity and temperature (not higher than 25°C) during 48-72 hours. These conditions allow the collagen molecules from gels to be structured and to form intermolecular bonds without any cross-linking agent. They have dense and microporous structure (Li et al., 1991).

Collagen matrices are obtained by lyophilisation (freeze-drying) of collagen solution/gel. The specificity of porous structure is the very low specific density, of approximately 0.02-0.3 g/cm^3 (Albu 2011, Zilberman & Elsner, 2008; Stojadinovic et al., 2008; Trandafir et al., 2007). The matrix porous structure depends significantly on collagen concentration, freezing rate, size of gel fibrils and the presence or absence of cross-linking agent (Albu et al., 2010b). The collagen matrix morphological structure is important, influencing the hydrophilicity, drug diffusion through network, degradation properties and interaction with cells. Figure 3 shows characteristic pore structure with a large variation in average pore diameter in collagen matrices.

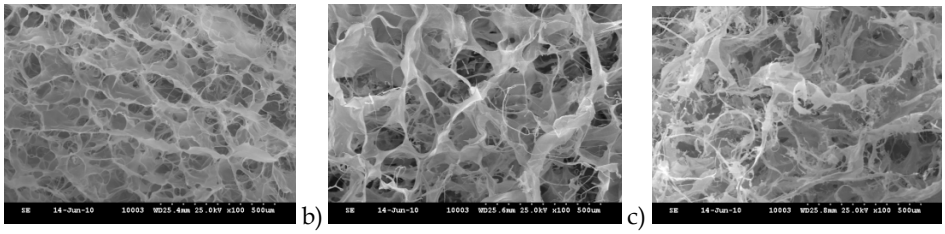

Fig. 3. SEM images of collagen matrices: (a) freeze at -40°C, (b) freeze at -10°C and (c) cross-linked with 0.25% glutaraldehyde.

Although the matrices presented in Fig. 3a,b have the same composition, their structure is different. Therefore, the low temperature (e.g. -40^{0}C) induces about 10 times smaller pore sizes than higher temperature (e.g. -10^{0}C). It can be noticed that lower freezing temperature produces more homogeneous samples than those obtained at high freezing temperature. Major differences of pore size and shape appear between un-cross-linked and cross-linked samples, the most homogeneous matrix with the smallest and inner pores being the un-cross-linked obtained at lowest freezing temperature.

Hydrophilic properties expressed by absorbing water and its vapor, are characteristic for collagen matrices, which can absorb at least 1500% water. Permeability for ions and macromolecules is of particular importance for tissues which are not based only on the vascular transport of nutrients. Diffusion of nutrients into the interstitial space ensures survival of the cells, continued ability to grow and to synthesize extracellular matrix specifically for tissue.

The infrared spectra of collagen exhibit several features characteristic for the molecular organization of its molecules: amino acids linked together by peptide bonds give rise to infrared active vibration modes amide A and B (about 3330 and 3080 cm-1, respectively) and amide I, II, and III (about 1629-1658 cm^{-1}, 1550-1560 cm^{-1} and 1235-1240 cm^{-1}, respectively) (Sionkowska et al., 2004).

Hydrothermal stability of collagen is characterized by its contraction when heated in water at a certain temperature at which the conformational transition of molecules from the triple helix statistic coil take place (Li, 2003).

Thermal behavior of collagen matrices depends on the number of intermolecular bonds. Generally, the number of bonds is higher, the shrinkage temperature is higher and the biomaterial is more stable *in vivo*.

Another method commonly used to assess the *in vivo* stability of collagen biomaterials, is the *in vitro* digestion of matrix with collagenase and other proteinases (trypsin, pepsin) (Li, 2003). Biodegradability of collagen matrices is dependent on the degree of cross-linking.

Collagen can form a variety of homogeneous collagen composites with ceramics, drugs, natural or synthetic polymers**.** The obtaining methods involve chemical cross-linking, physical loading and co-precipitation followed by free-drying, freeze-drying or electrospinning.

The most recent collagen composites used as medical devices, artificial implants, supports for drug release and scaffolds for tissue regeneration are presented in Table 1.

Collagen composites containing physiologically active substances acting as drug delivery systems (DDS) are discussed in Section 3.

Type of composite	Type of component from composite	Composite form
Collagen-natural polymer	Hyaluronic acid (Davidenko et al., 2010)	Matrix, membrane, hydrogel, fibers
	Silk fibroin (Zhou et al., 2010)	Membrane, fibers, matrix, microtubes
	Chondroitin-6-suphate (Stadlinger et al., 2008)	Tube, matrix
	Elastin (Skopinska-Wisniewska et al., 2009)	Tube, film, fibers, matrix
	Alginate (Sang et al., 2011)	Spongious, filler for bone,
	Chitosan (Sionkowska et al., 2004)	Matrix, membrane, tubular graft, nanofibers, hydrogel,
	Heparin (Stamov et al., 2008)	Matrix
Collagen-synthetic polymer	Poly-L-lactide (PLLA) (Chen et al., 2006)	Coating for composite
	Poly-lactic-co-glycolic-acid (PLGA) (Wen et al., 2007)	Fibers, matrix, coated tube
	ε-caprolactone (Schnell et al., 2007)	Nanofibers
	Poly(ethylene-glycol) (PEG) (Sionkowska et al., 2009)	Films, fibers
Collagen-ceramic	Calcium phosphates (Hong et al., 2011)	Matrix, filler
	Hydroxyapatite (Zhang et al., 2010; Hoppe et al., 2011)	Matrix, filler
	Tricalciumphosphate (Gotterbarm et al., 2006)	Matrix, filler

Table 1. Collagen-based composites

3. Collagen-based drug delivery systems

Nowdays, the field of drug delivery from topical biopolymeric supports has an increased development due to its advantages compared to the systemic administration. These biopolymers can release adequate quantities of drugs, their degradation properties being adjustable for a specific application that will influence cellular growth, tissue regeneration, drug delivery and a good patient compliance (Zilberman & Elsner, 2008). Among the biopolymers, collagen is one of the most used, being a suitable biodegradable polymeric support for drug delivery systems, offering the advantage of a natural biomaterial with haemostatic and wound healing properties (Lee et al., 2001).

Studies with collagen as support showed that *in vivo* absorption and degradability on the one hand and drug delivery on the other hand are controlled by the collagen chemical or physical cross-linking performed in order to control the delivery effect (Albu, 2011).

Among the incorporated drugs in the collagen biomaterials various structures are mentioned: antibiotics and antiseptic (tetracycline, doxycicline, rolitetracycline, minocycline, metronidazole, ceftazidine, cefotaxime, gentamicin, amikacin, tobramycin, vancomycin, clorhexidine), statines (rosuvastatin), vitamines (riboflavine), parasympathomimetic alkaloid (pilocarpine) etc. (Zilberman & Elsner, 2008; Goissis & De Sousa, 2009; Yarboro et al., 2007).

The most known collagen-based drug delivery systems are the hydrogels and matrices.
The literature in the field reveals the importance of modeling the drug release kinetics from systems with topical application. The topical preparations with antibiotics, anti-inflammtories, antihistaminics, antiseptics, antimicotics, local anaesthetics must have a rapid realease of the drug. The release kinetics has to balance the advantage of reaching a therapeutical concentration with the disadvantage of toxic concentrations accumulation (Ghica, 2010).
As far as the drug delivery kinetics from semisolid/solid systems generally is concerned, it has been widely studied only in the case of the hydrogels having quasi-solid structure (Lin & Metters, 2006; Albu et al., 2009b).
In the case of the matrices, there is scarce literature on the delivery and the delivery mechanism of the drug from such systems. In Fig. 4 the drug delivery from a spongious collagen support is schematically presented.
The delivery of the drug from polymeric formulations is controlled by one or more physical processes including: polymer hydration through fluid, swelling to form a gel, drug diffusion through the gel formed and eventual erosion of the polymeric gel. It is possible that, for the sponges, the swelling, erosion and the subsequent diffusion kinetics play an important role in the release of the drug from these systems upon contact with biological fluids (cutaneous wound exsudate/gingival crevicular fluid). Upon contact of a dry sponge with the wet surface at the application site, biological fluid from that region penetrates the polymer matrix. Thus, the solvent molecules' internal flux causes the subsequent sponge hydration and swelling and the formation of a gel at the application site surface. The swelling noticed is due to the polymeric chains solvation that leads to an increase of the distance between the individual molecules of the polymer (Peppas et al., 2000; Boateng et al., 2008).
For some of the spongious forms the drug release mechanism has been explained through the hydrolytic activity of the enzymes existing in biological fluids, different mathematical models of the collagen sponges' enzymatic degradation being suggested (Metzmacher et al., 2007; Radu et al., 2009).
It was shown that in an aqueous medium the polymer suffers a relaxation process having as result the direct, slow erodation of the hydrated polymer. It is possible that its swelling and dissolution happen at the same time as in the sponges' situation, each of these processes contributing to the global release mechanism. However, the quantity of the drug released is generally determined by the diffusion rate of the medium represented by biological fluid in the polymeric sponge. Factors such as polymeric sponge erosion after water diffusion and the swelling in other dosage forms are the main reason of kinetics deviation square root of time (Higuchi type, generally specific to the hydrogels as such) (Boateng et al., 2008).
Different methods have been suggested for the investigation of the drug controlled release mechanisms that combine the diffusion, the swelling and the erosion. It is assumed that the collagen sponge is made of a homogeneous polymeric support where the drug (dissolved or suspended) is present in two forms: free or linked to the polymeric chains. The drug as free form is available for diffusion, through the desorption phenomenon, for immediate release in a first stage, this being favored by the sponge properties behaving as partially open porosity systems. The drug amount partially imobilized in collagen fibrillar structure will be gradually released after the diffusion of the biologic fluid inside the sponge, followed by its swelling and erosion on the basis of polymers reaction in solution theory. This sustained release is favored by the matrix properties to act as partially closed porosity systems, as well as by the collagen sponge tridimensional structure, which is a barrier between the drug in the sponge and the release medium (Singh et al., 1995; Friess, 1998; Wallace & Rosenblatt, 2003; Ruszczak & Friess; 2003).

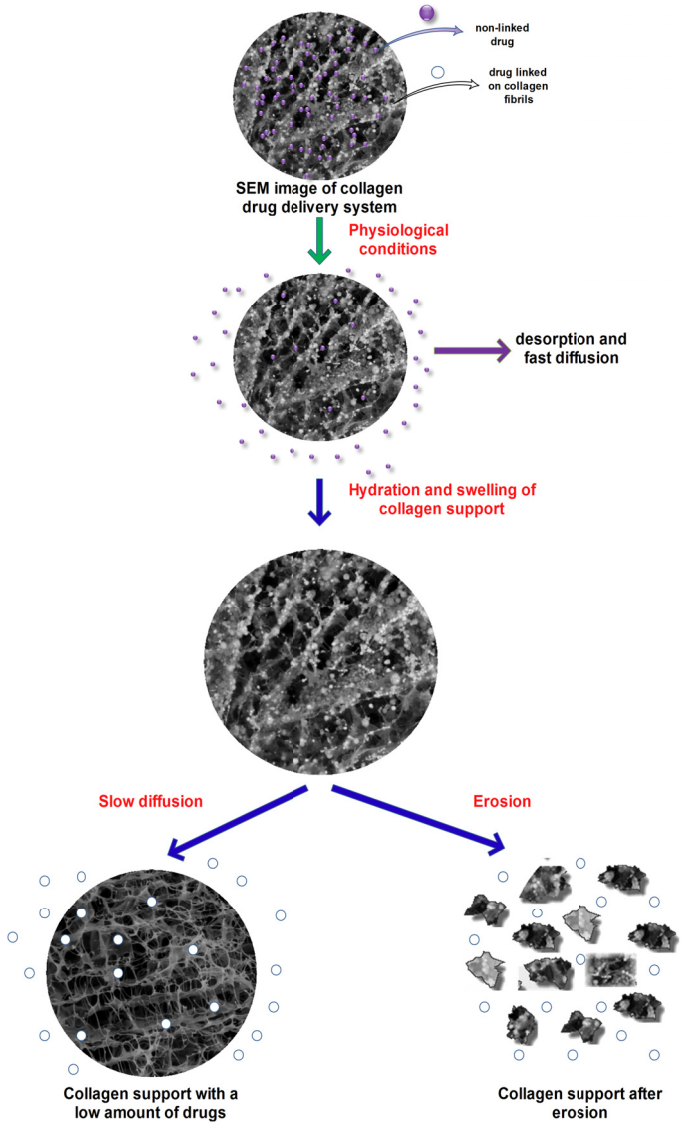

Fig. 4. Drug release from collagen matrix

In addition, the drug release kinetics can be influenced by the different chemical treatments that affect the degradation rate or by modifications of sponge properties (porosity, density) (M. Grassi & G. Grassi, 2005).

Among the chemical methods we can mention the cross-linking techniques. Thus, the different *in vivo* and *in vitro* behaviour, including the drug delivery profiles, can be obtained if the product based on collagen suffer in addition cross-linking with different

cross-linking agents. Among these agents, the most known and used is the glutaraldehyde that forms a link between the ε-amino groups of two lateral lysin chains. It was demonstrated that the treatment with glutaraldehyde reduces the collagen material immunogenicity, leading at the same time to the increase of resistance to enzymatic degradation (Figueiro et al., 2006).

Concerning the preparation of sponges with different porosities, those can be obtained by modifying the temperature during the collagen sponges lyophilization process (Albu et al., 2010a).

To understand the release process, both from hydrogels and from collagen sponges, and to establish the drug release mechanism implicitly, a range of kinetic models is used (Peppas, Higuchi, zero order). The general form of the kinetic equation through which the experimental kinetic data are fitted is the following: (eq. 1)

$$\frac{m_t}{m_\infty} = k \cdot t^n \tag{1}$$

where m_t is the amount of drug released at time t, m_∞ is the total drug contents in the designed collagen hydrogels, m_t/m_∞ is the fractional release of the drug at the time t, k is the kinetic constant, reflecting the structural and geometrical properties of the polymeric system and the drug, and n is the release exponent, indicating the mechanism of drug release.

If n=0.5 the release is governed by Fickian diffusion (the drug diffusion rate is much lower than the polymer relaxation rate, the amount of drug released being proportional to the release time square root, corresponding to Higuchi model). If n=1 the release is controlled by surface erosion (the drug diffusion rate is much higher than the polymer relaxation rate, the amount of drug released being proportional with the release time, corresponding to zero order model). If 0.5<n<1, the drug release mechanism is of non-Fickian type diffusion, the drug diffusion rate and the polymer relaxation rate being roughly equal. In this case the release is not based only on diffusion, being also associated with other release mechanisms due to the complex processes previousely described (Teles et al., 2010; Higuchi, 1962; Peppas et al., 2000; Singh et al., 1995; Ho et al., 2001).

The studied literature shows that Peppas, Higuchi and zero order models do not explain the mechanisms involved in the kinetic processes in the case of sponge forms, because the value of the apparent release order value (n) does not fit between the limits imposed by these aforesaid models, having values much lower than 0.5. This is why an extension of Peppas model to the Power law model (0<n<1) is generally applied in order to elucidate the complex kinetic mechanisms involved in the drug release from such natural supports. Practically, n value includes characteristics of each particular model previously described (Ghica et al., 2009; Albu et al., 2009a; Albu et al., 2010b; Phaechamud & Charoenteeraboon, 2008; Natu et al., 2007).

Our studies showed values of n equal to 0.5 for different collagen-based hydrogels with doxyciclyne, uncross-linked or cross-linked with glutaraldehyde, which confirms the respect of Higuchi model concerning the drug release from semisolid supports (Albu et al., 2009b). On the contrary, n values for doxycycline release from spongious supports were inferior to 0.5 (Ghica et al., 2009; Albu et al., 2010a; Albu et al., 2010b).

4. Collagen-based scaffolds for tissue engineering

It is known that collagen is the major component of the extracellular matrix of most tissues. As a natural molecule, collagen possesses a major advantage in being biodegradable, biocompatible presented low antigenicity, easily available and highly versatile. Collagen provides structural and mechanical support to tissues and organs (Gelse et al., 2003) and fulfils biomechanical functions in bone, cartilage, skin, tendon, and ligament. For this reason, allogenic and xenogenic collagens have been long recognized as one of the most useful biomaterials. Collagen can be prepared in a number of different forms with different application: shields used in ophthalmology (Rubinstein, 2003; Yoel & Guy, 2008) matrices for burns/wounds (Keck et al., 2009; Wollina et al., 2011), gel formulation in combination with liposomes for sustained drug delivery (Wallace & Rosenblatt, 2003; Weiner et al., 1985; Rao, 1996), as controlling material for transdermal delivery (Rao, 1996; Thacharodi & Rao, 1996), nanoparticles for gene delivery (Minakuchi et al., 2004) and basic matrices for cell culture systems. Therefore thin sheets and gels are substrates for smooth muscle (Dennis et al., 2007; Engler et al., 2004), hepatic (Hansen & Albrecht, 1999; Ranucci et al., 2000), endothelial (Albu et al., 2011; Deroanne et al., 2001; Titorencu et al., 2010), and epithelial cells (Haga et al., 2005), while matrices are often used to engineer skeletal tissues such as cartilage (Stark et al., 2006; Schulz et al., 2008), tendon (Gonçalves-Neto et al., 2002; Kjaer, 2004) and bone (Guille et al., 2005).

It is known that the goal of tissue engineering (TE) is to repair and restore damaged tissue function. The three fundamental "tools" for both morphogenesis and tissue engineering are responding cells, scaffolds and growth factors (GFs - regulatory biomolecules, morphogens), which, however, are not always simultaneously used (Badylak & Nerem, 2010; Berthiaume et al., 2011) (Fig. 5).

In tissue engineering, matrices are developed to support cells, promoting their differentiation and proliferation in order to form a new tissue. Another important aspect for the generation of 3D cell matrix constructs suitable for tissue regeneration is represented by cell seeding. Besides the seeding technique, the cellular density is a crucial factor to achieve a uniform distribution of a number of cells which is optimal for new tissue formation (Lode et al., 2008). Such strategies allow producing of biohybrid constructs that can be implanted in patients to induce the regeneration of tissues or replace failing or malfunctioning organs.

The advantage of tissue engineering is that small biopsy specimens can be obtained from the patient and cells can be isolated, cultured into a structure similar to tissue or organs in the living body, expanded into large numbers (Bruder & Fox, 1999; Levenberg & Langer, 2004; Mooney & Mikos, 1999; Service, 2005) and then transplanted into the patients.

The recent advances in collagen scaffold biomaterials are presented as follows:

Wound dressing and delivery systems

In the treatment of wounds the collagen-based dressings are intensely used. There are many studies which attest the benefits of topical collagen matrices on the wound healing (Inger & Richard, 1999; Ruszczak, 2003; Shih-Chi et al., 2008).

It is known that collagen matrices absorb excess wound exudate or sterile saline, forming a biodegradable gel or sheet over the wound bed that keeps the balance of wound moisture environment, thus promoting healing (Hess, 2005). Also, collagen breakdown products are chemotactic for a variety of cell types required for the formation of granulation tissue. Nowadays, many types of skin substitutes using living cells have been used clinically (Table 2).

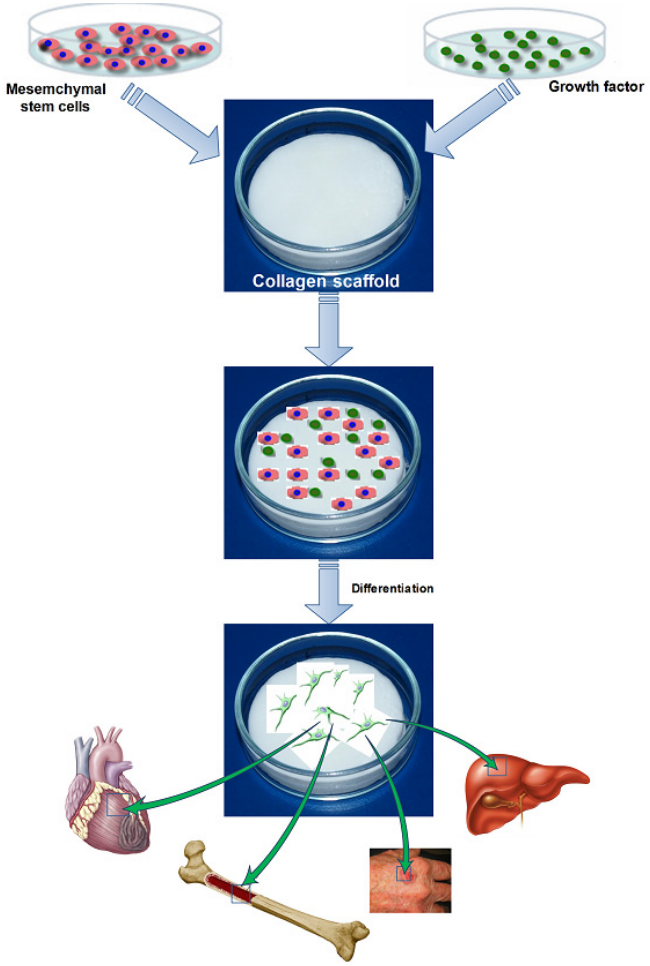

Fig. 5. Strategies for tissue engineering

Classification	Tissue replaced	Layers
TranCyte®	Epidermal	Silicone Nylon mesh Collagen seeded with neonatal fibroblasts
PermaDerm™	Dermal	Autologous fibroblasts in bovine collagen matrix with autologous keratinocytes
Apligraft®	Epidermal and dermal	Neonatal keratinocytes Collagen seeded with neonatal fibroblasts
OrCell™	Epidermal and dermal	Collagen (bovine type I) seeded with allogenic fibroblasts and keratinocytes

Table 2. Classification of collagen substitutes with living cells

These biomaterials can be divided into three groups depending on the type of layer cells which are substituted. The first type consists of grafts of cultured epidermal cells with no dermal components. The second type has only dermal components. The third type is a bilayer containing both dermal and epidermal elements.

Bone defects

Bone development and regeneration occurs as a result of coordinated cell proliferation, differentiation, migration, and remodeling of the extracellular matrix. In bone tissue engineering collagen scaffolds play an essential role in supporting bone regeneration. The implantation of these 3D biomaterials is necessary when osteochondral defects reach an important volume or when autografts have to be avoided for practical or pathological reasons. In order to promote bone healing scaffolds must have some properties: to promote the differentiation of immature progenitor cells into osteoblasts (*osteoinduction*), to induce the ingrowth of surrounding bone (*osteoconduction*) and to be integrated into the surrounding tissue (*osseointegration*) (Dickson et al., 2007). However there is still some ambiguity regarding the optimal porosity and pore size for a 3D bone scaffold. A literature review indicates that a pore size in the range of 10–400 μm may provide enough nutrient and osteoblast cellular infusion, while maintaining structural integrity (Bignon et al., 2003; Holmbom et al., 2005; Woodard et al., 2007).

Collagen scaffolds have the advantage of facilitating cell attachment and maintaining differentiation of cells (Fig. 6). Resorbable collagen sponges have been successfully used as carriers of BMP-2, BMP-4 and BMP-7 but they have the disadvantages of a fast degradation rate and low mechanical strength (Bessa et al., 2008; Higuchi et al., 1999; Huang et al., 2005; Huang et al., 2005; Kinoshita et al., 1997;).

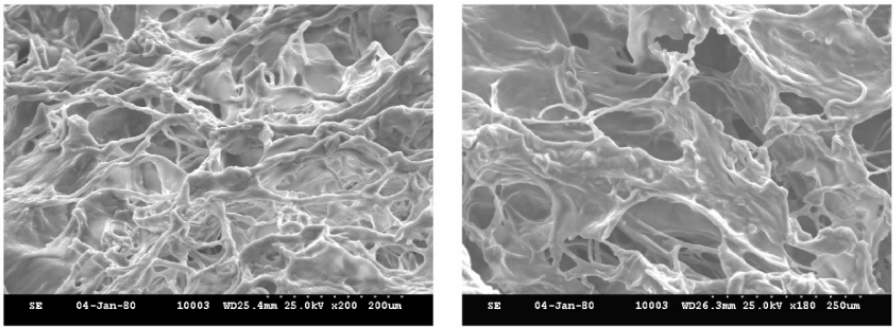

Fig. 6. Human osteoblasts precursor cells (hFOB1.19) grown seven days on collagen scaffolds

In order to increase mechanical strength and to improve the release of growth factors a combination between collagen and other natural polymer has been used such as chitosan (Arpornmaeklong et al., 2007), dextran (Fig. 7) or glycosaminoglycans (Harley & Gibson, 2008; Wang et al., 2010).

Another combination of collagen scaffolds is represented by mineralization with calcium phosphate (Du et al., 2000; Harley et al., 2010) and/or on cross-linking with other substances like hydroxyapatite (Dubey & Tomar, 2009; Liao et al., 2009.) or bushite (Tebb et al., 2006).

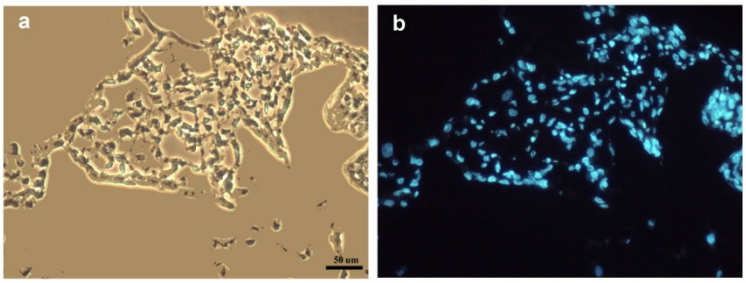

Fig. 7. Osteosarcoma cells (MG 63) grown on collagen-dextran scaffold: a – phase contrast, b – Hoechst nuclear staining

Urogenital system

Injuries of the genitourinary system can lead to bladder damage. Treatment in most of these situations requires eventual reconstructive procedures that can be performed with native non-urologic tissues (skin, gastrointestinal segments or mucosa), heterologous tissues or substances (bovine collagen) or artificial materials (Atala, 2011). Acellular collagen scaffolds were used in the treatment of bladder augmentation (Akbal et al., 2006; Liu et al., 2009; Parshotamet al., 2010) and urethral stricture (el-Kassaby et al., 2008; Farahat et al., 2009). Also collagen-composite scaffolds populated with the patient's own urothelial and muscle cells or self-assembled fibroblast sheets represent a promising strategy for bladder augmentation (Bouhout et al., 2010; Magnan et al., 2006). Trials of urethral tissue replacement with processed collagen matrices are in progress, and bladder replacement using tissue engineering techniques are intensely being studied (Atala et al., 2006).

Scaffolds for hepatic cells

Recent new strategies for treating liver diseases, including the extracorporeal bioartificial liver device and hepatocyte transplantation represent the future in hepatic diseases treatment. Recent advances in the field of tissue engineering have demonstrated that type I collagen matrices induced the differentiation of hepatic stem-like cells into liver epithelial cells and that biodegradable collagen matrices provide an appropriate microenvironment for hepatocytic repopulation (Uneo et al., 2004;Ueno et al., 2005.); also, a combination between collagen-chitosan-heparin scaffolds was used in order to obtain bioartificial liver (Xing et al., 2005).

Cornea and neural cells

Bioengineered corneas are substitutes for human donor tissue that are designed to replace part or the full thickness of damaged or diseased corneas. Collagen has been used successfully in reconstruction of artificial cornea alone by delivery of limbal epithelial stem cells to damaged cornea (Builles et al., 2010; De Miguel et al., 2010**)** or in combination with glycosaminoglycan (GAG) molecules (Auxenfans et al., 2009). The combination of collagen biomaterials and stem cells could be a valuable strategy to treat corneal defects also. Other strategies in collagen-based corneal scaffolds include the utilization of recombinant human collagen (Dravida et al., 2008; Griffith et al., 2009), the secretion of collagen by the fibroblasts themselves (Carrier et al., 2008) and surface modification to reduce extensive endothelialization (Rafat et al., 2009).

Nerve repairing

One of the major challenges in neurology is to be able to repair severe nerve trauma. It was observed that collagen scaffolds is a suitable nerve guidance material (Han et al., 2010) Most collagen nerve guides are engineered from crosslinked collagen with tubular shape such as commercially available NeuraGen® from Integra™. Recent tissue engineering strategies involve addition of neurotrophic factors into collagen scaffolds (Sun et al., 2007; Sun et al., 2009) and cell delivery (Bozkurt et al., 2009; Kemp et al., 2009) in order to attempt to enhance nerve guides.

5. Conclusion

Collagen biomaterials as matrices, hydrogels, composites have already been proved to be effective in tissue repairing, in guiding functional angiogenesis and in controlling stem cell differentiation. Also, collagen-based drug delivery systems were studied and their mechanisms of release were determined. Based on such good results, the promising next generation of engineered tissues is relying on producing scaffolds which can prolong the release rate of growth factors or cells in order to increase their therapeutic effect. This justifies the importance of drug delivery in tissue engineering applications.

6. Acknowledgment

The authors would like to thank Dr. Viorica Trandafir for guiding their steps in the collagen biomaterial field and for precious information from her own experience.

7. References

Akbal, C.; Lee, S.D.; Packer, S.C.; Davis, M.M.; Rink, R.C. & Kaefer, M. (2006). Bladder augmentation with acellular dermal biomatrix in a diseased animal model. *Journal of Urology,* Vol.176, No.4, (October 2006), pp. 1706–1711, ISSN 00225347

Albu, M.G. & Leca, M. (2005). Rheological behaviour of some cross-linked collagen hydrogels for drug delivery use. *European Cells and Materials*, Vol.10, Suppl.1, pp. 8, ISSN 1473-2262

Albu, M.G.; Ghica, M.V.; Giurginca, M.; Trandafir, V.; Popa, L. & Cotrut, C. (2009a). Spectral characteristics and antioxidant properties of tannic acid immobilized on collagen drug-delivery systems. *Revista de Chimie – Bucharest*, Vol.60, No.7, (July 2009), pp. 666-672, ISSN 0034-7752

Albu, M.G.; Ghica, M.V.; Popa, L.; Leca, M. & Trandafir, V. (2009b). Kinetics of in vitro release of doxycycline hyclate from collagen hydrogels, *Revue Roumaine de Chimie*, Vol.54, No.5, (May 2009), pp. 373-379, ISSN 0035-3930

Albu, M.G.; Ghica, M.V.; Ficai, A.; Titorencu, I..& Popa, L. (2010a). The influence of freeze-drying process on porosity and kinetics release of collagen-doxycycline matrices. *Proceedings of 3rd International Conference on Advanced materials and systems ICAMS*, ISBN 2068-0783, Bucharest, Romania, September, 2010

Albu, M.G.; Ficai, A. & Lungu, A. (2010b). Preparation and characterization of collagen matrices obtained at different freezing temperatures, *The Leather and Footwear Journal*, Vol. 10, No. 3, (September 2010), pp.39-50, ISSN 1583-4433

Albu, M.G.; Ghica, M.V.; Leca, M.; Popa, L.; Borlescu, C.; Cremenescu, E.; Giurginca, M. & Trandafir, V. (2010c). Doxycycline delivery from collagen matrices crosslinked with tannic acid. *Molecular Crystals & Liquid Crystals*, Vol.523, pp. 97/[669]-105[677], ISSN 1542-1406

Albu, M.G. (2011). *Collagen gels and matrices for biomedical applications,* LAP LAMBERT Academic Publishing GmbH & Co. KG, ISBN 978-3-8443-3057-1, Saarbrücken, Germany

Albu, M.G.; Titorencu, I. & Chelaru, C. (2011). The stability of some collagen hydrogels, *The Leather and Footwear Journal, Vol. 11, No.1, (March 2011), pp.11-20, ISSN* 1583-4433

Angele, P.; Abke, J.; Kujat, R.; Faltermeier, H.; Schumann, D.; Nerlich, M.; Kinner, B.; Englert, C.; Ruszczak, Z.; Mehrl, R. & Mueller, R. (2004), Influence of different collagen species on physico-chemical properties of crosslinked collagen matrices, *Biomaterials*, Vol.25, No.14, (June 2004), pp.2831-2841, ISSN 0142-9612

Arpornmaeklong, P.; Suwatwirote, N.; Pripatnanont, P. & Oungbho, K. (2008). Growth and differentiation of mouse osteoblasts on chitosan–collagen sponges. *Journal of Oral Maxillofacial Surgery*, Vol.36, No.4, (April 2007), pp. 328–337, ISSN 02782391

Atala A.; Bauer, S.B.; Soker, S.; Yoo, J.J. & Retik, A.B. (2006). Tissue-engineered autologous bladders for patients needing cystoplasty. *Lancet,* Vol. 367, No.9518, (April 2006), pp. 1241–1246, ISSN 0140-6736

Atala, A. (2011). Tissue engineering of human bladder. *British Medical Bulletin,* Vol.97, No.1, (February 2011), pp. 1–24, ISSN 1471-8391

Auxenfans, C.; Builles, N.; Andre, V.; Lequeux, C.; Fievet, A.; Rose, S.; Braye, F.M.; Fradette, J.; Janin-Manificat, H.; Nataf, S.; Burillon, C & Damour, O. (2009). Porous matrix and primary-cell culture: a shared concept for skin and cornea tissue engineering. *Pathologie Biologie (Paris),* Vol.57, No.4, (June 2009), pp. 290-298, ISSN 0369-8114

Badylak, S.F. & Nerem R.M. (2010). Progress in tissue engineering and regenerative medicine. *PNAS, V*ol.107, No.8, (February 2010), pp. 3285–3286, ISSN: 1529-24

Bazin, S. & Delaumay, A. Preparation of acid and citrate soluble collagen, In: *The Methodology of Connective Tissue Research*, Hall D.A., pp.13-18, Joynson–Bruvvers, ISBN 0903848066, Oxford

Berthiaume, F.; Maguire, T.J. & Yarmush, M.L. (2011). Tissue Engineering and Regenerative Medicine: History, Progress, and Challenges. *Chemical and Biomolecular Engineering* Vol.2, (June 2011), pp. 1-18, ISSN: 1307-7449

Bessa, P.C.; Casal, M. & Reis, R.L. (2008). Bone morphogenetic proteins in tissue engineering: the road from laboratory to clinic, part II (BMP delivery). *Journal of Tissue Engineering and Regenerative Medicine,* Vol.2, No.2-3, (March - April 2008), pp. 81–96, ISSN 1932-6254

Bignon, A.; Chouteau, J.; Chevalier, J.; Fantozzi, G.; Carret, J.P.; Chavassieux, P.; Boivin, G.; Melin, M. & Hartmann, D. (2003). Effect of micro- and macroporosity of bone substitutes on their mechanical properties and cellular response. *Journal of Matererial Science Material Medicine*, Vol.14, No.12, (December 2003), pp.1089–1097, ISSN 0957-4530

Boateng, J.S.; Matthews, K.H.; Stevens, H.N.E. & Eccleston, G.M. (2008). Wound healing dressings and drug delivery systems: a rewiev. *Journal of Pharmaceutical Sciences*, Vol.97, No.8, (August 2008), pp. 2892-2923, ISSN 0022-3549

Bouhout, S.; Perron, E.; Gauvin, R.; Bernard, G.; Ouellet, G.; Cattan, V. & Bolduc, S. (2010). *In vitro r*econstruction of an autologous, watertight and resistant vesical equivalent. *Tissue Engineering Part A,* Vol.16, No.5, (May 2010), pp.1539-1548, ISSN 1937-3341

Bozkurt, A.; Deumens, R.; Beckmann, C.; Olde Damink, L.; Schugner, F.; Heschel, I.; Sellhaus, B.; Weis, J.; Jahnen-Dechent, W.; Brook, G.A. & Pallua, N. (2009). *In vitro* cell alignment obtained with a Schwann cell enriched microstructured nerve guide with longitudinal guidance channels. *Biomaterials*, (January 2009), Vol.*30*, No.2, pp.169–179, ISSN 0142-9612

Bruder, S.P. & Fox, B.S. (1999). Tissue engineering of bone. Cell based strategies. *Clinical Orthopopaedics*, Vol.367, (October 1999), pp: S68–S83, ISSN 0095-8654

Builles, N.; Janin-Manificat, H.; Malbouyres, M.; Justin, V.; Rovère, M.R,; Pellegrini, G.; Torbet, J.; Hulmes, D.J.; Burillon, C.; Damour, O. & Ruggiero F. (2010). Use of magnetically oriented orthogonal collagen scaffolds for hemi-corneal reconstruction and regeneration. *Biomaterials*, Vol.31, No.32, (November 2010), pp. 8313-8322, ISSN 0142-9612

Carrier, P.; Deschambeault, A.; Talbot, M.; Giasson, C.J.; Auger, F.A.; Guerin, S.L. & Germain, L. (2008). Characterization of wound reepithelialization using a new human tissue-engineered corneal wound healing model. *Invesigation. Ophthalmology & Visual Science,* Vol.49, No.4, (April 2008), pp. 1376–1385, ISSN 1552-5783

Chen, S.; Hirota, N.; Okuda, M.; Takeguchi, M.; Kobayashi, H.; Hanagata, N. & Ikoma, T. (2011). Microstructures and rheological properties of tilapia fish-scale collagen hydrogels with aligned fibrils fabricated under magnetic fields, *Acta Biomaterialia*, Vol.7, No.2, (February 2011), pp. 644-652, ISSN 1742-7061

Chen, Y.; Mak, A.F.T; Wang, M.; Li, J. & Wong, M.S. (2006). PLLA scaffolds with biomimetic apatite coating and biomimetic apatite/collagen composite coating to enhance osteoblast-like cells attachment and activity, *Surface and Coatings Technology*, Vol.201, No.3-4, (October 2006), pp.575-580, ISSN 0257-8972

Cioca, Gh. (July 1981). *Process for preparing macromolecular biologically active collagen*, Patent No. 4279812, US

Davidenko, N.; Campbell, J.J.; Thian, E.S.; Watson, C.J. & Cameron, R.E. (2010). Collagen–hyaluronic acid scaffolds for adipose tissue engineering, *Acta Biomaterialia*, Vol. 6, No.10, (October 2010), pp.3957-3968, ISSN 1742-7061

De Miguel, M.P.; Alio, J.L.; Arnalich-Montiel, F.; Fuentes-Julian, S.; de Benito-Llopis, L.; Amparo, F. & Bataille, L. (2010). Cornea and ocular surface treatment. *Current Stem Cell Research Therapy,* Vol.5, No.2, (June 2010), pp. 195-204, ISSN 1574-888X

Deroanne, C.F.; Lapiere, C.M. & Nusgens, B.V. (2001). In vitro tubulogenesis of endothelial cells by relaxation of the coupling extracellular matrix-cytoskeleton. *Cardiovascular Research*, Vol.49, No.3, (September 2001), pp. 647-658, ISSN 0008-6363

Dickson, G.; Buchanan, F.; Marsh, D.; Harkin-Jones, E.; Little, U. & McCaigue M. (2007). Orthopaedic tissue engineering and bone regeneration. *Technology and Health Care,* Vol.15, No.1, (January 2007), pp.57-67, ISSN 0928-7329

Doillon, C. J. (1992). Skin replacement using collagen extracted from bovine hide, *Clinical Materials,* Vol.9, No.3-4, (April 2004), pp.189-193, ISSN 0267-6605

Dravida, S.; Gaddipati, S.; Griffith, M.; Merrett, K.; Lakshmi Madhira, S. & Sangwan, V.S. (2008). A biomimetic scaffold for culturing limbal stem cells: a promising

alternative for clinical transplantation. *Journal of Tissue Engineering Regenerative Medicine,* Vol.2, No.5, (July 2008), pp. 263–271, ISSN 1932-7005

Du, C.; Cui, F.Z.; Zhang, W.; Feng, Q.L.; Zhu, X.D. & de Groot, K. (2000). Formation of calcium phosphate/collagen composites through mineralization of collagen matrix. *Journal of Biomedical Materials Research Part A,* Vol.*50*, No.4, (April 2000), pp. 518–527, ISSN 1549-3296

Dubey, D.K. & Tomar, V. (2009). Role of the nanoscale interfacial arrangement in mechanical strength of tropocollagen-hydroxyapatite-based hard biomaterials. *Acta Biomaterialia,* Vol.5, No.7, (September 2009), pp. 2704–2716, ISSN 1742-7061

Edwards, G.A. & Roberts, G. (1992), Development of an ovine collagen-based composite biosynthetic vascular prosthesis, *Clinical Materials*, Vol.9, No.3-4, (April 2004), pp.211-223, ISSN 0267-6605

el-Kassaby, A.; AbouShwareb, T. & Atala, A. (2008). Randomized comparative study between buccal mucosal and acellular bladder matrix grafts in complex anterior urethral strictures. *Journal of Urology,* Vol.179, (April 2008), 1432–1436, ISSN 00225347

Engler, A.; Bacakova, L.; Newman, C.; Hategan, A.; Griffin, M. & Discher, D. (2004). Substrate Compliance versus Ligand Density in Cell on Gel Responses. *Biophysical Journal*; Vol.86, No.1, (January 2004), pp. 617–628, ISSN 0006-3495

Farahat, Y.A.; Elbahnasy, A.M.; El-Gamal, O.M.; Ramadan, A.R.; El-Abd, S.A. & Taha, M.R. (2009). Endoscopic urethroplasty using small intestinal submucosal patch in cases of recurrent urethral stricture: A preliminary study. *Journal of Endourology,* Vol.23, No.12, (December 2009), pp. 2001–2005, ISSN 0892-7790

Fielding, A.M. (1976). Preparation of neutral salt soluble collagen, In: *The Methodology of Connective Tissue Research*, Hall D.A., pp.9-12, Joynson–Bruvvers, ISBN 0903848066, Oxford

Figueiro, S.D.; Macedo, A.A.M.; Melo, M.R.S.; Freitas, A.L.P.; Moreira, R.A.; De Oliveira, R.S.; Goes, J.C. & Sombra, A.S.B. (2006). On the dielectric behaviour of collagen–algal sulfated polysaccharide blends: effect of glutaraldehyde crosslinking. *Biophysical Chemistry*, Vol.120, No.2, (March 2006), pp. 154-159, ISSN 0301-4622

Friess, W. (1998). Collagen – biomaterial for drug delivery. *European Journal of Pharmaceutics and Biopharmaceutics*, Vol.45, No.2, (March 1998), pp.113-136, ISSN 0939-6411

Ghica, M.V. (2010). *Physico-chemical and biopharmaceutical elements of semisolid systems with topical action. Applications to indomethacin hydrogels*, ISBN 978-606-521-436-1, Printech, Bucharest, Romania

Ghica, M.V.; Albu, M.G.; Popa, L.; Leca, M.; Brazdaru, L.; Cotrut, C. & Trandafir, V. (2009). Drug delivery systems based on collagen-tannic acid matrices. *Revue Roumaine de Chimie*, Vol.54, No.11-12, (November-December 2009), pp. 1103-1110, ISSN 0035-3930

Goissis, G. & De Sousa, M.H. (2009). Characterization and in vitro release studies of tetracycline and rolitetracycline imobilized on anionic collagen membranes. *Materials Research*, Vol.12, No.1, pp. 69-74, ISSN 1516-1439

Gonçalves-Neto, J.; Witzel, S.S.; Teodoro, W.R.; Carvalho-Júnior, A.E.; Fernandes, T.D. & Yoshinari, H.H. (2002). Changes in collagen matrix composition in human posterior tibial tendon dysfunction. *Joint Bone Spine*, Vol.69, No.2, (Martch 2002), pp.189-194, ISSN: 1297-319X

Gotterbarm, T; Richter, W.; Jung, M.; Vilei, S.B.; Mainil-Varlet, P.; Yamashita, T & Breusch, S.J. (2006). An in vivo study of a growth-factor enhanced, cell free, two-layered collagen–tricalcium phosphate in deep osteochondral defects, *Biomaterials*, Vol. 27, No.18, (June 2006), pp.3387-3395, ISSN 0142-9612

Grassi, M. & Grassi, G. (2005). Mathematical modelling and controlled drug delivery: matrix systems. *Current Drug Delivery*, Vol.2, No.1, (January 2005), pp. 97-116, ISSN 1567-2018

Griffith, M.; Jackson, W.B.; Lagali, N.; Merrett, K.; Li, F. & Fagerholm, P. (2009). Artificial corneas: A regenerative medicine approach. *Eye,* Vol.23, No.10, (October 2009), pp.1985–1989, 0950-222X

Guille, M.G.; Mosser, G.; Helary C. & Eglin, D. (2005). Bone matrix like assemblies of collagen: From liquid crystals to gels and biomimetic materials. *Micron*, Vol.36, No.7-8, (October-December 2005), pp. 602-608, ISSN 1463–9076

Haga, H.; Irahara, C.; Kobayashi, R.; Nakagaki, T. & Kawabata, K. (2005). Collective Movement of Epithelial Cells on a Collagen Gel Substrate. *Biophysical Journal,* Vol.88, No.3, (March 2005), pp. 2250–2256, ISSN 0006-3495

Han, Q.; Jin, W.; Xiao, Z.; Ni, H.; Wang, J.; Kong, J.; Wu, J.; Liang, W.; Chen, L.; Zhao, Y.; Chen, B. & Dai, J. (2010). The promotion of neural regeneration in an extreme rat spinal cord injury model using a collagen scaffold containing a collagen binding neuroprotective protein and an EGFR neutralizing antibody. *Biomaterials*, Vol.31, No.35, (December 2010), pp. 9212-9220, ISSN 0142-9612

Hansen, L.K. & Albrecht, J.H. (1999). Regulation of the hepatocyte cell cycle by type I collagen matrix: role of cyclin D1. *Journal of Cell Science,* Vol.112, (August 1999), pp. 2971-2981, ISSN 0021-9533

Harley B.A.C. & Gibson, L.J. (2008). *In vivo* and *in vitro* applications of collagen-GAG scaffolds. *Chemical Engineering Journal*, Vol.137, No.1, (March 2008), pp.102-121, ISSN 1385-8947

Harley, B.A.; Lynn, A.K.; Wissner-Gross, Z.; Bonfield, W.; Yannas, I.V. & Gibson, L.J. (2010). Design of a multiphase osteochondral scaffold. II. Fabrication of a mineralized collagenglycosaminoglycan scaffold. *Journal of Biomedical Materials Research Part A,* Vol. 92A, No.3, (March 2010), pp. 1066–1077, ISSN 1549-3296

Healy, K.E.; Rezania, A. & Stile, R.A. (1999). Designing biomaterials to direct biological responses, *Annals of the New York Academy of Sciences,* Vol. 875, (June 1999), pp.24-35, ISSN 1749-6632

Hess, C.T. (2005). *The art of skin and wound care documentation*. *Home Healthcare Nurse*, Vol.23, No.8, (August 2005), pp. 502-512, ISSN 0884741X

Higuchi, T.; Kinoshita, A.; Takahashi, K.; Oda, S. & Ishikawa, I. (1999). Bone regeneration by recombinant human bone morphogenetic protein-2 in rat mandibular defects. An experimental model of defect filling. *Journal of Periodontology*, Vol.70, No.9, (September 1999), pp. 1026–1031, ISSN 0022-3492

Higuchi, W.I. (1962). Analysis of data on the medicament release from ointments. *Journal of Pharmaceutical Sciences*, Vol.51, No.8, (August 1962), pp 802-804, ISSN 0022-3549

Ho, H.O.; Lin, C.W. & Sheu, M.T. (2001). Diffusion characteristics of collagen film. *Journal of Controlled Release*, Vol.77, No.1-2, (November 2001), pp. 97-105, ISSN 0168-3659

Holmbom, J.; Sodergard, A.; Ekholm, E; Martson, M.; Kuusilehto, A.; Saukko, P. & Penttinen, R. (2005). Long-term evaluation of porous poly(epsilon-caprolactone-co-

L-lactide) as a bone-filling material. *Journal of Biomedical Material Research A*, Vol.75, No.2, (November 2005), pp.308–315, ISSN 1549-3296

Hong, Y.J.; Chun, J-S. & Lee, W-K. (2011). Association of collagen with calcium phosphate promoted osteogenic responses of osteoblast-like MG63 cells, *Colloids and Surfaces B: Biointerfaces*, Vol.83, No.2, (April 2011), pp.245-253, ISSN 0927-7765

Hoppe, A.; Güldal, N.S. & Boccaccini, R.A. (2011). A review of the biological response to ionic dissolution products from bioactive glasses and glass-ceramics, *Biomaterials*, Vol.32, No.11, (April 2011), pp.2757-2774, ISSN 0142-9612

Huang, Y.C.; Kaigler, D.; Rice, K.G.; Krebsbach, P.H. & Mooney, D.J. (2005). Combined Angiogenic and Osteogenic Factor Delivery Enhances Bone Marrow Stromal Cell-Driven Bone Regeneration. *Journal of Bone and Mineral Research,* Vol.20, No.5, (May 2005), pp. 848–857, ISSN 1523-4681

Huang, Y.C.; Simmons, C.; Kaigler, D.; Rice, K.G. & Mooney, D.J. (2005). Bone regeneration in a rat cranial defect with delivery of PEI-condensed plasmid DNA encoding for bone morphogenetic protein-4 (BMP-4). *Gene Therapy,* Vol.12, No.5, (March 2005), pp. 418–426, ISSN 0969-7128

Hubbel, J.A. (1999). Bioactive biomaterials, *Current Opinion in Biotechnology*, Vol.10, No.2, (April 1999), pp.123-129, ISSN 0958-1669

Inger, A.J.S &. Clark, R.A.F. (1999). Cutaneus wound healing. *The New England Journal of Medicine* Vol.341, No.10, (September, 1999), pp.738-746, ISSN 1533-4406

Keck, M.; Haluza, D.; Burjak S.; Eisenbock, B.; Kamolz, L.-P. & Frey, M. (2009). Cultivation of keratinocytes and preadipocytes on a collagen-elastin scaffold (Matriderm®): First results of an in vitro study - Elastin Matrix (Matriderm®): Erste Ergebnisse einer In vitro Studie. *European Surgery,* Vol.41, No.4, (July 2009), pp.189-193, ISSN 1682-4016

Kemp, S.W.; Syed, S.; Walsh, W.; Zochodne, D.W. & Midha, R. (2009). Collagen nerve conduits promote enhanced axonal regeneration, schwann cell association, and neovascularization compared to silicone conduits. *Tissue Engineering Part A,* Vol.15, No.8, (August 2009), pp.1975–1988, ISSN 2152-4947

Ket, G.; Poschl, E. & Aigner, T. (2003). Collagens-structure, function, and biosynthesis. *Advanced Drug Delivery Review*, Vol.55, No.12, (November 2003), pp.1531–1546, ISSN 0169-409X

Kinoshita, A.; Oda, S.; Takahashi, K.; Yokota, S. & Ishikawa, I. (1997). Periodontal regeneration by application of recombinant human bone morphogenetic protein- 2 to horizontal circumferential defects created by experimental periodontitis in beagle dogs. *Journal of Periodontology,* Vol. 68, No.2, (February 1997), pp. 103–109, ISSN 0022-3492

Kjaer, M. (2004). Role of Extracellular Matrix in Adaptation of Tendon and Skeletal Muscle to Mechanical Loading. Physiology Review, Vol.84, No.2, (April 2004), pp. 649-698, ISSN 0031-9333

Kumar, M.S.; Kirubanandan. S.; Sripriya, R. & Sehgal, P.K. (2010). Triphala incorporated collagen sponge – a smart biomaterial for infected dermal wound healing. *Journal of Surgical Research*, Vol.158, No.1, (January 2010), pp. 162-170, ISSN 0022-4804

Lee, C.H.; Singla, A.& Lee, Y. (2001). Biomedical applications of collagen. *International Journal of Pharmaceutics*, Vol.221, No.1-2, (June 2001), pp. 1-22, ISSN 0378-5173

Levenberg, S. & Langer, R. (2004). Advances in tissue engineering. *Current Topics in Developmental Biology*, Vol.61, pp. 113–134, *ISBN* 9780080494340

Li, S.T.; Archibald, S.J.; Krarup, C. & Madison, R.D. (1991). The development of collagen nerve guiding conduits that promote peripheral nerve regeneration, In: *Biotechnology and Polymers,* Gebelein, C.G., pp.282-293, Plenum Press, ISBN 0-306-44049-0, New York

Li, S-T. (2003). Biologic Biomaterials: Tissue-Derived Biomaterials (Collagen), In: *Biomaterials Principle and Applications,* Park, J.B & Bronzino, J.D., pp.117-139, CRC Press, ISBN 0-8493-1491-7, Boca Raton, Florida

Liao, S.; Ngiam, M.; Chan, C.K. & Ramakrishna, S. (2009). Fabrication of nanohydroxyapatite/ collagen/osteonectin composites for bone graft applications. *Biomedical Materials,* Vol.4, No.2, (April 2009), pp. 025019, ISSN 1748-605X

Limpisophon, K.; Tanaka, M.; Weng, W.Y; Abe, S. & Osako, K. (2009), Characterization of gelatin films prepared from under-utilized blue shark (*Prionace glauca*) skin, *Food Hydrocolloids*, Vol. 23, No.7, (October 2009), pp.1993-2000, ISSN 0268-005X

Lin, C.C. & Metters, A.T. (2006). Hydrogels in controlled release formulations: Network design and mathematical modeling. *Advanced Drug Delivery Reviews*, Vol.58, No.12-13, (November 2006), pp. 1379-1408, ISSN 0169-409X

Lin, Y.-K; Lin, T-Y & Su, H.P. (2011). Extraction and characterisation of telopeptide-poor collagen from porcine lung, *Food Chemistry,* Vol.124, No.4, (February 2011), pp.1583-1588, ISSN 0308-8146

Liu, Y.; Bharadwaj, S.; Lee, S.J.; Atala, A. & Zhang, Y. (2009). Optimization of a natural collagen scaffold to aid cell-matrix penetration for urologic tissue engineering. *Biomaterials,*Vol.30, No.23-24, (August 2009), pp. 3865–3873, ISSN 0142-9612

Lode, A.; Bernhardt, A. & Gelinsky, M. (2008). Cultivation of human bone marrow stromal cells on three-dimensional scaffolds of mineralized collagen: influence of seeding density on colonization, proliferation and osteogenic differentiation. *Journal of Tissue Engineering and Regenenerative Medicine,* Vol.2, No.7, (October 2008), pp. 400–407, ISSN 1932-7005

Lungu, A.; Albu, M.G. & Trandafir, V. (2007). New biocomposite matrices structures based on collagen and synthetic polymers designed for medical applications. *Materiale Plastice*, Vol.44, No.4, pp. 273-277, ISSN 0025-5289

Magnan, M.; Berthod, F.; Champigny, M.F.; Soucy, F. & Bolduc, S. (2006). *In vitro* reconstruction of a tissue-engineered endothelialized bladder from a single porcine biopsy. *Journal of Pediatric Urology,* Vol.2, No.4, (August 2006), pp. 261–270, ISSN 1477-5131

McDaniel, D.P.; Gordon, A.; Shaw, J.; Elliott, T.; Bhadriraju, K.; Meuse, C.; Chung, K-H. & . Plant, A.L. (2007). The Stiffness of Collagen Fibrils Influences Vascular Smooth Muscle Cell Phenotype. *Biophysical Journal*, Vol.92, No.5, (March 2007), pp. 1759-1769, ISSN 0006-3495

Metzmacher, I.; Radu, F.; Bause, M.; Knabner, P. & Friess, W. (2007). A model describing the effect of enzymatic degradation on drug release from collagen minorods. *European Journal of Pharmaceutics and Biopharmaceutics*, Vol.67, No.2, (September 2007), pp. 349-360, ISSN 0939-6411

Minakuchi, Y.; Takeshita, F.; Kosaka, N.; Sasaki, H.; Yamamoto, Y.; Kouno, M.; Honma, K.; Nagahara, S.; Hanai, K.; Sano, A.; Kato, T.; Terada, M. & Ochiya T. (2004).

Atelocollagen-mediated synthetic small interfering RNA delivery for effective gene silencing *in vitro* and *in vivo*. *Nucleic Acids Research,* Vol.32, No.13, (July 2004), pp. e109, ISSN 0305-1048

Mooney, D.J. & Mikos, A.G. (1999). Growing new organs. *Scientific American*, Vol.280 (April 1999) pp. 60–65, ISSN 0036-8733

Nagai, T. & Suzuki, N. (2002). Preparation and partial characterization of collagen from paper nautilus *(Argonauta argo,* Linnaeus) outer skin, *Food Chemistry,* Vol.76, No.2, (February 2002), pp.149-153, ISSN 0308-8146

Natu, M.V.; Sardinha, J.P.; Correia, I.J. & Gil, M.H. (2007). Controlled release gelatine hydrogels and lyophilisates with potential applications as ocular inserts. *Biomedical Materials*, Vol.2, No.4, (December 2007), pp. 241-249, ISSN 1748-6041

Parker, D.M.; Armstrong, P.J; Frizzi, J.D & North Jr, J.H. (2006). Porcine Dermal Collagen (Permacol) for Abdominal Wall Reconstruction, *Current Surgery*, Vol.63, No.4, (July-August 2006), pp.255-258, ISSN 0149-7944

Parshotam Kumar, G.; Barker, A.; Ahmed, S.; Gerath, J. & Orford, J. (2010). Urinary bladder auto augmentation using INTEGRA((R)) and SURGISIS ((R)): An experimental model. *Pediatric Surgurgery Inernational,* Vol.26, No.3, (March 2010), pp. 275–280, ISSN 1437-9813

Peppas, N.A.; Bures, P.; Leobandung, W. & Ichikawa, H. (2000). Hydrogels in pharmaceutical formulations. *European Journal of Pharmaceutics and Biopharmaceutics*, Vol.50, No.1, (July 2000), pp. 27-46, ISSN 0939-6411

Phaechamud, T. & Charoenteeraboon, J. (2008). Antibacterial activity and drug release of chitosan sponge containing doxycycline hyclate. *AAPS PharmSciTech*, Vol.9, No.3 , (September 2008), pp. 829-835, ISSN 1530-9932

Piez, K.A. (1984). Molecular and aggregate structures of the collagens, In: *Extracellular Matrix Biochemistry*, Piez, K.A. & Reddi, A.H., pp.1-40, Elsevier, ISBN 978-0-4440-0799-5, New York

Radu, F.A.; Bause, M.; Knabner, P.; Friess, W. & Metzmacher, I.. (2009). Numerical simulation of drug release from collagen matrices by enzymatic degradation. *Computing and visualization in science*, Vol.12, No.8, pp. 409-420, ISSN 1432-9360

Rafat, M.; Matsuura, T.; Li, F. & Griffith, M. (2009). Surface modification of collagen-based artificial cornea for reduced endothelialization. *Journal of Biomedical Materials Research Part A,* Vol.*88*, (March 2009), pp. 755–768, ISSN 1549-3296

Ranucci, C.S.; Kumar, A.; Batra, S.P. & Moghe, P.V. (2000). Control of hepatocyte function on collagen foams: sizing matrix pores toward selective induction of 2-D and 3-D cellular morphogenesis. *Biomaterials,* Vol.21, (April 2000), pp.783-793, ISSN 0142-9612

Rao, P. K. (1996). Recent developments of collagen-based materials for medical applications and drug delivery systems. *Journal of Biomaterials Science, Polymer Edition*, Vol.7, No.7, (January 1996), pp. 623-645(23), ISSN 1568-5624

Raub, C.B.; Suresh, V.; Krasieva, T.; Lyubovitsky, J.; Mih, J.D., Putnam, A.J.; Tromberg, B.J. & George, S.C. (2007). Noninvasive assessment of collagen gel microstructure and mechanics using multiphoton microscopy. *Biophysical Journal*, Vol.92, No.6, (March 2007), pp. 2212-2222, ISSN 0006-3495

Renou, J.-P.; Foucat, L.; Corsaro, C.; Ollivier, J.; Zanotti, J.-M. & Middendorf H.D. (2004). Dynamics of collagen from bovine connective tissues, *Physica B: Condensed Matter,* Vol.350, No.1-3, (July 2004), pp.E631-E633, ISSN 0921-4526

Rodziewicz-Motowidło, S.; Śladewska, A.; Mulkiewicz, E.; Kołodziejczyk, A.; Aleksandrowicz, A.; Miszkiewicz, J. & Stepnowski, P. (2008), Isolation and characterization of a thermally stable collagen preparation from the outer skin of the silver carp *Hypophthalmichthys molitrix*, *Aquaculture*, Vol. 285, No.1-4, (December 2008), pp.130-134, ISSN 0044-8486

Roreger, M. (November 1995). *Collagen preparation for the controlled release of active substances,* Patent No. PCT/EP1995/001428, Germany

Rubinstein, M. P. (2003). Applications of contact lens devices in the management of corneal disease. *Eye* Vol.17, (February 2003), pp. 872–876, ISSN 0950-222X

Ruszczak, Z. & Friess, W. (2003). Collagen as a carrier for on-site delivery of antibacterial drugs. *Advanced Drug Delivery Reviews*, Vol.55, No.12, (November 2003), pp. 1679-1698, ISSN 0169-409X

Ruszczak, Z. (2003). Effect of collagen matrices on dermal wound healing. *Advanced Drug Delivery Reviews* (November 2003) Vol.55, No.12, pp. 1595-1611, ISSN 0169-409X

Sahoo, S.; Cho-Hong, J.G. & Siew-Lok, T. (2007). Development of hybrid polymer scaffolds for potential applications in ligament and tendon tissue engineering. *Biomedical Materials*, Vol.2, No.3, (September 2007), pp. 169-173, ISSN 1748-6041

Sang, L.; Luo, D.; Xu, S.; Wang, X. & Li, X. (2011). Fabrication and evaluation of biomimetic scaffolds by using collagen–alginate fibrillar gels for potential tissue engineering applications, *Materials Science and Engineering: C*, Vol.31, No.2, (March 2011), pp.262-271, ISSN 0928-4931

Satish, C.S.; Satish, K.P. & Shivakumar, H.G. (2006). Hydrogels as controlled drug delivery systems: synthesis, crosslinking, water and drug transport mechanism. *Indian Journal of Pharmaceutical Sciences*, Vol.68, No.2, (March 2006), pp. 133-140, ISSN 0250-474X

Schnell, E.; Klinkhammer, K., Balzer, S., Brook, G., Klee, D., Dalton, P. & Mey, J. (2007). Guidance of glial cell migration and axonal growth on electrospun nanofibers of poly-ε-caprolactone and a collagen/poly-ε-caprolactone blend, *Biomaterials*, Vol.28, No.19, (July 2007), pp.3012-3025, ISSN 0142-9612

Schulz, R.M.; Zscharnack, M.; Hanisch, I.; Geiling, M.; Hepp, P. & Bader, A. (2008). Cartilage tissue engineering by collagen matrix associated bone marrow derived mesenchymal stem cells. *Bio-medical materials and engineering,* Vol.18, No.1, (November 2008), pp. S55-70, ISSN: 1422-6405

Service, R.F. (2005). Tissue engineering. Technique uses body as 'bioreactor' to grow new bone. *Science,* Vol.309 No.5735, (July 2005), pp.683, ISSN 0036-8075

Singh, M.P.; Lumpkin, J.A. & Rosenblatt, J. (1995). Effect of electrostatic interactions on polylysine release rates from collagen matrices and comparison with model predictions. *Journal of Controlled Release*, Vol.35, No.2-3, (August 1995), pp. 165-179, ISSN 0168-3659

Singh, P.; Benjakul, S.; Maqsood, S. & Kishimura, H., Isolation and characterisation of collagen extracted from the skin of striped catfish (*Pangasianodon hypophthalmus*), *Food Chemistry*, Vol.124, No. 1, (January 2011), pp.97-105, ISSN 0308-8146

Sionkowska A.; Wisniewski, M; Skopinska, J., Kennedy, C.J. & Wess, T.J. (2004). The photochemical stability of collagen–chitosan blends, Journal of Photochemistry and Photobiology A: Chemistry, Vol.162, No. 2-3, (March 2004), pp.545-554, ISNN 1010-6030

Sionkowska, A.; Skopinska-Wisniewska, J., Wisniewski, M., Collagen–synthetic polymer interactions in solution and in thin films, *Journal of Molecular Liquids*, Vol.145, No.3, (May 2009), pp.135-138, ISSN 0167-7322

Skopinska-Wisniewska, J.; Sionkowska, A.; Kaminska, A.; Kaznica, A.; Jachimiak, R. & Drewa, T. (2009). Surface characterization of collagen/elastin based biomaterials for tissue regeneration, *Applied Surface Science*, Vol.255, No. 19, (July 2009), pp.8286-8292, ISSN 0169-4332

Smith, M.; McFetridge, P.; Bodamyali, T.; Chaudhuri, J.B.; Howell, J.A.; Stevens, C.R. & Horrocks, M. (2000). Porcine-Derived Collagen as a Scaffold for Tissue Engineering, *Food and Bioproducts Processing,* Vol.78, No.1, (March 2000), pp.19-24, ISSN 0960-3085

Stadlinger, B.; Pilling, E.; Huhle, M.; Mai, R.; Bierbaum, S.; Scharnweber, D.; Kuhlisch, E.; Loukota, R. & Eckelt, U. (2008) Evaluation of osseointegration of dental implants coated with collagen, chondroitin sulphate and BMP-4: an animal study, *International Journal of Oral and Maxillofacial Surgery*, Vol.37, No.1, (January 2008), pp. 54-59, ISSN 0882-2786

Stamov, D.; Grimmer, M.; Salchert, K.; Pompe, T. & Werner, C. (2008). Heparin intercalation into reconstituted collagen I fibrils: Impact on growth kinetics and morphology. *Biomaterials*, Vol.29, No.1, (January 2008), pp.1-14, ISSN 0142-9612

Stark, Y.; Suck, K.; Kasper, C.; Wieland, M.; van Griensven, M. & Scheper, T. (2006). Application of collagen matrices for cartilage tissue engineering. *Experimental and Toxicologic Pathology,* Vol.57, No.4, (March 2006), pp. 305-311, ISSN: 0940-2993

Stojadinovic, A.; Carlson, J.W.; Schultz, G.S.; Davis, T.A. & Elster, E.A. (2008). Topical advances in wound care. *Gynecologic Oncology*, Vol.111, No.3, Suppl.1, (November 2008), pp. S70-S80, ISSN 0090-8258

Su, S.-C.; Mendoza, E.A.; Kwak, H. & Bayless, K.J. (2008). Molecular profile of endothelial invasion of three-dimensional collagen matrices: insights into angiogenic sprout induction in wound healing. *American Journal of Physiology - Cell Physiology,* Vol. 29, (September 2008), pp.C1215–C1229, ISSN 1522-1563

Sun, W.; Lin, H.; Chen, B.; Zhao, W.; Zhao, Y. & Dai, J. (2007). Promotion of peripheral nerve growth by collagen scaffolds loaded with collagen-targeting human nerve growth factor-beta. *Journal of Biomedical Materials Research Part A,* Vol.83, No.4, (December 2007), pp. 1054–1061, ISSN 1549-3296

Sun, W.; Lin, H.; Chen, B.; Zhao, W.; Zhao, Y.; Xiao, Z. & Dai, J. (2009). NGF-beta accelerate ulcer healing. *Journal of Biomedical Materials Research Part A,* Vol.92A, No.3, (March 2009), pp.887–895, ISSN 1549-3296

Swatschek, D.; Schatton, W.; Müller, W.E.G. & Kreuter, J. (2002), Microparticles derived from marine sponge collagen (SCMPs): preparation, characterization and suitability for dermal delivery of all-*trans* retinol, *European Journal of Pharmaceutics and Biopharmaceutics,* Vol.54, No.2, (September 2002), pp.125-133, ISSN 0939-6411

Tebb, T.A.; Tsai, S.W.; Glattauer, V.; White, J.F.; Ramshaw, J.A. & Werkmeister, J.A. (2006). Development of porous collagen beads for chondrocyte culture. *Cytotechnology,* Vol.52, No.2, (October 2006), pp. 99–106, ISSN 0920-9069

Teles, H.; Vermonden, T.; Eggink, G.; Hennink, W.E. & de Wolf, F.A. (2010). Hydrogels of collagen-inspired telechelic triblock copolymers for the sustained release of proteins. *Journal of Controlled Release*, Vol.147, No.2, (October 2010), pp. 298-303, ISSN 0168-3659

Thacharodi D. & Rao, K.P. (1996). Rate-controlling biopolymer membranes as transdermal delivery systems for nifedipine: Development and *in vitro* evaluations. *Biomaterials,* Vol.17, No.13, (July 1996), pp. 1307-1311, ISSN 0142-9612

Tillman, B.W.; Yazdani, S.K.; Lee, S.J; Geary, R.L; Atala, A. & Yoo, J.J. (2009). The *in vivo* stability of electrospun polycaprolactone-collagen scaffolds in vascular reconstruction. *Biomaterials*, Vol.30, No.4, (February 2009), pp.583-588, ISSN 0142-9612

Titorencu, I.; Albu, M.G.; Giurginca, M.; Jinga, V.; Antoniac, I.; Trandafir, V.; Cotrut, C.; Miculescu, F. & Simionescu, M. (2010). In *Vitro* Biocompatibility of Human Endothelial Cells with Collagen-Doxycycline Matrices. *Molecular Crystals and Liquid Crystals,* Vol.523, (May 2010), pp. 82/[654] - 96/[668], ISSN 1542-1406

Trandafir, V.; Popescu, G.; Albu, M.G.; Iovu, H. & Georgescu, M. (2007). *Collagen based products*, Ars Docendi, ISBN 978-973-558-291-3, Bucharest, Romania

Trelstad, R.L. (1982). Immunology of collagens, In: *Immunochemistry of the extracellular matrix*, Furthmayer, H., pp.32-39, CRC, ISBN 978-0-8493-6196-8, Boca Raton, Florida

Ueno, Y.; Nagai, H.; Watanabe, G.; Ishikawa, K.; Yoshikawa, K.; Koizumi, Y.; Kameda, T. & Sugiyama, T. (2005). Transplantation of rat hepatic stem-like (HSL) cells with collagen matrices. *Hepatology Research,* Vol.33, No.4, (December 2005), pp. 277-84, ISSN 1386-6346

Uneo, Y.; Terada, K.; Nagai, H.; Watanabe, G.; Ishikawa, H.; Yoshikawa, K.; Hirayama, Y.; Endo, E.; Kameda, T.; Liu, Y. & Sugyiama, T. (2004). Application of collagen scaffolds for hepatic stem-like cells transplantation. *Akita Journal Medicine*, Vol.31, No.2, (January 2004) pp. 113-119, ISSN 0386-6106

Uriarte-Montoya, M.H; Arias-Moscoso, J.L.; Plascencia-Jatomea, M.; Santacruz-Ortega, H.; Rouzaud-Sández, O.; Cardenas-Lopez, J.L.; Marquez-Rios, E., Ezquerra-Brauer, J.M., Jumbo squid (*Dosidicus gigas*) mantle collagen: Extraction, characterization, and potential application in the preparation of chitosan–collagen biofilms, *Bioresource Technology*, Vol.101, No.11, (June 2010), pp.4212-4219, ISSN 0960-8524

Wallace, D. G. & Rosenblatt, J. (2003). Collagen in drug delivery and tissue engineering. *Advanced Drug Delivery Review,* Vol.55, No.12, (November 2003), pp. 1631-1649, ISSN 0169-409X

Wang, D-A.; Williams, C.G.; Yang, F. & Elisseeff, H. (2004). Enhancing the tissue-biomaterial interface: tissue-initiated integration of biomaterials, *Advanced Functional Materials*, Vol.14, No.12, (December 2004), pp.1152-1159, ISSN 1616-3028

Wang, L.; An, X.; Yang, F.; Xin, Z.; Zhao, L. & Hu, Q. (2008). Isolation and characterisation of collagens from the skin, scale and bone of deep-sea redfish (Sebastes mentella), *Food Chemistry*, Vol.108, No.2, (May 2008), pp.616-623, ISSN 0308-8146

Wang, Y.; Zhang, L.; Hu, M.; Wen, W.; Xiao, H. & Niu, Y. (2010). Effect of chondroitin sulfate modification on rhBMP-2 release kinetics from collagen delivery system. *Journal of*

Biomedical Materials Research Part A, Vol.92A, No. 2, (February 2010), pp. 693–701, ISSN 1549-3296

Weiner, A.L.; Carpenter-Green, S.; Soehngen, E.C.; Lenk, R.P. & Popescu, M.C. (1985). Liposome–collagen gel matrix: A novel sustained drug delivery system. *Journal of Pharmaceutical Sciences,* Vol.74, No.9, (September 1985), pages 922–925, ISSN 0022-3549

Wen, F.; Chang, S.; Toh, Y.C.; Teoh, S.H. & Yu, H. (2007). Development of poly (lactic-co-glycolic acid)-collagen scaffolds for tissue engineering, *Materials Science and Engineering: C*, Vol.27, No.2, (March 2007), pp. 285-292, ISSN 0928-4931

Williams, D.F. (May 1999). *The Williams Dictionary of Biomaterials,* Liverpool University Press, ISBN 978-0-8532-3921-5, Liverpool, United Kindom

Wollina, U.; Meseg, A. & Weber, A. (2011), Use of a collagen–elastin matrix for hard to treat soft tissue defects. *International Wound Journal*, Vol.8, (March 20110), pp. 1742-4801, ISSN 1742-4801

Woodard, J.R.; Hilldore, A.J.; Lan, S.K.; Park, C.J.; Morgan, A.W.; Eurell, J.A.; Clark, S.G.; Wheeler, M.B.; Jamison, R.D. & Wagoner, J.A.J. (2007). The mechanical properties and osteoconductivity of hydroxyapatite bone scaffolds with multi-scale porosity. *Biomaterials*, Vol.28, No.1,(August 2007), pp. 45–54, ISSN 0142-9612

Yarboro, S.R.; Baum, E.J. & Dahners, L.D. (2007). Locally administered antibiotics for prophylaxis against surgical wound infection. *The Journal of Bone and Joint Surgery*, Vol.89, No.5, (May 2007), pp. 929-933, ISSN 0021-9355

Yoel, G. & Guy, K. (2008). Use of collagen shields for ocular-surface drug delivery. *Expert Review of Ophthalmology*, Vol.3, No.6, (December 2008), pp. 627-633(7), ISSN 1746-9899

Yu, X.; Bichtelen, A.; Wang, X.; Yan, Y.; Lin, F.; Xiong, Z; Wu, R.; Zhang, R. & Lu, Q. (2005). Collagen/Chitosan/Heparin Complex with Improved Biocompatibility for Hepatic Tissue Engineering. *Follow Journal of Bioactive and Compatible Polymers*, Vol.20, No.1, (January 2005), pp. 15-28, ISSN 0883-9115

Zhang, L.; Tang, P.; Xu, M.; Zhang, W.; Chai, W. & Wang, W. (2010). Effects of crystalline phase on the biological properties of collagen–hydroxyapatite composites, *Acta Biomaterialia,* Vol.6, No.6, (June 2010), pp. 2189-2199, ISSN 1742-7061

Zhou, J.; Cao, C.; Ma, X. & Lin, J. (2010). Electrospinning of silk fibroin and collagen for vascular tissue engineering, *International Journal of Biological Macromolecules*, Vol.47, No. 4, (November 2010), pp. 514-519, ISSN 0141-8130

Zilberman, M.& Elsner, J.J. (2008). Antibiotic-eluting medical devices for various applications. *Journal of Controlled Release*, Vol.130, No.3, (September 2008), pp. 202-215, ISSN 0168-3659

18

The Use of Biomaterials to Treat Abdominal Hernias

Luciano Zogbi
Federal University of Rio Grande- FURG
Brazil

1. Introduction

Hernia is the most frequent abdominal surgery. Although hernia is a highly prevalent disease, with serious risks and well-known anatomy, there were high rates of recurrence after treatment until the mid-20th century. With the advent of biomaterials, also called prostheses or meshes, the definitive cure of this disease is close to 100%. Using an appropriate surgical technique, following the appropriate postoperative care, with good integration of the prosthesis, a person can safely return to normal life with all the usual activities, including sports and physical efforts. Meshes are indicated for the treatment of all kinds of abdominal wall hernias, such as umbilical, epigastric, femoral and, mainly, inguinal and incisional hernias. Just as the surgical technique to treat this disease has evolved with a significant number of modalities, so also research and the prostheses market are taking up an increasingly outstanding position in the world (Usher, 1958; Penttinen & Grönroos, 2008).

2. Abdominal wall hernias

2.1 Definition

Hernia is derived from the Latin word for rupture. A hernia is defined as an abnormal protrusion of an organ or tissue through a defect, an opening, in its surrounding walls (figs. 1 and 2). This opening is called hernial ring. Its content may be any abdominal viscera, most frequently the small bowel and omentum. When protruding through the hernial ring, the herniated structure is covered by the parietal peritoneum, here called hernial sac (Malangoni & Rosen, 2007).

2.2 Classification

Although hernias can occur in various regions of the body, the most common site is the abdominal wall, particularly in the inguinal and ventral regions. **Hernias of the inguinal region** are classified as direct, indirect and femoral hernia, depending on where the hernia orifice is located in the fascia transversalis, in the deep inguinal ring and in the femoral ring, respectively. A **ventral hernia** is defined by a protrusion through the anterior abdominal wall fascia. These defects can be categorized as spontaneous or acquired or by their location on the abdominal wall: epigastric hernia occurs from the xyphoid process to the umbilicus; umbilical hernia occurs at the umbilicus; hypogastric hernia is a rare spontaneous hernia that occurs below the umbilicus in the midline; and acquired hernia typically occurs after

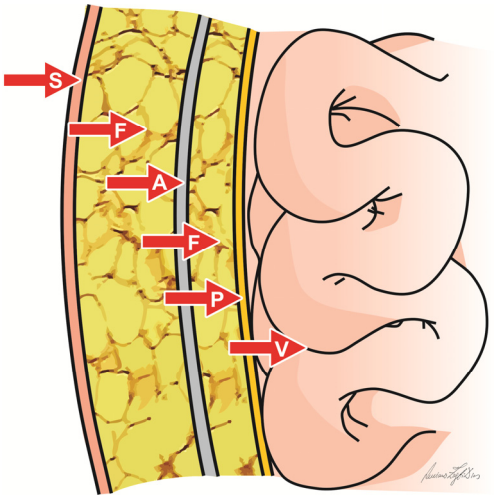

Fig. 1. Schematic drawing of a normal abdominal wall and their layers: Skin (S); Fat Tissue (F); Aponeurosis (A); Pre-peritoneal Fat Tissue (F); Peritoneun (P); and the abdominal viscera (V).

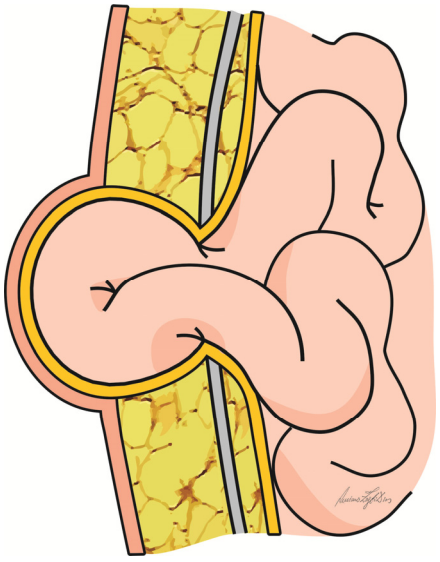

Fig. 2. Schematic drawing of a hernia. In this case, the bowel is the herniated viscera.

surgical incisions (figs 3 and 4). This is therefore termed *incisional hernia* and is the most common long-term complication after abdominal surgery (Franklin et al, 2003; Malangoni & Rosen, 2007; Penttinen & Grönroos, 2008).

Independently of the site, the principles of treatment are the same, only the surgical technique is different, according to regional anatomy.

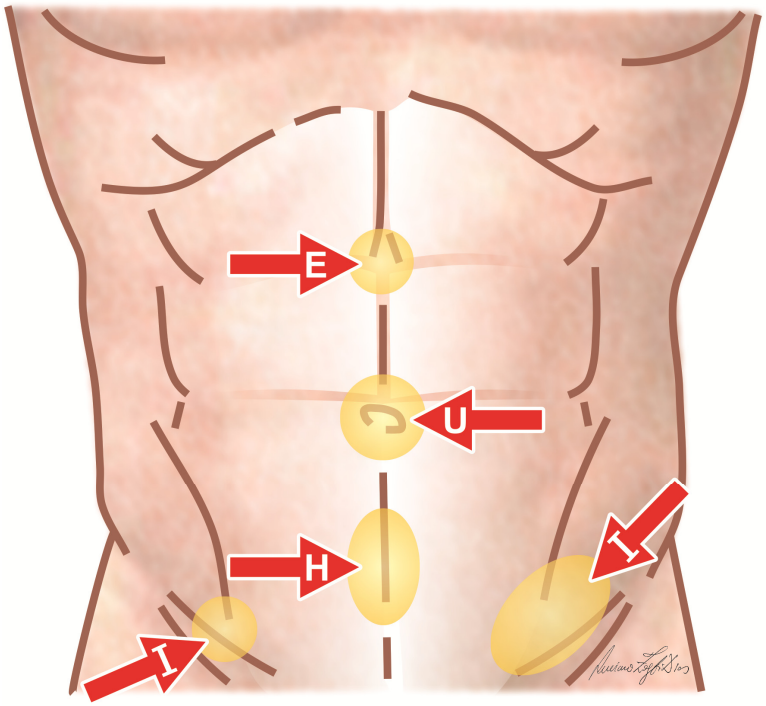

Fig. 3. Mainly places of abdominal wall hernia: Epigastric (E); Umbilical (U); Hypogastric (H); Inguinal (I).

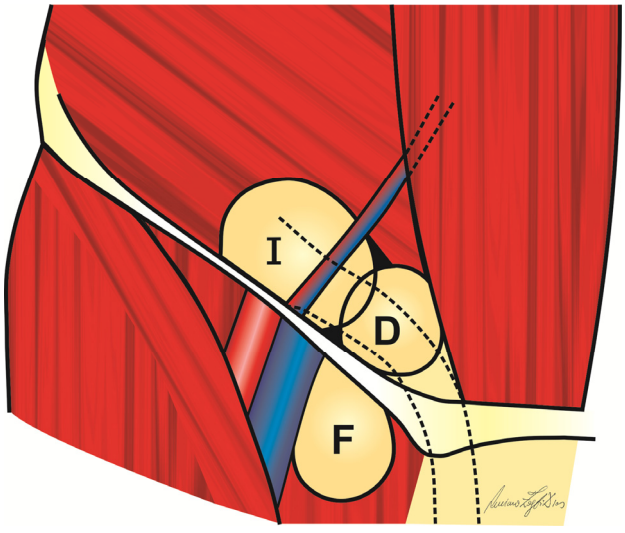

Fig. 4. Hernias of the groin area: Indirect (I); Direct (D); Femoral (F).

2.3 Epidemiology

Hernias are a common problem; however, their true incidence and prevalence are unknown. It is estimated that 5% of the population will develop an abdominal wall hernia, but the prevalence may be even higher. About 75% of all hernias occur in the inguinal region. Two thirds of these are indirect, and the remainder are direct inguinal hernias. The chance of a person having to undergo an inguinal hernia operation during his/her life is quite high, 27% in the case of men and 3% in the case of women. Men are 25 times more likely to have a groin hernia than are women. An indirect inguinal hernia is the most common hernia, regardless of gender. In men, indirect hernias predominate over direct hernias at a ratio of 2:1. Direct hernias are very uncommon in women. Although femoral hernias occur more frequently in women than in men, indirect inguinal hernias remain the most common hernia in women. About 3% to 5% of the population have epigastric hernias, and they are two to three times more common in men. The female-to-male ratio in femoral and umbilical hernias, however, is about 10:1 and 2:1, respectively (Malangoni & Rosen, 2007).

2.4 Risk factors

Hernias are characterized by the rupture of a wall that should be whole (incisional and inguinal direct hernias), or by the widening of a natural orifice (umbilical, femoral and direct inguinal hernias), generally due to excessive and sudden pressure on a fragile area. This weakening occurs because of biochemical and systemic changes in the collagen metabolism, weakening all the connective tissue. The best known risk factors are: old age, male sex, malnutrition, obesity, chemotherapy, radiotherapy, cortisone, sedentarism, decompensated diabetes mellitus, lack of vitamin C, anemia, smoking, chronic obstructive pulmonary disease, abdominal aortic aneurysm, long-term heavy lifting work, positive family history, pregnancy, appendicectomy, prostatectomy, peritoneal dialysis (Rodrigues et al., 2002; Wolwacz et al., 2003; Chan & Chan, 2005; Junge et al., 2006; Szczesny et al., 2006, Penttinen & Grönroos, 2008; Simons et al., 2009).

2.5 Complications if untreated

There is no spontaneous cure or medication to treat this disease. The only existing treatment is surgical correction. As long as it is not treated, the hernia defect will tend to become wider and increase progressively. Besides, herniated organs could be trapped by the hernial ring, and be unable to return to their usual site. When this happens it is called an **incarcerated** hernia. The risk of an inguinal hernia becoming incarcerated is less than 3% per year. The risk is greater in femoral hernias. The most serious risk of this disease is **strangulation**, which occurs when the incarcerated organ is deprived of a blood supply and becomes ischemic (fig.5). In this case, if the hernia is not treated urgently, its content may develop necrosis, infection, sepsis and death. When there is incarceration, the hernia must be reduced manually within 4 to 6 hours. After that, emergency surgery must be performed (Speranzini & Deutsch, 2001a).

Hernia surgery should ideally be performed electively, before these complications arise, making the procedure more effective and safe, since an emergency operation due to a strangulated inguinal hernia has a higher associated mortality (>5%) than an elective operation (<0.5%). Mortality increases about seven-fold after emergency operations and 20-fold if bowel resection was undertaken. After treatment, the risk of incarceration and/or strangulation disappears, as long as the hernia does not recur (Simons et al., 2009).

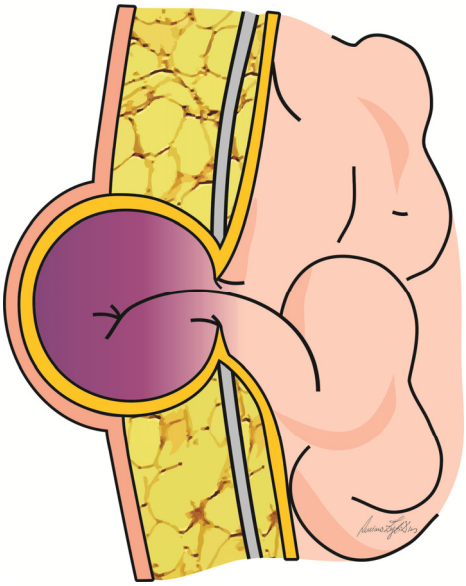

Fig. 5. Ischemic bowel due to strangulation

2.6 Treatment options

Although the only treatment is surgery, there are many effective surgical alternatives. However, merely correcting the hernia defect with sutures does not avoid the source of the problem, because the patient's tissues will still be fragile and predisposed to rupturing again at the same site. The recurrence rate for ventral hernia may be as high as 40–54% after open repair without meshes. Mesh repair is superior to suture repair, results in a lower recurrence rate and less abdominal pain. It does not cause more complications than suture repair (Burger et al. 2004; Penttinen & Grönroos, 2008).

For each type of hernia there are several techniques involving prostheses and different models of prosthesis. Surgeons in training, who see a variety of prosthetics in use, must recognize that the technique of prosthetic implantation is far more important than the type of prosthetic. To help the surgeon choose, it is helpful to look at the prosthetic landscape with a perspective based on (1) the prosthetic's raw material and design, (2) the implantation technique, and (3) the clinical scenario (Earle & Mark, 2008).

For treating inguinal hernia, the use of a polypropylene prosthesis is the best technique. Eighty-five percent of the operations, overall, are performed using an open approach and 15% are performed endoscopically. The surgeon should discuss the advantages and disadvantages of each technique with the patient. Endoscopic inguinal hernia techniques result in a lower incidence of wound infection, hematoma formation and an earlier return to normal activities or work than the Lichtenstein technique. When only considering chronic pain, endoscopic surgery is superior to open mesh. However, endoscopic inguinal hernia techniques need general anesthesia, result in a longer operation time and a higher incidence of seroma than the Lichtenstein technique (Simons et al., 2009).

Independently of the technique employed, after covering the hernia site adequately, the mesh must be fixed to the abdominal wall in order to prevent it from folding over or

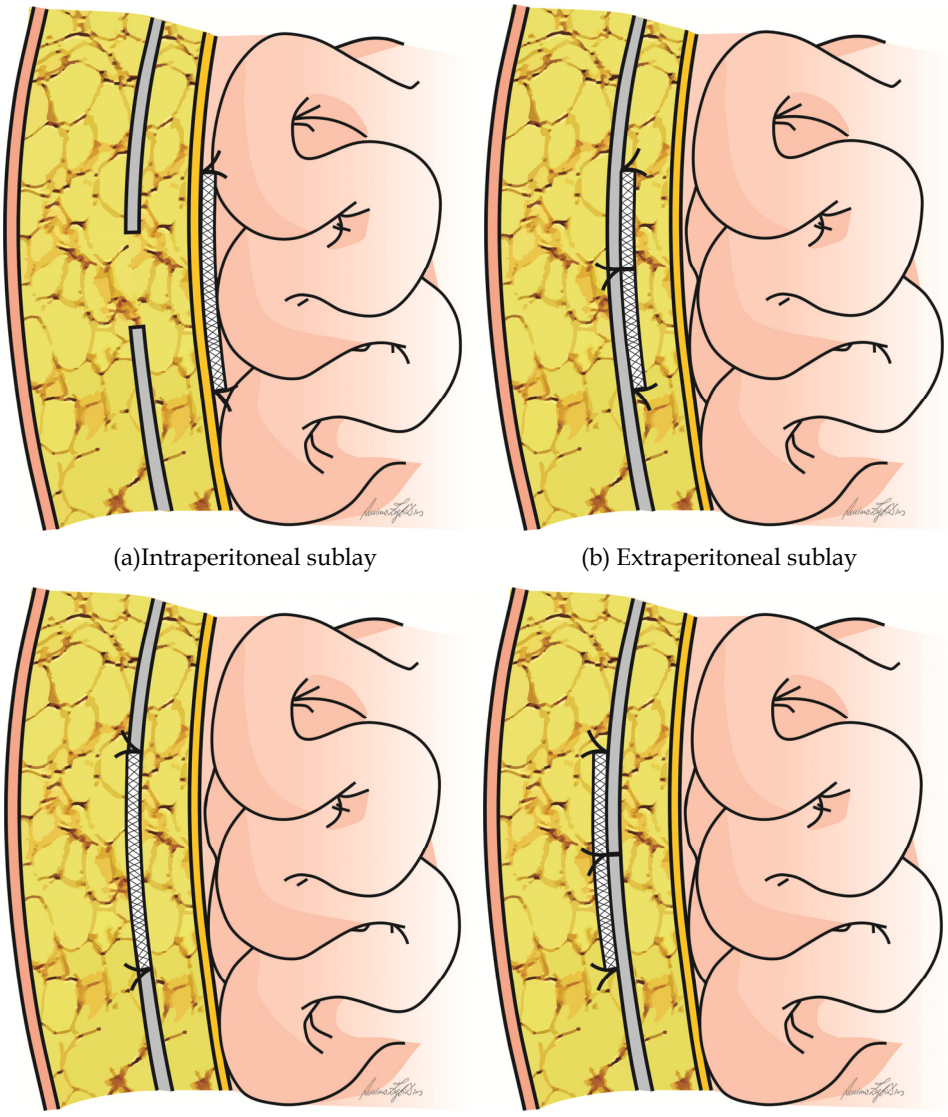

(a)Intraperitoneal sublay (b) Extraperitoneal sublay

(c)Inlay (d) Onlay

Fig. 6. Possible plans of the abdominal wall to insert the prosthesis.

migrating. It may be fixed simply by physical principles of pressure between layers of the abdominal wall (Stoppa & Rives, 1984), by means of a suture with inadsorbable thread (Lichtenstein et al., 1989), absorbable thread (Gianlupi & Trindade, 2004), clips (Read, 2011) or fibrin glue (Agresta & Bedin, 2008; Negro et al., 2011). For fixation of the mesh in ventral hernia repair, most authors have used an extraperitoneal – but intraperitoneal is also possible (fig.6a) - sub-lay technique, in which the mesh is sutured into place on the posterior

rectus sheath with approximately 4 cm of fascia overlap (fig.6b). The other two repair options include an inlay technique (fig.6c), such that the mesh is sutured to the fascial edges, and an onlay technique whereby the mesh is placed and sutured onto the anterior rectus sheath (Fig.6d). The inlay technique has the advantage of minimal soft-tissue dissection thus reducing devascularized tissue, but the disadvantage of high rate of recurrences, while the onlay technique has the disadvantage of vast soft tissue dissection above the rectus layer (Penttinen & Grönroos, 2008).

3. History of biomaterials

Trusses have been used for the treatment of inguinal hernia for thousands of years. In the 19th century, several surgical techniques were proposed to treat hernia, but all of them limited themselves to the raphe of the hernia defect. Until then, the rate of occurrence was high, even surpassing 50%. Cooper already suspected of the degenerative nature of the disease and, Billroth, ahead of his time, perceived that even if he knew everything about anatomy and surgery, he still lacked something. Even before the meshes were created he said that: "If we could artificially produce tissues of the density and toughness of fascia and tendon, the secret for the radical cure of hernia would be discovered" (Amid, 1997; Franklin et al., 2003; Read, 2004; Earle & Mark, 2008).

The first biomaterials were described in 1900, when Oscar Witzel used a silver mesh (Witzel, 1900). Handley developed silk meshes in 1918, but they were no longer used because they did not tolerate the organism (Handley, 1963). In 1928, Goepel inserted stainless steel prostheses, of a fine, flexible, easily manipulated material (Goepel, 1900). Its drawback was the tendency to become fragmented, injuring tissue and blood vessels. The attempt to make celluloid-based materials, by Mandl, in 1933, did not meet with success, since, despite its flexibility and resistance to tension, it easily developed abscesses from infection (Mandl, 1962). In 1946, another metal material was described, vitalium, which was no longer used because of its rigidity (McNealy & Glassman, 1946). Amos Koontz adopted tantalum to treat eventrations in 1948, and it was widely accepted (Koontz, 1948). This was a resistant metal, with a low tendency to corrosion, appropriate to the synthesis of granulation tissue and very safe against infection. Its disadvantages were fragility and high cost, and therefore it was no longer used. The fragmentation observed in these metal substances over time is due to a principle of physics called *point of metal fatigue* (Sans,1986).

The era of plastics began in the manufacture of prostheses when nylon mesh was introduced in 1944 (Acquaviva & Bourret, 1944). Mersilene mesh, a polyester polymer, was widely known as an alloplastic material in 1946 (Adler & Firme, 1959). In 1951, Kneise described the use of the Perlon meshes (Kneise, 1953). In 1958, Francis Usher introduced the first generation of polyethylene mesh to correct abdominal hernias. Despite its good resistance and inertia, the clinical application of this material was limited because it could not be easily sterilized. In 1962 the same author fulfilled Billroth's dream and presented to the worldwide surgical community the material that, with Lichtenstein's encouraging results decades later, became the best known and most used: It is Marlex, a high density propylene; it cannot be affected by acids, alkalis, or organic solvents; it is highly resistant; inert to the infectious process; non-toxic; it cannot be absorbed; it can be cut and modeled without deforming; in other words, all of the benefits of polyethylene added to the virtue of being possible to sterilize in the autoclave (Usher, 1958, 1962; Lichtenstein, 1989). Mesh screens of other materials, also published at the time, such as chromed catgut (Schönbauer & Fanta, 1958),

Silastic, based on silicone (Brown et al., 1960), and Supramid (Rappert , 1963), were not successful (table 1).

Year	Author	Material
1900	Witzel	Silver
1918	Handley	Silk
1928	Goepel	Stainless steel
1933	Mandl	Celluloid
1944	Acquaviva & Bourret	Nylon
1946	Mc Nealy & Glassman	Vitalium
1946	Adler & Firme	Mersilene
1948	Koontz	Tantalum
1951	Kneise	Perlon
1958	Schönbauer & Fanta	Chromed catgut
1958	Usher	Polyethylene
1960	Brown et al.	Silastic
1962	Rappert	Supramid
1962	Usher	Marlex

Table 1. Development of synthetic prosthesis over the course of history.

4. Mechanism of biomaterial integration to the organism

4.1 Normal healing

After tissue injury, such as surgery, the healing process occurs. It takes place in three phases. It begins with the **inflammatory, substrate or exudative phase,** characterized firstly by vasoconstriction and platelet aggregation. Fibrin is formed as the coagulation mechanism continues, in order to diminish loss to hemorrhage, and it lasts approximately 15 minutes. Then the opposite phenomenon is observed, with the consequent exudation of proteins and plasma cells in the zone affected. The cell response is processed 6 to 16 h after the onset of the lesion, when a large amount of polymorphonuclear neutrophils appear, as the *first wave of cell migration*. They stay from 3 to 5 days, with a peak within 68 h (Monaco & Lawrence, 2003). Already on the 1st day there is a monocyte incursion. These are macrophage precursors. Neocapillary growth and fibroblastic proliferation begin about 36 h after injury. The activated macrophages are the predominant leukocytes on day 3, when they peak and persist until healing is complete. This first phase lasts until the 2nd day (Castro & Rodrigues, 2007), and may last until the 4th day postoperatively (Pitrez, 2003).

Around the 3rd to 5th day the **proliferative or connective tissue phase** begins, in which angiogenesis and fibroplasia occur, from the proliferation of the endothelial cells and fibroblasts, respectively. They will build the *granulation tissue*. The lymphocytes appear around the 5th day, peaking on the 7th day , and they are mostly represented by T Lymphocytes. During the 2nd week, the fibroblasts become the dominant cells, especially on the 10th day. After this period they differentiate into fibrocytes. Fibroblasts synthetize collagen, which promotes repair resistance. Around the second week type III collagen is gradually replaced by type I collagen. The fibroblasts migrate into the wound from the surrounding tissue, differentiating into myofibroblasts, forming actin filaments, synthetizing a collagen that is periodically reabsorbed, and like the muscles, the scar tissue

has a centripetal movement, making the scar spheroid (Nien et al., 2003). Wound contraction is an essential aspect of healing. It diminishes the area of the defect making it easier to close. During this phase, tension resistance of the synthetized tissue is still low, no more than 25% to 30% of the original resistance (Junge et al., 2002; Klinge et al., 2002).
From the 21st day onwards, during the last phase of the healing process, called **molding, maturing, resolutive or differentiation phase,** tension resistance will reach its highest levels. The accumulation of collagen tissue peaks on the 21st day, and its value remains practically constant in the 3 following months. During this period, acute and inflammatory cells diminish, angiogenesis is suppressed, and fibroplasia ends. The balance between synthesis and degradation of collagen is restored, and *reformulation of collagens* is seen. In the mature matrix type I is 80% to 90%, and type III is 10 to 20% of the total collagen. This matrix undergoes continuous modification until a stable matrix is formed. The scar tissue takes on 40% of the tensile resistance around 6 weeks, 80% around 6 months, and its maximum resistance is achieved after many months, or even years, but it is not equal to the resistance of healthy tissue. (Monaco & Lawrence, 2003; Pitrez, 2003).

4.2 Healing with a prosthesis

The reinforcement given by the prosthesis does not occur due to the mere mechanical presence of the material at the surgical site. It is caused by the tissue that will be produced because it is there. After any prosthetic is implanted, an extraordinarily complex series of events takes place and the healing process described above will occur amidst the mesh. The architecture formed by its filaments and by its pores will act as a foundation for the deposition of connective tissue. The principle and phases of healing are similar, and on the mesh screen weave, a new tissue will be built similar to a dense aponeurosis (Zogbi et al., 2010).
Immediately after implantation, the prosthetic adsorbs proteins that create a coagulum around it. This coagulum consists of albumin, fibrinogen, plasminogen, complement factors, and immunoglobulins. Platelets adhere to this protein coagulum and release a host of chemoattractants that invite other platelets, polymorphonucleocytes (PMNs), fibroblasts, smooth muscle cells, and macrophages to the area in a variety of sequences. Activated PMNs drawn to the area release proteases to attempt to destroy the foreign body in addition to organisms and surrounding tissue. The presence of a prosthetic within a wound allows the sequestration of necrotic debris, slime-producing bacteria, and a generalized prolongation of the inflammatory response of platelets and PMNs. Macrophages then increasingly populate the area to consume foreign bodies as well as dead organisms and tissue. These cells ultimately coalesce into foreign body giant cells that stay in the area for an indefinite period of time (Earle & Mark, 2008). The histological examination of the mesh screens removed shows that all prostheses, independent of type of biomaterial, induce an acute and intense inflammatory reaction (Zogbi et al., 2010, whose quantity and quality depend on the type of material of which the mesh is made (Di Vita et al., 2000). The fibroblasts and smooth muscle cells subsequently secrete monomeric fibers that polymerize into the helical structure of collagen deposited in the extracellular space. The overall strength of this new collagen gradually increases for about 6 months, resulting in a relatively less elastic tissue that has only 70% to 80% of the strength of the native connective tissue. It is for this reason that the permanent strength of a prosthetic is important for the best long-term success of hernia repair (Earle & Mark, 2008).

Three aspects are valuable from the histological standpoint, in the interaction between the material and the organism: the size of the tissue reaction, the cell density and fibroblastic activity. The tissue reaction is 10mm on the 20th day and 20 mm on the 40th day. Cell censity is moderate to the 8th day and maximal after the 30th day. Fibroblastic activity begins on the 8th day on the intraperitoneal plane and 10th day on the extraperitoneal plane. It is maximal on days 30 and 35, respectively. The mechanical resistance of wall reconstruction is similar at the end of 30 days, independently of the material used. During the early postoperative period, between the first and second week, the permeable macroporous prostheses are significantly more resistant than the impermeable ones. This period, during which the prosthesis insertion zone is fragile, is called the Howes latency period (Sans, 1986; Zogbi et al., 2010).

5. Classification

Currently there are more than 70 meshes for hernia repair available on the market (Eriksen et al., 2007). They can be classified into different categories according to composition or type of material (Ponka, 1980), pore size (table 2) (Amid, 1997), density (Earle & Mark, 2008) and others. The classification below covers all these characteristics:

5.1 Synthetic nonabsorbable prosthesis

5.1.1 Type I: Totally macroporous prosthesis

The macroporous prostheses are characterized by a diameter larger than 75 (Amid, 1997) or 100μm (Annibballi & Fitzgibbons, 1994). Thus, they allow easy entry of macrophages, fibroblasts, collagen fibers, which will constitute the new connective tissue and integrate the prosthesis to the organism. They also allow more immunocompetent cells to enter, providing protection from infection-causing germs. The larger the pore diameter, the greater and faster will be the fibroplasia and angiogenesis (Gonzalez et al., 2005). On the other hand, there will also be a greater risk of adhesions when the screen is inserted in the intraperitoneal space, especially if it is in contact with the viscerae; it may also promote erosion and fistula formation (Hutchinson et al., 2004; Mathews et al, 2003; Melo et al., 2003). The main representative is **Polypropylene (PP)** (fig.7). Common brand names include **Marlex**® (Davol, Cranston, Rhode Island), **Prolene**® (Ethicon, Somerville, New Jersey), **Prolite**® (Atrium Medical, Hudson, New Hampshire), **Atrium**® and **Trelex**® (Erle & Mark, 2008). PP is the material most used to correct hernias, both anteriorly, retroperitoneally or laparoscopically (Bellón, 2009). PP is an ethylene with an attached methyl group, and it was developed and polymerized in 1954 by the Italian scientist, Giolo Natta. It is derived from propane gas. The position of the methyl groups during polymerization affects overall strength and it is at a maximum when they are all on the same side of the polymeric chain. This polymer is hydrophobic, electrostatically neutral, and resistant to significant biologic degradation (Earle & Mark, 2008). Since it is thermostable, with a fusion point of 335ºF, it can be sterilized repeatedly in an autoclave (Amid, 2001). Studies show that the tensile strength of PP implanted in organic tissue remains unchanged over time. Disposed in different makes and models, the mesh screens developed for use in hernioplasties are monofilamentary, rough, semi-rigid and allow elasticity in both directions (Speranzini & Deutsch, 2001b). The screen thickness varies according to the model. For instance, Atrium®, Marlex®, Prolene® are respectively, 0.048, 0.066 and 0.065 cm (Goldstein, 1999). It has a high tolerance to infection. When there is a infection at the surgical site, the mesh screen can be

preserved, as long as it is integrated to the fascia, thanks to its broad pores, and must only be drained and the infection treated. In open inguinal hernia repair, the use of a monofilament polypropylene mesh is advised to reduce the chance of incurable chronic sinus formation or fistula which can occur in patients with a deep infection (Simons et al., 2009).

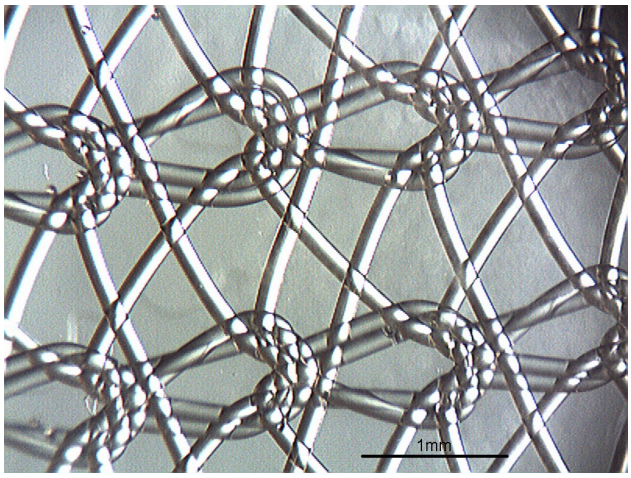

Fig. 7. Augmentation picture of polypropylene prosthesis

Considering the abdominal cavity as a cylinder, and according to Pascal's hydrostatic principle, the maximum load for its rupture is between 11 and 27N/cm. Abdominal pressures vary from 8 to 150mmHg. Klinge et al demostrated that the prostheses that were being used until that time can bear up to 10 times these rupture tensions, much higher than the resistance of the abdominal wall itself. Thus, there is a reduction of the natural elasticity in the aponeurosis after it is implanted, since the incorporation of tissue to the prosthesis gives rise to an incongruence of resistance between the receiving tissue and the biomaterial, and can cause patient more discomfort. Therefore, it would be more reasonable to implant materials with a lower resistance and greater elasticity (Bellón, 2009). Low weight density (LW) prostheses were then developed (fig.8), characterized by a lower concentration of synthetic material and larger pores (>1,000 μm). The first experimental tests were performed with a hybrid prosthesis of LW PP and polyglactine (Klinge et al., 1998), which was later sold under the name **Vypro II®** (Ethicon, Johnson&Johnson, Somerville, USA). Then pure LW PP prostheses were developed and disseminated, such as **Parietene®** (Tyco, Healthcare, Mansfield, MA), with a 38g/m^2 density and 1.15 +- 0.05 mm^2 pores and **Optilene elastic®** (Braun, Spangerwerg, Germany), with 48g/m^2 and 7.64 +- 0.32mm^2 pores (Bellón, 2009).
Hence, as to density, the prostheses can be classified as: Heavyweight (HW), when they are above 80g/m^2; Mediumweight (MW), between 50 and 80 g/m^2; Lightweight (LW), between 35 and 50 g/m^2; and Ultra-lightweight, below 35 g/m^2. Comparing them, it would be helpful to classify density (weight) and pore size uniformly in a standard fashion. Earle & Mark proposed a standard based on currently available data: Very large pore: >2,000 μm; Large pore: 1,000–2,000 μm; Medium pore: 600–1,000 μm; Small pore: 100–600 μm; Microporous (solid): <100 μm (Earle & Mark, 2008).

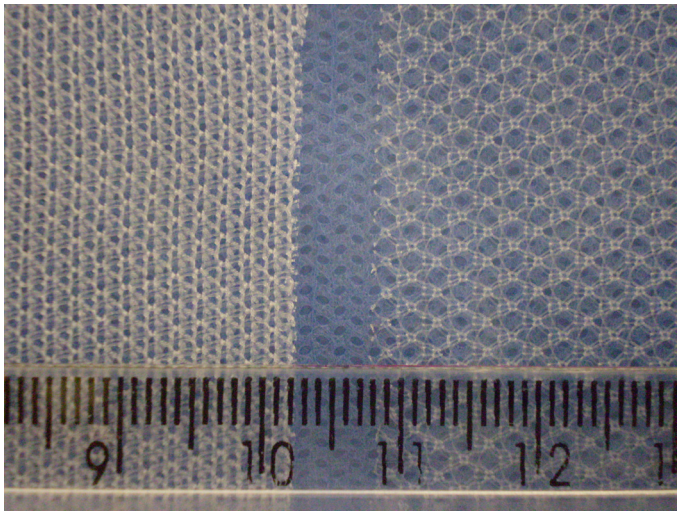

Fig. 8. Comparison between a HW (Marlex®), on the left, and a LW mesh (Parietene®), on the right.

Material-reduced (Weight-reduced mesh materials/ lightweight/oligofilament structures/largepore/macroporous>1,000 μm) meshes have some advantages with respect to long-term discomfort and foreign-body sensation in open hernia repair (when only chronic pain is considered), but are possibly associated with an increased risk for hernia recurrence in high-risk conditions (large direct hernia), perhaps due to inadequate fixation and/or overlap. They seem to shrink less, cause less inflammatory reaction and induce less extensive scar-tissue formation (Hollinsky et al., 2008; Simons et al., 2009).

5.1.2 Type II: Totally microporous prosthesis

The pores are smaller than 10μm in at least one of the three sizes. The main example is **expanded politetraflouroethylene (e-PTFE)**. It was discovered at a DuPont laboratory serendipitously by Roy Plunkett in 1938. While researching tetraflouroethylene gas as a refrigerant, he discovered that the gas spontaneously polymerized into a slippery, white, powdery wax. After some time on the shelf, it was eventually used as a coating for cables. While still working at DuPont, William Gore subsequently saw the potential for medical applications, and ultimately started his own company, W.L. Gore and Associates, in 1958. That company developed and manufactured e-PTFE under the brand name **Gore-Tex®** (W.L. Gore and Associates, Flagstaff, Arizona) for hernia repair products, among other things. There are other manufacturers of PTFE hernia prosthetics, each with a different manufacturing process, and hence a slightly different architecture (Earle & Mark, 2008). PTFE is not a mesh, but a flexible, impervious sheet. It is transformed into its expanded form (e-PTFE) after being submitted to an industrial process. It is a soft, flexible, slightly elastic material, and its smooth surface is not very adherent (Mathews et al., 2003). Therefore it must be carefully fixed with sutures, since its integration is very slow, taking about 30 to 40 days (Speranzini & Deutsch, 2001b). Its minuscule pores are actually complex fine canals,

through which fibroblasts penetrate and synthetize collagen. The e-PTFE is composed of columns of compact nodules, interconnected by fine fibers of the same material (Mathews et al., 2003). The intermodal distance is from 17 to 41μm, with a multidirectional fibrillar arrangement that provides equal strength on every plane (Amid, 2001). Bacteria, approximately 1μm in size, easily penetrate the micropores of the prosthesis and are thus protected from the macrophages or neutrophils, which are too voluminous to enter the site, perpetuating the infectious process. It is a mechanism similar to that of a foreign body which occurs with plaited threads or any materials with interstices (Amid, 1997). Therefore, when there is an infection, the mesh screen should always be removed, on the contrary of the macroporous screens. The main advantage of this material is the diminished risk of adhesions, even in direct contact with the viscerae. It is the prosthesis with the smallest tissue reaction (Speranzini & Deutsch, 2001b). Because of this, its use in laparoscopic hernia repair allows the surgeon to leave the peritoneum open once the prosthetic is in place (Earle & Mark, 2008).

5.1.3 Type III: Macroporous prosthesis with multifilament or microporous components

They are characterized as containing plaited multifilamentary threads in their composition, and the space between threads is less than 10 μm; but also because their pores are larger than 75 μm. They include plaited polyester mesh - **Mersilene®** (Ethicon, Johnson&Johnson, Somerville, USA) and **Parietex®** (Covidien, Mansfield, USA); plaited polypropylene - **SurgiPro®** (Covidien, Mansfield, USA); perforated PTFE - **Mycromesh®** and **MotifMESH®** (Amid, 1997; Eriksen et al., 2007).

The main disadvantage is during an infection, because the chance of complete wound healing after adequate drainage is difficult. When a multifilament mesh is used, bacteria (<1 μm) can hide from the leucocytes (>10 μm), because the mesh has a closer weave structure with a smaller pore diameter (<10 μm) (Simons et al., 2009).

Polyester (PE), the common textile term for polyethylene terephthalate (PET), is a combination of ethylene glycol and terephthalic acid, and it was patented by the English chemists J.R. Whinfield and J.T. Dickson in 1941 at the Calico Printers Association Ltd. in Lancashire, the United Kingdom. PET is hydrophilic and thus has the propensity to swell. PET is the same polymer used for plastic beverage bottles (Earle & Mark, 2008). It is a light, soft, flexible, elastic material, in a single direction. Its wide meshes encourage fibroblastic migration making it easier for tissue to incorporate – its pores are even greater than those of the PP, which is believed to allow faster cell migration and greater intensity of adherence to the underlying fascia (Gonzalez et al., 2005). It has good resistance to infection, although its threads are multifilament. It does not have the plastic memory of PP, which allows it to adapt to the structures on which it is placed. Another advantage is the cost, because it has a lower cost (Speranzini & Deutsch, 2001b). It is the mesh screen most used by European surgeons, especially the French (Stoppa & Rives, 1984).

In 1993 the MycroMesh® with pores all way through the mesh was introduced to allow better tissue ingrowth. MotifMESH® is a new macroporous non-woven mesh of condensed PTFE (cPTFE) for intraperitoneal application. Although the mesh is macroporous (fenestrated) it has a theoretically anti-adhesion barrier because of the PTFE content. The thickness of the MotifMESH® is reduced by 90% compared with older ePTFE meshes (Eriksen et al., 2007).

Prostheses	Definition	Examples
Type I	Pore diameter > 75 μm	Polypropyleno (PP)
Type II	Pore diameter < 10 μm	Expanded Polytetrafluorethylene (e-PTFE)
Type III	Pore diameter >75 μm Space between threads < 10 μm	Polyester (PE)
Type V	Submicromic pores	Pericardium, dura mater

Table 2. Classification of the biomaterials according to Amid (Amid, 1997)

5.2 Mixed prostheses

Also known as "second generation" screens, they are characterized by combining more than one type of material in the same prosthesis (Bachman & Ramchaw, 2008).

5.2.1 Partially absorbable prosthesis

One of the disadvantages of LW prostheses is the excessive malleability of the screen). The lack of memory, or lack of rigidity, makes them difficult to handle during surgery, especially laparoscopic surgery. To reduce the polymer density (and subsequent inflammatory response), yet maintain the intraoperative handling characteristics and long-term wound strength, prosthetics have been developed that mix nonabsorbable polymers (eg, PP) with absorbable polymers. Thus, screens composed by a LW PP structure are associated with biodegradable elements, such as **polyglactine – Vypro II®** mesh or **polyglecaprone-25 - Ultrapro®** mesh (Ethicon, Johnson&Johnson, Somerville, USA). This confers on the screen an appropriate malleability for better surgical handling, without, however, leaving a high weight of unabsorbed tissue in the organism (Earle & Romanelli, 2007; Earle & Mark, 2008; Hollinsky et al., 2008; Bellón, 2009).

5.2.2 Coated nonabsorbable prosthesis

In order to avoid visceral adhesions, erosion and even fistula formation which are possible complications of macroporous screens when inserted on the peritoneal side, screens covered with low tissue reaction material were developed to remain in direct contact with the viscerae. The two-sided **DualMesh®** was introduced in 1994, made in e-PTFE, and it was later modified with large interstices and an irregular "corduroy-like" surface on the parietal side to increase tissue ingrowth. Other available brands are: **Intramesh T1®**; **Dulex®**; and **Composix®**. The DualMesh® is also available with incorporated antimicrobial agents (silver–chlorhexidine film, type "Plus"). **TiMesh®** (GfE Medizintechnik GmbH, Nürnberg, Germany) is a titanium-coated lightweight (macroporous) PP mesh. Titanium is known for its good biocompatibility and should theoretically reduce adhesions. It is manufactured for intraperitoneal use although it has no "real" solid anti-adhesion barrier or micro-pore/no-pore site against the bowel loops. **Parietene Composite®** (Covidien, Mansfield, USA) is a woven PP mesh with a protective collagen-oxidized film (collagen-coating) on the visceral side. **Sepramesh®** is a PP mesh coated on the visceral side with an absorbable barrier of sodium hyaluronate and carboxymethylcellulose. **Proceed®** (Ethicon, Johnson&Johnson, Somerville, USA) is a Prolene® soft mesh encapsulated in a polydioxanone polymer film (PDS®) covered by a layer of absorbable oxidised regenerated cellulose (ORC); **Glucamesh®** (Brennen Medical, St. Paul, Minnesota) is a midweight PP mesh (50 g/m^2) coated with the absorbable complex carbohydrate, oat beta glucan; **Dynamesh®** (FEG Textiltechnik, Aachen, Germany) is a PP mesh with polyvinylidene fluoride (PVDF) monofilament; **C-QUR®**

(Atrium Medical) is a mediumweight PP mesh (50 or 85 g/m^2) coated with an absorbable omega-3 fatty acid preparation derived from fish oil, because omega-3 fatty acids have anti-inflammatory properties. The coating is about 70% absorbed in 120 days and has had all protein removed to avoid an immune response. The same mesh without the coating has been analyzed in the laboratory and found to be acceptable in terms of inflammatory response compared with more heavyweight polypropylene prosthetics (Mathews et al., 2003; Abaza et al., 2005; Eriksen et al., 2007; Earle & Mark, 2008; Schreinemacher et al., 2009).
The **Parietex Composite®** mesh is composed of multifilament PE with a resorbable collagen-oxidized film made of oxidized atelocollagen type I, polyethylene glycol and glycerol, against the viscera. **Intramesh W3®** is a PE mesh with silicone layer (Eriksen et al., 2007; Schreinemacher et al., 2009).
In the mixed prostheses in general, weight is usually smaller and porosity greater. For instance, a conventional PP prosthesis PP (HW) such as Surgipro®, weighs 84g/m^2 and has small pores (0.26 +- 0.03mm^2). Conversely, Ultrapro®, weighs 28g/m^2 with 3.45 +- 0.19mm^2; pores; and VyproII® weighs 35g/m^2 with 4.04 +- 0,54mm^2 pores(Bellón, 2009).

5.3 Biologic prosthesis

Biologic mesh materials are based on collagen scaffolds derived from a donor source and they represent so-called ''third-generation'' mesh. According to Amid's classification they are included in the **type IV** prostheses, **biomaterials with submicronic pore size.** Dermis from human, porcine, and fetal bovine sources are decellularized to leave only the highly organized collagen architecture with the surrounding extracellular ground tissue. Other natural collagen sources in addition to the dermal products include porcine small intestine submucosa (which is layered for strength) and bovine pericardium. The collagen in these materials can be left in its natural state or chemically crosslinked to be more resistant to the collagenase produced in wounds. By increasing crosslinking, the persistence of the mesh is also increased. Uncrosslinked mesh can be totally incorporated and reabsorbed within 3 months, whereas a highly crosslinked mesh can persist for years (Amid, 1997; Bachman & Ramshaw, 2008).
Most of the human studies published on biologic materials are from difficult clinical situations. Because angiogenesis is a part of the remodeling of the mesh, these materials can potentially resist infection (Blatnik et al., 2008; Deprest et al., 2009), and they have a moderately good success rate for salvaging contaminated and infected fields, especially when placed with wide overlap. Other findings demonstrate some resistance to adhesion formation (Bachman & Ramchaw, 2008).
The basic concept behind these types of prosthetics is that they provide a matrix for native cells to populate and generate connective tissue that will replace the tissue in the hernia defect. Given that newly formed connective tissue is only 70% to 80% as strong as native connective tissue, and that hernia patients may have an inherent defect in their native connective tissue, biologic (or absorbable synthetic) prosthetics would theoretically have a higher risk of recurrence than would permanent prosthetics. With a theoretically increased risk of long-term recurrence, relatively high cost, and no clear benefit, the use of these products for elective inguinal hernia repair should be considered investigational, and are not routinely indicated (Earle & Mark, 2008; Simons et al., 2009).

5.3.1 Heterografts

These are biomaterials produced from animal tissue. Porcine heterografts, whose main and most studied example is **Surgisis®** (Cook Biomedical, Bloomington, IN, USA), derived from

porcine small bowel submucosa was one of the initial biologic grafts used and was FDA approved in 1999. Surgisis is an acellular xenograft consisting primarily of type I porcine collagen. It is harvested from slaughterhouse pigs, processed with paracetic acid, and terminally sterilized with ethylene oxide. It does not undergo crosslinking during processing. The graft is available in different thickness including four ply, for hiatal hernias and groin hernias; and eight ply, for ventral hernias. This material seems to be biodegradable and manufacturers claim it is completely replaced with native tissue at 6 months. Surgisis has been extensively studied in animal models. Agresta & Bedin say that, besides diminishing the chances of adhesions on the peritoneal side, another advantage to using a biological mesh is that the persistence of a synthetic mesh in the preperitoneal inguinal area, where scar formation can result in the possible complications of infertility and difficulties in future vascular and urological surgical procedures, is that the biological mesh does not lead to a persistent foreign body in this region and these complications may, therefore, be avoided. This is especially important in the young patient or in athletes. The theoretical benefits of its use include: resistance to infection in contaminated surgical fields; avoidance of a permanent foreign body in the inguinal region; and a reconstruction that results in the formation of natural tissue. These characteristics, together with the results of several human clinical studies which have demonstrated its safety, let us suggest its possible use in young patients without any fear of possible future complications (Agresta & Bedin, 2008).

Several porcine dermal products are also available using different processing techniques: **Permacol**® (Covidien, Norwalk, CT) was initially approved for pelvic floor reconstruction in 2000. It is manufactured by Tissue Sciences Laboratory (Aldershot, UK) and was acquired by Covidien in 2008. It is processed with Diisocynate to achieve collagen cross-linking, and is terminally sterilized with gamma irradiation. It is not freeze dried and requires no rehydration before use. There are several peer reviewed publication evaluating Permacol in gynecologic, urological, plastic surgical, and ventral hernia repairs. **Collamend**®, distributed by Davol Inc, (Warwick, RI), was approved for use in 2006. It is freeze dried, requires 3 minutes of rehydration before use, and is heavily crosslinked. LifeCell Inc, (Branchburg, NJ) introduced **Strattice**® in 2007; it is, noncrosslinked, terminally sterilized, and requires a 2 minute soak before usage. **XenMatrix**® is another porcine dermal product that received approval in 2003, and is manufactured by Brennen Medical (St, Paul, MN). It is noncrosslinked and terminally sterilized with E-beam radiation. It is stored at room temperature and does not require rehydration before usage (Rosen, 2010).

Bovine donors constitute the remainder of the heterografts and sources include pericardium or fetal dermis. **Tutopatch**® is a bovine pericardial product, is manufactured by Tutogen (Alachua, FL), and received FDA approval in 2000. Tutogen processing is a proprietary technique that involves osmotic contrast bathing, hydrogen peroxide, sodium oxide, and gamma irradiation for terminal sterilization. It is stored at room temperature and requires rehydration before use. Two other bovine pericardial products are manufactured by Synovis Surgical Innovations (St, Paul, MN): **Veritas**® received approval in 2003, and is a noncrosslinked bovine pericardium that is harvested from an isolated Midwestern slaughterhouse from cows younger than 30 months. It is processed with sodium hydroxide, propylene oxide, and ethanol. It does not require rehydration and is ready to use out of the package. **Peri-guard**® is treated with gluteraldehyde to initiate collagen crosslinking. It requires a 2 min soak before usage (Rosen, 2010).

5.3.2 Allografts

Several cadaveric allografts are presently available. Because these grafts have been minimally altered from the initial starting material, they are classified as "minimally processed human tissue" by the FDA. This is an important distinction from the heterografts, which are classified as medical devices and are under closer scrutiny by the FDA. Tissue banks typically regulate these allografts. **AlloDerm®** (LifeCell Corporation, Branchburg, NJ) is created from cadaveric skin using proprietary processing techniques that reportedly maintain the biochemical and structural components of the extracellular matrix promoting tissue regeneration. Cells are then removed by deoxycholate, and the residue is washed and lyophilized. The remnant material is an insoluble matrix composed mainly of collagen, elastin and laminin and closely resembles the composition of normal skin connective tissue (Penttinen & Grönroos, 2008). The graft is noncrosslinked, and is freeze dried, and requires a 20 to 30 minutes soak before use. The ability of AlloDerm to withstand hostile environments has been well documented. However, the graft's durability and the prevention of hernia recurrence have been less clear. **AlloMax®** (Tutogen Medical Inc., Alachua, FL) is another acellular human dermal product that is marketed through Davol Inc. It is noncrosslinked and undergoes a proprietary processing developed by Tutoplast similar to the Tutopatch previously described. **Flex HD®** is manufactured by Musculoskeletal Tissue Foundation (Edison, NJ) and is distributed by Ethicon Inc. (Somerville, NJ). It is stored in a 70% ethanol solution and remains in a hydrated form and therefore does not require rehydration before use. It does not require refrigeration (Rosen, 2010).

Implantation of a **fibroblast growth factor (bFGF)**-releasing polygalactone polymer rod into the fascial wound of rats has been carried out. This approach reduced the development of primary incisional hernias from 60 to 30%, and recurrent incisional hernias from 86 to 23%. This study also reported that type I collagen staining was significantly increased around the bFGF treated fascia, which was thought to contribute to the results (Dubay et al., 2004).

The use of the patient's hernial sac as biomaterial to correct the hernia and reinforce the surgery has also been described, since it also induces fibroplasia (Silva et al., 2004).

6. Complications from the use of mesh screens

The overall risk of complications reported after inguinal hernia operations varies from 15 to 28% in systematic reviews. The most frequent early complications were hematomas and seromas (8–22%), urinary retention and early pain, and late complications were mainly persistent pain and recurrences. Those are the two most important outcome measures. Chronic pain is an issue that primarily affects patient quality of life, and is the most common complication of otherwise successful inguinal hernia surgery (Perenttinen & Grönroos, 2008). A truly successful hernia repair requires effective bridging or augmentation that will prevent recurrence. If reoperation is required in the event of a recurrence, the incidence of chronic pain increases. Other complications described are foreign body reactions, infection, discomfort, dislocation, migration, erosion and shrinkage of the prosthesis (Junge et al., 2006; Zogbi et al., 2010). The risk of infertility has been considered significant in inguinal mesh operations (Penttinen & Grönroos, 2008). Chronic pain, stiff abdomen, and foreign body sensation are least often observed with the use of a lightweight mesh and a laparoscopic approach (Klosterhalfen et al., 2005). Besides these specific complications caused by the prosthesis, complications common to any surgical procedure, such as

respiratory or urinary infection, vomiting, constipation, urine retention, venous thrombosis, hemorrhage, anesthetic complications and even death should not be underestimated. Fortunately, lifethreatening complications were rarely reported (Simons et al., 2009).

7. Measures to avoid complications

First it should be recalled that surgical techniques using mesh result in fewer recurrences than techniques which do not use mesh (Simons et al., 2009). Besides, mesh repair appears to reduce the chance of chronic pain rather than increase it (Collaboration, 2002).
During any surgery, a meticulous, anatomical, precise and aseptic surgical technique should be used. The mesh should be positioned adequately when it is fixed, and it should go 2 cm or more beyond the limits of the margins of existing defects, so that a possible retraction or displacement will not compromise the entire coverage of the hernial defect (Amid, 2001). After all recurrences in humans invariably occurred at the mesh margin, where the mesh interfaced with tissue (Bachman & Ramchaw, 2008). Contact with bowel loops should be avoided, because the adhesions resulting from this contact may cause irreversible damage such as necrosis, digestive fistula and elimination of the material (Mathews et al, 2003). Contact with subcutaneous cell tissue should be avoided to reduce the risk of seroma and infection. It should be placed between two myoaponeurotic layers, not only to avoid contact with the viscerae, or with the subcutaneous, as described above, but also so that the mesh will not fold over and will be directly integrated to these tissues, strengthening them (Falci 1997, 2003).
After surgery, the patient should return gradually to his activities, without intense, abrupt efforts. Risk factors described at the beginning of the chapter should be controlled.

8. The ideal mesh for hernia repair: defining characteristics

Classically the first desirable qualities in the biomaterials described were resistance, durability, good tissue tolerance, flexibility, easy manipulation, non-migration, stability, pervious pores, sterilizability and economic feasibility, besides not producing cysts or malignant changes. All this is still accepted (Cumberland, 1952; Scales, 1953). Other needs were found over time, namely, they should not restrict postimplantation function or future access, they should perform well in the presence of infection and block transmission of infectious diseases, resist shrinkage or degradation over time and be easy to manufacture. (Earle & Mark, 2008). Saberski et al added another characteristic called anisotropy, and they found striking differences between elastic properties of perpendicular axes for most commonly used synthetic meshes (Saberski et al., 2011). From the surgeons' and patients' point of view, the optimal mesh should have minimal adhesion formation, excellent tissue ingrowth with minimal shrinkage, no fistula formation and promote minimal pain and seroma formation. Furthermore, it is important that the mesh causes no change in abdominal wall compliance (Eriksen et al., 2007). The mesh should be flexible but also have a good memory, and it should have elasticity in more than one dimension, allowing it to stretch in more than one direction and then return to its original shape. In this way, the mesh should match the abdominal wall dynamics as closely as possible. Flexibility and memory, which make a mesh more adaptable, are also important to optimize the surgical handling of the mesh. The mesh should have an adequate adhesive quality that requires minimal or no additional fixation, even for large defects. An ideal mesh would be a

monofilament mesh that would prevent adhesions yet still enable growth of the adjacent tissue for optimal augmentation (Bringman et al., 2010).

In healthy volunteers, documented measured intra-abdominal pressure via intravesicular measurements was up to 252 mmHg in a variety of maneuvers, including lifting, coughing, and jumping. This correlates to forces of up to 27 N/cm (Cobb et al, 2006). A tensile strength of 16 N was probably more than sufficient to augment the abdominal wall; for bridging of large defects, an increased tensile strength of 32 N may be necessary (Bringman et al., 2010). With these numbers in mind, compare a maximum force on the abdominal wall of 27 N/cm with the measured burst force of some of the more common synthetic mesh materials: Marlex® has a tensile strength of 59 N/cm, Atrium® 56 N/cm, and VyproII® 16 N/cm. Marlex® and Prolene® were both over five times stronger than the calculated abdominal wall strength, and Mersilene® was at least twice as strong (Kinge et al, 1998). A similar trend was noted in an animal study conducted by Cobb. Mesh was implanted into swine for 5 months and then tested for burst strength. Native tissue ruptured at 232 N, LW PP mesh burst at 576 N, MW at 590 N, and HW mesh at 1218 N (Cobb et al, 2006). These data have lent scientific support to the theory that synthetic mesh materials, especially traditional HW PP mesh, are overengineered for their purpose. This excess prosthetic can lead to more complications, including decreased mesh flexibility, loss of abdominal wall compliance, inflammation, and scarring of surrounding tissues, potentially leading to pain, a sensation of feeling the mesh in the abdominal wall, and mesh contraction and wadding, which in turn may result in a recurrent hernia (Bachman & Ramchaw, 2008). Actually, all commercially available synthetic prosthetics today have long-term foreign-body reactions. Given the existing products and body of evidence, the overall density should probably be somewhere between 28 g/m^2 and 90 g/m^2 to minimize recurrence and adverse effects of the host foreign-body response. Methods to decrease the density of the prosthetic include reduction in fiber diameter (ie, strength) and number of fibers (ie, increase in pore size). Studies have also shown that a PP mesh with a pore size greater than 600 to 800 mm should result in more of a scar ''net'' rather than a scar ''plate''. The ''net'', compared to the ''plate'', is less prone to contracture and stiffness of the abdominal wall. Not all small-pore prosthetics are stiff. Consider what is seen clinically with microporous PTFE, and the maintenance of pliability even with encapsulation. It may then be that the architecture (woven versus solid) of the prosthetic is a more significant contributor to performance than the polymer itself. The upper limits of pore size for adequate fixation to prevent recurrence have not been appropriately investigated. Very large pore size (4,000 mm) combined with a partially absorbable component doesn't appear to have any clinical benefits in terms of pain, and may not be sufficient to prevent higher recurrence rates when used with a Lichtenstein technique (Earle & Mark, 2008). An ideal portfolio of meshes would have the benefits of both HW and LW meshes, such as the strength of an HW mesh and the flexibility of an LW mesh with none of the adverse events. The HW microporous meshes have a lower risk of tissue-to-mesh adhesion but carry a risk of encapsulation and foreign body reaction, resulting in decreased integration. LW macroporous mesh results in better tissue ingrowth and lower (ou less) foreign body reaction but may lead to a higher risk of adhesions (Eriksen et al., 2007). A larger pore size also provides optimal flexibility for improved physical properties, allowing a better activity profile post-surgery, but relinquishes memory, which is important for handling during the procedure. A monofilament mesh with a pore size of > 2.5 mm seems ideal. In all hernia repair techniques, a strong mesh is important for augmentation of the abdominal wall and to prevent recurrences (Bringman et al., 2010).

9. Charity campaigns involving biomaterials for low income patients.

Publications on campaigns performed in Africa show encouraging results with the use of sterilized mosquito net mesh. Clarke et al. report their results, implanting sterilized polyester mosquito net mesh in 95 poor patients in Ghana, with 2% infection and no recurrences. They concluded that PE mosquito net mesh is a cost-effective alternative to commercial mesh for use in inguinal hernia repair in developing countries (Clarke et al., 2009). Optimistic results were also described in a study performed before this one, in Burkina Faso, using Nylon (100% Polyamide 6-6) mosquito net mesh, this time describing the complete absence of infection (Freudenberg et al., 2006).

10. Establishing animal models for the development of biomaterials

Animal models resembling the human hernia are a useful tool for researchers to investigate hernia treatment options. The current animal models used to study hernia repair are not perfect. Artificially created hernias in animals are poor hernia models as they do not truly recreate the biological defects that cause hernias, such as collagen defects. Furthermore, the defects that are created to test mesh products are not real-life defects that surgeons would encounter. In order to serve as a useful model, the pathology in the animal must be similar to the human hernia equivalent. One factor when considering an animal model is similarities in the elasticity of the abdominal wall. Although there is no consensus for the most appropriate test or animal model, animal models are useful when comparing different meshes in the same species either in vivo or ex vivo. Studies in humans and large animals are the only way that most issues, such as elasticity, chronic pain, foreign body reaction, and adhesion, will be observed. What problems animal models can solve and which animals are the most appropriate for use will differ depending on the purpose of the study. Small animals or even cell cultures are instructive for studying the inflammatory reaction and biocompatibility, but for abdominal wall function and elasticity, larger animals are more suitable. Although ineffective for other comparisons, pigs are useful to simulate mesh implantation within the human body as pigs have a similar body size to humans. Sheep and rabbits are reasonable models to mimic vaginal operating conditions; potentially, they are also useful models for pelvic floor damage due to pregnancy and birth (Penttinen & Grönroos, 2008; Bringman et al., 2010).

11. Conclusion

Operation techniques using mesh result in fewer recurrences than techniques which do not use mesh.

12. Acknowledgment

The author declares no conflict of interest; none of the mesh manufacturers was involved in any way in this chapter. He particularly thanks three Brazilian herniologists who have guided him throughout his career: Prof. Antonio Portella, Prof. Fernando Pitrez and Prof. Manoel Trindade.

13. References

Abaza, R.; Perring, P. & Sferra, J.J. (2005). Novel parastomal hernia repair using a modified polypropylene and PTFE mesh. *J Am Coll Surg*.; 201(2): 316-17.

Acquaviva, D.E. & Bourret, P. (1944). Cure d'une volumineuse éventration par plaque de nylon. *Bull Méd Soc Chir Marseille*; 5: 17.

Agresta, F. & Bedin, N. (2008). Transabdominal laparoscopic inguinal hernia repair: is there a place for biological mesh? *Hernia*, 12: 609–612 DOI 10.1007/s10029-008-0390-0

Annibballi, R. & Fitzgibbons, J.R. (1994). Prosthetic material and adhesions formation. In: Arregui ME, Nagan RF: in Inguinal hernia: advances or controversies? Oxford: Radcliffe; pp. 115-124.

Adler, R.H. & Firme, C.N. (1959). Use of pliable synthetic mesh in the repair of hérnias and tissue defects. *Surg Gyn Obst*; 108: 199-206.

Amid, P.K. (1997). Classification of biomaterials and their related complications in abdominal wall hernia surgery. *Hernia* 1:15–21

Amid, P.K. (2001). Polypropylene prostheses. In R. Bendavid (Ed), Abdominal Wall Hernias. New York: Springer- Verlag Inc, 2001, Pp. 272-277.

Bachman, S. & Ramshaw, B. (2008). Prosthetic Material in Ventral Hernia Repair: How Do I Choose? *Surg Clin N Am,* 88: 101–112

Bellón, J.M. (2009). Implicaciones de los nuevos diseños protésicos de baja densidad en la mejora de la reparación de defectos herniarios. Revisión de conjunto. *Cir Esp*. 85(5) :268–273

Blatnik, J.; Jin, J. & Rosen, M. (2008). Abdominal hernia repair with bridging acellular dermal matrix—an expensive hernia sac. *Am J Surg* 196:47–50

Bringman, S.; Conze, J.; Cuccurullo, D.; Deprest, J.; Junge, k.; Klosterhalfen, B.; Parra-Davila, E. Ramshaw, B. & Schumpelick, V. (2010). Hernia repair: the search for ideal meshes. *Hernia* 14:81–87. DOI 10.1007/s10029-009-0587-x

Brown, J.B.; Fryer, M.P. & Ohlwiler, D.A. (1960). Study and use of sinthetic materials such as silicones and teflon, as subcutaneous prostheses. *Plast Reconst Surg*; 26: 264-279.

Burger, J.W.; Luijdendijk, R.W.; Hop, W.C.; Halm, J.A.; Verdaasdonk, E.G. & Jeekel, J. (2004). Long-term follow-up of a randomized controlled trial of suture versus mesh repair of incisional hernia. *Ann Surg* 240:578–585

Castro, C.C. & Rodrigues, S.M.C. (2007). Cicatrização de feridas. In Programa de atualização em cirurgia. Porto Alegre. Artmed, 2007; 2(4): 35-50.

Clarke, M.G.; Oppong, C.; Simmermacher, R.; Park, K.; Kurzer, M.; Vanotoo, L. & Kingsnorth, A.N. (2009). The use of sterilised polyester mosquito net mesh for inguinal hernia repair in Ghana. *Hernia* 13:155–159 DOI 10.1007/s10029-008-0460-3

Chan, G. & Chan, C.K. (2005). A review of incisional hernia repairs: preoperative weight loss and selective use of the mesh repair. *Hernia;* 9: 37-41.

Cobb, W.S.; Burns, J.M.; Peindl, R.D. (2006). Textile analysis of heavy weight, mid-weight, and light weight polypropylene mesh in a porcine ventral hernia model. *J Surg Res*, 136(1):1–7.

Collaboration, E.H. (2002). Repair of groin hernia with synthetic mesh: meta-analysis of randomized controlled trials. *Ann Surg* 235:322–332

Cumberland, V.H. (1952) A preliminary report on the use of prefabricated nylon weave in the repair of ventral hernia. *Med J Aust* 1:143–144

Deprest, J.; De Ridder, D. & Roovers, J.P. et al (2009). Medium term outcome of laparoscopic sacrocolpopexy with xenografts compared to synthetic grafts. *J Urol* 182:2362–2368

Dubay, D.A.; Wang, X.; Kuhn, M.A.; Robson, M.C. & Franz, M.G. (2004). The prevention of incisional hernia formation using a delayed-release polymer of basic fibroblast growth factor. *Ann Surg* 240:179–186.

Earle, D. & Romanelli, J. (2007). Prosthetic materials for hernia: what's new. *Contemporany Surgery*; 63(2): 63-69.

Earle, D.B. & Mark, L.A. (2008). Prosthetic material in inguinal hernia repair: How do I choose? *Surg Clin N Am*; 88:179–201.

Eriksen, J.R.; Gogenur, I. & Rosenberg, J. (2007). Choice of mesh for laparoscopic ventral hernia repair. *Hernia* 11:481–492. DOI 10.1007/s10029-007-0282-8

Falci, F. (1997) Análise crítica das próteses na região inguinal. In: Silva, A.L. Hérnias da parede abdominal. Clin Bras Cir CBC. Rio de Janeiro, Atheneu, 1997 ano III. V.1, p 141-151.

Falci, F. (2003) Utilização das próteses em hérnias da parede abdominal. In: Lira, O.B. & Franklin, R. *Hérnias – Texto e Atlas*. 1ª ed, Rio de Janeiro, Rubio, 2003, pp. 199-202.

Franklin, R.; Lira, O.B. & Filho, A.M. Introdução ao estudo das hérnias. In: Lira, O.B. & Franklin, R. *Hérnias – Texto e Atlas*. 1ª ed, Rio de Janeiro, Rubio, 2003, pp. 1-18

Gianlupi, A. & Trindade, M.R.M. (2004) Comparação entre o uso de fio inabsorvível (polipropileno) e fio absorvível (poliglactina 910) na fixação da prótese de polipropileno em correção de defeitos músculo-aponeuróticos da parede abdominal. Estudo experimental em ratos. *Acta Cir Bras*; 19(2): 94-102.

Goepel, R. (1900). Über die Verschliessung von Bruchpforten durch Einheilung geflochtener, fertiger Silberdrahtnetze. Gesellschaft für Chirurgie XXIX Congress 1900, 174-177.

Goldstein, H.S. (1999). Selecting the right mesh. *Hernia*. 3:23-26.

Gonzalez, R.; Fugate, K.; McClusky, D.; Ritter, E.M.; Lederman, A. & Dillehay, D. (2005). Relashionship between tissue ingrowth and mesh contraction. *World J Surg*; 29: 1038-1043.

Handley, W.S. (1963). En: Behandlung der Bauchnarbenbrüche. Reitter, H. *Langenbecks Arch Klin Chir*; 304: 296-297.

Hollinsky, C.; Sandberg, S.; Koch, T. & Seidler, S. (2008). Biomechanical properties of lightweight versus heavyweight meshes for laparoscopic inguinal hernia repair and their impact on recurrence rates. Surg Endosc (2008) 22:2679–2685. DOI 10.1007/s00464-008-9936-6

Hutchinson, R.W.; Chagnon, M. & Divilio, L. (2004). Pre-clinical abdominal adhesion studies with surgical mesh. Current Issues Technology. Business Briefing: Global Surgery: 29-32.

Junge, K.; Klinge, U.; Rosch, R.; Klosterhalfen, B. & Schumpelick, V. (2002). Functional and morphologic properties of a modified mesh for inguinal hernia repair. *World J Surg* 26:1472–1480

Junge, K.; Rosch, R. & Klinge, U. (2006). Risk factors related to recurrence in inguinal hernia repair: a retrospective analysis. *Hernia* 10:309–315

Klinge, U.; Klosterhalfen, B.; Conze, J.; Limberg, W.; Obolenski, B. & Ottinger, A.P. (1998). Modified mesh for hernia repair that is adapted to the physiology of the abdominal wall. *Eur J Surg*;164:951–60.

Klinge, U.; Klosterhalfen, B.; Birkenhauer, V.; Junge, K.; Conze, J. & Schumpelick, V. (2002). Impact of polymer pore size on the interface scar formation in a rat model. *J Surg Res*; 103: 208-214.

Klosterhalfen, B.; Junge, K. & Klinge, U. (2005). The lightweight and large porous mesh concept for hernia repair. *Expert Rev Med Devices* 2:103–117

Koontz, A.R. (1948). Premilinary report on the use of tantalum mesh in the repair of ventral hernias. *Ann Surg*; 127: 1079-1085.

Kneise, G. (1953). Erfahrungen und neue Erkenntnise bei der Perlonnetzimplantation. *Centralblatt für Chirurgie*; 12: 506-511.

Lemchen, H. & Irigaray, J.H. (2003). Ferida pós-operatória: conduta na evolução normal e nas complicações. In: Pitrez FAB. Pré e pós-operatório em cirurgia geral e especializada. 2ª ed. Artmed, 2003. Cap. 15. pp 130-136.

Lichtenstein, I.L.; Shulman, A.G.; Amid, P.K. & Montllor, M.M. (1989) The tension-free hernioplasty. *Am J Surg* 157:188–193

Malangoni, M.A. & Rosen, M.J. (2007). Hernias. :In Townsend: Sabiston Textbook of Surgery, 18th ed. Chapter 44. Copyright © 2007 Saunders, An Imprint of Elsevier

Mandl, W. (1962). Diskussionsbemerkung. Osterr Ges für Chirurgie und Unfallheilkunde. Salzburg, 1962, 6-8.

Mathews, B.D.; Pratt, B.L.; Pollinger, H.S.; Backus, C.L.; Kercher, K.W.; Sing, R.F. et al. (2003). Assessment of adhesion formation to intra-abdominal polypropylene mesh and polytetrafluoroethilene mesh. *J Surg Research*; 114: 126-132.

McNealy, R.W. & Glassman, J.A. (1946). Vitallium plates used in repair of large hernia. *Illinois Med Jour* 1946; 90: 170-173.

Melo, R.S.; Goldenberg, A.; Goldenberg, S.; Leal, A.T. & Magno, A. (2003). Effects of polypropylene prosthesis placed by inguinotomy in the preperitonial space, in dogs: evaluation laparoscopic and microscopic. *Acta Cir Bras 2003*; 18(4): 289-296

Monaco, J.L. & Lawrence, W.T. (2003). Acute wound healing an overview. *Clin Plast Surg*. 30 (1): 1-12.

Negro, P.; Basile, F.; Brescia, A.; Buonanno, G.M; Campanelli, G.; Canonico, S.; Cavalli, M.; Corrado, G.; Coscarella, G. & Di Lorenzo, N. et al. (2011). Open tension-free Lichtenstein repair of inguinal hernia: use of fibrin glue versus sutures for mesh fixation. *Hernia* Volume 15, Number 1, 7-14, DOI: 10.1007/s10029-010-0706-8

Nien, Y.D.; Man, Y.P. & Tawil, B. (2003). Fibrinogen inhibits fibroblast-mediated contraction of colagen. *Wound Repair Regen*; 11: 380-385.

Penttinen, R. & Grönroos, J.M. (2008). Mesh repair of common abdominal hernias: a review on experimental and clinical studies. *Hernia*. 12:337–344 DOI 10.1007/s10029-008-0362-4

Ponka, J.L. (1980). Hernia of abdominal wall. WB Saunders Company 1980. Philadelphia.

Rappert, E. (1963). Supramidnetze bei Bauchbrüchen. *Langenbecks Arch Klin Chir*; 304: 296-297.

Read, R.C. (2004). Milestones in the history of hernia surgery: prosthetic repair. *Hernia*; 8(1): 8-14.

Read, R.C. (2011). Crucial steps in the evolution of the preperitoneal approaches to the groin: an historical review. *Hernia*. Volume 15, Number 1, 1-5, DOI: 10.1007/s10029-010-0739-z.

Rodrigues, Jr.A.J.; Rodrigues, C.J.; Cunha, A.C.P. & Yoo, J. (2002). Quantitative analysis of collagen and elastic fibers in the transversalis fascia in direct and indirect hernia. *Rev Hosp Clín Fac Méd S Paulo*; 57(6): 265-270.

Rosen, M.J. (2010). Biologic Mesh for Abdominal Wall Reconstruction: A Critical Appraisal, *The American Surgeon.* Vol. 76, (January 2010), pp 1-6.

Saberski, E.R.; Orenstein, S.B. & Novitsky, Y.W. (2011). Anisotropic evaluation of synthetic surgical meshes. *Hernia.* Volume 15, Number 1, 47-52, DOI: 10.1007/s10029-010-0731-7.

Sans, J.V. (1986). Eventraciones – Procedimientos de reconstrucción de la pared abdominal. 1ª ed. Editorial Jims, 1986. Barcelona España, p 108-116.

Scales, J.T. (1953) Discussion on metals and synthetic material in relation to soft tissues; tissue reactions to synthetic materials. *Proc R Soc Med* 46:647–652

Schönbauer, L. & Fanta, H. (1958) Versorgung grosser Bauchwanddefecte mit implantiertem Chromeatgutnetz. *Brun's Beitr Klin Chir*; 196: 393-401.

Schreinemacher, M.H.F.; Emans, P.J.; Gijbels, M.J.J.; Greve, J.W.M.; Beets, G.L. & Bouvy, N.D. (2009). Degradation of mesh coatings and intraperitoneal adhesion formation in an experimental model. *Br J Surg*; 96: 305–313. DOI: 10.1002/bjs.6446

Silva, H.C.; Silva, A.L. & Oliveira, C.M. (2004). Peritoneum autogenous graft fibroblast: an experimental study. *Rev Col Bras Cir*; 31(2): 83-89.

Simons, M.P.; Aufenacker, T.; Bay-Nielsen, M.; Bouillot, J. L.; Campanelli, G.; Conze, J.; de Lange, D.; Fortelny, R.; Heikkinen, T.; Kingsnorth, A.; Kukleta, J.; Morales-Conde, S.; Nordin, P.; Schumpelick, V.; Smedberg, S.; Smietanski, M.; Weber, G. & Miserez, M. (2009). European Hernia Society guidelines on the treatment of inguinal hernia in adult patients. *Hernia*; 13:343–403. DOI 10.1007/s10029-009-0529-7

Speranzini, M.B. & Deutsch, C.R. (2001). Complicações das Hérnias: Encarceramento/Estrangulamento. In: Tratamento cirúrgico das hérnias das regiões inguinal e crural. 1ª ed. Atheneu, 2001. Cap 4. pp 43-55.

Speranzini, M.B. & Deutsch, C.R. (2001). Biomateriais. In: Tratamento cirúrgico das hérnias das regiões inguinal e crural. 1ª ed. Atheneu, 2001. Cap 5. pp 57-67.

Stoppa, R.G. & Rives, J. (1984). The use of dacron in the repair of hernias of the groin. *Surg Clin North América*; 64: 269-285.

Szczesny, W.; Cerkaska, K.; Tretyn, A. & Dabrowiecki, S. (2006). Etiology of inguinal hérnia: ultrastructure of rectus sheath revisited. *Hernia*; 10: 266-271.

Usher, F.C.; Ochsner, J. & Tuttle, L.L. Jr. (1958). Use of Marlex mesh in the repair of incisional hernias. *Am Surg* 24:969–974.

Usher, F.C. (1962) Hernia repair with Marlex Mesh. An analysis of 541 cases. *Arch Surg*; 84: 73-76.

Witzel, O. (1900). Über den Verschluss von Bauchwunden und Bruchpforten durch versenkte Silberdrahtnetze (Einheilung von Filigranpelotten). *Centralblatt für Chirurgie*; 10: 258-260.

Wolwacz, Jr.I.; Trindade, M.R.M. & Cerski, C.T. (2003). O colágeno em fáscia transversal de pacientes com hérnia inguinal direta submetidos à videolaparoscopia. *Acta Cir Bras*; 18(3): 196-202.

Zogbi, L.; Portella, A.O.V.; Trindade M.R.M. & Trindade, E.N. (2010). Retraction and fibroplasia in a polypropylene prosthesis: experimental study in rats. *Hernia* 14:291–298 DOI 10.1007/s10029-009-0607-x

19

Biopolymers as Wound Healing Materials: Challenges and New Strategies

Ali Demir Sezer[1] and Erdal Cevher[2]
[1]*Faculty of Pharmacy, Marmara University,*
[2]*Faculty of Pharmacy, Istanbul University,*
Turkey

1. Introduction

Wound healing is a multi-factorial physiological process. The complexity of this phenomenon makes it prone to several abnormalities. Apart from cellular and biochemical components, several enzymatic pathways also become active during repair and help the tissue to heal. The goal of this chapter is to introduce the biomaterials community to the emerging field of self-healing materials, and also to suggest how one could utilize and modify self-healing approaches to develop new classes of biomaterials. On the other hand, natural and synthetic gel-like materials, films/membranes, composites, micro-/nanoparticulate systems have featured heavily in the development of biomaterials for wound healing and other tissue-engineering purposes. Nanofibrous membranes are highly soft materials with high surface-to-volume ratios, and therefore can serve as excellent carriers for therapeutic agents or accelerate wound healing. Biocompatible and biodegradable polymer scaffolds combined with cells or biological signals are being investigated as alternatives to traditional options for tissue reconstruction and transplantation. These approaches are already in clinical use as engineered tissues that enhance wound healing and skin regeneration. This chapter covers the recent reports on the preparation and biomedical applications of biopolymers and biomaterials based on pharmaceutical dosage forms and wound dressing.

2. Skin structure

Skin is the largest organ of the integumentary system, comprising 15 % of the body weight. It protects the organism against injury and damage, and prevents passing of microorganisms and lets water vapour permeation. Substances secreted by glands in the epidermis contribute to the preservation of water - electrolyte balance of the body. The skin regulates body temperature by vasodilation and vasoconstriction of cutaneous blood vessels, and is formed by two main layers, including epidermis covering the body surface, and the dermis involving the connective tissue (Junqueria et al, 1992).

2.1 Epidermis

The epidermis consists of two different cell layers. It comes into existence whereas ectoderm is taking its form. Cells forming the top layer of epithelium undergo keratinisation and form

the dead layer of skin. Whereas dead cells are being pushed from the deeper portion of the epidermis toward the surface, they are replaced by proliferating cells by mitosis in the basal layer. This change is called cytomorphosis. Cytomorphosis takes an average of 15 to 30 days for a healthy individual. The basic cell type of epidermis is keratinocytes. The content of the keratin constantly changes in the epidermis because keratinocytes undergo changes in epidermis and consists of 85 % of total protein of the *Stratum corneum* (Gartner et al., 2001). Keratinocytes synthesize different keratins in different stages of cytomorphosis. Whereas basal layer cells include only low molecular weight keratins, cells with high molecular weight keratin begin to build the heap structure of the *Stratum corneum* as the cells move upward. Keratins in this layer are cross-connected by disulphide bonds at the same time.
The epidermis consists of five layers. These are, respectively, from the inside to out (Junqueria et al., 1992).
Stratum basale (germinativum): This layer consists of a single row of cylindrical cells sitting on the basal membrane, located on the dermis and basal lamina. This layer is responsible for continuous renewal of the epidermis due to the proliferation of cells. Cytoplasmic fibrillar protein is found in all cells that form the structure. As proliferating cells migrate towards the upper layer, the number of protein filaments increases.
Stratum spinosum: This is a multi-storey layer composed of polygonal or squamous epithelial cells. The cytoplasm and cytoplasmic extensions are filled with bundles of fibrils and connected to each other with bridges on the cell surface. These cells are called spino-cellular cells, due to the spine-like structures around this layer of cells. All the layers of both *Stratum basale* and *Stratum spinosum* are called the Malpighian layer.
Stratum granulosum: This layer consists of small, flat, polygonal-shaped cells. These cells contain keratohyalin granules. The number of lamellar structures emerging in the *Stratum spinosum* increases in the *Stratum granulosum*, their contents are secreted to intercellular spaces as accumulating in the periphery of the cell, providing intercellular lipids, which are essential for the barrier function of the epidermis.
Stratum lucidum (Transparent layer): This layer is composed of flat, transparent, and tightly gathered cells ranging from 3 to 5 rows. It is a thin layer that is only found in regions where the epidermis is thick. The cytoplasm of the *transparent layer* is filled with a substance refracting light called eleidin and cell organelles decrease in this layer. As tonofibrils become more numerous and regular, they make the cell membrane thicker. Desmosomes are located between cells and the amount of intercellular materials increases.
Stratum corneum: It is a dead cell layer having no nucleus. Keratin is found in the cytoplasm of these cells. Intercellular gaps are full of lipids which are secreted from the lamellar structures in the *Stratum spinosum* and *Stratum granulosum*. Superficial cells of the *Stratum corneum* shed continuously (desquamation) and new tissue is produced by mitosis of cells in the germinal layer. Keratinization occurs with the formation of disulfide groups from sulphydryl groups of protein fibrils during migration to the upper layer. These protein fibrils make reticulated bundles, forming a substantial long chain by disulfide bonds and also including a dense, amorphous matrix between them, composed of keratohyalin granules. At this stage, the cell membrane thickens. This layer, formed by the thickening of the cell membrane, takes the shape of cornified cells losing its core and other organelles after reaching of keratohyalin granules to maximum point and forming of keratin lipids (Gartner et al., 2001; Junqueria et al., 1992).

2.2 Dermis

The dermis is a type of elastic, flexible bond tissue locating under epidermis and is vascularised, enabling it to provide energy and nutrition to the epidermis. The dermis extends limitlessly by integrating to the subcutaneous layer and its thickness varies according to the region (Leeson & Leeson, 1981). Its surface contacting the epidermis is rough and composed of papillae. Papillae are named *Stratum papillare* by integrating deep surface of the epidermis. Some papillae also contain special nerve endings, called vascular papillae (Young & Heath, 2000). The deepest part of dermis is called as *Stratum reticulare*. This layer consists of irregular, dense connective tissue and has rather weak cells, primarily fibroblasts and macrophages. Hair follicles are concentrated around sebaceous and sweat glands in the dermis (Leeson & Leeson, 1981).

2.3 Hypodermis

Hypodermis, the subcutaneous layer, is a loose connective tissue located under the dermis and containing varying amounts of flat cells. Collagen and elastic fibrils within its structure continue into the dermis. Hair roots also are found in this layer (Junqueria et al., 1992; Leeson et al., 1988). The increase in the number of fibrils results in a rigid binding of dermis to hypodermis and thus affects the mobility of the skin.

3. Wounds and burns

3.1 Types of wounds

A wound is the disruption of the integrity of anatomical tissues caused by exposure to any factor. Wounds are examined under two groups:

Closed Wounds: This group includes contusion, hematoma and abrasion. Contusion-type injuries involve damage to soft tissues, small blood vessels and deep tissue layers, resulting in their separation, but the anatomy of the skin remains intact. Oedema, and in later periods, atrophy and defective pigmentation are observed in wound and the healing is delayed. Vessel rupture or hyperaemia due to vessel damage is called hematoma and wounds such as scrapes are termed abrasions. The healing process is very painful because this type of wound involves damage to sensory nerves and the wound can easily become infected (Mutsaers et al., 1997).

Open Wounds: This group includes lacerations, cutting-pricking tool wounds, gunshot wounds, surgical wounds, insect bites and stings, radionecrosis, vascular neurological and metabolic wounds. Wounds except for lacerations cause serious damage to tissues beneath the skin. In laceration type wounds, skin and subcutaneous tissue have been destroyed, but deep tissues remain healthy. The anatomical integrity of tissues is damaged in cutting-pricking tool wounds without any tissue damage at the edges of the wound (Aydın, 2000; Kapoor & Appleton, 2005).

Wounds are also classified according to tissue loss.

Wounds with Tissue Loss: These types of wounds involve damage or loss in some or all of the skin layers. Healing occurs *via* filling of the wound area by granulation tissue typically growing from the base of a wound. Wounds that involve tissue loss are collected in two groups in proportion to the loss. In superficial wounds, the entire epidermis and the papillar layer of the dermis are damaged. The epidermis, all the layers of the dermis and even

subcutaneous tissue are damaged in full-thickness wounds covering second group (Mutsaers et al., 1997; Porth, 1998; Chanson et al., 2005).
Wounds without Tissue Loss: These kinds of wounds occur as a result of tissue crushing. The severity of bleeding occurring in tissue varies according to the condition of the wound. Tissues exposed to this kind of wound heal after granulation tissue formation in minimal level in first phase of healing process (Ruszczak, 2003).

3.2 Types of burns

Burn is a kind of wound that occurs when skin or organs are damaged by an electrical current, heat, chemical or flammable agent effect. It is known that burn-initiated pathophysiological events differ from other traumas, may cause death risks and lead to increasing capillary permeability, resulting in hypovolemia. Burn causes changes of vascular permeability, extravasation of plasma proteins, aggregation of platelets and increased fibrinolysis (Yenerman, 1986; Madri, 1990; Atiyeh et al., 2005).
Burns are divided into 4 groups according to the depth and the affected skin layers:

3.2.1 First-degree burns

Only the outer layer of the epidermis and *Stratum corneum* are damaged in this type of burn, and there is no damage in the dermis. First-degree burns generally occur as a result of short-term heat or flame contact or long-term exposing to intense sunlight. First-degree burn areas are characterised by slight oedema, which diminishes after 24 hours. At this stage the skin begins to dry, there is no vesicle and infection is not seen. The wound heals within a week (Whitney & Wickline, 2003).

3.2.2 Second-degree burns

These types of burns are deeper than first-degree burns and necrosis spread into the dermis. Damage covers the entire epidermis and some part of dermis. The wound is clinically characterised by pain, erythema and bullae. The recovery rate depends on the depth of skin injury and formation of infection. Generally, second-degree burns heal spontaneously in a short period if infection does not occur. If infection occurs in the wound, it can easily convert to third degree burn.
The burns in this group may be divided into two categories, termed superficial and deep dermal second-degree burns (Sparkes, 1997; Whitney & Wickline, 2003):
Superficial Second Degree Burns: These occur due to short period contact with flame or hot liquids. Generally, the upper portion of the *Stratum germinativum* is damaged in superficial second-degree burns. The surface is generally humid because of the leakage of liquid plasma from the burned area. Generally, less scarring than the deep dermal burns occurs. Recovery usually occurs within 3-4 weeks with zero or very mild scarring (Madri, 1990).
Deep Dermal Burns: These occur due to contact with chemicals such as flame, hot liquids or acids, or exposure to high electrical current. In these types of burns, whereas the epidermis is completely burned, damage extends to the *Stratum germinativum* and the bottom section of the dermis. In deep dermal burns, fluid loss and metabolic effects are the same as in third-degree burns. Wound pain is very severe during burning and hyperanesthesia may occur in some areas. The wound may develop into a third-degree burn if infection occurs in the burn area. The time required for re-epithelialisation depends on degradation in the dermis, the amount of burnt hair follicles and sweat

glands, and the width of infected areas. If the wound is properly preserved, it usually closes within 2 months, leaving some scarring on the skin surface. Scarring and contracture occur in healing areas where closing lasts longer than 2 months. In this case, it is very difficult to distinguish the wound from third-degree burns and treatment of this kind of wound will last longer (Porth, 1998; Shakespeare, 2001).

3.2.3 Third-degree burn

These kinds of burns result from hot water, fire and prolonged contact with electrical current. The wound area exhibits tautness and brightness as the elasticity of the skin is lost, causing abnormal shrinkage. In such cases, all structures within the skin sustain damage. The dermis and subcutaneous fat are destroyed as a result of coagulation necrosis. Thrombosis occurs in vessels under the skin. Increased capillary permeability and oedema is much higher in third-degree burns than second-degree burns. Skin is damaged in all layers and is characterised by autolysis and leukocytoclastic infiltration for 2 or 3 weeks. This event is usually associated with suppuration. Capillary bundles and fibroblasts are organised in granulation tissue under scar. If the burn affects subcutaneous fat, healing can take much longer. Burn affecting the muscle causes increasing in degradation of red blood cells. The care of third-degree burns requires removing scar tissue and covering the wound with a graft. If grafting is not carried out, a thick layer of granulation is shaped and the contraction of the area follows it. At this stage, re-epithelialisation, slightly, occurs on the edge of wound granulation is soft, can be infected and healing continues over several months. Permanent deep scars in the skin occur following healing in these kinds of wounds and surgical intervention is usually required to restore normal appearance (Moulin et al., 2000; Shakespeare, 2001).

3.2.4 Fourth-degree burns

This refers to the carbonization of burned tissues.

4. Wound and burn treatment

4.1 Developments in the treatment of wounds and burns

A range of methods has been used to treat wounds, dating back to ancient times. The earliest information on wound treatment is found in Egyptian medical documents, called the Ebers Papyrus. It is known that ancient Egyptians treated wounds by covering them frog skin and castor oil. The results have been limited and partially misleading, although humans have used many materials of biological origin in wound and burn treatment throughout history and have conducted various experiments on animals. The first wide-ranging microscopic study was conducted by Hartwell in the 1930s. Hartwell compared human wounds to those in pigs, rabbits, dogs and guinea pigs and found that the wound healing progress is different in human epithelial and subepithelial surfaces, compared to those of animals. If the pathological table of wound healing is also taken into account, it was confirmed that pig physiopathology was most similar to humans, followed by that of rabbits. Later, Gangjee et al. (1985) conducted studies of percutaneous wound healing. Winter et al. (1965) developed animal models of wounds and burns using pigs as a subject for wound treatment and concluded that, as the histology of skin and the wound healing mechanism differs between animals and humans, animal models or experiments can only provide a general indication of wound healing phases.

Researchers subsequently sought new materials for use in wound healing, due to the disadvantages of traditional dressings such as gauze, paraffin gauze, biological dressings, etc. The first synthetic material used for wound coverage was methyl cellulose. The common feature of all these materials is the necessity of physical protection from external factors and conditions. Many new materials have been used as the wound healing mechanism has become better understood. The usage of artificial dressing materials in forms such as film, spray, foam and gel have increased significantly in recent years (Shakespeare & Shakespeare, 2002; Stashak et al., 2004; Merei, 2004)

The following characteristics are required for ideal wound and burn dressing (Sheridan & Tompkins, 1999; Balasubramani et al., 2001; Jones et al., 2002);

- ease of application
- bioadhesiveness to the wound surface
- sufficient water vapour permeability
- easily sterilised
- inhibition of bacterial invasion
- elasticity and high mechanical strength
- compatibility with topical therapeutic agents
- optimum oxygen permeability
- biodegradability
- non-toxic and non-antigenic properties

Average water loss from normal human skin is 250 g/m^2/day. In wounded skin, this figure can reach up 5000 g/m^2/day according to the type of wound. If a wound dressing material is thin and has extreme water vapour permeability, it causes accumulation of liquid, bacterial growing and delay in recovery (Alper et al., 1982; Fansler et al., 1995). Wound coverings should be adequately adhesive to the wound surface and edges. At the end of treatment, cover material should also permit removal in such a manner that it does not harm any tissues, must not cause toxic or antigenic reactions, and must be biocompatible. The materials used should not cause contamination of microorganisms on the wound surface and, if possible, it should also prevent the proliferation of bacteria in normal skin flora. Wound dressing materials should be easy to apply and have sufficient elasticity and mechanical strength to be used in areas especially close to the joints. The surface of the dressing material that is in contact with the wound should support the development of fibrovascular tissue as creating a convenient platform for wound healing. Adequate oxygenation is important in wound healing, so dressing material should provide contact the wound with oxygen. In addition, major desirable characteristics are that wound dressing materials should be easily sterilised, have a long shelf-life, and be cost-effective (Quinn et al., 1985; Lloyd et al., 1998; Stashak et al., 2004).

4.2 Classification of dressings used in wound and burn treatment

Materials used to cover wounds and burns are also called artificial skin, as they fulfil the functions of normal skin within areas with wounds and partly destroyed skin.

Wound and burn covering materials are classified as follows (Freyman et al., 2001; Stashak et al., 2004);

1. Traditional dressing
2. Biomaterial-based dressings
3. Artificial dressings

4.2.1 Traditional dressing

These are still the most commonly used materials for wound and burn dressings (Balasubramani et al, 2001). The traditional dressings, which are generally used during first intervention in wound treatment, prevent wound's contact with outer environment and bleeding (Sheridan & Tompkins, 1999; Stashak et al., 2004). The best sample of this group is gauze and gauze-cotton composites which have very high absorption capacity. As they cause rapid dehydration whereas they are being removed from the wound surface, they can cause bleeding and damage of newly formed epithelium (Naimer & Chemla, 2000; Stashak et al, 2004). Therefore, gauze composites with a non-adhesive inner surface are prepared to reduce the pain and trauma which can occur when removing traditional wound dressings from the wound surface.
Traditional wound dressings in the world market are shown in Table 1.

Dressing material	Brand name	Manufacturer
Paraffin gauze dressing containing 0.5% chlorhexidine acetate	Bactigras	Smith & Nephew
Paraffin gauze dressing	Jelonet	Smith & Nephew
Petrolatum gauze	Xeroform	Chesebrough-Pond's Inc.
Petrolatum gauze containing 3% bismuth tribromophenate	Xeroform	Chesebrough-Pond's Inc.
Scarlet Red dressing	Scarlet Red	Chesebrough-Pond's Inc.
Sterile hydrogel dressing	2nd skin®	Spenco
Highly absorbent cotton wool pad	Gamgee® pad	3M
Highly absorbent rayon/cellulose blend sandwiched with a layer of anti-shear high density polyethylene	Exu Dry Dressing	Smith & Nephew
Absorbent cotton pad	Telfa "Ouchless" Nonadherent Dressings	Kendall (Covidien)

Table 1. Traditional wound dressings in the world market.

Exudate leaking from traditional dressing materials usually increases the risk of infection and is one of the most significant problems of these type dressings. Antibacterial agents are added into the dressings to eliminate the infection. In addition, one of the most significant problems encountered in this material is foreign body reaction in the wound caused by cotton fibres. The biggest advantage of these materials is their low cost (Lim et al., 2000; Price et al., 2001; Stashak et al., 2004).

4.2.2 Biomaterial-based dressings

The most convenient method used in complete closure of wounds and burns is autografting. However, inadequate donor areas for large wounds led to the search for a new tissue source (Sheridon et al., 2001). Biological dressings are natural dressings with collagen-type structures, generally including elastin and lipid.
Such dressings can mainly be categorised under the following groups (Sheridon et al., 2001; Kearney, 2001).

1. Allografts
2. Tissue derivatives
3. Xenografts

Some biomaterial-based dressings, which were used for the treatment of wounds and burns, is shown in Table 2.

Type of dressing	Dressing material	Brand name	References/ Manufacturer
Allograft	Scalp tissue	-------	Barnett et al. (1983)
	Amniotic membrane	-------	Peters and Wirth (2003)
Xsenograft	Porcine tissue	Mediskin	Genetic Lab.
	Silver impregnated porcine tissue	E-Z derm	Genetic Lab.
Skin derivatives	Highly purified bovine collagen	-------	Chvapil et al. (1973)
	Formaline fixed skin	-------	Chvapil et al. (1973)

Table 2. Biomaterial-based dressings.

Allografts

The most common source for this type of dressing is fresh or freeze-dried skin fragments taken from the patient's relatives or cadavers. Immune reaction as a result of the use of allograft can be seen and the body may reject the tissue. Infection risk also increases with suppression of the immune system to prevent the body's rejection of transplanted tissue.
The other disadvantages of these dressings include the difficulty of preparation, lack of donors, high cost and limited shelf life (Nanchahal et al., 2002; Ruszczak, 2003).
Amniotic membrane, which is separated from chorion, generally uses in superficial partial thickness burns as a dressing material for many years (Ravishanker et al., 2003). Though it has advantages such as ease of preparation and use, it has disadvantages like causing cross-infection and dehydration of the wound (Freyman et al., 2001; Jones et al., 2002). Amniotic membrane derived from a healthy donor is shown in Figure 1.

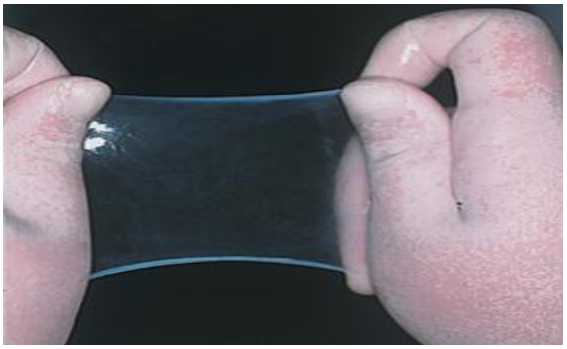

Fig. 1. The cryo-preserved amniotic membrane was thawed prior to its application (Hasegawa et al., 2007).

The effectiveness of amniotic membranes as dressing materials in burn treatment is summarized in Table 3.

Dressing quality	Amniotic membrane
Pain relief	+++
Infection prevention	+++
Good adherence to wound bed	+++
Promotion of re-epithelialisation	+++
Cost factor	++
Moist wound healing environment	++
Elasticity/conformability	+++
Easy application	++
Prevention of heat loss	+
Availability	++

+++, very good; ++, average; +, below average

Table 3. Qualities of an ideal dressing for partial-thickness burns (Branski et al., 2008).

In vitro epidermal cell cultures are new and currently expensive systems used to prepare dressing materials. These can be applied in the form of autologous or homologous epithelial cell cultures and are still at the development stage (Beckenstein et al., 2004; Manwaring et al., 2004).

Xenografts

Xenografts are commercially available materials contrary to autografts and allografts. The most common of xenografts is the ones derived from pig skin (Sheridan et al., 2001) which have a long shelf-life and can be sterilized easily (Sheridan & Tompkins, 1999). Although pig skin is not microscopically similar to human skin, it shows close similarity in terms of adhesion and collagen content. Its disadvantage is the risk of triggering an immune response due to the foreign tissue.

Tissue derivatives

These materials, derived from different forms of collagen, have the advantages like ease of preparation, low contamination risk and weak antigenic features. The greatest disadvantage of these materials is the risk of infection, particularly in long term usage (Jones et al., 2002; Stashak et al., 2004).

4.2.3 Artificial dressings

The usage of traditional dressing materials and biomaterial-based dressings is restricted due to factors such as their stability problems and risk of infection. These conditions brought up the use of wound and burn dressing materials being cheaper and more effective, and having long shelf-life. Many dressing materials have ideal features for the treatment of wounds and burns; however, due to the variations between pathophysiology of the wound and burn, it is difficult to develop an artificial dressing material that meets all the criteria for optimum healing. Much research is currently being undertaken studies to develop wound dressing materials that can provide optimum healing conditions, taking into account all of these factors and healing mechanisms (inflammation, tissue replacement, fibrosis, coagulation, etc.) (Still et al., 2003; Stashak et al., 2004).

Some of artificial wound and burn dressing materials in world market are shown in Table 4.

Type	Dressing material	Brand name	Company
Film/membrane	Polyurethane	Omiderm	Omicron Scientific
		Opsite	Smith & Nephew
		Bioclusive	Johnson & Johnson
		Tegaderm	3M
	Polyvinyl chloride	Strech Neal	Colgate
	Nylon velour	Capran77C	Allied Chemical Corp.
	Polyvinylidene chloride	Saran Wrap	Asahi Kasei
	Polyurethane hydrocolloid	Granuflex	ConvaTec
	Synthetic fibre + aluminium	Aluderm	Söhngen
	Synthetic fibre + metal	Scanpore tape	Norgeplaster
	Activated charcoal	Carbopad	Charcoal
Foam	Formalinized polyvinyl alcohol	Ivalon	Chardack
	Polyurethane	Lyofoam	Ultra Labs
	Poly(dimethylsiloxane)	Silastic	Dow Corning
Gel	Calcium alginate	Kaltostat	ConvaTec
	Polyurethane with grafted acrylamide and hydroxyethylmethacrylate	Omiderm	Omicron Scientific
Composite	Polyprophylene film and polyurethane foam	Epigard	Parke-Davis
	Silicone film with a nylon fabric	Biobrane	Smith & Nephew
Spray	Methacrylic acid ethoxyethyl ester	Nobecutane	Astra Zeneca
	Polyhydroxyethylmethacrylate and polyethylene glycol 400	Hydron	Hydron Lab.

Table 4. Artificial wound and burn dressings in world market.

4.2.3.1 Polymers used for artificial dressings

Many natural and synthetic polymers are being used in the preparation of artificial dressing materials.
The most widely used of these includes:

a. Natural polymers

Collagen

Collagen is a biodegradable and biocompatible protein mostly found in connective tissue. The first medical usage of collagen in humans was reported by Knapp et al. (1977) and was used to provide co-reaction of contour deformities. Bovine collagen was used as suture and hemostatic agents after years. In 1980, Zyderm 1 was released, a suspension form containing sterilised fibrillar bovine collagen that was used for injecting under the dermis in wounds. Today, collagen is used in numerous biomedical applications (Hafemann et al., 1999; Ortega & Milner, 2000). These include collagen suspensions for dermal injection, topical haemostatic agents, wound dressing materials, collagen suture and catguts, collagen gels for periodontal reconstruction, collagen sponges for the hemostasis and coating of joint, and collagen rich pig skin wound dressing materials (Gingras et al., 2003; Park et al., 2004).

Alginic acid and its salts

Alginic acid, is a natural polysaccharide derived from brown algae such as *Laminaria* and *Ascophyllum* species. Alginic acid are formed by linear block copolymerization of D-mannuronic acid and L-guluronic acid. Alginic acid and its salts are used for the treatment of wound and burn due to their haemostatic properties. Their first applications were in the form of a gel, but sponges produced from calcium alginate are also used effectively in the treatment of wounds. It is also indicated that calcium alginate increases cellular activity properties such as adhesion and proliferation (Thomas, 2000a, 2000b and 2000c).

Hyaluronic acid and its derivatives

Hyaluronic acid is a natural biopolymer that alternately consists of D-glucuronic acid and 2-acetamido-2-deoxy-D-glucose and is generally found in mammal's bond tissues and synovial fluids (Saliba, 2001; Kirker et al., 2002). It has been reported that hyaluronic acid interacts with proteins, proteoglycans, growth factors and tissue components called biomolecules which has vital importance in healing of various types of wounds (Park et al., 2003). This interaction plays an important role in acceleration of tissue repair and wound healing. Hyaluronic acid and its derivatives also play a role in the protection of the injured area against microorganisms due to their bacteriostatic activity (Miller et al., 2003; Lobmann et al., 2003).

Chitosan

Chitosan, which is produced by deacetylation of kitin, is a linear polysaccharide composed of randomly distributed β-(1-4)-linked D-glucosamine (deacetylated unit) and N-acetyl-D-glucosamine (acetylated unit) (Muzzarelli & Muzzarelli, 2002; Krajewska, 2004). Chitosan is used in the treatment of wounds and burns due to its haemostatic effect (Ueno et al., 1999; Khor & Lim, 2003; Şenel & McClure, 2004). It is thought that chitosan accelerates the formation of fibroblasts and increases early phase reactions related to healing (Paul & Sharma, 2004). Chitosan can be prepared in a variety of forms, namely films, hydrogels, fibres, powders and micro-/nanoparticles. Applications of this biopolymer in commercial and biomedical fields have increased due to the low toxicity of chitosan and its biodegradation products, and its biocompatibility with blood and tissues (Berthold et al., 1994; Cho et al., 1999; Tan et al., 2001; Ishihara et al., 2002; Kim et al., 2002; Mi et al., 2002).

Fucoidan

Fucoidan is a sulphated polyfucose polysaccharide and has attracted considerable biotechnological research interest since the discovery that it possessed anti-coagulant activity similar to that of heparin and also reported to possess other properties including anti-thrombotic, anti-inflammatory, anti-tumoral and anti-viral effects (Patankar et al., 1993). Many of these effects are thought to be due to its interaction with growth factors such as basic fibroblast growth factor (bFGF) and transforming growth factor-β (TGF-β). Fucoidan may, therefore, be able to modulate growth factor-dependent pathways in the cell biology of tissue repair (O'Leary et al., 2004). In recent years, the research on drug and gene delivery systems, diagnostic microparticles and wound and burn healing formulations of fucoidan has been increasing in course of time (Sezer et al., 2008a and 2008b, Sezer & Akbuğa, 2009).

Poly-N-acetyl glucosamine

Poly-N-acetyl glucosamine which is produced from marine microalgae, has hemostatic activity and are used as a support material in the treatment of burns and wounds (Pietramaggiori et al., 2008).

b. Synthetic polymers

Polyurethanes and their derivatives

Polyurethanes are copolymers containing urethane groups in their structures. In general, they are formed by conjugation of diol groups and diisocyanate groups with polymerisation reaction (Trumble et al., 2002). A large number of non-toxic polyurethanes are synthesized for use in biomedical applications. One of these, Pellethane 2363-80A which accelerates re-epithelialisation was used as dressing material in the treatment of burn and wound (Wright et al., 1998; Pachulski et al., 2002).

Teflon

Teflon is a polymer that is synthesized by polymerization of tetrafluoroethylene at high temperature and pressure. Teflon is an inert material which is non-carcinogenic, insoluble in polar and nonpolar solvents, and which can be sterilized. It can take the desired shape by application of low-pressure and can easily be applied to the injured area (Raphael et al., 1999; Lee & Worthington, 1999).

Proplast

Proplast which is the first synthetic biomaterial, specially developed for implant applications. It is among the particularly preferred materials in wound, burn and surgical applications due to its high biocompatibility with tissue (Şenyuva et al., 1997).

Methyl methacrylate

Methyl methacrylate is a non-biodegradable synthetic polymer that is resistant to heat and UV. It is used as a dressing and supporting material in plastic surgery and the treatment of injuries (Nakabayashi, 2003).

Silicon

Silicon is used extensively for biomedical purposes. It has low toxicity, low allergic properties and high biocompatibility in the body (O'Donovan et al., 1999; Jansson & Tengvall, 2001). This polymer, which is resistant to biodegradation, is used in the preparation of implant elastomers used in soft tissue repair and in the production of hypodermic needles and syringes (Van den Kerckhove et al., 2001; Park et al., 2002). In addition, silicon is also often used as wound support material in severe wounds and burns due to its high tissue compatibility (Whelan, 2002; Losi et al., 2004).

4.3 Pharmaceutical formulations used as dressings for wounds and burns

Many pharmaceutical formulations have been recently developed as synthetic dressing material for wound and burn treatment.

4.3.1 Films/membranes

These pharmaceutical dosage forms, which are available in thickness ranging from μm to mm, are prepared by different methods using one or more polymers. Films are ideal dressing materials and available in commercial. Films/membranes with a homogeneous polymeric network structure are used to treat the damaged area and generally protect the wound and burn area against external factors (Verma & Iyer, 2000; Stashak et al., 2004). The polymers used in the preparation of films include; polyurethane, polyvinylpyrrolidone (Yoo

& Kim, 2008), hyaluronic acid (Xu et al., 2007; Uppal et al., 2011), collagen (Boa et al., 2008), sodium alginate (Kim et al., 2008a and 2008b) chitosan and its derivatives (Tanigawa et al., 2008), poly-N-acetyl glucosamine (Pietramaggiori et al., 2008) and fucoidan (Sezer et al., 2007). In a clinical study, as a result of *in vitro* studies of polyurethane / poly (N-vinylpyrrolidone) composite film combinations, it was reported that their water absorption capacity was high and water vapour permeability was between 1816-2728 g /m^2 /day. It was seen that recovery in the injured area was significantly increased and a new epithelial tissue was formed in 15 day period following application of these prepared formulations to full-thickness wounds induced in a rat model (Yoo & Kim, 2008). Tanigawa et al. (2008) prepared scaffold formulations by using chitosan citrate and chitosan acetate, which are natural polymers, and examined the effectiveness of the formulations on wound healing in mice with damaged epidermis. The scaffold, prepared by a lyophilisation method, gave quite a distinct pore structure especially inside it, depending on the type of the acid used for the preparation of chitosan solution; the pore consisted of fibrous networks appeared in chitosan citrate, whereas the pore surround by cell walls occurred in chitosan acetate. Despite the large difference in the pore structure, both scaffolds were effective in regeneration of the outher skin. However, chitosan citrate scaffold provided better facilitation in wound healing than the chitosan acetate one (Tanigawa et al., 2008). Commercially available collagen-based film formulations also used in the treatment of dermal burns (Boa et al., 2008). In a recent study, the treatment efficacy of collagen-based films was investigated in second-degree burns created in 45 Wistar rats. The prepared collagen film formulations were applied to the wound alone or in combination with liposome formulations containing usnic acid, and then examined after 14 and 21 days. The use of the usnic acid provided more rapid substitution of type-III for type-I collagen on the 14th day, and improved the collagenisation density on the 21st day. It was concluded that the use of reconstituted bovine type-I collagen-based films containing usnic acid improved burn healing process (Nunes et al., 2011). Differences in healing of wounds are summarized in histological sections in Figure 2.

In another study, the researchers hypothesized that a poly-N-acetyl glucosamine (pGlcNAc) fibre patch might enhance wound healing in diabetic (db/db) mice. Wounds dressed with pGlcNAc patches for 1 h closed faster than control wounds, reaching 90% closure in 16.6 days, 9 days faster than untreated wounds. Granulation tissue showed higher levels of proliferation and vascularization after 1 h treatment than the 24 h and left-untreated groups. Foreign body reaction to the material was not noted in applications up to 24 h (Pietramaggiori et al., 2008).

The primary negative factor affecting healing of burns and wounds is the loss of skin integrity. It is indicated in the literature that wound and burn healing occur much more quickly with the help of a dressing material (Mutsaers et al., 1997; Kapoor & Appleton, 2005). Therefore, in recent years, the use of biopolymers has gained priority in tissue engineering and biotechnology, both as dressing material and in terms of enhancing treatment efficiency (Atiyeh et al., 2005).

A biopolymer, fucoidan, consisting of fucose and sulphate groups has been used for the treatment of burns and wounds (Sezer et al., 2007, 2008a and 2008b). It was reported that fucoidan shows anticoagulant effect and heparin activity (Sezer & Cevher 2011). It was also reported that films prepared with fucoidan do not prevent contact of the wound surface with air oxygen, provide the moisture balance in wound/burn area, accelerate the migration of fibroblasts and provide re-epithelialisation (Sezer et al., 2007) (Table 5).

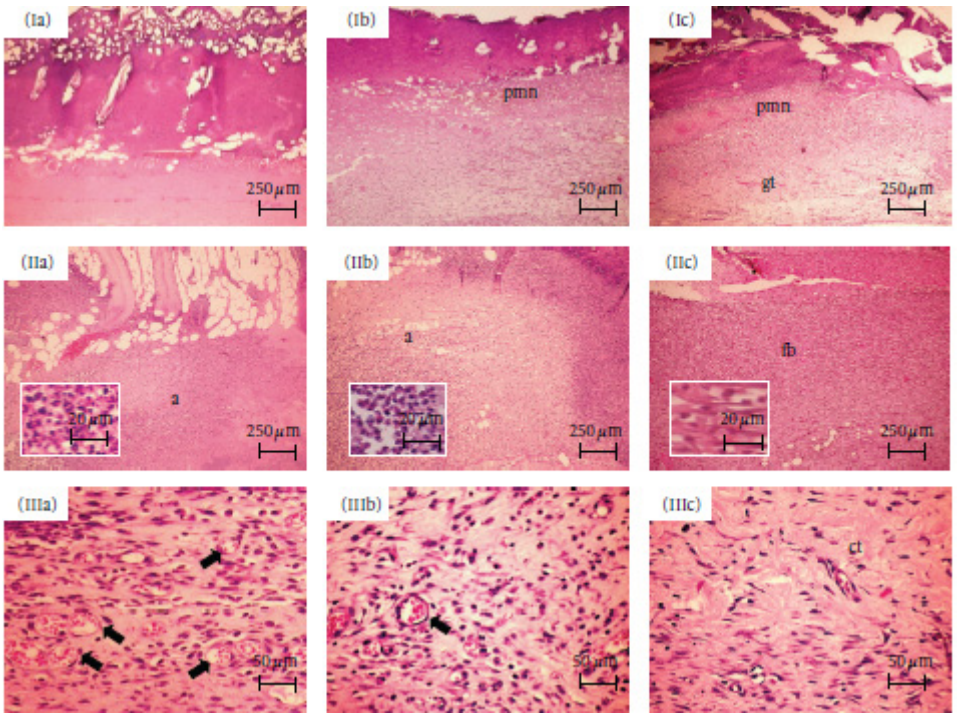

Fig. 2. Histological sections stained in hematoxylen-eosin. Seven days: (Ia) Lack of inflammatory response in the center of the burned area in COL. (Ib) Inflammatory infiltrate rich in polymorphonuclear neutrophils (pmn) in PHO. (Ic) Expressive content of polymorphonuclear neutrophils (pmn) in the top of the wound, and early granulation tissue (gt) formation in the bottom, in UAL. Fourteen days: (IIa and IIb) Intense acute inflammatory reaction (a) scattered within the burned area in COL and PHO, respectively. Neutrophils seen in detail. (IIc) Moderate infiltrate of neutrophils and lymphocytes in association to expressive fibroblastic proliferation (fb) in UAL. Fibroblasts seen in detail. Twentyone days: (IIIa and IIIb) Vascular component (arrows), and chronic inflammatory infiltrate, still evident in COL and PHO, respectively. (IIIc) Scanty inflammatory cells are seen within the cicatricial tissue (ct) in UAL. *COL—animals treated with collagen-based films; PHO—animals treated with collagen films containing empty liposomes; UAL—animals treated with collagen-based films containing usnic acid incorporated into liposomes (Nunes et al., 2011).

	Day 7				Day 14				Day 21			
Codes	Fibroblast	Collagen	MN	PMNL	Fibroblast	Collagen	MN	PMNL	Fibroblast	Collagen	MN	PMNL
Control	+ (6/6)	− (5/6) + (1/6)	− (5/6) + (1/6)	+ (2/6) ++ (2/6) +++(2/6)	+ (4/6) ++ (2/6)	− (4/6) + (2/6)	− (4/6) + (2/6)	+ (3/6) ++ (2/6) +++ (1/6)	+ (4/6) ++ (1/6) +++(1/6)	+ (3/6) ++(3/6)	+ (6/6)	+ (5/6) ++ (1/6)
FS	++ (6/6)	− (1/6) + (5/6)	− (5/6) + (1/6)	− (2/6) + (4/6)	+ (1/6) ++ (5/6)	+ (3/6) ++ (3/6)	− (2/6) + (4/6)	− (4/6) + (2/6)	+ (6/6)	+ (4/6) ++ (2/6)	− (4/6) + (2/6)	− (4/6) + (2/6)
CF	+ (6/6)	− (4/6) + (2/6)	− (5/6) + (1/6)	+ (4/6) ++ (2/6)	+ (4/6) ++ (2/6)	+ (6/6)	− (4/6) + (2/6)	+ (4/6) ++ (2/6)	++ (5/6) +++(1/6)	++ (4/6) +++(2/6)	− (2/6) + (3/6) ++ (1/6)	− (3/6) + (3/6)
CFF	+ (6/6)	+ (6/6)	− (3/6) + (2/6) ++(1/6)	+ (3/6) ++ (3/6)	+ (1/6) ++ (1/6) +++(4/6)	++ (4/6) +++(2/6)	+ (3/6) ++ (2/6) +++(1/6)	− (6/6)	− (4/6) + (2/6)	− (5/6) + (1/6)	− (6/6)	− (6/6)

*MN indicates mononuclear leukocyte; PMNL, polymorphonuclear leukocyte; —, absent; +, mild; ++, moderate; +++, severe; FS, fucoidan solution; CF, chitosan film without fucoidan; and CFF, chitosan film containing fucoidan.

Table 5. The score of the wound cells and collagen (Sezer et al., 2007).

4.3.2 Gels

Gels are viscous semi-solid preparations formed by dispersion of inorganic or organic substances that have larger size than colloidal particles in a liquid phase. Hydrogels are semi-solid systems, formed by a combination of one or more hydrophilic polymer. They are among the dressing materials frequently used in the treatment of wounds and burns. As they are capable of absorbing much more water than their weight, they act as dressing, reducing potential irritation when in contact with tissue and other similar structures. They keep moisture at the application site and permit oxygen penetration (Hoffman, 2002; Jeong et al., 2002). Hydrogels have many advantages including patient compliance, treatment efficacy and ease of application. The advantages of hydrogels in wound and burn treatment can be listed as follows (Kumar et al., 2001; Hoffman, 2002; Jeong et al., 2002; Byrne et al., 2002);

- Bioadhesion of gels to the surface of the wound is high and this also eases the treatment due to increased contact with the wound
- Their structures facilitate the moisture and water vapour permeability necessary to heal the wound area
- Difficulties that are particularly related to the application to open wounds are not seen in these preparations
- They can easily be removed from the application site when adverse events seen

Natural polymers are generally preferred in the preparation of hydrogels. Hyaluronan is a biopolymer widely used in the treatment of wounds. It is non-toxic, non-immunogenic, and has very good resorption characteristics in biomedical applications, which allow this biopolymer to be used in the treatment of wounds. In a study, cross-linked glycol chitosan/hyaluronan hydrogels was prepared and found that they displayed the characteristics required of an ideal wound dressing material (Wang, 2006). Chitosan is obtained by partial deacetylation of the amines of chitin. Its use has been explored in various biomaterial and medical applications. Chitosan has desirable qualities, such as hemostasis, wound healing, bacteriostatic, biocompatibility, and biodegradability properties. Chitosan appears to have no adverse effects after implantation in tissues and, for this reason, it has been used for a wide range of biomedical applications. Chitosan was also used to inhibit fibroplasia in wound healing and to promote tissue growth and differentiation in culture (Alsarra, 2009).

The efficacy of chitosans with different molecular weights and deacetylation degrees was investigated in the treatment of wounds (Sezer, 2011). The treatment efficacy of gels prepared with chitosans with low, medium and high molecular weight was examined in a rat full-thickness wound model in which the epidermis and dermis had been damaged. Chitosan gel formulations were also compared with Fucidin® ointment containing fusidic acid. Chitosan was found to promote the migration of the inflammatory cells which are capable of the production and secretion of a large repertoire of pro-inflammatory products and growth factors at a very early phase of healing. Fucidin® ointment-treated rats revealed a site that was not completely healed but more improved and with a smaller lesion than that of untreated groups. In comparison with high molecular weight chitosan-treated wounds (after 12 days), the wound site was so perfectly healed that it was difficult to distinguish it from normal skin (Figure 3) (Alsarra, 2009).

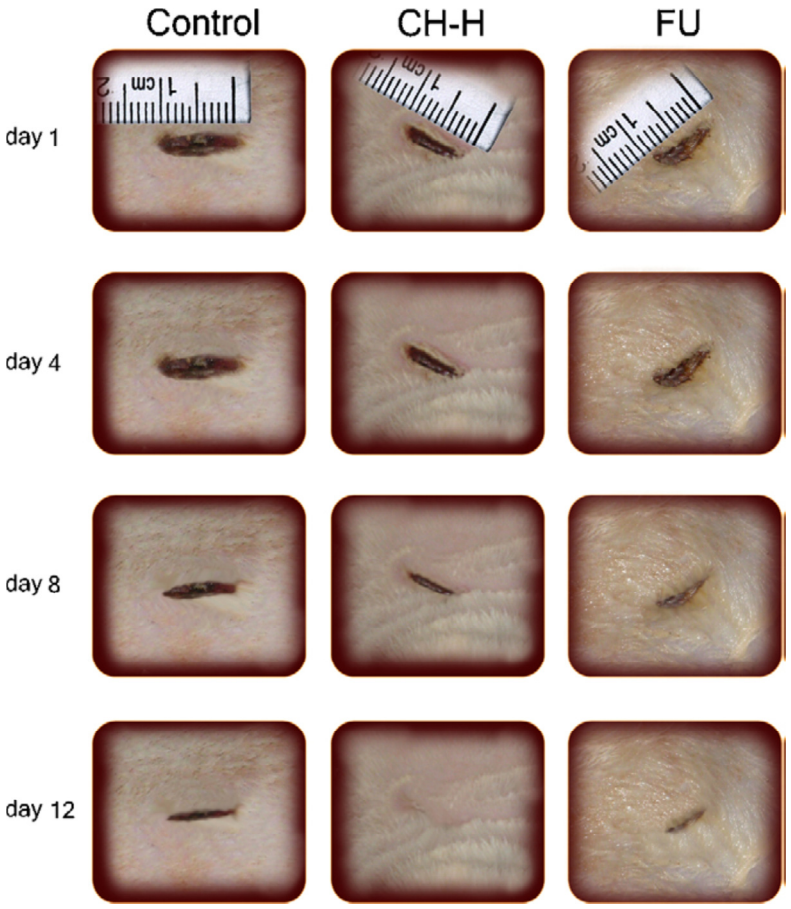

Fig. 3. Photographs of macroscopic appearances of wound excised from rats that were untreated (control), treated with high molecular weight chitosan (CH-H), or treated with Fucidin® ointment (FU) (Alsarra, 2009).

The efficacy of chitosan gel formulations containing silver sulfadiazine in the treatment of burn was examined. Due to its pseudoplastic characteristic and high bioadhesiveness, the chitosan gels with and without silver sulfadiazine showed a satisfactory retention time over the wounds. Wounds treated with chitosan gel with silver sulfadiazine showed a higher fibroblast production and a better angiogenesis than that of commercially available silver sulfadiazine cream, which are important parameters on the evolution of the healing process (Nascimento et al., 2009).

Polyvinyl alcohol hydrogels with different combinations, prepared with chitosan and dextran, are also used as wound dressing material. It was recorded that these cross-linked hydrogels are capable of ideal water absorption and swelling and provide an ideal moist environment necessary for wound healing. In addition, it has been reported in the literature that cross-linking of polyvinyl alcohol with dextran and chitosan increases the flexibility and elasticity of the gel (Sung et al., 2010; Hwang et al., 2010).

In another study, the novel thermoreversible wound gel formulation containing Polyhexadine showed good results for wound treatment and represented an alternative to silver sulfadiazine cream and iodine-based ointment, which are toxic and associated with many allergic reactions. The open randomized controlled single-center study was carried out on 44 patients in 2 parallel groups (Traumasept®wound covering gel vs. Flammazine®). The transparency of the thermosensitive gel formulation and absence of staining allowed for good wound assessment, without the need for painful cleaning, and the change from the fluid to the gel state enabled easy handling and filling the wound cavities (Goertz et al., 2010).

One of the most important parameters of the injured tissue pathology is to stop the bleeding and to protect the area with a protective support material in the first step. It is reported that hydrogels prepared using oxidised dextran and allylamine hydrochloride decreased coagulation and increased cloth strength and consequently are able to decrease the haemorrhage in clinical use (Peng & Shek, 2009).

The use of various proteins in topical wound treatment is also recorded in the literature (Ji et al., 2009). Wound treatment efficacy of methylcellulose gel dressings including recombinant human vascular endothelial growth factor (rhVEGF) have been examined by Ji et al. (2009). The dressings being studied were Adaptic®, Non-stick Dressing, Conformant 2®, Opsite®™ and Tegapore™. The criteria to select a compatible dressing include protein stability, absence of leachables from the dressing, and ability to retain gel on wound. Results showed that rhVEGF was significantly oxidized by Adaptic dressing in 24 h. Protein oxidation was likely due to the peroxides, as determined by ferrous oxidation with xylenol orange (FOX) assay, released into the protein solution from the dressing. In conclusion, Tegapore™ was considered suitable for the rhVEGF topical gel (Ji et al., 2009).

A similar study determined the gel properties of sodium carboxymethyl cellulose and fusidic acid and aimed to improve them as wound dressings. It was reported that swelling, flexibility and elasticity properties of sodium carboxymethyl cellulose (Na-CMC) gels was changed depending on sodium fucidate and the cross linker (PVA) content in the formulation. Hydrogel formulation containing 2.5% PVA, 1.125% Na-CMC and 0.2% sodium fucidate adsorbed exudate from the wound surface adequately and kept the moisture sufficiently in wound area and consequently, it was recommended as an ideal wound dressing material. (Lim et al., 2010).

Hydroxyapatite (HA) and silk fibroin (SF) composites are biomaterials used in wound treatment. It was reported that the polarized HA (pHA) transforms the SF structure into a porous three-dimensional scaffold. SF gel containing pHA was found to be higher promotive effects on wound healing, re-epithelialisation and matrix formation (Okabayashi et al., 2009).

Gelatine is commonly used in the treatment of wounds and burns, and acts as supportive tissue when used in the treatment of dermal burns with various biopolymers. Balakrishnan et al. (2005) applied hydrogel formulations containing oxidised alginate and gelatine to the 1 cm^2 full-thickness skin wounds created in rat model and the results evaluated histologically. At 15th day, test wounds appeared reduced in size with new epithelium noted at both the edges of the defect with the proliferation of basal layer and formation of the rete pegs. New collagen formed in the dermis appeared mature. Granulation tissue was seen in dermis. Granulation tissue formation is essential for permanent wound closure, since it fills the defects and prepares the way for re-epithelialisation. These findings support that alginate/gelatin hydrogel is able to provide suitable condition for granulation tissue formation. At 15th day, in test wounds, the defect area became smaller and filled with fibro-proliferative tissue. Inflammatory cells were absent. However, for some control wounds though the entire surface of the defect was covered with new epithelium, moderate number of inflammatory cells, predominantly lymphocytes and macrophages, were still present in the upper dermis. Though superficially neither control nor test wounds showed any reduction in defect area at 5th day, on measuring the wound re-epithelialisation it was found that both wounds have started healing (Balakrishnan et al., 2005).

In a previous study has shown successful treatment with fucoidan-chitosan hydrogels which were tested in New Zealand rabbits with second degree burn (Sezer et al., 2008a). In another study, chitin/chitosan, fucoidan and alginate hydrogel blends were prepared and the granulation tissue and capillary formation were found to be increased in the first 7 days of the treatment of induced wounds (Murakami et al., 2010).

4.3.3 Sprays and foams

Sprays are pharmaceutical forms containing the solvent and polymer, forming a film layer on the surface of the wound when sprayed. The best example of a spray-based artificial wound and burn dressing is Hydron. It is prepared with polyhydroxyethyl methacrylate powder and liquid polyethylene glycol. When it is sprayed on the surface of the wound, it creates a thin and transparent film layer. In studies it was found that sprays reduce the pain of the wound, but have disadvantages including loss of integrity of the dressing and accumulation of sub-membrane fluid. Researchers stated that Hydron provides an effective treatment when applied to small partial thickness wounds and to areas which are away from joints (Dressler et al., 1980; Pruitt & Levine, 1984). Another example of aerosol sprays is papain-pectin sprays. The spray-on topical wound debrider composition consisting of 0.1% papain immobilized in 6% pectin gel was formulated for skin wound healing. The stability of the enzyme activity of this new formulated spray was compared with the 0.1% papain in water solution at the refrigerated temperature of 4C. and 75°C. Prepared formulations were tested on experimental wounds created on rabbits. In the study groups treated by pectin-papain aerosol spray compared with a control group.

During the experiment, no obvious healing process inhibition or side effects were visually observed. Upon spray application on the surgical wound, the aerosol formed a thin, smooth, and even film staying in place on the wound bedwithout dripping, promoting wound healing after drying versus an untreated wound (as control). The spray bottle was easy to maneuver; making it possible to reach areas of each wound that otherwise might receive inadequate coverage. The progress of healing was overall higher with the spray at 2 times more in the first four days of treatment. The difference was calculated to be significant based on the Student´s t-test method with the resulting $p < 0.05$. It was concluded that papain immobilized in pectin can be used for the development of effective aerosol spray system for wound healing in the areas of enzymatic debridement of necrotic tissue and liquefaction of slough to remove dead or contaminated tissue in acute and chronic lesions, such as diabetic ulcers, pressure ulcers, varicose ulcers, and traumatic infected wounds, postoperative wounds, burns, carbuncles, and pilonidal cyst wounds (Jáuregui et al., 2009).
Lyofoam, polyurethane foam, is normally hydrophobic; however, when applying heat and pressure, it becomes hydrophilic and, in this form, while providing blood and exudates absorption, it also prevents drying the wound surface completely (Johnson et al., 1998; Catarino et al., 2000; Fenn & Butler, 2001; Lehnert & Jhala, 2005).

4.3.4 Composites

Composites developed for wound treatment may involve an elastic outer layer with high mechanical strength, which is resistant to the effects of the environment and provides moisture by preventing evaporation; in contrast, the inner layer provide adhesion of the composite to the surface of the wound. Telfa™ is a dressing material, including cotton, covered by polyester film and is used both for providing absorption and preventing dehydration of the wound surface (Kickhöfen et al., 1986). Clinical studies have been conducted of chitin nanofibrils/chitosan glycolate composites (Muzzarelli et al., 2007), salmon milt DNA/salmon collagen composites (Shen et al., 2008), polymer-xerogel composites (Costache et al., 2010), and autologous cellular gel matrix systems (Weinstein-Oppenheimer et al., 2010). Chitin and chitosan composites were found to be very promising in the treatment of wounds. Muzzarelli et al. (2007) tested the wound treatment activity of spray, gel and gauze forms of nanofibrils chitin/chitosan glycolate composites on both Wistar male rats and 75 patients between the ages of 45-70. Recovery was particularly good when applied gauze to gangrenous tissue (Figure 4).
It was shown that the nanofibrillar chitin/chitosan glycolate composites appeared to be most suitable as medicaments able to exert control over various biochemical and physiological processes involved in wound healing besides haemostasis. Whereas chitosan provided antimicrobial activity, cell stimulation capacity and filmogenicity, chitin nanofibrils restructured the gel, released N-acetylglucosamine slowly and recognised proteins and growth factors.
In another study, Shen et al. (2008) examined the neovascularization and fibrillogenesis effects of salmon milt DNA and salmon collagen (SC) composites when used for the treatment of wounds. Tissue loss of wounds treated with composites was repaired quickly and the epidermal layer was formed quickly by means of sDNA (Shen et al., 2008).
Biobrane, is a collagen-silicone based composite, uses as a skin graft to treat injuries (Figure 5). The outer layer of the membrane is a thin and semi-permeable layer consisting of silicon. This layer allows water permeation but prevents the entry of microorganisms. Type I pig collagen forms an inner layer with an inert, hydrophilic network structure and provides a

suitable platform for the development of granulation tissue. Water transfer can be maintained similar to that of natural skin by modifying the membrane thickness (Suzuki et al., 1990; Ou et al., 1998; Still et al., 2003).

Fig. 4. Gangrenous pyoderma on tibial surface. Treated with Gauze and i.v. therapy of steroids and cyclosporine to ameliorate the wound bed. Complete healing in 40 days (Muzzarelli et al., 2007).

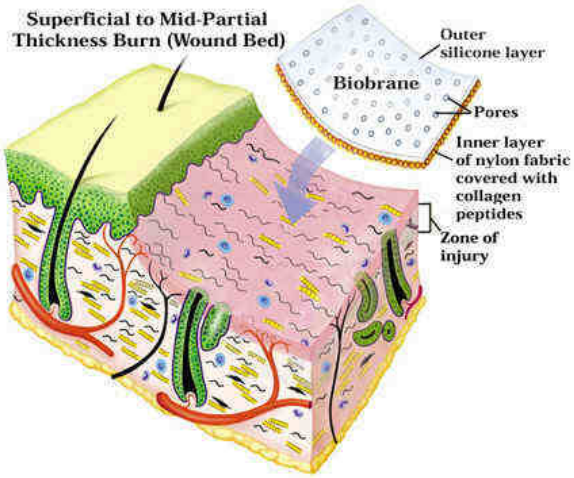

Fig. 5. Schematic observation of biobrane application on superficial to mid-partial thickness burn (http://www.burnsurgery.com).

Bilaminar composite membranes containing bovine collagen-based dermal analogue and silastic epidermis has been developed for the treatment of wounds and burns. It is stated that biocompatible bovine collagen-based dermal analogue slowly degrades and provides a suitable environment for the development of the patient's connective tissue; in addition, the epidermal layer's water vapour permeability is close to the skin and protects the wound from trauma and microorganisms (Still et al., 2003).
There are certain restrictions in the areas in which skin source materials can be applied as dressings. Biodegradable or non-biodegradable unilaminar and bilaminar composite membranes function as a serous crust and reduce pain but can not prevent infection. It is stated that synthetic composites do not constitute infection, are suitable for use with antimicrobial solutions and are easily applied to wound tissue (Van den Kerckhove et al., 2001; Van Zuijlen et al., 2003).

4.3.5 Particulate systems

The biggest advantages of particulate systems are that, when applied locally to open wounds, they easily provide water vapour and oxygen permeability of the wound; and have large contact surfaces and high bioadhesiveness due to their multiparticulate structures. Drug release in the wound area can be controlled with particulate system, and this increases the speed of wound healing (Kawaguchi, 2000; Date & Patravale, 2004).
In recent studies on micro-/nanoparticulate systems in wound and burn treatment, the use of nitric oxide nanoparticles (Martinez et al., 2009), poly (ethylene-co-vinyl alcohol) nanofiber (Xu et al., 2011), silver nanoparticles (Lakshmana et al., 2010; Xu et al., 2011), fucoidan microparticles (Sezer et al., 2008b), collagen sponges (Still et al., 2003; Lee, 2005), and liposomes containing epidermal growth factor (Alemdaroglu et al., 2008) have examined. *Staphylococcus aureus* is a gram-positive bacteria, capable of rapidly proliferating in the injured area and causing infection, causes superficial and invasive skin infections. Wounded skin is suitable media for the growth of such pathogenic microorganisms. Various clinical studies have attempted to develop strategies and formulations to address this common issue of pathogenic infection. Topically applied nitric oxide (NO) is a potentially useful preventive and therapeutic strategy against superficial skin infections, including methicillin-resistant *Staphylococcus aureus* infections. NO modulates immune responses and is a significant regulator of wound healing (Martinez et al., 2009). NO nanoparticles were prepared by combination of sodium nitrite with tetramethylorthosilicate, polyethylene glycol, chitosan, glucose. The mechanisms through which the NO nanoparticles accelerate wound healing were further determined by establishing whether NO nanoparticles prevented collagen degradation by MRSA in the infected tissue. Collagen content was highest in both uninfected and infected wounds treated with NO nanoparticles, although nanoparticles-treated uninfected tissue also had high collagen content. The dispersed blue stain indicated thicker and more mature tissue collagen formation in wounds treated with NO nanoparticles, suggesting that NO nanoparticles exposure maintained dermal architecture through bacterial clearance, and ultimately by guarding collagen (Figure 6) (Martinez et al., 2009).
Silver has been used in wound treatment since ancient times. Ointments including silver sulfadiazine are also frequently used in the treatment of burns. Silver affects pathogenic bacteria in wound and burn areas in different ways. Silver ions interacting with bacterial enzymes are taken up inside the bacterial cells, impair the DNA of the bacteria and prevent cell proliferation. Silver ions also attach the cell wall and disrupt the integrity of cell

membrane and kill the bacteria (Klasen, 2000a and 2000b). Poly (ethylene-co-vinyl alcohol) fibre systems including silver nanoparticles were prepared for the treatment of wounds. The results showed that the nanofibre size can be controlled by regulating polymer solution concentration. It has been reported that high concentration of silver might change the fibre morphology. Results of bacterial tests showed that pathogen-restraining ability of the silver-encapsulated nanofibres was effective and proportional over a range of silver concentration, indicating its inflammation control capacity and the potential for applications in skin wound treatment (Xu et al., 2011).

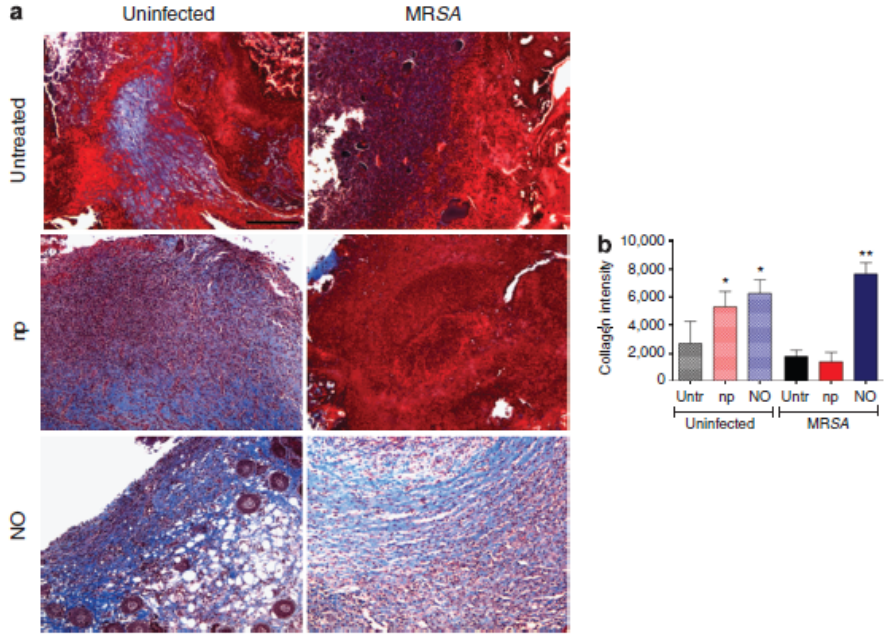

Fig. 6. NO-nps decrease collagen degradation in skin lesions of Balb/c mice. (a) Histological analysis of Balb/c mice uninfected and untreated, uninfected treated with nanoparticles without nitric oxide (NO) (np), uninfected treated with NO-nps (NO), untreated methicillin-resistant Staphylococcus aureus (MRSA)-infected, np-treated MRSA-infected, and MRSA-infected treated with NO, day 7. Mice were infected with 107 bacterial cells. The blue stain indicates collagen. Bar ¼ 25 mm. (b) Quantitative measurement of collagen intensity in 16 representative fields of the same size for uninfected and untreated, uninfected treated with nanoparticles without NO (np), uninfected treated with NO, untreated MRSA-infected, np-treated MRSA-infected, and MRSA-infected treated with NO wounds. Bars are the averages of the results, and error bars denote SDs. *P<0.01 in comparing the untreated groups with the uninfected np- and NO-treated groups; **P<0.001 in comparing the untreated groups with the MRSA + NO group (Martinez et al., 2009).

In another study, silver nanoparticles were synthesized by aqueous and organic methods and incorporated into electrospun polyurethane (PU) nanofibre to enhance the antibacterial as well as wound healing properties. The electrospinning parameters were optimized for PU

with and without silver nanoparticles. The water absorption, antibacterial and cytocompatibility of the PU-silver nanofibers were studied and compared to that of conventional PU foam. The results indicated that the PU-Ag nanofibers could be used for wound dressing applications (Lakshmana et al., 2010).

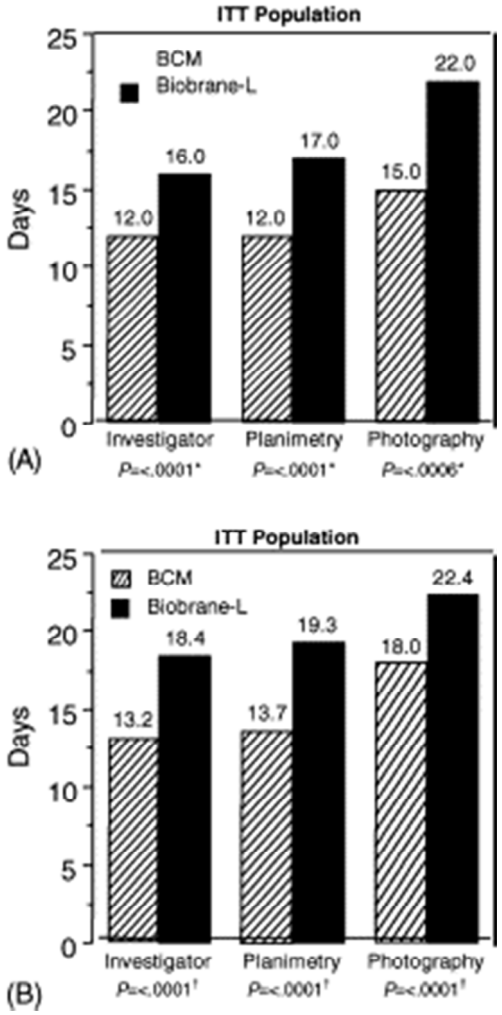

Fig. 7. Days to 100% wound closure. Median times to wound closure is shown in (A) and mean times are shown in (B). BCM indicates bilayered cellular matrix (OrCelTM); intent-to-treat (ITT). ∗Log-rank test of the difference between treatment healing times, stratified by patient. †Paired t-test (Still et al., 2003).

In different stages of wound healing, various cell types, cytokines, coagulation factors, growth factors, complement activation and matrix proteins are involved in different extents. Collagen is one of the most important structural protein components of connective tissue. It is difficult to say at which stage collagen predominates because wound healing is a dynamic

event involving many stages. There are many different clinical applications of collagen. For example, collagen gel is often used to treat haemophilia patients due to its haemostatic effects (Tan et al., 2001; Lee et al., 2002; Ruszczak, 2003; Beckenstein et al., 2004). By using microsponge technology, which is a new type of pharmaceutical dosage form, collagen-based particles are clinically tested in the treatment of wounds and burns and were reported to have positive results compared with commercial preparations (Ruszczak, 2003; Beckenstein et al., 2004). Still et al. (2003) examined the safety and efficacy of porous collagen sponge containing co-cultured allogeneic donor epidermal keratinocytes and dermal fibroblasts from human neonatal foreskin tissue (OrCel™) in facilitating timely wound closure of split-thickness donor sites in severely burned patients. Utilized a matched pairs design; each patient had two designated donor sites of equivalent surface area and depth. Sites were randomized to receive a single treatment of either OrCel™ or the standard dressing Biobrane-L®. The treatment of donor site wounds with OrCel™ is well tolerated, promotes more rapid healing, and results in reduced scarring when compared with conventional therapy with Biobrane-L® (Still et al., 2003). Data on wound closure as a result of the treatment are given in Figure 7. As seen in Figure 7, the cell based-membrane sponges improved the healing of the wound.

The efficacy of microsponges containing epidermal growth factor (EGF) was investigated clinically. It was found that the application of EGF microsponges to the burn surface increased the activity of fibrinogen and thus fibroblast synthesis and migration were seen at the injury site (Lee, 2005). Also, liposome systems in which EGF had been encapsulated was used as particulate carrier systems in the treatment of wounds and burns. Positive results were reported in terms of eschar tissue formation and wound healing with these systems, when especially used in the treatment of second-degree burns (Alemdaroglu et al., 2008).

5. Conclusion

The biopolymers are more effective as a wound-healing accelerator than synthetic polymers. The wound treated with biopolymers and biomaterials shows accelerated healing. Biopolymers structural arrangement is similar to that of normal skin. Consequently, the biopolymers are considered to be one of ideal materials with biocompatibility, biodegradability, and wound healing property as well as easy application.

6. References

Alemdaroglu, C.; Degim, Z.; Çelebi, N.; Şengezer, M.; Alömeroglu, M. & Nacar, A.(2008). Investigation of epidermal growth factor containing liposome formulation effects on burn wound healing, *Journal of Biomedical Materials Research*, Vol.85A, pp.271–283.

Alper, J.C.; Welch, E.A.; Ginsberg, M.; Bogaars, H. & Maguire, P. (1983). Moist wound healing under a vapor permeable membrane, *Journal of the American Academy of Dermatology*, Vol.8, pp.347-353.

Alsarra, I.A. (2009). Chitosan topical gel formulation in the management of burn wounds, *International Journal of Biological Meacromolecules*, Vol.45, pp.16-21.

Atiyeh, B.S.; Hayek, S.N. & Gunn, S.W. (2005). New technologies for burn wound closure and healing-review of the literature, *Burns*, Vol.31, pp.944-956.

Balasubramani, M.; Kumar, T.R. & Babu, M. (2001). Skin substitutes: a review. *Burns*, Vol.27, pp.534-544.

Balakrishnan, B.; Mohanty, M.; Umashankar, P.R. & Jayakrishnan, A. (2005). Evaluation of an in situ forming hydrogel wound dressing based on oxidized alginate and gelatin, *Biomaterials*, Vol.26, No.32, pp.6335-6342.

Bao, L.; Yang, W.; Mao, X.; Mou, S. & Tang, S. (2008). Agar/collagen membrane as skin dressing for wounds, *Biomedical Materials*, Vol.3, pp.1-7.

Barnett, A; Berkowitz, R.L.; Mills, R. & Vistnes, L.M. (1983). Scalp as skin graft donor site: rapid reuse with synthetic adhesive moisture vapour permeable dressings, *Journal of Trauma*, Vol.23, pp.148-151.

Beckenstein, M.S.; Kuniaki, T. & Matarasso, A. (2004). The effect of scarguard on collagenase levels using a full-thickness epidermal model, *Aesthetic Surgery Journal*, Vol.24, pp.542-546.

Berthod, F.; Saintigny, G.; Chretien, F.; Hayek, D.; Collombel, C. & Damour, O. (1994). Optimization of thickness, pore size and mechanical properties of a biomaterial designed for deep burn coverage, *Clinical Materials*, Vol.15, pp.259-265.

Branski, L.K.; Herndon, D.N.; Celis, M.M.; Norbury, W.B.; Masters, O.E. & Jeschke, M.G. (2008). Amnion in the treatment of pediatric partial-thickness facial burns, *Burns*, Vol.34, No.3, pp.393-399.

Byrne, M.E.; Park, K. & Peppas, N.A. (2002). Molecular imprinting within hydrogels, *Advanced Drug Delivery Reviews*, Vol.54, pp.149-161.

Catarino, P.A.; Chamberlain, M.H.; Wright, N.C.; Black, E.; Campbell, K.; Robson, D. & Pillai, R.G. (2000). High-pressure suction drainage via a polyurethane foam in the management of poststernotomy mediastinitis, *Annals of Thoracic Surgery*, Vol.70, pp.1891-1895.

Chanson, M.; Derouette, J.; Roth, I.; Foglia, B.; Scerri, I.; Dudez, T. & Kwak, B.R. (2005). Gap junctional communication in tissue inflammation and repair, *BBA*, Vol.1711, pp.197-207.

Cho, Y.W.; Cho, Y.N.; Chung, S.H.; Yoo, G. & Ko, S.W. (1999). Water-soluble chitin as a wound healing accelerator, *Biomaterials*, Vol.20, pp.2139-2145.

Chvapil, M.; Kronenthal, R,L. & Van Winkle, W. (1973). Medical and surgical applications of collagen, *International Review of Connective Tissue Research*, Vol.6, pp.1–61.

Costache, M.C.; Qu, H.; Ducheyne, P. & Devore, D.I. (2010). Polymer-xerogel composites for controlled release wound dressings, *Biomaterials*, Vol.31, No.24, pp.6336-6343.

Date, A.A. & Patravale, V.B. (2004). Current strategies for engineering drug nanoparticles, *Current Opinion in Colloid and Interface Science*, Vol.9, pp.222-235.

Dressler, D.P.; Barbee, W.K. & Sprenger, R. (1980). The effect of Hydron® burn wound dressing on burned rat and rabbit ear wound healing, *Journal of Trauma*, Vol.20, pp.1024-1028.

Fansler, R.F.; Taheri, P.; Cullinane, C.; Sabates, B. & Flint, L.M. (1995). Polypropylene mesh closure of the complicated abdominal wound, *American Journal of Surgery*, Vol.170, pp.15-18.

Fenn, C.H. & Butler, P.E.M. (2001). Abdominoplasty wound-healing complications: assisted closure using foam suction dressing, *British Journal of Plastic Surgery*, Vol.54, pp.348-351.

Freyman, T.M.; Yannas, I.V. & Gibson, L.J. (2001). Cellular materials as porous scaffolds for tissue engineering, *Progress in Materials Science*, Vol.46, pp.273-282.

Gangjee, T.; Colaizzo, R. & Von Recum, A.F. (1985). Species-related differences in percutaneous wound healing, *Annals of Biomedical Engineering*, Vol.13, No.5, pp.451-467.

Gingras, M.; Paradis, I. & Berthod, F. (2003). Nerve regeneration in a collagen-chitosan tissue-engineered skin transplanted on nude mice, *Biomaterials*, Vol.24, pp.1653-1661.

Goertz, O.; Abels, C.; Knie, U.; May, T.; Hirsch, T.; Daigeler, A.; Steinau, H.U. & Langer, S. (2010). Clinical safety and efficacy of a novel thermoreversible polyhexanide-preserved wound covering gel, *European Surgical Research*, Vol. 44, No.2, pp.96-101.

Hafemann, B.; Ensslen, S.; Erdmann, C.; Niedballa, R.; Zühlke, A.; Ghofrani, K. & Kirkpatrick, C.J. (1999). Use of a collagen/elastin-membrane for the tissue engineering of dermis, *Burns*, Vol.25, pp.373-384.

Hasegawa, T.; Mızoguchi, M.; Haruna, K.; Mizuno, Y.; Muramatsu, S.; Suga, Y.; Ogawa, H. & Ikeda, S. (2007). Amnia for intractable skin ulcers with recessive dystrophic epidermolysis bullosa: report of three cases, *Journal of Dermatology*, Vol. 34, pp.328–332.

Hoffman, A.S. (2002). Hydrogels for biomedical applications, *Advanced of Drug Delivery Reviews*, Vol.43, pp.3-12.

http://www.burnsurgery.com

Hwang, M.R.; Kim, J.O.; Lee, J.H.; Kim, Y.I.; Kim, J.H.; Chang, S.W.; Jin, S.G.; Kim, J.A.; Lyoo, W.S.; Han, S.S.; Ku, S.K.; Yong, C.S. & Choi, H.G. (2010). Gentamicin-loaded wound dressing with polyvinyl alcohol/dextran hydrogel: gel characterization and *in vivo* healing evaluation, *AAPS PharmSciTech*, Vol.11, No.3, pp.1092-1103.

Integument. (2001). Ed, L.P. Gartner & J.L. Hiatt, Color Textbook of Histology. Vol. 14, pp. 325-342, W.B. Saunders Company, Philadelphia, USA.

Jansson, E. & Tengvall, P. (2001). *In vitro* preparation and ellipsometric characterization of thin blood plasma clot films on silicon, *Biomaterials*, Vol.22, pp.1803-1808.

Jáuregui, K.M.G.; Cabrera, J.C.C.; Ceniceros, E.P.S.; Hernández, J.L.M. & Ilyina, A. (2009). A new formulated stable papain-pectin aerosol spray for skin wound healing, *Biotechnology and Bioprocess Engineering,* Vol.14, pp.450-456.

Jeong, B.; Kim, S.W. & Bae, Y.H. (2002). Thermosensitive sol-gel reversible hydrogels, *Advanced of Drug Delivery Reviews*, Vol.54, pp.37-51.

Ji, J.A.; Borisov, O.; Ingham, E.; Ling, V. & Wang, Y.J. (2009). Compatibility of a protein topical gel with wound dressings, *Journal of Pharmaceutical Sciences*, Vol.98, No.2, pp.595-605.

Johnson, P.A.; Fleming, K. & Avery, C.M.E. (1998). Latex foam and staple fixation of skin grafts, *British Journal of Oral and Maxillofacial Surgery*, Vol. 36, pp.141-142.

Jones, I.; Currie, L. & Martin, R. (2002). A guide to biological skin substitutes, *British Journal of Plastic Surgery*, Vol.55, pp.185-193.

Kapoor, M. & Appleton, I. (2005). Wound healing: abnormalities and future therapeutic targets, *Current Anaesthesia & Critical Care*, Vol.16, pp.88-93.

Kawaguchi, H. (2000). Functional polymer microspheres. *Progress in Polymer Science*, Vol.25, pp.1171-1210.

Kearney J.N. (2001). Clinical evaluation of skin substitutes, *Burns*, Vol.27, pp.545-551.

Khor, E.; Lim, L.Y. (2003). Implantable applications of chitin and chitosan, *Biomaterials*, Vol.24, pp. 2339-2349.

Kickhöfen, B.; Wokalek, H.; Scheel D. & Ruh, H. (1986). Chemical and physical properties of a hydrogel wound dressing, *Biomaterials*, Vol.7, pp.67-72.

Kim, I.; Park, J. W.; Kwon, I.C.; Baik, B.S. & Cho, B.C. (2002). Role of BMP βig-h3, and chitosan in early bony consolidation in distraction osteogenesis in a dog model, *Plastic and Reconstructive Surgery*, Vol.109, pp.1966-1977.

Kim, J.O.; Choi, J.Y.; Park, J.K.; Kim, J.H.; Jin, S.G.; Chang, S.W.; Li, D.X.; Hwang, M.R.; Woo, J.S.; Kim, J.A.; Lyoo, W.S.; Yong, C.S. & Choi, H.G. (2008). Development of clindamycin-loaded wound dressing with polyvinyl alcohol and sodium alginate, *Biological and Pharmaceutical Bulletin,* Vol. 31, No.12, pp.2277-2282.

Kim, J.O.; Park, J.K.; Kim, J.H.; Jin, S.G.; Yong, C.S.; Li, D.X.; Choi, J.Y.; Woo, J.S.; Yoo, B.K.; Lyoo, W.S.; Kim, J. & Choi, H. (2008). Development of polyvinyl alcohol–sodium alginate gel-matrix-based wound dressing system containing nitrofurazone, *International Journal of Pharmaceutics*, Vol.359, pp.79–86.

Kirker, K.R.; Luo, Y.; Nielson, J.H.; Shelby, J. & Prestwich, G.D. (2002). Glycosaminoglycan hydrogel films as bio-interactive dressings for wound healing, *Biomaterials*, Vol.23, pp.3661-3671.

Klasen, H.J. (2000a). A historical review of the use of silver in the treatment of burns. I. early uses, *Burns*, Vol.26, pp.117-130.

Klasen, H.J. (2000b). A historical review of the use of silver in the treatment of burns. II. renewed interest for silver, *Burns*, Vol.26, pp.131-138.

Knapp, T.R.; Kaplan, E.N. & Daniels, J.R. (1977). Injectable collagen for soft tissue augmentation, *Plastic and Reconstructive Surgery*, Vol.60, pp.398-405.

Krajewska, B. (2004). Application of chitin and chitosan based materials for enzyme immobilizations: a review, *Enzyme and Microbial Technology*, Vol.35, pp.126-139.

Kumar, N.; Ravikumar, M.N.V. & Domb, A.J. (2001). Biodegradable block copolymers, *Advanced of Drug Delivery Reviews*, Vol.53, pp.23-44.

Lakshmana, L.R.; Shalumona, K.T.; Naira, S.V.; Jayakumara, R. & Nair, S.V. (2010). Preparation of silver nanoparticles ıncorporated electrospun polyurethane nano-fibrous mat for wound dressing, *Journal of Macromolecular Science, Part A: Pure and Applied Chemistry*, Vol.47, pp.1012–1018.

Lee, A.R. (2005). Enhancing dermal matrix regeneration and biomechanical properties of 2nd degree-burn wounds by EGF-impregnated collagen sponge dressing, *Archives of Pharmacal Research*, Vol.28, No.11, pp.1311-1316.

Lee, C.H.; Singla, A. & Lee, Y. (2001). Biomedical application of collagen, *International Journal of Pharmaceutics*, Vol.221, pp.1-22.

Lee, J.J. & Worthington, P. (1999). Reconstruction of the temporomandibular joint using calvarial bone after a failed teflon-proplast implant, *Journal of Oral and Maxillofacial Surgery*, Vol.57, pp.457-461.

Lehnert, B. & Jhala, G. (2005). The use of foam as a postoperative compression dressing, *Journal of Foot and Ankle Surgery*, Vol.44, pp.68-69.

Lim, J.K.; Saliba, L.; Smith, M.J.; McTavish, J.; Raine, C. & Curtin, P. (2000). Normal saline wound dressing-is it really normal?, *British Journal of Plastic Surgery*, Vol.53, pp.42-45.

Lim, S.J.; Lee, J.H.; Piao, M.G.; Lee, M.K.; Oh, D.H.; Hwang, du H.; Quan, Q.Z.; Yong, C.S. & Choi, H.G. (2010). Effect of sodium carboxymethylcellulose and fucidic acid on the gel characterization of polyvinylalcohol-based wound dressing, *Archives of Pharmacal Research*, Vol.33, No.7, pp.1073-1081.

Lloyd, L.L.; Kennedy, J.F.; Methacanon, P.; Paterson, M. & Knill, C.J. (1998). Carbohydrate polymers as wound management aids, *Carbohydrate Polymers*, Vol. 37, pp.315-322.

Losi, P.; Lombardi, S.; Briganti, E. & Soldani, G. (2004). Luminal surface microgeometry affects platelet adhesion in small-diameter synthetic grafts, *Biomaterials*, Vol.25, pp.4447-4455.

Madri J.A. (1990). Inflammation and healing. Ed: J. M. Kıssane, Anderson's Pathology. Vol. 1, pp. 67-110, The C.V. Mosby Company, St. Louis, USA.

Manwaring, M.E.; Walsh, J.F. & Tresco P.A. (2004). Contact quidance induced organization of extracellular matrix, *Biomaterials*, Vol.25, pp.3631-3638.

Martinez, L.R.; Han, G.; Chacko, M.; Mihu, M.R.; Jacobson, M.; Gialanella, P.; Friedman, A.J.; Nosanchuk, J.D. & Friedman J.M. (2009). Antimicrobial and healing efficacy of sustained release nitric oxide nanoparticles against *Staphylococcus aureus* skin infection, *Journal of Investigative Dermatology*, Vol. 129, No. 10, pp.2463-2469.

Mi, F.; Wu, Y.; Shyu, S.; Schoung, J.; Huang, Y.; Tsai, Y. & Hao J. (2002). Control of wound infections using a bilayer chitosan wound dressing with sustaniable antibiotic delivery, *Journal of Biomedical Materials Research*, Vol.59, pp.438-449.

Miller, R.S.; Steward, D.L.; Tami, T.A.; Sillars, M.J.; Seiden, A.M.; Shete, M.; Paskowski, C. & Welge, J. (2003). The clinical effects of hyaluronic acid ester nasal dressing (Merogel) on intranasal wound healing after functional endoscopic sinus surgery, *Otolaryngology-Head and Neck Surgery*, Vol.128, pp.862-869.

Moulin, V.; Auger, F.A.; Garrel, D. & Germain, L. (2000). Role of wound healing myofibroblasts on re-epithelialization of human skin, *Burns*, Vol.26, pp.3-12.

Mutsaers, S.E.; Bishop, J.E.; McGrouther, G. & Laurent, G.J. (1997). Mechanisms of tissue repair: from wound healing to fibrosis, *International Journal of Biochemistry & Cell Biology*, Vol.29, pp.5-17.

Murakami, K.; Aoki, H.; Nakamura, S.; Nakamura, S.; Takikawa, M.; Hanzawa, M.; Kishimoto, S.; Hattori, H.; Tanaka, Y.; Kiyosawa,, T.; Sato, Y. & Ishihara, M. (2010). Hydrogel blends of chitin/chitosan, fucoidan and alginate as healing-impaired wound dressings, *Biomaterials*, Vol.31, No.1, pp.83-90.

Muzzarelli, C. & Muzzarelli, R.A.A. (2002). Natural and artificial chitosan-inorganic composites, *Journal of Inorganic Biochemistry*, Vol.92, pp.89-94.

Muzzarelli, R.A.A.; Morganti, P.; Morganti, G.; Palombo, P.; Palombo, M.; Biagini, G.; Belmonte, M.M.; Giantomassi, F.; Orlandi, F. & Muzzarelli, C. (2007). Chitin nanofibrils/chitosan glycolate composites as wound medicaments, *Carbohydrate Polymers*, Vol. 70, pp. 274–284.

Naimer, S.A. & Chemla, F. (2000). Elastic adhesive dressing treatment of bleeding wounds in trauma victims, *American Journal of Emergency Medicine,* Vol.18, pp.816-819.

Nakabayashi, N. (2003). Dental biomaterials and the healing of dental tissue, *Biomaterials*, Vol.24, pp.2437-2439.

Nanchahal, J.; Dover, R. & Otto, W.R. (2002). Allogeneic skin substitutes applied to burns patients, *Burns*, Vol.28, pp.254-257.

Nascimento, E.G.; Sampaio, T.B.; Medeiros, A.C. & Azevedo, E.P. (2009). Evaluation of chitosan gel with 1% silver sulfadiazine as an alternative for burn wound treatment in rats, *Acta Cirurgica Brasileira*, Vol.24, No.6, pp.460-465.

Nunes, P.S.; Albuquerque-Júnior, R.L.C.; Cavalcante, D.R.R.; Dantas, M.D.M.; Cardoso, J.C.; Bezerra, M.S.; Souza, J.C.C.; Serafini, M.R.; Quitans-Jr, L.J.; Bonjardim, L.R. & Araújo A.A.S. (2011). Collagen-based films containing liposome-loaded usnic acid as dressing for dermal burn healing, *Journal of Biomedicine and Biotechnology*, Article ID. 761593.

O'Donovan, D.A.; Mehdi, S.Y. & Eadie, P.A. (1999). The role of mepitel silicone net dressings in the managment of fingertip injuries in children, *Journal of Hand Surgery*, Vol.24, pp.727-730.

Okabayashi, R.; Nakamura, M.; Okabayashi, T.; Tanaka, Y.; Nagai, A. & Yamashita, K. (2009). Efficacy of polarized hydroxyapatite and silk fibroin composite dressing gel on epidermal recovery from full-thickness skin wounds, *Journal of Biomedical Materials Research Part B: Applied Biomaterials*, Vol.90B, pp.641–646.

O'Leary, R.; Rerek, M. & Wood, E.J. (2004). Fucoidan modulates the effect of transforming growth factor (TGF)-beta1 on fibroblast proliferation and wound repopulation in in vitro models of dermal wound repair, *Biological and Pharmaceutical Bulletin*, Vol.27, No.2, pp.266-270.

Ortega, M.R. & Milner, S.M. (2000). Human beta defensin is absent in burn blister fluid, *Burn*, Vol.26, pp.724-726.

Ou, L.F.; Lee, S.Y.; Chen, Y.C.; Yang, R.S. & Tang, Y.W. (1998). Use of biobrane in pediatric scald burns-experience in 106 children, *Burns*, Vol.24, pp.49-53.

Pachulski, R.; Zasadil, M.; Adkins, D. & Hanif, B. (2002). High incidence of Pellethane 90A lead malfunction, *Europace*, Vol.4, pp.45-47.

Park, S.; Lee, K.C.; Song, B.S.; Cho, J.H.; Kim, M.N. & Lee, S.H. (2002). Microvibration transducer using silicon elastic body for an implantable middle ear hearing aid, *Mechatronics*, Vol.12, pp.1173-1184.

Park, S.N.; Kim, J.K. & Suh, H. (2004). Evaluation of antibiotic-loaded collagen-hyaluronic acid matrix as a skin substitute, *Biomaterials*, Vol.25, pp.3689-3698.

Park, S.N.; Lee, H.J.; Lee, K.H. & Suh, H. (2003). Biological characterization of EDC-crosslinked collagen-hyaluronic acid matrix in dermal tissue restoration, *Biomaterials*, Vol.24, pp.1631-1641.

Patankar, M,S.; Oehninger, S.; Barnett, T.; Williams, R.L. & Clark, G.F. (1993). A revised structure for fucoidan may explain some of its biological activities, *Journal of Biological Chemistry*, Vol. 268, No.29, pp.21770-21776.

Paul, W. & Sharma, C.P. (2004). Chitosan and alginate wound dressings: a short review, *Trends in Biomaterials & Artificial Organs*, Vol.18, pp.18-23.

Peng, H.T. & Shek, P.N. (2009). Development of in situ-forming hydrogels for hemorrhage control, *Journal of Materials Science: Materials in Medicine*, Vol.20, No.8, pp.1753-1762.

Peters, G. & Wirth, CJ. (2003). The current state of meniscal allograft transplantation and replacement, *Knee,* Vol.10, No.1, pp.19-31.

Pietramaggiori, G.; Yang, H.J.; Scherer, S.S.; Kaipainen, A.; Chan, R.K.; Alperovich, M.; Newalder, J.; Demcheva, M.; Vournakis, J.N.; Valeri, C.R.; Hechtman, H.B. & Orgill, D.P. (2008). Effects of poly-N-acetyl glucosamine (pGlcNAc) patch on wound healing in db/db mouse, *Journal of Trauma*, Vol.64, No.3, pp.803-808.

Price, R.D.; Das-Gupta, V.; Frame, J.D. & Navsaria, H.A. (2001). A study to evaluate primary dressings for the application of cultured keratinocytes, *British Journal of Plastic Surgery*, Vol.54, pp. 687-696.

Pruitt, B.A. & Levine, N.S. (1984). Characteristics and uses of biologic dressings and skin substitutes, Archives of Surgery, Vol.119, pp.312-322.

Rao, S.B. & Sharma, C.P. (2007). Use of chitosan as a biomaterials: studies on its safety and hemostatic potential, *Journal of Biomedical Materials Research*, Vol.34, pp.21-28.

Raphael, K.G.; Marbach, J.J.; Wolford, L.M.; Keller, S.E. & Bartlett, J.A. (1999). Self-reported systemic, immune-mediated disorders in patients with and without proplast-teflon

implants of the temporomandibular joint, *Journal of Oral and Maxillofacial Surgery*, Vol.57, pp.364-370.

Ravishanker, R.; Bath, A.S. & Roy, R. (2003). Amnion Bank the use of long term glycerol preserved amniotic membranes in the management of superficial and superficial partial thickness burns, *Burns*, Vol. 29, No.4, pp.69-74.

Ruszczak, Z. (2003). Effect of collagen matrices on dermal wound healing, *Advanced of Drug Delivery Reviews*, Vol.55, pp.1595-1611.

Saliba, M.J. (2001). Heparin in the tratment of burns: a review, *Burns*, Vol.27, pp.349-358.

Sezer, A.D. (2011). Chitosan: properties and its pharmaceutical and biomedical aspects. In: Focus on chitosan research, Samuel P. Davis, editor pp.377-398, Nova Publisher, ISBN: 978-1-61324-454-8, Hauppauge, Newyork, USA.

Sezer, A.D. & Akbuğa, J. (2006). Fucosphere--new microsphere carriers for peptide and protein delivery: preparation and in vitro characterization, *Journal of Microencapsulation*, Vol.23, No.5, pp.513-522.

Sezer, A.D. & Akbuğa, J. (2009). Comparison on in vitro characterization of fucospheres and chitosan microspheres encapsulated plasmid DNA (pGM-CSF): formulation design and release characteristics, *AAPS PharmSciTech*, Vol.10, No.4, pp.1193-1199.

Sezer, A.D. & Cevher, E. (2011). Fucoidan: is a versatile biopolymer for biomedical applications, In: Biomaterials and nanostructures are for active implants, Meital Zilberman, editor. pp.377-406, Springer-Verlag Publisher, ISBN: 978-3-642-18064-4, Heidelberg, Berlin, Germany.

Sezer, A.D.; Cevher, E.; Hatipoğlu, F.; Oğurtan, Z.; Baş, A.L. & Akbuğa, J. (2008). Preparation of fucoidan-chitosan hydrogel and its application as burn healing accelerator on rabbits, *Biological and Pharmaceutical Bulletin*, Vol.31, No.12, pp.2326-2333.

Sezer, A.D.; Cevher, E.; Hatipoğlu, F.; Oğurtan, Z.; Baş, A.L. & Akbuğa, J. (2008). The use of fucosphere in the treatment of dermal burns in rabbits, *European Journal of Pharmaceutics and Biopharmaceutics*, Vol.69, No.1, pp.189-198.

Sezer, A.D.; Hatipoğlu, F.; Cevher, E.; Oğurtan, Z.; Baş, A.L. & Akbuğa, J. (2007). Chitosan films containing fucoidan as a wound dressing for dermal burn healing: Preparation and in vitro/in vivo evaluation, *AAPS PharmSciTech*, Vol.8, No.2, Article 39, E1-E8.

Shakespeare, P. & Shakespeare V. (2002). Survey: use of skin substitute materials in UK burn treatment centres, *Burns*, Vol.28, pp.295-297.

Shakespeare, P. (2001). Burn wound healing and skin substitutes, *Burns*, Vol.27, pp.517-522.

Shen, X.; Nagai, N.; Murata, M.; Nishimura, D.; Sugi, M. & Munekata, M. (2008). Development of salmon milt DNA/salmon collagen composite for wound dressing, *Journal of Materials Science: Materials in Medicine*, Vol.19, pp.3473–3479.

Sheridan, R.L. & Tompkins, R.G. (1999). Skin substitutes in burns, *Burns*, Vol.25, pp.97-103.

Sheridon, R.L.; Morgan, J.R. & Mohammad R. (2001). Biomaterials in burn and wound dressing. Ed: Severian D., Polymeric Biomaterials, Dumitriu Severian, editor. pp.451-458, Marcel Dekker, ISBN: 0-8247-8969-5, New York, USA.

Singer, A.J.; Mohammad, M.; Thode, H.C. & Mcclain, S.A. (2000). Octylcyanoacrylate versus polyurethane for treatment of burns in swine: a randomized trail, *Burns*, Vol.26, pp.388-392.

Skin. Ed: Junqueria, L.C.; Carneiro, J. & Kelley, O.R., Basic Histology. Vol. 18, pp.357-370, Prentice-Hall International Inc., Rio de Janerio, Brasil.

Skin. Ed: Young, B. & Heath J.W., Wheather's Functional Histology. Vol. 9, pp.157-171, Churchill Livingstone, Philadelphia, USA.

Sparkes, B.G.: Immunological responses to termal injury, *Burns*, Vol.23, pp.106-113.

Stashak, T.S.; Farstvedt, E. & Othic, A. (2004). Update on wound dressings: indications and best use, *Clinical Techniques in Equine Practice*, Vol.3, pp.148-163.

Still, J.; Glat, P.; Silverstein, P.; Griswold, J. & Mozingo, D. (2003). The use of a collagen sponge/living cell composite material to treat donor sites in burn patients, *Burns*, Vol.29, No.8, pp.837-841.

Suh, J.K.F. & Matthew, H.W.T. (2000). Application of chitosan-based polysaccharide biomaterials in cartilage tissue engineering: a review, *Biomaterials*, Vol.21, pp.2589-2598.

Sung, J.H.; Hwang, M.R.; Kim, J.O.; Lee, J.H.; Kim, Y.I.; Kim, J.H.; Chang, S.W.; Jin, S.G.; Kim, J.A.; Lyoo, W.S.; Han, S.S.; Ku, S.K.; Yong, C.S. & Choi, H.G. (2010). Gel characterisation and in vivo evaluation of minocycline-loaded wound dressing with enhanced wound healing using polyvinyl alcohol and chitosan, *International Journal of Pharmaceutics,* Vol.392, No.1-2, pp.232-240.

Suzuki, S.; Matsuda, K.; Isshiki, N.; Tamada, Y. & Ikada, Y. (1990). Experimental study of a newly developed bilayer artificial skin, *Biomaterials*, Vol.11, pp.356-360.

Şenel, S. & McClure, S.J. (2004). Potential applications of chitosan in veterinary medicine, *Advanced of Drug Delivery Reviews*, Vol.56, pp.1467-1480.

Şenyuva, C.; Yücel, A.; Erdamar, S.; Çetinkale, O.; Seradjmir, M. & Özdemir, C. (1997). The fate of alloplastic materials placed under a burn scar: an experimental study, *Burns*, Vol.23, pp.484-489.

Tan, W.; Krishnaraj, R. & Desai, T.A. (2001). Evaluation of nanostructured composite collagen-chitosan matrices for tissue engineering, *Tissue Engineering*, Vol.7, pp.203-210.

Tanigawa, J.; Miyoshi, N. & Sakurai, K. (2008). Characterization of chitosan/citrate and chitosan/acetate films and applications for wound healing, *Journal of Applied Polymer Science*, Vol.110, pp.608–615.

The skin and its appendages (The Integument). (1981). Ed: Leeson T.S. & Leeson C.R., Histology. Vol. 10, pp. 308-327, W.B. Saunders Company, Philadelphia, USA.

The skin and its appendages (The Integument). (1988). Ed: Leeson T.S., Leeson C.R., Paparo A.A., Text/Atlas of Histology. Vol. 10, s. 362-393, W.B. Saunders Company, Philadelphia, USA.

Thomas, S. (2000a). Alginate dressings in surgery and wound management-Part 1, *Journal of Wound Care*, Vol. 9 No.2 pp.56-60.

Thomas, S. (2000b). Alginate dressings in surgery and wound management-Part 2, *Journal of Wound Care*, Vol. 9 No.3 pp.115-119.

Thomas, S. (2000c). Alginate dressings in surgery and wound management-Part 3, *Journal of Wound Care*, Vol. 9 No.4 pp.163-166.

Tissue repair and wound healing. (1998). Ed: Porth C.M., Pathophysiology. Vol. 2, pp.43-48, Lippincott, Philadelphia, USA.

Tissue repair and wound healing. (1998). Ed: Porth C.M., Pathophysiology., Vol. 2, pp.289-293, Lippincott, Philadelphia, USA.

Trumble, D.R.; McGregor, W.E. & Magovern, J.A. (2002). Validation of a bone analog model for studies of sternal closure, *Annals of Thoracic Surgery,* Vol.74, pp.739-745.

Ueno, H.; Mori, T. & Fujinaga, T. (2001). Topical formulation and wound healing applications of chitosan. *Advanced of Drug Delivery Reviews*, Vol.52, pp.105-115.

Ueno, H.; Yamada, H.; Tanaka, I.; Kaba, N.; Matsuura, M.; Okumurai, M.; Kadosawa T. & Fujinaga, T. (1999). Accelerating effects of chitosan for healing at, early phase of experimental open wound in dogs, *Biomaterials*, Vol.20, pp.1407-1414.

Uppal, R.; Ramaswamy, G.N.; Arnold, C.; Goodband, R. & Wang, Y. (2011). Hyaluronic acid nanofiber wound dressing: Production, characterization, and in vivo behavior, *Journal of Biomedical Materials Research Part B: Applied Biomaterials*, Vol.97B, pp.20–29.

Van den Kerckhove, E.; Stappaerts, K.; Boeckx, W.; Van den Hof B.; Monstrey, S.; Van der Kelen, A. & Cubber J. (2001). Silicones in the rehabilitation of burns: a review and overview, *Burns*, Vol.27, pp. 205-214.

Van Zuijlen, P.P.M.; Ruurda, J.J.B.; Van Veen, H.A.; Marle, J.V.; Van Trier, A.J.M.; Groenevelt, F.; Kreis, R.W. & Middelkoop, E. (2003). Collagen morphology in human skin and scar tissue: no adaptations in response to mechanical loading at joints, *Burns*, Vol.29, pp.423-431.

Verma, P.R.P. & Iyer, S.S. (2000). Controlled transdermal delivery of propranolol using HPMC matrices: design and *in-vitro* and *in-vivo* evaluation, *Journal of Pharmacy and Pharmacology*, Vol.52, pp.151-156.

Wang, W. (2006). A novel hydrogel crosslinked hyaluronan with glycol chitosan, *Journal of Materials Science: Materials in Medicine*, Vol.17, No.12, pp.1259-1265.

Weinstein-Oppenheimer, C.R.; Aceituno, A.R.; Brown, D.I.; Acevedo, C.; Ceriani, R.; Fuentes, M.A.; Albornoz, F.; Henríquez-Roldán C.F.; Morales, P.; Maclean, C.; Tapia, S.M. & Young, M.E. (2010). The effect of an autologous cellular gel-matrix integrated implant system on wound healing, *Journal of Translational Medicine*, Vol.8, No.59, pp.1-11.

Whelan, J. (2002). Smart bandages diagnose wound infection, *DDT*, Vol.7, pp.9-10.

Whitney, J.D. & Wickline, M.M. (2003). Treating chronic and acute wounds with warming: review of the science and practice implications, *Journal of Wound Care*, Vol.30, pp.199-209.

Winter, G.D. (1965). A note on wound healing under dressings with special reference to perforated-film dressings, *Journal of Investigative Dermatology*, Vol.45, pp.299-302.

Wright, K.A.; Nadire, K.B.; Busto, P.; Tubo, R.; McPherson, J.M. & Wentworth, B.M. (1998). Alternative delivery of keratinocytes using a polyurethane membrane and the implications for its use in the treatment of full-thickness burn injury, *Burns*, Vol.24, pp.7-17.

Xu, C.; Xu, F.; Wang, B. & Lu, T. (2011). Electrospinning of poly(ethylene-co-vinyl alcohol) nanofibres encapsulated with ag nanoparticles for skin wound healing, *Journal of Nanomaterials,* Article ID 201834.

Xu, H.;, Ma, L.; Shi, H.; Gao, C. & Han, C. (2007). Chitosan–hyaluronic acid hybrid film as a novel wound dressing: *in vitro* and *in vivo* studies, *Polymers for Advanced Technologies*, Vol.18, pp.869–875.

Yenerman, M. (1986). Genel Patoloji. 1st edition, pp.271-294, Istanbul Üniversitesi, Istanbul, Turkey.

Yoo, H. & Kim, H. (2008). Characteristics of Waterbornepolyurethane/poly (nvinylpyrrolidone) composite films for wound-healing dressings, *Journal of Applied Polymer Science*, Vol.107, pp.331–338.

20

Cellular Systems and Biomaterials for Nerve Regeneration in Neurotmesis Injuries

Ana Colette Maurício[1,2] et al.[*],
[1]*Centro de Estudos de Ciência Animal (CECA), Instituto de Ciências e Tecnologias Agrárias e Agro-Alimentares (ICETA), Universidade do Porto (UP),*
[2]*Instituto de Ciências Biomédicas Abel Salazar (ICBAS), UP, Portugal*

1. Introduction

A relevant number of peripheral nerve injuries can only be dealt through reconstructive surgical procedures. Despite continuous refinement of microsurgery techniques, peripheral nerve repair still stands as one of the most challenging tasks in neurosurgery. Particularly problematic is the fact that despite the good regenerative ability of peripheral nerves and successful surgical nerve repair functional recovery is most often disappointing in these patients (Lundborg, 2002). While direct nerve repair should be the procedure of choice whenever tension-free suturing is possible, in many cases there is a significant loss of nerve tissue and resulting nerve gap. In these cases a nerve graft might be necessary for adequate nerve repair (Lundborg, 2002). Nerve grafting, however have some disadvantages, the most prominent being donor site morbidity that may lead to a secondary sensory deficit and occasionally neuroma and pain. In addition, non-matching donor and recipient nerve diameters often occur, which might be at the basis of poor functional recovery (May, 1983). Entubulation offers advantages over autographs, including the potential to manipulate the regeneration environment within the tube-guide (Fields et al., 1989). Consequently, guidance of regenerating axons is not only achieved by a mechanical effect but also by a chemical effect (such as accumulation of neurotrophic factors) (Meek & Coert, 2002). Nerve guides can be made of biological or synthetic materials and, among the latter, both non-absorbable (e.g. silicon) and biodegradable tubes have been used (Schmidt & Leach, 2003). Biodegradable nerve guides must be preferred since no foreign body material will be left in

[*]Andrea Gärtner[1,2], Paulo Armada-da-Silva[3], Sandra Amado[3], Tiago Pereira[1,2], António Prieto Veloso[3], Artur Varejão[4], Ana Lúcia Luís[1,2] and Stefano Geuna[5]
[1] *Centro de Estudos de Ciência Animal (CECA), Instituto de Ciências e Tecnologias Agrárias e Agro-Alimentares (ICETA), Universidade do Porto (UP), Portugal.*
[2] *Instituto de Ciências Biomédicas Abel Salazar (ICBAS), UP, Portugal.*
[3] *Faculdade de Motricidade Humana (FMH), Universidade Técnica de Lisboa (UTL), Portugal.*
[4] *Departamento de Ciências Veterinárias, CIDESD, Universidade de Trás-os-Montes e Alto Douro (UTAD), Portugal*
[5] *Neuroscience Institute of the Cavalieri Ottolenghi Foundation & Department of Clinical and Biological Sciences, University of Turin, Italy*

the host after the device has fulfilled its task. Four types of nerve guides attracted particular attention of our research group: those made of PLGA (Luis et al., 2007b; Luis et al., 2008) and poly-ε-caprolactone (Luis et al., 2008; Varejao et al., 2003a), collagen (Amado et al., 2010) and chitosan (Amado et al., 2008). In particular, chitosan has recently attracted particular attention because of its biocompatibility, biodegradability, low toxicity, low cost, enhancement of wound-healing and antibacterial effects and its potential usefulness in nerve regeneration have been demonstrated both *in vitro* and *in vivo* (Amado et al., 2010; Shirosaki et al., 2005; Simoes et al., 2010). Chitosan is a partially deacetylated polymer of acetyl glucosamine obtained after the alkaline deacetylation of chitin (Senel & McClure, 2004). While chitosan matrices have low mechanical strength under physiological conditions and are unable to maintain a predefined shape after transplantation, their mechanical properties can be improved by modification with a silane agent, namely γ-glycidoxypropyltrimethoxysilane (GPTMS), one of the silane-coupling agents which has epoxy and methoxysilane groups. The epoxy group reacts with the amino groups of chitosan molecules, while the methoxysilane groups are hydrolyzed and form silanol groups, and the silanol groups are subjected to the construction of a siloxane network due to the condensation. Thus, the mechanical strength of chitosan can be improved by the cross-linking between chitosan, GPTMS and siloxane network. We have previously obtained by adding GPTMS, chitosan type III membranes (hybrid chitosan membranes) which have about 110 μm pores and about 90% of porosity, due to the employment of freeze-drying technique, and which were successful in improving sciatic nerve regeneration after axonotmesis (Amado et al., 2008). Wettability of the material surfaces is one of the key factors for protein adsorption, cell attachment and migration (Amado et al., 2008). The addition of GPTMS improves the wettability of chitosan surfaces, and therefore chitosan type III membranes are more hydrophilic than types of chitosan membranes (Shirosaki et al., 2005). In addition, chitosan type III was developed to be more porous, with a larger surface to volume ratio, and to preserve mechanical strength and ability to adapt to different shapes. Significant differences in water uptake between commonly used chitosan and our hybrid chitosan type III were previously reported and it has been shown that they retain about two times as much biological fluid (Tateishi et al., 2002). The Neurolac® and the PLGA90:10 tube-guides guides show several different physical-chemical properties, namely Neurolac® is stiffer than PLGA due to structural reinforcement of the ester bonds and does not degrade so quickly. The biodegradation rate of PLGA tubes is estimated to be around 3 months while that complete resorption of Neurolac® is estimated to be of 16 months approximately (Geuna et al., 2009; Luis et al., 2007b; Luis et al., 2008). The degradation products of Neurolac® are less acidic, which may cause less damage to the surrounding tissue, and they are transparent so that the correct positioning of the nerve stumps may be confirmed after suturing. On the other hand, the biodegradable non woven structure of PLGA tubes may offer some advantages in terms of microporosity which may enhance nerve repair (Luis et al., 2007b; Luis et al., 2008). *In vitro* studies have shown that the four types of tube-guides, namely, the PLGA, the collagen, the hybrid chitosan and the Neurolac® are biocompatible to nerve cells and can facilitate nerve cell attachment, differentiation and growth (Amado et al., 2008; Luis et al., 2007b; Luis et al., 2008; Luis et al., 2008; Wang et al., 2008). Our research group tested the PLGA90:10, the hybrid chitosan type III and the collagen tube-guides covered with the neural cells *in vitro* differentiated for 48 hours in the presence of DMSO (Amado et al., 2010; Amado et al., 2008; Luis et al., 2008; Simoes et al., 2010). The Neurolac® tubes were not tested with the cellular system, since the

cell adherence was more difficult to obtain and imply the previous covering with poli-l-lysine (Amado et al., 2010; Amado et al., 2008; Luis et al., 2008; Simoes et al., 2010). It is expected that tissue engineering associating these biomaterials to cellular systems, capable of differentiating into neuron-like cells, may improve peripheral nerve regeneration, in terms of motor, sensory and histomorphometric parameters. The N1E-115 cells derived from mouse neuroblastomas (Amano et al., 1972) can *in vitro* differentiate into neural-cells (Amano et al., 1972; Rodrigues et al., 2005) and were used as a cellular model for stem cells. In addition, mesenchymal cells isolated from the Wharton's jelly of the umbilical cord, were used by our research group (data not published yet). Stem cells can be loosely classified into 3 broad categories based on their time of isolation during ontogenesis: embryonic, fetal and adult (Marcus & Woodbury, 2008). Recent years have witnessed an explosion in the number of adult stem cells populations isolated and characterized. While still multipotent, adult stem cells have long been considered restricted, giving rise only to progeny of their resident tissues. Recently, and currently controversial studies have challenged this dogma, suggesting that adult stem cells may be far more plastic than previously appreciated (Marcus & Woodbury, 2008). Extra-embryonic tissues as stem cell reservoirs offer many advantages over both embryonic and adult stem cell sources. Extra-embryonic tissues, collectively known as the afterbirth, are routinely discarded at parturition, so little ethical controversy attends the harvest of the resident stem cell populations. Most significantly, the comparatively large volume of extra-embryonic tissues and ease of physical manipulation theoretically increases the number of stem cells that can be isolated (Marcus & Woodbury, 2008). The umbilical cord contains two arteries and one vein protected by a proteoglycan rich connective tissue called Wharton's jelly. Within the abundant extracellular matrix of Wharton's jelly resides a recently described stem cell population called Umbilical Cord Matrix Stem Cells. It can be isolated around 400,000 cells per umbilical cord, which is significantly greater than the number of MSCs that can be routinely isolated from adult bone marrow. *In vitro* the Wharton's jelly MSCs cells are capable of differentiation to multiple mesoderm cell types including skeletal muscle and neurons (Fu et al., 2006; Wang et al., 2004). Human MSCs (HMSCs) isolated from Wharton's jelly of the umbilical cord can be easily and ethically obtained and processed compared with embryonic or bone marrow stem cells. These cells may be a valuable source in the repair of the peripheral nerve system. HMSCs from Wharton's jelly of the umbilical cord possess stem cell properties (Yang et al., 2008) and it was previously demonstrated that HMSCs could be induced to differentiate into neuron-like cells (Fu et al., 2006). The transplanted cells were able to promote local blood vessel formation and expression of the neurotrophic factors, brain-derived neurotrophic factor (BDNF) and glial cell line-derived neurotrophic factor (GDNF) (Wang et al., 2004). Therefore, the purpose to cover the PLGA 90:10, hybrid chitosan, and collagen tube-guides used in reconstructed nerves after neurotmesis with a cellular system differentiated *in vitro* into neuronal cells, was to produce locally neurotrophic factors in a physiological concentration. The role of neurotrophic factors in neural regeneration has been the focus of extensive research (Amado et al., 2010; Hu et al., 1997). The influence of these factors in neural development, survival, outgrowth, and branching has been explored on various levels, from the molecular level to the macroscopic tissue responses. Neurotrophic factors promote a variety of neural responses, like the survival and outgrowth of the motor and sensory nerve fibers, and are implicated in spinal cord and peripheral nerve regeneration (Geuna et al., 2009; Johnson et al., 2008). However, *in vivo*, the efficacy of neurotrophic factors might vary greatly due to the method used for their delivering and it is thus

important to deliver them near the regenerating site, in the physiologic concentrations. In this view, association of a cellular system producing neurotrophic factors to biodegradable membranes may greatly improve the nerve regeneration in neurotmesis (Geuna et al., 2009). N1E-115 cell line established from a mouse neuroblastoma (Kerns et al., 1991), might be a useful cellular system to locally produce and deliver these neurotrophic factors (Geuna et al., 2001). *In vitro*, the N1E-115 cells undergo neuronal differentiation in response to dimethylsulfoxide (DMSO), adenosine 3′, 5′- cyclic monophosphate (cAMP), or serum withdrawal (Koka & Hadlock, 2001; Luis et al., 2007b; Luis et al., 2008; Luis et al., 2008). Upon induction of differentiation, proliferation of N1E-115 cells ceases, extensive neurite outgrowth is observed and the membranes become highly excitable (Koka & Hadlock, 2001; Luis et al., 2007b; Luis et al., 2008). The ideal interval period of 48 hours of differentiation was determined by measurement of the intracellular calcium concentration ($[Ca^{2+}]_i$), when the N1E-115 cells presented already the morphological characteristics of neuronal cells but at a time, cell death due to increased $[Ca^{2+}]_i$ was not still occurring (Rodrigues et al., 2005).

2. Biomaterial for tube-guides fabrication

The tube-guides or scaffold of tissue engineered nerve grafts serve in neurotmesis injuries to direct axons sprouting from the proximal to the distal stump, to maintain adequate mechanical support for the regenerating nerve fibers. Yet, they provide a conduit channel for the diffusion of neurotrophic and neurotropic factors secreted in the regeneration local and provide a conduit wall for the exchange of nutrients and waste products with the surrounding media, limiting the infiltration of fibrous scar tissue that hinders axonal regeneration (Johnson & Soucacos, 2008;). The neural scaffolds should be easy to be fashioned in different lengths and diameters, to be sterilized and implanted using microsurgical techniques. The neural scaffold has to satisfy many biological and physicochemical requirements like biocompatibility, biodegradability, permeability to ions, metabolites and for the revascularization of the regenerated nerve, biomechanical properties and surface properties that modulate the cellular system adhesion (Huang & Huang, 2006). A wide variety of biomaterials has been attempted which are of either natural or synthetic origin.

2.1 Natural biomaterials

The natural biomaterials are known by stimulating cell adhesion, migration, growth and proliferation. The natural biomaterials have also a very good biocompatibility and less toxic effects. Our research group has tested the collagen and the chitosan.

Collagen, laminin and fibronectin play an important role in the development and growth of axons (Grimpe & Silver, 2002). So, these components have become very important candidates for neural scaffolds, these materials can also serve as delivery vehicles for support cells, growth factors and drugs. For example, silicone tubes filled with laminin, fibronectin, and collagen led to a better regeneration over a 10 mm rat sciatic nerve gap compared to empty silicone controls (Chen et al., 2007). Collagen filaments have also been used to guide regenerating axons across 20–30 mm defects in rats (Itoh et al., 2003; Yoshii & Oka, 2001). Further studies have shown that oriented fibers of collagen within gels, aligned using magnetic fields, provide an improved template for neurite extension compared to randomly oriented collagen fibers (Ceballos et al., 1999). Finally, rates of regeneration comparable to those using a nerve autograft have been achieved using collagen tubes

containing a porous collagen-glycosaminoglycan matrix (Archibald et al., 1995; Chamberlain et al., 2000). In our studies we have used equine collagen type III membrane (GentaFleece®; Baxter, Nuremberg, Germany) in axonotmesis and neurotmesis lesion of the rat sciatic nerve with very promising results (Amado et al., 2010; Luis et al., 2008).

Chitin is the second most abundant polysaccharide found in nature next to cellulose. It is a biopolymer of N-acetyl-D-glucosamine monomeric units and it has been used in a wide range of biomedical devices. Chitosan is a copolymer of D-glucosamine and N-acetyl-D-glucosamine and it has a very similar molecular structure with lamin, fibronectin and collagen. So, the chitosan has favorable biological properties for the nerve regeneration and it is easier to process than the chitin. Chitosan is quite fragile in its dry form, so, it has to undergo chemical cross-linking or to be used with other biomaterials before scaffold fabrication. The chitosan (high molecular weight, Aldrich®, USA) tested by our research group was dissolved in 0.25M acetic acid aqueous solution to a concentration of 2% (w/v). To obtain type III membranes, GPTMS (Aldrich®, USA) was also added to the chitosan solution and stirred at room temperature for 1h. The drying process for type III chitosan membrane was as follows: the solutions were frozen for 24h at -20°C and then transferred to the freeze-dryer, where they were left 12h to complete dryness. The chitosan type III membranes were soaked in 0.25N sodium hydroxide aqueous solution to neutralize remaining acetic acid, washed well with distilled water, and freeze dried (Amado et al., 2008). All membranes used in vivo testing, were sterilized with ethylene oxide gas, considered by some authors the most suitable method of sterilization for chitosan membranes (Marreco et al., 2004). Prior to their use *in vivo*, membranes were kept 1 week at room temperature to clear any ethylene oxide gas remnants (Amado et al., 2008; Simoes et al., 2010) (see Fig.1).

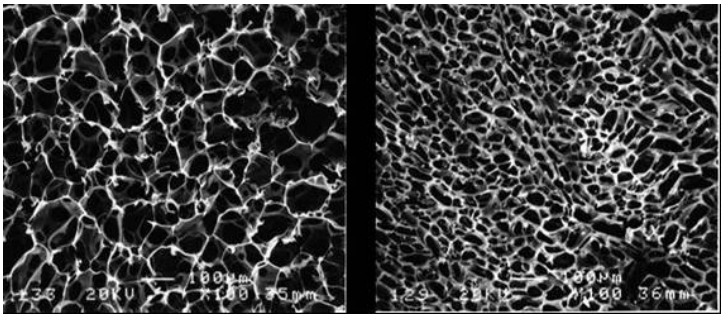

Fig. 1. SEM microstructure of chitosan membranes. Type II chitosan membrane (A). Type III chitosan membrane, showing a more porous microstructure, when compared to type II chitosan membrane (B) (Amado et al., 2008).

2.2 Synthetic biomaterials

The synthetic biopolymers constitute a group of promising biomaterials for the fabrication of neural tube-guides. However, the biocompatibility of some synthetic materials can be low since the difficulty of cell adhesion and survival can be a negative issue. Historically, non degradable synthetic materials were tested before the degradable ones. For instance, the silicone has been tested for peripheral nerve repair since 1960. Although it is not degradable in the body and it is impermeable to large molecules, the silicone tube-guide was an

important model system for studying nerve regeneration. It was also applied in several clinical trials to bridge short nerve gaps with some success (Gu et al., 2011). The use of non-degradable tube-guides implies a second surgery time, which has clear disadvantages for the patient. In order to overcome the disadvantages associated with non-degradable materials, research has been focused in biodegradable synthetic biomaterials that should degrade within a reasonable time span. The degradation products absorbed should not be toxic or induce a foreign body reaction. Moreover, the physiochemical and biological properties of biodegradable synthetic materials can be tailored to match different application requirements, like to entrap some molecules or serve as a support for a cellular system. Aliphatic polyesters represent a class of the common degradable synthetic polymers, among which poly(L-lactic acid) (PLLA) (Wang et al., 2009), polyglycolic acid (PGA) (Waitayawinyu et al., 2007), polycaprolactone (PCL) (Mligiliche et al., 2003) and their copolymers, including poly(lactic-ε-caprolactone (Neurolac®) (Den Dunnen et al., 1998; Luis et al., 2007b) and poly(L-lactic-co-glycolic acid (PLGA) (Bini et al., 2004; Luis et al., 2007b; Luis et al., 2008). Among synthetic biodegradable tubes, two types attracted particular attention: those made of PLGA and those made of Poly (DL-lactide-ε-caprolactone) copolyester (Neurolac®) (see Fig.2).

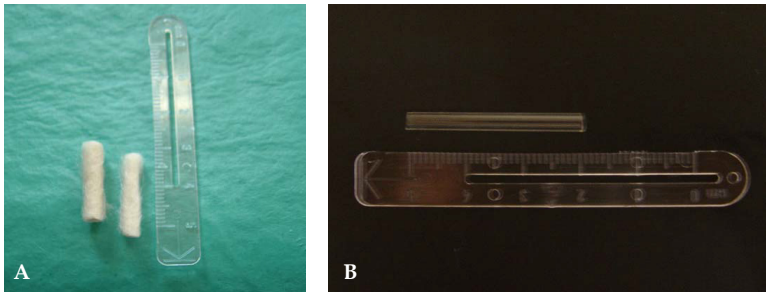

Fig. 2. PLGA 90:10 (A) and poly (DL-lactide-e-caprolactona) copolyester (Neurolac®) tube-guides (B) (Luis et al., 2007b).

These two types of nerve guides showed several different physical-chemical properties. The Poly (DL-lactide-ε-caprolactone) tube-guides (Neurolac®), 16 mm long, internal diameter of 2 mm and thickness wall of 1.5 mm, were purchased from Polyganics BV, Groningen, The Netherlands (Luis et al., 2007b; Luis et al., 2008). Poly (dl-lactide-co-glycolide) copolymers with ratio of 90PLA:10PLG were obtained from their cyclic dimers, dl-lactide and glycolide. Non-woven constructs were used to prepare tube-guides 16 mm long, internal diameter of 2.0 mm and thickness wall of 1.5mm, to be applied in a 10-mm sciatic nerve gap. These fully synthetic non-woven materials are extremely flexible, biologically safe and are able to sustain the compressive forces due to body movement after implantation. They have also some degree of porosity to allow for influx of low molecular nutrients required for nerve regeneration. The non-woven structure allowed the tube-guide to hold suture without difficulties, however greater care had to be taken in order to ensure its integrity. These tube-guides of PLGA are expected to degrade to lactic and glycolic acids through hydrolysis of the ester bonds (Luis et al., 2007b; Luis et al., 2008).

The polyvinyl alcohol hydrogel (PVA) tube-guides are now starting to be tested by our research groups. Previous studies showed the PVA potential to several biomedical

applications (Grant et al., 2006). The PVA gathers a set of exceptional properties, based in a nanofibrilar 3D structure, namely its high biocompatibility: it practically does not induce any foreign body or inflammatory reaction; it has high capacity to absorb water, mechanical resistance, elasticity, mobility and suturability (Bichara et al., 2010). The PVA are prepared in a tubular form, with 16 mm long, an internal diameter of 2 mm and thickness wall of 1.5 mm. These forms are prepared by a casting route to a mould that allows the final shape and thickness. Among the several methods described for the preparation of PVA material, the physical cross-linking of PVA by cyclic freezing and thawing is the one with better mechanical results (data not published by our research group). PVA from Aldrich (Mowiol 10-98: Mw 61,000, 98.0-98.8 mol% hydrolysis) is used. The tube-guides are produced using a solution of 20%(m/v) of PVA submitted to 3 repetitions of a freeze/thaw cycle, using 8 hours of freezing at –20.0°C and 4 hours of thawing at 22°C. However, several freeze/thaw cycling schemes must be tested to evaluate their effect on the final physical and mechanical properties, and choose the best one. The possible involvement of a final annealing step in the production process is being considered. This type of nerve guides can have unlimited availability in terms of diameters and lengths.

3. Cellular systems

The use of neural scaffolds alone to repair peripheral nerve defects have achieved variable success, but only small gap nerve repair (of 10 mm in rat sciatic nerve and of 30 mm in primate ulnar nerve) demonstrated evident functional and morphologic recovery (Amado et al., 2010; Gu et al., 2011; Hood et al., 2009; Luis et al., 2007b; Luis et al., 2008; Simoes et al., 2010). When the length of nerve gaps are increased, neural scaffolds alone only permit the bridging between the stumps, but for an effective regeneration, supporting cells or growth factors should be incorporated. The cellular systems implanted into the injury nerve may produce growth factors or ECM molecules, or may modulate the inflammatory process, to improve nerve regeneration (Amado et al., 2010; Gu et al., 2011; Luis et al., 2007b; Luis et al., 2008; Simoes et al., 2010). Schwann cells, mesenchymal stem cells, embryonic stem cells, marrow stromal cells are the most studied candidates of support cells among others. We focused our research in N1E-115 cell line *in vitro* differentiated (Amado et al., 2010; Luis et al., 2007b; Luis et al., 2008; Simoes et al., 2010) and in mesenchymal stem cells from Wharton's jelly of the umbilical cord (data not published yet).
To implant cultured cells (N1E-115 cells, MSCs, Schwann cells, and other cellular systems) into defective nerves (with axonotmesis and neurotmesis injuries), there are two main techniques. The cellular system may be directly injected to the neural scaffold which has been interposed between the proximal and distal nerve stumps or around the crush injury (in neurotmesis and axonotmesis injuries, respectively). In alternative, implant can also be achieved by pre-adding the cells to the neural scaffold via injection or co-culture (in most of the cellular systems, it is allowed to form a monolayer) and then the biomaterial with the cellular system is implanted in the injured nerve (Amado et al., 2010; Luis et al., 2008; Luis et al., 2008; Simoes et al., 2010).

3.1 Cell culture of N1E-115 cells – a cellular model for stem cells transplantation

The role of neurotrophic factors in neural regeneration has been the focus of extensive research in nerve regeneration (Schmidt & Leach, 2003). The influence of these factors in neural development, survival, outgrowth, and branching has been explored on various

levels, from molecular interactions to macroscopic tissue responses. One family of neurotrophic factors, the neurotrophins, has been heavily investigated in nerve regeneration studies, including the nerve growth factor (NGF), brain-derived neurotrophic factor (BDNF), neurotrophin-3 (NT-3), and neurotrophin-4/5 (NT-4/5) (Lundborg et al., 1994). Neurotrophic factors promote a variety of neural responses: survival and outgrowth of the motor and sensory nerve fibers, spinal cord and peripheral nerve regeneration (Schmidt & Leach, 2003). However, *in vivo* responses to neurotrophic factors can vary due to the method of their delivering. Therefore, the development and use of highly controlled delivery devices are required for the study of these extremely complex systems. For that reason, N1E-115 cell line established from neuroblastoma, that undergo neuronal differentiation in response to dimethylsul-foxide (DMSO), adenosine 3';5'-cyclic monophosphate (cAMP), or serum withdrawal (Amado et al., 2010; Rodrigues et al., 2005) was a cellular system tested in axonotmesis and neurotmesis lesions to locally produce and deliver these neurotrophic factors. Upon induction of differentiation, proliferation of N1E-115 cells ceases, extensive neurite outgrowth is observed and the membranes become highly excitable (Amado et al., 2010; Rodrigues et al., 2005). During differentiation, cyclin-dependent kinase (cdk) activities decline and phosphorylation of the retinoblastoma gene product (pRb) is lost, leading to the appearance of a pRb-containing E2F DNA-binding complex. The molecular mechanism by which pRb inhibits cell proliferation is becoming increasingly clear. pRb inhibits the activity of proteins that function as inducers of DNA synthesis (Kranenburg et al., 1995). Ca^{2+} serves as an important intracellular signal for cellular processes such as growth and differentiation. Free calcium levels within neural cells control many essential neural functions including neurotransmitter release, membrane conductance, nerve fibber excitability, coupling between neuronal cells, and axonal transport. Although regulation of the intracellular Ca^{2+} concentration ($[Ca^{2+}]_i$) is important for normal cell functioning, its deregulation has been linked to cellular pathologies and cell death (Trump & Berezesky, 1995). Deregulation in $[Ca^{2+}]_i$ can be toxic to cells and is involved in the triggering of events leading to excitotoxic cell death in neurons, through the activation of calpain, phospholipases and endonucleases (Smith & Hall, 1988). Because of the importance of $[Ca^{2+}]_i$ in neuronal health and disease, a relatively simple cell model system, where $[Ca^{2+}]_i$ regulation can be studied fairly easily, is desirable. We have tested a non-expensive and easy method to culture neural-like cell line capable of producing locally, nerve growth factors and of growing inside PLGA90:10, chitosan and collagen tubular/membrane nerve guides (Amado et al., 2010; Amado et al., 2008; Luis et al., 2008; Luis et al., 2008; Simoes et al., 2010), in order to use them to promote nerve regeneration across a peripheral nerve gap. To correlate the neuronal cells' ability to promote nerve regeneration across a gap, through their differentiation grade and survival capacity, the $[Ca^{2+}]_i$ of non-differentiated and DMSO differentiated N1E-115 cells was determined by the epifluorescence technique using the Fura-2-AM probe (Tsien, 1989). The measurement of $[Ca^{2+}]_i$ permitted to determine an ideal period of differentiation of 48 hours, when the N1E-115 cells presented already the morphological characteristics of neuronal cells and at the same time, the death process was not initiated by the $[Ca^{2+}]_i$ modifications. This cellular system was used in axonotmesis and neurotmesis injuries associated to chitosan, equine collagen type III and PLGA membranes or tube-guides in order to improve the functional and morphologic recovery of the nerve (Amado et al., 2010; Gu et al., 2011; Luis et al., 2007b; Luis et al., 2008; Simoes et al., 2010).

3.2 Wharton's jelly mesenchymal cells

After peripheral nerve injury, many neurons die. Because neurons cannot be easily expanded in vitro, there is a wide difficulty in applying primary cultured neurons to nerve tissue engineering. Embryonic stem cells (ESCs) have a great potential to proliferate unlimitedly and differentiate into neural cells using several differentiation protocols (Gu et al., 2011). The differentiation of ESCs can be modulated by growth factors and retinoic acid (Gu et al., 2011). Extensive research has been focused on the implantation of these stem cells in Central Nervous System (CNS) disorders, but in Peripheral Nerve System (PNS) injuries only a few studies were published. Cui and co-workers, in 2008, implanted ESC-derived neural progenitor cells into a 10-nm sciatic nerve gap, resulting in substantial axonal regrowth and nerve repair (Cui et al., 2008). The implanted cells survived for 3 months and could differentiate into myelinating cells. The nerve stumps presented almost normal diameter with longitudinally oriented, densely packed Schwann cell-like arrangement. The regenerated nerves also showed recovery of the functional activity, determined by electrophysiological records (Cui et al., 2008). Although these promising results, the ESCs have serious ethical issues, especially when obtained by somatic nuclear transfer technique or from embryos produced for assisted medical reproduction.

Recent years have witnessed a great expansion in the number of adult stem cell populations isolated and characterized. Adult stem cells have long been considered restricted, considering their multipotency. Many studies have challenged this dogma, suggesting that adult stem cells may be more plastic than previously appreciated (Beer et al., 2001). Extra-embryonic tissues as stem cell reservoirs offer many advantages over embryonic and adult stem cell sources, and are routinely discarded at parturition. Little ethical controversy attends the harvest of the resident stem cell populations. Human umbilical cord (UC) consists of three tissue components including the (1) amniotic membrane, (2) stroma (namely, Wharton's jelly), and (3) blood vessels (two arteries and one vein). The stroma is also further divided into three histological zones including the (1) subamniotic zone, (2) intervascular zone, and (3) perivascular zone (Can & Karahuseyinoglu, 2007). Wharton´s jelly (WJ) is a proteoglycan rich connective tissue of the UC. Within the abundant extracellular matrix of WJ resides a recently described stem cell population called UC Matrix Stem Cells. Can be isolated around 400,000 cells per UC, which is significantly greater than the number of MSCs that can be routinely isolated from adult bone marrow. Isolated MSCs express CD29 and CD54, consistent with a mesenchymal cell type, and can be propagated in culture for more than 80 population doublings (Marcus & Woodbury, 2008). *In vitro* the WJ MSCs cells are capable of differentiation to multiple mesodermal cell types. This cells have been successfully differentiated into various cell types including adipocytes (Karahuseyinoglu et al., 2008), chondrocytes (Baksh et al., 2007; Wang et al., 2004), osteocytes (Baksh et al., 2007; Conconi et al., 2006; Wang et al., 2004), cardiomyocytes (Kadivar et al., 2006; Wang et al., 2004), skeletal myocytes (Conconi et al., 2006), hepatocytes (Kadivar et al., 2006), insulin-producing cells (Wu et al., 2009) as well as neuron-like cells (Fu et al., 2006; Weiss et al., 2006) (see Fig.3).

Generation of clinically important dopaminergic neurons has been also reported by other groups (Fu et al., 2006; Wang et al., 2004). MSCs isolated from WJ may be a valuable cellular system to improve peripheral nerve regeneration, since they possess stem cell properties and are able to differentiate *in vitro* into neuron-like cells (Fu et al., 2006; Yang et al., 2008). The transplanted cells are able to promote local blood vessel formation and to locally

produce neurotrophic factors like BDNF and GDNF (Wang et al., 2004). Transformed MSCs are still viable 4 months after transplantation without the need for immunological suppression, suggesting them as good source for Regenerative Medicine (Fu et al., 2006).

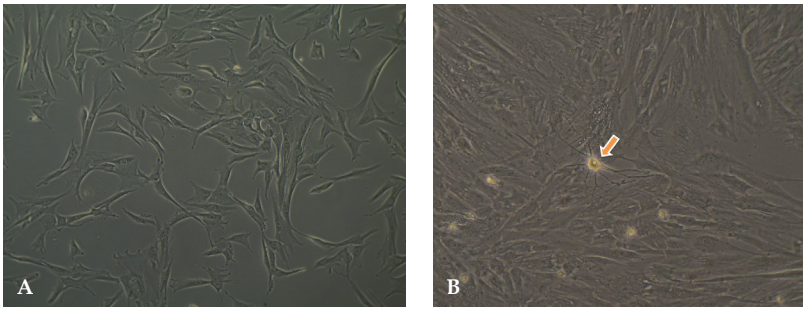

Fig. 3. Undifferentiated mesenchymal stem cells, from Wharton's jelly, exhibiting a star-like shape with a flat morphology (A) and neural-like cells, differentiated after 96 hours with neurogenic medium, formation of typical neural-like multi-branches (B) (100X magnification).

4. Microsurgical procedures

Rodents, particularly the rat and the mouse, have become the most frequently utilized animal models for the study of peripheral nerve regeneration because of the widespread availability of these animals as well as the distribution of their nerve trunks which is similar to humans (Mackinnon et al., 1985; Rodriguez & Navarro, 2004). Although other nerve trunks, especially in the rat forelimb, are getting more and more used for experimental research (Papalia et al., 2006), the rat sciatic nerve is still the far more employed experimental model as it provides a nerve trunk with adequate length and space at the mid-thigh for surgical manipulation and/or introduction of grafts or guides (Rodriguez & Navarro, 2004). Although sciatic nerve injuries themselves are rare in humans, this experimental model provides a very realistic testing bench for lesions involving plurifascicular mixed nerves with axons of different size and type competing to reach and reinnervate distal targets (Mackinnon et al., 1985). Common types of experimentally induced injuries include focal crush or freeze injury that causes axonal interruption but preserves the connective sheaths (axonotmesis), complete transection disrupting the whole nerve trunk (neurotmesis) and resection of a nerve segment inducing a gap of certain length. For these reasons our experimental work, concerning the *in vivo* testing of neurotmesis injury regeneration, was based on the use of Sasco Sprague-Dawley rat sciatic nerve. Usually, the surgeries are performed under an M-650 operating microscope (Leica Microsystems, Wetzlar, Germany). Under deep anaesthesia (ketamine 9 mg/100 g; xylazine 1.25 mg/100 g, atropine 0.025 mg/100 body weight, intramuscular), the right sciatic nerve is exposed through a skin incision extending from the greater trochanter to the distal mid-half followed by a muscle splitting incision. After nerve mobilisation, a transection injury is performed (neurotmesis) using straight microsurgical scissors, at a level as low as possible, in general, immediately above the terminal nerve ramification. The proximal and distal nerve stumps are inserted 3 mm into the tube-guide (not covered or covered with cells) and

held in place, maintaining a nerve gap of 10mm, with two epineurial sutures using 7/0 monofilament nylon. For neurotmesis without gap, the nerve is reconstructed with an end-to-end suture, with two epineural sutures using de 7/0 monofilament nylon. Finally the skin and subcutaneous tissues are closed with a simple-interrupted suture of a non-absorbable filament (Synthofil®, Ethicon). An antibiotic (enrofloxacin, Alsir® 2.5 %, 5 mg / kg b.w., subcutaneously) is always administered to prevent any infections. To prevent autotomy a deterrent substance must be applied to rats' right foot (Kerns et al., 1991; Sporel-Ozakat et al., 1991). All procedures must be performed accordance with the European Communities Council Directive of November 1986 (86/609/EEC).

5. Functional evaluation

Our studies of sciatic nerve regeneration after neurotmesis include a post-surgery follow-up period of 20 weeks based on the assumption that, by the end of this time, functional and morphological recovery are complete (Amado et al., 2010; Luis et al., 2007b; Luis et al., 2008; Simoes et al., 2010). Although both morphological and functional data have been used to assess neural regeneration after induced neurotmesis and axonotmesis injuries, the correlation between these two types of assessment is usually poor (Dellon & Mackinnon, 1989; Shen & Zhu, 1995). Classical and newly developed methods of assessing nerve recovery, including histomorphometry, retrograde transport of horseradish peroxidase and retrograde fluorescent labelling (Mackinnon et al., 1985; Mackinnon SE, 1988) do not necessarily predict the reestablishment of motor and sensory functions (de Medinaceli et al., 1982; Shen & Zhu, 1995). Although such techniques are useful in studying the nerve regeneration process, they generally fail in assessing functional recovery (Shen & Zhu, 1995). In this sense, research on peripheral nerve injury needs to combine both functional and morphological assessment. The use of biomechanical techniques and rat's gait kinematic evaluation is a progress in documenting functional recovery (Varejao et al., 2003b). Indeed, the use of biomechanical parameters has given valuable insight into the effects of the sciatic denervation/reinnervation, and thus represents an integration of the neural control acting on the ankle and foot muscles (Varejao et al., 2003b; Varejao et al., 2002).

5.1 Evaluation of motor performance (EPT) and nociceptive function (WRL)

Motor performance and nociceptive function were evaluated by measuring extensor postural thrust (EPT) and withdrawal reflex latency (WRL), respectively. The animals are tested pre-operatively (week-0), at weeks 1, 2, and every two weeks thereafter until week-20. The EPT was originally proposed by Thalhammer and collaborators, (Thalhammer et al., 1995) as a part of the neurological recovery evaluation in the rat after sciatic nerve injury. For this test, the entire body of the rat, excepting the hind-limbs, is wrapped in a surgical towel. Supporting the animal by the thorax and lowering the affected hind-limb towards the platform of a digital balance, elicits the EPT. As the animal is lowered to the platform, it extends the hind-limb, anticipating the contact made by the distal metatarsus and digits. The force in grams (g) applied to the digital platform balance is recorded. The same procedure is applied to the contra-lateral, unaffected limb. Each EPT test must be repeated 3 times and the average result is considered. The normal (unaffected limb) EPT (NEPT) and experimental EPT (EEPT) values are incorporated into a equation (Equation 1) to derive the percentage of functional deficit (Koka & Hadlock, 2001).

$$\text{Percentage motor deficit} = [(\text{NEPT} - \text{EEPT}) / \text{NEPT}]*100$$

The EPT data, originally measured in grams of weight borne by each hindlimb, is expressed as percentage deficit from total bearing weight as determined by the weight borne by the unoperated limb. Potential pitfalls of the EPT do exist. It takes a certain training period for the tester to become comfortable handling the animals, and this comfort level is critical for the animal to behave in a non frightened way. There is also a level of recognition of when the animal is bearing its maximum weight, which is critical since the tester is supporting the body of the animal at all times. Once this recognition takes place, through training by an experienced tester, the examination becomes highly reproducible (Koka & Hadlock, 2001).
To assess the nociceptive withdrawal reflex (WRL), the hotplate test was modified as described by Masters and collaborators (1993). The rat is wrapped in a surgical towel above its waist and then positioned to stand with the affected hind paw on a hot plate at 56ºC and with the other on a room temperature plate. WRL is defined as the time elapsed from the onset of hotplate contact to withdrawal of the hind paw and measured with a stopwatch. Normal rats withdraw their paws from the hotplate within 4.3 s or less (Hu et al., 1997). The affected limbs are tested 3 times, with an interval of 2 min between consecutive tests to prevent sensitization, and the three latencies are averaged to obtain a final result (Campbell, 2001). If there is no paw withdrawal after 12 s, the heat stimulus is removed to prevent tissue damage, and the animal is assigned with the maximal WRL of 12 s (Varejao et al., 2003a).

5.2 Sciatic functional index (SFI) and static sciatic index (SSI)

For SFI, animals are tested in a confined walkway measuring 42-cm-long and 8.2-cm-wide, with a dark shelter at the end. A white paper is placed on the floor of the rat walking corridor. The hind paws of the rats are pressed down onto a finger paint-soaked sponge, and they are then allowed to walk down the corridor leaving its hind footprints on the paper. Often, several walks are required to obtain clear print marks of both feet. Prior to any surgical procedure, all rats are trained to walk in the corridor, and a baseline walking track is recorded. Subsequently, walking tracks are recorded pre-operatively (week-0), at weeks 1, 2, and every two weeks thereafter until week-20. Several measurements are taken from the footprints: (I) distance from the heel to the third toe, the print length (PL); (II) distance from the first to the fifth toe, the toe spread (TS); and (III) distance from the second to the fourth toe, the intermediary toe spread (ITS). The static footprints are obtained at least during four occasional rest periods. In the static evaluation (SSI) only the parameters TS and ITS, are measured. For both dynamic (SFI) and static assessment (SSI), all measurements are taken from the experimental and normal sides. Four steps should be analyzed per rat. Prints for measurements should be chosen at the time of walking based on clarity and completeness at a point when the rat was walking briskly. The mean distances of three measurements are used to calculate the following factors (dynamic and static):

$$\text{Toe spread factor (TSF)} = (\text{ETS} - \text{NTS})/\text{NTS}$$

$$\text{Intermediate toe spread factor (ITSF)} = (\text{EITS} - \text{NITS})/\text{NITS}$$

$$\text{Print length factor (PLF)} = (\text{EPL} - \text{NPL})/\text{NPL}$$

Where the capital letters E and N indicate injured and non-injured side, respectively.
The SFI was calculated as described by Bain et al. (1989) (Bain et al., 1989) according to the following equation:

$$SFI = -38.3\ (EPL - NPL)/NPL + 109.5(ETS-NTS)/NTS + 13.3(EIT-NIT)/NIT - 8.8 = (-38.3 \times PLF) + (109.5 \times TSF) + (13.3 \times ITSF) - 8.8$$

The SSI is a time-saving and easy technique for accurate functional assessment of peripheral nerve regeneration in rats and is calculated using the static factors, not considering the print length factor (PL), according to the equation (Bervar, 2000; Meek et al., 2004)

$$SSI = [(108.44 \times TSF) + (31.85 \times ITSF)] - 5.49$$

For both SFI and SSI, an index score of 0 is considered normal and an index of -100 indicates total impairment. When no footprints are measurable, the index score of -100 is given. In each walking track three footprints must be analyzed by a single observer, and the average of the measurements are used in SFI calculations.

5.3 Kinematic analysis

Locomotion is also of higher functional relevance since it involves integrated function of both the motor and sensory systems and their respective components, such as skeletal muscles, sensory endings, efferent and afferent nerve fibers and integrative centers within the central nervous system. Muscles innervated by sciatic nerve branches include both dorsiflexors and plantarflexors and, although in previous studies we focused our kinematic analysis only in the stance phase (Amado et al., 2010; Amado et al., 2008; Luis et al., 2008), we now prefer to include analysis of the ankle joint motion also during the swing phase in order to provide additional information (Joao et al., 2010).

In our previous studies we analyzed ankle kinematics in the sagittal plane during the stance phase of walking either after sciatic nerve transection and repair (Amado et al., 2010; Luis et al., 2008) or after sciatic nerve crush (Amado et al., 2008). The two-dimensional (2D) ankle motion analysis was conducted during voluntary level walking along a corridor with darkened cages at both ends to attract the animals. The lateral walls of the corridor were made of Perspex and a high speed video camera (JVC GR-DVL9800, Nex Jersey, USA) was placed orthogonally to corridor length in order to record ankle motion during walking. Sagittal records of the rat walking were obtained at a frame rate of 100 frames per second and images were semi-automatically digitized using marks at reference points of the rat hindlimb and foot (see Fig. 4B).

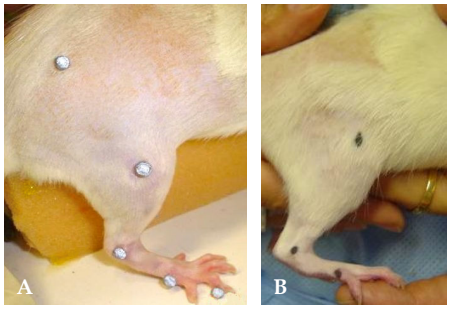

Fig. 4. Reflective markers with 2mm diameter were attached to the right hindlimb at bony prominences (from bottom to top): (1) tip of fourth finger, (2) head of fifth metatarsal, (3) lateral malleolus, (4) lateral knee joint, (5) trochanter major (A). Tattoo marks at bony prominences of the right hindlimb: (1) head of fifth metatarsal, (2) lateral malleolus, (3) lateral knee joint (B).

The trajectories of the segments leg and hindfoot were obtained through this procedure and ankle joint angle was derived by using dot product computation. Ankle kinematics parameters proposed by Varejão et al. (2003) were employed in order to assess functional recovery after sciatic nerve transection and repair and to compare treatments using our tested biomaterials and cellular system. Our ankle joint kinematic analysis generally showed profound walking dysfunction in the weeks after sciatic neurotmesis. Changes affected the whole stance phase and were best characterized by an inability of the animals to perform the normal ankle push off action during the second half of this walking phase (see Fig 5 and Fig.6). Profound ankle kinematic changes during the stance phase of walking were also evident when taking into account angular velocity data. Uninjured animals show a clear ankle angular velocity peak both at the initiation and end of the stance phase. After sciatic transection these two peaks are not observed and the stance phase is characterized by a rather steady increase in positive ankle velocity that corresponds to a progressive augment in ankle dorsiflexion. This abnormal pattern of ankle motion during the stance phase of walking was interpreted as caused by denervation and paralysis of the ankle plantarflexors that were unable to actively extend the ankle against the load of the body weight. In sciatic nerve transected and repaired animals, the recovery of the normal ankle motion pattern of walking is slow and largely incomplete. After 20 weeks of recovery, abnormal ankle motion is still noticed after sciatic nerve neurotmesis (Amado et al., 2010; Luis et al., 2008). In our recent study (Amado et al., 2010), investigating the role of a collagen membrane with and without differentiated N1E-115 cells enwrapped around the transected and end-to-end repaired sciatic nerve, the shape of ankle joint motion during the stance phase showed little improvements until three months after injury (see Fig 5 and Fig.6).

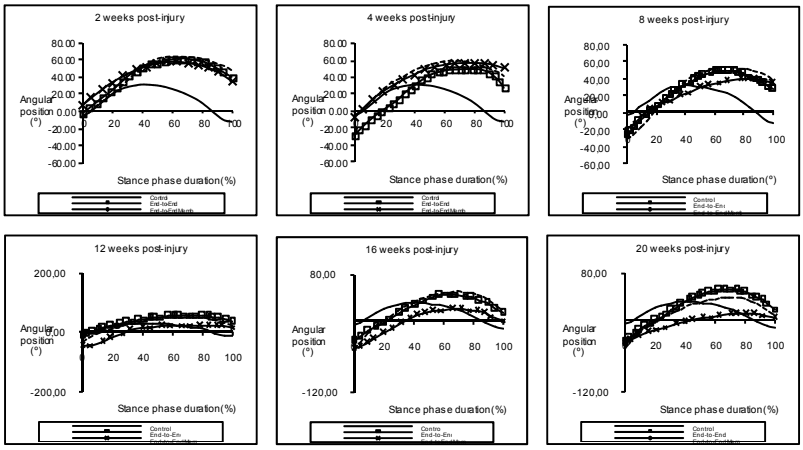

Fig. 5. Kinematics plots in the sagittal plane for the angular position (º) of the ankle as it moves through the stance phase, during the healing period of 20 weeks. The mean of each group is plotted.

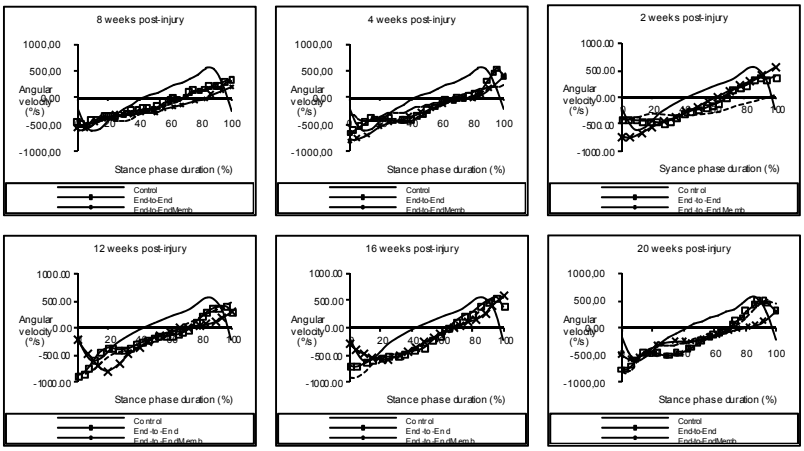

Fig. 6. Kinematics plots in the sagittal plane for the angular velocity (°/s) of the ankle as it moves through the stance phase, during the healing period of 20 weeks. The mean of each group is plotted.

A progressive improvement in ankle kinematics occurred from this time point up to the end of the 20 weeks recovery time. Such improvement consisted mainly in a slight recovery of ankle plantarflexion at the end of stance phase and lesser peak dorsiflexion at midstance. These changes in ankle kinematics are suggestive of muscle reinnervation and increased force generation ability by the ankle pantarflexor muscle group. In this study, ankle kinematics data were in general agreement with the results of the EPT and WRL tests. The latter tests also demonstrated progressive recovery of motor and sensory function along the follow up time that in the case of the WRL test was accelerated beyond the 12 weeks time point. As for ankle kinematics, the EPT and WRL results also demonstrated incomplete functional recovery in these animals, with slightly better recovery in the end-to-end repair group compared to other two groups. However, ankle kinematics must be envisaged merely as an indirect measure of muscle function. It should be noticed that walking requires fine coordination of limbs motion and definitely quadruped animals have many movement strategies to compensate for deficit in one of the hindlimbs. Through plasticity of integrative structures, animals may develop adaptive patterns that persist even if significant reinnervation takes place. Also, no direct relation exists between more simple tests of muscle strength or of sensory function and a complex action such as walking (Varejao et al., 2003b). Indeed, ankle kinematics data poses a fundamental question. Does recovery of ankle motion during walking signals successful muscle reinnervation and regain of muscle function or else is a product of compensatory changes at whole hindlimb level? To answer this question satisfactorily, walking analysis has to be improved by extending the analysis to hip and knee joints and should be combined with direct measures of muscle activity (Gramsbergen et al., 2000a) and to measures of the force applied to the ground by the walking animal (Howard et al., 2000). To better assess hindlimb joint kinematics during walking, we recently analyzed hip, knee and ankle joint kinematics during recovery of less severe sciatic nerve crush injury, using a more sophisticated motion capture system to track the motion of reflective markers attached to the rat hindlimb (unpublished observations) (see Fig. 4A).

After this kind of injury, functional recovery is often deemed as complete even on the basis of ankle kinematic analysis with only minor walking changes observed after 12 weeks of recovery. However, after 12 weeks of recovery from complete sciatic nerve crush, changes in hip and knee kinematics during walking were present, when compared to sham-operated control animals. Importantly, such altered hip and knee kinematics were in contrast with total reestablishment of the normal pattern of ankle motion in sciatic-crushed animals.
Individual joint kinematics either in control or nerve-injured animals is characterized by high variability, with notable differences between different animals and even from step to step (Chang et al., 2009). Such high level of variability, which seems to be an intrinsic property of normal quadruped walking, seriously affects the precision of joint kinematic measures of functional recovery after nerve injury. Reducing this variability is a challenge for efficient use of walking analysis to assess functional recovery. Attempts to overcome this limitation include constraining walking velocity by using treadmill walking instead of self-paced locomotion (Pereira et al., 2006). This, of course, is likely to reduce step-by-step variability in joint kinematics but has the disadvantage of requiring expensive equipment and limits the possibility of combining kinematic analysis with other data, such as ground reaction forces. Other possibilities look at a global, limb-level movement analyses as an alternative to individual joints kinematics (Chang et al., 2009; Sabatier et al., 2011). Also, systematic changes in the biomechanical and movement control constraints of the locomotor task, such as using up- and down-slope walking might also increase the accuracy of walking analysis within the context of peripheral nerve research (Sabatier et al., 2011).
In summary, walking analysis is a promising method to assess functional recovery after hindlimb nerve injury. However, in order to provide accurate measures of functional recovery, walking analysis after hindlimb peripheral nerve injury will have to evolve from simply analyzing ankle kinematics to reach a full biomechanical description of hindlimb motion including analysis of hip, knee and ankle joints. Further refinements of walking analysis in the field of peripheral nerve research using the rat model will probably include the combined use of joint kinematics, ground reaction forces and electromyographical data of muscle activity.

6. Morphological analysis

It has been recently pointed out that morphological analysis is the far most common method for the study of peripheral nerve regeneration (Raimondo et al., 2009). Actually, the investigation of nerve morphology can give us important information on various aspects of the regeneration processes which relates with nerve function (Geuna et al., 2009).
Although different types of fixatives can be used for peripheral nerve histology, we fix nerve samples in a solution of 2.5% purified glutaraldehyde (Histo-line Laboratories s.r.l., Milano, Italy) and 0.5% saccarose (Merck, Darmstadt, Germany) in 0.1M Sörensen phosphate buffer, pH 7.4, for 6-8h. Nerves are then washed and stored in 0.1M Sörensen phosphate buffer added with 1.5% saccarose at 4-6°C prior to embedding. Sörensen phosphate buffer is made with 56g di-potassium hydrogen phosphate 3-hydrate (K2HPO4-3H2O) (Fluka, Buchs, Switzerland) and 10.6 g sodium di-hydrogen phosphate 1-hydrate (NaH2PO4-H2O) (Merck, Darmstadt, Germany) in 1 litre of doubly-distilled water. Just before the embedding, nerves are washed for few minutes in the storage solution and then immersed for 2 h in 2% osmium tetroxide (Sigma, St.Louis, MO) in the same buffer solution. The specimens are then carefully dehydrated in passages in ethanol and embedded in

Glauerts' mixture of resins which is made of equal parts of Araldite M and the Araldite Härter, HY 964 (Merck, Darmstad, Germany). At the resin mixture, 2% of accelerator 964, DY 064 is added (Merck, Darmstad, Germany). Finally, the plasticizer (0.5% of dibutylphthalate) is added to the resin.

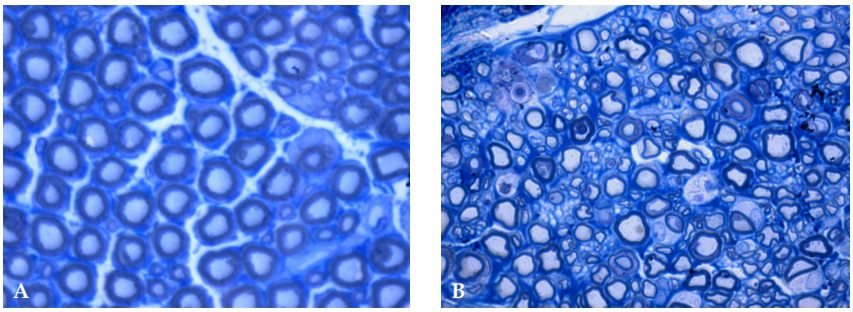

Fig. 7. Representative high resolution photomicrographs of nerve fibers from normal (A) and regenerated (B) rat sciatic nerves after entubulation with collagen nerve guide. Original magnification = 1,000x.

In our laboratory, histomorphometry (stereology) is carried out on toludine-blue-stained semi-thin sections (2.5 micron-thick) of nerve samples using a DM4000B microscope equipped with a DFC320 digital camera and an IM50 image manager system (Leica Microsystems, Wetzlar, Germany). We adopt a final magnification of 6,600x in order to enable accurate identification of myelinated nerve fibers (Figure 9). A 2D-disector method, (Raimondo et al., 2009) is finally used for estimating the total number of myelinated fibers (N), the mean diameter of fiber (D) and axon (d) as well as mean [(D-d)/2] and g-ratio (D/d) (see Fig.7).

7. Synopsis of results and discussion

Peripheral nerve regeneration can be studied in a number of different experimental models based on the use of nerves from both forelimb and hindlimb (Hu et al., 1997). The experimental animal model of choice for many researchers remains the rat sciatic nerve. It provides an inexpensive source of mammalian nervous tissue of identical genetic stock that it is easy to work with and well studied (Geuna et al., 2009) and shows a similar capacity for regeneration in rats and sub-humans primates (Johnson et al., 2008). The rat sciatic nerve is a widely used model for the evaluation of motor as well as sensory nerve function at the same time. One of the most addressed issues in experimental nerve repair research is represented by entubulation (Chen et al., 2006). While early studies were more directed towards biological material (Kerns et al., 1991) recent studies have focused more on synthetic materials that are biodegradable. The majority of natural biomaterials used in clinical applications such as hyaluronic acid, collagen, and gelatin are derived from animal sources. In spite of thorough purification methods these materials bear the inherent risk of transfer of viral and prionic diseases and may cause immunological body reactions (Koka & Hadlock, 2001; Luis et al., 2007b). Synthetic biomaterials are not associated with these risks (Koka & Hadlock, 2001; Luis et al., 2007b).

Our group has assessed two types of nerve guides made of a different type of biodegradable synthetic biomaterial, PLGA and caprolactone (Neurolac®). Our data showed that both types of nerve guides were a mean to help in the growth of axons and didn't deleteriously interfere with the nerve regeneration process. While the information on the effectiveness of Neurolac® tubes for allowing nerve regeneration was already provided experimentally (; Geuna et al., 2009; Luis et al., 2008) and with patients (Bertleff et al., 2005), the PLGA tubes with the polymers proportion of 90 PLA:10 PLG used in that study have never been tested *in vivo* before (Luis et al., 2007b). Results of the comparative functional assessment showed that the differences between the two experimental groups were not significant in terms of motor and nociceptive recovery. The EPT proposed by Thalhammer and coworkers (Geuna, 2005) to evaluate the motor function in rats is used routinely by veterinarian neurologists to evaluate the nervous system of small domestic animals. This reflex is initiated by a stretching of the spindles in the interosseous muscles and stimulation of sensory receptors of the foot (Lundborg, 2002). A steady recover of motor deficit occurred throughout the 20-week post-surgery period in the group of animals where PLGA and Neurolac® tube-guides were used. As expected, the motor recovery in animals of the end-to-end group occurred significantly faster and to a larger extent when compared to the entubulation groups. Similarly, nociception recovered to a significantly larger extent in the end-to-end group compared to both entubulation groups which, on the contrary, did not differ significantly between them (Luis et al., 2007b). Interestingly, when the nerve is transected and the regenerating axons must bridge a gap, sensory neurons exhibit a faster regenerative pattern than motor neurons (Lundborg, 2002). Morphological analysis showed a different pattern of biodegradation of the two tubes. In fact, while in the nerves repaired by Neurolac® the structure of the polymer was still well preserved at week-20, in the nerves repaired by PLGA guides, the polymer was largely substituted by a connective matrix rich in collagen fibbers and fibroblasts resembling a normal epineurium. These results may suggest that PLGA can be a better biomaterial for fashioning nerve guides since nerves regenerated inside it were more similar to a normal nerve than those regenerated inside Neurolac® guides, although the results of the motor and sensory functional assessment did not disclose significant differences between the two tube-guides and thus both should be considered a good substrate for preparing tubular nerve guides. We have also used the rat sciatic nerve model for investigating the effects of chitosan type III membranes after neurotmesis followed by surgical repair either by direct suture, or autograft or tubulization. Morphological results showed that nerve regeneration occurred when the chitosan type III tube-guide was used and that, at time of withdrawal, Wallerian degeneration was almost completed and substituted by re-growing axons and the accompanying Schwann cells. The results obtained with chitosan type III tube-guides were significantly better, in terms of functional and morphologic recovery, when compared with PLGA90:10 where the regeneration pattern was worse (Simoes et al., 2010). The synergistic effect of a more favorable porous microstructure and physicochemical properties (more wettable and higher water uptake level) of chitosan type III compared to common chitosan, as well as the presence of silica ions, may be responsible for the good results in promoting post-traumatic nerve regeneration (Amado et al., 2008) suggesting that this material may not just work as a simple mechanical scaffold but instead may work as an inducer of nerve regeneration (Amado et al., 2008). The neuroregenerative property of chitosan type III might be explained

by a direct stimulation of Schwann cell proliferation, axon elongation and myelination (Shirosaki et al., 2005). Yet, the expression of established myelin genes such as PMP22, PO and MBP (Pietak et al., 2007) may be influenced by the presence of silica ions which exert an effect on several glycoprotein expression (Pietak et al., 2007). Taken together, results of this study support the view that hybrid chitosan type III membranes can be a valuable tool for fashioning nerve guides aimed to bridge nerve defects. We also investigated the effects on nerve regeneration of the employment PLGA90:10 nerve guide tubes covered with N1E-115 cells *in vitro* differentiated in the presence of DMSO for 48 hours (Geuna et al., 2001). Results showed that both motor and sensory functions improved significantly similarly to what occurs in PLGA tubes alone (Luis et al., 2008). Nerve recovery of around 60% was achieved by week-20, in both groups, reconstructed with PLGA 90:10 tube-guides with or without the cellular system. The pattern of degradation and the degradation products of PLGA90:10 more acidic than the collagen ones do not seem to influence negatively the degree of nerve regeneration during the healing period. On the other hand, the biodegradable non-woven structure of PLGA tubes may offer some advantages in terms of microporosity which may enhance nerve repair. It is not surprising that recovery was significantly better in the group where the gap was reconstructed using the autologous graft since this is still considered the gold standard for peripheral nerve regeneration (Matsuyama et al., 2000). The rationale for the use of the N1E-115 cells was to take advantages of the properties of these cells as a neural-like cellular source of neurotrophic factors (Geuna et al., 2001).

Although tube guides are a suitable choice for peripheral nerve reconstruction, it is known that nerve regeneration and functional recovery are less satisfactory than when nerve repair is done by using an end-to-end neurorraphy or when an autologous nerve graft is applied (Geuna et al., 2009). For example, the risk of neuroma formation in neurotmesis injury is considerable, which is clearly avoided with tube-guide technique. In this sense, enhancing the rate of axonal growth might prevent the occurrence of side effects and might turn nerve regeneration faster, thus improving functional recovery. Neurotrophic factors play an important role in nerve regeneration after injury or disease and it is conceivable that if neurotrophic factors are applied in the close vicinity of the injured nerve their healing potency is optimized. In spite of these premises and contrary to our initial hypothesis, the N1E-115 cells did not facilitate either nerve regeneration or functional recovery and, as far as morphometrical parameters are concerned, results showed that the presence of this cellular system reduced the number and size of the regenerated fibers. These results suggest that this type of nerve guides can partially impair nerve regeneration, at least from a morphological point of view (Luis et al., 2008). The impaired axonal regeneration seems to be the result of N1E-115 cells surrounding and invading the regenerating nerve, since numerous of these cells where seen colonizing the nerve and might have deprived regenerated nerve fibers blood supply (Luis et al., 2008). The use of N1E-115 cells did not promote nerve healing and their use might even derange the nerve regenerating process. Whereas the effects on nerve regeneration were negative, an interesting result of this study was the demonstration that the cell delivery system that we have used was effecting in enabling long-term colonization of the regenerated nerve by transplanted neural cells. Whether the negative effects of using N1E-115 cells as a cellular aid to peripheral neural tissue regeneration extends to other types of cells is not known at present and further studies are warranted to assess the role of other cellular systems, e.g. mesenchymal stem cells, as a foreseeable therapeutic strategy in peripheral nerve regeneration. Our

experimental results with this cellular system are also important in the perspective of stem cell transplantation employment for improving posttraumatic nerve regeneration with patients (Luis et al., 2008). Undoubtedly, great enthusiasm has raised among researchers and in the general public about cell-based therapies in regenerative medicine (Geuna et al., 2009; Thalhammer et al., 1995). There is a widespread opinion that this type of therapy is also very safe in comparison to other pharmacological or surgical therapeutic approaches. By contrast, recent studies showed that cell-based therapy might be ineffective for improving nerve regeneration (Varejao et al., 2003b) or even have negative effects by hindering the nerve regeneration process after tubulisation repair. Whereas the choice of the cell type to be used for transplantation is certainly very important for the therapeutic success, our present results suggest that the paradigm that donor tissues guide transplanted stem cells to differentiate in the direction that is useful for the regeneration process it is not always true and the possibility that transplanted stem cells choose another differentiation line potentially in contrast with the regenerative process should be always taken in consideration.

8. Acknowledgements

This work was supported by the Fundação para a Ciência e Tecnologia (FCT) through the PhD grant SFRH/BD/70211/2010. Financial support was also provided by the European Regional Development Fund, through the QREN Project BIOMAT&CELL No. 1372.

9. References

Amado, S., Rodrigues, J. M., Luis, A. L., Armada-da-Silva, P. A., Vieira, M., Gartner, A., Simoes, M. J., Veloso, A. P., Fornaro, M., Raimondo, S., Varejao, A. S., Geuna, S., & Mauricio, A. C. (2010). Effects of collagen membranes enriched with in vitro-differentiated N1E-115 cells on rat sciatic nerve regeneration after end-to-end repair. *J Neuroeng Rehabil*, 7: 7. ISSN 1743-0003.

Amado, S., Simoes, M. J., Armada da Silva, P. A., Luis, A. L., Shirosaki, Y., Lopes, M. A., Santos, J. D., Fregnan, F., Gambarotta, G., Raimondo, S., Fornaro, M., Veloso, A. P., Varejao, A. S., Mauricio, A. C., & Geuna, S. (2008). Use of hybrid chitosan membranes and N1E-115 cells for promoting nerve regeneration in an axonotmesis rat model. *Biomaterials*, 29(33): 4409-4419. ISSN 0142-9612.

Amano, T., Richelson, E., & Nirenberg, M. (1972). Neurotransmitter synthesis by neuroblastoma clones (neuroblast differentiation-cell culture-choline acetyltransferase-acetylcholinesterase-tyrosine hydroxylase-axons-dendrites). *Proc Natl Acad Sci U S A*, 69(1): 258-263. ISSN 0027-8424.

Archibald, S. J., Shefner, J., Krarup, C., & Madison, R. D. (1995). Monkey median nerve repaired by nerve graft or collagen nerve guide tube. *J Neurosci*, 15(5 Pt 2): 4109-4123. ISSN 0270-6474.

Bain, J. R., Mackinnon, S. E., & Hunter, D. A. (1989). Functional evaluation of complete sciatic, peroneal, and posterior tibial nerve lesions in the rat. *Plast Reconstr Surg*, 83(1): 129-138. ISSN 0032-1052.

Baksh, D., Yao, R., & Tuan, R. S. (2007). Comparison of proliferative and multilineage differentiation potential of human mesenchymal stem cells derived from umbilical cord and bone marrow. *Stem Cells*, 25(6): 1384-1392. ISSN 1384-1392.

Beer, G. M., Steurer, J., & Meyer, V. E. (2001). Standardizing nerve crushes with a non-serrated clamp. *J Reconstr Microsurg*, 17(7): 531-534. ISSN 0743-684X.

Bertleff, M. J., Meek, M. F., & Nicolai, J. P. (2005). A prospective clinical evaluation of biodegradable neurolac nerve guides for sensory nerve repair in the hand. *J Hand Surg Am*, 30(3): 513-518. ISSN 0363-5023.

Bervar, M. (2000). Video analysis of standing--an alternative footprint analysis to assess functional loss following injury to the rat sciatic nerve. *J Neurosci Methods*, 102(2): 109-116. ISSN 0165-0270.

Bichara, D. A., Zhao, X., Hwang, N. S., Bodugoz-Senturk, H., Yaremchuk, M. J., Randolph, M. A., & Muratoglu, O. K. (2010). Porous poly(vinyl alcohol)-alginate gel hybrid construct for neocartilage formation using human nasoseptal cells. *J Surg Res*, 163(2): 331-336. ISSN 1095-8673.

Bini, T. B., Gao, S., Xu, X., Wang, S., Ramakrishna, S., & Leong, K. W. (2004). Peripheral nerve regeneration by microbraided poly(L-lactide-co-glycolide) biodegradable polymer fibers. *J Biomed Mater Res A*, 68(2): 286-295. ISSN 1549-3296.

Campbell, J. N. (2001). Nerve lesions and the generation of pain. *Muscle Nerve*, 24(10): 1261-1273. ISSN 0148-639X.

Can, A., & Karahuseyinoglu, S. (2007). Concise review: human umbilical cord stroma with regard to the source of fetus-derived stem cells. *Stem Cells*, 25(11): 2886-2895. ISSN 1549-4918.

Ceballos, D., Navarro, X., Dubey, N., Wendelschafer-Crabb, G., Kennedy, W. R., & Tranquillo, R. T. (1999). Magnetically aligned collagen gel filling a collagen nerve guide improves peripheral nerve regeneration. *Exp Neurol*, 158(2): 290-300. ISSN 0014-4887.

Chamberlain, L. J., Yannas, I. V., Hsu, H. P., & Spector, M. (2000). Connective tissue response to tubular implants for peripheral nerve regeneration: the role of myofibroblasts. *J Comp Neurol*, 417(4): 415-430. ISSN 0021-9967.

Chang, Y. H., Auyang, A. G., Scholz, J. P., & Nichols, T. R. (2009). Whole limb kinematics are preferentially conserved over individual joint kinematics after peripheral nerve injury. *J Exp Biol*, 212(Pt 21): 3511-3521. ISSN 3511-3521.

Chen, X., Wang, X. D., Chen, G., Lin, W. W., Yao, J., & Gu, X. S. (2006). Study of in vivo differentiation of rat bone marrow stromal cells into schwann cell-like cells. *Microsurgery*, 26(2): 111-115. ISSN 0738-1085.

Chen, Z. L., Yu, W. M., & Strickland, S. (2007). Peripheral regeneration. *Annu Rev Neurosci*, 30: 209-233. ISSN 0147-006X.

Conconi, M. T., Burra, P., Di Liddo, R., Calore, C., Turetta, M., Bellini, S., Bo, P., Nussdorfer, G. G., & Parnigotto, P. P. (2006). CD105(+) cells from Wharton's jelly show in vitro and in vivo myogenic differentiative potential. *Int J Mol Med*, 18(6): 1089-1096. ISSN 1107-3756.

Cui, L., Jiang, J., Wei, L., Zhou, X., Fraser, J. L., Snider, B. J., & Yu, S. P. (2008). Transplantation of embryonic stem cells improves nerve repair and functional recovery after severe sciatic nerve axotomy in rats. *Stem Cells*, 26(5): 1356-1365. ISSN 1549-4918.

de Medinaceli, L., Freed, W. J., & Wyatt, R. J. (1982). An index of the functional condition of rat sciatic nerve based on measurements made from walking tracks. *Exp Neurol*, 77(3): 634-643. ISSN 0014-4886.

Dellon, A. L., & Mackinnon, S. E. (1989). Sciatic nerve regeneration in the rat. Validity of walking track assessment in the presence of chronic contractures. *Microsurgery*, 10(3): 220-225. ISSN 0738-1085.

Den Dunnen, W. F., Meek, M. F., Robinson, P. H., & Schakernraad, J. M. (1998). Peripheral nerve regeneration through P(DLLA-epsilon-CL) nerve guides. *J Mater Sci Mater Med*, 9(12): 811-814. ISSN 0957-4530.

Fields, R. D., Le Beau, J. M., Longo, F. M., & Ellisman, M. H. (1989). Nerve regeneration through artificial tubular implants. *Prog Neurobiol*, 33(2): 87-134. ISSN 0301-0082.

Fu, Y. S., Shih, Y. T., Cheng, Y. C., & Min, M. Y. (2004). Transformation of human umbilical mesenchymal cells into neurons in vitro. *J Biomed Sci*, 11(5): 652-660. ISSN 1021-7770.

Geuna, S. (2005). The revolution of counting "tops": two decades of the disector principle in morphological research. *Microsc Res Tech*, 66(5): 270-274. ISSN 1059-910X.

Geuna, S., Raimondo, S., Ronchi, G., Di Scipio, F., Tos, P., Czaja, K., & Fornaro, M. (2009). Chapter 3: Histology of the peripheral nerve and changes occurring during nerve regeneration. *Int Rev Neurobiol*, 87: 27-46. ISSN 0074-7742.

Geuna, S., Tos, P., Guglielmone, R., Battiston, B., & Giacobini-Robecchi, M. G. (2001). Methodological issues in size estimation of myelinated nerve fibers in peripheral nerves. *Anat Embryol (Berl)*, 204(1): 1-10. ISSN 0340-2061.

Gramsbergen, A., Ijkema-Paassen, J., & Meek, M. F. (2000). Sciatic Nerve Transection in the Adult Rat: Abnormal EMG Patterns during Locomotion by Aberrant Innervation of Hindleg Muscles. *Experimental Neurology*, 161(1): 183-193. ISSN 0014-4886.

Grant, C., Twigg, P., Egan, A., Moody, A., Smith, A., Eagland, D., Crowther, N., & Britland, S. (2006). Poly(vinyl alcohol) hydrogel as a biocompatible viscoelastic mimetic for articular cartilage. *Biotechnol Prog*, 22(5): 1400-1406. ISSN 8756-7938.

Grimpe, B., & Silver, J. (2002). The extracellular matrix in axon regeneration. *Prog Brain Res*, 137: 333-349. ISSN 0079-6123.

Gu, X., Ding, F., Yang, Y., & Liu, J. (2011). Construction of tissue engineered nerve grafts and their application in peripheral nerve regeneration. *Prog Neurobiol*, 93(2): 204-230. ISSN 1873-5118.

Hood, B., Levene, H. B., & Levi, A. D. (2009). Transplantation of autologous Schwann cells for the repair of segmental peripheral nerve defects. *Neurosurg Focus*, 26(2): E4. ISSN 1092-0684.

Howard, C. S., Blakeney, D. C., Medige, J., Moy, O. J., & Peimer, C. A. (2000). Functional assessment in the rat by ground reaction forces. *J Biomech*, 33(6): 751-757. ISSN 0021-9290.

Hu, D., Hu, R., & Berde, C. (1997). Neurologic evaluation of infant and adult rats before and after sciatic nerve blockade. *Anesthesiology*, 86: 957-965. ISSN 003-3022.

Huang, Y. C., & Huang, Y. Y. (2006). Biomaterials and strategies for nerve regeneration. *Artif Organs*, 30(7): 514-522. ISSN 0160-564X.

Itoh, S., Suzuki, M., Yamaguchi, I., Takakuda, K., Kobayashi, H., Shinomiya, K., & Tanaka, J. (2003). Development of a nerve scaffold using a tendon chitosan tube. *Artif Organs*, 27(12): 1079-1088. ISSN 0160-564X.

Joao, F., Amado, S., Veloso, A., Armada-da-Silva, P., & Mauricio, A. C. (2010). Anatomical reference frame versus planar analysis: implications for the kinematics of the rat hindlimb during locomotion. *Rev Neurosci*, 21(6): 469-485. ISSN 0334-1763.

Johnson, E. O., & Soucacos, P. N. (2008). Nerve repair: experimental and clinical evaluation of biodegradable artificial nerve guides. *Injury*, 39 Suppl 3: S30-36. ISSN 1879-0267.

Johnson, W. L., Jindrich, D. L., Roy, R. R., & Reggie Edgerton, V. (2008). A three-dimensional model of the rat hindlimb: musculoskeletal geometry and muscle moment arms. *J Biomech*, 41(3): 610-619. ISSN 0021-9290.

Kadivar, M., Khatami, S., Mortazavi, Y., Shokrgozar, M. A., Taghikhani, M., & Soleimani, M. (2006). In vitro cardiomyogenic potential of human umbilical vein-derived mesenchymal stem cells. *Biochem Biophys Res Commun*, 340(2): 639-647. ISSN 0006-291X.

Karahuseyinoglu, S., Kocaefe, C., Balci, D., Erdemli, E., & Can, A. (2008). Functional structure of adipocytes differentiated from human umbilical cord stroma-derived stem cells. *Stem Cells*, 26(3): 682-691. ISSN 1549-4418.

Kerns, J. M., Braverman, B., Mathew, A., Lucchinetti, C., & Ivankovich, A. D. (1991). A comparison of cryoprobe and crush lesions in the rat sciatic nerve. *Pain*, 47(1): 31-39. ISSN 0304-3959.

Koka, R., & Hadlock, T. A. (2001). Quantification of functional recovery following rat sciatic nerve transection. *Exp Neurol*, 168(1): 192-195. ISSN 0014-4886.

Kranenburg, O., Scharnhorst, V., Van der Eb, A. J., & Zantema, A. (1995). Inhibition of cyclin-dependent kinase activity triggers neuronal differentiation of mouse neuroblastoma cells. *J Cell Biol*, 131(1): 227-234. ISSN 0021-9525.

Luis, A. L., Amado, S., Geuna, S., Rodrigues, J. M., Simoes, M. J., Santos, J. D., Fregnan, F., Raimondo, S., Veloso, A. P., Ferreira, A. J., Armada-da-Silva, P. A., Varejao, A. S., & Mauricio, A. C. (2007a). Long-term functional and morphological assessment of a standardized rat sciatic nerve crush injury with a non-serrated clamp. *J Neurosci Methods*, 163(1): 92-104. ISSN 0165-0270.

Luis, A. L., Rodrigues, J. M., Amado, S., Veloso, A. P., Armada-Da-Silva, P. A., Raimondo, S., Fregnan, F., Ferreira, A. J., Lopes, M. A., Santos, J. D., Geuna, S., Varejao, A. S., & Mauricio, A. C. (2007b). PLGA 90/10 and caprolactone biodegradable nerve guides for the reconstruction of the rat sciatic nerve. *Microsurgery*, 27(2): 125-137. ISSN 0738-1085.

Luis, A. L., Rodrigues, J. M., Geuna, S., Amado, S., Simoes, M. J., Fregnan, F., Ferreira, A. J., Veloso, A. P., Armada-da-Silva, P. A., Varejao, A. S., & Mauricio, A. C. (2008). Neural cell transplantation effects on sciatic nerve regeneration after a standardized crush injury in the rat. *Microsurgery*, 28(6): 458-470. ISSN 1098-2752.

Lundborg, G. (2002). Enhancing posttraumatic nerve regeneration. *J Peripher Nerv Syst*, 7(3): 139-140. ISSN 1085-9489.

Lundborg, G., Dahlin, L., Danielsen, N., & Zhao, Q. (1994). Trophism, tropism, and specificity in nerve regeneration. *J Reconstr Microsurg*, 10(5): 345-354. ISSN 0743-684X.

Mackinnon, S. E., Hudson, A. R., & Hunter, D. A. (1985). Histologic assessment of nerve regeneration in the rat. *Plast Reconstr Surg*, 75(3): 384-388. ISSN 0032-1052.

Marcus, A. J., & Woodbury, D. (2008). Fetal stem cells from extra-embryonic tissues: do not discard. *J Cell Mol Med*, 12(3): 730-742. ISSN 1582-1838.

Marreco, P. R., da Luz Moreira, P., Genari, S. C., & Moraes, A. M. (2004). Effects of different sterilization methods on the morphology, mechanical properties, and cytotoxicity

of chitosan membranes used as wound dressings. *J Biomed Mater Res B Appl Biomater*, 71(2): 268-277. ISSN 1552-4973.

Masters, D., Berde, C., Dutta, S., Griggs, C., Hu, D., Kupsky, W., & Langer, R. (1993). Prolonged regional nerve blockade by controlled release of local anesthetic from a biodegradable polymer matrix. *Anesthesiology*, 79: 340-346.

Matsuyama, T., Mackay, M., & Midha, R. (2000). Peripheral nerve repair and grafting techniques: a review. *Neurol Med Chir (Tokyo)*, 40(4): 187-199. ISSN 0470-8105.

May, M. (1983). Trauma to the facial nerve. *Otolaryngol Clin North Am*, 16(3): 661-670. ISSN 0030-6665.

Meek, M. F., & Coert, J. H. (2002). Clinical use of nerve conduits in peripheral-nerve repair: review of the literature. *J Reconstr Microsurg*, 18(2): 97-109. ISSN 0743-684X.

Meek, M. F., Jansen, K., Steendam, R., van Oeveren, W., van Wachem, P. B., & van Luyn, M. J. (2004). In vitro degradation and biocompatibility of poly(DL-lactide-epsilon-caprolactone) nerve guides. *J Biomed Mater Res A*, 68(1): 43-51. ISSN 1549-3296.

Mligiliche, N. L., Tabata, Y., Kitada, M., Endoh, K., Okamato, K., Fujimoto, E., & Ide, C. (2003). Poly lactic acid--caprolactone copolymer tube with a denatured skeletal muscle segment inside as a guide for peripheral nerve regeneration: a morphological and electrophysiological evaluation of the regenerated nerves. *Anat Sci Int*, 78(3): 156-161. ISSN 1447-6959.

Papalia, I., Tos, P., Scevola, A., Raimondo, S., & Geuna, S. (2006). The ulnar test: a method for the quantitative functional assessment of posttraumatic ulnar nerve recovery in the rat. *J Neurosci Methods*, 154(1-2): 198-203. ISSN 0165-0270.

Pereira, J. E., Cabrita, A. M., Filipe, V. M., Bulas-Cruz, J., Couto, P. A., Melo-Pinto, P., Costa, L. M., Geuna, S., Mauricio, A. C., & Varejao, A. S. (2006). A comparison analysis of hindlimb kinematics during overground and treadmill locomotion in rats. *Behav Brain Res*, 172(2): 212-218. ISSN 0166-4328.

Pietak, A. M., Reid, J. W., Stott, M. J., & Sayer, M. (2007). Silicon substitution in the calcium phosphate bioceramics. *Biomaterials*, 28(28): 4023-4032. ISSN 0142-9612.

Raimondo, S., Fornaro, M., Di Scipio, F., Ronchi, G., Giacobini-Robecchi, M. G., & Geuna, S. (2009). Chapter 5: Methods and protocols in peripheral nerve regeneration experimental research: part II-morphological techniques. *Int Rev Neurobiol*, 87: 81-103. ISSN 0074-7742.

Rodrigues, J. M., Luis, A. L., Lobato, J. V., Pinto, M. V., Faustino, A., Hussain, N. S., Lopes, M. A., Veloso, A. P., Freitas, M., Geuna, S., Santos, J. D., & Mauricio, A. C. (2005). Intracellular Ca2+ concentration in the N1E-115 neuronal cell line and its use for peripheric nerve regeneration. *Acta Med Port*, 18(5): 323-328. ISSN 1646-0758.

Rodriguez JF, V.-C. A., Navarro X. (2004). Regeneration and funcional recovery following peripheral nerve injury. *Drugs Discovery Today: Disease Models*, 1(2): 177-185.

Sabatier, M. J., To, B. N., Nicolini, J., & English, A. W. (2011). Effect of slope and sciatic nerve injury on ankle muscle recruitment and hindlimb kinematics during walking in the rat. *J Exp Biol*, 214(Pt 6): 1007-1016. ISSN 1007-1016.

Schmidt, C. E., & Leach, J. B. (2003). Neural tissue engineering: strategies for repair and regeneration. *Annu Rev Biomed Eng*, 5: 293-347. ISSN 1523-9829.

Senel, S., & McClure, S. J. (2004). Potential applications of chitosan in veterinary medicine. *Advanced Drug Delivery Reviews*, 56(10): 1467-1480.

Shen, N., & Zhu, J. (1995). Application of sciatic functional index in nerve functional assessment. *Microsurgery*, 16(8): 552-555. ISSN 0738-1085.

Shirosaki, Y., Tsuru, K., Hayakawa, S., Osaka, A., Lopes, M. A., Santos, J. D., & Fernandes, M. H. (2005). In vitro cytocompatibility of MG63 cells on chitosan-organosiloxane hybrid membranes. *Biomaterials*, 26(5): 485-493.

Simoes, M. J., Amado, S., Gartner, A., Armada-Da-Silva, P. A., Raimondo, S., Vieira, M., Luis, A. L., Shirosaki, Y., Veloso, A. P., Santos, J. D., Varejao, A. S., Geuna, S., & Mauricio, A. C. (2010). Use of chitosan scaffolds for repairing rat sciatic nerve defects. *Ital J Anat Embryol*, 115(3): 190-210. ISSN 1122-6714.

Smith, K. J., & Hall, S. M. (1988). Peripheral demyelination and remyelination initiated by the calcium-selective ionophore ionomycin: in vivo observations. *J Neurol Sci*, 83(1): 37-53. ISSN 0022-510X.

Sporel-Ozakat, R. E., Edwards, P. M., Hepgul, K. T., Savas, A., & Gispen, W. H. (1991). A simple method for reducing autotomy in rats after peripheral nerve lesions. *Journal of Neuroscience Methods*, 36(2-3): 263-265.

Tateishi, T., Chen, G., & Ushida, T. (2002). Biodegradable porous scaffolds for tissue engineering. *J Artif Organs*, 5: 77-83.

Thalhammer, J. G., Vladimirova, M., Bershadsky, B., & Strichartz, G. R. (1995). Neurologic evaluation of the rat during sciatic nerve block with lidocaine. *Anesthesiology*, 82(4): 1013-1025. ISSN 0003-3022.

Trump, B. F., & Berezesky, I. K. (1995). Calcium-mediated cell injury and cell death. *FASEB J*, 9(2): 219-228. ISSN 0892-6638.

Tsien, R. Y. (1989). Fluorescent probes of cell signaling. *Annu Rev Neurosci*, 12: 227-253. ISSN 0147-006X.

Varejao, A. S., Cabrita, A. M., Geuna, S., Patricio, J. A., Azevedo, H. R., Ferreira, A. J., & Meek, M. F. (2003a). Functional assessment of sciatic nerve recovery: biodegradable poly (DLLA-epsilon-CL) nerve guide filled with fresh skeletal muscle. *Microsurgery*, 23(4): 346-353. ISSN 0738-1085.

Varejao, A. S., Cabrita, A. M., Meek, M. F., Bulas-Cruz, J., Filipe, V. M., Gabriel, R. C., Ferreira, A. J., Geuna, S., & Winter, D. A. (2003b). Ankle kinematics to evaluate functional recovery in crushed rat sciatic nerve. *Muscle Nerve*, 27(6): 706-714. ISSN 0148-639X.

Varejao, A. S., Cabrita, A. M., Meek, M. F., Bulas-Cruz, J., Gabriel, R. C., Filipe, V. M., Melo-Pinto, P., & Winter, D. A. (2002). Motion of the foot and ankle during the stance phase in rats. *Muscle Nerve*, 26(5): 630-635. ISSN 1652-1670.

Waitayawinyu, T., Parisi, D. M., Miller, B., Luria, S., Morton, H. J., Chin, S. H., & Trumble, T. E. (2007). A comparison of polyglycolic acid versus type 1 collagen bioabsorbable nerve conduits in a rat model: an alternative to autografting. *J Hand Surg Am*, 32(10): 1521-1529. ISSN 0363-5023.

Wang, H. B., Mullins, M. E., Cregg, J. M., Hurtado, A., Oudega, M., Trombley, M. T., & Gilbert, R. J. (2009). Creation of highly aligned electrospun poly-L-lactic acid fibers for nerve regeneration applications. *J Neural Eng*, 6(1): 016001. ISSN 1751-2560.

Wang, H. S., Hung, S. C., Peng, S. T., Huang, C. C., Wei, H. M., Guo, Y. J., Fu, Y. S., Lai, M. C., & Chen, C. C. (2004). Mesenchymal stem cells in the Wharton's jelly of the human umbilical cord. *Stem Cells*, 22(7): 1330-1337. ISSN 1330-1337.

Wang, W., Itoh, S., Matsuda, A., Ichinose, S., Shinomiya, K., Hata, Y., & Tanaka, J. (2008). Influences of mechanical properties and permeability on chitosan nano/microfiber mesh tubes as a scaffold for nerve regeneration. *J Biomed Mater Res A*, 84(2): 557-566. 1549-3296.

Weiss, M. L., Medicetty, S., Bledsoe, A. R., Rachakatla, R. S., Choi, M., Merchav, S., Luo, Y., Rao, M. S., Velagaleti, G., & Troyer, D. (2006). Human umbilical cord matrix stem cells: preliminary characterization and effect of transplantation in a rodent model of Parkinson's disease. *Stem Cells*, 24(3): 781-792. ISSN 1066-5099.

Wu, L. F., Wang, N. N., Liu, Y. S., & Wei, X. (2009). Differentiation of Wharton's jelly primitive stromal cells into insulin-producing cells in comparison with bone marrow mesenchymal stem cells. *Tissue Eng Part A*, 15(10): 2865-2873. ISSN 1937-335X.

Yang, C. C., Shih, Y. H., Ko, M. H., Hsu, S. Y., Cheng, H., & Fu, Y. S. (2008). Transplantation of human umbilical mesenchymal stem cells from Wharton's jelly after complete transection of the rat spinal cord. *PLoS One*, 3(10): e3336. ISSN 1932-66203.

Yoshii, S., & Oka, M. (2001). Peripheral nerve regeneration along collagen filaments. *Brain Res*, 888(1): 158-162. ISSN 0006-8993.

21

Extracellular Matrix Adjuvant for Vaccines

Mark A. Suckow[1], Rae Ritchie[2] and Amy Overby[2]
[1]*University of Notre Dame;*
[2]*Bioscience Vaccines, Inc.*
United States of America

1. Introduction

In 1796, Edward Jenner first used the term, "vaccination," to describe his studies which used poxvirus derived from lesions in cows to protect humans against infection with smallpox (Barquet & Domingo, 1997). Later, Louis Pasteur demonstrated that animals and people could be protected against disease when administered microbes that had been attenuated to reduce pathogenicity. From this early work, it became evident that stimulation of the immune system by exposure to specific antigens associated with pathogens could lead to a response that would protect individuals from infection and, of paramount importance, disease associated with infection.

Since the times of Jenner and Pasteur, vaccination has proved over time to be one of the most cost-effective means to control infectious disease (Kaufmann, 2007). For example, in humans smallpox has been eradicated, and the incidence of polio has been greatly reduced; and in cattle, rinderpest has been eradicated (Kieny & Girard, 2005; Normile, 2008). Indeed, stimulation of the immune system by vaccination has proved to be a cornerstone of preventive medical strategies for several decades in both human and veterinary medicine.

The targets within a vaccine, and against which the immune response is directed, are referred to as "antigens." Often, antigens consist of proteins, though some vaccines utilize polysaccharides, nucleic acids, toxoids, peptides, and inactivated whole or fractions of microorganisms or cells as antigens (Liljeqvist & Ståhl, 1999). Great effort has been given to identification and production of purified recombinant protein subunit vaccines as a way to drive the immune system to target specific antigens key to the colonization, survival, and pathogenesis of infectious agents. Similar work has recently extended to the use of vaccination as an approach to cancer treatment, with vaccines based upon antigens ranging from recombinant subunit proteins to whole, inactivated cancer cells being evaluated in preclinical models and, in some cases, clinical trials (Buonaguro et al., 2011; Melenhorst & Barrett, 2011). In spite of significant progress in identification and production of vaccine antigens, many antigens stimulate only a weak immune response insufficient to offer protection to the patient.

2. Vaccine adjuvants

Adjuvants are compounds added to vaccines to improve the immune response to vaccine antigens. Indeed, the word 'adjuvant' derives from the Latin 'adjuvans' which means 'to help.' Adjuvants exert their action in a number of different ways, such as by increasing the

immunogenicity of weak antigens; strengthening the immune responses of individuals with weak immune systems; reducing the amount of antigen needed in the vaccine, thus reducing the cost; extending the duration of the immune response; modulating antibody avidity, specificity, or isotype distribution; and promoting specific forms of immunity, such as humoral, cell-mediated, or mucosal immunity.

2.1 Types of vaccine aduvants

A variety of compounds have been investigated for potential use as vaccine adjuvants. For example, immunostimulatory molecules such as the cytokines IL-2, IL-12, gamma-interferon, and granulocyte-macrophage colony-stimulating factor (GM-CSF) have all been shown to enhance aspects of the immune response following vaccination (Coffman et al., 2010). However, because these molecules are proteins that are relatively expensive, have short half-lives *in vivo*, and may exert a variety of other, often unpredictable systemic effects, their practical application as vaccine adjuvants is unlikely.

Compounds which lack the challenges that restrict the application of cytokines, but which in turn enhance immunostimulatory cytokines, have also been studied. Monophosphoryl lipid A (MPL), a molecule derived from bacterial lipopolysaccharide (LPS), stimulates the release of cytokines, likely through interaction with toll-like receptor 4. MPL induces the synthesis and release of IL-2 and gamma-interferon (Gustafson & Rhodes, 1992; Ulrich & Myers, 1995). In contrast, saponins are derived from the bark of a Chilean tree, *Quillaja saponaria*. The saponin QS21 is a potent adjuvant for IL-2 and gamma-interferon; and it appears to act by intercalating into cell membranes through interaction with structurally similar cholesterol. This interaction results in formation of pores in the cell membrane, and it is thought that this may allow antigens a direct pathway for presentation to the immune system (Glaueri et al., 1962). QS21 has been associated with pain on injection and local reactions, and the balance between potency and adverse events is an important consideration (Kensil & Kamer, 1998). More recently, unmethylated CpG dinuclelotides have been evaluated for potential use as vaccine adjuvants. Such CpG molecules are common in bacterial DNA, but not in vertebrate DNA, and it is thought that the interaction of the immune system with these moieties is related to an evolutionary characteristic of vertebrate defense against microbial infection (McKluskie & Krieg, 2006). In this way, then, it may be that cells of the immune system are particularly adept at recognizing antigens conjugated to CpG DNA. Responses to CpG DNA are mediated by binding to toll-like receptor 9 (Hemmi et al., 2000). Further, it is believed that CpG conjugates are taken up by non-specific endocytosis and that endosomal maturation is necessary for cell activation and release of pro-inflammatory cytokines (Sparwasser, et al., 1998).

One approach toward vaccine adjuvants has been to focus on delivery of antigens to the immune system. In this regard, a variety of methods for delivery of antigens have been investigated, including oil-in-water liposomes, alginate microparticles, and inclusion of antigens in live viral or bacterial vectors. For example, the MF59 squalene oil-in-water emulsion has shown an adjuvant effect in animal models for an influenza vaccine (Cataldo & Van Nest, 1997) and hepatitis B vaccine (Traquina et al., 1996). Microparticles produced by polymerization of alginate by divalent cations have been used to vaccinate animals against bacterial respiratory pathogens (Suckow et al., 1999). Alginate microparticles enhance antibody responses when administered with incorporated antigens by either the subcutaneous or mucosal (intra-nasal or peroral) routes. Adjuvants based upon delivery of antigens via live viral or bacterial vectors have gained recent interest, particularly for

stimulation of immunity at mucosal surfaces. For example, modified intestinal pathogens such as *Salmonella typhimurium*, *S. cholerasuis*, *Listeria monocytogenes*, and *Escherichia coli* have all been used to deliver antigens, most often through vaccination at mucosal surfaces (Becker et al., 2008). Similarly, poxvirus and adenovirus have been used as a means of delivering antigens for vaccination purposes (Liu, 2010). A primary advantage of vaccination using a live vector is that the replication of the vector within the host can lead to a heightened and sustained immune response to the vectored antigens.

2.2 Aluminum salt adjuvants

The use of aluminum salts (alum) as vaccine adjuvants to boost the immune response to vaccine antigens has a long record of success over the past 70 years (Clapp et al., 2011). In this regard, both aluminum phosphate and aluminum hydroxide have been used, in varying ratios and concentrations specific to different vaccines. Typically, the antigen is adsorbed to alum through electrostatic charge, and the degree of antigen adsorption by aluminum-containing adjuvants is generally considered to be an important characteristic of vaccines that is related to immunopotentation by the adjuvant. In this regard, the World Health Organization (WHO) requires that at least 80% of the antigens in alum-precipitated diphtheria and tetanus toxoid vaccines be adsorbed (Clapp et al, 2011); however, others have found that there appears to be no correlation between the percentage of antigen adsorbed and subsequent antibody production following vaccination (Clausi et al., 2008). Further, antigen presenting cells have been demonstrated to take up desorbed antigen from the interstial fluid as well as antigen adsorbed to aluminum-containing adjuvants (Iver et al., 2003); and aluminum-containing adjuvants potentiate the immune response to non-adsorbed protein antigens (Romero-Mendez et al., 2007), suggesting that adsorption may not be a requirement for adjuvancy by alum.

The most widely accepted theory for the mechanism of alum adjuvancy is the repository effect, whereby the antigen adsorbed by the aluminum-containing adjuvant is slowly released after intramuscular or subcutaneous administration (Seeber, et al., 1991). However, it has been demonstrated using ^{28}Al in rabbits that aluminum quickly appears in the interstitial fluid and is rapidly eliminated from the body (Flarend et al., 1997). The best information regarding the mechanism of action for alum suggests that alum activates a complex of proteins, termed the inflammasome, in lymphocytes and that these proteins initiate a complex cascade of actions which result in an enhanced immune response to antigens (Eisenbarth et al., 2008).

At present, aluminum salts are the only adjuvants that are currently approved for use in human vaccines by the United States Food and Drug Administration (FDA). The FDA limits the amount of aluminum in biological products, including vaccines, to 0.85 mg/dose. However, in spite of this regulatory oversight and a widespread acceptance of safety, aluminum adjuvants have been associated with severe local reactions such as erythema, induration, formation of subcutaneous granulomas, and pain. A further major limitation of aluminum adjuvants is their inability to elicit cell-mediated Th1 responses that are required to control most intracellular pathogens such as those that cause tuberculosis, malaria, leishmaniasis, leprosy, and AIDS ; and to elicit Th1 responses typical of immunity to cancer. Additionally, failure of alum to augment the humoral antibody immune response in some circumstances, such as with influenza immunization in the elderly (Parodi et al., 2011), clearly illustrates the need for additional safe and effective vaccine adjuvants.

3. Extracellular matrix

Extracellular matrix (ECM) is a network of macromolecules, largely proteins and polysaccharides, that aggregate to form a complex meshwork that acts as a both physical lattice and a biologically active promoter for the cellular component of tissue. Proteins typically found in ECM include collagen, elastin, fibronectin, and laminin all of which contribute structural strength to the ECM and adhesive attraction for the cells. Complementing these proteins are glycosaminoglycans, a class of polysaccharide which are often found covalently linked to proteins to constitute proteoglycans. The proteoglycans exist as a highly hydrated, gel-like ground substance in which the proteins are embedded. The proteoglycan gel allows diffusion of nutrients and molecular signals important for cell survival and growth. Several glycosaminoglycans are typically present in ECM, including hyaluronan; chondroitin sulfate and dermatan sulfate; heparan sulfate; and keratan sulfate. The glycosaminoglycans are active participants in the maintenance and survival of cells and exhibit a variety of biological functions. For example, hyaluronan is thought to facilitate migration of cells during the process of tissue repair. Further, proteoglycans are believed to have a major role in chemical signaling between cells. An example is heparan sulfate which binds to fibroblast growth factors which subsequently stimulates proliferation by a variety of cells. Heparan sulfate proteoglycans immobilize secreted chemotactic attractants called chemokines on the endothelial surfaces of blood vessels at sites of inflammation. In this way, the chemokines remain there for a prolonged period, stimulating white blood cells to leave the bloodstream and migrate into the inflamed tissue. In short, the extracellular matrix is an active participant in the dynamic process of tissue function.

3.1 Small intestinal submucosa

Small intestinal submucosa (SIS) is a natural, bioactive extracellular matrix that has proven successful as a tissue graft material in a variety of clinical applications related to tissue repair (Ellis, 2007; Mostow et al., 2005). The material is processed, using porcine intestine as a raw material, into an acellular, multilaminar medical-grade material that serves as a bioscaffold for in-growth of, and subsequent incorporation into, normal, repaired tissue (Fig. 1).

SIS has been found to be a suitable material for tissue engineering applications at varied sites, including the lower urinary tract, the body wall, tendon, ligament, flat bone, cutaneous wounds and blood vessels. One common cause of tissue defects that might benefit from augmentation is tumor resection. It is interesting that, in spite of its tissue growth promoting characteristics, SIS has been shown not to promote re-growth of tumors when added to the remaining tumor bed following surgical tumor resection in a pre-clinical model (Hodde et al., 2004).

It is known that bioactive growth factors are retained in the SIS following lyophilization and sterilization. These growth factors include transforming growth factor-beta (TGF-β), which is important in wound healing, and the highly angiogenic growth factor, basic fibroblast growth factor (FGF-2). In addition, it has been demonstrated that SIS contains glycosaminoglycans such as hyaluronic acid, dermatan sulfate, chondroitin sulfate A, and heparan sulfate (Hodde et al., 1996). Because some of the gylcosaminoglycans endogenous to SIS assist chemotactic cytokines, it is not surprising that antigen-processing cells such as macrophages are drawn to sites where SIS has been implanted (Badylak et al., 2008).

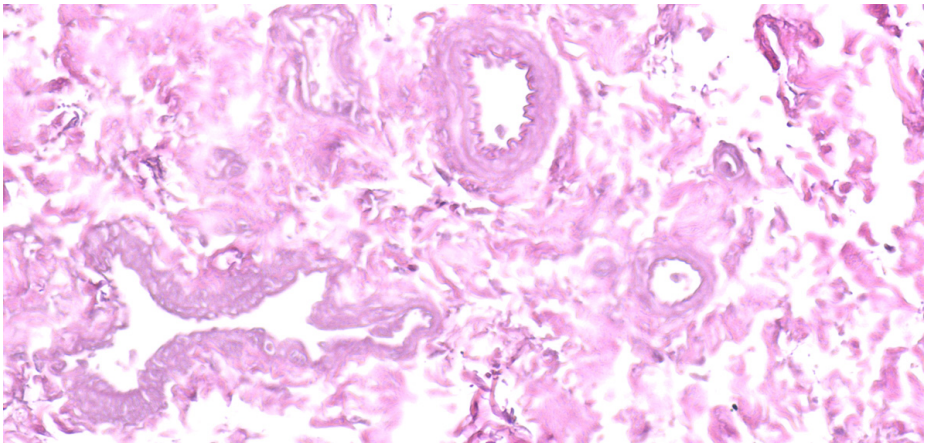

Fig. 1. Photomicrograph of small intestinal submucosa, demonstrating lack of cellular components but with remnant acellular matrix and vascular structures.

4. Use of SIS as a vaccine adjuvant and immune modulator

Because small intestinal submucosa has biological activities that are known to include attraction of antigen-presenting cells, such as macrophages, to sites of implantation, the potential application of the material as a vaccine adjuvant is obvious. That SIS is available as a medical-grade material in sheet form (Fig. 2) and has been safely used in a variety of applications in a large number of patients supports the idea that it could be safely applied as a vaccine adjuvant as well.

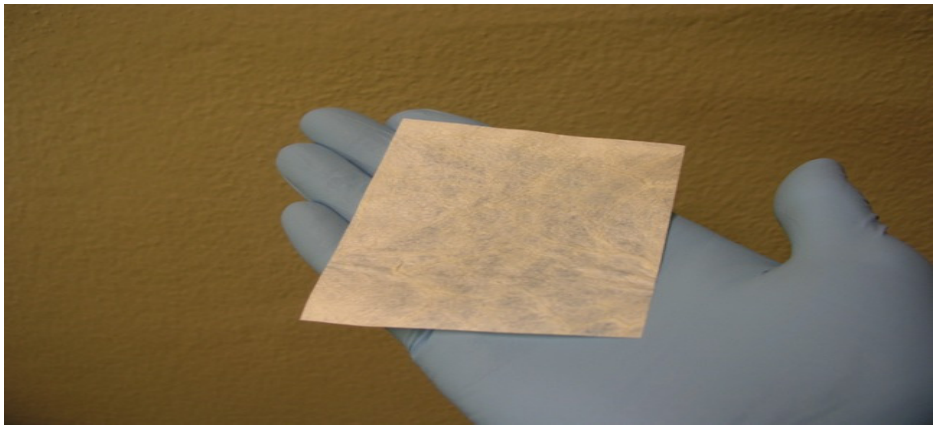

Fig. 2. A sheet of medical-grade SIS.

4.1 SIS enhances the performance of whole cell cancer vaccines

The idea that cancer is a disease that can be treated by vaccination is relatively new, and great effort has been given to development of therapeutic, and in some cases prophylactic,

vaccines. For example, the Provenge® dendritic cell-based vaccine for treatment of prostate cancer was recently approved by the U. S. Food and Drug Administration (Madan & Gulley, 2011); and the Gardasil® and Cervarix® vaccines for prevention of cervical cancer are approved as well (Harper, 2009). Indeed, it is believed by many that the age of cancer immunotherapy has dawned and offers entirely new possibilities for the clinical approach to cancer.

The use of whole tumor cells as vaccine components allows a greatly increased menu of antigens to be presented to the immune system. Although many antigenic moieties in such vaccine preparations may be unidentified, it can be presumed that the rich choice of antigenic targets facilitates the likelihood of a successful immune response. As an example, allogeneic (from the same species) human prostate cancer cells have been examined for potential use in vaccination therapy of prostate cancer patients. The basic reasoning for this approach is that because tumor antigens are often conserved between tumors, allogeneic vaccines might stimulate cross-protective immunity. To test this idea, monthly intradermal administrations of a vaccine composed of three inactivated (irradiated) allogeneic prostate cancer cell lines were given for 1 year to patients having progressive disease as defined by two consecutive increases in prostate-specific antigen (PSA). The treatment did not produce any evidence of toxicity and resulted in decreased PSA velocity, as well as a cytokine response profile consistent with a Th1 immune response (Simons et al., 1999). In addition, median time to disease progression was 58 weeks in vaccinated patients compared with 28 weeks for historical controls.

Tissue vaccines represent an expansion on the idea of whole cell vaccines. Tissue vaccines are produced directly from harvested tumor material and do not undergo any *in vitro* culture (Suckow et al., 2007a). In this regard, tissue vaccines include an enormous menu of antigen targets composed of various stages of an evolving, growing population of cancer cells; antigens associated with an evolving and expanding extracellular matrix; and antigens expressed uniquely *in vivo* but not *in vitro*. In the Lobund-Wistar rat model of hormone-refractory prostate cancer, a tissue vaccine was demonstrated to reduce the incidence of autochthonous prostate cancer by 90% (Suckow et al., 2005); reduce metastasis to the lungs by 70% (Suckow et al., 2008a); and augment tumor reduction by external beam irradiation by approximately 50% (Suckow et al., 2008b). Further, a xenogeneic tissue vaccine was demonstrated to reduce growth by 70% of tumors associated with human prostate cancer cells xenotransplanted in immunodeficient mice (Suckow et al., 2007b).

4.1.1 SIS as an adjuvant for prostate cancer whole cell vaccines

Melanoma is a cancer of pigment-producing skin cells referred to as melanocytes. Often aggressive with metastasis to the lymph nodes, lungs, liver, and brain, melanoma is usually first treated by surgical resection of the primary tumor. Though often curative, return of the tumor is not infrequent and can result in a particularly aggressive form of cancer.

To evaluate the ability of SIS to enhance the protective effect conferred by vaccination with a whole cell melanoma vaccine, C57Bl6/J mice were administered B16 mouse melanoma cells to produce subcutaneous tumors. When the tumors were palpable they were harvested, dissociated with a 80-mesh stainless steel screen and allowed to incubate on 2 x 2 cm sections of sterile SIS for three days. Sections of SIS with cells were then treated with 2.5% glutaraldehyde to produce a tissue vaccine as previously described (Suckow et al., 2008c). A separate portion of cells was used to make a tissue vaccine without added SIS, and separate

sections of SIS were treated with glutaraldehyde and washed to produce an SIS control treatment.

Groups of naïve mice were administered B16 cells to produce subcutaneous melanoma tumors. Fourteen days after administration of cells, all mice had palpable tumors and were prepared for aseptic surgical debulking of the tumor masses. Mice were anesthetized with a mixture of ketamine hydrochloride, acepromazine maleate, and xylazine; the hair overlying the tumor mass was shaved; and the skin scrubbed with an iodophore. Following incision of the skin, tumors the tumors were carefully dissected free of attachments except for a residual portion of the underlying tumor bed. Groups of mice then either received no further treatment other than wound closure and routine post-surgical care; direct administration onto the tumor bed of 1 x 10^6 glutaraldehyde-fixed tumor (GFT) cells; application onto the tumor bed of glutaraldehyde-fixed SIS (ECM) with no added cells; or application onto the tumor bed of glutaraldehyde-fixed SIS on which tumor cells had been grown and then fixed (GFT/ECM). Fourteen days after surgery, mice were euthanized and necropsied to assess the re-growth of tumors. As demonstrated in Fig. 3, the combination of GFT/ECM reduced the mass of re-grown tumors by approximately 70% compared to all other treatment groups.

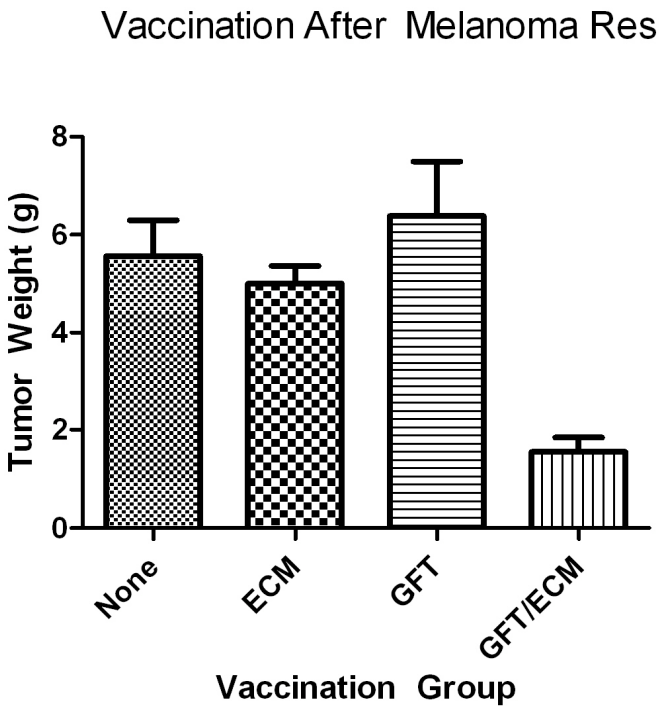

Fig. 3. Neither a melanoma tissue vaccine (GFT) nor SIS (ECM) alone reduced the size of re-grown melanoma tumors compared to controls following surgical resection, however the combination of the tissue vaccine with SIS (GFT/ECM) led to an approximately 70% reduction in tumor mass.

The idea that cancer immunotherapy might be enhanced by inclusion of SIS in the vaccine preparation needed further validation in additional models of cancer. In this regard, prostate cancer was viewed as a likely system for validation, as it is a common cancer and one which has been shown to be responsive to immunotherapy as demonstrated by the Provenge® vaccine. The Lobund-Wistar (LW) rat model of prostate cancer closely replicates the disease in man in that it progresses to a hormone-refractory cancer and readily metastasizes through the circulatory system (Pollard & Suckow, 2005). The LW rat develops autochthonous tumors, and a transplantable cell line (PAIII cells) has been isolated and characterized. When transplanted subcutaneously, PAIII cells rapidly produce aggressive tumors that metastasize to the lungs. Following surgical resection, PAIII tumors become exceptionally aggressive and there is little that can be done to ameliorate consequent growth and spread of the tumor.

As in the mouse melanoma model, subcutaneous tumors were produced as a source of vaccine material. PAIII cells administered subcutaneously rapidly grew into palpable tumors that were harvested 14 days after administration of cells. Following similar procedures as for the melanoma tissue vaccine, harvested tumor cells were added to 2 x 2 cm sections of SIS and allowed to grow for three days at 37° C, followed by glutaraldehyde fixation and extensive washing. Separate groups of rats which were administered PAIII cells 14 days earlier underwent surgical debulking of subcutaneous PAIII tumors then received no treatment other than standard peri-operative care; direct administration onto the tumor bed of 1 x 10^6 glutaraldehyde-fixed tumor (GFT) cells; application onto the tumor bed of glutaraldehyde-fixed SIS (ECM) with no added cells; or application onto the tumor bed of glutaraldehyde-fixed SIS on which tumor cells had been grown and then fixed (GFT + ECM). Histological examination of a section of the GFT + ECM vaccine material shows that cells readily grow along the edge of SIS (Fig. 4) and within the substance of the SIS (Fig. 5). Rats were euthanized 28 days later and tumors weighed to assess the effect of vaccination on tumor re-growth.

Microscopic examination of SIS upon which harvested tumor tissue was cultured demonstrated robust growth of tumor cells. Cells readily grew along the margin of SIS as shown in Fig. 4 and were arranged as a monolayer along the edge.

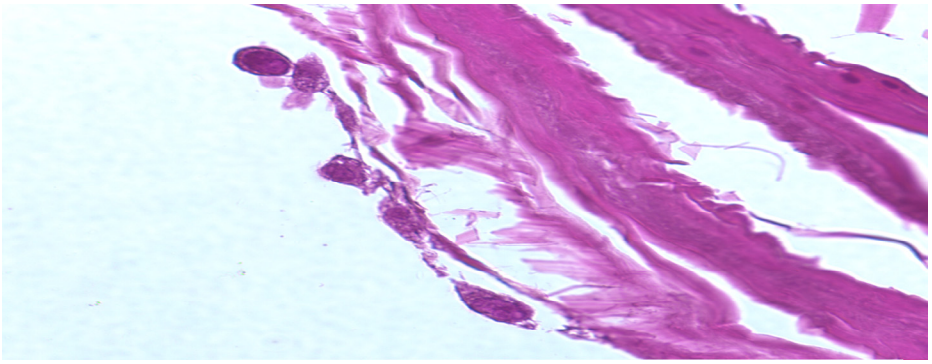

Fig. 4. Photomicrograph demonstrating growth of harvested PAIII tumor cells along the edge of SIS.

In contrast, within the substance of the SIS, cells were present as islands of piled-up cells (Fig. 5). Some islands of cells formed what appeared to be primitive vascular structures, consistent with the highly angiogenic character of PAIII tumors.

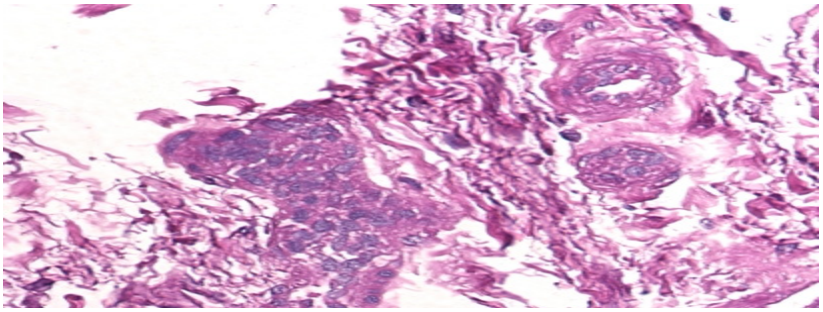

Fig. 5. Photomicrograph demonstrating growth of harvested PAIII tumor cells within the substance of SIS.

The requirement for delivery of nutrients and removal of waste metabolic products characteristic of a rapidly dividing and growing tissue is what drives the need for an expanded blood supply; thus, it is not surprising that cells from a harvested tumor would have an angiogenic phenotype. Indeed, vascular endothelial growth factor (VEGF) has been implicated in a number of aspects of cancer growth, including angiogenesis, remodeling of the ECM, generation of inflammatory cytokines, and hematopoietic stem cell development. Rats vaccinated with the GFT vaccine to which SIS was added had tumors that had a mean weight of 3.91 g, while tumors from rats that had not been vaccinated had a mean weight of 11.63 g (Fig. 6). Similarly, tumors from rats vaccinated with SIS only had a mean weight of 13.04 g and those from rats vaccinated with the GFT vaccine only had a mean weight of 9.96 g. While there was a significant ($P < 0.01$) reduction in tumor weight of rats vaccinated with GFT plus SIS compared to all other groups, tumors from rats of all other treatment groups did not significantly differ in this very aggressive model of cancer (Suckow et al., 2008c).

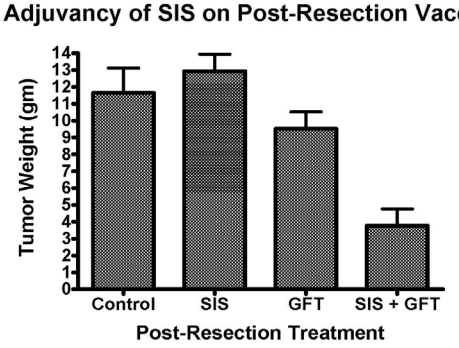

Fig. 6. Neither a PAIII prostate cancer tissue vaccine (GFT) nor SIS (ECM) alone reduced the size of re-grown prostate tumors compared to controls following surgical resection, however the combination of the tissue vaccine with SIS (GFT/ECM) led to an approximately 65% reduction in tumor mass.

Vaccination also reduced the number of rats which had foci of metastasis in the lungs. Specifically, only 40% of rats vaccinated with SIS + GFT had pulmonary metastatic foci, compared to 70% of rats immunized with the GFT vaccine and 100% of rats which were administered only SIS or those receiving no treatment (Fig. 7).

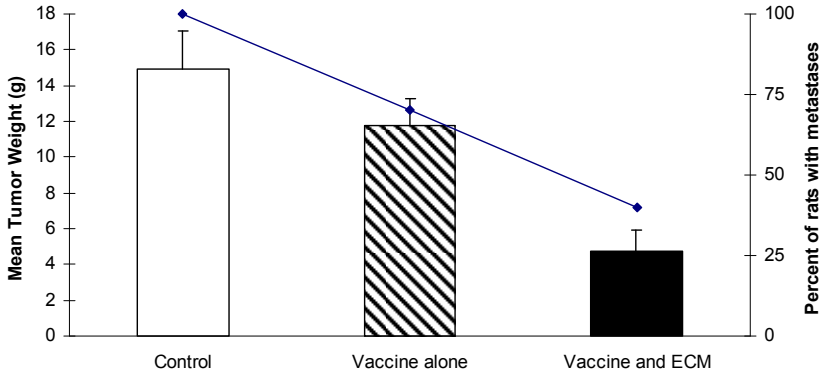

Fig. 7. Reduction in the number of PAIII prostate tumor-bearing rats having pulmonary metastasis (right X-axis). For reference, the mean tumor weight is indicated on the left X-axis.

4.1.2 Gel SIS exhibits adjuvancy for whole cell prostate cancer vaccine

Though vaccines produced from growth of cells directly on SIS extracellular matrix demonstrated remarkable stimulation of anti-tumor responses, it requires surgical implantation. The advantages of a similar vaccine that could be easily and quickly administered are clear. In particular, multiple doses could be given to patients without the requirement for repeated surgery.

Vaccination involving injection into the subcutaneous or intramuscular tissues is rapid and has relatively few adverse outcomes other than acute discomfort at the site of injection. Compounds administered in this way must be of a size and consistency that allow passage through a relatively narrow needle, typically 21-gauge or smaller. Obviously, a sheet of SIS is not amenable to administration in this manner. In this regard, a gel form of SIS, produced by chemical digestion, was developed and evaluated for vaccine adjuvancy. Of note, this same gel preparation has been found to be safe and effective for myocardial infarct repair in rats (Okada et al., 2010).

A tissue vaccine produced from harvested LW rat PAIII prostate tumors, as described earlier, was mixed with SIS gel such that each dose contained 1 x 10^6 GFT cells. In this case, groups of naïve LW rats were vaccinated with either saline; GFT cells; SIS gel; or GFT cell plus SIS gel. Vaccines were given subcutaneously once before challenge with live PAIII cells, and weekly for two doses afterward. The ability of vaccination to prevent growth of PAIII tumors was assessed by weighing tumors 28 days following PAIII cell challenge. As shown in Fig. 8, neither saline, GFT, nor SIS gel alone demonstrated a protective effect against development of PAIII prostate tumors; however, rats vaccinated with the GFT vaccine combined with SIS gel had tumors which were approximately 75% smaller than those in rats from other vaccination groups.

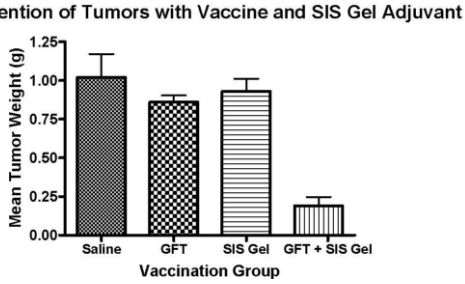

Fig. 8. SIS gel has an adjuvant effect on a tissue vaccine used to prevent prostate cancer.

An obvious concern with use of SIS as an adjuvant for cancer vaccines is whether a material that is known to promote tissue growth, and is used clinically for such applications, would also promote the growth of cancer tissue. Interestingly, when PAIII cells were administered directly onto implanted SIS sections in LW rats, no difference in tumor growth or metastasis was noted compared to control rats that did not have SIS implants (Hodde et al., 2004). This result demonstrates that the SIS extracellular matrix material is capable of promoting growth of normal tissue, but not neoplastic tissue. It may be that the mild inflammatory process which accompanies implantation of SIS facilitates growth of normal tissue, but recognizes foreign material or abnormal cells which happen to be in the vicinity of SIS, thereby alerting the immune system and stimulating an immune response to combat the challenge presented by tumor cells or other pathogenic agents.

4.2 SIS enhances the performance of vaccines for diseases associated with infectious agents

While the idea of vaccination to prevent or treat cancer is relatively new, the concept of vaccination for prevention of diseases associate with infectious agents is not. In 1796, Edward Jenner inoculated an eight-year-old boy with material taken from an active cowpox lesion on another individual and discovered that this strategy could be used to confer protection to smallpox (Barquet & Domingo, 1997). Since that time, vaccines have been developed for a variety of diseases related to infectious agents, including polio, tetanus, influenza, whooping cough (pertussis), measles, diphtheria, and hepatitis (Stern & Markel, 2005).

In spite of the many successes with vaccination, there are some infectious agents for which successful vaccination has proved elusive. For example, malaria and HIV are both important diseases caused by infectious agents and for which there are a lack of viable vaccination strategies. Because SIS proved to be a powerful adjuvant for vaccines designed to protect against cancer, it was reasoned that the material might also have value as an adjuvant for vaccines designed to protect against disease associated with infectious agents.

4.2.1 Particulate SIS vaccine adjuvant

Although sheet SIS and gel SIS were effective as adjuvants for cancer vaccines, it was reasoned that an adjuvant composed of particulate SIS would allow greater surface area of SIS to be exposed and interact with the cellular immune system. This was seen as an advantage because many antigens associated with vaccines for infectious diseases are composed of proteins or sub-units that are more rapidly degraded and processed than

whole, inactivated cells (as with whole cell cancer vaccines). Thus, a more rapid and robust adjuvant stimulation was expected to offer greater efficacy for infectious disease vaccines.
Particulate SIS was produced by mechanical grinding of medical grade sheet SIS. Sterility of the preparation was maintained and final particulate size was limited to 150 μm. The resulting product was a fine, white dust-like particulate (Fig. 9).

Fig. 9. Particulate SIS. Individual particles in this preparation are no greater than 150 μm in diameter.

4.2.2 Particulate SIS is an effective adjuvant for tetanus vaccine

Though relatively rare in the developed world, tetanus remains an important cause of death worldwide, with up to 1 million deaths estimated annually (Dietz et al., 1996). The disease, characterized by cardiovascular complications which result from autonomic dysfunction, is caused by a Gram-positive bacillus, *Clostridium tetani*. This microorganism is ubiquitous in soil; and under the anaerobic conditions found in necrotic tissue, the bacterium secretes two toxins: tetanolysin, which damages local tissues and optimizes conditions for further bacterial multiplication; and tetanospasmin, which is responsible for development of the clinical disease. Tetanospasmin, also commonly referred to as tetanus toxin, is a two-chain polypeptide of 150,000 Da which, when cleaved by tissue proteases, yields a light chain that acts pre-synaptically to prevent neurotransmitter release (Wright et al., 1989).
Vaccination for the prevention of tetanus has been available since 1923, with routine vaccination beginning later, mostly during the 1950s and 1960s. The vaccine is most commonly a suspension of alum-precipitated (aluminum potassium sulfate) tetanus toxoid. Though vaccination stimulates strong protective immunity in most cases, serological surveys have demonstrated an increasing proportion of patients with inadequate immunity with advancing age (Cook et al., 2001). Though some of these individuals were never vaccinated, a substantial number simply lost immunity over time (Prospero, et al., 1998).
Because immunization with alum-adjuvanted tetanus toxoid is very effective at stimulating protective antibody titers, it represents a good model against which to compare other vaccine adjuvants. In this regard, we undertook studies to evaluate the ability of ECM (SIS) adjuvant to stimulate anti-tetanus toxin antibody and protective responses in a mouse model.
Groups of 15 adult female balb/c mice were vaccinated subcutaneously with 0.03 μg/dose of tetanus toxoid (TT) in sterile saline either with no adjuvant; with 300 μg of alum

(Alhydrogel®); or with 300 μg of particulate ECM. In addition, an untreated control group was included in these studies. Mice were vaccinated initially and received booster vaccinations five weeks later. In addition, serum samples for evaluation of antibody responses were obtained immediately prior to challenge with tetanus toxin, 10 weeks after initial vaccination.

Serum IgG anti-tetanus toxin antibody responses were evaluated by enzyme-linked immunosorbent assay (ELISA). While control animals demonstrated no appreciable anti-tetanus toxin antibody titers, samples from mice vaccinated with alum-adjuvanted tetanus toxoid had measureable antibody levels. In contrast, serum samples from mice vaccinated with tetanus toxoid that was adjuvanted with ECM had five-fold higher titers compared to samples from mice vaccinated with alum-adjuvanted tetanus toxoid (Fig. 10)

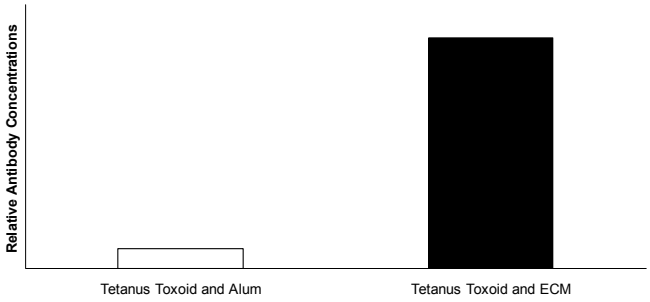

Fig. 10. Relative antibody concentrations in mice immunized with the tetanus toxoid combined with alum or ECM adjuvant.

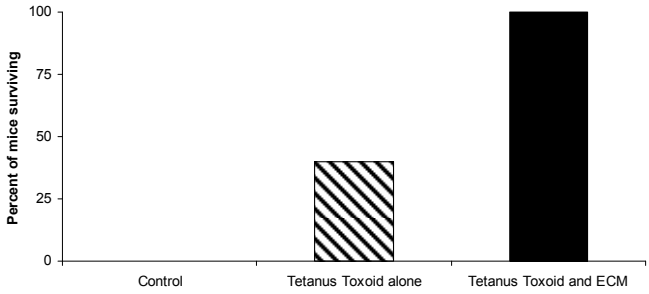

Fig. 11. Survival of mice following challenge with 1 ng/mouse of tetanus toxin

The strength of the anti-tetanus toxin serum antibody response is a reasonable measure of the likely protective effect; however, to assure that vaccination correlated with protection, vaccinated mice were challenged with 1 ng of tetanus toxin administered intraperitoneally. Mice were then observed over the next 96 hours and the number of surviving mice recorded for each group. All mice vaccinated with tetanus toxoid in alhydrogel of ECM survived challenge, while only one-third of mice vaccinated with tetanus toxoid alone, and no untreated control mice survived. Figure 11 shows the percent of surviving mice in mice

vaccinated with tetanus toxoid and ECM compared to the non-vaccinated and non-adjuvanted tetanus toxoid-vaccinated control mice.

5. Conclusion

Vaccination has greatly reduced the incidence of many infectious diseases. Currently, a variety of new vaccines based on nucleic acids or other subunits are in development. Further, great promise is offered by vaccination for the treatment and prevention of cancer. With these new vaccines comes a need for improved adjuvants which are safe and effective. Though aluminum salts have been used for adjuvant purposes with great success, there are some vaccines and some patient populations for which alum is not effective.

We have demonstrated the powerful adjuvant effect of SIS, a medical grade ECM. SIS demonstrated a powerful adjuvant effect for vaccines against two types of cancer, melanoma and prostate cancer, and we believe that it will likely prove efficacious with vaccines for other cancers. We further used SIS adjuvant with tetanus toxoid vaccine as a model for evaluation in a vaccine for disease associated with infectious pathogens. We found that the ECM-adjuvanted vaccine stimulated markedly higher anti-tetanus toxin antibody levels than, and offered clinical protection that was at least as good as that conferred by, the alum-adjuvanted vaccine.

In summary, the ECM material, SIS, is an effective vaccine adjuvant and offers an outstanding alternative to the current standard, alum. SIS has a proven safety record when used in humans for a variety of other applications, and we believe that it has unlimited potential for use as a vaccine adjuvant.

6. References

Badylak, S. F., Valentin, J. E., Ravindra, A. K., McCage, G. P., & Stewart-Akers, A. M. (2008). Macrophage phenotype as a determinant of biologic scaffold remodeling. *Tissue Engineering Part A*, Vol. 14, No. 11, (November, 2008), pp. 1835-1842, ISSN 1937-3341.

Barquet, N., & Domingo, P. (1997). Smallpox: the triumph over the most terrible of the ministers of death. *Annals of Internal Medicine*, Vol. 127, No. 8, (October, 1997), pp.635- 642, ISSN 0003-4819.

Becker, P. B., Noerder, M., & Guzman, C. A. (2008). Genetic immunization: bacteria as DNA vaccine delivery vehicles. *Human Vaccines*, Vol. 4, No. 3, (May, 2008), pp. 189-202, ISSN 1554-8600.

Buonaguro, L., Petrizzo, A., Tornesello, M. L., & Buonaguro, F. (2011). Translating tumor antigens into cancer vaccines. *Clinical and Vaccine Immunology*, Vol. 18, No. 1, (January, 2011), pp. 23-34, ISSN 1556-6811.

Cataldo, D. M., & Van Nest, G. (1997). The adjuvant MF59 increases the immunogenicity and protective efficacy of subunit influenza vaccine in mice. *Vaccine*, Vol. 15, No. 16, (November, 1997), pp. 1710-1715, ISSN 0264-410X.

Clapp, T., Siebert, P., Chen, D., & Braun, L. J. (2011). Vaccines with aluminum-containing adjuvants: optimizing vaccine efficacy and thermal stability. *Journal of Pharmaceutical Sciences*, Vol. 100, No. 2, (February, 2011), pp. 388-401, ISSN 1520-1617.

Clausi, A., Cummiskey, J., Merkley, S., Carpenter, J. F., Braun, L. J., & Randolph, T. W. (2008). Influence of particle size and antigen binding on effectiveness of aluminum salt adjuvants in a model lysozyme vaccine. *Journal of Pharmaceutical Sciences*, Vol. 97, No. 12, (December, 2008), pp. 5252-5262, ISSN 1520-1617.

Coffman, R. L., Sher, A., & Seder, R. A. (2010). Vaccine adjuvants: putting innate immunity to work. *Immunity*, Vol. 33, No. 4, (October, 2010), pp. 492-503, ISSN 1074-7613.

Cook, T. M., Protheroe, R. T., & Handel, J. M. (2001). Tetanus: a review of the literature. *British Journal of Anaesthesia*, Vol. 87, No. 3, (September, 2001), pp. 477-487, ISSN 0007- 0912.

Dietz, V., Milestien, J. B., Van Loon, F., Cochi, S., & Bennett, J. (1996). Performance and potency of tetanus toxoid: implications for eliminating neonatal tetanus. *Bulletin of the World Health Organization*, Vol. 74, No. 6, (June, 1996), pp. 619-628, ISSN 0042-9686.

Eisenbarth, S. C., Colegio, O. R., O'Connor, W., Sutterwala, F. S., & Flavell, R. A. (2008). Crucial role for the Nalp3 inflammasome in the immunostimulatory properties of aluminum adjuvants. *Nature*, Vol. 453, No. 7198, (June, 2008), pp. 1122-1126, ISSN 0028-0836.

Ellis, C. N. (2007). Bioprosthetic plugs for complex anal fistulas: an early experience. *Journal of Surgical Education*, Vol. 64, No. 1, (January, 2007), pp. 36-40, ISSN 1931-7204.

Flarend, R. E., Hem, S. L., White, J. L., Elmore, D., Suckow, M. A., Rudy, A. C., & Dandashli, E. (1997). In vivo absorption of aluminum-containing vaccine adjuvants using ^{26}Al. *Vaccine*, Vol. 15, No. 12-13, (August, 1997), pp. 1314-1318, ISSN 0264-410X.

Glaueri, A. M., Dingle, J. T., & Lucy, J. A. (1962). Action of saponins on biologic membranes. *Nature*, Vol. 196, (December, 1962), pp. 953-959, ISSN 0028-0836.

Gustafson, G. L., & Rhodes, M. J. (1992). Bacterial cell wall products as adjuvants: early interferon gamma as a marker for adjuvants that enhance protective immunity. *Research in Immunology*, Vol. 143, No. 5, (June, 1992), pp. 483-488, ISSN 0923-2494.

Harper, D. M. (2009). Currently approved prophylactic HPV vaccines. *Expert Review of Vaccines*, Vol. 8, No. 12, (December, 2009), pp. 1663-1679, ISSN 1476-0584.

Hemmi, H., Takeuchi, A., Kawai, T., Kaisho, T., Sato, S., Sanjo, H., Matsumoto, M., Hoshino, K., Wagner, H., Takeda, K., Akira, S., & Moingeon, P. (2000). A toll-like receptor recognizes bacterial DNA. *Nature*, Vol. 408, No. 6813, (December, 2000), pp. 740-745, ISSN 0028-0836.

Hodde, J. P., Badylak, S. F., Brightman, A. O., & Voytik-Harbin, S. L. (1996). Glycosaminoglycan content of small intestinal submucosa: a bioscaffold for tissue replacement. *Tissue Engineering*, Vol. 2, No. 3, (Fall, 1996), pp. 209-217, ISSN 2152-4947.

Hodde, J. P., Suckow, M. A., Wolter, W. R., & Hiles, M. C. (2004). Small intestinal submucosa does not promote PAIII tumor growht in Lobund-Wistar rats. *Journal of Surgical Research*, Vol. 120, No. 2, (August, 2004), pp. 189-194, ISSN 0022-4804.

Iver, S., HogenEsch, H., & Hem, S. L. (2003). Relationship between the degree of antigen adsorption to aluminum hydroxide adjuvant in interstitial fluid and antibody production. *Vaccine*, Vol. 21, No. 11-12, (March, 2003), pp. 1219-1223, ISSN 0264-410X.

Kaufmann, S. H. E. (2007). The contribution of immunology to the rational design of novel antibacterial vaccines. *Nature Reviews Microbiology*, Vol. 5, No. 7, (July, 2007), pp. 491- 504, ISSN 1740-1526.

Kensil, C. R., & Kamer, R. (1998). QS-21: a water-soluble triterpine glycoside adjuvant. *Expert Opinion on Investigational Drugs*, Vol. 7, No. 9, (September, 1998), pp. 1475-1482, ISSN 1744-7658.

Kieny, M. P., & Girard, M. P. (2005). Human vaccine research and development: an overview. *Vaccine*, Vol. 23, No. 50, (December, 2005), pp. 5705-5707, ISSN 0264-410X.

Liljeqvist, S., & Stahl, S. (1999). Production of recombinant subunit vaccines: protein immunogens, live delivery systems and nucleic acid vaccines. *Journal of Biotechnology*, Vol. 73, No. 1, (July, 1999), pp. 1-33, ISSN 0717-3458.

Liu, M. A. (2010). Immunologic basis of vaccine vectors. *Immunity*, Vol. 33, No. 4, (October, 2010), pp. 504-515, ISSN 1074-7613.

Madan, R. A., & Gulley, J. L. (2011). Sipleucel-T: harbinger of a new age of therapeutics for prostate cancer. *Expert Review of Vaccines*, Vol. 10, No. 2, (February, 2011), pp. 141-150, ISSN 1476-0584.

McKluskie, M. L., & Krieg, A. M. (2006). Enhancement of infectious disease vaccines through TLR9-dependent recognition of CpG DNA. *Current Topics in Microbiology and Immunology*, Vol. 311, pp. 155-178, ISSN 0070-217X.

Melenhorst, J. J., & Barrett, A. L. (2011). Tumor vaccines and beyond. *Cytotherapy*, Vol. 13, No. 1, (January, 2011), pp. 8-18, ISSN 1465-3249.

Mostow, E. N., Haraway, G. D., Dalgin, M. Hodde, J. P., & King, D. (2005). Effectiveness of an extracellular matrix graft (OASIS Wound Matrix) in the treatment of chronic leg ulcers: a randomized clinical trial. *Journal of Vascular Surgery*, Vol. 41, No. 5, (May, 2005), pp. 837-843, ISSN 0741-5214.

Normile, D. (2008). Rinderpest driven to extinction. *Science*, Vol. 319, No. 5870, (March, 2008), pp. 1606-1609, ISSN 1095-9203.

Okada, M., Payne, T. R., Oshima, H., Momoi, N., Tobita, K., & Huard, J. (2010). Differential efficacy of gels derived from small intestinal submucosa as an injectable biomaterial for myocardial infarct repair. *Biomaterials*, Vol. 31, No. 30, (October, 2010), pp. 7678- 7683, ISSN 0142-9612.

Parodi, V., de Florentis, D., Martini, M., & Ansaldi, F. (2011). Inactivated influenza vaccines: recent progress and implications for the elderly. *Drugs & Aging*, Vol. 28, No. 2, (February, 2011), pp. 93-106, ISSN 1170-229X.

Pollard, M., & Suckow, M. A. (2005). Hormone-refractory prostate cancer in the Lobund-Wistar rat. *Experimental Biology & Medicine*, Vol. 230, No. 8, (September, 2005), pp. 520- 526, ISSN 1535-3702.

Prospero, E., Appignanesi, R., E'Errico, M. M., & Carle, F. (1998). Epidemiology of tetanus in the Marshes Region of Italy. *Bulletion of World Health Organization*, Vol. 76, No. 1, (January, 1998), pp. 47-54, ISSN 0042-9686.

Romero-Mendez, I. Z., Shi, Y., HogenEsch, H., and Hem, S. L. (2007). Poentiation of the immune response to non-adsorbed antigens by aluminum-containing adjuvants. *Vaccine*, Vol. 25, No. 5 (January, 2007), pp. 825-833, ISSN 0264-410X.

Seeber S. J., White, J. L., & Hem, S. L. (1991). Solubilization of aluminum-containing adjuvants by constituents of interstitial fluid. *Journal of Parenteral Science and Technology*, Vol. 45, No. 3, (May, 1991), pp. 156-159, ISSN 0279-7976.

Simons, J. W., Mikhak, B., Chang, J. F., DeMarzo, A. M., Carducci, M. A., Lim, M., Weber, C. E., Baccala, A. A., Goemann, M. A., Clift, S. M., Ando, D. G., Levitsky, H. I., Cohen, L. K., Sanda, M. G., Mulligan, R. C., Partin, A. W., Carter, H. B., Piantadosi, S., Marshall, F. F., & Nelson, W.G. (1999). Induction of immunity to prostate cancer antigens: results of a clinical trial of vaccination with irradiated autologous prostate tumor cells engineered to secrete granulocyte-macrophage colony-stimulating factor using ex vivo gene transfer. *Cancer Research*, Vol. 59, No. 20, (October, 1999), pp. 5160- 5168, ISSN 1010-4283.

Sparwasser, T., Koch, E. S., Vabulas, R. M., Heeg, K., Lipford, G. B., Ellwart, J. W., & Wagner, H. (1998). Bacterial DNA and immunostimulatory CpG oligonucleotides trigger maturation and activation of murine dendritic cells. *European Journal of Immunology*, Vol. 28, No. 6, (June, 1998), pp. 2045-2054, ISSN 0014-2980.

Stern, A. M., & Markel, H. (2005). The history of vaccines and immunization: familiar patterns, new challenges. *Health Affairs*, Vol. 24, No. 3 (May, 2005), pp. 611-621, ISSN 0278-2715.

Suckow, M. A., Hall, P., Wolter, W., Sailes, V., & Hiles, M. C. (2008c). Use of an extracellular matrix material as a vaccine carrier and adjuvant. *Anticancer Research*, Vo. 28, No. 5, (September, 2008), pp. 2529-2534, ISSN 0250-7005.

Suckow, M. A., Heinrich, J., & Rosen, E. D. (2007). Tissue vaccines for cancer. *Expert Review of Vaccines*, Vol. 6, No. 6, (December, 2007), pp. 925-937, ISSN 1476-0584.

Suckow, M. A., Rosen, E. D., Wolter, W. R., Sailes, V., Jeffrey, R., & Tenniswood, M. (2007). Prevention of human PC-346C prostate cancer growth in mice by a xenogeneic vaccine. *Cancer Immunology & Immunotherapy*, Vol. 56, No. 8, (January, 2007), pp. 1275-1283, ISSN 0340-7004.

Suckow, M. A., Siger, L., Bowersock, T. L., Turek, J. J., Van Horne, D., Borie, D., Taylor, A., Park, H., & Park, K. (1999). *Polysaccharide Applications: Cosmetics and Pharmaceuticals* (1st Edition), American Chemical Society, ISBN 0-8412-3641-0, Washington, D. C.

Suckow, M. A., Wheeler, J. D., Wolter, W. R., Sailes, V., & Yan, M. (2008b) Immunization with a tissue vaccine enhances the effect of irradiation of prostate tumors. *In Vivo*, Vol. 22, No. 2, (March, 2008), pp. 171-177, ISSN 0258-851X.

Suckow, M. A., Wolter, W. R., & Pollard, M. (2005). Prevention of autochthonous prostate cancer by immunization with tumor-derived vaccines. *Cancer Immunology & Immunotherapy*, Vol. 54, No. 6, (June, 2005), pp. 571-576, ISSN 0340-7004.

Suckow, M. A., Wolter, W. R., & Sailes, V. T. (2008a). Inhibition of prostate cancer metastasis by administration of a tissue vaccine. *Clinical & Experimental Metastasis*, Vol. 25, No. 8, (August, 2008), pp. 913-918, ISSN 0262-0898.

Traquina, P., Morandi, M., Contorni, M., & Van Nest, G. (1996). MF59 adjuvant enhances the antibody response to recombinant hepatitis B surface antigen vaccine in primates. *Journal of Infectious Diseases*, Vol. 174, No. 6, (December, 1996), pp. 1168-1175, ISSN 0022-1899.

Ulrich, J. T., & Myers, K. R. (1995). Monophosphoryl lipid A as an adjuvant: past experiences and new directions. *Pharmaceutical Biotechnology*, Vol. 6, pp. 495-524, ISSN 1078-0467.

Wright, D. K., Lalloo, U. G., Nayaiger, S., & Govender, P. (1989). Autonomic nervous system dysfunction in severe tetanus: current perspectives. *Critical Care Medicine*, Vol. 17, No. 4, (April, 1989), pp. 371-375, ISSN 1530-0293.